UNIVERSITAT POLITÈCNICA DE CATALUNYA BARCELONATECH

Morpho-functionality of the toothed whale external ear canal

by
Steffen De Vreese

Joint PhD programme in Veterinary and Marine Sciences

MORPHO-FUNCTIONALITY of the TOOTHED WHALE EXTERNAL EAR CANAL

Thesis submitted to obtain the title of Doctor in Veterinary Sciences by the Università degli Studi di Padova and Doctor in Marine Sciences by the Universitat Politècnica de Catalunya

Doctoral dissertation by
Steffen De Vreese

Supervisors
Prof. Dr. Sandro Mazzariol
Prof. Dr. Michel André

Coordinators
Prof. Dr. Valentina Zappulli
Prof. Dr. Agustín Sanchez-Arcilla

Department of Comparative Biomedicine and Food Science (BCA), Università degli Studi di Padova (UniPd), Italy
Laboratory of Applied Bioacoustics (LAB), Universitat Politècnica de Catalunya (UPC), Spain

University with Administrative Responsibility: Università degli Studi di Padova
Hosting University: Universitat Politècnica de Catalunya
Performed with the financial contribution of the Cariparo Foundation

ACKNOWLEDGEMENTS

ACKNOWLEDGEMENTS

This work is the result of three years in a joint PhD between the Department of Comparative Biomedicine and Food Science of the University of Padova and the Laboratory of Applied Bioacoustics of the Technical University of Catalonia. The time I spent was divided between both, besides occasional collaborations with other institutions. The results are the fruit of an international effort, shared among many talented people.

I would like to thank my supervisors, Prof. Dr. Sandro Mazzariol and Prof. Dr. Michel André, for the absolute faith, unconditional support, and the countless opportunities you provided. For the ideas, for the inspiration to aim high, for thinking years ahead while living here and now. For sharing your knowledge, energy and motivation, and for putting things into context and showing the bigger picture when I ended up cockeyed and lost in details.

None of this could have been possible without the most amazing colleagues in both of the institutions where I spent the last years. *Muchisimas gracias* to the proficient and diverse group of colleagues with whom I have had the pleasure to work with at the LAB. Thank you Marta Solé, Mike van der Schaar, Rocio Prieto González, Antonio M. Sanchez, Alba Solsona Berga, Pablo Pla Caro, Ludwig Houegnigan, Serge Zaugg, and Florence Erbs for supporting me in too many ways to express here.

Many thanks to the most wonderful colleagues at BCA. Your passion for the work is transcendent and the smiles are infectious. A *grazie mille* is not sufficient to thank you all, Dr. Cinzia Centelleghe, Giorgia Corazzola, Ksenia Orekhova, Cristina Otero Sabio, Dr. Federico Bonsembiante, Ginevra Brocca, Dr. Diana Gianuzzi, Dr. AlessanDro Sammarco, Dr. Silvia Ferro, Prof. Dr. Massimo Castagnaro, Prof. Dr. Laura Cavicchioli, Prof. Dr. Maria Elena Gelain, Dr. Valentina Moccia, Nicolò Rensi, Filippo Torrigiani, Prof. Dr. Ranieri Verin, Prof. Dr. Valentina Zappulli. Also, the most sincere thanks and respect to Drs. Davide Trez, Enrico Gallo, Rosella Zanetti, Giuseppe Palmisano, Michele Povinelli, Letizia Moro, and AlessanDro Calore, for more than just technical support in the necropsy room and in the laboratories. It was a pleasure working with such fantastic and energetic colleagues. You have taught me so much, from technical protocols to classical music, Italian proverbs and dialects, and the simple act of enjoying the work and singing while doing it. To Davide PeDrotti, for constructing the antithetic slicer and for his unsalted opinion on the philosophy of being a student. Thanks to Prof. Dr. Mauro Dacasto, Prof. Dr. AlessanDra Piccirillo, Roberta Tolosi, Giorgia Guerra, MariaLaura Gallo, and Dr. Morgan Smits, and a special thanks to Matteo Tuzzato for all computer-related technical assistance, always ready to help, for being weird and calling me the same. My most sincere appreciation to Prof. Dr. Bruno Cozzi for sharing his wisdom, patience and trust. A merci beaucoup to the wise Dr. Jean-Marie Graïc for his brilliance, and to Tommaso Gerussi, Dr. Giovanni Caporale, and Prof. Dr. Federica Marcher, for technical assistance in the lab. Warm regards to Stefano Bianchini and his colleagues for administrative help.

My most sincere respect and gratitude to Dr. Eduard Degollada (Associación Edmaktub) for sharing his ideas on the morphofunctionality and anatomical research in cetaceans, for the practical and theoretical skills, and for preparing me to carry out the intense and stressful work that is a doctoral dissertation.

A most incredible and sincere 'grazie mille' to Prof. Dr. Giovanni Di Guardo (Università degli Studi di Teramo) for the celestial conversations, stimulating ideas, and inexhaustible curiosity.

My sincerest thanks to Dr. Enrico Orvieto (Dipartimento dei Servizi di Diagnosi e Cura, Direttore UOC Anatomia Patologica, hospital of Rovigo) for helping with the digitization of the histological slides used for 3D reconstruction, by offering his valuable time and facilities.

Muchissimas gracias to Prof. Dr. Mariano Domingo (Department of Health and Anatomy, Faculty of Veterinary Medicine, Autonomous University of Barcelona, Bellaterra) for a fruitful collaboration, for involving me in the cetacean necropsies, and to Dr. Lola Perez for always making me feel welcome in the necropsy room, for technical assistance, for being the warm-hearted person she is.

Danke schön to Prof. Dr. Hansjörg Schröder, Dr. Stefan Huggenberger, Dr. Lennart Mueller-Thomsen, and dear Sofia Schroeder, for a very interesting time and collaboration at the Department of Anatomy II of the University of Köln, Germany, and elsewhere such as in Barcelona, for being warm, open and welcoming, in mind and heart.

Hartelijk dank to Lonneke IJsseldijk (Department of Pathobiology, Faculty of Veterinary Medicine, Utrecht University) for sharing samples of harbour porpoise ears, and to her colleague Dr. Dorien Willems for the CT images of a single animal. Also, thanks to Prof. Dr. AlessanDro Zotti (Department of Animal Medicine, Production and Health, UniPD) for the CT images of a bottlenose dolphin.

The immunofluorescence study with confocal microscopy is an on-going collaboration, but I already express my gratitude here to Prof Dr. Federico Luzzati and Dr. Marco Fogli (Dipartimento di Scienze della Vita e Biologia dei Sistemi, Università degli Studi di Torino, Turin, Italy; & Neuroscience Institute Cavalieri Ottolenghi (NICO)), and to Dr. Cristiano Corona, Dr. Cristina Casalone, Dr. Carla Grattarola, Dr. Elena Valentina Costassa, and Claudia Palmitessa (S.C. Neuroscienze, Lab. di Neurobiologia Sperimentale - Centro di Referenza per le TSE, Istituto Zooprofilattico Sperimentale del Piemonte Liguria e Valle d'Aosta) for the very interesting collaboration, and to Dr. Giacomo carta (Istituti Clinici di Perfezionamento, Department of Rehabilitation, Milan, Italy) for a fascinating discussion on the somatosensory system.

Many thanks to all people that are part of the sampling network and who dissected and provided the valuable samples for this research, in particular Dr. Giuseppe Lucifora, Dr. Walter Mignone, Dr. Giuliana Terraciano, and Dr. Antonio Pintore (IZS del Mezzogiorno, Portici; IZS del Piemonte, Liguria e Valle d'Aosta, Torino; IZS del Lazio e Toscana, Pisa; and IZS della Sardegna, respectively).

I would also like to acknowledge Josep Maria Rebled, Eva Prats, Adriana Martínez Gené, and Rosa Rivera (Unitat de Microscopia Electrònica, Hospital Clínic, Universitat de Barcelona) for technical support for the TEM studies.

Lastly, big hugs to all the residents of Cas'Alaska and particularly to the most warm-hearted and extraordinary Dr. Gaia Pagani and Martina Libanora, for welcoming me into their home and hearts.

To all my friends, family, and other loved ones.

GENERAL TABLE OF CONTENTS

Detailed tables of contents are provided at the beginning of each chapter

ABSTRACTS

ABSTRACT (EN)

While marine, anthropogenic noise pollution is a scientific and societal matter of concern, there is limited knowledge on how sea animals, particularly cetaceans, perceive their environment through sounds. Toothed whales, like all cetaceans, show a series of astonishing morphological and physiological evolutionary adaptations, of which one of the most striking can be found in the complex configuration of the hearing apparatus. The external ear canal, although no longer considered a direct actor in the sound reception process, also shows surprising adaptation with many active structures and a complex peripheral innervation, although basic knowledge on its morphology is inconclusive at the moment.

This study aimed at providing fundamental knowledge on the morphology of the external ear canal in various toothed whales, associated to its sensory capabilities with in-depth morphological descriptions of its shape and course, lumen and content, epithelium, glands, lymphoid tissue, vascularization, innervation, muscular tissue, cartilage, fat and connective tissue. Furthermore, specific attention was given to the identification and morphological characterization of the sensory formations associated with the external ear canal, and the comparison with the terrestrial cetartiodactyl external ear canal, to gain perspective of a comprehensive understanding of the cetacean sensory abilities.

Post-mortem samples were gathered during necropsies of wild toothed whales, in an international collaborative effort. The tissues were inspected macroscopically and subjected to microscopic studies including immunohistochemical analyses using antibodies specific for nervous tissue, various histochemical techniques, ultrastructural investigation using transmission electron microscopy, and 3D reconstruction from histological slides of the ear canal and associated tissues.

The winding structure of the external ear canal revealed a complex organ that comprises a physiological function reflected in its delicate anatomical structures, all of which are discussed in detail. Remarkably, the innervation showed an extensive intramural nervous plexus with the predominant presence of simple lamellar corpuscles, similar to Pacinian corpuscles although without an outer core or capsule. There were differences in conformation along the canal, from a network that fully encompasses the ear canal to a nervous tissue ridge that bulges into the lumen.

The work elaborates on hypotheses related to the external ear canal's function and the somatosensory system in toothed whales, taking into account the importance of the perspective of sensory modalities in the marine environment. The results indicate it plays an important physiological function, which impairment may have direct effects on their sensory capabilities and compromise essential physiological processes. It also puts into question to what extent there might be an adverse effect from various sources of anthropogenic noise, as it can cause physical changes in the sensory tissues in cetaceans and other marine fauna.

Keywords: Toothed whales, External ear canal, Morphology, Pathology, Peripheral nervous system, Sensory nerve formations, Lamellar corpuscles

ABSTRACT (IT)

Studio morfo-funzionale del canale uditivo esterno negli odontoceti

Nonostante l'inquinamento acustico marino sia una questione che induce una crescente preoccupazione scientifica e sociale, la conoscenza su come gli animali marini, in particolare i cetacei, percepiscono il loro ambiente attraverso i suoni è ancora limitata. Gli odontoceti in particolare mostrano una serie di notevoli adattamenti evolutivi morfologici e fisiologici, di cui uno dei più eclatanti si trova nella complessa configurazione dell'apparato uditivo. Il condotto uditivo esterno, sebbene non sia più considerato una parte direttamente interessata nel processo di ricezione del suono, mostra un sorprendente adattamento con molte strutture attive e una complessa innervazione periferica. Tuttavia, le conoscenze basilari sulla sua morfologia e funzione sono incomplete al momento.

Questo studio mira ad approfondire la morfologia del condotto uditivo esterno in vari odontoceti, con descrizioni morfologiche fornendo dettagli sulla sua forma e decorso, lume e contenuto, epitelio, ghiandole, tessuto linfoide, vascolarizzazione, innervazione, tessuto muscolare, cartilagine, tessuto adiposo e connettivo. Inoltre, una particolare attenzione è stata data all'identificazione e caratterizzazione morfologica delle formazioni sensoriali associate al condotto uditivo esterno, e al confronto con la medesima struttura in altri ceto-artiodattili terrestri, per ottenere una prospettiva di comprensione complessiva delle capacità sensoriali dei cetacei.

I campioni sono stati raccolti durante necroscopie di odontoceti spiaggiati, in uno sforzo di collaborazione internazionale. I tessuti sono stati valutati macroscopicamente e quindi sottoposti a studi microscopici, comprendenti analisi immunoistochimiche utilizzando anticorpi specifici per il tessuto nervoso, insieme a varie tecniche istochimiche e indagini ultrastrutturali mediante microscopia elettronica a trasmissione. Ciò ha inoltre portato alla ricostruzione 3D partendo da vetrini istologici del condotto uditivo e dei tessuti associati.

Il condotto uditivo esterno si è rivelato un organo complesso che comprende una funzione fisiologica riflessa nella sua delicata struttura anatomica. L'innervazione mostrava un esteso plesso nervoso intramurale con la presenza predominante di semplici corpuscoli lamellari, simili ai corpuscoli del Pacini, sebbene senza strato esterno o capsula. Lungo il decorso del condotto si sono notate alcune differenze nella sua architettura e distribuzione, da una rete che racchiude completamente il condotto uditivo a una papilla di tessuto nervoso che si gonfia nel lume.

Grazie a questo studio si è potuto, al termine del lavoro, elaborare ipotesi relative alla funzione del condotto uditivo esterno e del sistema somatosensoriale nelle balene dentate, tenendo conto dell'importanza della prospettiva delle modalità sensoriali nell'ambiente marino. I risultati indicano che svolge una rilevante funzione fisiologica, la cui compromissione può avere effetti diretti sulla capacità sensoriali dei odontoceti e possibilmente compromettere i processi fisiologici essenziali. Questo studio sottolinea come potrebbe esserci effetti da varie fonti di rumore antropico, che possono causare cambiamenti fisici nei tessuti sensoriali dei cetacei e di altra fauna marina.

ABSTRACT (CAT)

Morfo-funcionalitat del canal auditiu extern en odontocets

Si bé la contaminació acústica marina antropogènica és un assumpte que preocupa la comunitat científica i la societat en general, el coneixement sobre com els animals marins, en particular els cetacis, perceben el seu entorn a través dels sons és limitat. Els odontocets, com tots els cetacis, presenten una sèrie de sorprenents adaptacions evolutives morfològiques i fisiològiques. Entre elles, una de les més notables es troba en la complexa configuració de l'aparell auditiu. El canal auditiu extern, tot i que no es considera que tingui un paper directe en el procés de recepció de el so, també mostra una sorprenent adaptació al medi marí, mostrant moltes estructures actives i una complexa innervació perifèrica. Malgrat això, els coneixements bàsics sobre la seva morfologia no són concloents de moment.

Aquest estudi tenia com a objectiu la descripció fonamental de la morfologia del conducte auditiu extern en diversos odontocets, associant-la a les seves capacitats sensorials a través de descripcions morfològiques en profunditat de la seva forma i curs, lumen i contingut, epiteli, glàndules, teixit limfoide, vascularització, innervació, teixit muscular, cartílag, teixit adipós i connectiu. A més, es va parar especial atenció a la identificació i caracterització morfològica de les formacions sensorials associades al canal auditiu extern, i es va fer una comparació amb el conducte auditiu extern de cetartiodáctilos terrestres, per tal d'assolir una comprensió integral de les capacitats sensorials dels cetacis.

Es van recol·lectar mostres post-mortem durant necròpsies d'odontocets salvatges, en un esforç de col·laboració internacional. Els teixits es van inspeccionar macroscòpicament i es van sotmetre a estudis microscòpics, incloent anàlisis immunohistoquímics amb anticossos específics per teixit nerviós, diverses tècniques histoquímiques, investigació ultraestructural mitjançant microscòpia electrònica de transmissió i reconstrucció 3D a partir de talls histològics de canal auditiu i teixits associats.

L'estructura sinuosa de canal auditiu extern va revelar un òrgan complex, la funció fisiològica del qual es reflecteix en les seves delicades estructures anatòmiques, que presenten una morfologia que es discuteix en detall. Sorprenentment, la innervació va mostrar un extens plexe nerviós intramural amb la presència predominant de corpuscles lamelares simples, similars als corpuscles de Pacini, encara que sense capa externa o càpsula. Es van observar diferències en la conformació dels corpuscles al llarg del canal auditiu, des d'una xarxa que abasta completament el conducte fins a una cresta de teixit nerviós que sobresurt en el lumen.

El treball desenvolupa hipòtesis relacionades amb la funció del conducte auditiu extern i el sistema somatosensorial en odontocets, tenint en compte la importància de la perspectiva de les modalitats sensorials en el medi marí. Els resultats indiquen que el canal exerceix una funció fisiològica important, el deteriorament del qual pot tenir efectes directes sobre les seves capacitats sensorials i comprometre processos fisiològics essencials. També qüestiona fins a quin punt les diverses fonts de soroll antropogènic poden tenir un efecte advers, ja que poden provocar canvis físics en els teixits sensorials en cetacis i altra fauna marina.

ABSTRACT (ES)

Morfo-funcionalidad del canal auditivo externo en odontocetos

Si bien la contaminación acústica marina antropogénica es un asunto que preocupa a la comunidad científica y a la sociedad en general, existe un conocimiento limitado sobre cómo los animales marinos, en particular los cetáceos, perciben su entorno a través de los sonidos. Los odontocetos, como todos los cetáceos, presentan una serie de asombrosas adaptaciones evolutivas morfológicas y fisiológicas. Entre ellas, una de las más notables se encuentra en la compleja configuración del aparato auditivo. El canal auditivo externo, aunque no se considera que tenga un rol directo en el proceso de recepción del sonido, también muestra una sorprendente adaptación al medio marino, mostrando muchas estructuras activas y una compleja inervación periférica. No obstante, los conocimientos básicos sobre su morfología no son concluyentes por el momento.

Este estudio tuvo como objetivo la descripción fundamental de la morfología del conducto auditivo externo en diversos odontocetos, asociandola a sus capacidades sensoriales a través de descripciones morfológicas en profundidad de su forma y curso, lumen y contenido, epitelio, glándulas, tejido linfoide, vascularización, inervación, tejido muscular, cartílago, tejido adiposo y conectivo. Además, se prestó especial atención a la identificación y caracterización morfológica de las formaciones sensoriales asociadas al canal auditivo externo, y se hace una comparación con el conducto auditivo externo de cetartiodáctilos terrestres, con el fin de alcanzar una comprensión integral de las capacidades sensoriales de los cetáceos.

Se recolectaron muestras post-mortem durante necropsias de odontocetos salvajes, en un esfuerzo de colaboración internacional. Los tejidos se inspeccionaron macroscópicamente y se sometieron a estudios microscópicos, incluyendo análisis inmunohistoquímicos con anticuerpos específicos para tejido nervioso, diversas técnicas histoquímicas, investigación ultraestructural mediante microscopía electrónica de transmisión y reconstrucción 3D a partir de cortes histológicos del canal auditivo y tejidos asociados.

La estructura sinuosa del canal auditivo externo reveló un órgano complejo cuya función fisiológica se refleja en sus delicadas estructuras anatómicas, la morfología de las cuales se discuten en detalle. Sorprendentemente, la inervación mostró un extenso plexo nervioso intramural con la presencia predominante de corpúsculos lamelares simples, similares a los corpúsculos de Pacini, aunque sin capa externa o cápsula. Se observaron diferencias en la conformación de los corpúsculos a lo largo del canal auditivo, desde una red que abarca completamente el conducto hasta una cresta de tejido nervioso que sobresale en el lumen.

El trabajo desarrolla hipótesis relacionadas con la función del conducto auditivo externo y el sistema somatosensorial en odontocetos, teniendo en cuenta la importancia de la perspectiva de las modalidades sensoriales en el medio marino. Los resultados indican que el canal desempeña una función fisiológica importante, cuyo deterioro puede tener efectos directos sobre sus capacidades sensoriales y comprometer procesos fisiológicos esenciales. También cuestiona hasta qué punto las diversas fuentes de ruido antropogénico pueden tener un efecto adverso, ya que pueden provocar cambios físicos en los tejidos sensoriales en cetáceos y otra fauna marina.

INTRODUCTION

INTRODUCTION

Table of contents

1 Preface - motivation

1.1 Topic

Toothed whales are fully aquatic mammals for whom the use of acoustics is essential for navigation, foraging and communication (Richardson et al., 1995). As top-chain predators, they have been considered umbrella and flagship species indicating the health status of the marine acoustic environment. Indeed, there are indications that cetaceans can be affected by underwater noise overexposure, particularly individual animals, with indirect and direct impacts on sensory organs and in particular the hearing apparatus, similar to terrestrial mammals (e.g. Fernández et al., 2005). The sources of underwater noise include military activities (explosions, sonar), oil and gas prospection, construction, maritime transport, and commercial and private fishing, all of which produce distinct types of sound that can have various effects on toothed whales and other fauna (André et al., 2009). This issue has been of global concern for the last decade and has led to the development of noise exposure criteria for marine mammals (Southall et al., 2019), which in time leads to the implementation of effective mitigation measures and guidelines for operators (e.g. MSFD, Fernández et al., 2013).

The European Commission decided in September 2010, under the Marine Strategy Framework Directive (MSFD)(Van der Graaf et al., 2012), to start addressing this concern by introducing two indicators for underwater noise that would help to describe ocean Good Environmental Status (GES). Although they represent a necessary base to homogenise and standardise measurements, these two indicators are centred on the physical aspects of noise but do not yet help monitor the impact of these sources on the marine environment, nor include other forms of energy like EMF.

Although it is generally accepted that exposure to anthropogenic noise can sometimes trigger behavioural and physiological changes, and there is a consensus amongst the scientific community that toothed whales could suffer from *acoustic trauma* after sound exposure, the direct effects anthropogenic noise can have on biological tissues are still unclear, particularly regarding sound reception mechanisms and organs, since very scarce data is currently available to assess their status, such as during mass stranding events (Morell et al., 2017). Therefore, it is essential to have a clear understanding of the functional morphology of the tissues associated with the auditory pathways, and to discern pathologies and apprehend how they develop and can affect the sensory system. However, this understanding must also involve all the tissues directly or indirectly associated with the hearing apparatus. In toothed whales, this includes the peripheral acoustic pathway, the middle and inner ear, and the central pathway through the cranial nerves and the central nervous system. Also, one has to consider the entirety of the body and its peculiar and sometimes extreme morphological and physiological adaptations to the fully aquatic life. It is also important to note and investigate the mechanisms of self-mitigation and adaptation to the variable circumstances such as the changes in pressure, which can impact the physiological mechanisms used for adaptation and auto-protection.

The role of the veterinarians in this regard is essential, nonetheless complex and pertinently multidisciplinary. They contribute in two primary fields: evidence-based medicine from a forensic pathological perspective (IJsseldijk et al., 2019; Mazzariol et al., 2018), and, fundamental research on the morphofunctional aspects of these enigmatic animals (Cozzi et al., 2017).

Atypical stranding events, particularly mass stranding of live animals, have been associated in time and space with anthropogenic activity such as military exercises with the use of low- and mid-frequency active sonar, which has a potential to induce functional-structural damage (Jepson et al., 2003, 2013). The lesions found during post-mortem investigations in spatiotemporal association with such acoustic events range from alterations caused by a systemic gas and fat embolic syndrome with haemorrhages and gas and fat emboli in various vital organs and locations, accompanied by haemorrhages in the acoustic fat bodies, around ears, in the brain, and in the kidneys (Balcomb III and Claridge, 2001; Fernández et al., 2005). While some of the investigative efforts focus on the sensitive structure of the hearing apparatus and the analysis of alterations inside the inner ear (Morell et al., 2017), these investigations emphasised again the role of the veterinarian and the value of performing complete post-mortem investigations as part of a multidisciplinary approach in order to understand the cause of the stranding events (Mazzariol et al., 2018; IJsseldijk et al., 2019).

1.2 Purpose

The first purpose is to get a better understanding of the functional morphology of the external ear canal. As such, this will include both a general morphological assessment of the external ear canal and associated soft tissues and more detailed investigations of the peripheral nervous system.
Second, is to investigate if there is any pathology associated with the external ear canal and associated tissues, with the purpose to get an understanding of pathological processes in these animals, and the defence mechanisms and the immune system, the flexibility and resilience of the tissues to drastic changes in environmental parameters (pressure) and the physiological adaptations.

2 Sound reception in toothed whales

2.1 Brief overview

Odontocetes can perceive sounds through their mandible and the associated acoustic fat bodies, which are in physical contact with the tympanic bulla and the ear bones (Nummela et al., 2007). However, the exact pathway of how sound waves reach the inner ear is still under debate. Moreover, the involved tissues have been described in only a few species, and as there are significant interspecific differences in the acoustic spectrum, this constitutes interspecific morphological differences in both the sound production and reception pathways (Nummela et al., 2007). Furthermore, the function of tissues such as the external ear canal is unknown, which is often regarded as vestigial, an evolutionary remnant that is considered functionally insignificant. Although it has been suggested that it can serve as an effective sound wave transductor (Lipatov, 1978, In: Popov and Supin, 1990), a vibratory wave could enter all soft tissues of the head of toothed whales as their impedance is close to that of seawater (Hemilä et al., 2010).
Such investigations are characteristic for morpho-functional studies in cetaceans, because of the difficulties implied in obtaining conclusive outcome when starting a paucity of samples with often a poor tissue preservation state.
Consequently, there is a paucity of information on the sensory system in the peripheral tissues associated with the auditory apparatus in toothed whales. The cranial nerves have been studied in few species while only in detail in Pantropical spotted dolphin (*Stenella attenuata*) (Rauschmann, 1992), and the middle ear, inner ear and vestibulocochlear nerve have been subject of several anatomical studies (e.g. Ketten, 1992). At the same time, the peripheral nervous system has been of little interest, and there is little to no in-depth information on its functional morphology. Few authors have mentioned the presence of lamellar corpuscles in cetaceans (Bryden and Molyneux, 1986; Giacometti, 1967; Palmer and Weddell, 1964; Wickham, 1980) and these have been mostly studied using basic histological techniques. The tissues in these studies include various parts of the skin including the trunk, fluke and pectoral fins, the nasal sac system, the blowhole, and the iridocorneal

angle in several species of odontocetes. However, there is an essential need for detailed information on the morphology of the sensory nerve formations related to the ear canal in order to understand the functionality of the ear canal and the peripheral sensory system, and any pathologies associated with it. A preliminary study showed indications of an exceptional sensitivity of the external ear canal with the abundant presence of likely mechanoreceptors in an odontocete (*Lagenorhynchus albirostris*) and mysticete (*Balaenoptera acutorostrata*) species (De Vreese et al., 2014), but failed to draw any conclusions on the functional morphology of the entire organ.

2.2 Evolution of hearing in cetaceans and studies on hearing in toothed whales

After the hearing apparatus of terrestrial mammals evolved for the detection of sound vibration in the air with the development of more complex system than in fish, amphibians, reptiles, and even birds, some mammals returned to the water, only to have to adapt again to a different medium. The first of these mammals were cetaceans, in the Early Eocene, more than 50 million years ago (Berta et al., 2006), later to be followed by the sirenians, the only other mammal with a fully aquatic lifestyle, and various other mammals, including pinnipeds. In this transition from air to water, instead of devolution of the complexity of the hearing apparatus to a more primitive state, it evolved and adapted to the dispositions imposed by the water medium and its physical, acoustic (sound transmission) characteristics to form a highly complex and efficient hearing system unlike any other (Reysenbach de Haan, 1956).

As cetaceans descend from land mammals, the structure of their hearing apparatus consists of the three main components: outer, middle and inner ear, from where the signal changes modality from physical to electrical, containing information that to be processed in the central nervous system. All three components show specific adaptations to the fully aquatic life, one more extreme than next. Reysenbach de Haan (1957), who was one of the first to describe the entire hearing apparatus in various cetaceans, mentioned that all three components show morphological characteristics that are *typically 'whalish' in every respect*, which means they show adaptations that can be found among cetaceans but not in other mammals. Among cetaceans, there are several significant differences in the hearing apparatus of toothed whales and baleen whales. One of the most enigmatic adaptations of toothed whales to aquatic life is the use of high-frequency sounds used for navigation or foraging, in contrast to the apparent absence of echolocation in baleen whales. As such, toothed whales have developed acoustic fat bodies both involved in sound production and reception, the melon and the mandibular fat bodies respectively. The latter takes up the prominent part of the peripheral sound conduction pathway in toothed whales, but the specific mechanisms are not fully understood yet. Reysenbach de Haan (1956), and Dudok van Heel (1962) were the first to propose that the soft tissues of the head could assist in the sound reception process. These soft tissues included a 'huge' fat body

that filled the mandibular hiatus from caudal, and which was in direct contact with the lateral side of the tympanic, rostral to the external ear canal. A few years later, Norris (1968) gave rise to the jaw hearing theory, which is sound conduction through the fatty channels associated with the mandible.
There exist various sound reception pathway theories, most of which do not exclude any of the others. There are even indications that not a single pathway would be responsible for the conduction of all sounds, but rather a segmented pathway, in which the 'acoustic windows' (i.e. the sound receiving area, the location where sound enters the head) and the underlying tissues through which the sound propagates are sensitive to the frequency characteristics of the incoming sound. As such, the reception of lower-frequency sounds could be spatially associated with an acoustic window near the external ear canal and tympanic bone, while higher frequency sounds would be associated with a pathway that involves the mandibles and the related fat bodies (Ketten, 1994, 1997; Popov and Supin, 1990; Popov et al., 2008)(Figure 1).

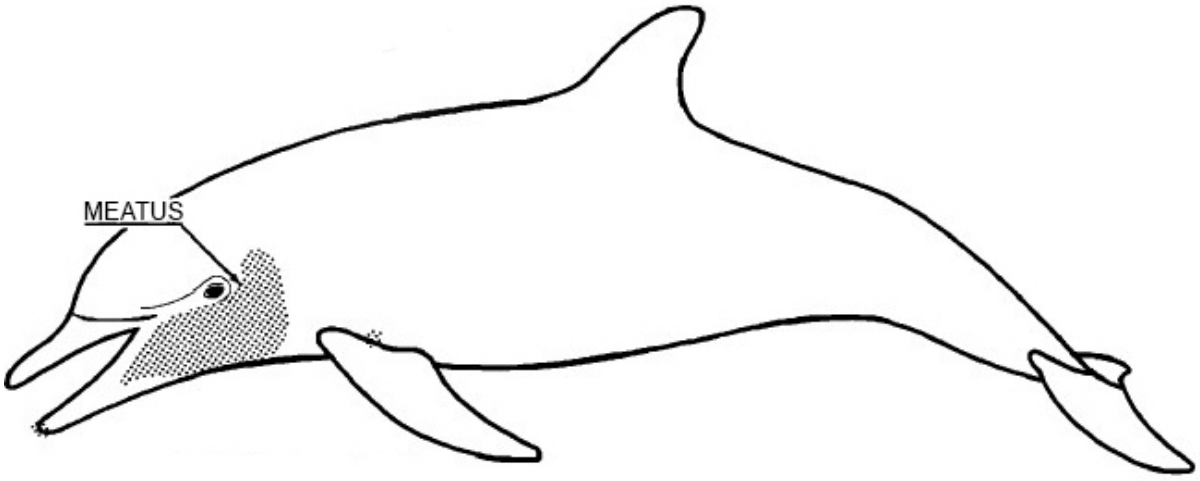

Figure 1. McCormick et al., 1970. Dots represent the areas of greatest sensitivity to acoustic stimuli, according to McCormick et al. (1970).

The mandibular fat bodies stretch in and around the lower jaws: inside the mandibular canal and over almost the entire length of the mandible, and lateral and caudolateral to the mandibles and in close contact with the mandibular fossae but medial to the blubber[1].
An incoming sound wave could pass through the skin and underlying soft tissues, which is possible because of the impedance matching between the water medium and soft tissues, and it enters the mandibular fat bodies (Cranford et al., 2010; Ketten, 1997; Norris, 1968). One way sound can travel, first described as the '*jaw hearing' theory* (Norris, 1968) is through the thin bony plate of the caudolateral side of the mandible, named the 'pan bone', called that way initially by sailors and described by (Norris, 1968). The pan bone, as an 'acoustic window', provides an acoustic pathway of

[1] The blubber in this region has a different chemical composition that the adjacent blubber, and is similar to the acoustic fat as it contains high concentrations of molecules (iso-acids). These chemical observations support that this region can act as an acoustic window (Zahorodny Duggan et al., 2009).

low impedance from the external environment through the soft and fatty tissues (Norris, 1968), confirmed using AEP's (Møhl et al., 1999), and cochlear window movements (McCormick et al., 1970), at least for high-frequency sounds. On passing the pan bone, the sound enters the intramandibular fat body, which passes through the mandibular foramen, i.e. the absent caudomedial bony wall of the mandible, from where it can be coupled to the middle ears. As such, both sides of the mandible are 'acoustically transparent'. Another pathway is through the oral cavity and gular region, labelled as the *gular pathway* (Cranford and Krysl, 2012; Cranford et al., 2008a)(described in Cuvier's beaked, *Ziphius cavirostris*), in which the incoming sound enters the soft tissues of the head from below and between the mandibles and enters the internal mandibular fat bodies 'through' the mandibular foramen (Figure 2). The gular pathway and the dental pathway were both derived from models, while the other pathways were derived from physical experiments. In the 'dental pathway,' the teeth act as high-frequency resonators and the teeth innervation (mandibular nerve) as part of a pressure sensor system that could play a role in the sound reception mechanism, at least valid for species that possess teeth (Goodson and Klinowska, 1990). The *lateral acoustic pathway* is spatially closely associated with the extramandibular or lateral fat body in which the sound would not travel through the pan bone, but passes the mandible caudally (Ketten, 1997; Popov and Supin, 1990). Finally, (Ryabov, 2010) considered the *mental foramina of the lower jaw*, through which the mental nerves and vascularisation innervate and provide the skin of the rostral part of the lower jaw of vascularisation, as possible holes through which the incoming sound wave could enter and pass to the internal mandibular fat body. All of these studies agree on the internal part of the peripheral sound reception pathway, which is from the internal mandibular fat body to the middle ear (Cranford et al., 2010; Hemilä et al., 1999, 2010). This fat body has two branches that contact the middle ear in two locations (Cranford et al., 2008b, 2010): one along the ventrolateral aspect of the tympanic (cfr. Norris, 1968) and one in a sulcus anterior to the sigmoid process (sulcus for chorda tympani) (Mead and Fordyce, 2009).

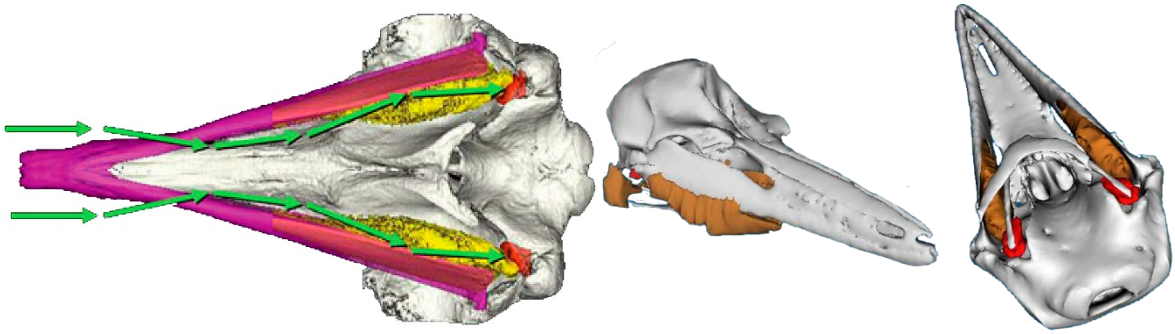

Figure 2. Left: The gular pathway in Cuvier's beaked whale (Source: Cranford and Krysl, 2012). Right the mandibular fat bodies in a bottlenose dolphin (Source: Darlene Ketten, Woods Hole Oceanographic Institution and Harvard Medical School, https://csi.whoi.edu/)

The internal mandibular fat body is composed of an inner and outer core, with the outer being denser (Montie et al., 2011), similar to the melon fat configuration (Norris, 1968; Soldevilla, 2005), which is also reflected in the biochemical composition (Varanasi and Malins, 1971; Koopman et al., 2006; Zahorodny Duggan et al., 2009). The chemical composition influence the sound speed (Varanasi et al., 1982), and as such, both in the melon and in the internal mandibular fat bodies, sound waves are focused into the core of the fat bodies, to propagate to the external environment or the middle ear respectively (Koopman, 2018). Although there are interspecific and inter-age differences in the molecular composition of the mandibular fat, the relative spatial arrangement of the lipids is highly consistent among species and age classes

In this work, the focus is put on adult toothed whales, although results obtained from striped dolphin foetus and references from the literature on baleen whales are added appropriately to put findings into perspective. Much more is known about toothed whale functional morphology related to both sound production and reception mechanisms, than what is known in baleen whales, due to the availability of animals and samples, and the logistics associated with the size of the animals.

Most morphological studies put into perspective the relevance of the findings to the functionality associated with the acoustic spectrum and use for a specific species. However, a certain amount of extrapolation between morphologically similar species in acoustically similar habitats is accepted.

Few studies have looked at the entire hearing apparatus in both toothed and baleen whales (e.g. Ketten, 1997, 2000), which provide essential 'points of overview', while other studies have provided essential knowledge of fine-scale and complex structures such as the inner ear (e.g. Morell Ybarz, 2012), the middle ear (e.g. Hemilä et al., 1999; Nummela et al., 1999), and the mandibular fat bodies (e.g. Cranford et al., 2010; Barroso et al., 2012).

The techniques used to study the hearing apparatus in cetaceans range from purely observational morphological studies, from the macroscopic level down to the ultrastructural level, and accompanied fairly recently by modelling techniques starting from medical imaging techniques to predict the behaviour of the tissues, are complemented by studies that assess hearing-thresholds (e.g. Finneran et al., 2008) using behavioural methods, and brainstem auditory evoked potentials (BAEPs or ABRs). These also are accompanied by pathological studies, and physiological studies, and can benefit from the extrapolation of more advanced knowledge in laboratory animals and humans. More than often, there exists no single technique to provide conclusive answers regarding the functionality of an entire organ, especially when it is as complex as the odontocete hearing apparatus.

The peripheral parts of the hearing apparatus in toothed whales no longer comprises the pinna and external ear canal as in terrestrial mammals, but rather, the *outer ear* as a whole has to be reconsidered with the incorporation of the additional components such as the mandibular fat bodies,

which serve in the sound received from the external environment to the middle ear. In contrast, the role of inherited organs such as the external ear canal has been put into question.

2.1 The odontocete external ear canal

2.1.1 Morphology, shape, and associated tissues

Both Aristotle (384–322 BC, Τῶν περὶ τὰ ζῷα ἱστοριῶν, Historia *Animālium*) and Plinius (*Naturalis Historia*, Published 77-79 AD) were aware of the fact that dolphins could hear, as they could be attracted or chased away using sound (e.g. trumpets), or could be attracted by a flute or a lyre according to Pindar (522-422 BC), but they did not understand the mechanisms behind it (In: Slijper, 1958). Aristotle wrote that dolphins do not have an opening in the skin associated with hearing, and although Rondelet (*Libri de piscibus marinis, in quibus veræ piscium effigies expressæ sunt*, Published 1554-1555) lent faith to many of Aristotle's words, he described the presence an external ear opening immediately caudal to the eyes, without a pinna, subtle as in seals, and surrounded by so much fat that one can barely detect it. This opening is hardly noticeable in live animals, but evident during post-mortem investigation, and there is a continuation from the ear opening to the brain. Two centuries later, also Hunter (1787) described the absence of a pinna and gave a brief and general description of the external ear canal in *Phocoena phocoena*, *Grampus griseus*, *Delphinus delphis*, *Monodon Monoceros*, *Balaenoptera acutorostrata*, *Balaena mysticetus* and *Physeter macrocephalus.* He stated that there was a small external opening, situated little caudal to the eye, connected to the ear canal, which had a serpentine course, starting horizontal, then ventral, then horizontal again, and terminating at a tympanic membrane. It was not until the beginning of the 20th century that the ear canal morphology was described in more detail, (e.g. Boenninghaus, 1903; Hanke, 1914)(Figure 3).

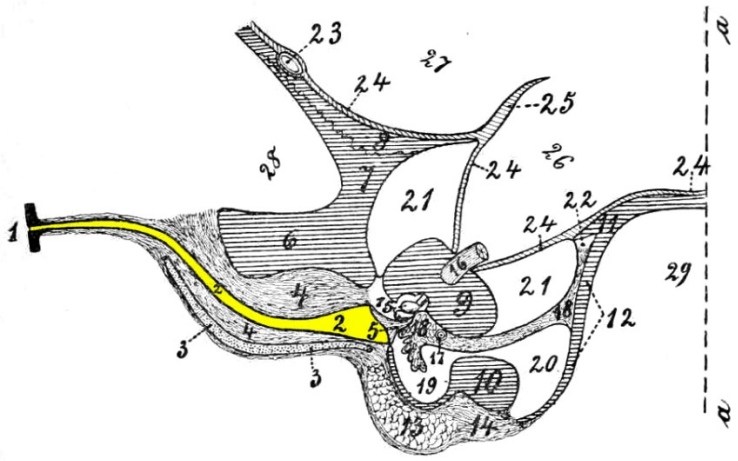

Figure 3. (Source: Boennighaus, 1903; and adapted with external ear canal in yellow; nomenclature compared with Cozzi et al., 2017). Schematic drawing of a transverse/axial cut through the soft and hard tissue of the ear region of an adult harbour porpoise. 1: external ear opening; 2: external ear canal; 3: cartilage; 4: connective tissue; 5: tympanic membrane; 6: zygomatic process of squamosal; 7: squamosal; 8: parietal; 9: periotic; 10: tympanic; 11: basioccipital; 12: basioccipital process; 13: mandibular fat body; 14: thickened periost of tympanic bone; 15: middle ear ossicles; 16: vestibulocochlear nerve; 17: internal carotid artery; 18: corpus spongiosum tympanicum; 19: tympanic cavity; 20: peribullar sinus; 21: sinus

pneumaticus peripetrosus; 22: sinus petrosus internus; 23: spinal meningeal artery; 24: dura mater; 25: tentorium cerebelli; 26: posterior cranial fossa; 27: middle cranial fossa; 28: temporal fossa; 29: pharyngeal groove; 30: contour of the cerebellum; aa': mediosagittal plane of the skull.

The first most apparent evolutionary adaptation, as can be seen from externally, is the absence of the pinna (Rondelet, 1554), which has been sacrificed to optimise (or at least it removes an impediment in) the hydrodynamics of cetaceans.

The external ear opening (*porus acusticus externus*) is present in all species of odontocetes subjected to study. However, it is tiny and often very hardly detectable, although it can be noted by as a minute indent in the skin, situated caudoventral to the eye. The diameter of the opening reaches a maximum of a few millimetres, even in the most massive whales (Ketten, 2000; Reysenbach de Haan, 1956).

It is generally accepted that the ear canal in toothed whales forms a small, spiralling canal with a continuous lumen, which can contain cellular debris and glandular product, and which ends blindly at the tympanic membrane (e.g. Boenninghaus, 1903; Sassu and Cozzi, 2007)(Figure 4). However, there is inconsistency about many structures, including the lumen or its content. For example, Solntseva (2007) noted a 'constantly closed' lumen at the level of the glands in bottlenose dolphin and short-short-beaked common dolphin. Ketten (2000) wrote that the external ear canal in toothed whales becomes narrower towards medial, that it is *filled* with cellular debris and cerumen, and that no connection was observed with the tympanic membrane or tympanic bones[2].

In contrast, most sources state the opposite: the odontocete ear canal is a tortuous canal with gradually increasing diameter towards medial, with cellular and ceruminous content but only in superficial sections, and a connection with the tympanic membrane, which shows adaptations into a tympanic conus (= tympanic membrane + tympanic ligament; see below)(Reysenbach de Haan, 1956).

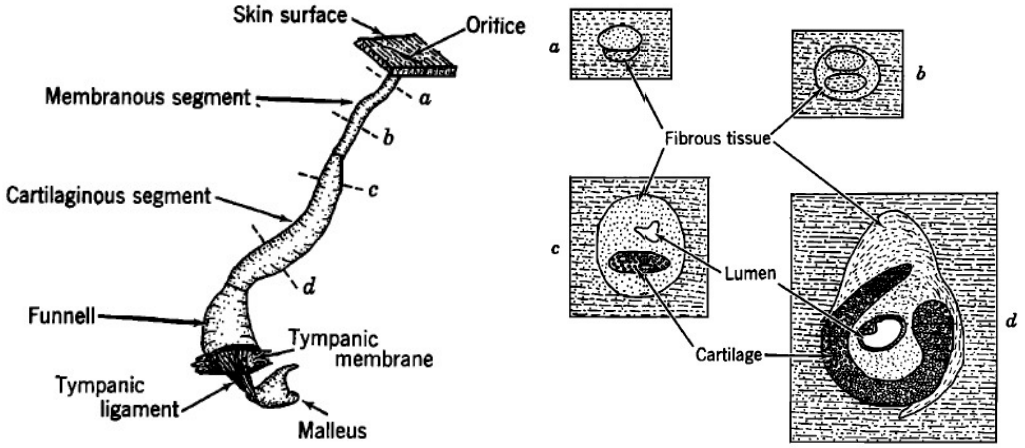

Figure 4. Source: McCormick et al., 1970. Left: schematic drawing of the external ear canal in a bottlenose dolphin from the skin to the middle ear. Right: schematic drawings of cross-sections of the ear canal at four levels of depth beneath the skin (a-d)

[2] A statement that has also been adapted by the DOSITS website: https://dosits.org/animals/sound-reception/marine-mammals-hear/hearing-in-cetaceans/

In brief comparison, in baleen whales, the ear canal is equally tortuous, but it is fully closed for a short length in the deep blubber layer while it opens up again further medially (De Vreese et al., 2014; Fraser and Purves, 1960), although it is reported to have a continuous lumen according to others (e.g. Buchanan 1928, *Balaena mysticetus*, In: Fraser and Purves, 1960). The lumen contains an earplug or "wax plug" (Purves, 1955, In: Fraser and Purves, 1960; Trumble et al., 2013), which is made up of layers of secreted cerumen (ear wax) and keratinised epithelial cells, forming a mass that accumulates inside the ear canal because it is closed off.

In all toothed whales, the wall of the ear canal is delineated by a pigmented to non-pigmented, stratified, squamous, epithelium (Figure 5). The surrounding tissue constitutes a prominent blood supply, well-developed musculature, glandular structures, a rich innervation, and a complex cartilaginous structure with variety in shape.

Auricular glands accompany the canal at the level of the deep blubber layer. The glands are simple or compound tubuloacinar/-alveolar glands that form a simple to complex body of glandular structures, from several glandular pockets to a full *glandular ring*, which surrounds the ear canal like a scarf (De Vreese et al., 2014; Solntseva, 2007). The secretory cells contain basal nuclei with a pyknotic aspect as well as 'normal' nuclei and secrete in a 'holomerocrine' manner. They are connected to excretory ducts that open into epithelial folds in the external ear canal. All secretory units are accompanied by myoepithelial cells. The secretion product is eosinophilic with basophilic granules and degenerated cell products, and it mixes in the ear canal with desquamated epithelial cells to form a mass that can fill the ear canal at this level (De Vreese et al., 2014; Solntseva, 2007).

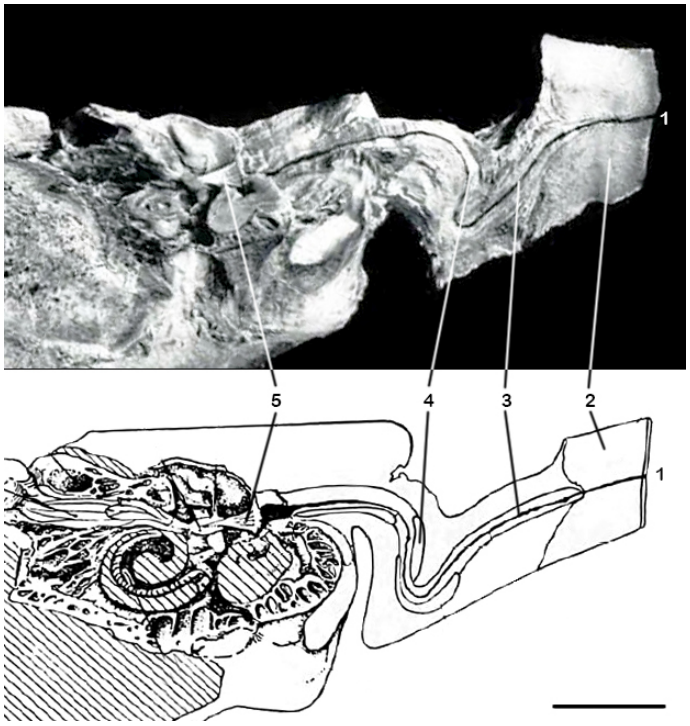

Figure 5. (Source top: Fraser and Purves, 1966; source bottom: Purves, 1966). Photograph and schematic drawing of a preparation of the ear region of a long-finned pilot whale (Globicephala melas). Note the external ear canal as a

pigmented sinuous tube from the opening in the skin (1) to the tympanic annulus. 2: blubber; 3: external auditory meatus; 4: cartilage of the meatus; 5: tympanic ligament; Scale bar 1 cm

Where the glands end medially, the canal takes a ventral turn and from here on is accompanied by cartilage down to the middle ear (Fraser and Purves, 1960, 1960; Hanke, 1914; Reysenbach de Haan, 1956; Yamada, 1953). Hunter (1787) was one of the first to note the presence of an auricular cartilage associated with the external ear canal. He described it as several irregular cartilages that are connected by a 'cellular membrane', which could allow for a movement of the ear canal, as it could lengthen and shorten with varying body conditions. Also Reysenbach de Haan (1956) described the possibility of the ear canal varying in length, although he did this in the context of hearing, which was later proven inconsistent. These 'several cartilages' were later found to consist of a main cartilaginous body with various flanges that could appear as seemingly separate structures in conventional histology (Purves, 1966; Reysenbach de Haan, 1956)(Figure 6). Cartilage was found in all cetaceans studied, although it was not always obvious or well-described. E.g. Buchanan (1928) described a "globular substance" in bowhead whale (*Balaena mysticetus*) and narwhal (*Monodon monoceros*), which was later interpreted as the auricular cartilage by Fraser and Purves (1960)

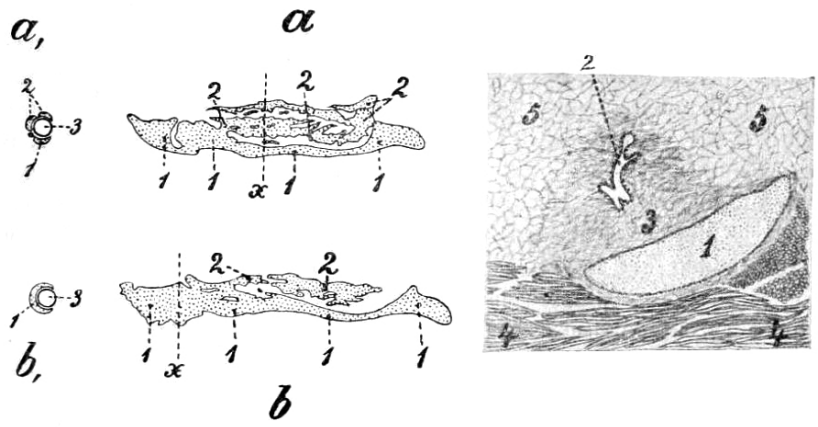

Figure 6. (Source: Boennighaus, 1903) Left: schematic drawings of the cartilage of the right ear canal in harbour porpoise in transverse and longitudinal views. It shows a main cartilaginous body (1) with variations in the amounts of cartilaginous lobes (2). Right: drawing of a transverse section through the ear canal in harbour porpoise, at the level of the distal part of the cartilage (1) (see 'x' in the left image); 2: ear canal; 3: connective tissue between ear canal and cartilage; 4: m. occipito-auricularis profundus; 5: fat.

The embedding soft tissues consist for the most part of fat and connective tissue, in which muscles insert in various areas (Boenninghaus, 1903; Hanke, 1914; Purves, 1966)(For figure examples see Figure 7, Figure 8, **Error! Reference source not found.**). Because of their small size and the uncertain homologies with auricular muscles in terrestrial mammals, muscle identification or nomenclature is not clear (Cozzi et al., 2017; Solntseva, 2007). Various hypotheses have been provided on the function of these muscles either in the context of hearing, or associated with physiological adaptations to varying body conditions (e.g. Reysenbach de Haan, 1956; Slijper, 1958; Fraser and Purves, 1960).

Although all authors assume that the muscles could play a role in adjusting the tension on the ear canal in some way, their exact movement and significance are still under debate.

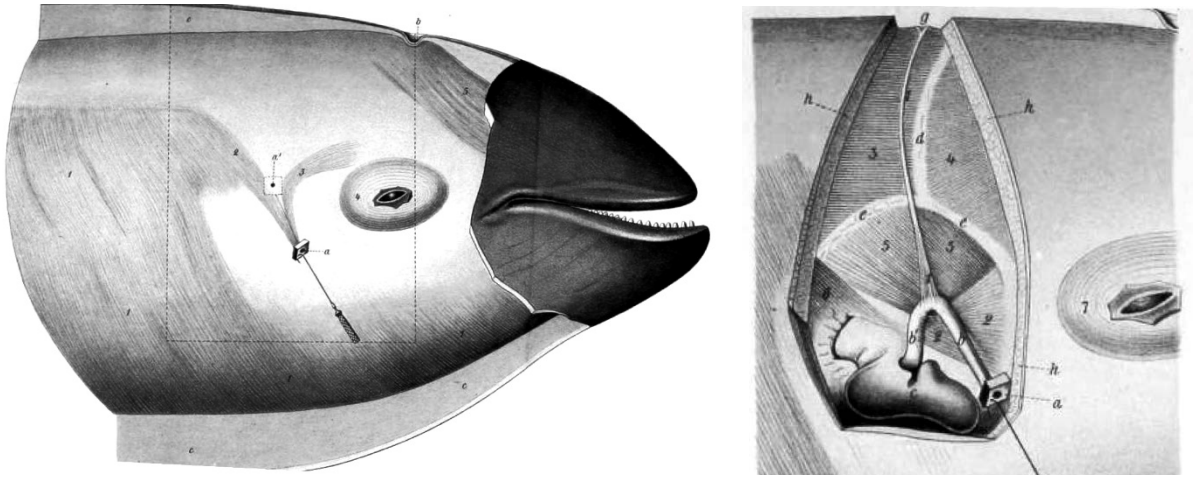

Figure 7. (Source: Boenninghaus, 1903) Drawing of the superficial and deep musculature around the right external ear canal in a harbour porpoise.

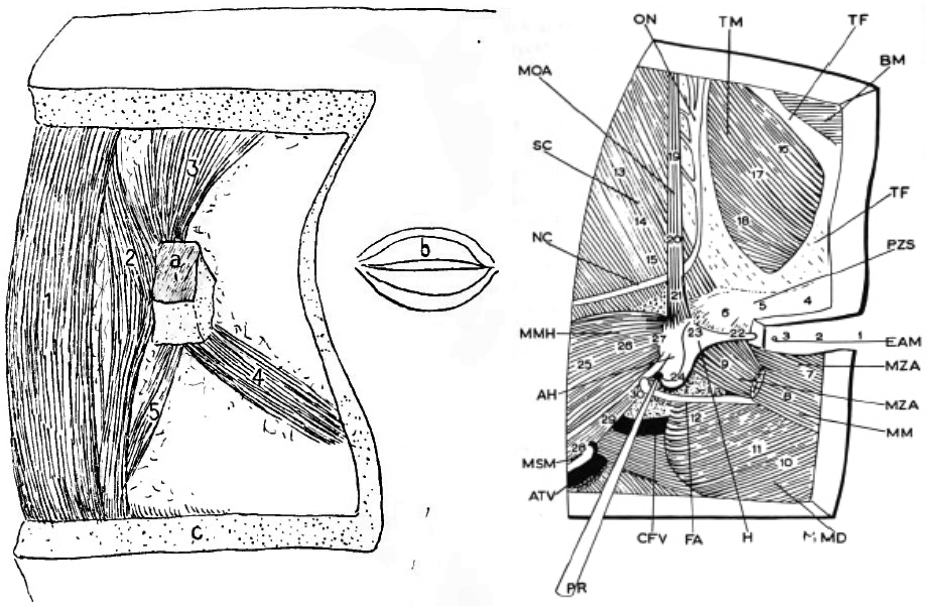

Figure 8. Drawing of the musculature associated with the right external ear canal in a short-beaked common dolphin (Delphinus delphis) left (source: Hanke, 1914), and a bottlenose dolphin (Tursiops truncatus) right (source: Purves, 1966 after Purves and van Utrecht). LEFT: 1. m. subcutaneous nuchae; 2. m. occipito-auricularis; 3. m. orbito-auricularis; 4. m. auriculo-labialis inferior; 5. m. mandibulo-auricularis; a. external ear opening; b. eye; c. subcutaneous fat layer; RIGHT: AC: auricular cartilage; AH: fibroelastic lobe as antihelix; CM: cartilage of the meatus; EAM: external auditory meatus; ET: Eustachian tuba; FVP: fibrovenous plexus; GF: glenoid fossa; H: helix; MM: m. masseter; MMH: m. mastohumeralis; MSH: m. sternomastoideus; MTP: m. tensor palatini; MZA: m. zygomatico-auricularis; NF: facial nerve (mandibular branch); PBS: peribullar air spaces; MOA: m. occipitoauricularis; ON: lesser occipital nerve; PS: periost; PZS: zygomatic process of the squamosal; STC: styloid cartilage; TB: tympanic bulla; TH: tail of the helix; (Some abbreviations are missing since the explanations were not provided in the text by Purves, 1966).

The tympanic membrane in the odontocete species is smooth and concave on the side of the ear canal (Reysenbach de Haan, 1956), while in baleen whales the pars flaccida protrudes into the ear canal, is firm in texture and hollow on the side of the middle ear cavity (Purves, 1966). Because of its peculiar structure in baleen whales, it has been called the “glove finger” (e.g. Home, 1812 for beautiful

lithographs). In all toothed whales studied, the tympanic membrane is connected to the malleus of the middle ear.

2.1.2 Innervation

Few publicly available sources describe the topography of the cranial nerves in delphinids, and only one mentions the innervation of the region of the ear canal. Rauschman (1992), meticulously described the topographic anatomy and course of the cranial nerves in *Stenella attenuata*. The region of the external ear canal is innervated by the auriculotemporal nerve, as a branch of the mandibular nerve (V3)(Figure 9). The auriculotemporal is also mentioned in Risso's dolphin by Barthelmess (Barthelmess, 2017), who describes it as a 3 mm thick nerve that branches from the mandibular nerve and runs in caudoventral direction towards the tympanic bulla, where it gave off several rami, too small to dissect.

The mandibular nerve is a mixed sensory nerve. It exits the neurocranium through a fissure formed by the alisphenoid, the periotic and the squamosal. Perinatal, this fissure is closed rostral and caudal by connective tissue, and postnatally, it becomes a foramen ovale (not to be confused with foramen ovale of the inner ear). Extracranially, the mandibular nerve appears medial to the processus falciformis of the squamosal and divides into its main branches. The auriculotemporal nerve is a weak branch that turns ventrolateral in the direction of the tympanic bone. Near the mandibular joint, the nerve turns dorsally and gives off very thin branches into the area of the external ear canal (Rauschmann, 1992).

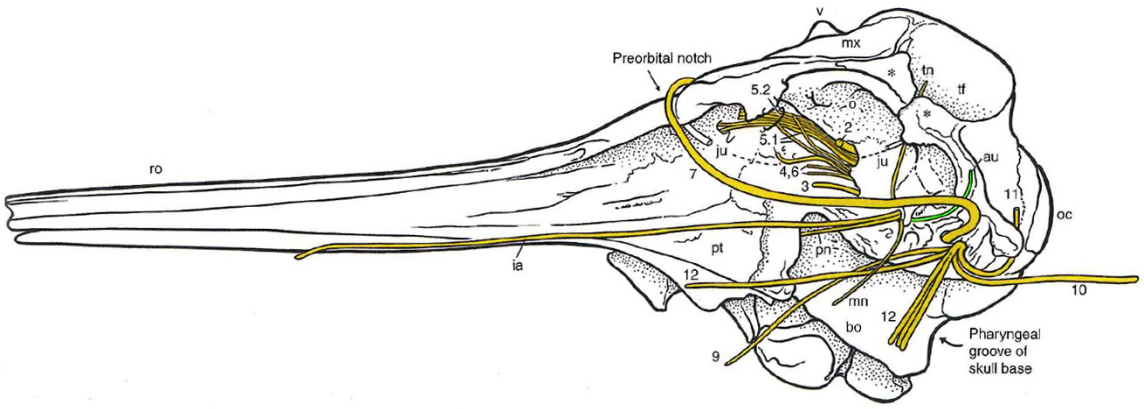

Figure 9. *(From: Rauschmann, 1992). Drawing of the cranial nerves in a slightly oblique left lateroventral view of a Stenella species skull. The cranial nerves are indicated according to their conventional numbers. The auriculotemporal nerve (au) is coloured in green.*

The peripheral nervous system associated with the external ear canal in cetaceans has been mentioned to feature abundant specialised nerve endings, i.e. lamellar or encapsulated sensory nerve formations in the subepithelial tissue (De Vreese et al., 2014; Yamada, 1953). Even though these have only been studied using traditional histological staining, their morphology shows a certain similarity to Pacinian corpuscles. The same sensory nerve formations have been found in the skin, in the nasal sac system, and inside the eye (Bryden and Molyneux, 1986; Giacometti, 1967; Palmer and Weddell,

1964; Wickham, 1980). The tissues in these studies include various parts of the skin including the trunk, fluke and pectoral fins, the nasal sac system, the blowhole, and the iridocorneal angle in several species of odontocetes.

Although the nature of the cells and tissues that make up these corpuscles has not yet been studied, it is assumed they act as mechanoreceptors. They occur in the skin of the head, particularly around the eyes and snout, in the skin of blowhole, anus, genital slit, flippers, and fluke, and they are scantly present in the skin of the dorsal and ventral side of the body. The same corpuscles are also present in the iridocorneal angle of the eyes. The presence of lamellar corpuscles in various superficial locations could presuppose an involvement in a general mechanosensory context and specifically have been proposed to play a part in the hydrodynamic control of the skin and in pressure regulation in the eyes (Giacometti, 1967; Harrison and Thurley, 1974; Ling, 1974; Palmer and Weddell, 1964; Wickham, 1980). The quantitative differences have been alluded with higher concentrations of corpuscles in the eye and the ear canal, although with significant individual variation (De Vreese et al., 2014; Wickham, 1980; Yamada, 1953). The alluded mechanosensory nature of the corpuscle and their role in the various organs in which they can be found has not been studied to date.

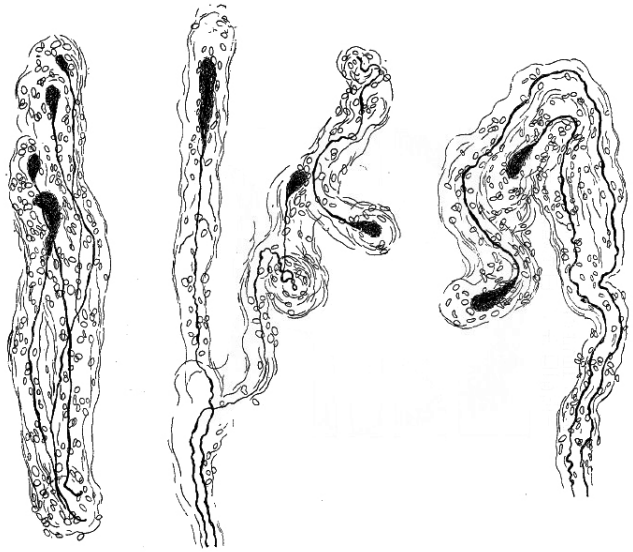

Figure 10. (Source: Yamada, 1953) Drawing of variation in perimeatal corpuscles in Baird's beaked whale.

2.1.1 Function

Past halfway the 20th century, various researchers reasoned that the external ear canal in toothed whales had lost its function as a sound conductor by taking into account the alternative pathways, but it was not until McCormick et al. (1970), that conclusive evidence was provided. Electrophysiological methods including various parts of the soft tissues around the ear canal concluded that the external ear canal played no role into the system of sound conduction from the external environment to the inner ear as it did not provide an increased input to the soft tissue conduction.

Consequently, the external ear canal was regarded as vestigial in this matter and has ever since been considered as such, an evolutionary remnant that has lost its function as a sound conductor with the development of alternative acoustic pathways (McCormick et al., 1970; Ketten, 1997; Nummela et al., 2007).

However, the ear canal proved a well-innervated, well-vascularised complex structure with many active components (Hanke, 1914; Yamada, 1953; Reysenbach de Haan, 1956; Fraser and Purves, 1960; De Vreese et al., 2014). Although most of the studies to date were carried out with an excellent eye for detail, no commonly accepted conclusions could be drawn from the findings because of various reasons: first of all, the differences in morphology of the external ear canal of toothed and baleen whales are substantial and should not be mixed. Also, the inconsistencies in methodology between studies, the interspecific or interindividual differences, and the fact that most studies had only a few specimens available of varying condition states complicates the meta-comparison that would allow for a correct interpretation of the morphological features of the ear canal. Combined with a further muddled confusion in terminology, to date, the function of the external ear canal in cetaceans is still under debate, and the knowledge on its morphology is mostly incomplete.

2.1.2 Pathology

To date, there exist no publications on pathology associated with the external ear canal in marine mammals. As such, this study will be the first to describe possible pathological alterations associated with the external ear canal in toothed whales.

3 Bibliography of Introduction

André, M., Morell, M., Alex, M., Solé, M., van der Schaar, M., Houégnigan, L., Zaugg, S., and Castell, J.V. (2009). Best practices in management, assessment and control of underwater noise pollution.

Balcomb III, K.C., and Claridge, D.E. (2001). A mass stranding of cetaceans caused by naval sonar in the Bahamas. Bahamas Journal of Science 2, 2–12.

Barroso, C., Cranford, T.W., and Berta, A. (2012). Shape analysis of odontocete mandibles: Functional and evolutionary implications. Journal of Morphology 273, 1021–1030.

Barthelmess, N.G. (2017). Topographic Anatomy and Course of Cranial Nerves in the Risso's Dolphin (Grampus griseus). Bachelor thesis. University of Cologne.

Berta, A., Sumich, J.L., and Kovacs, K.M. (2006). Marine Mammals - Evolutionary Biology (Elsevier Inc.).

Boenninghaus, G. (1903). Das Ohr des Zahnwales, zugleich ein beitrag zur theorie der Schalleitung: eine biologische studie. Zoologische Jahrbücher. Abteilung Für Anatomie Und Ontogenie Der Tiere 19, 189–360.

Bryden, M.M., and Molyneux, G.S. (1986). Ultrastructure of encapsulated mechanoreceptor organs in the region of the nares. In Research on Dolphins, M.M. Bryden, and R. Harrison, eds. (Oxford: Clarendon Press), pp. 99–107.

Cozzi, B., Huggenberger, S., and Oelschläger, H.H.A. (2017). Anatomy of Dolphins (Academic Press).

Cranford, T.W., and Krysl, P. (2012). Acoustic Function in the Peripheral Auditory System of Cuvier's Beaked Whale (Ziphius cavirostris). In The Effects of Noise on Aquatic Life, A.N. Popper, and A. Hawkins, eds. (New York, NY: Springer New York), pp. 69–72.

Cranford, T.W., Krysl, P., and Hildebrand, J.A. (2008a). Acoustic pathways revealed: simulated sound transmission and reception in Cuvier's beaked whale (Ziphius cavirostris). Bioinspiration & Biomimetics 3, 016001.

Cranford, T.W., Mckenna, M.F., Soldevilla, M.S., Wiggins, S.M., Goldbogen, J.A., Shadwick, R.E., Krysl, P., St. Leger, J.A., and Hildebrand, J.A. (2008b). Anatomic Geometry of Sound Transmission and Reception in Cuvier's Beaked Whale (Ziphius cavirostris). The Anatomical Record: Advances in Integrative Anatomy and Evolutionary Biology 291, 353–378.

Cranford, T.W., Krysl, P., and Amundin, M. (2010). A New Acoustic Portal into the Odontocete Ear and Vibrational Analysis of the Tympanoperiotic Complex. PLoS ONE 5, e11927.

De Vreese, S., Doom, M., Haelters, J., and Cornillie, P. (2014). Heeft de uitwendige gehoorgang van walvisachtigen nog enige functie? Vlaams Diergeneeskundig Tijdschrift 83, 284–292.

Dudok van Heel, W.H. (1962). Sound and Cetacea. Netherlands Journal of Sea Research 1, 407–510.

Fernández, A., Edwards, J.F., Rodriguez, F., De Los Monteros, A.E., Herraez, P., Castro, P., Jaber, J.R., Martin, V., and Arbelo, M. (2005). "Gas and fat embolic syndrome" involving a mass stranding of beaked whales (family Ziphiidae) exposed to anthropogenic sonar signals. Veterinary Pathology 42, 446–457.

Fernández, A., Arbelo, M., and Martín, V. (2013). Whales: No mass strandings since sonar ban. Nature 497, 317–317.

Finneran, J.J., Houser, D.S., Blasko, D., Hicks, C., Hudson, J., and Osborn, M. (2008). Estimating bottlenose dolphin (Tursiops truncatus) hearing thresholds from single and multiple simultaneous auditory evoked potentials. The Journal of the Acoustical Society of America 123, 542–551.

Fraser, F.C., and Purves, P.E. (1960). Anatomy and Function of the Cetacean Ear. Proceedings of the Royal Society of London B: Biological Sciences 152, 62–77.

Giacometti, L. (1967). The skin of the whale (Balaenoptera physalus). The Anatomical Record 159, 69–75.

Goodson, A.D., and Klinowska, M. (1990). A Proposed Echolocation Receptor for the Bottlenose Dolphin (Tursiops mincatus): Modelling the Received Directivity from Tooth and Lower Jaw Geometry. In Sensory Abilities of Cetaceans: Laboratory and Field Evidence, J.A. Thomas, and R.A. Kastelein, eds. (Boston, MA: Springer US), pp. 255–267.

Hanke, H. (1914). Ein Beitrag zur Kenntnis der Anatomie des Äusseren und Mittleren Ohres der Bartenwale. Jenaische Zeitschrifte Fur Naturwissenschaft 51, 487–524.

Harrison, R.J., and Thurley, K.W. (1974). Structure of the Epidermis in Tursiops, Delphinus, Orcinus and Phocoena. In Functional Anatomy of Marine Mammals, R.J. Harrison, ed. (London: Academic Press), pp. 45–71.

Hemilä, S., Nummela, S., and Reuter, T. (1999). A model of the odontocete middle ear. Hear. Res. 133, 82–97.

Hemilä, S., Nummela, S., and Reuter, T. (2010). Anatomy and physics of the exceptional sensitivity of dolphin hearing (Odontoceti: Cetacea). Journal of Comparative Physiology A 196, 165–179.

Home, E. (1812). An Account of Some Peculiarities in the Structure of the Organ of Hearing in the Balaena Mysticetus of Linnaeus. Philosophical Transactions of the Royal Society of London Series I 102, 83–88.

Hunter, J. (1787). Observations on the Structure and Oeconomy of Whales. Philosophical Transactions of the Royal Society of London 77, 371–450.

IJsseldijk, L.L., Brownlow, A., and Mazzariol, S. (2019). Best practice for cetacean post mortem investigation and tissue sampling. ASCOBANS/AC25/Inf.3.2/Rev1 71.

Jepson, P.D., Arbelo, M., Deaville, R., Patterson, I.A.P., Castro, P., Baker, J.R., Degollada, E., Ross, H.M., Herráez, P., Pocknell, A.M., et al. (2003). Gas-bubble lesions in stranded cetaceans. Nature 425, 575–576.

Jepson, P.D., Deaville, R., Acevedo-Whitehouse, K., Barnett, J., Brownlow, A., Brownell Jr., R.L., Clare, F.C., Davison, N., Law, R.J., Loveridge, J., et al. (2013). What Caused the UK's Largest Common Dolphin (Delphinus delphis) Mass Stranding Event? PLoS ONE 8, e60953.

Ketten, D.R. (1992). The cetacean ear: form, frequency, and evolution. In Marine Mammal Sensory Systems, J.A. Thomas, R.A. Kastelein, and A.Y. Supin, eds. (New York: Springer Science+Business Media), pp. 53–75.

Ketten, D.R. (1994). Functional analyses of whale ears: adaptations for underwater hearing. In OCEANS'94.'Oceans Engineering for Today's Technology and Tomorrow's Preservation.'Proceedings, (IEEE), p. I–264.

Ketten, D.R. (1997). Structure and Function in Whale Ears. Bioacoustics 8, 103–135.

Ketten, D.R. (2000). Cetacean Ears. In Hearing by Whales and Dolphins, W.W.L. Au, A.N. Popper, and R.R. Fay, eds. (New York: Springer-Verlag), pp. 43–108.

Koopman, H.N. (2018). Function and evolution of specialised endogenous lipids in toothed whales. Journal of Experimental Biology 221.

Koopman, H.N., Budge, S.M., Ketten, D.R., and Iverson, S.J. (2006). Topographical Distribution of Lipids Inside the Mandibular Fat Bodies of Odontocetes: Remarkable Complexity and Consistency. IEEE Journal of Oceanic Engineering 31, 95–106.

Ling, J.K. (1974). The Integument of Marine Mammals. In Functional Anatomy of Marine Mammals, R.J. Harrison, ed. (London: Academic Press), pp. 1–44.

Lipatov, N. V., in: Morskiye Mlekopitayushchiye (in Russ.), p. 112. Ed. V. E. Sokolov. Nauka Press 1978. In: Popov and Supin (1990. "Localisation of the Acoustic Window at the Dolphin's Head," in Sensory Abilities of Cetaceans NATO ASI Series. (Springer, Boston, MA), 417–426. doi:10.1007/978-1-4899-0858-2_28.

Mazzariol, S., Centelleghe, C., Cozzi, B., Povinelli, M., Marcer, F., Ferri, N., Di Francesco, G., Badagliacca, P., Profeta, F., Olivieri, V., et al. (2018). Multidisciplinary studies on a sick-leader syndrome-associated mass stranding of sperm whales (Physeter macrocephalus) along the Adriatic coast of Italy. Scientific Reports 8, 1–18.

McCormick, J.G., Wever, E.G., Palin, J., and Ridgway, S.H. (1970). Sound Conduction in the Dolphin Ear. The Journal of the Acoustical Society of America 48, 1418–1428.

Mead, J.G., and Fordyce, R.E. (2009). The Therian Skull A Lexicon with Emphasis on the Odontocetes. Smithsonian Contributions to Zoology 627, 261.

Møhl, B., Au, W.W.L., Pawloski, J., and Nachtigall, P.E. (1999). Dolphin hearing: relative sensitivity as a function of point of application of a contact sound source in the jaw and head region. The Journal of the Acoustical Society of America 105, 3421–3424.

Montie, E.W., Manire, C.A., and Mann, D.A. (2011). Live CT imaging of sound reception anatomy and hearing measurements in the pygmy killer whale, Feresa attenuata. Journal of Experimental Biology 214, 945–955.

Morell, M. (2012). Ultrastructural analysis of odontocete cochlea. Universitat Politécnica de Catalunya.

Morell, M., Brownlow, A., McGovern, B., Raverty, S.A., Shadwick, R.E., and André, M. (2017). Implementation of a method to visualise noise-induced hearing loss in mass stranded cetaceans. Scientific Reports 7, 41848.

Norris, K.S. (1968). Evolution of Acoustic Mechanisms in Odontocetes. In Evolution and Environment, E.T. Drake, ed. (New Haven: Yale University Press), pp. 297–324.

Nummela, S., Reuter, T., Hemilä, S., Holmberg, P., and Paukku, P. (1999). The anatomy of the killer whale middle ear (Orcinus orca). Hearing Research 133, 61–70.

Nummela, S., Thewissen, J.G.M., Bajpai, S., Hussain, T., and Kumar, K. (2007). Sound transmission in archaic and modern whales: Anatomical adaptations for underwater hearing. The Anatomical Record: Advances in Integrative Anatomy and Evolutionary Biology 290, 716–733.

Palmer, E., and Weddell, G. (1964). The Relationship Between Structure, Innervation and Function of the Skin of the Bottlenose Dolphin (Tursiops truncatus). Proceedings of the Zoological Society of London 143, 553–568.

Popov, V., and Supin, A. (1990). Localisation of the Acoustic Window at the Dolphin's Head. In Sensory Abilities of Cetaceans, (Springer, Boston, MA), pp. 417–426.

Popov, V.V., Supin, A.Ya., Klishin, V.O., Tarakanov, M.B., and Pletenko, M.G. (2008). Evidence for double acoustic windows in the dolphin, Tursiops truncatus. The Journal of the Acoustical Society of America 123, 552–560.

Purves, P.E. (1955). The Wax Plug in the external auditory meatus of the Mysticeti. Discovery Reports, 27, 293-302. In: Fraser and Purves (1960). Fraser, F. C., and Purves, P. E. (1960). Anatomy and Function of the Cetacean Ear. Proceedings of the Royal Society of London B: Biological Sciences 152, 62–77. doi:10.1098/rspb.1960.0024.

Purves, P.E. (1966). Anatomy and Physiology of the Outer and Middle Ear in Cetaceans. In Whales, Dolphins and Porpoises, K.S. Norris, ed. (Berkeley, California, USA: University of California Press), pp. 320–380.

Rauschmann, M.A. (1992). Morphologie des Kopfes beim Schlanken Delphin Stenella attenuata mit besonderer Berücksichtigung der Hirnnerven. Makroskopische Präparation und moderne bildgebende Verfahren. Johann Wolfgang Goethe-Universität.

Reysenbach De Haan, F.W. (1957). Hearing in whales. Acta Otolaryngol Suppl 134, 1–114.

Reysenbach de Haan, W.F. (1956). De ceti auditu: over de gehoorzin bij walvissen. Dissertation. Universiteit Utrecht.

Richardson, W.J., Green Jr., C.R., Malme, C.I., and Thomson, D.H. (1995). Marine Mammals and Noise (New York: Academic Press).

Rondelet, G.A. du texte (1554). Libri de piscibus marinis, in quibus verae piscium effigies expressae sunt (Montpellier, France).

Ryabov, V. (2010). Role of the mental foramens in dolphin hearing. NS 02, 646–653.

Sassu, R., and Cozzi, B. (2007). The External and Middle Ear of the Striped Dolphin Stenella coeruleoalba (Meyen 1833). Anatomia, Histologia, Embryologia: Journal of Veterinary Medicine Series C 36, 197–201.

Slijper, E.J. (1958). Walvissen (Amsterdam - Hilversum - den Helder: C. de Boer Jr. N.V.).

Soldevilla, M.S. (2005). Cuvier's beaked whale (Ziphius cavirostris) head tissues: physical properties and CT imaging. Journal of Experimental Biology 208, 2319–2332.

Solntseva, G.N. (2007). Morphology of the auditory and vestibular organs in mammals, with emphasis on marine species (Bulgaria: Russian Academy Of Sciences & Pensoft Publishers & Brill Academic Publishers).

Southall, B.L., Finneran, J.J., Reichmuth, C., Nachtigall, P.E., Ketten, D.R., Bowles, A.E., Ellison, W.T., Nowacek, D.P., and Tyack, P.L. (2019). Marine Mammal Noise Exposure Criteria: Updated Scientific Recommendations for Residual Hearing Effects. Aquat Mamm 45, 125–232.

Trumble, S.J., Robinson, E.M., Berman-Kowalewski, M., Potter, C.W., and Usenko, S. (2013). Blue whale earplug reveals lifetime contaminant exposure and hormone profiles. Proceedings of the National Academy of Sciences 110, 16922–16926.

Van der Graaf, A.J., Ainslie, M.A., Brensing, K., Dalen, J., Dekeling, René, Robinson, S., Tasker, M.L., Thomsen, F., and Werner, S. (2012). European Marine Strategy Framework Directive Good Environmental Status (MSFD-GES): Report of the Technical Subgroup on Underwater Noise and other forms of energy.

Varanasi, U., and Malins, D.C. (1971). Unique lipids of the porpoise (Tursiops gilli): Differences in triacyl glycerols and wax esters of acoustic (mandibular canal and melon) and blubber tissues. Biochimica et Biophysica Acta (BBA) - Lipids and Lipid Metabolism 231, 415–418.

Varanasi, U., Markey, D., and Malins, D.C. (1982). Role of isovaleroyl lipids in channeling of sound in the porpoise melon. Chemistry and Physics of Lipids 31, 237–244.

Wickham, M.G. (1980). Irido-corneal angle of mammalian eyes: Comparative morphology of encapsulated corpuscles in odontocete cetaceans. Cell and Tissue Research 210, 501–515.

Yamada, M. (1953). Contribution to the Anatomy of the Organ of Hearing of Whales. The Scientific Reports of the Whales Research Institute 8, 79.

Zahorodny Duggan, Z.P., Koopman, H.N., and Budge, S.M. (2009). Distribution and development of the highly specialised lipids in the sound reception systems of dolphins. Journal of Comparative Physiology B 179, 783–798.

OBJECTIVES AND METHODOLOGICAL CONCEPT

OBJECTIVES

This project involves strategic partnerships between multiple international institutions involved in the assessment of functional morphology, health status and pathology of vibration-sensitive tissues in the head of small odontocetes.

The practical objectives of this study are to use descriptive research to provide basic knowledge on the morphology of the ear canal in a variety of toothed whales, on the specialisations of the peripheral nervous in those animals, on the functionality of the external ear canal as a distinct sensory organ, and to provide ground for premises on its role in the hearing apparatus or the local and systemic physical and physiological processes, and to make a gateway for future morphofunctional and pathological studies.

The focus is put on assessing the morphology of the peripheral nervous tissues associated with the external auditory meatus and tissues related to the auditory pathways for sound reception in conjunction with establishing a standardised necropsy sampling protocol of the aforementioned tissues in the scope of possible sound or pressure-related pathologies.

Previous research has shown the presence of specialised nerve endings that show similarities to Pacinian corpuscles (lamellar corpuscles), a type of mechanoreceptor, in the vicinity of the external ear canal in cetaceans (see above)(De Vreese et al., 2014; Yamada, 1953). The function of these corpuscles is equally enigmatic as the function of the ear canal itself. In this study, the somatosensory system is regarded as a gateway into the understanding of the ear canal's functionality.

Therefore, the objectives of the research are

- To assess the mechanosensory nature of the ear canal lamellar corpuscles through various techniques, including electron-microscopy imaging and immunohistochemical staining methods. Complementary techniques include confocal microscopy (in combination with immunohistochemical primary and secondary labelling), and clinical imaging techniques.
- To assess the presence and relative abundance of the ear canal lamellar corpuscles between and among species, and in other tissues presumptively sensitive to mechanical deformation (vibration/pressure) such as tissues of the ocular region, the blowhole, the muzzle and dorsal side of the nose (vibrissal crypts), the pectoral and dorsal fins, the fluke, the belly skin, urogenital folds, clitoris, penis, and mammary glands, and particularly in the soft tissues associated with the intra- and extramandibular fat bodies, and the air sinuses in contact with the tympanoperiotic complex

- To assess the morphological characteristics of the external ear canal and to compare intra- and interspecific features, by use of various histological techniques and staining, and extrapolating results using 3D reconstruction of the ear canal and the surrounding soft tissues.

These objectives are brought to bear on several toothed whale species, and results are compared to land mammals as control species.

- To assess any pathology occurring in the external ear canal and the peripheral hearing apparatus and to develop a specific sampling protocol as part of the general routine necropsy protocol.

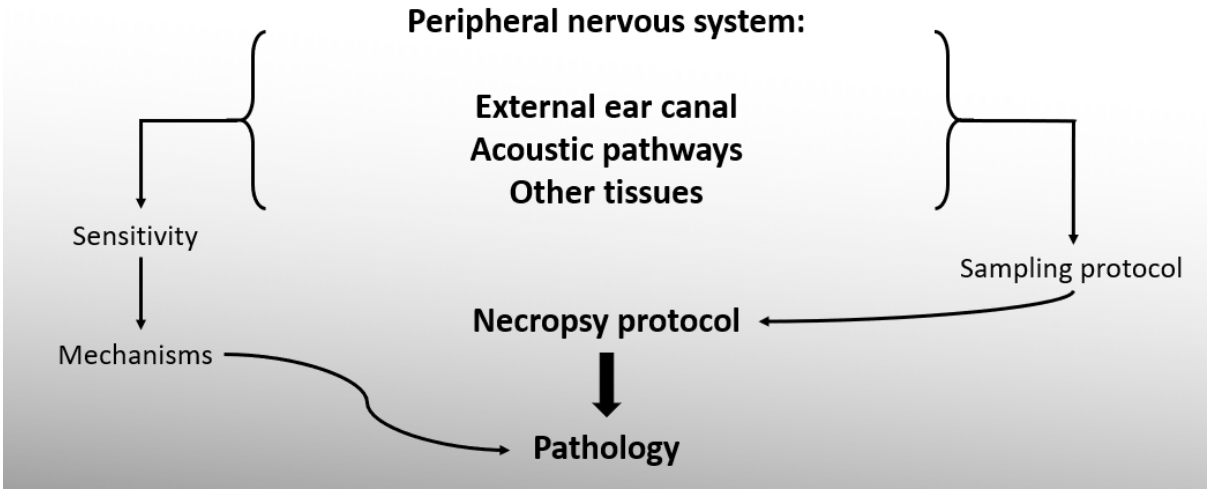

Figure 11. A simple diagram of the objectives of anatomy and pathology. This diagram explains the logical approach of obtaining pathological results by making use of the same techniques used for other objectives. The morphological studies, which focus on the peripheral nervous system in the external ear canal and other tissues of the auditory pathways, will give an idea of the sensitivity of the systems and possibly also indications of the physical and physiological mechanisms that are at play. The results give rise to a sampling protocol that is complementary to the general necropsy protocol and other protocols such as for the inner ear studies. As such, a simultaneous understanding of the functional morphology and the pathological findings could provide exciting findings in the scope of the general pathological assessment of the animal.

METHODOLOGICAL CONCEPT

In this study, we observed the macro- and microscopic morphological features of the ear canal of many specimens of striped dolphin of various ages and condition states, and compared the findings with other small delphinids such as the common and the bottlenose dolphins, and also long-finned pilot whale and Cuvier's beaked whale. This study aimed at getting a broad understanding of the morphological features of the external ear canal in a variety of species, highlighting the common features, interspecific differences, and intraspecific variations and drawing attention to how all of the soft tissues interact and play an essential part in this unique sensory organ. Based on the comparative morphology, and the interpretation of scanty literature, we provided a hypothetical deviation on the role of the external ear canal in toothed whales.

Before the description of the methodologies of the different chapters, it is relevant to explain the network that has been developed for the gathering of samples of a variety of toothed whale species. The focus was initially put on the two most common species in the Mediterranean: the striped (*Stenella coeruleoalba*) and bottlenose (*Tursiops truncatus*) dolphins, which was complemented by studies on harbour porpoise (*Phocoena phocoena*) from the North Sea. Samples were gathered from several European countries. In Italy, this work was integrated into the Italian stranding network and in collaboration with the Instituti Zooproofilatici Sperimentali (Venezia, Emilia Romagna, Abruzzo e Toscana and Lìguria). In Spain, the samples came through a collaborative effort with the Veterinary Faculty of the Autonomous University of Barcelona. Next, an international network was established to gather more samples of these species and to include other species for comparative anatomy studies, which proved to be most fruitful, particularly through a collaboration with the University of Utrecht in the Netherlands.

The first chapter describes the abundance and topographical distribution of the lamellar structures in toothed whales external ear canal and tissues of primary interest. It consists of gross anatomical studies and microscopical studies. A histological assessment with particular attention to sensory nerve formations will allow for a distinction between tissues of primary and secondary interest.

A specific and detailed necropsy protocol is developed in parallel that focuses on the tissues of the head. In parallel, mentioned in chapter 2, a gross anatomical study is performed for a mapping of the macroscopically visible nervous tissues such as the cranial nerves, musculature, course of the ear canal and relation with bony tissues.

The second chapter includes an in-depth study on the lamellar corpuscles in tissues of primary interest on the three main anatomical levels: gross anatomy, light microscopy and ultramicroscopy. The sampling will be executed together with & similar as for the first chapter, but for this in-depth study, specifically fresh cadavers are selected. The freshest animals will enter the microscopical studies; the remaining animals are used for the gross anatomical study.

The gross anatomical study is performed either immediately after discovery of a fresh cadaver or, in case the latter is not immediately possible, on the fresh frozen & thawed animal (unfixed, unprocessed cadaver). Photo logged anatomical dissections are performed to expose and topographically map the primary tissues and to identify and track the macroscopically visible nerve fibres.

For the light microscopical study, the primary tissues are sampled in an area that is, based on the results of chapter 1, known to contain a high density of lamellar corpuscles. Tissue samples are formalin-fixed for 24h and subsequently further processed for paraffin embedding according to standard and experimental histological procedures that could provide information on the nature of the corpuscles.

Identification of the nature of the lamellar corpuscles: 4 µm thick paraffin sections are processed for immunohistochemical staining. In a preliminary study, samples and sections are used to optimise the protocol, primarily to test the activity of the selected antibodies, and to determine the optimal concentration and accompanying agents of the different reagents.

By use of transmission electron microscopy (TEM), the ultrastructure of the different layers of a lamellated corpuscle is evaluated and compared with TEM-studies on Pacinian corpuscles (e.g. Pease and Quilliam, 1957). Tissue samples of a single, or in the best case multiple, fresh cadavers are collected from an area of the external ear canal containing high numbers of lamellated corpuscles (based on the results of chapter 1).

A third chapter focuses on the construction of the three-dimensional micro-architecture of the external ear canal. Consecutive serial sections of the formalin-fixed and paraffin-embedded tissues are made and stained according to several staining protocols including Masson's trichrome or haematoxylin-eosin, and specific stainings for tissues of interest. Digital pictures of every section can be used to create a three-dimensional reconstruction of the fine microanatomy of the external ear canal.

In the fourth chapter, the presence of sensory nerve formations is compared among the toothed whale species that were included in the study and with other marine mammals (if available) and terrestrial mammals. Also, tissue samples of secondary interest will be gathered opportunistically following the developed sampling protocol, and they will be processed similarly to the other tissues up to the level histological identification of the relative presence of any sensory nerve formations.

A fifth, optional chapter includes two experimental designs and techniques. First, by combining immunohistochemical staining techniques with confocal microscopy, further detailed information on the ultrastructure of the lamellar corpuscles can be obtained. Moreover, this can provide additional information on the physiology of the lamellar corpuscles. Using a combination of confocal microscopy studies and the knowledge gained from other chapters, and in collaboration with partner institutions, a biomechanical model of the lamellar corpuscles could be reconstructed, which can help gain information on the physiology and the specificity of the triggering signals for these corpuscles.

MATERIALS AND METHODS

MATERIAL AND METHODS

1 Animals

1.1 Cetaceans

The animals used in this study included a variety of toothed whales of which most samples came from striped dolphin, harbour porpoise, bottlenose dolphin, and single specimens of common dolphin, long-finned pilot whale, and Cuvier's beaked whale. These animals were not subjected to any scientific or commercial testing. They were all free-living animals that were found stranded, either dead or euthanized by the appropriate responsible. Samples gathered in Italy were either taken by myself, on

site or in the necropsy room, or sent through collaborations with the Zooprofilactic Insititutes of Venezia, Lazio e Toscana, Piemonte, Lìguria e Valle d'Aosta, and Sardinia. All samples gathered in Spain were taken under the direction of Prof. dr. Mariano Domingo. All harbour porpoise ear samples were provided by Lonneke IJsseldijk of Utrecht University, the Netherlands). A detailed list of the examined animals is reported in Table 2.

Also, there was no requirement for any consent from an Animal Use or Ethical Committee.

Decomposition Condition Codes (DCC) of the animals were assessed following standardised guidelines (Jauniaux et al., 2019; Mazzariol et al., 2015).

We obtained 2 CT images, one of an entire single harbour porpoise (provided by Utrecht University) and one of the head of a single bottlenose dolphin (L'ospedale veterinario didattico universitario (OVUD), University of Padova)

1.2 Terrestrial mammals

The terrestrial mammals that were used in this study included cow, roe deer, northern giraffe, and mouse, of which samples were taken during routine necropsy at the University of Padova. Two mice heads (Strain BL6) with intact external ear canals, but with the brain already dissected, were provided by the University Hospital of Köln (Prof. dr. Schröder, Dept of Anatomy II).

2 Tissue sampling and processing.

A sampling protocol was developed to identify tissues of primary and secondary interest, together with a specific focus on the ear canal and associated tissues (See Annex). According to the animal's conservation code, different actions were suggested (Table 1).

Table 1. Sampling action according to the conservation code of the animal.

CONSERVATION CODE	ACTION
1 - 2	• Samples gathered by CERT-team • Samples*, fixed in formalin • Entire head, frozen
2 - 3	• Samples, fixed in formalin • Entire head frozen
4	• Ear canal, fixed in formalin • Nothing

The external ear canals of all animals were obtained during routine necropsy. The odontocete samples were taken according to the following protocol: First, the external ear opening was located and soft tissues were dissected in a rectangle of about 1 cm2 around the opening down to the level of the osseous cove that is delineated by the mandible rostrally, the squamosal dorsally, and the exoccipital bone dorsocaudally. Next, the soft tissues that hold the TP-complex in place were cut and the

combined tissues of the ear canal, surrounding soft tissues and TP-complex were dissected and extracted. The entire structure was fixed in 10% neutral-buffered formalin for 24 hours after which the fixative was refreshed. The time from fixation to tissue processing ranged from several days to 18 months. The TP-complex, together with the far-most medial end of the ear canal was separated and decalcified using a commercial decalcifier (Biodec R, Bio-Optica®). For the terrestrial mammals, we dissected the cartilaginous portion of the external ear canal, which was fixated in the same manner as the odontocete samples.

3 Macroscopic studies

3.1 Animals and samples

The macroscopic morphology of the ear canal and associated tissues were studied and mapped during routine necropsies in the necropsy room and on site (on the beach or in designated areas such as a garbage disposal centre). On one occasion, two striped dolphin heads with the rostrum, brain and soft tissues of the neck region removed (ID5386, ID2926), were kindly provided by the Istituto Zooprofilattico Sperimentale del Piemonte, Liguria e Valle d'Aosta. These were subjected to a more in-depth study of the shape of the ear canal and the inserting musculature, both through macroscopic dissection and transverse slabs.

A detailed macroscopic study of the cranial nerve distribution, with special attention to the innervation of the peripheral auditory apparatus and associated structures, was performed at the Department II of Anatomy (Neuroanatomy), University of Cologne (50924 Cologne, Germany), under direction of Dr. Stefan Huggenberger and Prof. dr. Hansjörg Schröder. There, a single Pantropical spotted dolphin foetus (*Stenella attenuata*) that had been fixed in formalin for more than 40 years, was dissected macroscopically for a mapping of the cranial nerves associated with the region of the outer ear canal and tympanic membrane. Simultaneously, a less well-preserved harbour porpoise head (ID 230704A) was cut lengthwise in slabs of about 10 cm, which provided the opportunity for assessing the macroscopic course of the ear canal in harbour porpoise.

3.2 Camera

Macroscopic images were taken with camera Olympus (550 D) or a Sony Xperia Z5 Compact cell phone.

Table 2. Animals

Animal ID	Species	CC	Origin	Country	Management	Date of necropsy	Alive/ dead	Spont/ Euth	Sex	Length (cm)	Weight (kg)	Ear canal	
												Left	Right
N-00419-16	*S. coeruleoalba*	2	Port de la Selva	Spain	Wild	16/11/2016	D	S	M	103	14	Y	N
N-00044-17	*S. coeruleoalba*	2	Port Ginesta	Spain	Wild	10/02/2017	D	S	M	153	37	Y	Y
N-00168-17	*S. coeruleoalba*	2	L´Escala	Spain	Wild	19/04/2017	D	S	M	193	79	Y	N
N-00169-17	*D. delphis*	2	L´Escala	Spain	Wild	20/04/2017	A	S	M	179	72	Y	Y
N-00488-17	*S. coeruleoalba*	2	Gavà	Spain	Wild	28/09/2017	A	E	F	198	70	Y	Y
N-00509-17	*S. coeruleoalba*	2-3	Tarragona	Spain	Wild	10/10/2017	D	S	M	183	87	Y	Y
12691	*S. coeruleoalba*	2	Bibona, Livorno	Italy	Wild	19/12/2017	D	S	M	193,5	62,4	Y	Y
12693	*S. coeruleoalba*	3	Livorno	Italy	Wild	19/12/2017	D	S	F	160	40	Y	Y
12694/429	*Z. cavirostris*	2	Livorno	Italy	Wild	23/12/2017	D	S	M	503	na	Y	Y
12703/2926	*S. coeruleoalba*	2	Bagni Buraxen, Imperia	Italy	Wild	13/01/2018	D	S	M	133	34,5	Y	Y
N-00021-18	*S. coeruleoalba*	2-3	Calella de palafrugell	Spain	Wild	15/01/2018	D	S	M	182	73	Y	N
12708/5386	*S. coeruleoalba*	2	Porto Genova Pra, Genova	Italy	Wild	21/01/2018	D	S	M	192	69	Y	Y
N-00042-18	*S. coeruleoalba*	2	Viladecans	Spain	Wild	25/01/2018	D	S	M	178	62	Y	N
N-00077-18	*S. coeruleoalba*	2	Delta del Ebro	Spain	Wild	19/02/2018	D	S	M	220	97,5	Y	Y
441	*G. melas*	4	Aglientu, Sardegna	Italy	Wild	20/03/2018	D	S	M	525	na	Y	Y
444	*T. truncatus*	3	Pellestrina, Venezia	Italy	Wild	24/03/2018	D	S	M	264	260	Y	Y
N-00145-18	*S. coeruleoalba*	2	Palamós	Spain	Wild	26/03/2018	D	S	F	195	91	Y	N
N-00232-18	*S. coeruleoalba*	1	Tarragona	Spain	Wild	24/05/2018	A	S	M	180	51,5	Y	N
N-00274-18	*S. coeruleoalba*	3	Delta del Ebro	Spain	Wild	24/06/2018	A	S	M	152	38	Y	Y
N-00292-18	*S. coeruleoalba*	2	Tarragona	Spain	Wild	06/07/2018	D	S	M	194	59,5	Y	Y
N-00293-18	*S. coeruleoalba*	3	Port Ginesta	Spain	Wild	09/07/2018	A	E	F	187	85	Y	Y
N-00620-17	*S. coeruleoalba*	2	Vilanova i la Geltrú	Spain	Wild	24/07/2018	A	S	M	196	75,5	Y	N
N-00362-18	*S. coeruleoalba*	2	Riumar	Spain	Wild	12/09/2018	A	E	M	181	78	Y	Y
109064/449	*S. coeruleoalba*	2	Groticelle, Calabria	Italy	Wild	13/10/2018	A	S	M	102	12,23	Y	Y
N-00177-19	*Z. cavirostris*	4	Tossa de Mar	Spain	Wild	20/04/2019	D	S	M	520	1200	Y	Y
127565	*S. coeruleoalba*	2	Calabria	Italy	Wild	28/11/2018	D	S	M	200	na	Y	Y
AE565/457	*T. truncatus*	2	Bibione, Venezia	Italy	Wild	29/01/2019	D	S	M	285	260	Y	Y
UT1664	P. phocoena	2	Ouddorp	the NL´s	Wild	09/07/2018	D	S	F	92	11	Y	N
UT1692	P. phocoena	1	Kats	the NL´s	Wild	25/07/2018	D	S	M	90	12.5	Y	N
UT1709	P. phocoena	2	Oostkapelle	the NL´s	Wild	19/09/2018	D	S	M	95	10.5	Y	Y
UT1711	P. phocoena	2	Petten	the NL´s	Wild	25/09/2018	D	S	M	146	37.5	Y	Y
UT1712	P. phocoena	3	Dishoek	the NL´s	Wild	04/10/2018	D	S	M	124.5	30.5	Y	Y
UT1718	P. phocoena	2	Vlieland thv KNRM huisje Vliehors	the NL´s	Wild	05/01/2019	D	S	M	113	24	Y	N
UT1727	P. phocoena	2	Ijmuiden Seport Marina	the NL´s	Wild	13/01/2019	D	S	F	141	37	Y	Y
UT1728	P. phocoena	1	Egmond paal 38.750	the NL´s	Wild	17/01/2019	D	S	F	155	64.5	Y	Y
UT1734	P. phocoena	1	Terschelling paal 4	the NL´s	Wild	27/01/2019	D	S	M	103	24.5	Y	Y
UT1740	P. phocoena	1	Terschelling West	the NL´s	Wild	27/02/2019	D	S	M	102	22.2	Y	Y

**CC/CS: conservation code or status; Death: natural or euthanized after veterinary consultation; na: not available; Age profile estimation based on (Mazzariol et al., 2015)*

4 Histology

For histology, tissue slabs with a diameter of about 3–4 mm were dissected manually from the gross sample, transverse to the local orientation of the ear canal lumen, or, in some cases, parallel to the direction of the ear canal. Next, they were embedded in paraffin, sectioned to a thickness of 4 µm, and mounted on polarized glass slides. Sections for staining with haematoxylin-eosin were obtained from all slabs and dried overnight at 70 °C, followed by automated staining using a Leica Autostainer XL (Leica Biosystems Nussloch GmbH):

- Deparaffinizing in xylene, isopropylalcohol, en decreasing concentrations of alcohol
- Staining with haematoxylin and eosin
- Dehydrating in increasing concentrations of alcohol, isopropylalcohol and xylene

The slides were coverslipped using a mixture of Eukitt® (ORSAtec GmbH) and xylene.

4.1 Types of stains

Slides for routine histological evaluation were stained with haematoxylin eosin, while slides for 3D reconstruction were stained with Masson's trichrome with Aniline blue.

Slides for other histochemical stains were obtained in the same manner as for standard haematoxylin-eosin, and the techniques included: Luxol Fast Blue stain (protocol was empirically adapted, with variations in time (1s-5s) in the lithium carbonate solution to obtain a better differentiation), Cresyl Violet Stain, Spaethe's Silver stain modified after Richardson (Spaethe, 1984) (with and without bleaching), Palmgren's silver stain (Bancroft and Gamble, 2002), 2 types of Bielschowski's silver stain (Bancroft and Gamble, 2002)(Paul Polak and Douglas Feinstein, University of Illinois, Chicago), Masson's Trichrome Goldner, Masson's Trichrome with Aniline blue, Alcian Blue (either with pH 2.6 or pH 1), PAS staining (Pernick, 2019a), Giemsa (Pernick, 2019b), 2 types of GRAM staining, Prussian blue, Weigert's stain, and Acid Orceid Giemsa.

5 Immunohistochemistry

5.1 Immunolabelling

For immunohistochemistry, tissues were sectioned (thickness 4 µm) and captured on polarized glass slides. Next, the slides were labelled with a barcode and dried overnight at room temperature, and incubated at 37 °C 30 min before the start of the semi-automatic staining procedures using Benchmark® GX and Ventana software, using Polyclonal anti-bovine S-100 (Dako, Z0311), Monoclonal anti-human Neurofilament M Protein (NF)(Dako, M0762), Monoclonal anti-human Neuron-Specific Enolase (NSE)(Dako, M0873), and Polyclonal anti-bovine PGP 9.5 (Dako, Z5116) as primary antibodies in several dilutions with and without blocking agent (Table 3). The sections for anti-PGP 9.5 were stained with a protocol modified from Sematovica et al. (2008), which, in some odontocete cases, was

preceded by a melanin bleaching procedure (See below)(modified from Luna (1968)). Other antibodies, which were applied in specific cases, were von Willebrand factor (factor VIII), and Pancytokeratin. The antibodies were diluted with Ventana® Antibody Diluent with or without casein blocking buffer. After staining, all slides were washed with standard dishwashing soap and rinsed with tap water for several repetitions during 10–15 min. Next, the slides were dehydrated in increasing concentrations of alcohol, coverslipped and dried overnight at room temperature inside the extraction hood. The specificity of the immunohistochemical reaction was checked using a) negative control (internal and external control with epithelium, muscle, fat, and connective tissue), and b) white control sections (primary antibody absent)(See Antibodies).

All slides were examined with an Olympus BX41 microscope (Olympus Italia S.r.l., Milan, Italy) at up to x600 magnification, and scanned with D-sight scanning microscope at x400 magnification (A. Menarini Diagnostics, S.r.l., Florence, Italy) and uploaded to a server (Telepathology, Visia Imaging S.r.l., San Giovanni Valdarno (AR), Italy), and pictures were taken either as screenshots from the server or with a Leica DMD108 Microscope (Leica Microsystems CMS GmbH, Milan, Italy). Images were edited using Fiji software (ImageJ 1.52i) for adding the scale bar, for appropriate brightness and contrast when insufficient, and montages were made using the Magic Montage plugin. For the classification of the SNF, we compared morphology with literature (See Malinovský, 1996, for a review).

5.2 Protein extraction and western blotting analysis

For protein extraction, 150 µg of frozen brain tissue from bottlenose dolphin, striped dolphin and bovine (closest phylogenetic species in which cross-reactivity tissue controls were possible) were homogenized using Potter glass (Vetrotecnica, Italia) in 5 ml of buffer A (10 mM Tris-Base, 150 mM NaCl, 5 mM EDTA, pH 7.2 and cocktail inhibitor - Sigma, Milan, Italy) and centrifuged at 10000 g for 30 minutes. The supernatant was then centrifuged at 125000 g for 1 hour (Optima L-90K, Beckman, Italy) and the pellet proteins were dissolved in 0.5 ml of buffer B (10 mM Tris, 150 mM pH 7.2 NaCl). Total protein concentration was calculated using the Pierce BCA Protein Assay Kit (ThermoFisher Scientific). In order to evaluate PGP 9.5, NF, NSE and S-100 antibody specificity, a Western Blot analysis has been performed according to the following protocol. Twenty-five micrograms of the extracted proteins were denatured at 70 °C for 10 minutes. Proteins were resolved using NuPAGE 4–12% Bis-Tris gel (ThermoFisher Scientific) and transferred to the nitrocellulose membrane. Nonspecific binding sites were blocked for 1 hour in 5% nonfat dry milk in TBS-T (TBS containing 0.05% Tween-20) at room temperature. Blot was incubated at 4 °C overnight with antibodies against PGP, NF, NSE and S-100, respectively (Dako). Then, the membrane was incubated for 1 hour at room temperature with anti-rabbit peroxidase-conjugate secondary antibody (ThermoFisher Scientific, #32260) for PGP and S-110

and with anti-mouse peroxidase-conjugate secondary antibody for NF and NSE (ThermoFisher Scientific, #32230). Reactive bands were visualized with a chemiluminescent detection kit (SuperSignal West Pico Chemiluminescent Substrate, ThermoFisher Scientific) using the iBright instrument (ThermoFisher Scientific).

5.3 Antibodies

A list of the primary antibodies used in this study, and to which animal's ear canal tissues they have been applied, can be found in Table 3 and Table 4 respectively.

White sections were cut consecutively to the sample sections and processed in the same way except for using diluent without adding the primary antibodies. As such, those sections only demonstrated background staining. The negative control was considered to be internal as all samples contained epithelial tissue, adipose tissue, connective tissue and muscle tissue, none of which were stained in any of the stains performed. For positive control slides, we used either standard positive control samples from the lab or an internal control such as for NF (with the presence of large nerve bundles in the section). Details on positive and negative and control samples are depicted in Table 5.

***Table 3*. Primary Antibodies**

Antibody	Origin	Code	Validation	Cross-reactivity	Ag sequence conservation**	Dilution + agent
Polyclonal Anti-Bovine S-100	Rabbit	Z0311	Human*	bovine, cat, horse, mouse, swine, rat*	Sperm whale - human 100% Sperm whale - bovine 97% Beluga whale - bovine 98%	1:1000 (with and without block) 1:2000 (no block)
Monoclonal Anti-Human NF (Clone 2F11) Interacts with the NF-M subunit (Klück et al., 1984)	Mouse	M0762	Human*	bovine, swine, rabbit, mouse, horse, dog, cat*, opossum(Breckenridge et al., 1997)	Bovine - human >99% Swine - human 97%	1:100 (with and without block)
Monoclonal Anti-Human NSE (γγ-isoenzyme)	Mouse	M0873	Human*, guinea pig*, dog(Fyfe et al., 2010)· (Aoki et al., 1992)	bovine(Aoki et al., 1992), dog(Fyfe et al., 2010)·(Aoki et al., 1992), goat(Aoki et al., 1992), pig(Aoki et al., 1992), rabbit(Aoki et al., 1992), rat(Aoki et al., 1992), fish (*Oryzias latipes*)(Uemura et al., 2015), domestic ferret (*Mustela putorius furo*)[5], cat(van Sprundel et al., 2014), African green monkey (*Macaca fascicularis*)(Cabo et al., 2015), mouse(Kestell et al., 2015), Tasmanian devil (*Sarcophilus harrisii*)(Stammnitz et al., 2018)	Goat - human >98% Rat - human >98%	1:250 (with and without block)
Polyclonal Anti-Bovine PGP 9.5 (UCT-H1)	Rabbit	Z5116	Human, mouse*	None	Bovine - human >97% Bovine - rat/mouse >97%	1:500 (with/without block/melanin bleaching) 1:2000 (with/without block, with melanin bleaching)

NF: Neurofilament Protein
NSE: Neuron-Specific Enolase
PGP: Protein Gene Product
All antibodies were supplied by DakoCytomation (Dako Denmark A/S, Denmark)
**** Manufacturer data sheet***
*****Calculated with use of the database of the United States' National Center for Biotechnology Information (https://www.ncbi.nlm.nih.gov/).***

Table 4. Animals for IHC

Animal ID	Species	PGP9.5	NF	S100	NSE
12691	*S. coeruleoalba*	x	x	x	x
12708	*S. coeruleoalba*	x	x	x	
N-293\18	*S. coeruleoalba*	x	x		x
N-274\18	*S. coeruleoalba*		x	x	x
N-488\17	*S. coeruleoalba*	x		x	x
444	*Tursiops truncatus*	x			
N-169\17	*Delphinus delphis*	x			
429	*Ziphius cavirostris*	x			
441	*Globicephalus melas*	x			
AE246	*Bos taurus*	x	x	x	x
CP11	*Capreolus capreolus*	x	x	x	x
AB959	*Giraffa camelopardalis*	x	x	x	x

Table 5. **IHC: positive and negative controls**

	CTRL+	*CTRL-*
PGP 9.5	Bovine cerebrum; Bovine sciatic nerve	Bovine skin and muscle (epithelium, connective tissue, adipose tissue, striated muscle, blood vessels)
S100	Bovine cerebrum; Bovine sciatic nerve; Canine mammary gland (myoepithelial cells)	Bovine skin and muscle (epithelium, connective tissue, adipose tissue, striated muscle, blood vessels)
NF	Cat thalamus Internal positive control	Cat skin with epithelium, connective tissue, striated muscle, and fat tissue
NSE	Cat thalamus	Cat skin with epithelium, connective tissue, striated muscle, and fat tissue

5.4 Melanin bleach

In the cases where we used bleaching methods to remove to melanin from the epithelium, the following protocols were applied after drying, and before the semi-automatic immunohistochemical labelling (Modified after (Luna, 1968)):

- Deparaffinize and hydrate all slides to distilled water.
- Place slides to be bleached in 0.25% aq. potassium permanganate solution, for 2-4 hours. Leave the slides to be used as controls in distilled water until step 6.
- Place the slide in 1% aqueous oxalic acid for 1-2 minutes, or until colourless.
- Wash in tap water.
- Rinse in deionized water
- Start IHC protocols in the same manner as mentioned above, but without the first steps of deparaffination.

6 Corpuscle core quantification

We did a relative quantification of the number of cross-sections through corpuscle cores over the course of the external ear canal in striped dolphin. Histological slides were obtained as described above. In each slide, the corpuscle cores were manually counted at a magnification of 200×, in all fields of view of the subepithelial tissue around the ear canal, always including the basal layer of the epithelium within the field of view. Each corpuscle core was labelled as positive only when a central axon and surrounding lamellar structure were recognized, independent of the occurrence as single corpuscles or as multiple corpuscles that were adjacent to each other or embedded within the same peripheral layer. The tissue sections were labelled as belonging to one of five distinguishable regions along the course of the ear canal (see Table 6 for a schematic representation of the presence of the different types of soft tissues over the course of the canal). Because there was a limited amount of good quality samples, we included all possible animals and sections that allowed for a reliable counting of the corpuscles. We assumed that the number of corpuscle cores would not be affected by age,

length, sex, left versus right, and that it would not change within a region. We took the maximum value of all slabs in each of the five regions for further analysis, as it was considered to be most representative of the true number of corpuscles and less influenced by artefacts.

6.1 Animals

For the present study, we used several specimens of striped dolphin, and two bottlenose dolphins.

6.2 Tissue sampling and processing

The external ear canals of all animals were obtained during routine necropsy. The odontocete samples were taken according to the following protocol: First, the external ear opening was located and soft tissues were dissected in a rectangle of about 1 cm^2 around the opening down to the level of the osseous cove that is delineated by the mandible rostrally, the squamosal dorsally, and the exoccipital bone dorsocaudally. Next, the soft tissues that hold the tympano-periotic complex (TP complex) in place were cut and the combined tissues of the ear canal, surrounding soft tissues and TP complex were dissected and extracted. The entire structure was fixed in 10% neutral-buffered formalin for 24 hours after which the fixative was refreshed. The time from fixation to tissue processing ranged from several days to 18 months. The TP complex, together with the far-most medial end of the ear canal was separated and decalcified using …. For the terrestrial mammals, we dissected the cartilaginous portion of the external ear canal, which we fixated in the same manner as the odontocete samples. Next, slabs with a diameter of about 3-4 mm were dissected, transverse to the local orientation of the ear canal lumen, embedded in paraffin, sectioned to a thickness of 4 µm, and mounted on polarized glass slides. At least two sections for hematoxylin-eosin staining were obtained from all slabs, and dried overnight at 70°C, followed by automated staining using a Leica Autostainer XL (Leica Biosystems Nussloch GmbH). The slides were coverslipped using a mixture of Eukitt® (ORSAtec GmbH) and xylene. Next, we assessed the preservation state of the tissue, and discarded the animals that showed too many artefacts as this impeded a confident identification of the corpuscles.

6.3 Quantification of the corpuscles

The corpuscle cores were manually counted by one experienced investigator (SDV), at a magnification of 200X, in a field of view which included the basal layer of the epithelium. The corpuscles were labeled as positive only when a central axon and surrounding lamellar core could be identified, independent of the occurrence as single corpuscles or as multiple corpuscles that were adjacent to each other or embedded within the same peripheral layer. The sections were labelled as belonging one of five clearly distinguishable regions along the course of the ear canal (See Table 6 for a schematic representation of the soft tissues over the course of the canal). Of each of the regions we took the maximum value for further analysis, as we considered this to be most representative of the sensitivity of the region and less influenced by artefacts.

1. Blubber: From the external ear opening to the distal end of the glands (excluding glands)
2. Glands: containing glandular structures
3. Muscle: From the proximal end of the glands to the proximal end of the cartilage
4. Cartilage: From the distal end of the cartilage to the proximal end of the ´nervous button´
5. Button: from the distal end of the nervous button to the medial end of the canal

TABLE 6. Schematic representation of soft tissues associated with the ear canal (rows), from left to right representing the course from the external ear opening to the tympanic conus. The columns represent the regions used for quantification.

		External ear opening	***Regions for quantification***							*Tympanic conus*
			Blubber	*Glands*		*Muscle*	*Cartilage*		*Nervous button*	
Soft tissue	*Blubber*		*X*	*X*						
	Glands			*X*	*X*					
	Muscle				*X*	*X*	*X*			
	Cartilage						*X*	*X*	*X*	
	Button								*X*	

7 Transmission electron microscopy

The ear canals of a striped dolphin stranded in Delta de l'Ebre, Paya del Serrallo, Sant Jaume d'Enveja, Tarragona, Spain, and a bottlenose dolphin stranded in Bibione, Venice, Italy (See Table 7) were dissected during routine necropsy.

- Fresh tissue samples of the ear canals of a striped dolphin stranded in Delta de l'Ebre, Paya del Serrallo, Sant Jaume d'Enveja, Tarragona, Spain (23/06/2018, N-274/18, male, condition code 3, 38 kg, 152 cm length) were dissected during routine necropsy at the Veterinary Faculty of the Autonomous University of Barcelona (UAB, Bellaterra) about 22 h after the animal died on the beach without human intervention.
- Samples of the ear canal of a bottlenose dolphin (ID457) were gathered during routine necropsy at the Veterinary Faculty of the University of Padova.

Of both samples, subsamples were taken from a tissue zone medial to the blubber layer and fixed for at least 48h at 4 °C in a solution of 2.5% glutaraldehyde in 0.1 M cacodylate buffer solution (Karnovsky's fixative; for 10ml = 1ml glutaraldehyde + 2.5ml buffer + 6.5ml distilled water), subsequently post-fixed with 1% osmium tetroxide, and dehydrated with increasing concentrations of acetone in water. Semi-thin sections (1 mm) were obtained with a glass knife, then stained with methylene blue, covered with Durcupan, and observed by light microscopy for identification of the region of interest. Ultrathin slides, about 100 nm thick, were cut with an Ultracut E ultramicrotome (Reichert-Jung). Sections were double-stained with uranyl acetate and lead citrate and observed with a Jeol JEM-1010 Electron Microscope (JEOL Corp. Ltd., Tokyo, Japan) at 80 kV. Images were obtained with a Bioscan camera model 792 (Gatan) at the University of Barcelona (Unitat de Microscòpia Electrònica (TEM/SEM), Centres Científics i Tecnològics).

Table 7. Animals for TEM

ID	*Species*	*Origen*	*Country*	*Man*	*Alive/Dead*	*Frozen/fresh*	*Date of necropsy*	*CC*	*Sex*	*Length*	*Weight*
N-00274-18	*S. coerulealba*	*Delta de l'Ebre, Tarragona*	*Spain*	*Wild*	*A*	*Fresh*	*23/06/2018*	*3*	*M*	*152*	*38*
ID457-AE565	*T. truncatus*	*Bibione, Venezia*	*Italy*	*Wild*	*A*	*Fresh*	*29/01/2019*	*2*	*M*	*285*	*260*

8 Image Processing and Analysis

All histological slides were examined with an Olympus BX41 microscope (Olympus Italia S.r.l., Milan, Italy) at up to x600 magnification, and scanned with D-sight scanning microscope at x400 magnification (A. Menarini Diagnostics, S.r.l., Florence, Italy) and uploaded to a server (Telepathology, Visia Imaging S.r.l., San Giovanni Valdarno (AR), Italy). Pictures were taken either as screenshots from the server or with a Leica DMD108 Microscope (Leica Microsystems CMS GmbH, Milan, Italy).

Whenever needed, .jp2 images were batch converted to .tiff using the open source software gdal (https://gdal.org/), specifically the programme *gdal_translate*, with a bash script (Link). In contrast, .svs images were assessed manually and a region of interest was exported to .tiff format, using Aperio ImageScope software[1].

9 3D reconstruction from histological slides

9.1 Tissue preparation

For the reconstruction of the focal nervous tissue network, we took a tissue block of a transverse section of the ear canal of a striped dolphin (Sc1), about halfway between the skin and the ventral curvature, proximal to the blubber layer, and prepared and scanned 100 consecutive HE-stained slides of 4 µm thickness, good for a total length of 400 µm. Every slide was stained with H&E, digitalized and grouped in pairs of two, of which the slide with the best tissue quality was chosen for further investigation. As such, we ended up with 50 digital slides of transverse sections through the ear canal, with an average distance of 8 µm between the center of consecutive slides (i.e. 4 µm between each slide), which were digitalized as mentioned in '8. Image Processing and Analysis'.

For the general 3D reconstruction of the entire ear canal and associated tissues, the ear canals of several specimens striped dolphin and harbour porpoise were prepared as for standard histological evaluation. The tissue preparation was either fully manual, or coordinated and systemic using a custom-built antithetic slicing device (built in collaboration with D. Pedrotti, BCA UniPD). As such, the cutting planes of the tissue blocks were always orientated in the same plane relative to the general orientation of the ear canal tissue, were consequently all parallel to each other, and had on average the same thickness of 5 mm (4 mm plexiglass + 1 mm metal washer). Tissue slides were taken with an interval of either 100, 200 or 500 µm, stained according to Masson's trichrome protocol with Aniline blue.

9.2 Focal nervous tissue network

[1] https://www.leicabiosystems.com/digital-pathology/manage/aperio-imagescope/

After scanning, images were downloaded from the D-sight software in .jp2 format and converted to .tiff files using custom built code written in BASH language, and using the OpenJpeg library, and DLAG translation software. These images were uploaded into the Software ImageJ (1.52n, Wayne Rasband, National Institute of Health, United States), cropped, aligned using the ´Register Virtual Stack Slides´ plugin, cropped again, and the distinguishable nervous structures around the ear canal were annotated and tracked using the Trackmate plugin (Tinevez et al., 2017). Next, the data, which included coordinates and size of each annotated structure and the connections between the structures, was exported to a csv-file, imported into Matlab® and Rhino® for a preliminary visual representation, and later processed via custom-built Python code for visual representation in Blender 2.8.

9.1 Ear canal and associated tissues

9.1.1 Slide digitization

Although some of the slides were digitized using the same methods as mentioned above, the largest batch was scanned automatically at 20x magnification at the Dipartimento dei Servizi di Diagnosi e Cura, UOC Anatomia Patologica at the Human Hospidal of Rovigo, Italy. The scanner was a Scanscope XT, which could process batches of up to 120 slides, with fully automatic focus. The images were saved on an external hard disk in .svs format (resolution 0.555 µm/pixel), and were cropped and saved as .tif files using Leica ImageScope Pathology slide viewing software (version 12.4.0), while also while also renaming the automatically assigned name to the appropriate animal specimen and slide labels.

9.1.2 Tissue segmentation

In order to facilitate the manual identification of nervous tissue in histological slides, we tested various silver impregnation techniques, including Spaethe's silver stain (with and without bleaching), Luxol fast blue/Cresyl violet, and Bielschowksy's silver stain (Chan, unpublished). Then, we applied Masson's trichrome with Aniline blue, in combination with automatic image segmentation techniques using ImageJ's Trainable Weka segmentation (Arganda-Carreras et al., 2017) or ILastik (v.1.3.3; Copyright (C) 2011-2019, www.ilastik.org).

9.1.3 Image processing

Several image processing workflows were tested before deciding on the final methods described below. These methods included the conversion of image to DICOM images as some software applications such as 3DSlicer (Kikinis et al., 2014, [CSL STYLE ERROR: reference with no printed form.]) handle such image formats well, or the colour separation according to the colour spectra in order to segment the tissues according to the colours of the staining (Masson's trichrome). For the first 3D model (ID127575), the .svs images were cropped and renamed and saved as two files, one full

resolution (100%) .tiff image that was cropped centred around the EAM, and one low resolution (10%) image that encompassed all of the tissue present on the slide. For the sequential models, only the full resolution images were saved in tiff format, before automated reduction of the resolution to 10%.

Next, the images were first (semi-)automatically aligned (rigid registration) using ImageJ's TRAKEM2 plugin (Cardona et al., 2012), sometimes in combination with the Virtual Stack Registration plugin (Cardona et al., 2017), followed by a manual alignment using the TrakEM2 plugin[2] for manual correction of the alignment, or for alignment from scratch in case of fail of the previous alignment.

In parallel, Ilastik (Berg et al., 2019) was used for a machine-learning-based image segmentation of the various soft and hard tissues (see list below). From the tiff sequences (either aligned or unaligned) a random set of 500 by 500, or 1000 x 1000 pixel sized images, cropped either around the centre of the images and in other locations of interest, in every tenth image of the sequence, starting at a random number less than 10, or starting from a full sequence of all images, converted to h5 format, were used as training data. The classifier was constantly re-evaluated within the program, until satisfactory. In the case of ID127565, additional images were loaded into the software to allow for the trained segmentation of less common tissues. The tissue labels were:

- Lumen
- Epithelium
- Nervous tissue
- Vascular tissue (which included vascular lacunae and lymphoid tissue)
- Glands (only in distal high resolution of ID127565)
- Connective tissue
- Fat
- Muscle
- Cartilage and bone (not in distal)
- Arterial wall (not in ID127565)
- Background

The classifiers (one for tissue segment (distal, curvature, proximal) per image resolution, so 6 classifiers per specimen in total) were then applied to all images, which resulted in each image (.tiff format) being segmented with distinct grey-scales or colours for each of the tissues to which the classifier was trained.

The images were then 'despeckled' 5 times using ImageJ, which removed small speckles in the images,, in order to keep the resolution of the models, to be created in a following step, manageable.

---

[2] *Cardona, A.; Saalfeld, S. & Schindelin, J. et al. (2012), "TrakEM2 software for neural circuit reconstruction.", PloS one **7(6)**: e38011, PMID 22723842*

Next, the images were downsized and cropped using ImageJ, without averaging or interpolation, so that 500x500 pixel (= best max size for 3DSlicer), up to 2500x2500 pixel images with resolutions of 1, 5, 10, 12.5, or 25% of the original image could be loaded as volumes into 3DSlicer where the image spacing (x, y and z) and origin (x, y and z) were adjusted for each stack.

In 3DSlicer, each colour was used as a mask for the segmentation and modelling of the various tissues. In most cases, the segmentations were smoothed by a factor of 10% within 3DSlicer, before they were exported as an .stl file, which was then loaded into Meshlab (latest version v2020.04)(Cignoni et al., 2008), for a systematic reduction of the size of the models. First, the models were cleaned and repaired by removing eventual duplicate or non-manifold vertices and faces. The models were simplified using consecutive Quadric Edge Collapse Decimation (standard parameters) of 50%. After each simplification step the model was exported, saved and reloaded until the raw of the file came to a manageable size (preferably <10Mb, but if distortion became too noticeable, a maximum size of 50Mb was acceptable) to be imported into Blender (latest version used v.2.81).

Within Blender, single vertices were removed, the models were smoothly shaded, and textures, materials and lighting were applied, together with camera settings and movement, to fit the visual requirements for the various representations and levels of morphological detail. Whenever available, macroscopic images were added as references into Blender to cross-check the topography.

10 Tissue evaluation

For the development of the sampling protocol, we wanted to evaluate in what grade the process of freezing and thawing would affect the morphology of the tissues of interest. As is known, the intra- and extracellular fluids expand and contract during these processes which can distort the tissue appearance. We examined histological sections of fresh samples (Condition code 2) immediately fixed in formalin (ID 12691), fresh frozen samples fixed in formalin (ID 2926 Left side), and fresh frozen samples that were defrosted before fixing in formalin (ID 2926 Right side). As such we could asses the impact of freezing by comparing results from animal ID12691 to ID2926 and ID5396, and assess the impact of defrosting by comparing the left side and right side of animal ID2926.

Histological markers included the degree to which tissues could be identified, with special attention to the morphology of the sensory nerve formations, and the general degree of tissue conservation in the epithelium, the musculature, etc.

11 Bibliography of Materials and Methods

Aoki, T., Tanaka, T., and Watabe, H. (1992). Purification and characterization of gamma-enolase from various mammals. Chem. Pharm. Bull. 40, 1236–1239.

Arganda-Carreras, I., Kaynig, V., Rueden, C., Eliceiri, K.W., Schindelin, J., Cardona, A., and Sebastian Seung, H. (2017). Trainable Weka Segmentation: a machine learning tool for microscopy pixel classification. Bioinformatics 33, 2424–2426.

Bancroft, J.D., and Gamble, M. (2002). Palmgren's method for nerve fibers in paraffin-embeddd material (Palmgren, 1948). In Theory and Practice of Histological Techniques, (London: Elsevier Science Limited), p. 378.

Bancroft, J.D., and Gamble, M. (2002). Bielschowsky's silver stain for neurofibrils, dendrites, and axons in paraffin and frozen sections, modified (Chan, unpublished). In Theory and Practice of Histological Techniques, (London), pp. 376–377.

Berg, S., Kutra, D., Kroeger, T., Straehle, C.N., Kausler, B.X., Haubold, C., Schiegg, M., Ales, J., Beier, T., Rudy, M., et al. (2019). ilastik: interactive machine learning for (bio)image analysis. Nat Methods 16, 1226–1232.

Breckenridge, L.J., Sommer, I.U., and Blackshaw, S.E. (1997). Developmentally regulated markers in the postnatal cervical spinal cord of the opossum Monodelphis domestica. Developmental Brain Research 103, 47–57.

Cabo, R., Alonso, P., José, I.S., Vázquez, G., Pastor, J.F., Germanà, A., Vega, J.A., and García-Suárez, O. (2015). Brain-Derived Neurotrofic Factor and its Receptor TrkB are Present, but Segregated, Within Mature Cutaneous Pacinian Corpuscles of Macaca fascicularis. The Anatomical Record 298, 624–629.

Cardona, A., Saalfeld, S., Schindelin, J., Arganda-Carreras, I., Preibisch, S., Longair, M., Tomancak, P., Hartenstein, V., and Douglas, R.J. (2012). TrakEM2 Software for Neural Circuit Reconstruction. PLOS ONE 7, e38011.

Cardona, A., Schindelin, J., Eglinger, J., Saalfeld, S., and Arganda-Carreras, I. (2017). Register Virtual Stack Slices.

Cignoni, P., Callieri, M., Corsini, M., Dellepiane, M., Ganovelli, F., and Ranzuglia, G. (2008). MeshLab: an Open-Source Mesh Processing Tool (The Eurographics Association).

Fyfe, J.C., Al-Tamimi, R.A., Castellani, R.J., Rosenstein, D., Goldowitz, D., and Henthorn, P.S. (2010). Inherited neuroaxonal dystrophy in dogs causing lethal, fetal-onset motor system dysfunction and cerebellar hypoplasia. The Journal of Comparative Neurology 518, 3771–3784.

Jauniaux, T., André, M., Dabin, W., De Vreese, S., Gillet, A., and Morell, M. (2019). Marine Mammals Stranding Guidelines For Post-Mortem Investigations Of Cetaceans & Pinnipeds & 13rd Cetacean Necropsy Workshop Special Issue On Necropsy And Samplings (Liege 2019) (Liège).

Kestell, G.R., Anderson, R.L., Clarke, J.N., Haberberger, R.V., and Gibbins, I.L. (2015). Primary afferent neurons containing calcitonin gene-related peptide but not substance P in forepaw skin, dorsal root ganglia, and spinal cord of mice. Journal of Comparative Neurology 523, 2555–2569.

Kikinis, R., Pieper, S.D., and Vosburgh, K.G. (2014). 3D Slicer: A Platform for Subject-Specific Image Analysis, Visualization, and Clinical Support. In Intraoperative Imaging and Image-Guided Therapy, F.A. Jolesz, ed. (New York, NY: Springer), pp. 277–289.

Klück, P., Van Muijen, GoosN.P., Van Der Kamp, ArthurW.M., Tibboel, D., Warnaar, SvenO., Van Hoorn, WopkeA., and Molenaar, JanC. (1984). Hirschsprung's disease studied with monoclonal antineurofilament antibodies on tissue sections. The Lancet 323, 652–654.

Luna, L.G. (1968). Manual of histologic staining methods of the Armed Forces Institute of Pathology (New York: Blakiston Division, McGraw-Hill).

Malinovský, L. (1996). Sensory nerve formations in the skin and their classification. Microsc. Res. Tech. 34, 283–301.

Mazzariol, S., Cozzi, B., and Centelleghe, C. (2015). Handbook for cetacean's stranding.

Pernick, N. (2019a). PAS stain (Periodic Acid-Schiff). http://www.pathologyoutlines.com/topic/stainspas.html. Accessed 2020-05-14

Pernick, N. (2019b). Giemsa stain. http://www.pathologyoutlines.com/topic/stainsgiemsa.html. Accessed 2020-05-14

Sematovica, I., Pilmane, M., and Jemeljanovs, A. (2008). Vascular endothelial growth factor, nerve growth factor receptor p75, protein gene product 9.5, tumor necrosis factor-α and apoptosis in the cow endometrium in post partum period. 5.

Spaethe, A. (1984). Eine Modifikation der Silbermethode nach Richardson für die Axonfärbung in Paraffinschnitten. Verh. Anat. Ges. 78, 101–102.

van Sprundel, R.G.H.M., van den Ingh, T.S.G.A.M., Guscetti, F., Kershaw, O., van Wolferen, M.E., Rothuizen, J., and Spee, B. (2014). Classification of primary hepatic tumours in the cat. The Veterinary Journal 202, 255–266.

Stammnitz, M.R., Coorens, T.H.H., Gori, K.C., Hayes, D., Fu, B., Wang, J., Martin-Herranz, D.E., Alexandrov, L.B., Baez-Ortega, A., Barthorpe, S., et al. (2018). The Origins and Vulnerabilities of Two Transmissible Cancers in Tasmanian Devils. Cancer Cell 33, 607-619.e15.

Tinevez, J.-Y., Perry, N., Schindelin, J., Hoopes, G.M., Reynolds, G.D., Laplantine, E., Bednarek, S.Y., Shorte, S.L., and Eliceiri, K.W. (2017). TrackMate: An open and extensible platform for single-particle tracking. Methods 115, 80–90.

Uemura, N., Koike, M., Ansai, S., Kinoshita, M., Ishikawa-Fujiwara, T., Matsui, H., Naruse, K., Sakamoto, N., Uchiyama, Y., Todo, T., et al. (2015). Viable Neuronopathic Gaucher Disease Model in Medaka (Oryzias latipes) Displays Axonal Accumulation of Alpha-Synuclein. PLOS Genetics 11, e1005065.

RESULTS

RESULTS

To locate a specific figure, please refer to the corresponding sections in the table of contents.

1 Macroscopic morphology of the ear canal and associated tissues

The ear canal followed a spiralling course through the soft tissues between the external ear opening at its lateral end, and the tympanic conus and TP complex on the medial end (Figure 12, Figure 13). The external ear opening was tiny and situated several centimetres caudoventral to the eye. The pigmented ear canal followed a horizontal course, slightly angled caudoventrally, penetrating the blubber layer and superficial soft tissues including muscles, and showed gradually increasing density (connective tissue) until being surrounded by a notable connective tissue sheath, which housed the cartilage as well. The canal then spiralled in rostroventral direction before turning back horizontal and continuing a horizontal course to the middle ear. The connective tissue sheath at this level turned from oval to triangular in shape, with the ear canal in the centre of the triangle´s base, and overlaying a lateral or extramandibular fat body, separated from the ear canal by the ear canal cartilage, while the deep occipito-auricular muscle was touching the caudodorsal margin of the connective tissue triangle´s margin (Figure 14). As the canal enters the parotic cavity in the caudodorsal margin of the

trench created by the caudal ramus of the mandible rostrally, the retroarticular (postglenoid) and retrotympanic process of the squamosal dorsally, and the exoccipital bone caudally (Figure 15), and it arrived at the lower tympanic aperture of the tympanic bone.

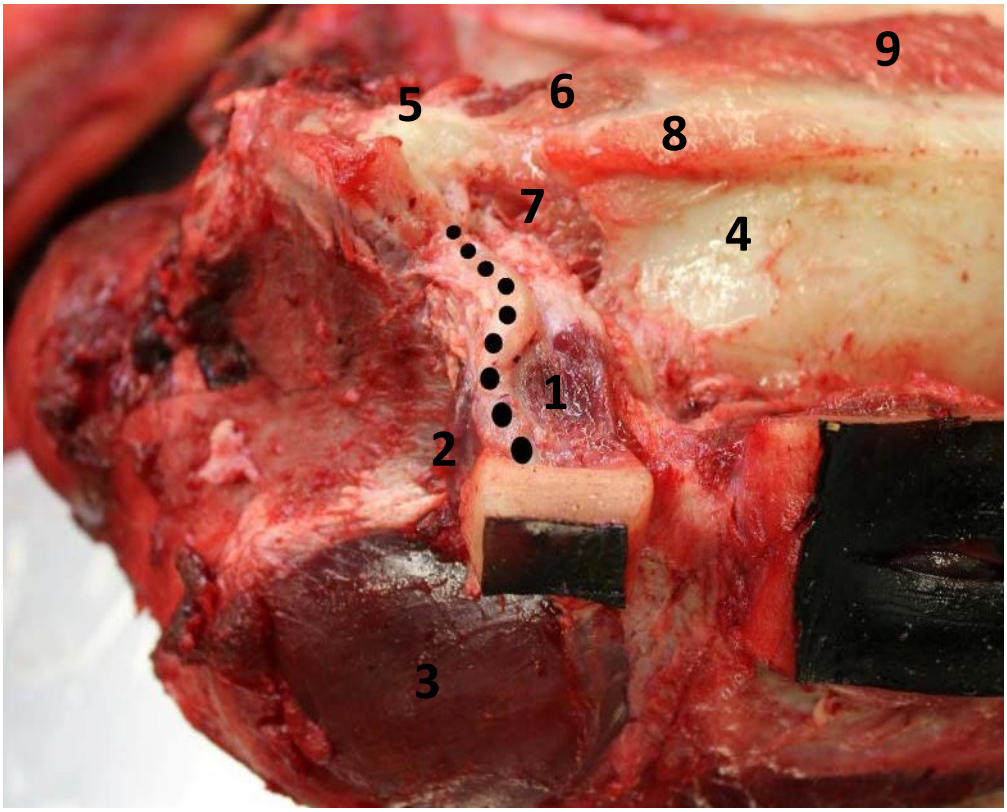

Figure 12. Left lateral view of the external ear canal from the external opening to the tympano-periotic complex. Note the spiralling course starting (from lateral to medial) in caudoventral direction, then in rostroventral direction, then back in caudoventral direction (±45°) and horizontally reaching the tympanic bone. The canal enters the paraotic cavity in the caudodorsal margin of the trench (dotted line) created by the caudal ramus of the mandible rostrally, the retrotympanic and retroarticular (postglenoid) process of the squamosal dorsally, and the lateral margin of the exoccipital bone caudally. 1. Zygomatico-auricular muscle; 2. Occipito-auricular muscle; 3. Temporal muscle; 4. Mandible; 5. Middle ear (tympanic bone); 6. Internal mandibular fat body; 7. fibrovenous plexus; 8. Remnants of the dissected m. hyomandibularis; 9. M. pterygoideus medialis

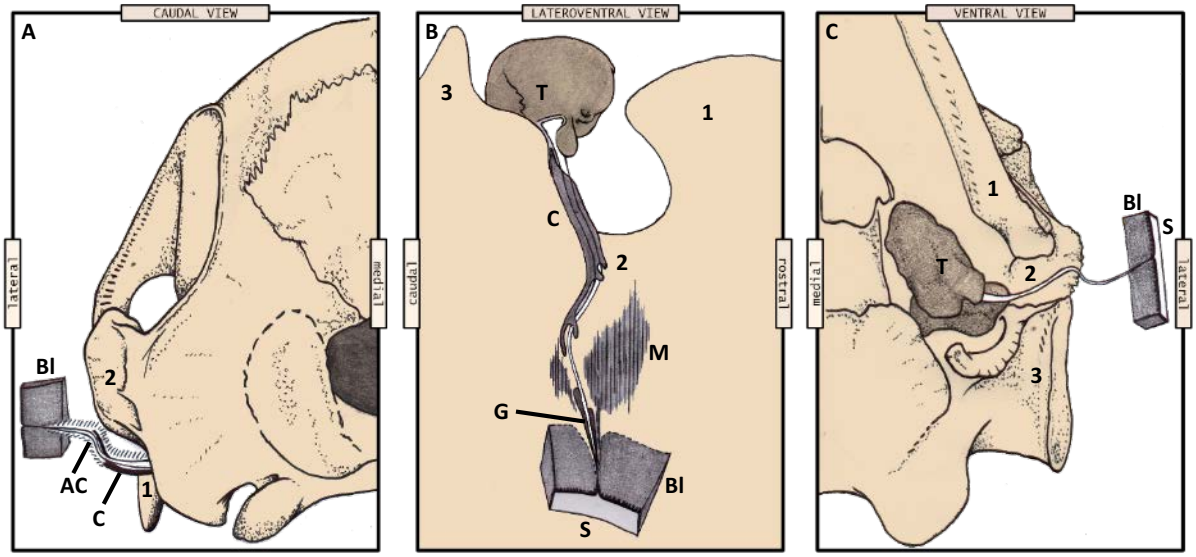

Figure 13. Drawings of the macroscopic course of the external ear canal in a striped dolphin from three different points of view: caudal, lateroventral and ventral. The drawings display the external ear opening in the skin (S) and the underlying blubber layer (Bl), and demonstrate the sigmoid course of the external ear canal (white), which is accompanied by an adipoconnective tissue capsule (AC, in A), local glands (G, in B) and musculature (M, in B), and cartilage (C, in A & B), before reaching the tympanic bone (T, in B & C). 1: Mandible; 2: squamosal bone; 3: exoccipital bone. (Source: De Vreese et al., 2020b)

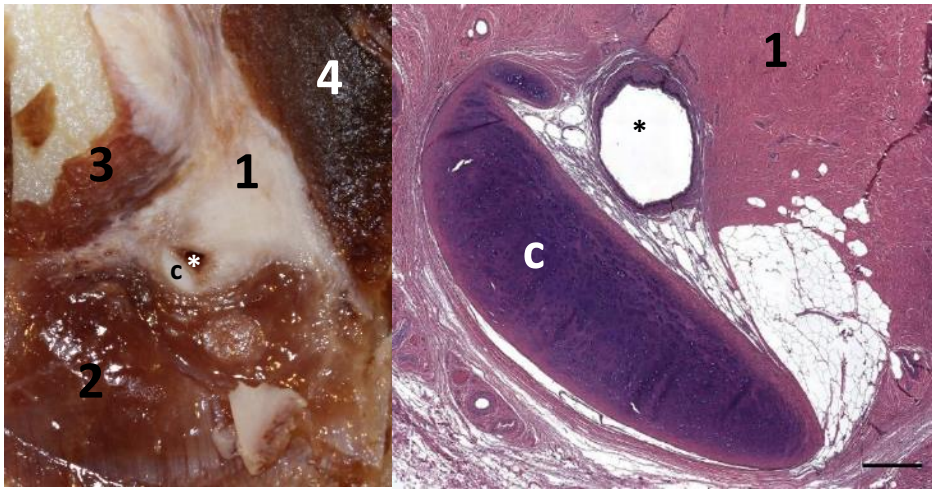

Figure 14. Macroscopic (left) and microscopic (right, HE staining) preparation of a lateral view of the external ear canal (asterisk) in a striped dolphin medial to the ventral curvature. The ear canal, supported by a bean-shaped cartilage (c) on its rostroventral side, is embedded in triangular soft tissue (1), which overlays (likely acoustic) fatty tissue (2)(degenerated). The zygomatico-auricular muscle (3) shows insertions into the connective tissue and runs towards rostral in the direction of the zygomatic. Caudal to the connective tissue runs the deep occipito-auricular muscle (4) caudosagitally in the direction of the crista occipitalis. Scale bar right 0.5 mm.

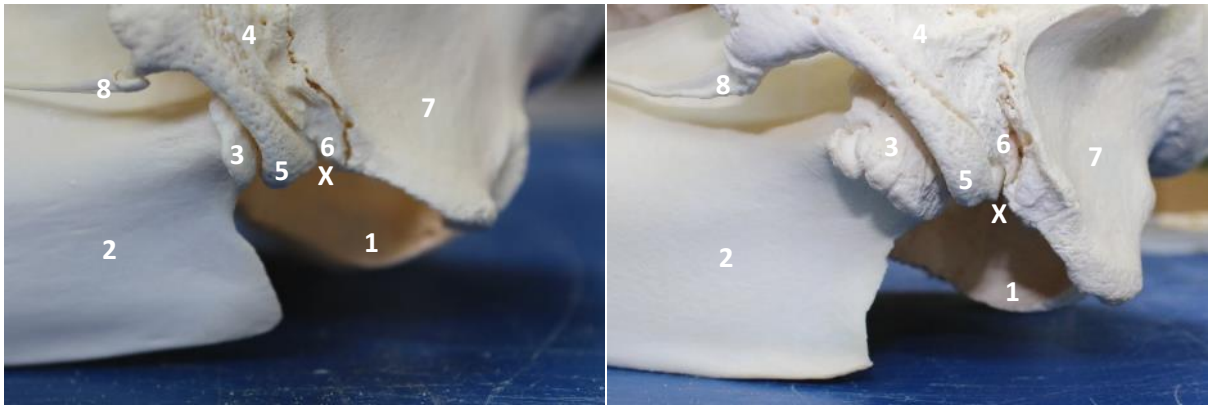

Figure 15. Left lateral view of a close-up of the ear region in the skull of a striped dolphin (left) and a bottlenose dolphin (right). X marks the location of the ear canal on entering the paraotic cavity. Note that the tympanoperiotic complex is missing, and the basioccipital bone (1) is visible; 2. Mandible with condyle (3) situated in the mandibular fossa of the squamosal (4) and part of the temporomandibular joint with the latter; 5. Retroarticular process of the squamosal; 6. Retrotympanic process of the squamosal; 7. Exoccipital; 8. Jugal bone.

1.1 External ear opening – porus acusticus externus

The external ear opening in all species and specimens was situated in a small indentation of the skin located caudoventral to the posterior commissure of the eye at an angle of about 25-30° (Figure 16, Figure 17, Figure 18, Figure 19, Figure 20, Figure 21). The distance between the eye and the ear opening was seemingly larger in larger species and specimens, although no statistical relations between such distance and the size and length of the animal were analysed.

In striped dolphin, the location of the external ear opening in striped dolphin was often indicated by a linear pigmentation, that ran from the external ear opening in rostroventral direction for few centimetres until the colour merged with the darker pigmentation ventral to the eye, making it relatively easy to find in this species, at least in well-preserved specimens (Figure 16, Figure 17, Figure 18). This pigmentation was absent in the striped dolphin foetus (Figure 19), but also in some adult specimens we did not observe such linear pigmentation, but rather the entire area was pigmented, which could have masked the line. In some fresh specimens, we noted macroscopically that the lumen was slightly compressed dorsoventrally, while in other more dehydrated specimens the opening was detected as a dorsoventrally oriented slit. In all mature striped dolphin, the ear opening had a diameter of about 1 mm that quickly tapered to 0.5 mm on the progression through the skin. In two specimens of adult bottlenose dolphin, the location of the ear opening was visible as a minute orifice located at about 6.5 cm and 7.5 caudoventral to the caudal commissure of the eye at an angle of less than 20° to the horizontal. No geometrical measurements were taken for harbour porpoise.

Also, the ear opening was often difficult or impossible to locate, especially in specimens with local dark skin pigmentation, and in bad preservation state. In the pilot whale and the Cuvier's beaked whales, neither of the two external ear openings could be identified macroscopically, partly because of the complete dark pigmentation but mostly because of the preservation state of the animal's skin (Figure 22, Figure 23).

Figure 16. Macroscopic images of the region of the eye and ear in a striped dolphin (N-00293-18). The arrow indicates the external ear opening, situated about 3.5 cm ventrocaudal to the lateral commissure of the eye. It is easily noticeable because of the striped pigmentation, despite the livor mortis. Scale bar 1 cm.

Figure 17. Macroscopic image of the left eye and external ear opening (arrow) of a striped dolphin with marked linear pigmentation running from the external ear opening in rostroventral direction. Scale bar 1 cm.

Figure 18. Left lateral view of the eye and external auditory opening of a striped dolphin (Sc2). The right image is a detail of the left. Note the location of the external ear opening ±5 cm caudoventral to the caudal commissure of the eye. Note the marked linear pigmentation that runs from the ear opening in the direction of the angle of the commissure of the mouth.

Figure 19. Macroscopic left lateral image of the region of the ear in a striped dolphin foetus (ID293/18). The arrow points to the external ear opening. The distance between the ear opening and caudal eye commissure was 22 mm. Scale bar 1 mm

Figure 20. Macroscopic picture of the left eye and external ear opening (arrow) in a bottlenose dolphin (ID444). The opening was situated at 6.5 cm caudoventral to the lateral commissure of the eye.

Figure 21. Right lateral macroscopic picture of the location of the external ear opening situated 7.6 cm caudoventral to the lateral commissure of the eye in a bottlenose dolphin.

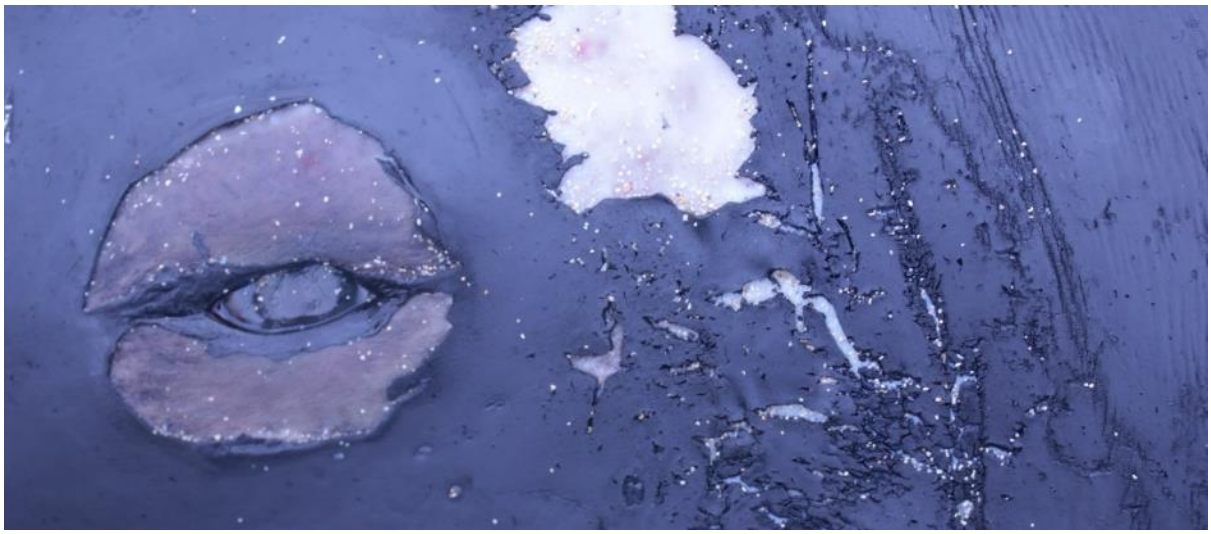

Figure 22. Macroscopic picture of the left lateral side of a long-finned pilot whale (ID441). Note the bad preservation state of the skin around the eye and the area caudal to the eye. The external ear opening could not be located with a thorough external inspection.

Figure 23. Macroscopic picture of the right lateral side of a Cuvier's beaked whale (ID429). The external ear opening was not identifiable with certainty based on macroscopic inspection.

1.2 External auditory meatus (EAM)

In all toothed whales examined, the EAM ran a spiralling course from the external opening in the skin to the TP-complex (Figure 12). The total length was about 4-5 cm in striped dolphin, and the macroscopic dimensions were larger in larger specimens and species, up to an estimated 9-10 cm ear canal length in Cuvier´s beaked whale. From the opening, the ear canal travelled through the blubber layer in a slight caudoventral angle. At this level, the ear canal was detectable as a small dark-pigmented string, which in apparent close contact with the surrounding fat, while there was increasingly more connective tissue around the ear canal over the course towards the middle ear (Figure 24). Various striped muscles inserted into the ear canal´s surrounding connective tissue, from about the medial end of the blubber layer, and particularly at the level of the ventral curvature of the ear canal. As such, medial to the blubber layer, the canal took a ventrorostral turn before continuing horizontally in a slight caudal direction, entered into the paraotic cavity through the caudodorsal margin of the bony sulcus formed by the caudal ramus of the mandible rostrally, the retroarticular (postglenoid) and retrotympanic process of the squamosal dorsally, and the exoccipital bone caudally, before entering into the lower tympanic aperture of the middle ear (Figure 12, Figure 13)(De Vreese et al., 2020a).

In all toothed whales subjected to the macroscopic studies, the general configuration of the EAM and associated soft tissues was very similar to the anatomy in striped dolphin. No macroscopic differences could be discerned except for the differences in size. From superficial to deep, the course of the canal was sigmoid in ventromedial direction with a slight tendency towards rostral. The association with surrounding soft tissue seemed the same. For example, there was the bean-shaped cartilage situated

rostro- to caudoventral (with individual variation) to the EAM, medial to its ventral curvature, before incompletely encircling the EAM in the deepest sections before reaching the middle ear. There were macroscopically visible, small, muscles inserting in the connective tissue around the EAM. These muscles included what we identified as the zygomatico-auricular and occipito-auricular muscles (Figure 12, Figure 24), differentiated from other muscles in the region such as the temporal muscle and the (ventral) scalenus muscle (Figure 25).

There was the presence of fatty tissue with macroscopic similarity to the acoustic fat bodies, situated ventral to the canal from about halfway its course (Figure 25, Figure 14, Figure 27, Figure 28, Figure 29). It was broadly funnel-shaped, tapering towards medial (Figure 27), where it made physical contact with the tympanic bone (Figure 28). Although we could not dissect the exact location properly, it coincided roughly with the location of the insertion of the dorsal branch of the mandibular fat body (reported in Cuvier´s beaked whale, Cranford et al., 2008b)(Figure 28). The fat body ran parallel to the ear canal, was situated ventral to ventrocaudal to it, and was detectable from about the same parasagittal level as the caudal part of the mandible and continued further medially (Figure 27). A dense connective tissue capsule surrounded it, and the whole was suspended in a combination of vascular tissue, with the facial vein and associated (fibro-)venous plexus situated rostrodorsal to the fat body, and the posterolateral lobe of the peribullar sinus dorsocaudally (Figure 27). It also had a seemingly denser core as can be seen in Figure 27 and Figure 28, although this was not subjected to histological evaluation, and therefore the nature of the core and how it differed from the rest of the adipose tissue was not investigated.

There was a fibrovenous plexus situated ventral to the canal at the level of the mandible, between the ear canal and the facial vein (Figure 27). This venous plexus was in continuation with the fibrovenous plexuses of the peribullar and pterygoid sinuses (cfr. Fraser and Purves, 1960; Costidis, 2012; Costidis and Rommel, 2016). Dorsal to the facial vein, the facial nerve ran ventral to the ear canal, from the TP complex towards rostro-lateral, and continued laterally to the mandibles before turning dorsal and innervating the nasal complex (Figure 27, Figure 29), which was also often visible in the microscopical studies (see below).

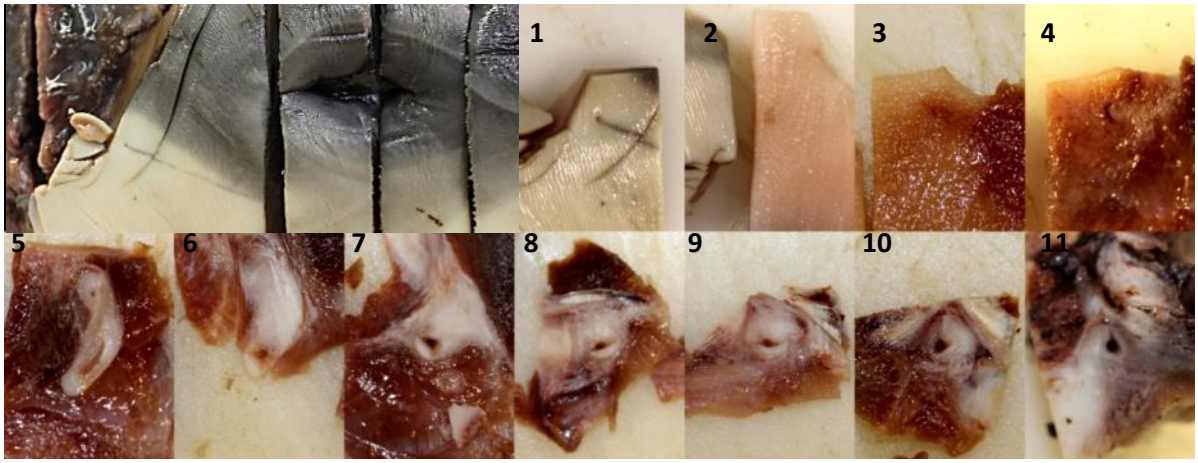

Figure 24. Macroscopic images of right external ear canal tissue slabs of a striped dolphin. Top left: undissected right lateral view (the animal was cut into transverse sections for macroscopic studies). Image sequence: 11 dissected tissue slabs of the ear canal from lateral to medial. Note the ventral curvature of the canal in slab 5-6 and the appearance of the cartilage, which then supports the lumen from ventral in slab 7-11 while gradually enveloping the lumen. The striated muscle visible in 7-8 is likely the deep occipito-auricular muscle.

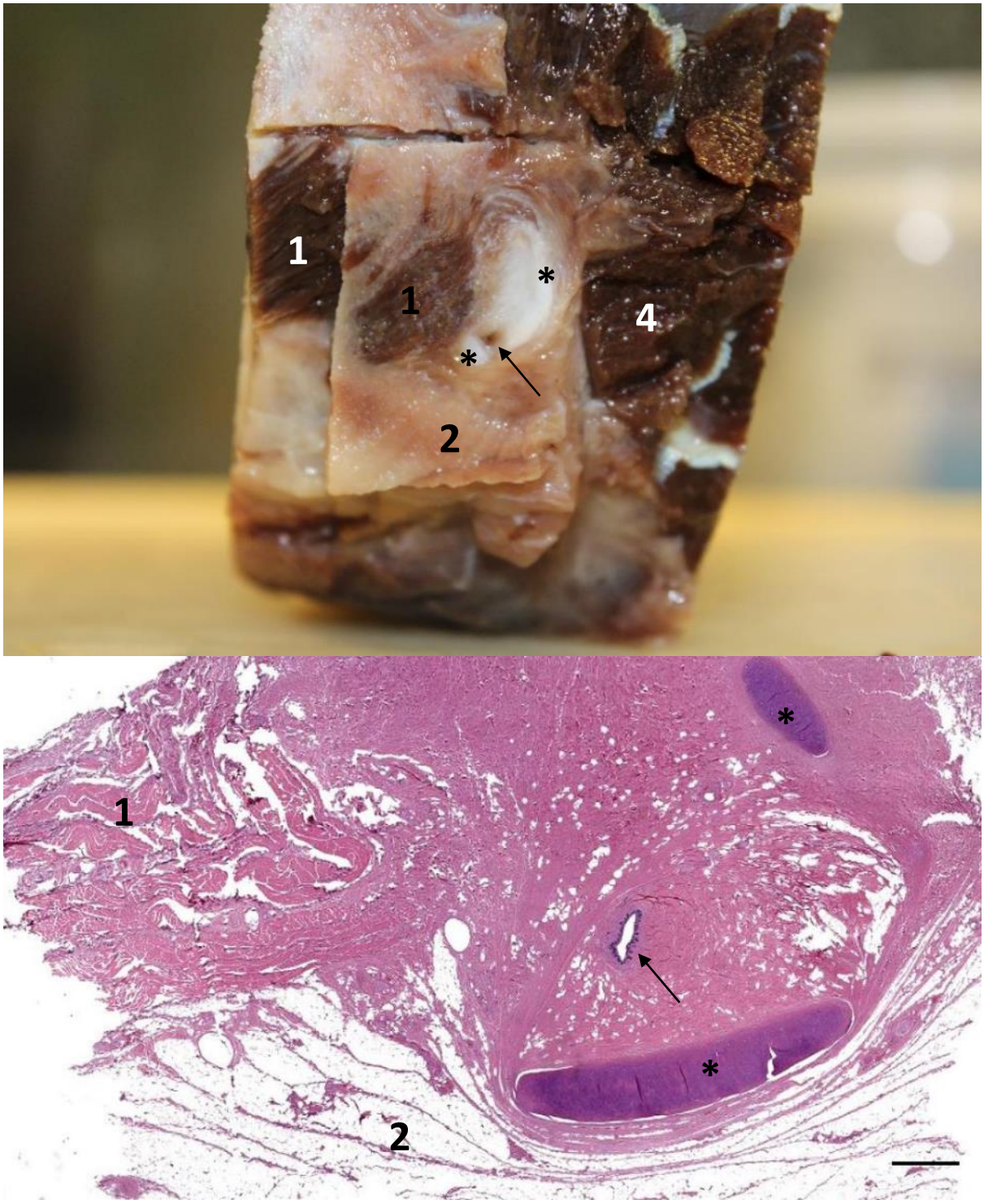

Figure 25. Macroscopic and microscopic (HE staining) lateral view of the left ear canal (arrow) with cartilage (asterisk) at the level of the bottom of the ventral curvature where the ear canal turns horizontal again. Rostral to the ear canal, there is the m. zygomatico-auricularis (1) with insertion into the connective tissue sheath of the canal. The same muscle is sectioned twice at different depths. The muscle fibres run rostroventrally from the around the ear canal. The connective tissue around the ear canal of the ventral curve is visible and the ear canal continuous its course further horizontal, supported by the cartilage (asterisk) on the ventral side. Ventral to the canal and cartilage, there is the lateral/extramandibular fat body (2). Caudal to the canal, although without direct insertions into common connective tissue, there are the insertions of the (ventral) scalenus muscle (4) and possibly also the sternocephalicus into the cavity of the exoccipital bone (Top: striped dolphin; Bottom: bottlenose dolphin; Scale bar 1 mm

*Figure 26. Macroscopic left lateral image of the ear canal and surroundings. 1: ear canal; 2; mandible, with the extramandibular fat body (3) arching around the angular process ('gonion') of the mandible. 4: fat body; 5: posterolateral sinus (cfr. Mead and Fordyce, 2009), the most posterolateral extension of the peribullar sinus. Caudally, there is the paraoccipital process of the exoccipital; 6: stylohyoid (cut through); 7: pterygoid muscle; 8. Ventral scalenus muscle; * continuation of the dense core of the fat body, see Figure 27*

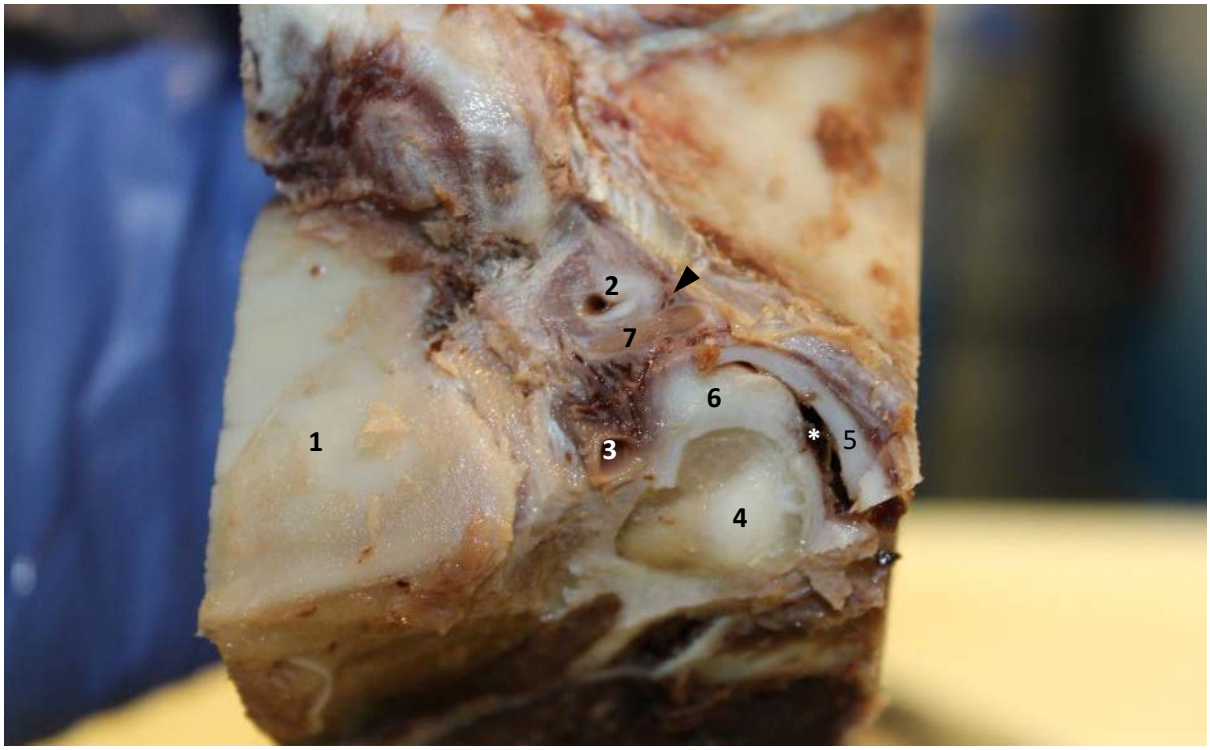

*Figure 27. Stenella coeruleoalba. Left lateral picture. 1: Mandible; 2: ear canal; 3: facial vein with the mandibular fibrovenous plexus dorsal to it, similar to the veins caudal to the ear canal (arrowhead); 4; fat body a core of denser tissue (white tissue); 5: cartilage at the medial end of the stylohyoid; 6: connective tissue surrounding the channel of the fat body; 7: Facial nerve running ventral to the ear canal; The ventral scalenus muscle has been removed. * Posterolateral (lobe of the peribullar) sinus*

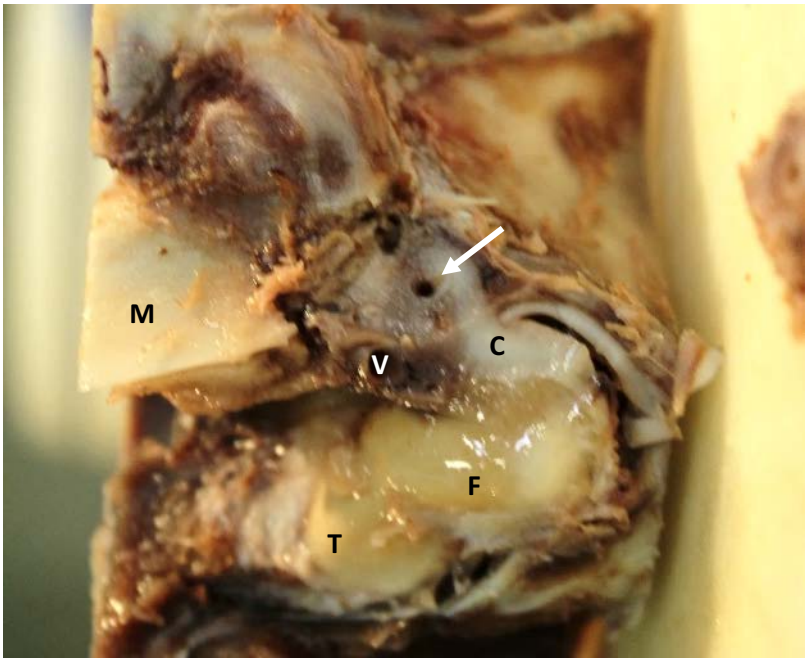

Figure 28. Macroscopic image of the left lateral side of the region of the ear. The mandible (m) has been cut horizontally and removed together with the mandibular fat body and other soft tissues. Note that there is a fat body (F) ventral to the ear canal, making contact with the tympanic bone (T). The dense connective tissue (C) (number 6 in the previous picture) connects to the dense connective tissue and cartilage posterior to the ear canal (arrow). V: facial vein.

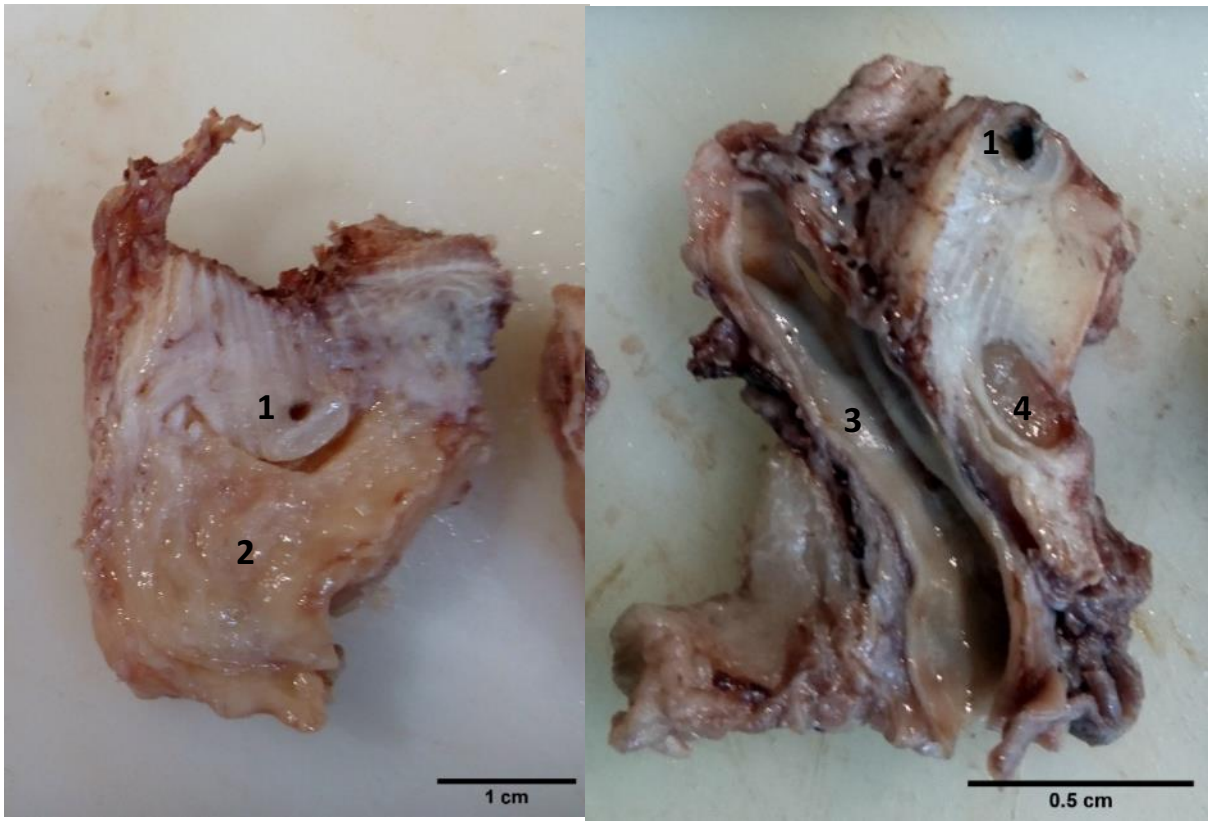

Figure 29. Macroscopic pictures of lateral aspects of sections through the left ear canal and surrounding tissue in a superficial and a deeper section, about 2 and 4 cm beneath the skin, respectively. 1. Ear canal and cartilage; 2. Acoustic fat body; 3. Facial vein; 4. Facial nerve.

1.3 Cranial nerve innervation and mapping in the region of the ear

The following results were obtained from a Pantropical spotted dolphin dissection (Figure 30, Figure 31, Figure 32).

The medial end of the ear canal was located at the base of the skull, rostral-lateral to where the mandibular nerve (V3) exits the skull. The tissue between V3 and the ear canal medial end was tough to prepare. The anterolateral part of the tympanic bone was removed, and V3 was tracked from its origin to caudal(dorsal). There was at least one branch of V3 that ran caudolateral in the direction of the external ear canal. This branch bifurcated near its base, and both branches ran towards the medial end of the ear canal, one slightly more lateral than the other. As such, both were considered part of the auricular nerve and likely innervated the EAM in its medial part, together with the external surface of the tympanic membrane.

Further dissection of the tissues towards medial showed that the trigeminal gave rise to one nerve going to the middle ear, entering between tympanic and periotic, and ran in the anterior incisure of the periotic (between the anterior process of the periotic and the part that contains the cochlea), in the direction of the malleus.

The mandibular ganglion gave off two branches in caudal direction, one dorsal and a ventral branch, the dorsal being bigger, and both innervated the region of the middle ear. The mandibular ganglion also gave off a lateral nerve that ran in the direction of the ear canal, which in its turn gave off a small branch that innervated the medial end of the ear canal, and a second larger branch that continued in caudolateral direction while giving off various branches that innervated the course of the canal. At this point, they became too small to dissect macroscopically.

Although the medial side of the tympanic conus would likely be innervated by the glossopharyngeal nerve, we did not identify any such innervation. There were arterial branches of what was likely the stylomastoid artery, which supplied the tympanic ligament or part of the inner lining of the tympanic with blood. These branches also entered the bony walls of the tympanic and were part of a vascular network that was partially supplied by the a. caroticotympanicae (< a. carotis interna), as also described in humans (Benninghoff et al., 1994).

The vagus nerve was prepared, and no macroscopically visible branch ran in the direction of the ear canal. There were other branches such as the one that is responsible for the innervation of the larynx, running parallel to the hypoglossal nerve (XII).

We could not identify any chorda tympani branching from the facial nerve, although this might have been due to the small size of the area, and possibly removed together with the *corpus spongiosum* of the middle ear. This *corpus spongiosum* showed an intense innervation. It consisted of a plexus of nerves that originated from the inferior ganglion of the glossopharyngeal nerve, although not

distinguishable from the superior ganglion of the vagus nerve, due to artefacts of the tissue drying out. Possibly, the innervation was provided by the tympanic branch of the glossopharyngeal nerve, as this also forms a tympanic plexus in humans (Watanabe et al., 2016).

In summary, the macroscopic innervation of the ear canal region showed the main innervation by the mandibular nerve (V3), through the auriculotemporal nerve and several of its branches. No other macroscopically visible nerves were identified that might supply the region of the outer ear canal.

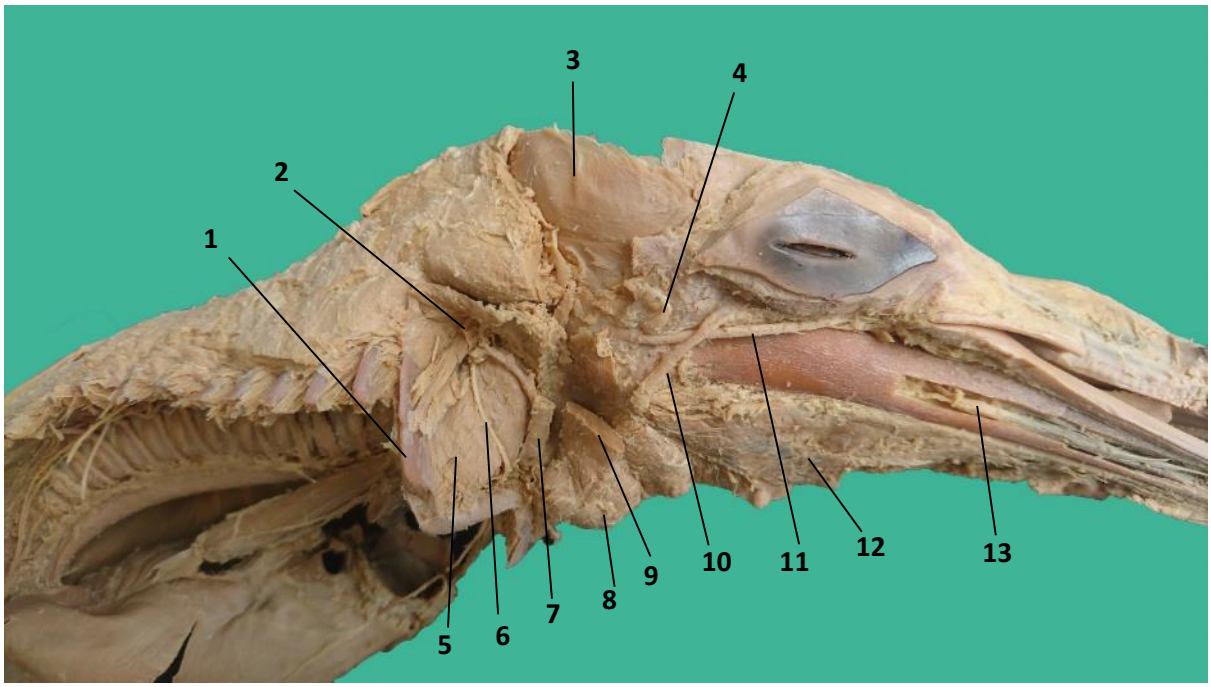

Figure 30. Macroscopic image of a tissue preparation of the region of the right ear in a Pantropical spotted dolphin foetus. 1. First rib; 2. Plexus brachialis; 3. Temporal muscle; 4. EAM with part of the ventral curvature; 5. Dorsal scalenus muscle; 6. Phrenic nerve; 7. Common carotid artery; 8. Sternohyoid muscle; 9. Sternocephalic muscle; 10. Facial vein; 11. Facial nerve; 12. Mylohyoid muscle; 13. Alveolar nerve

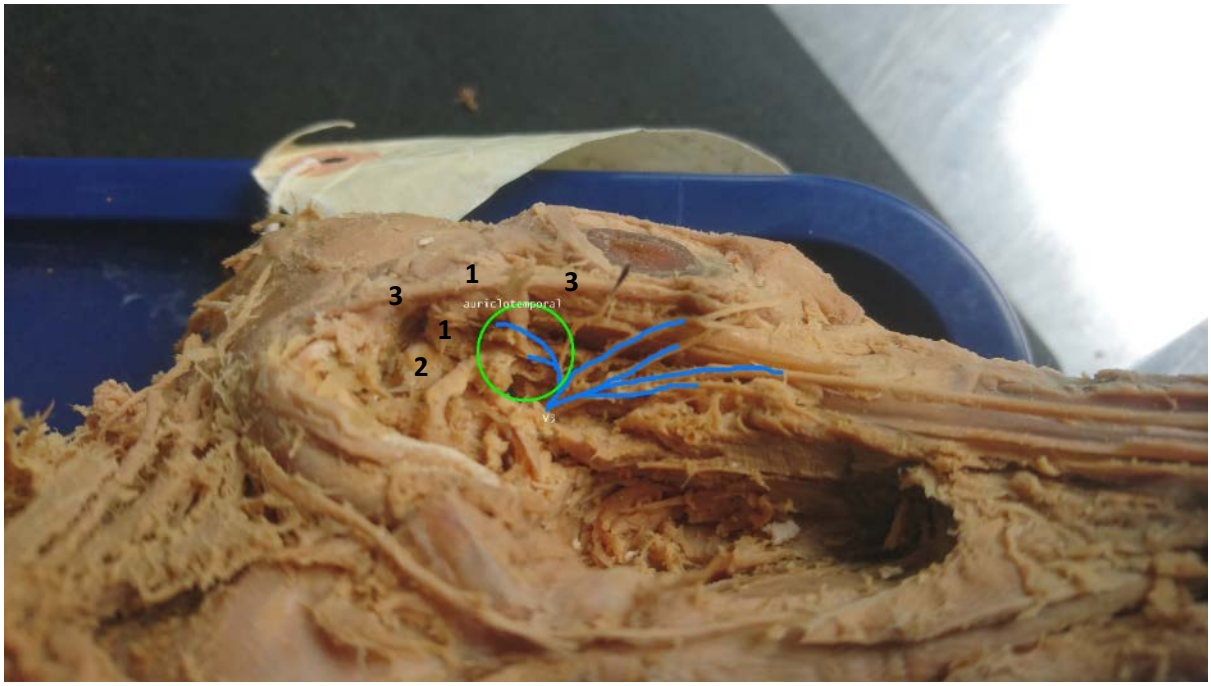

Figure 31. Macroscopic image of the ventrolateral aspect of the mandibular nerve branches. The caudal branches are considered auriculotemporal branches innervating the region of the external ear canal. 1. EAM in connective tissue; 2. Tympanic bone; 3. Facial nerve.

Figure 32. Macroscopic image of a medioventral view of a part of the trigeminal ganglion (asterisk) and the auriculotemporal nerve that branches off in caudolateral direction (indication).

2 Microscopic morphology of the external ear canal and associated tissues

General configuration (Link Video 3D reconstruction – striped dolphin)

The configuration and relationship of the various soft tissues changed along the course of the canal. Medial to the external ear opening, the lumen tapered rapidly to where the canal presented an absent lumen in all but a few ear canals. This absence of a lumen constituted itself in various forms, either by an apparent collapse with the epithelium of opposite sides touching (Figure 59), or an evenly

distributed growth of the epithelium to an almost complete closure of the lumen or with a dense luminal content consisting of desquamated epithelial cells and glandular products as was the case for a Cuvier's beaked whale (Figure 66) but also for several dolphins (e.g. Figure 75). There was variety among individuals in the configuration of the absent lumen from collapsed opposite sides, to a complex and star-shaped closure of the walls, to an onion-like shape where the distinction between luminal content and intact epithelium was vague. In deeper sections, the lumen was either empty or contained desquamated epithelial cells coming from the ear canal lining. In all species, the epithelium was a continuation of the external skin. It consisted of a variable pigmented stratified squamous epithelium with incomplete keratinization, configured in three strata (basale, intermedium, and superficiale) and resting on a basement membrane, which diminished in size throughout the canal from lateral to medial (Figure 41).

Surrounding the ear canal was fat and connective tissue in variable ratios, depending on the cut, with more fat around the ear canal in lateral sections, and more connective tissue in medial sections. The connective tissue near the ear canal was loose and nuclei-dense without elastic fibres, while the more peripheral connective tissue was dense, contained elastic fibres, and formed a sort of capsule.

In cross-sections medial to the artificial lumen, the lumen opened up in shapes of various complexity, together with the presence of glandular structures and the insertion of striated muscles into the adipoconnective tissue capsule (Figure 62). Striped and common dolphin showed a complex star-shaped lumen in transverse sections, while the beaked whales presented an oval to a triangular lumen, with less inward folding of the epithelium and papillary layer into the luminal space, except for few sections in one of the two specimens (Figure 44). Bottlenose dolphin and pilot whale showed an intermediate situation in terms of lumen complexity, and there was also a clear interspecific difference in the size of the ear canal between different species (Figure 75). Little deeper, the amount of surrounding connective tissue increased, and various striated muscles, inserting into the adipoconnective tissue around the ear canal. Concurrent with the most lateral muscle insertion, slightly medial to the artificial lumen, glandular structures were present in the soft connective tissue around the ear canal in all animals, except for the Cuvier´s beaked whale (in which the glands might have been missed). They were presented in various parenchymous bodies, often distributed around the ear canal, although most consistently located on one side of the canal. These were composed of compound, multilobar and –lobular, acinar or acinotubular secretory units, connected to excretory ducts lined with a thin stratified (at least three layers) squamous epithelium containing melanin, and which opened onto the ear canal lumen in a slight angle in the direction of the skin. Their product, present within the secretory units, excretory ducts, and in the ear canal lumen, stained positive for Alcian blue, which indicates the presence of mucinous substances. The glandular structures in striped

dolphin were distinguishable from the ear canal and presented excretory ducts that ran in the direction of the artificial lumen and external ear opening. In other species, we noted the same, although with a less clear distinction between glandular secretory cells, and the squamous epithelium of the ear canal itself. The common dolphin presented several separate glandular structures, but the distinction with the ear canal was not always possible using standard stain techniques. This was partly due to the tissue conservation state, but mainly because of the unique configuration. In one bottlenose dolphin and a pilot whale the same situation was found, while in another bottlenose dolphin, there were indications that the epithelium of the ear canal itself showed a transition from squamous to columnar and likely secretory (although not clearly positive for Alcian Blue) for a distance of about 1 cm before turning again squamous. The epithelium in the medial half of the ear canal in all animals had a similar squamous multilayered configuration with incomplete keratinization but was thin in comparison with the epithelium lateral to the glands.

As we followed the ear canal towards medial, the glandular structures disappeared, the amount of fat diminished and was gradually replaced by dense connective tissue, and hyaline cartilage appeared in the connective tissue around the canal (Figure 41). The cartilage presented various ´fingers´ (cartilaginous plates) that projected towards lateral, with usually one larger than the other. These ´fingers´ then converged into the main body of the cartilage, which escorted the ear canal down its ventral spiral. At the bottom of the spiral, with the canal turning back horizontal, the cartilage took on a bean-shaped in cross-section which supported the ear canal from ventral. At this level, the ear canal lumen was bigger and rounder and embedded in a dense connective tissue capsule with few adipocytes, separating the canal from an adipose tissue body that was present in all species and which could be noted both macro- and microscopically (Figure 25). This fat body showed a connection to the mandibular fat body, and made contact with the tympanic bone, although the exact relations between the soft and hard tissues were not mapped in detail.

The cartilage was present down to the tympanic membrane and gradually enveloped the canal over its course, until forming an incomplete, dorsally open trench that had the shape of a horseshoe on transverse sections. This configuration was similar for all species, although with individual variation.

The ear canal passed dorsal to the facial nerve in all species, where the nerve turns rostral after having travelled laterally through the bony cove formed by the mandible, the ventral processes of the squamosal, and the exoccipital bone.

The area between the ear canal lumen and the cartilage contained pronounced vascular lacunae which were embedded in a network of possible reticular fibres loosely arranged, and with a large amount of ground substance (Figure 193, Figure 197). These lacunae were lined with epithelium (endothelium) that stained positive for anti-von Willebrand factor (vWf, Factor VIII). They were present along the

entire medial half of the ear canal and were subjectively larger in deeper tissue, and continuous with a sizeable vascular plexus that was embedded in the same fibrinous network of connective tissue situated in the centre of the tympanic conus.

There was lymphoid tissue present in the form of scattered resident mononuclear cells in the same area between ear canal and cartilage, in the medial third of the canal where the cartilage changes from kidney- to horseshoe-shaped, and also in medial sections in the subepithelial tissue at the level of the glands. In both locations, we often noted the multifocal presence of lymphocytes, with scant plasma cells and macrophages.

The entire ear canal was richly innervated with many small nerves running along the ear canal, giving off branches into the subepithelial soft tissue layer, which contained abundant lamellar corpuscles. In the superficial half of the canal, the corpuscles were distributed evenly in the subepithelial tissue around the ear canal and interspersed with the glandular structures wherever present. With the appearance of the cartilage, the corpuscles concentrated on one side of the ear canal, more or less opposite to the cartilage. At this stage, there are few adipocytes in the surrounding tissue, which consists of dense connective tissue with fibres orientated as in the shape of a hammock in which the ear canal is suspended. Towards medial, the cartilage gradually enveloped the ear canal, and the amount of subepithelial tissue decreased except for the location of the corpuscles, where the epithelium and subepithelial tissue showed an interdigitating pattern (in contrast to the smooth course of basement membrane around the rest of the ear canal). Here, the subepithelial tissue with corpuscles formed a tissue bulge that protruded into the canal lumen. This tissue bulge was present down to the tympanic conus, where it showed a spatial/vectorial association with the structures of the middle ear.

The external ear canal varied in shape and size over the course of the canal from the external ear opening to the tympanic membrane (Figure 34). The ear opening was presented as a concavity in the skin that progressed through the blubber as a very narrow canal with a lumen that was either absent due to the collapse of opposing epithelial walls, was filled with desquamated epithelial cells and glandular product, or was presented with a minute diameter of a few tens of microns. In deeper sections, the canal opened up and had a complex shape that extended into the excretory ducts of the neighbouring mucinous glandular structures, which were situated in the adipoconnective tissue around the ear canal. From about halfway through the course of the canal, medial to the glandular structures, at the level of the ventral curvature, the lumen opened up more, took on an oval to a round shape, and had a gradually increasing diameter before arriving at the tympanic membrane (De Vreese et al., 2020a).

The ear canal was lined by a stratified squamous epithelium, a continuation of the skin, which diminished in the number of layers as the canal progressed deeper. It contained melanin, although not constantly present throughout the entire course.

The epithelium was encompassed by a relatively thin lamina propria with which it showed an intricate interaction, particularly in the lateral half of the canal. This layer was intensely vascularized and presented a prominent innervation with the presence of sensory nerve formations, simple lamellar corpuscles, which were present throughout the entire course of the canal. The corpuscles were distributed around the ear canal in the superficial half down to the ventral curvature, while they appeared concentrated into a tissue bulge on one side of the canal in the inner half of the ear canal.

Surrounding the canal, was an adipoconnective tissue capsule, which was present throughout the entire course, although with varying ratios of fat and connective tissue. From superficial to deep, the adipose tissue of this capsule was gradually replaced by connective tissue until it was almost completely absent in the deepest sections. Various striped muscles inserted into the adipoconnective tissue, at least in the superficial two-thirds of the canal, and were especially prominent at the level of the ventral curvature and the lateral projections of the cartilage.

The cartilage supported the ear canal from ventral and progressively enveloped the canal in deeper sections, although never fully closing. The cartilage ends at the level where the ear canal enters between the tympanic and periotic bone and the canal curves around the sigmoid process and ends as a blind sac at the tympanic membrane (De Vreese et al., 2020a).

Table 8. Schematic representation of soft tissues associated with the ear canal (rows), from left to right representing the course from the external ear opening to the tympanic conus. The columns represent the regions used for quantification.

		External ear opening	***Regions for quantification****							*Tympanic conus*
			Blubber	*Glands*		*Muscle*	*Cartilage*		*Nervous tissue ridge*	
Soft tissue	*Blubber*		*X*	*X*						
	Glands			*X*	*X*					
	Muscle				*X*	*X*	*X*			
	Cartilage						*X*	*X*	*X*	
	Button								*X*	

**Blubber: From the external ear opening to the lateral end of the glands (excluding glands); Glands: containing glandular structures; Muscle: From the medial end of the glands to the medial end of the cartilage; Cartilage: From the lateral end of the cartilage to the medial end of the ´nervous tissue ridge´; Button: from the lateral end of the nervous tissue ridge to the medial end of the ear canal*

The tissue regions, as mentioned in Table 8, are derived from an analysis done for most of the specimens as can be seen in Figure 33.

	A	B	C	D	E	F	G	H	I	J	K	L	M	N	O	P	Q	R	S	T	U	V
1	**Sample block**	Right	**1**	**2**	**3**	**4**	**5**	**6**	**7**	**8**	**9**	**10**	**11**	**12**	**13**	**14**	**15**	**16**	**17**	**18**	Lx1	Lx2
2	**# of single corpuscles**		A	6	6	3	1	9	5	12	8	3	9	7	9	1	10	A	A	24		
3	**# of corpuscle complexes**		A	0	1	1	0	5	3	2	1	1	2	1	3	0	1	A	A	1		
4	**average # cores per complex**		A		2	2		2	2.67	2.5	2	2	2.5	2	3		2	A	A	2		
5	**# of corpuscle cores in complexes**		A	0	2	2	0	10	8	5	2	2	5	2	9	0	2	A	A	2		
6	**Total number of corpuscle cores**		A	6	8	5	1	19	13	17	10	5	14	9	18	1	12	A	A	26		
7																						
8	**Artificial lumen**		1	1	1	1	0	0	0	0	0	0	0	0	0	0	0	0	0	0		
9	**Melanin**		0	0	1	1	1	1	1	1	1	1	1	1	1	1	1	1	1	1		
10	**Blubber**		0	1	1	1	1	0	0	0	0	0	0	0	0	0	0	0	0	0		
11	**Muscle**		0	0	0	1	1	1	0	1	1	1	0	0	0	0	0	0	0	0		
12	**Glands (Y/N)**		0	0	0	0	0	1	0	0	0	0	0	0	0	0	0	0	0	0		
13	**Cartilage (Y/N)**		0	0	0	0	0	0	1	1	1	1	1	1	1	1	1	1	1	1		
14	**Vascular lacunae (Y/N)**		0	0	0	0	0	0	0	0	0	0	0	1	1	1	1	1	1	1		
15	**Nervous button (Y/N)**		0	0	0	0	0	0	0	0	1	1	1	1	1	1	1	1	1	1		
16	**Pathology (Y/N)**		0	0	0	0	0	1	1	0	0	0	0	0	0	0	0	0	0	0		
17	**Cellular infiltration (Y/N)**		0	0	1	1	1	1	1	0	0	0	0	0	0	0	1	1	1	1		
18																NF					TM	CC

	A	B	C	D	E	F	G	H	I	J	K	L	M	N	O	P	Q	R	S
1	**Sample block**	**RIGHT**	**1 - skin**	**2**	**3**	**4**	**5**	**6**	**7**	**8**	**9**	**10**	**11**	**12**	**13**	**14**	**15**	**Rx1**	**Rx2**
2	**# of single corpuscles**		MANY	10	10	A	10	13	12	9	10	A	16	A	9	7	11	26	
3	**# of corpuscle complexes**			2	1	A	7	5	0	4	1	A	3	A	1	3	0	3	
4	**average # cores per complex**			2	2	A	2.71	2.8		2.5	2	A	2.33	A	2	2		2	
5	**# of corpuscle cores in complexes**			4	2	A	19	14		10	2	A	7	A	2	6		6	
6	**Total number of corpuscle cores**			14	12	A	29	27	12	19	12	A	23	A	11	13	11	32	
7																			
8	**Artificial lumen**		1	1	1	0	0	0	0	0	0	0	0	0	0	0	0	0	0
9	**Melanin**		1	0	0	0	0	1	1	1	1	1	1	1	1	1	1	1	1
10	**Blubber**		1	1	1	1	1	0	0	0	0	0	0	0	0	0	0	0	0
11	**Glands (Y/N)**		0	0	1		1	1	0	0	0	0	0	0	0	0	0	0	0
12	**Muscle**		0	0	0	0	1	1	0	0	0	0	0	0	0	0	0	0	0
13	**Cartilage (Y/N)**		0	0	0	0	0	0	1	1	1	1	1	1	1	1	1	1	0
14	**Vascular lacunae (Y/N)**		0	0	0	0	0	0	1	1	1	1	1	1	1	1	1	1	1
15	**Nervous button (Y/N)**		0	0	0	0	0	0	0	0	1	A	1	A	1	1	1	1	1
16	**Pathology (Y/N)**		0	0	0	0	0	0	0	0	0	0	0	A	0	0	0	0	0
17	**Cellular infiltration (Y/N)**		0	0	1	0	0	0	0	0	1	A	1	A	1	1	1	0	0
18															NF	NF			

Figure 33. Two examples of the recorded data in a bottlenose (top) and striped dolphin (bottom) specimens with the individual analysis of the quantitive data for corpuscles and qualitative data for tissue regions per block.

We treated the ear canal as consisting of three different portions between the external opening and the tympanic membrane. From superficial to deep, there is the portion that travels through the blubber layer (BP). Then, there is what we called the 'soft tissue portion' (SP) that consists of only soft tissues and includes the glandular structures (although the latter could not be found in *bottlenose dolphin* nor Cuvier´s beaked whale). Finally, the 'cartilaginous portion' (CP) started from the most peripheral protrusion of the cartilage down to the start of the tympanic bone. In general, the cartilaginous portion made up about half of the total length in small toothed whales, and its size was not fully ascertainable in large toothed whales due to sampling bias (Table 9).

Table 9. The length of each part is expressed as a percentage of the overall length, calculated as the means of the # of individuals values. (* sampling was incomplete, so the CP is underrepresented)

SPECIES	EAM OVERALL LENGTH (CM)	BP (%)	SP (%)	CP (%)
S. coeruleoalba (#20)	4-5	19	25	56
T. truncatus (#2)	7	25	20	55
G. melas* (#1)	10	53	32	16
Z. cavirostris* (#2)	10	35	26	39

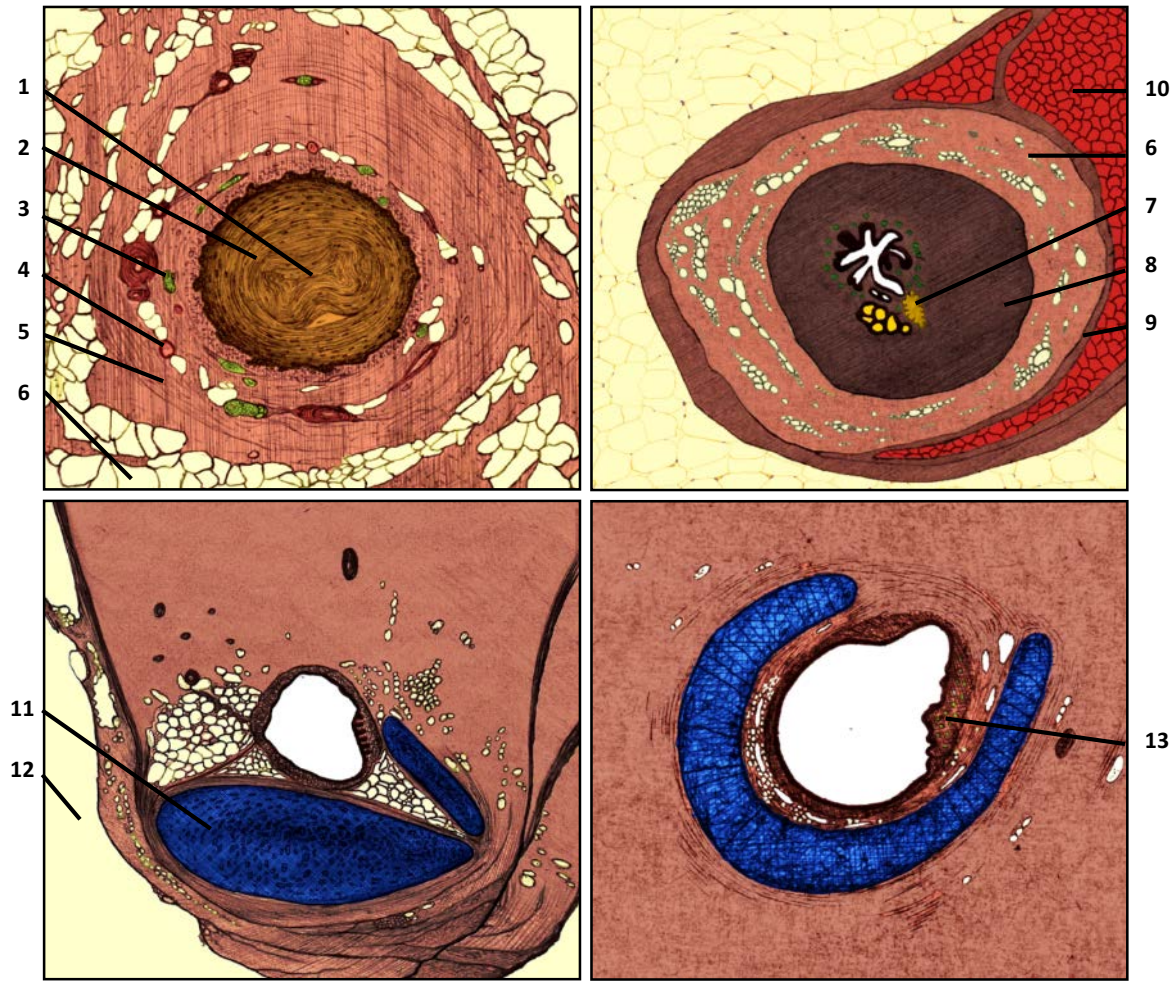

Figure 34. (From De Vreese et al., 2020b) Schemato-artistic drawings of transverse sections through the external ear canal in four distinct regions in a generalized toothed whale, made to demonstrate the configuration of the canal lumen and the surrounding the soft tissues.

A. Section through the ear canal immediately medial to the external ear opening. The lumen (1) is collapsed and there is only a minute or even no physical connection between the external environment and the deeper ear canal lumen. The epithelium (2) is consists of many layers at this level. The subepithelial tissue contains many nervous structures (3), including lamellar corpuscles and small nerves, and vascular structures (4). The connective tissue is infiltrated by fat cells and forms an adipoconnective tissue sheath (5), which separates the ear canal from the surrounding blubber layer (6).

B. Section through the ear canal at the level of the glands. There is a true lumen with a complex shape that is connected to the surrounding glandular structures (7), situated in the subepithelial tissue, together with nervous and vascular structures (similar to A). The connective tissue in the vicinity of the ear canal contains fewer fat cells (8). Surrounding this, although not always clearly distinguishable from the previous, there is the adipoconnective tissue sheath (6), which itself is surrounding by a fibro-elastic tissue capsule (9) in which striated muscles (10) insert.

C. Section through the ear canal medial to the ventral curvature. The lumen widens and is oval to round in shape. The epithelium consists of only a few layers, and the subepithelial tissue containing nervous and vascular structures is sparse and gradually concentrates on one side of the canal. The ear cartilage (11) appears and consists of a main body with several 'fingers' in various configurations. The adipoconnective tissue sheath consists of a large number of fat cells in the vicinity of the canal and dense connective tissue further peripheral. The entire structure is suspended from the skull dorsally and separated from acoustic fat (12) ventrally.

D. Section through the ear canal at the medial end before reaching the tympanic membrane. At this level the lumen is round and large, the epithelium is thin and so is the subepithelial tissue layer, except for the location of the nervous tissue ridge (13) (See Figure 3). The cartilage (10) is horseshoe-shaped and incompletely envelops the ear canal.

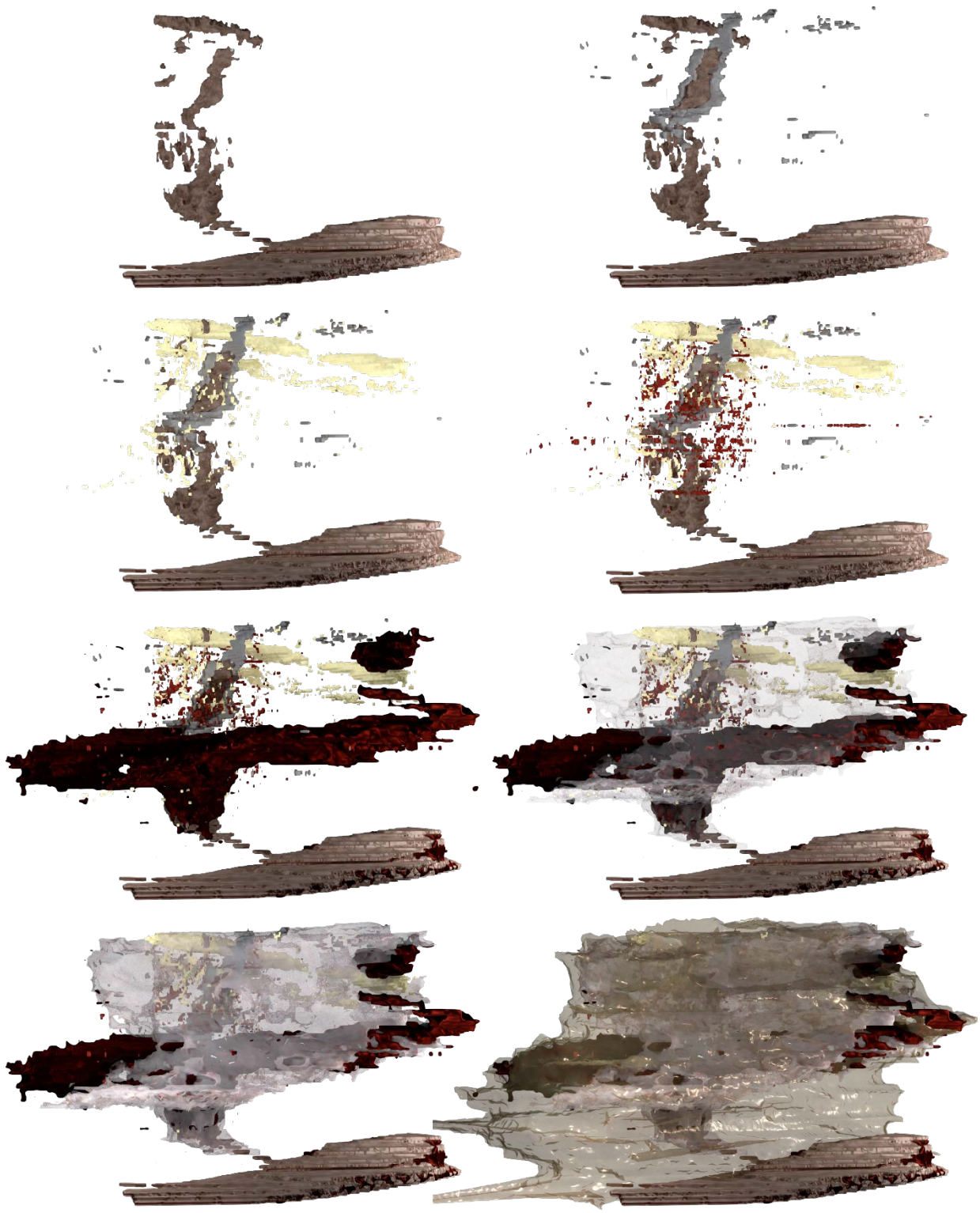

Figure 35. Images of a 3D rendering of a caudodorsal view of the right ear canal of a harbour porpoise (UT1727R). The bottom of each image is lateral, while the top is the medial end of the ear canal. Each image is the same as the previous with the addition of one type of tissue. 1: ear canal lumen and epithelium; 2: cartilage; 3: nervous tissue (most obvious is the facial nerve running ventral to the ear canal); 4: vascular tissue; 5: muscle tissue; 6: connective tissue (95% transparent); 7: connective tissue (50% transparent); 8: adipose tissue (70% transparent). See also a video (LINK).

2.1 External ear opening

The external ear opening was a funnel-shaped continuation of the skin that varied in diameter depending on the location of the measurement, although it always tapered down to an (almost) artificial lumen (Figure 36). In any case, it was always very small, with a value of 0.5 mm about halfway the funnel, and reduced even further to about 100-200 µm in adult striped dolphin and harbour porpoise (Figure 38). The shape was usually round, especially in fresh specimens, although varied in shape from round to oval and was usually a slit in dehydrated animals.

Histologically, we sometimes found erythrocytes unilateral inside the external ear opening (e.g. Figure 39), which was likely associated with the tissue manipulation during necropsy and could be considered an artefact, particularly because it was also noted in the ear opening of a striped dolphin foetus (Figure 40).

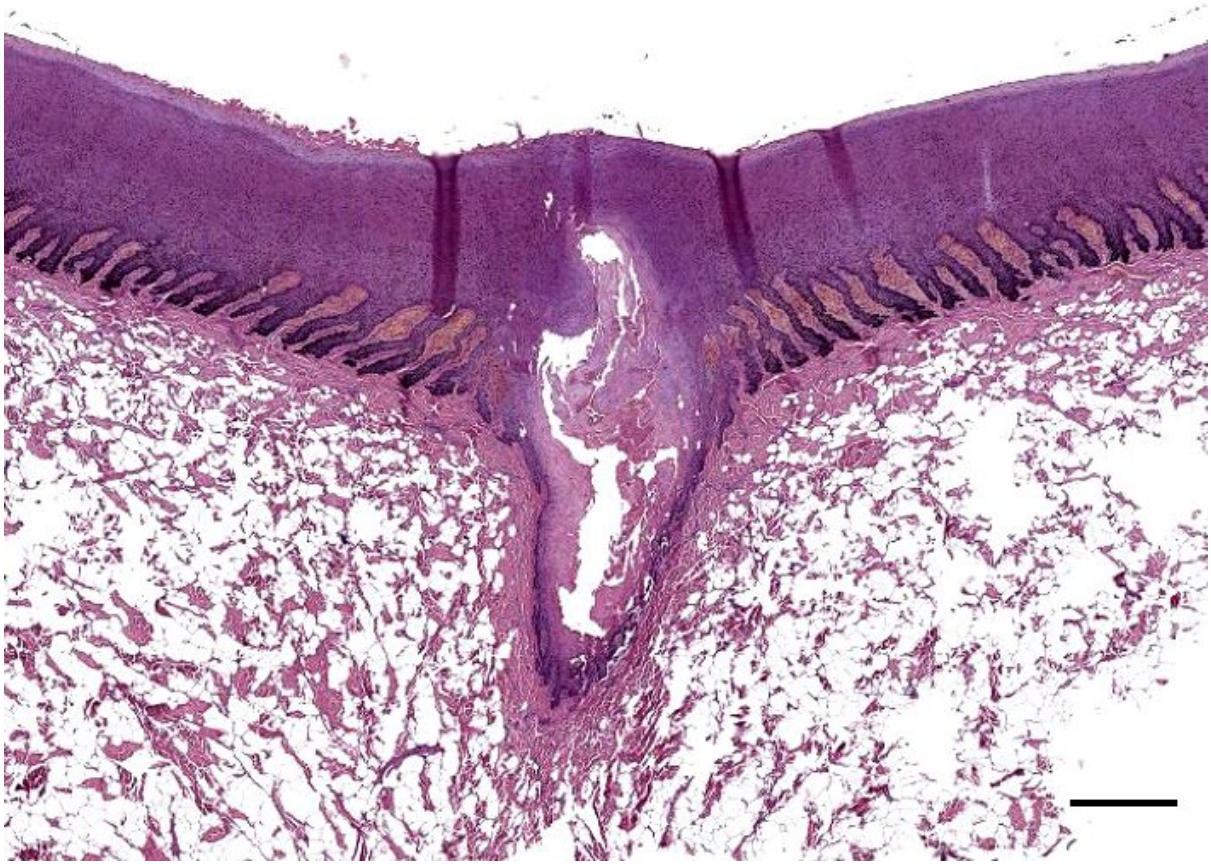

Figure 36. Histological image (HE stain) of a longitudinal section through the ear opening in a bottlenose dolphin (ID444_L1). Scale bar 500 µm

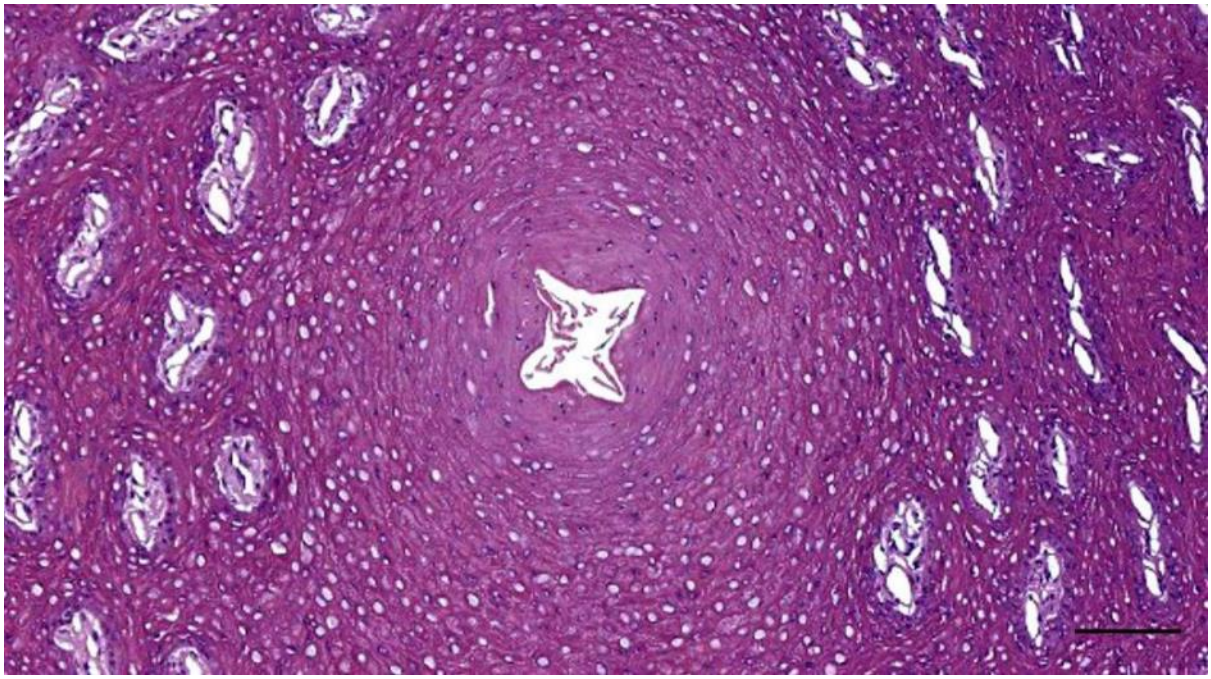

Figure 37. Histological image (HE stain) of the left external ear opening in the skin of a striped dolphin (ID5386). Scale bar 100 µm

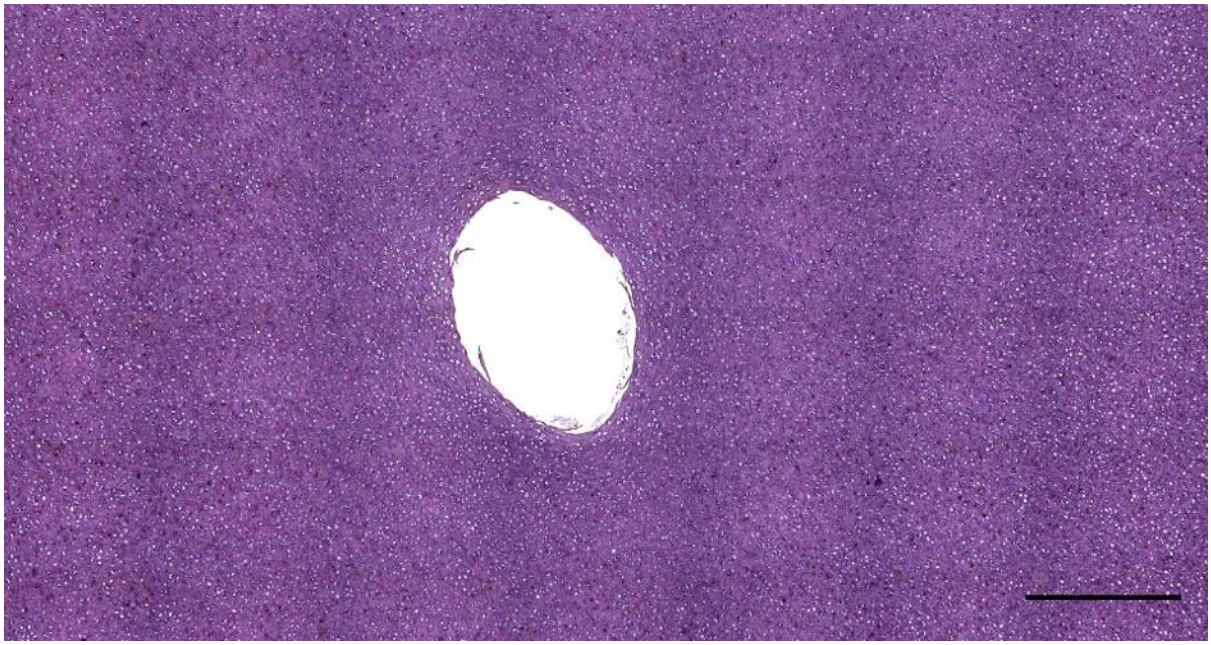

Figure 38. Histological image (HE) of a cross-section through the external ear opening of a harbour porpoise (UT1692_R0101). Scale bar 500 µm

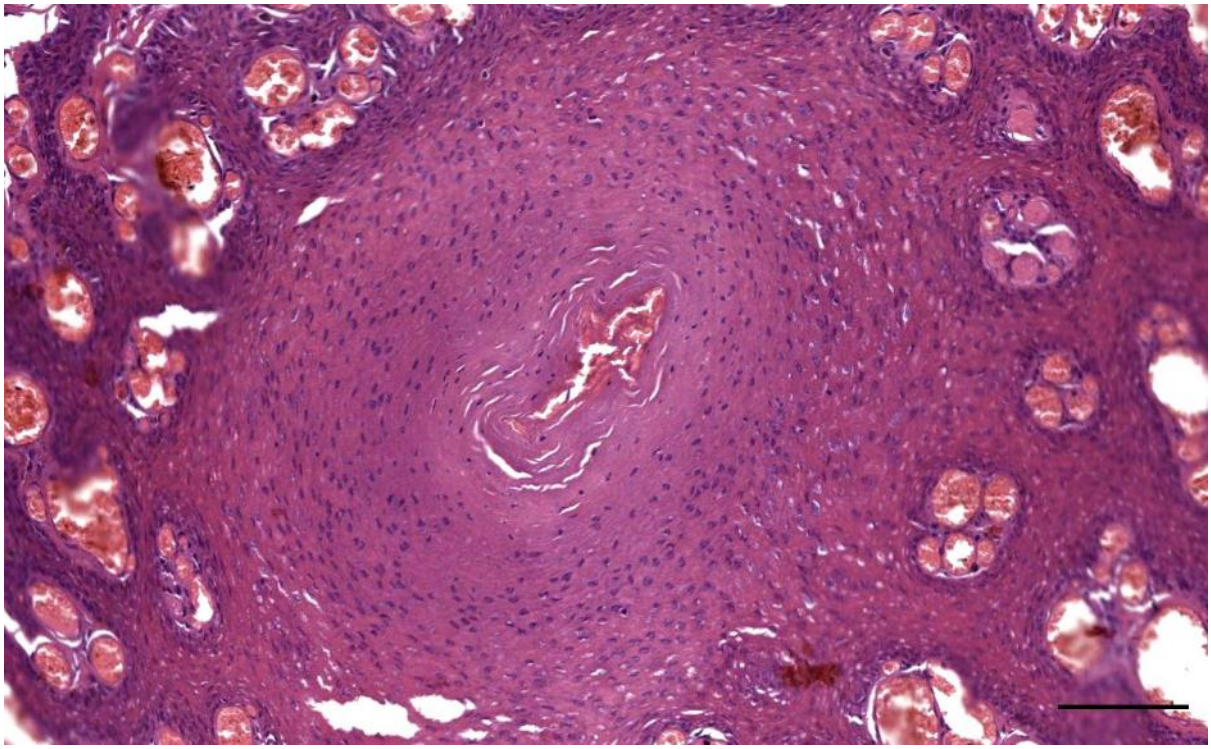

Figure 39. Histological transverse section of the external ear opening in a striped dolphin (ID274/18 Note the red blood cells in the lumen of the ear opening. Note the blood sinuses or enlarged vessels in the dermal papillae (likely associated with the active stranding event). Scale bar 100 µm.

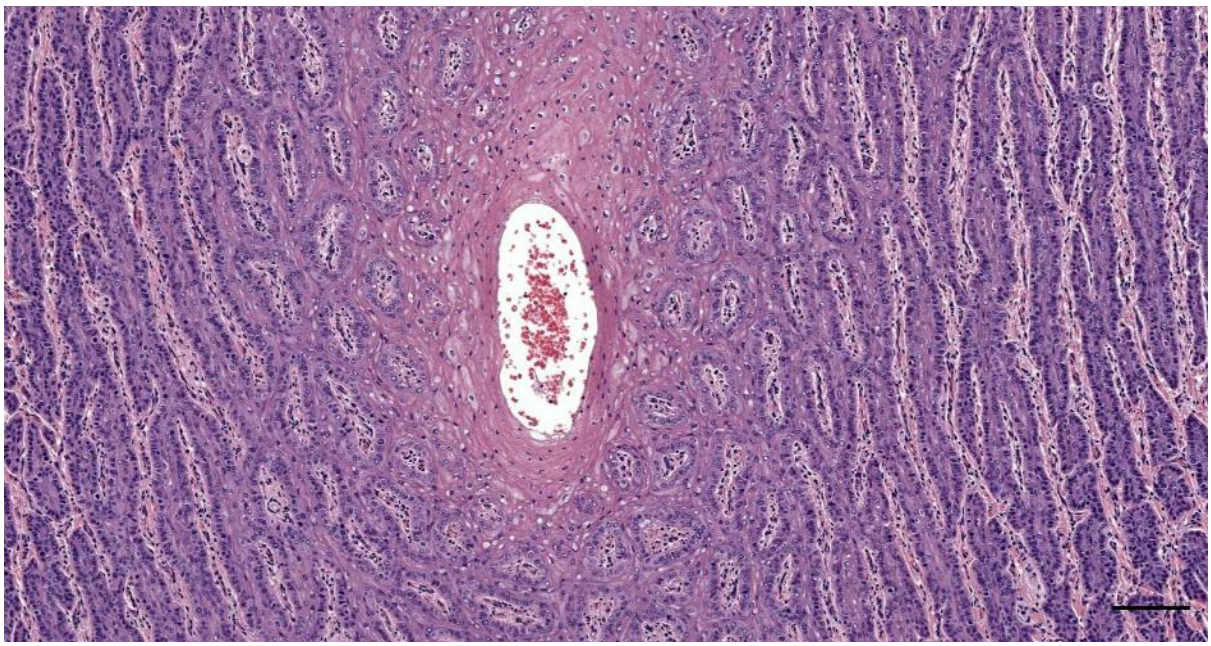

Figure 40. Histological transverse section of the external ear opening in a striped dolphin foetus. Note the red blood cells in the lumen. Scale bar 100 µm.

2.2 Lumen

Shape and content

The lumen of the ear canal changes in shape and size over its course from the external ear opening to the blind end at the tympanic membrane. A generalized model for the lumen morphology from lateral to medial could be described as follows: 1. very small to artificial at the medial end of the external ear opening. 2. round and filled with content lateral to the location of the glands. 3. complex star-shaped with large epithelial folds at the level of the glands. 4. Elliptical to round in the ear canal´s ventral curvature. 5. Round and small at the base of the ventral curvature. 6. Round to elliptical and gradually increasing in size before reaching the middle ear. See Figure 41 for a visualization of a typical progression in striped dolphin.

The same configuration was confirmed in other species, although with variation in size and shape.

- In both Cuvier´s beaked whale specimens, the lumen varied in shape over the course from round/oval, to a simple triangle at the level where we would expect glands in other species (See chapter Glands)(Figure 42), to semilunar in deeper sections (Figure 43), and complex with small excavations lateral to the appearance of the cartilage at least in one of the two specimens (Figure 44). The content of the canal consisted solely of desquamated epithelial cells with an occasional nucleus and also some melanin. We did not observe any glandular cells inside the ear canal as noted in other species.
- In harbour porpoise, the shape varied from round to oval to spindle-shaped in sections taken parallel to the skin (Following Boenninghaus, 1903). The content was similar to delphinids, with desquamated epithelial cells, seemingly glandular content and glandular cells.

The lumen was continuous in most specimens, but presented an almost complete closure or obstruction in the superficial transverse sections of the EAM, seemingly shrunken and filled with cellular debris at the same time. The lumen was filled with epithelial cells that do not seem to be desquamated as they form a continuation with the epithelial stratum superficiale, although there are cracks, which indicate a desquamation process with less strong bonds (desmosomes) between cells. We labelled this as an ‘artificial lumen´, or a ´virtual space´, as the lumen was not present in histological slides from post-mortem samples, but might have been present under different (natural, physiological) conditions (Figure 45, Figure 47, Figure 46, Figure 48)(See Discussion). There was a lot of variation in the configuration of the lumen and its content at this level of transverse sections. In some cases, there was never a full closure, but rather a minute lumen (few microns) (Figure 49, Figure 50). In other cases the lumen was filled with cellular debris, desquamated or not fully desquamated epithelial cells, together with glandular secrete coming from glands situated more medial and also glandular cells with (pyknotic) nuclei (see chapter Glands)(Figure 51, Figure 52, Figure 53). The nuclei

of the epithelial cells are normal in the stratum spinosum (although with slight shrinkage and perinuclear vacuoles), while flattened and hyperchromatic in the stratum superficiale and the centre of the canal (Figure 54)(parakeratosis). In deeper sections, there was a clear difference between the stratum superficiale and the ´more conventional´ intraluminal desquamated cells (Figure 55), which was also noted in the beaked whale (Figure 56).

In other specimens, the lumen was absent due to what seemed like a compression of the surrounding tissue (Figure 57). In other cases, the situation was not so obvious due to the presence of artefacts of the preparation, such as in the epithelium (Figure 58), similar to the situation found in a long-finned pilot whale specimen (Figure 60). The artificial lumen was located lateral to the location of the glands, and sometimes also overlapping spatially, as observed both in striped and common dolphin (Figure 49, Figure 61). However, in most specimens, the lumen was artificial or almost entirely absent lateral to the glands, and opened up together with the appearance of glandular structures (e.g. Figure 62). The same counted for harbour porpoise, there was often an ´artificial lumen´ in the superficial sections through the ear canal, between the external ear opening and the glands (Figure 45). The common dolphin also presented an artificial lumen in superficial sections (Figure 63), while the other side was continuous.

At the medial side of the glands, the ear canal took its ventral turn, the lumen is continuous, small and round, and from the base of the curvature continues in trumpet shape that gets gradually wider towards until reaching the tympanic membrane in a club-like expansion (See 2.10).

In striped dolphin, the diameter was about 0.3 to 0.7 mm in superficial sections and gradually increased in deeper sections to maximum dimensions of 0.7 x 2.2 mm.

The luminal content observed, besides the occasional presence of red blood cells which were considered artefacts, consisted of desquamated epithelial cells, both intact and as undiscernible debris and granular content, (eosinophilic) glandular content and glandular cells (Figure 64). This was seen mainly in sections from the surface to few millimetres medial to the blubber layer, where it partially to fully filled the ear canal lumen. In a specimen of bottlenose dolphin, there was exogenous content present in superficial sections through the ear canal (Figure 65)(possibly an artefact of the tissue preparation).

In deeper sections, the lumen was present and gradually increasing in diameter towards the middle ear. In the dolphins, the lumen contained, or was filled with, a combination of epithelial cells, glandular cells, and homogenous (glandular) content in the lateral third of the canal. In deeper sections, the lumen was empty except for sparse desquamated epithelial cells.

In Cuvier´s beaked whale, the ear canal contained epithelial cells in the superficial sections. It was unclear whether there might also have been a component of a glandular product together with the

desquamated epithelial cells, while we also did not note any glandular structures in the investigated sections (although these could have been missed)(Figure 66).

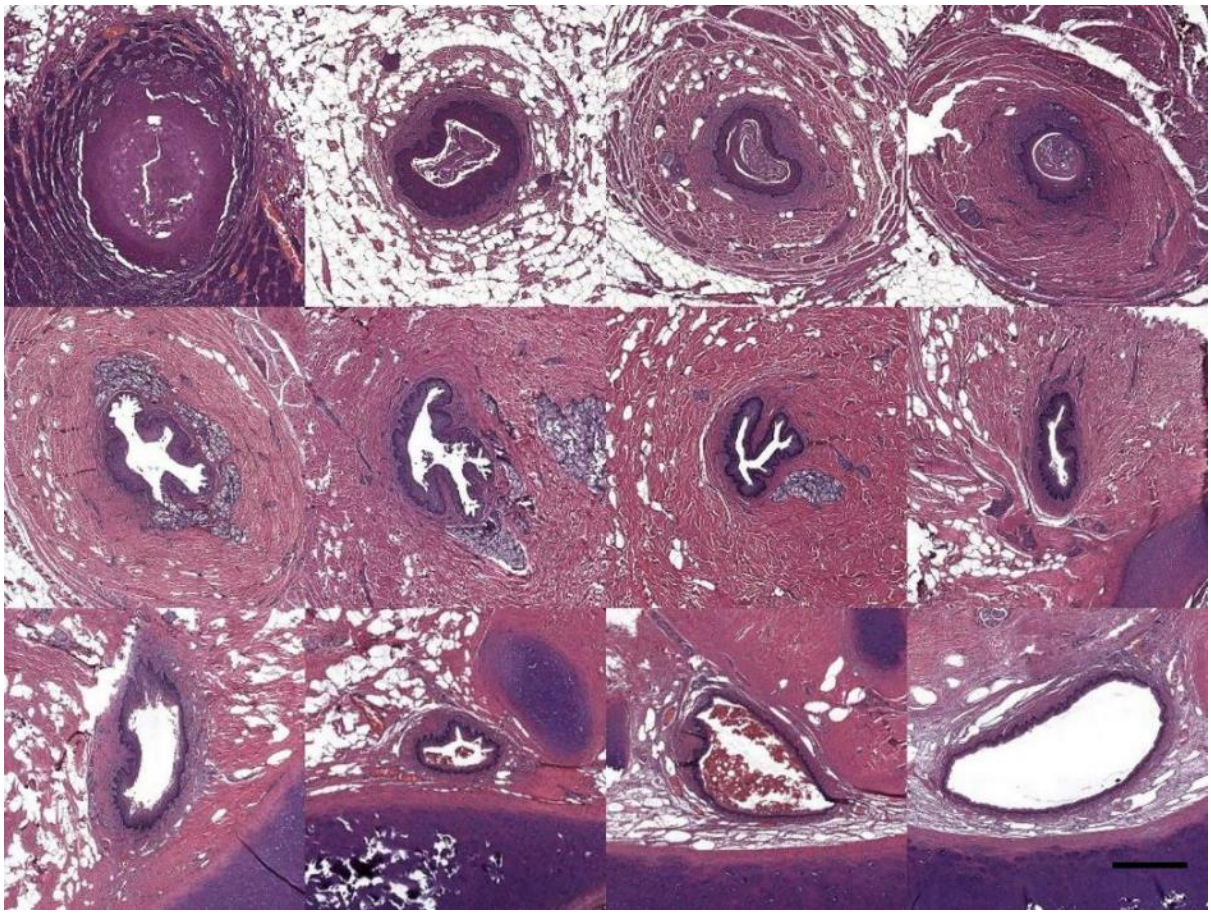

Figure 41. Montage of HE-stained cross-sections through the external ear canal of a striped dolphin. From top left to bottom right, the intersectional distance is about 4 mm. The medial end is missing, but the configuration can be seen in other figures. A: Section through the external ear ´opening´ and dermal papillae, with a lumen that is filled with desquamated epithelial cells. Note the highly vascularized sections through dermal papillae, and the epithelium of the skin. B-C-D: Ear canal filled with desquamated cells and glandular product, embedded in an adipoconnective tissue sheath. Immediately medial to the external ear opening, there is very little connective tissue surrounding the ear canal, and this gradually increases in size and over a distance of about 0.5 cm. E-F-G: external ear canal with glandular structures. H: the appearance of the cartilage; I: ventral curvature of the canal; J: the ear canal turns back horizontal and is supported from ventral by the cartilage body; K-L: the lumen gradually increases in size, and becomes rounder with less epithelial indents; In deeper sections, the cartilage changes shape and the ´nervous tissue ridge´ appears. Scale bar 0.5 mm

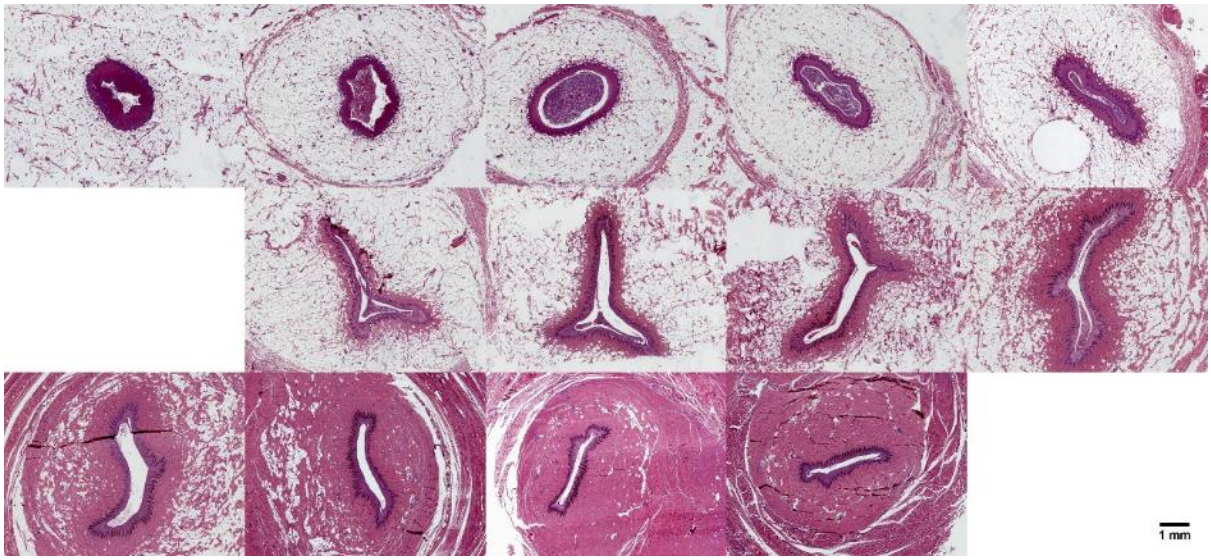

Figure 42. Sequence of histological transverse sections through the ear canal of a Cuvier´s beaked whale (ID429). The sixth image is blank because of very bad tissue quality, and the final field is blank because the sampling was only done down to this level. Scale bar 1 mm

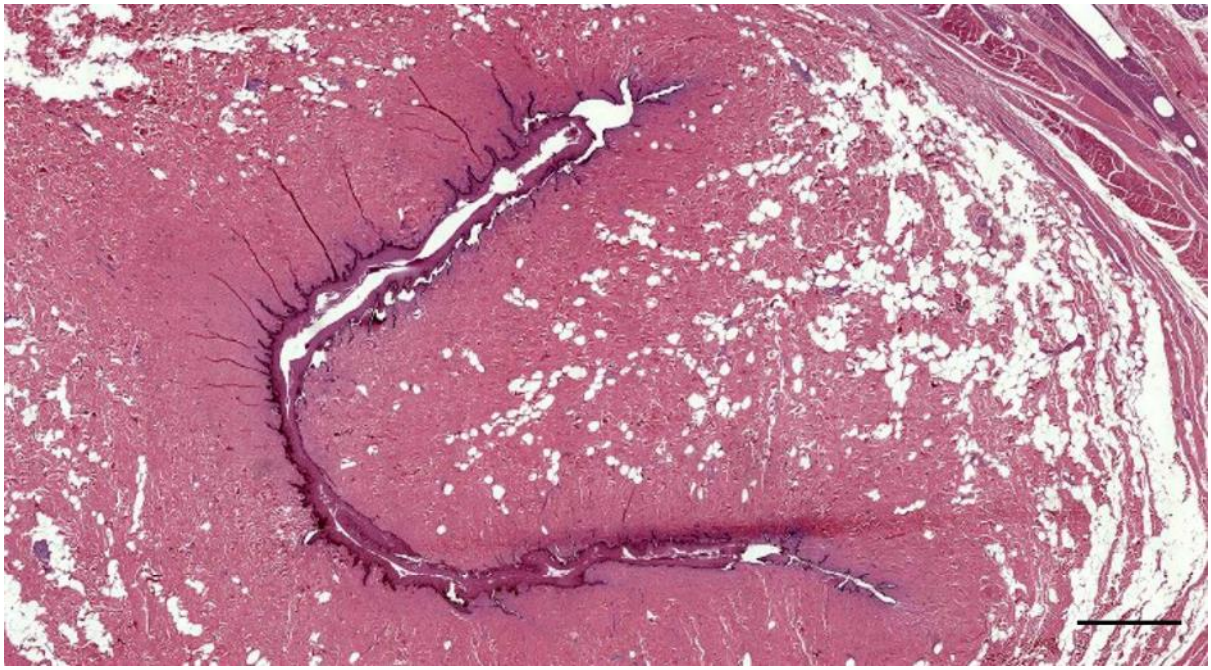

Figure 43. Histological transverse section through the external ear canal of a Cuvier´s beaked whale about 6 cm beneath the ski (177/19). Scale bar 100 µm.

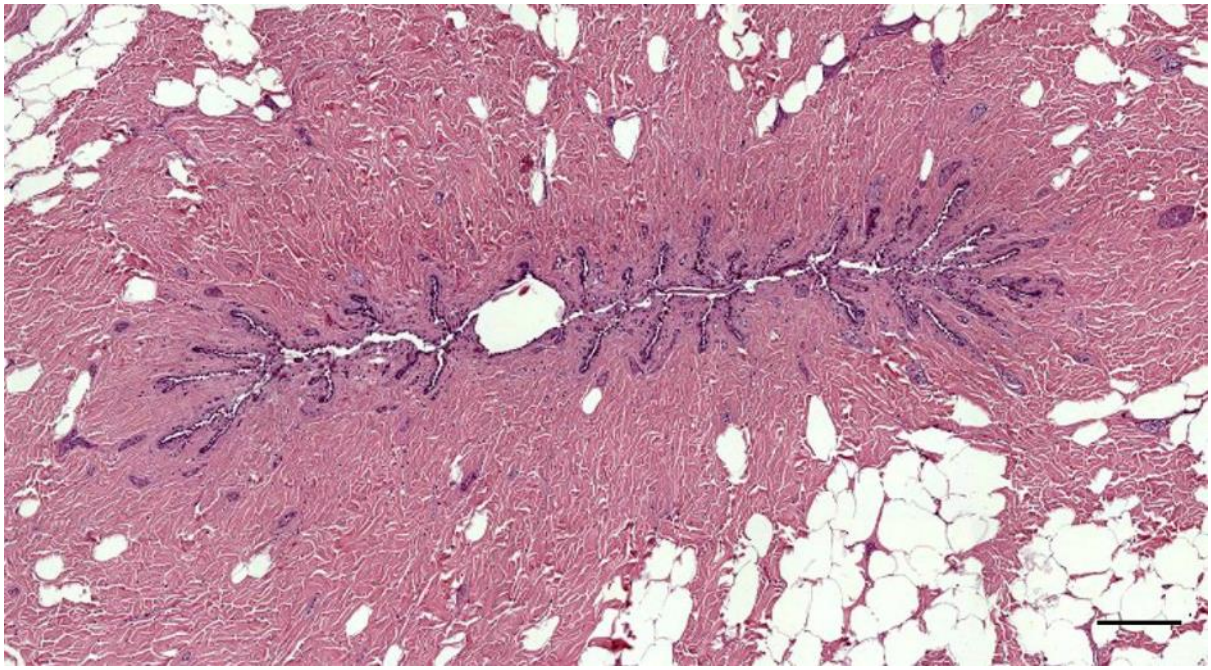

Figure 44. Histological transverse section through the external ear canal of a Cuvier´s beaked whale about 7 cm beneath the ski (177/19). Scale bar 200 µm.

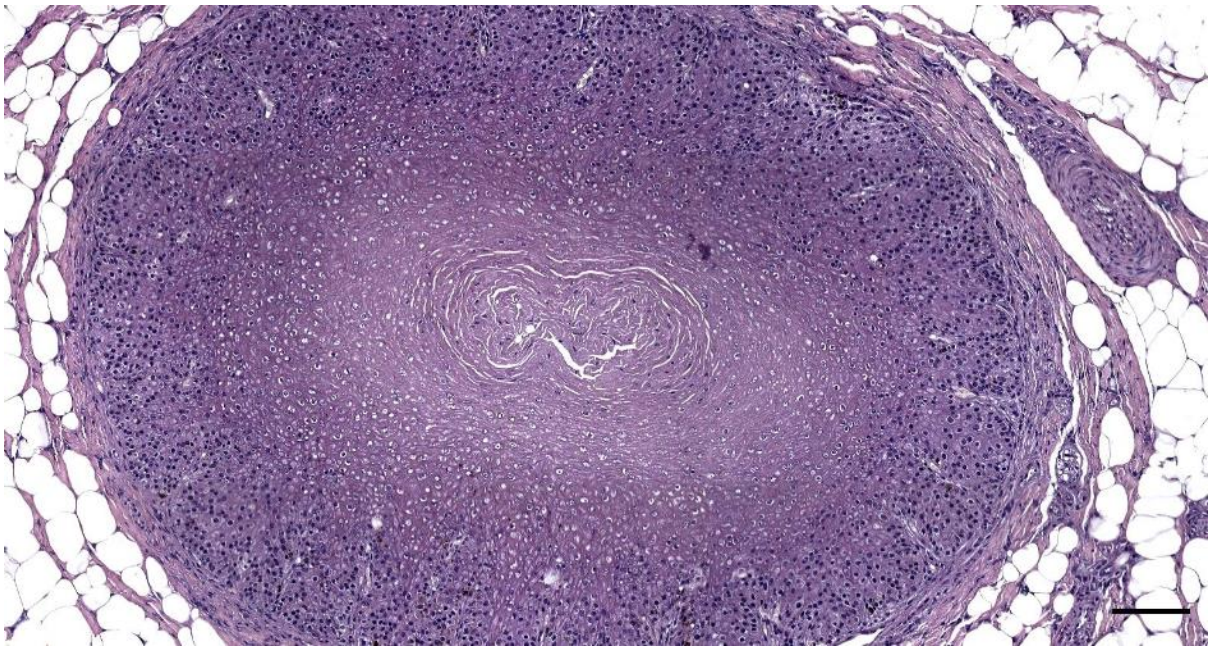

Figure 45. Histological image of a transverse section through the external ear canal of a harbour porpoise (UT1664). Scale bar 100 µm

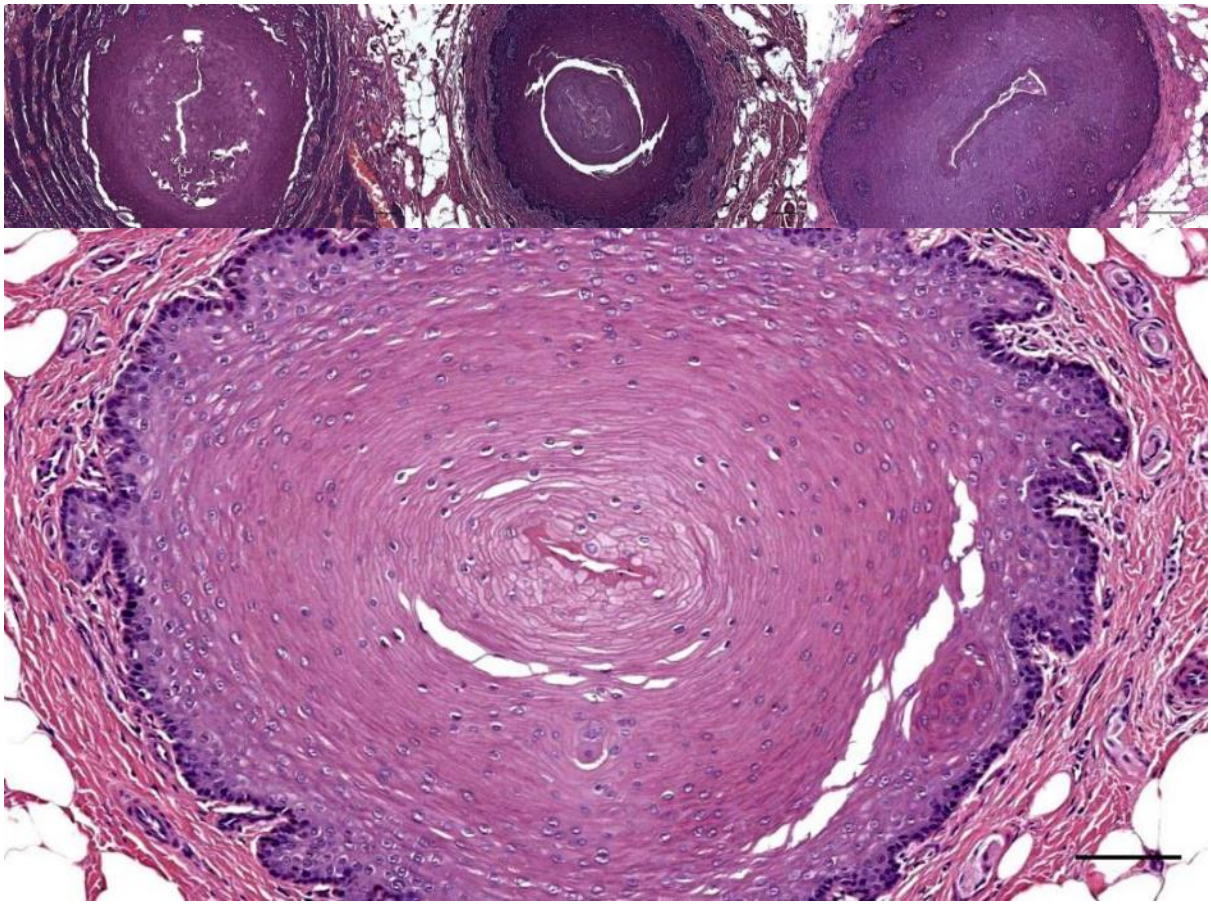

Figure 46. Four HE-stained cross-sections through the ear canals, close to the skin, in striped dolphin (about 0.5 cm beneath the skin), showing the variation in lumina and luminal content. Top Left: Lumen is filled with desquamated epithelial cells and likely glandular content. Middle: Same as left but with a much smaller lumen filled with desquamated cells, surrounded by epithelial layers (the empty space is the epithelial layer is likely an artefact). Right: small and longitudinal lumen with some desquamated epithelial cells; Bottom: Similar to top right, with a lumen of about 90 by 10 µm. Scale bars Top LTR: 100 µm, 100 µm, 200 µm; Bottom 100 µm

Figure 47. HE staining of a transverse section through the ear canal of a striped dolphin (ID488/17). Note the very small lumen. The spaces between the epithelial layers are artefacts due to tissue conservation and processing. Scale bar 100 µm.

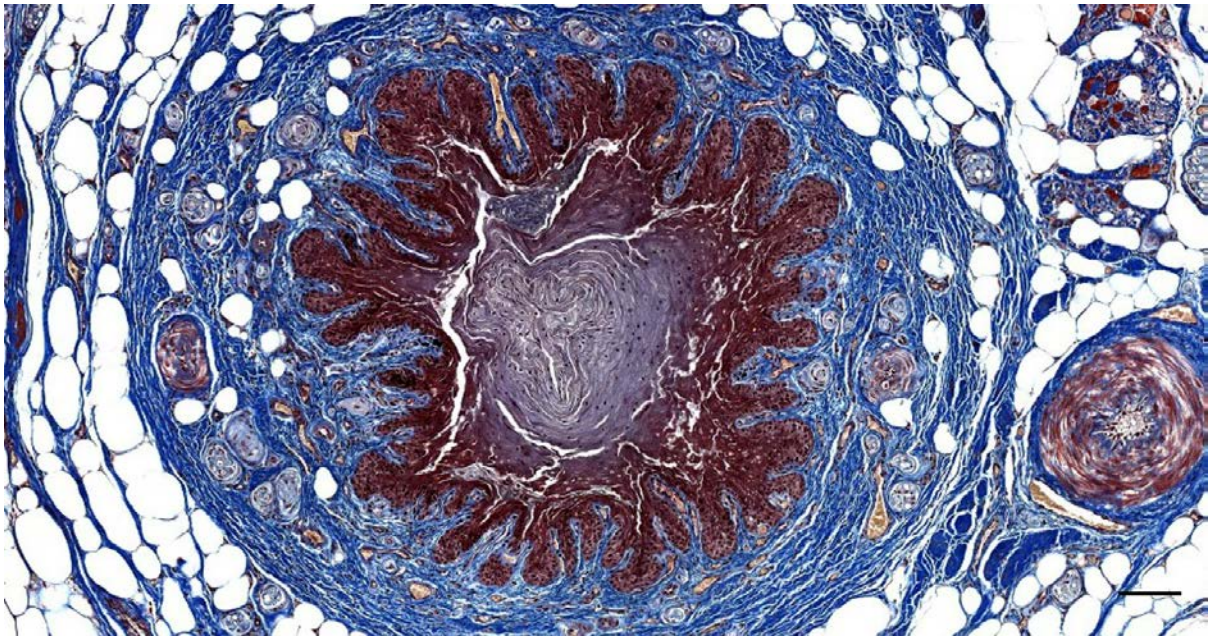

Figure 48. Histological image (Masson´s trichrome) of a transverse section through the external ear canal in a harbour porpoise, at about 1 cm beneath the skin (UT1711_R0401). Scale bar 100 µm

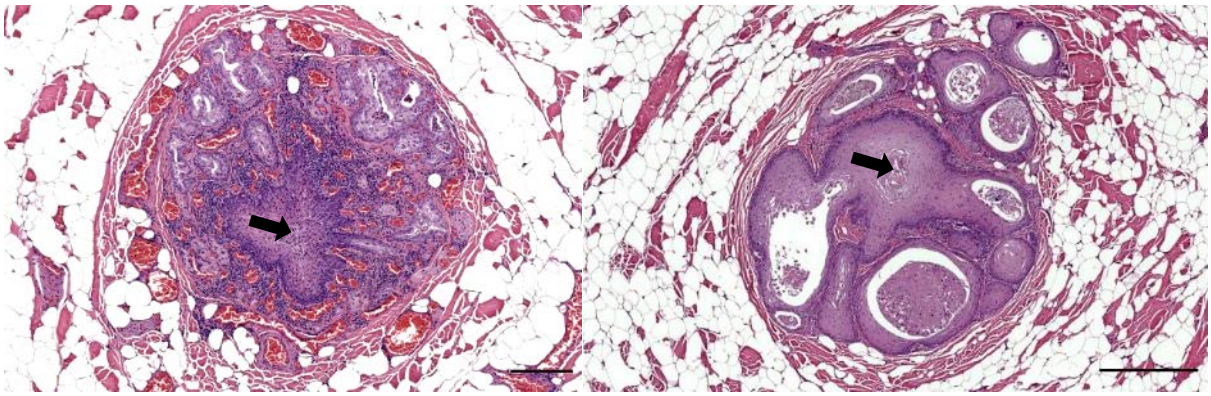

Figure 49. Two histological images (HE staining) of transverse sections through the ear canal of a striped dolphin (ID293/18)(left) and a common dolphin (ID169/17)(right) at the level of the glands. Note that in both cases, the ear canal itself present an artificial lumen (arrows). In the striped dolphin, there was also the presence of many mononuclear cells and a very intense vascularization in the subepithelial tissue, indicating a pathological condition. Scale bar 0.2 mm

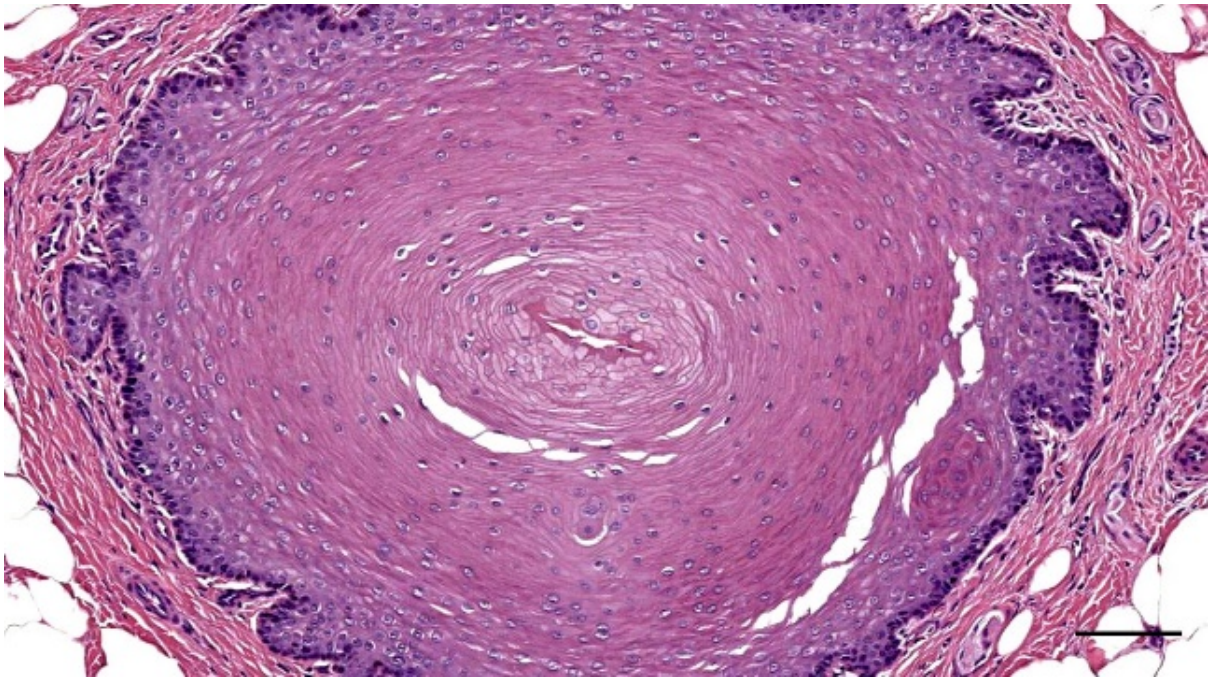

Figure 50. Histological transverse section through the ear canal of a striped dolphin at about 1 cm beneath the skin (ID168/17). Note the very small lumen. Scale bar 100 µm

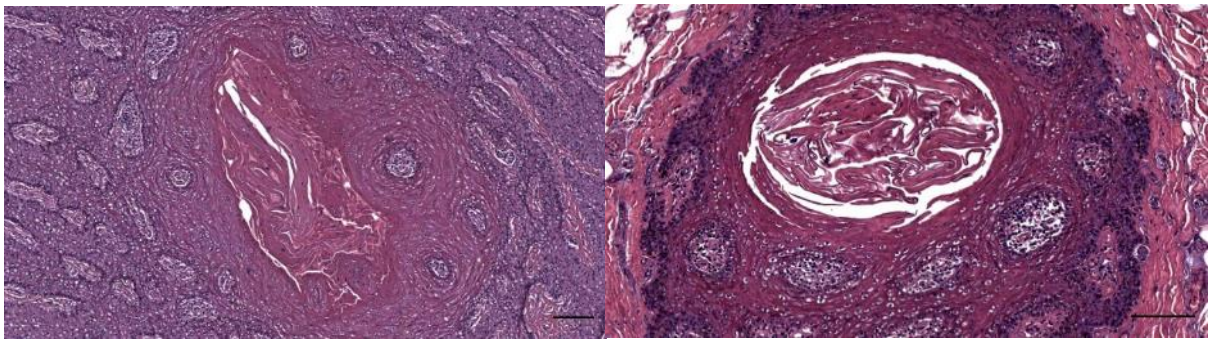

Figure 51. Two histological detail section of the ear canal lumen at the medial end of the funnel-shaped ear opening, on the transition between ear opening and ear canal, in a striped dolphin (ID362/18). The lumen is (almost) filled with desquamated epithelial layers with sparse nuclei. It is unsure to what extent the epithelial cracks are artefacts or not. Scale bars 100 µm.

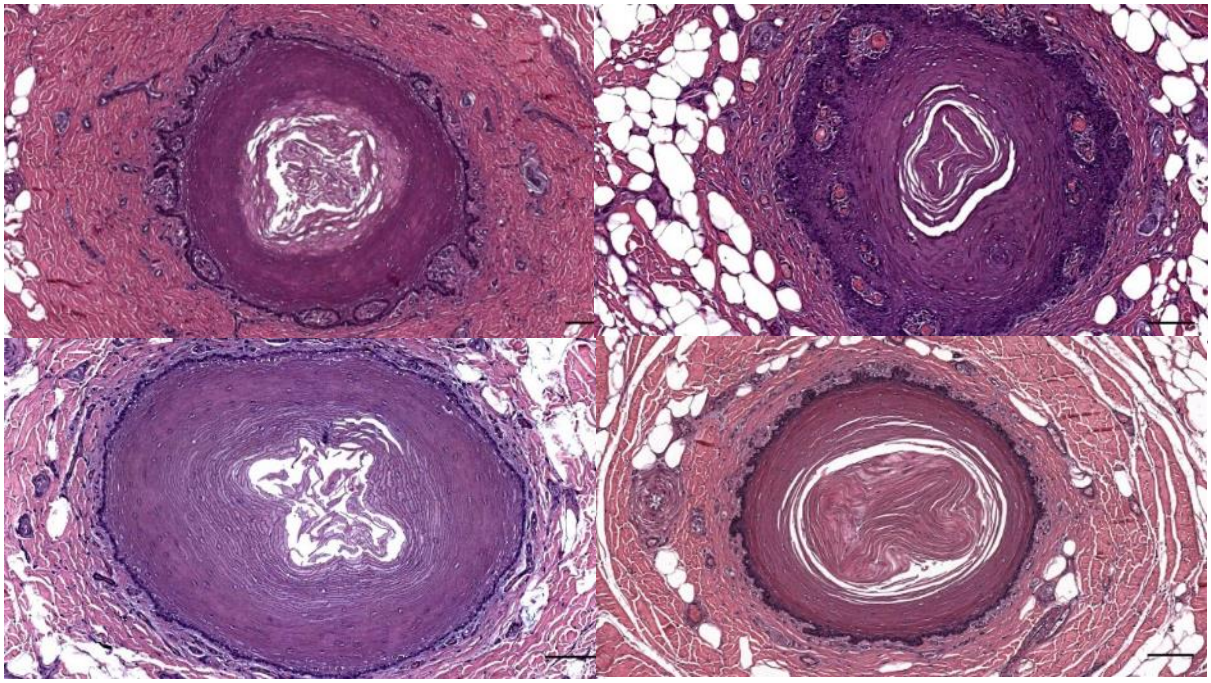

Figure 52. Histological transverse sections () through the ear canal of four striped dolphins, at about 1-2 cm beneath the skin. Scale bar 100 µm. (ID´s 457; 509/17; 620/17; 362/18)

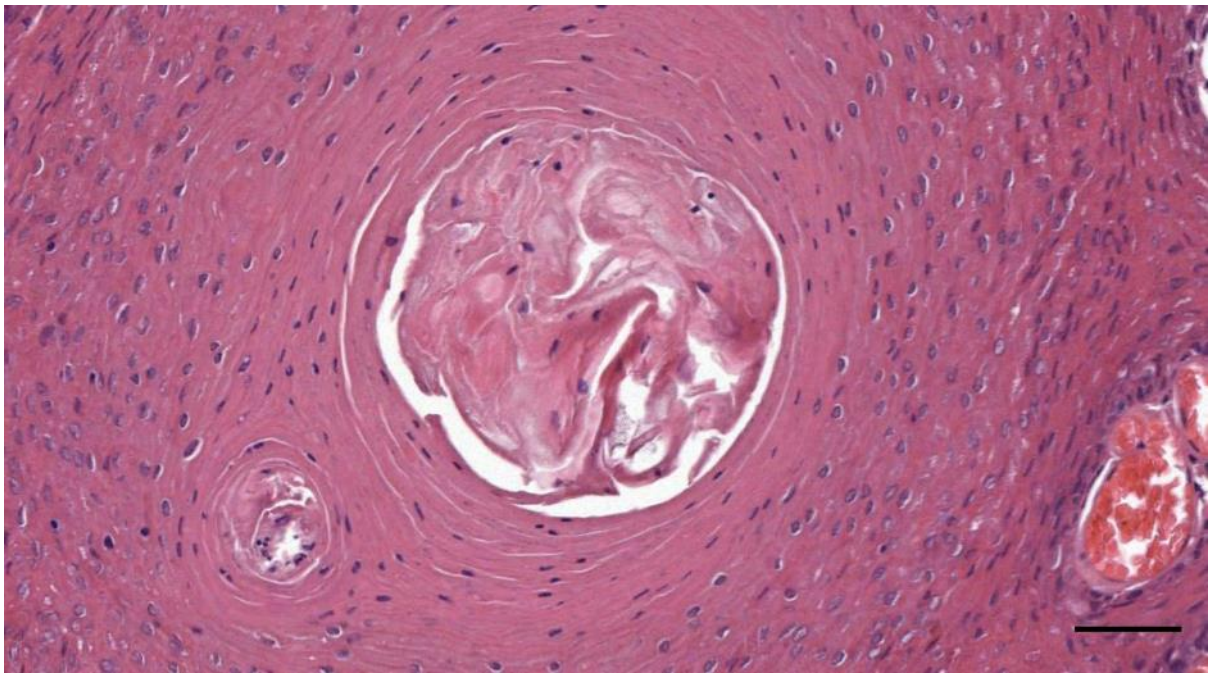

Figure 53. Histological transverse section through the ear canal of a striped dolphin at about 1 cm beneath the skin (ID274/18). The lumen is filled with an incompletely desquamated layer of epithelial cells. Scale bar 100 µm

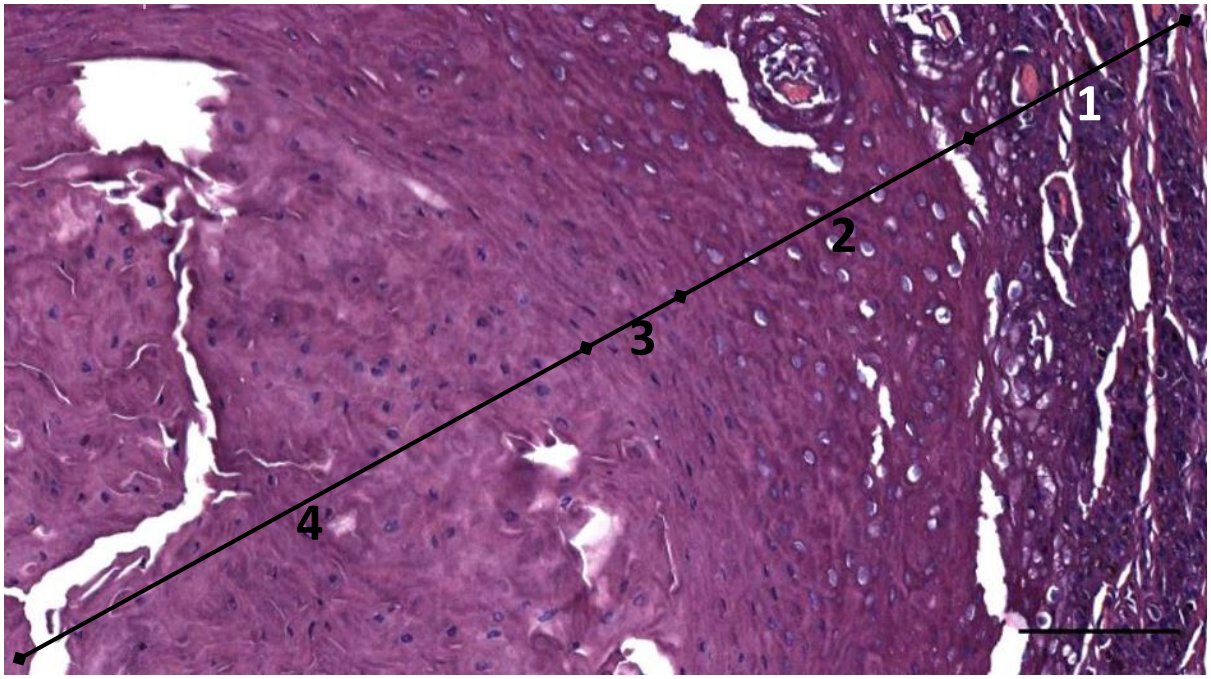

Figure 54. Histological detail image of the ear canal of a striped dolphin (44/17_L1) with an artificial lumen. HE-stain. 1: dermal papillae and stratum basal; 2: str. Spinosum; 3: stratum superficial; 4: ´desquamated´ cells as a continuation of 3. Scale bar 100 µm

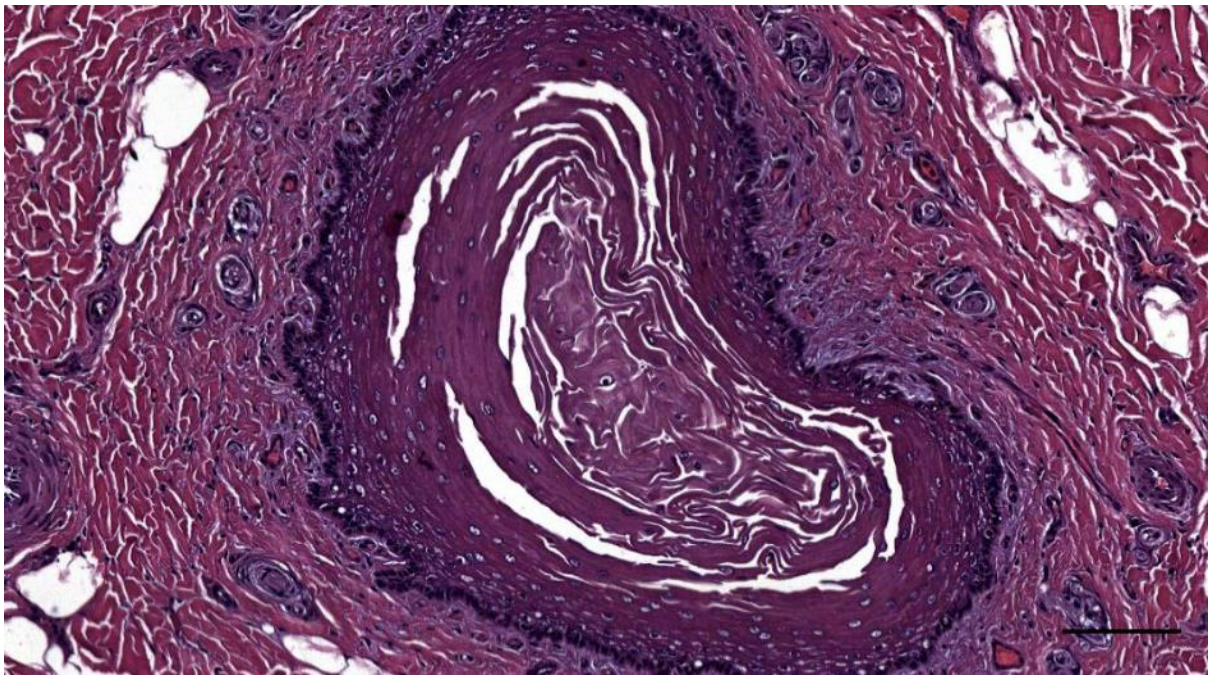

Figure 55. (44/17_L3, HE) Ear canal with intraluminal desquamated nucleated epithelial cells, with many blood vessels and lamellar corpuscles in the superficial propria. Scale bar 100 µm

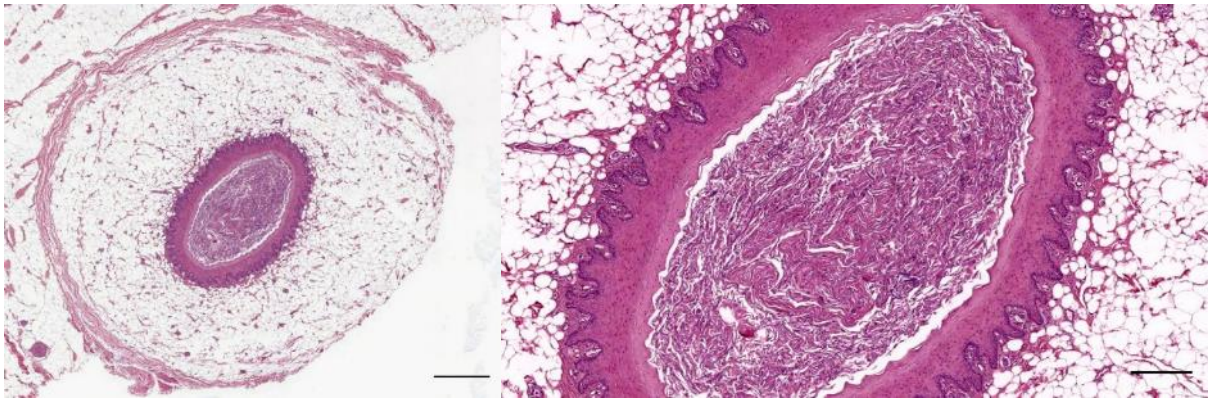

Figure 56. Two magnifications of a transverse histological section of the external ear canal in a Cuvier´s beaked whale (ID429) about 3 cm beneath the skin. The ear canal embedded in adipoconnective tissue surrounded by a tunnelled connective tissue capsule lumen is almost filled with desquamated epithelial cells and possible glandular product. Scale bar 1 mm left, and 0.5 mm right

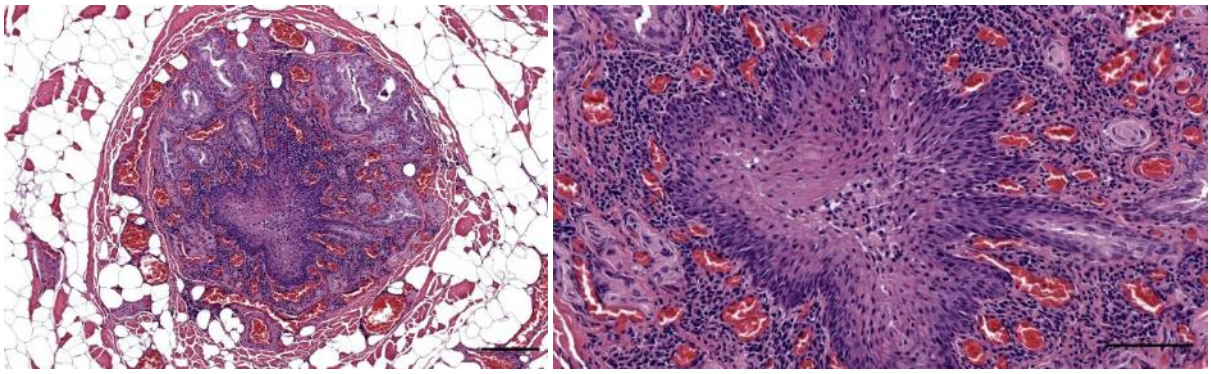

Figure 57. Two magnifications of a transverse histological section through the ear canal and associated glands at about 1cm beneath the skin in a striped dolphin (ID293/18). The lumen is absent due to a combination of a seeming compression of the ear canal walls and the presence of epithelial or and/or glandular cells at the location where we would expect a lumen to be present. Also note the subepithelial presence of an extraordinary amount of mononuclear cells, intense blood accumulation in the venules, and the presence of simple lamellar corpuscles.

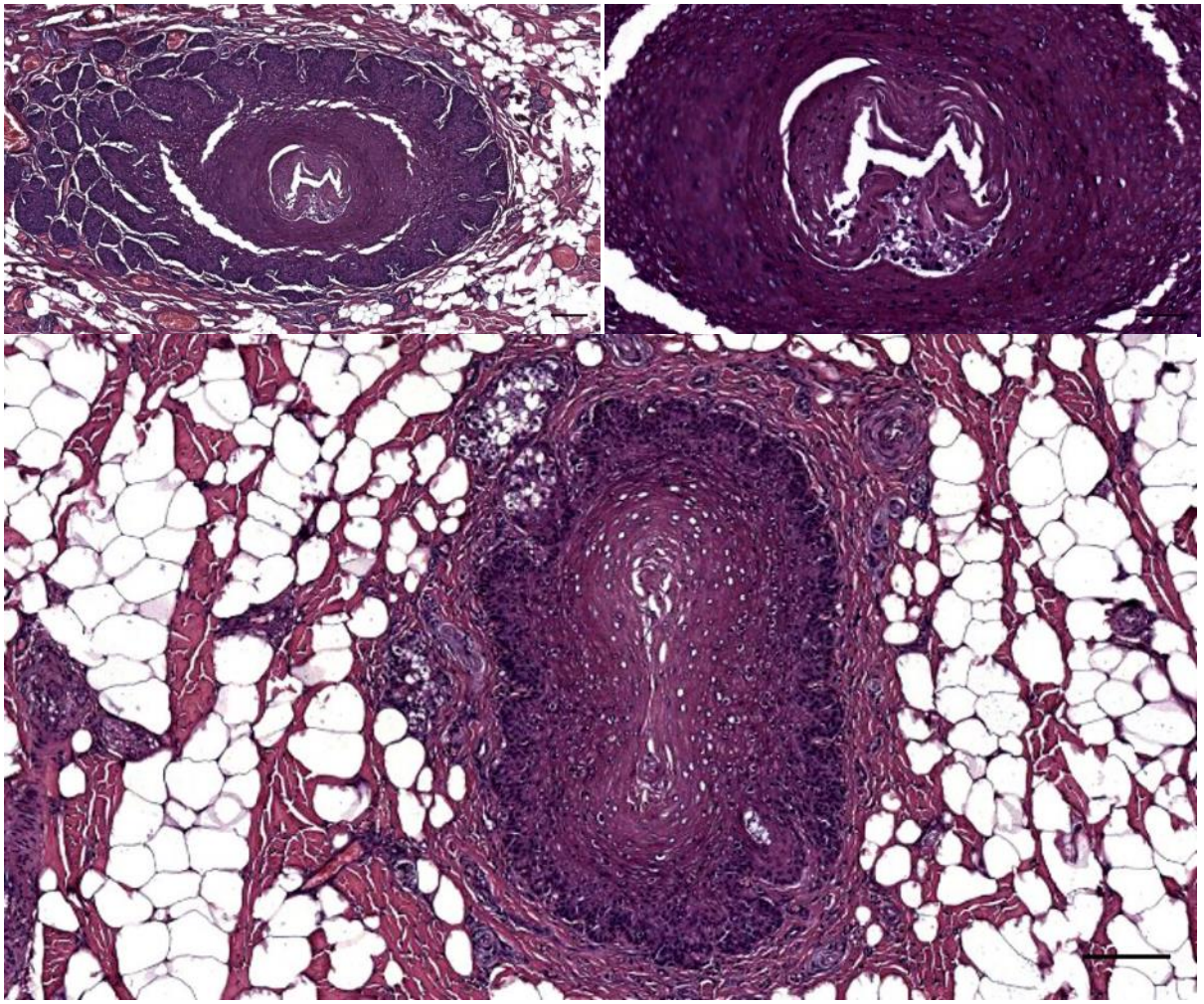

Figure 58. Top: Top: two histological transverse sections through the ear canal of a striped dolphin (ID449) at the medial end of the external ear opening (top), and about 1 cm beneath the skin (bottom). Top right is a detail of the top left image. Scale bars 500 µm top left, 100 µm top right and bottom.

Figure 59. HE stained cross-section of the ear canal of a striped dolphin about 1 cm beneath the surface. The lumen is absent as space is wholly taken up with stratum superficiale of the epithelium. The white spaces are likely artefacts of the preparation, which disrupted the intercellular connections (Cfr. Figure 46 Top Middle). Beneath the epithelium, there is a loose connective tissue layer comprising lamellar corpuscles, and surrounding that there is a denser connective tissue layer containing fat cells, larger blood vessels, and nerves. Scale bar 100 µm

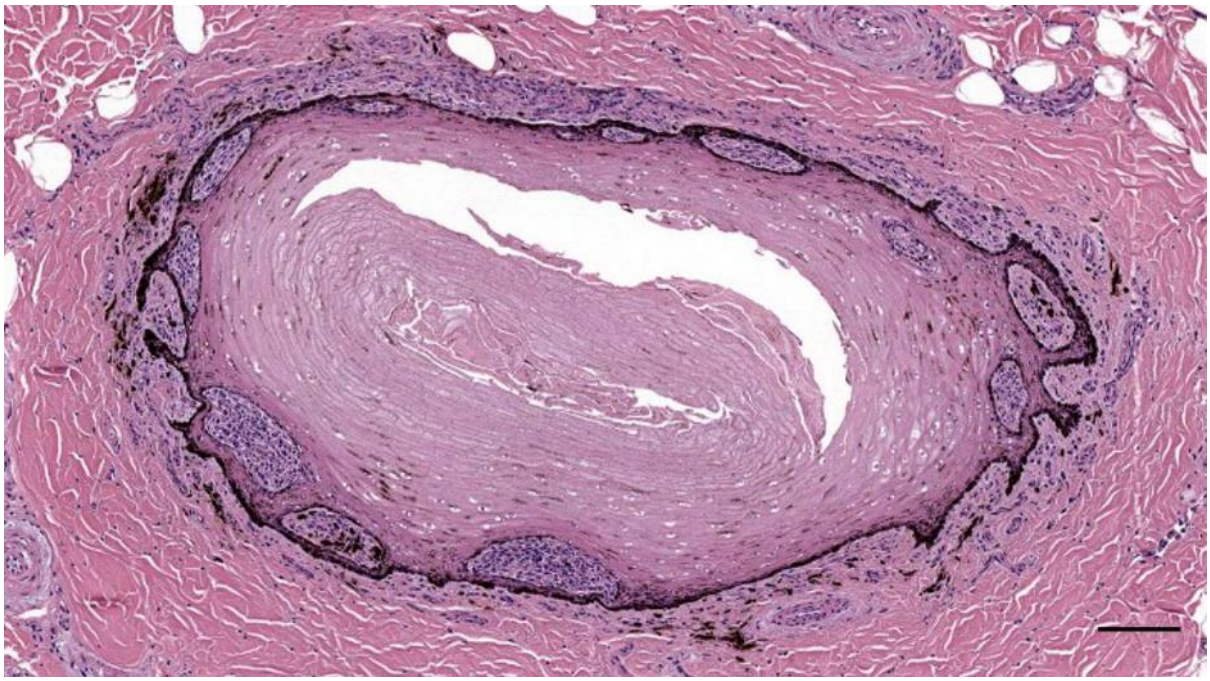

Figure 60. Histological cross-section (HE staining) of the left ear canal with subepithelial mononuclear cells (lymphocytes, plasmacells, macrophages) in a long-finned pilot whale (441_L4). Scale bar 300 µm

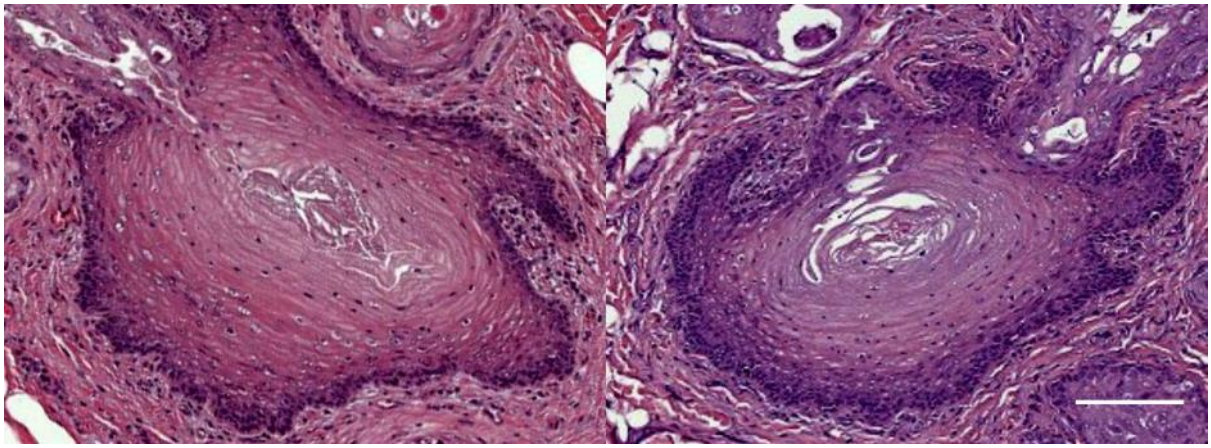

Figure 61. Histological transverse sections through the left and right ear canal of a striped dolphin (ID274/18) at about 1 cm beneath the skin. Both sides present an artificial lumen at the level of the glandular excretory ducts. Scale bar 100 µm

Figure 62. Histological transverse section (HE staining) through the ear canal of a striped dolphin (Sc1) at about 1.5 cm beneath the skin. The lumen is star-shaped, and the surrounding contain glandular unit, both secretory acini and excretory ducts. Scale bar 100 µm

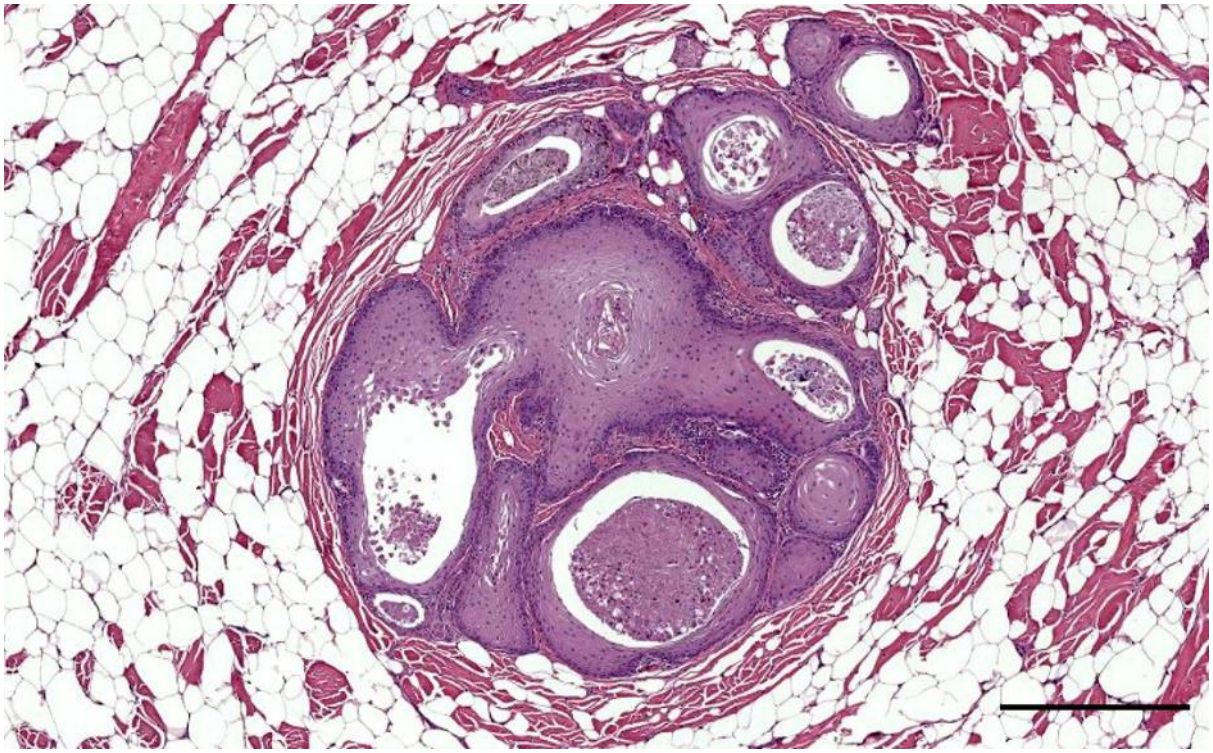

Figure 63. Histological image (HE staining) of a transverse section through the right ear canal of a common dolphin at about 1 cm beneath the skin (169/17_R2). The ear canal with artificial lumen (centre of image) is surrounded by glandular structures with fresh and degenerated glandular cells and lipid content. Scale bar 200 µm

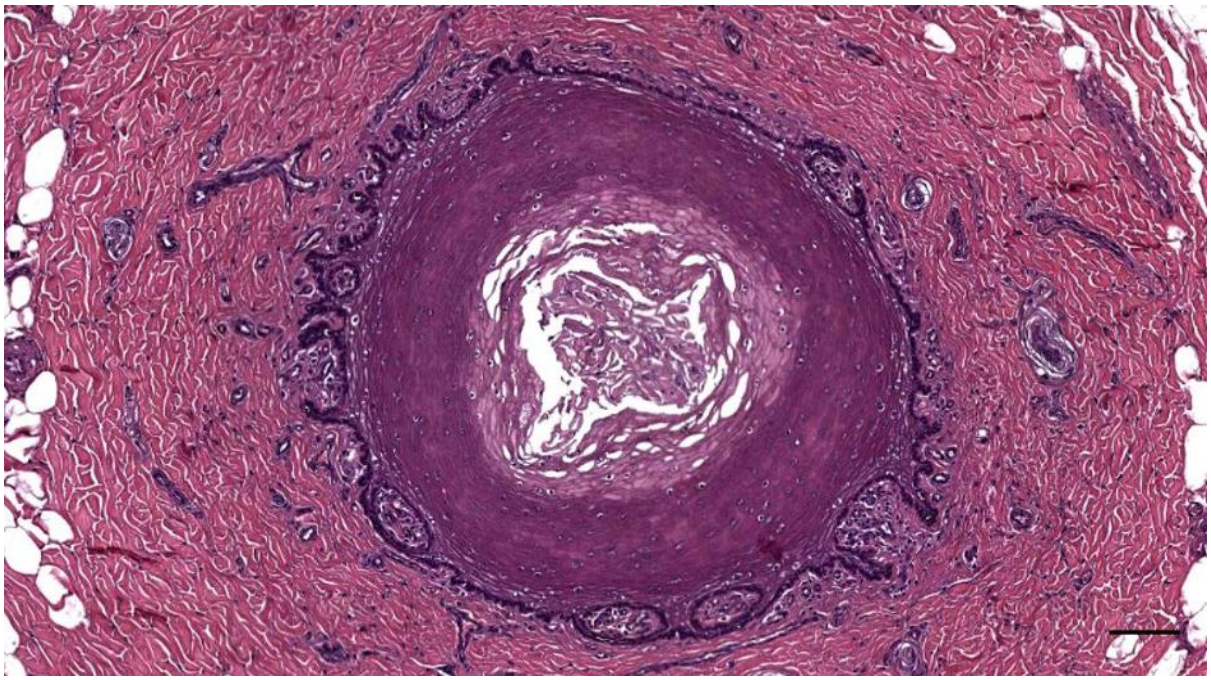

Figure 64. HE-stained cross-section of the right ear canal in a bottlenose dolphin, about 1 cm beneath the skin (457_R3). The lumen contains desquamated and layered epithelial cells. Scale bar 100 µm

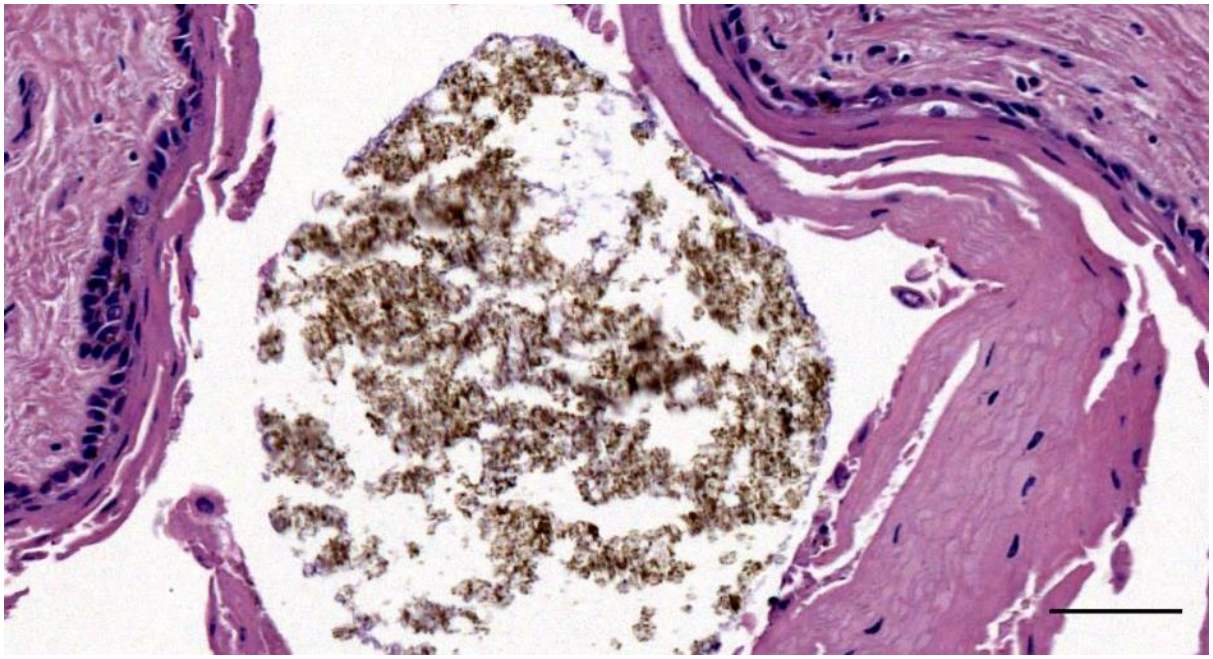

Figure 65. HE-stained cross-section of the ear canal in bottlenose dolphin (444_L4) Ear canal with exogenous content. Scale bar 50 µm

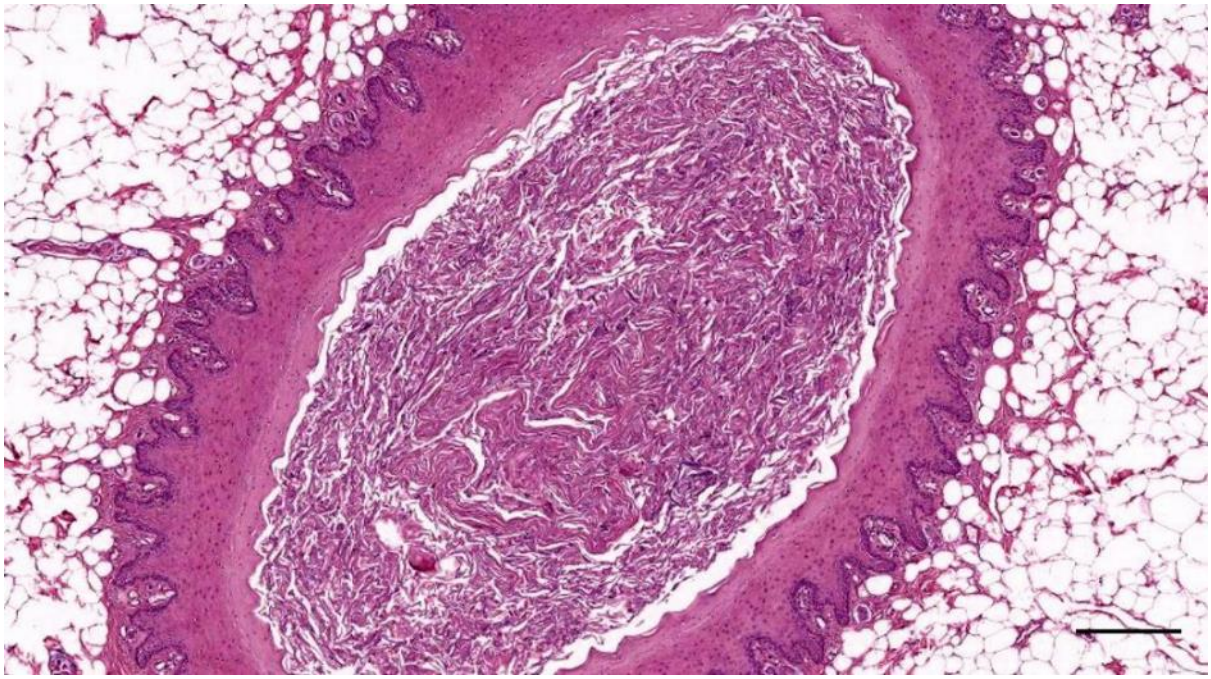

Figure 66. HE stained cross-section of the ear canal of a Cuvier´s beaked whale in the superficial blubber layer about 1.5 cm beneath the surface. The lumen is filled with desquamated epithelial cells and possible glandular product. Scale bar 300 µm

Table 10. Presentation of the change in shape and size of the external ear canal at different depths beneath the skin in a well-preserved striped dolphin specimen with typical common characteristics (top), and a Cuvier´s beaked whale (bottom). All values are in mm. SNF: sensory nerve formations; CT: connective tissue

Depth	*Diameter*	*Shape*	*Content*	*SNF*	*CT*	*Fat*
0	1.0 – 1.4	Oval-star	Desquamated cells			
5	0.3 – 0.7	Star	Desquamated cells	+++	+	++ +
10	0.3 – 0.6	Star	-	+++	++	++
20	0.5 – 1.3	Oval-star	-	+++	+++	+
30	0.8 – 1.3	Oval	-	+++	+++	+
40	0.9 – 2.0	Triangular	-	+++	+++	+/-
50	0.7 – 2.2	Oval	-	++	+++	-

Depth	*Diameter*	*Shape*	*Content*	*SNF*	*CT*	*Fat*
0	0.4	Pentagon	-	-	-	-
10	0.3 – 1.4	Pentagon	Desquamated cells	+	+/-	+++
20	1.4 – 2.3	Oval	Desquamated cells	+	+/-	+++
30	1.0 – 2.4	Oval	Desquamated cells	+	+	+++
40	2.4	Flat triangle	Desquamated cells	++	+	+++
50	3.2	Flat triangle	Desquamated cells	+	+	+++
60	4.5-5.0	Oval stretched	Desquamated cells	+	++	++
70	4.0	Oval stretched	Desquamated cells	+	++	++
80	3.0	Oval stretched	Desquamated cells	+	+++	+
90	2.7	Oval stretched	Desquamated cells	+	+++	+/-

2.3 Epithelium and papillary layer

The external ear canal, throughout its entire course, in all species, was lined with stratified squamous epithelium. This epithelium was a continuation of the skin that funnelled down through the external ear opening. We noted an incomplete cornification (parakeratosis) in the species that presented glands (striped dolphin, bottlenose dolphin, common dolphin, long-finned pilot whale, harbour porpoise), with para- to full orthokeratosis (true keratinization) in the ear canal of the beaked whales (Figure 67, Figure 68). In that species, we did not observe any glandular structures. In contrast, in the common dolphin and bottlenose dolphin (best-preserved specimen of the two), the epithelium of the canal was parakeratotic for most of its course, except for the region of the glands, where the epithelium changed, and the difference between the ear canal and glandular structures was sometimes not discernible (Figure 69, Figure 70)(See also Glands and Annex (ID444, ID169/17)). All animals demonstrated a process of desquamation of the epithelial layers, which seemed to occur

more uniformly in Cuvier´s beaked whale than in other species (possibly due to the greater thickness of the epithelium)

The nature of the epithelium of the ear canal of these animals, in the region of the glands, was either glandular, or transitory between squamous and glandular, thin with few layers and in some locations even pseudostratified, or at least it seemed to be, taking into account that the tissue was not in optimal condition states and artefacts could not be excluded.

Due to the glandular presence, the epithelium could be considered a mucous membrane, at least on a local scale. However, as it is a continuation of the skin, it could be considered otherwise. Table 11 presents a comparison of nomenclature and structure of the skin and the external ear canal in toothed whales.

Table 11. Comparison of the layers of skin and external ear canal, based on (Palmer and Weddell, 1964; Harrison and Thurley, 1974; Ling, 1974; Cozzi et al., 2017).[1]

<table>
<tr><td rowspan="11">INTEGUMENT</td><td rowspan="6">SKIN</td><td rowspan="4">epidermis</td><td>str. externum[2]</td><td colspan="3"></td><td>str. superficiale[3]/externum</td><td rowspan="3">epithelium</td><td rowspan="11">EXTERNAL EAR CANAL</td></tr>
<tr><td>(str. intermedium[4])</td><td rowspan="3">rete ridges and pegs[5]</td><td rowspan="3">Papillary layer[6]</td><td rowspan="3">epithelial ridges and pegs</td><td>str. spinosum/intermedium</td></tr>
<tr><td>str. spinosum</td><td rowspan="2">str. basale/germinativum</td></tr>
<tr><td>str. basale/germinativum</td></tr>
<tr><td colspan="2">basal lamina</td><td>basal lamina</td><td colspan="2">basal lamina</td></tr>
<tr><td rowspan="2">corium (dermis)</td><td></td><td>dermal papillae and ridges</td><td>propria papillae and ridges</td><td colspan="3" rowspan="3">tunica propria-submucosa:
- a subepithelial layer with loose connective tissue (papillary layer)(contained lamellar corpuscles; relatively cell-dense with fibrocytes, fibroblasts, and in certain locations also concentrations of histiocytes, plasma cells, and lymphocytes), well-vascularized
- loose and dense connective tissue, fat, muscles</td></tr>
<tr><td>str. reticulare</td><td colspan="3" rowspan="4"></td></tr>
<tr><td rowspan="2">hypodermis</td><td>hypodermal fat = blubber</td></tr>
<tr><td>loose connective tissue (well-vascularized) and wandering fat cells</td></tr>
<tr><td colspan="2">skin musculature (panniculus carnosus)
subcutaneous fat,
superficial fascia</td><td colspan="3">In some parts of the canal, there could be considered t. adventitia, e.g. between ear canal and cartilage</td></tr>
</table>

In the ear canal of several terrestrial mammals, i.e. northern giraffe, roe deer, cow, sheep, and mouse, we found only complete ortokeratosis, independent of the presence of glands (Figure 72, Figure 73, Figure 74). The epithelial thickness, as formed by the number of epithelial layers, was subjectively thin in terrestrial mammals compared to toothed whales. In all toothed whales, the thickness of the epithelium changed throughout the ear canal. Beneath the skin, the epithelium consisted of many

[1] For more information on the morphological characteristics of the skin in toothed whales, see Japha, 1905; Bonin and Vladikov, 1940; Parry, 1949; E. Sokolov, 1955, 1960; W. Sokolov, 1960, Narkhov, 1962; Geraci et al., 1986; Shoemaker and Ridgway, 1991; Pabst et al., 1999; Zabka and Romano, 2003; Struntz et al., 2004; For information on the skin in baleen whales, see e.g. Giacometti, 1967; Reeb et al., 2007

[2] Also called stratum corneum, although not preferred due to the incomplete cornification (parakeratosis) (Cozzi et al., 2017)

[3] Like in a stratified, squamous, uncornified epithelium like the oral mucosa in carnivores, or the inside of the eyelid (cfr. Figure 296)

[4] Only described by Harrison and Thurley (1974) as a separate layer; other authors consider this part of the stratum spinosum

[5] A.k.a. epidermal ridges and protuberances

[6] In the ear canal, the papillary layer is mostly present in vicinity of the skin, and in the nervous ridge

layers (Figure 75), similar to the epidermis, while the number of layers and the thickness of the epithelium gradually decreased in thickness towards medial (Figure 41).

The presence and amount of melanin pigment in the epithelium varied among individuals. There was pigment present in all animals (except for the single striped dolphin foetus), evident over the bulk of the ear canal, although it was often missing in the most superficial and deepest tissues. The amount of melanin showed individual variation, ranging from a fully melanotic epithelium over the entire length of the ear canal (e.g. ID457), to a complete absence of melanin. However, the most common configuration was the presence of melanin pigment in the skin around the ear opening and the ear canal as it travelled through the blubber, adjoined by the absence of melanin in deeper sections, lateral to the cartilage, and a reoccurrence of melanin in the medial half of the canal together with the presence of cartilage. The striped dolphin individuals that had an external linear pigmentation in the skin associated with the external ear opening (Figure 16, Figure 17, Figure 18), presented more obvious pigmentation in the lateral part of the ear canal as well. There was sometimes also pigment in the glandular excretory ducts with a squamous epithelium in continuation with that of the ear canal itself (e.g. ID274/18).

The epithelium in the lateral third of the canal contained many papillae, together with an elaborate germinal layer, which would be suitable for a sloughing rate that is higher than in deeper tissue.

The epithelium consisted of a pigmented stratified squamous epithelium. The epithelial layers that could be distinguished were the same as in the epidermis, namely stratum basale (stratum germinativum), stratum spinosum, stratum corneum with parakeratotic cells. The stratum basale consisted of basal cells visible as large columnar cells and melanocytes.

In striped dolphin the height of the epithelium was constant over the entire course, measuring 20-40 µm. On the contrary, in Cuvier's beaked whale, the height measured about 500 µm in superficial section, gradually diminishing to 50-200 µm in the deepest section. Also, in striped dolphin, the peripheral layers of the epithelium showed vacuolization with compression of the nucleus, while in Cuvier´s beaked whale, the same was present in deeper layers.

Although the general construction of the wall was the same, there was an interspecific difference in the ratio of the wall thickness versus the underlying connective tissue (Figure 76).

There was a prominent presence of epithelial ridges and pegs, and propria ridges and papillae, suggesting a strong interaction between epithelium and subepithelial tissue, similar to the skin (See eyelid Figure 296). In superficial sections, this occurred all around the ear canal although with variability in the prominence (e.g. Figure 58, Figure 77), while in deeper sections, this occurred mostly in two opposite sides of the canal (Figure 78) and in the ridge of tissue that bulged into the ear canal lumen (Figure 79, Figure 80**,** Figure 81), although with individual variability (e.g. Long-finned pilot

whale (Figure 82, Figure 83). In the most superficial sections, there was a gradual transition between the dermal papillary layer and the one of the ear canal (Figure 84). A similar configuration was found in all species.

Transmission Electron Microscopic analysis

The epithelium in striped dolphin was identified as a stratified squamous epithelium in which the most apical cells had a nucleus with one or multiple nucleoli and eu- and heterochromatin (Figure 85). However, it could have been that superficial cell layers were missing due to post-mortem degeneration. The different epithelial layers could not be distinguished (Figure 86), also because of post-mortem degeneration. The apical plasma membrane of all epithelial cells lining the lumen showed an extensive glycocalyx, and most of the cells displayed the presence of small membrane-bound structures in the form of vesicles, bulges or knobs (Figure 87). These protrusions and intraluminal vesicles are not omnipresent on every cell (E.g. Figure 88). The separate vesicles in the lumen had a clear centre, a double-layered plasma membrane and an extensive glycocalyx, and were only present in the vicinity of the epithelium. There were various thread-like connections between and amongst the knobs and intraluminal vesicles (Figure 89). This glycocalyx was not only present in association with the vesicles, but occurred on the plasma membrane of all cells, including the ones that did not present any knobs or vesicles (Figure 90), and also in the artefactual intracellular spaces between the epithelial cells (Figure 91).

Also, there was a single, large proteinaceous structure of unknown origin in the lumen of the striped dolphin (Figure 92, Figure 93). There seemed to be a spatial relation with the exocytotic processes of the epithelium, both in small magnification, where the epithelium shows the most activity in the plasma membranes close to the structure (Figure 92) and on large magnification, where the exocytotic vesicles make contact with the membrane of the structure and seem to make physical indentations (Figure 93).

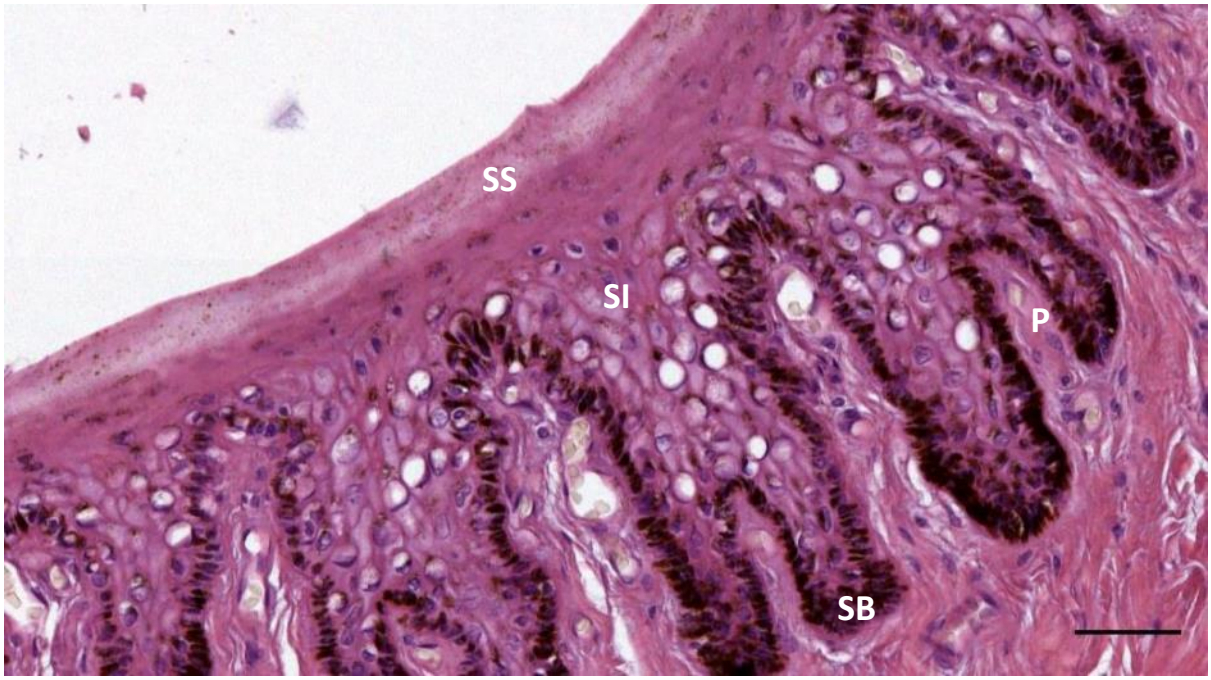

Figure 67. HE stained detail section of the epithelium of the ear canal of a Cuvier´s beaked whale. SL: Stratum basale with pigment; SI: str. intermedium; SS: str. superficiale. P: papillary layer. Scale bar 50 µm.

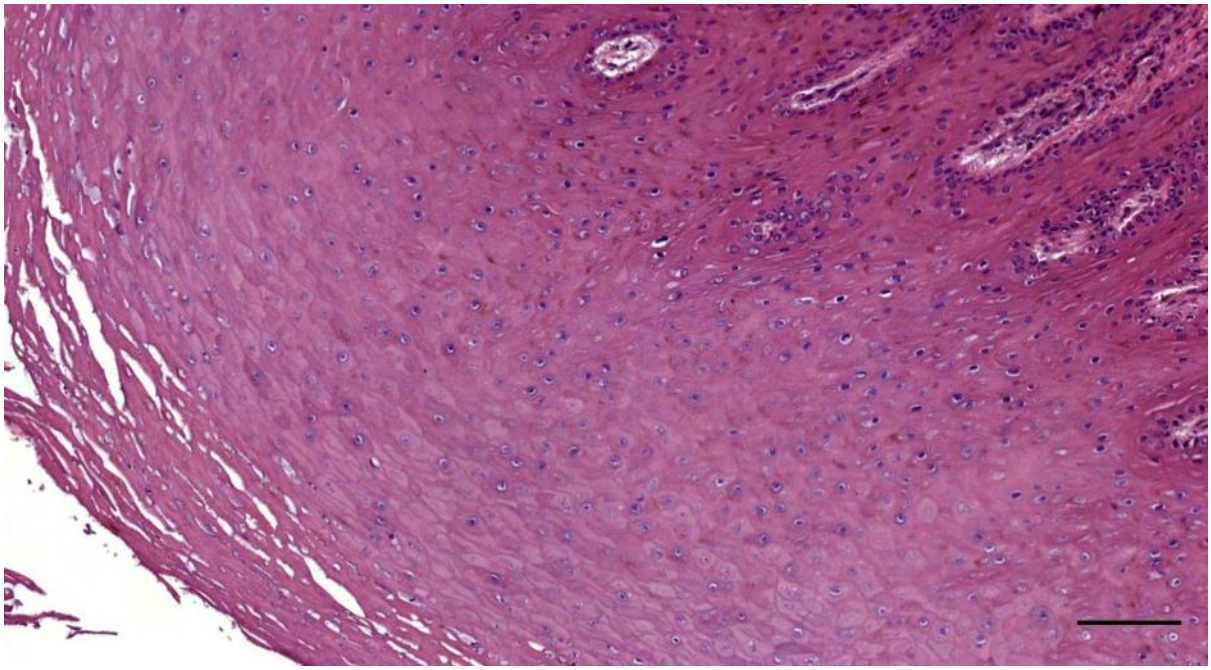

Figure 68. Detail of the epithelium in a histological transverse section through the external ear canal of a Cuvier´s beaked whale about 1 cm beneath the skin (ID177/19). Scale bar 100 µm

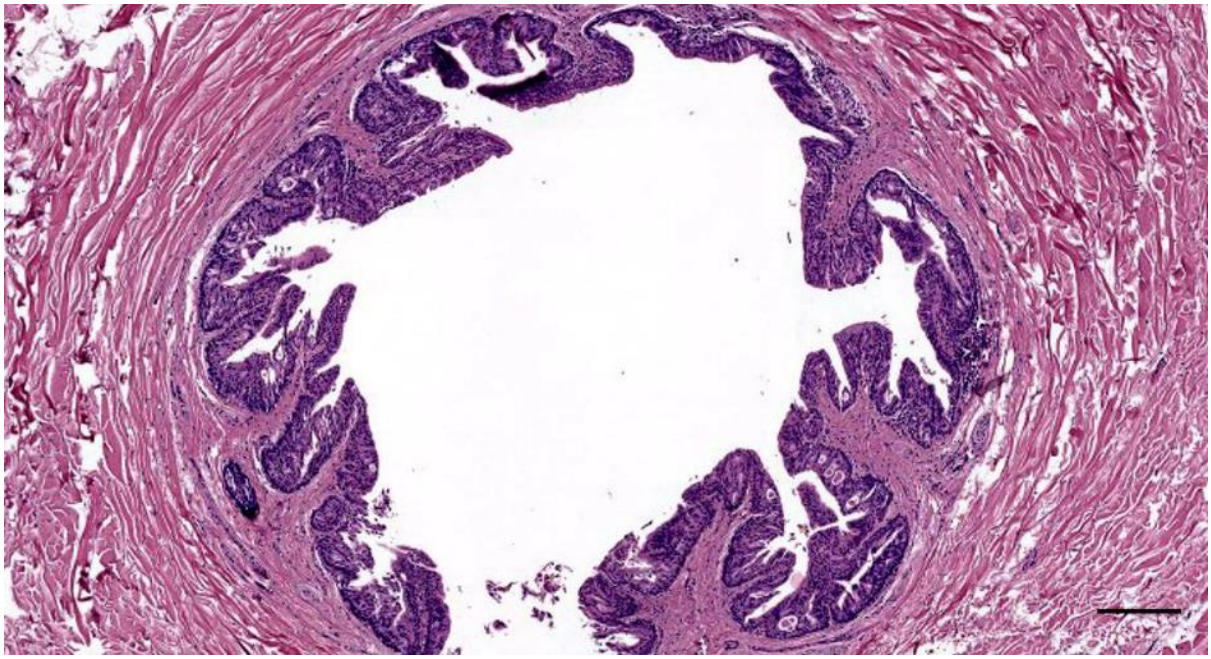

Figure 69. Histological transverse section (HE staining) through the ear canal of a bottlenose dolphin at about 3.5 cm beneath the skin (ID444). The distinction between the ear canal and glandular structures, and both of the epithelia, is not clear. Scale bar 200 µm

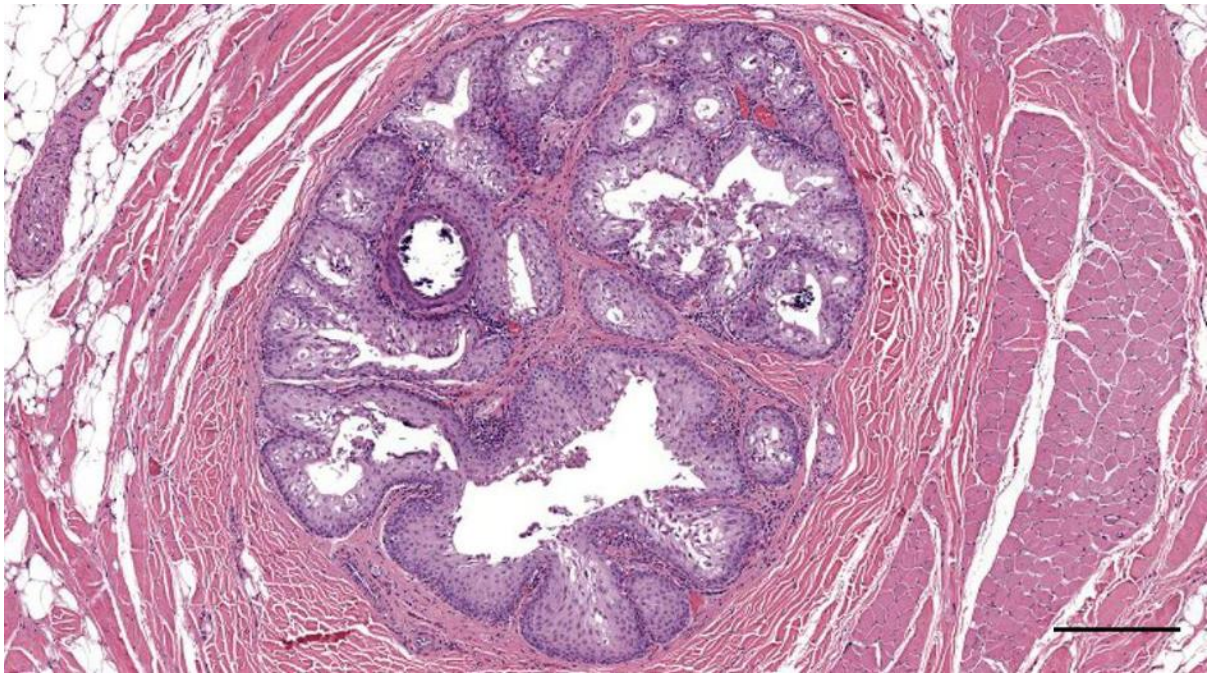

Figure 70. Histological transverse section through (HE staining) the ear canal of a common dolphin at about 2 cm beneath the skin (ID169/17) The distinction between ear canal and glands is not clear. Scale bar 300 µm

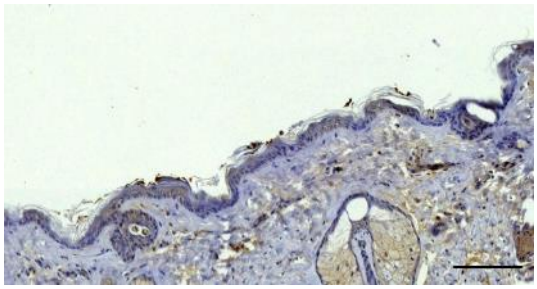

Figure 71. Immunohistological transverse section through the ear canal of a roe deer (CP11)(IHC, anti-S100). Note the fully keratinized stratified squamous epithelium. Scale bar 100 µm

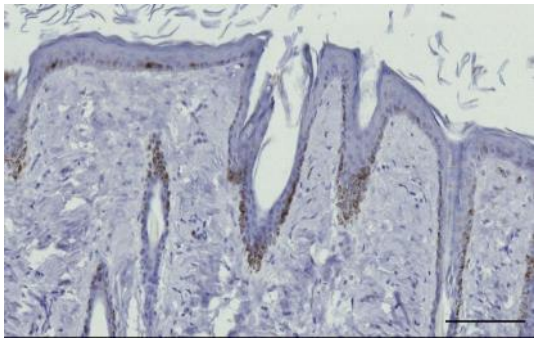

Figure 72. Immunohistological transverse section through the ear canal of a Northern Giraffe (IHC – anti-NF). The epithelium is a stratified squamous epithelium with full keratinization. Scale bar 100 µm

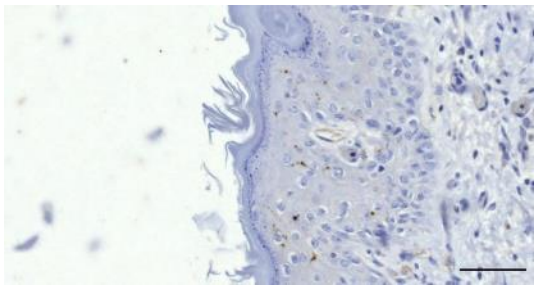

Figure 73. Immunohistological transverse section (HE staining) through the ear canal of a cow (AE246)(IHC, anti-PGP9.5). Note the fully keratinized stratified squamous epithelium. Scale bar 50 µm

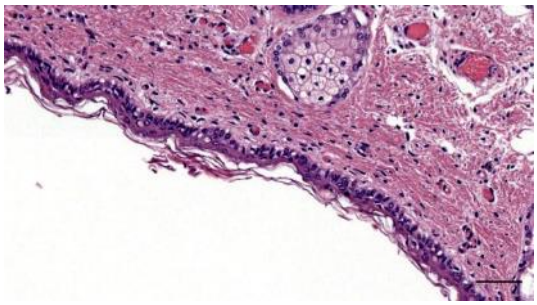

Figure 74. Histological transverse section through the ear canal of a sheep foetus (AE069)(HE staining). Note the thin but fully keratinized stratified squamous epithelium. Scale bar 50 µm

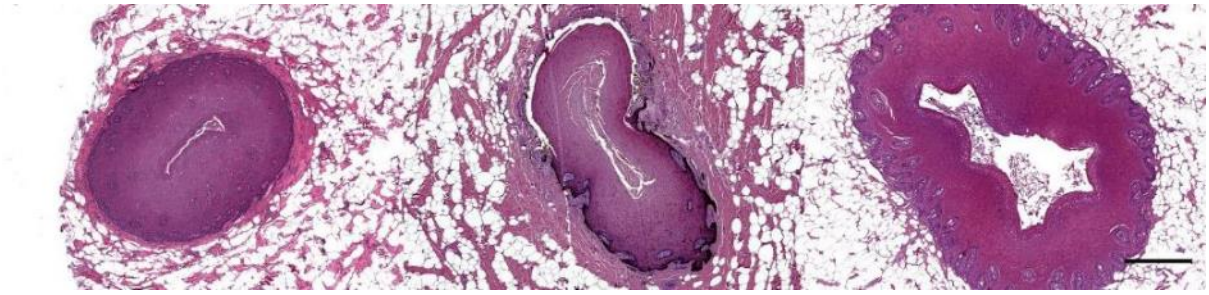

Figure 75. Montage of three HE-stained cross-sections through the ear canal, medial to the external ear opening in a striped dolphin (left), long-finned pilot whale (middle), and Cuvier´s beaked whale (right). The configuration is very similar in the three species, with a thick epithelium and little amount of surrounding connective tissue embedded within the blubber layer. Scale bar 500 µm

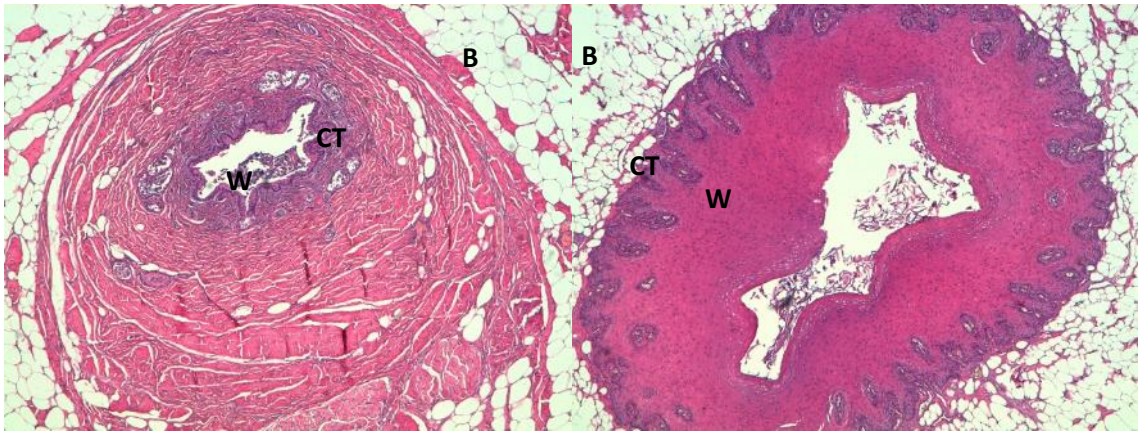

Figure 76. Histological overview (HE staining) of two cross-sections of the external ear canal of striped dolphin (left) and Cuvier's beaked whale (right). Both sections are embedded in the blubber layer (B), just underneath the skin. Although the overall size is similar, note the extreme difference in the ratio of the height of the wall (W) versus the surrounding connective tissue (CT). In striped dolphin, the wall is very thin, while in the beaked whale, the connective tissue layer is almost non-existing (Same magnification but scale bar missing).

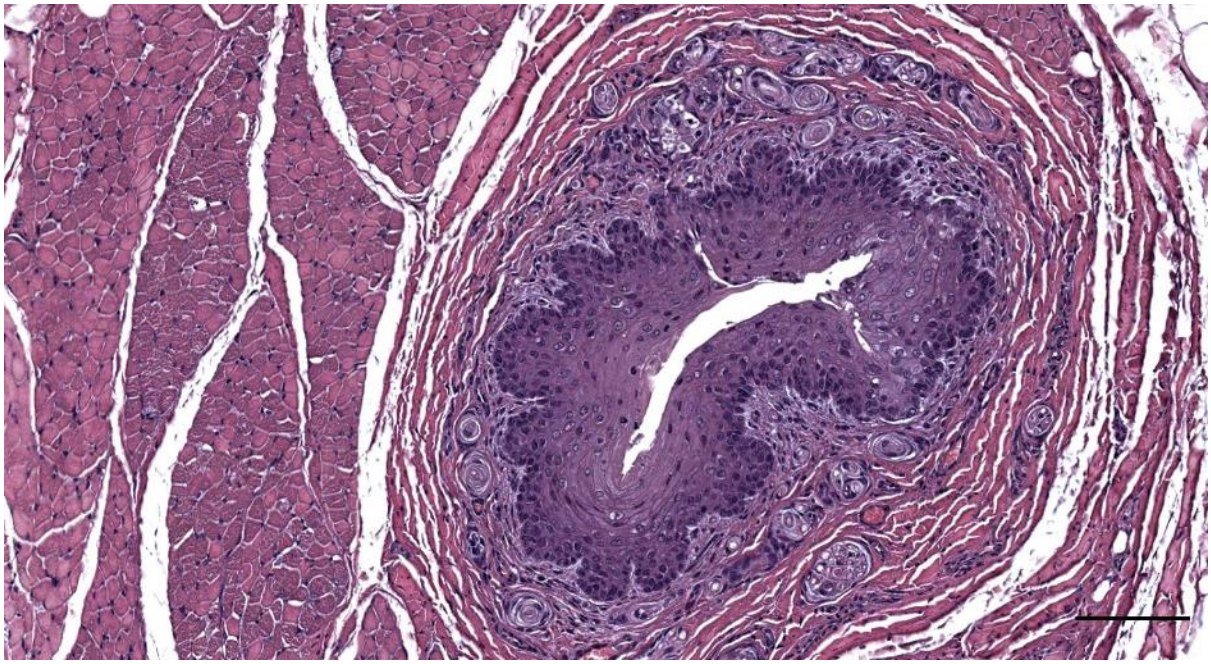

Figure 77. Histological transverse section (HE staining) through the ear canal of a striped dolphin about 2.5 cm beneath the skin (419_16_5). Scale bar 100 µm

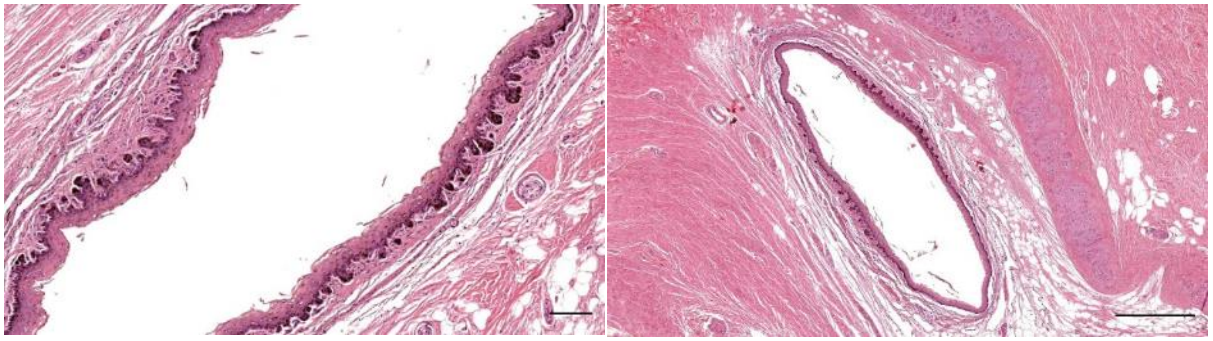

Figure 78. Histological images (HE staining) of transverse sections through the ear canal in a common dolphin (ID169/17) at about 3.5 and 4 cm beneath the skin. Scale bars 100 µm left, 500 µm right

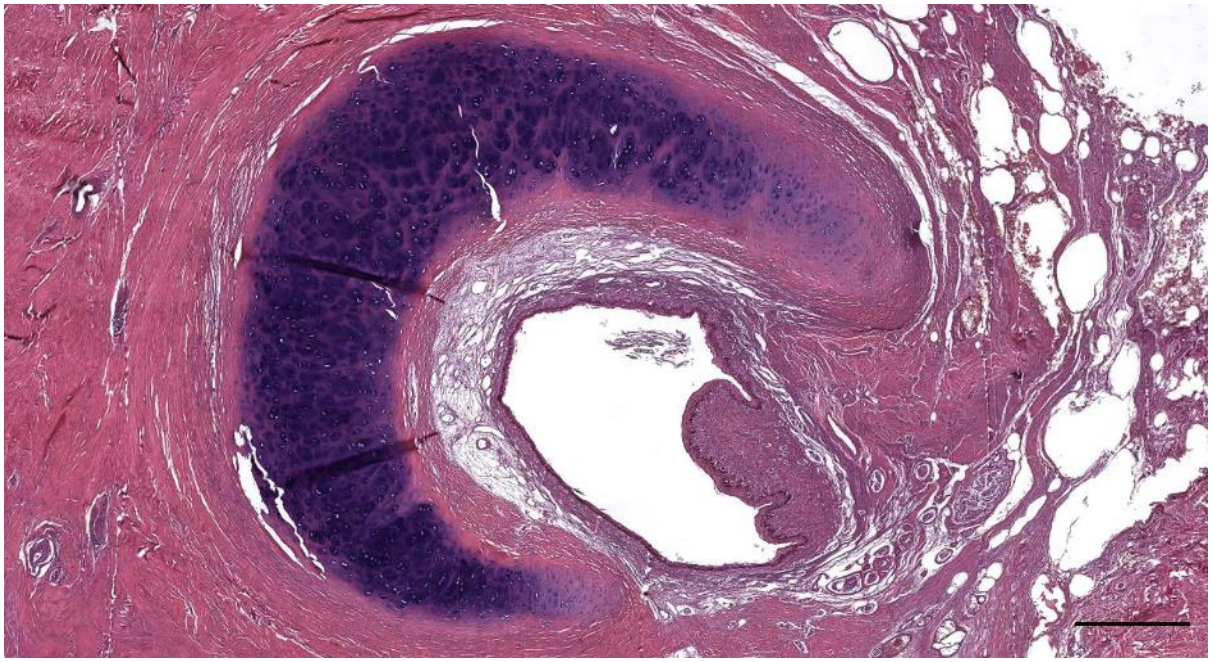

Figure 79. HE-stained cross-section of the ear canal and cartilage of a striped dolphin (ID509/17_Lx1), close to the TP complex. Scale bar 0.5 mm

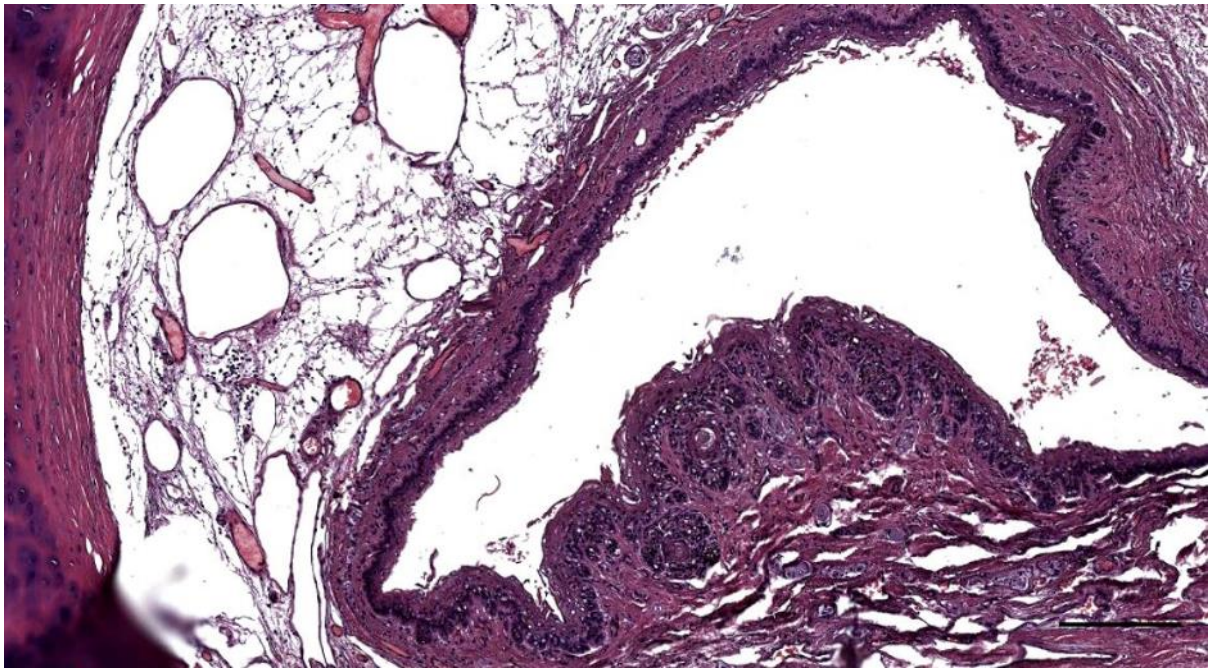

Figure 80. Histological image (HE staining) of a transverse section through the ear canal of a striped dolphin (292/18_L11) Mononuclear cells (lymphocytes) between ear canal and cartilage, situated in the reticular connective tissue network with vascular lacunae. Note the ridge of tissue bulging into the ear canal lumen. Scale bar 200 µm

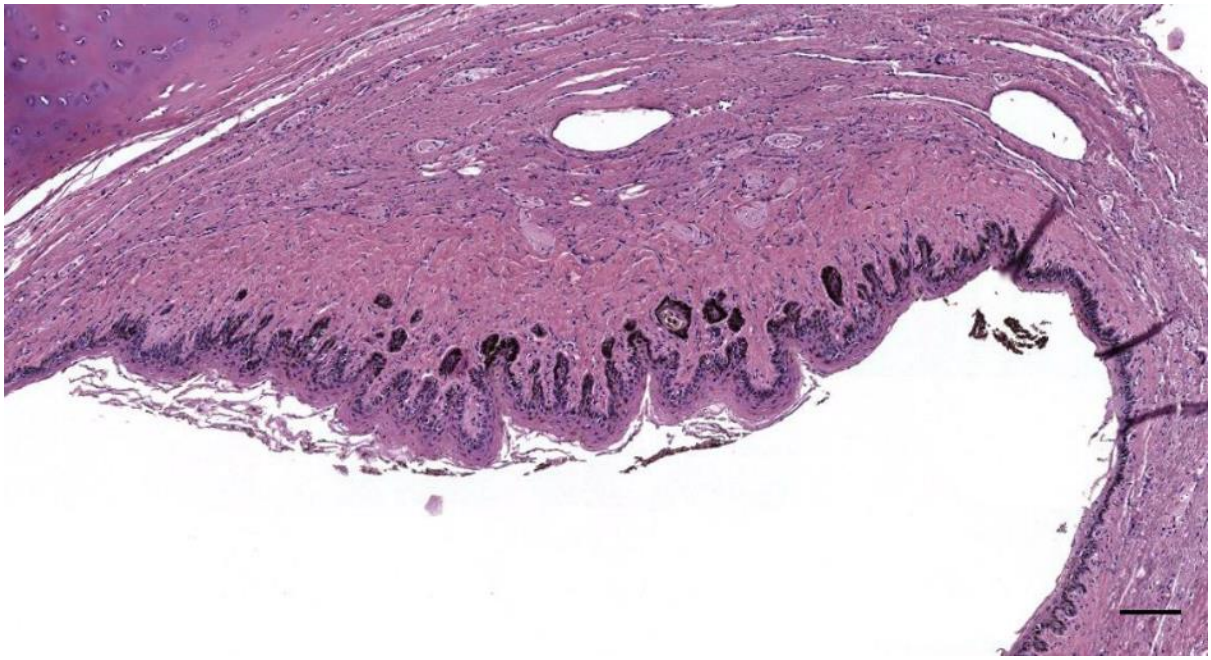

Figure 81. Histological image (HE staining) of the ear canal in a bottlenose dolphin (444_L19). Detail of the nervous tissue ridge. Scale bar 100 µm

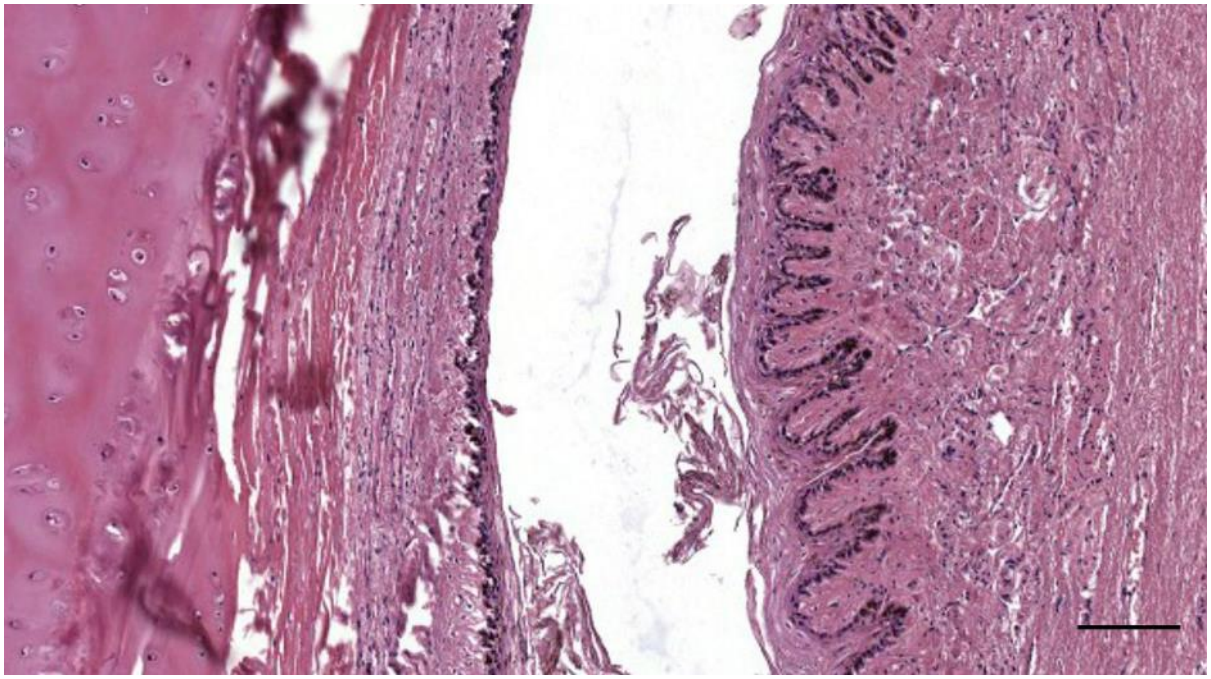

Figure 82. Histological transverse section (HE staining) through the ear canal of a pilot whale (441_L19). Ear canal with intricate epithelium-subepithelial tissue interaction in the form of dermal papillae and epithelial ridges, on one side of the ear canal, opposite the cartilage. It is also on this side of the ear canal that many nervous structures can be found, which are absent between canal and cartilage. Scale bar 100 µm

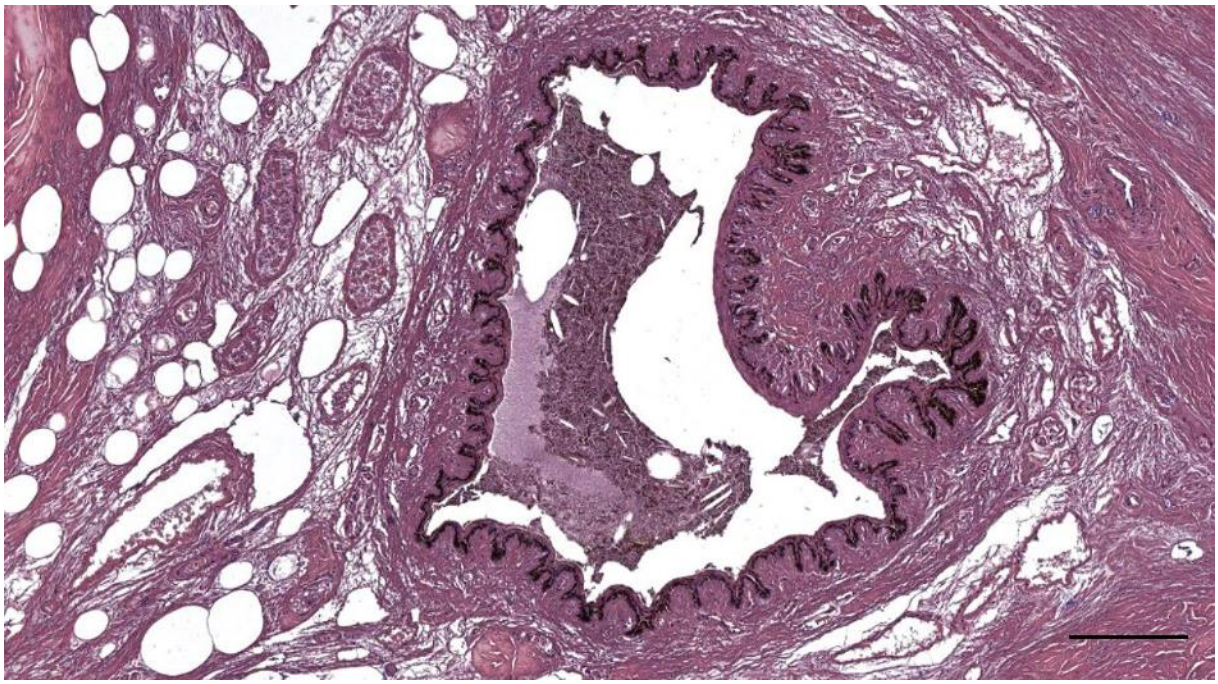

Figure 83. Histological image (HE staining) of the ear canal in a long-finned pilot whale (441_R21). Detail image of Figure 166. Note, the ear canal with content and nervous tissue ridge, and the intense epithelium-subepithelial interaction. Scale bar 200 µm

Figure 84. Two histological images of transverse sections through the left and right external ear opening in a common dolphin immediately beneath the skin. The zoomed-in image is a detail of the left, and shows the ear canal lumen besides a separate artificial lumen situated in the epithelium, and which is filled with epithelial cell layers. This is possibly a section through an epidermal ridge, or it is the obstructed excretory duct of a glandular unit (See chapter Glands). Scale bar top left 300 µm, top right 200 µm, and bottom 100 µm

All TEM images presented here are from a striped dolphin. The results were the same for striped and bottlenose dolphin, but the images of bottlenose dolphin were not included here due to the lousy tissue conservation state which often did not allow for a clear distinction between structures that make up the lamellar corpuscles. Therefore, the latter images are not presented here.

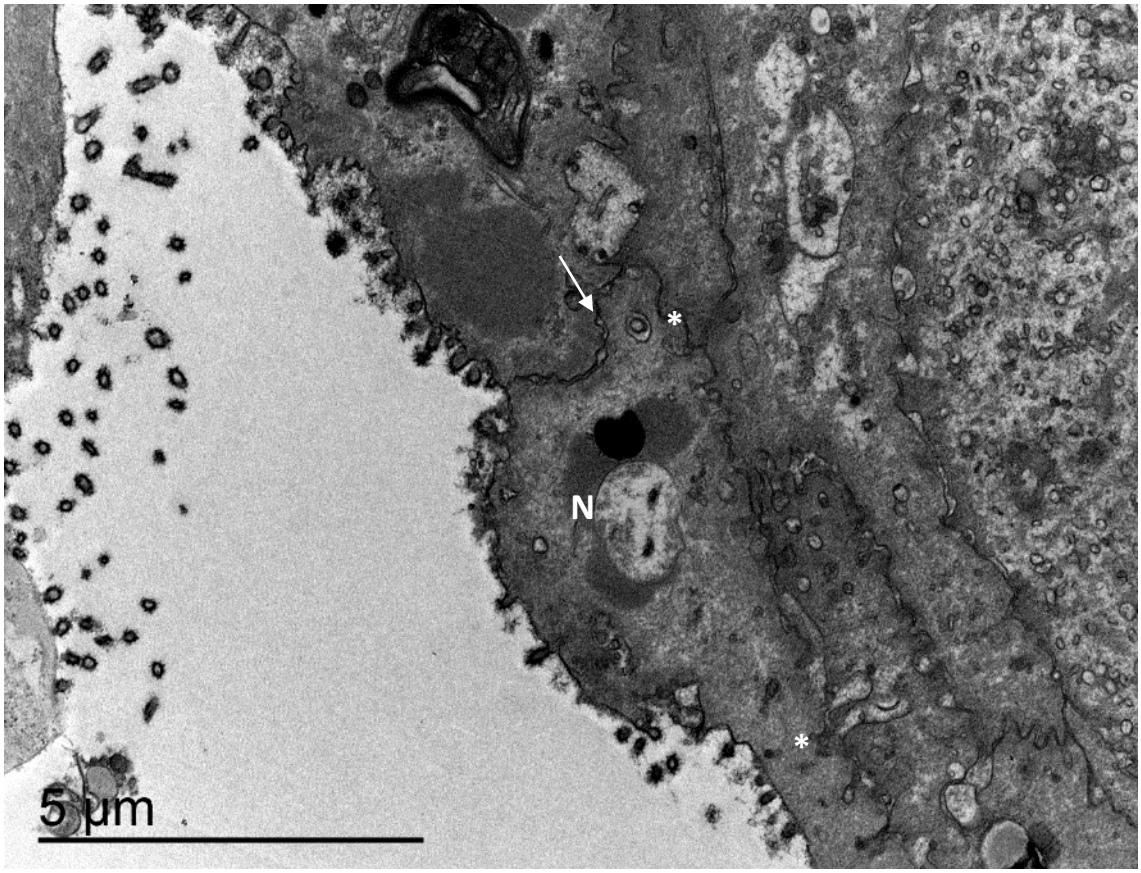

Figure 85. Image of the ear canal lumen and epithelium. Note the intraluminal vesicles. The apical epithelial cells have nuclei (N) with eu- and heterochromatin and nucleoli. There are also double-coated intracytoplasmic vesicles (e.g. arrow), and indications of desmosome-like connections between epithelium cells (asterisk). (TEM x 12000).

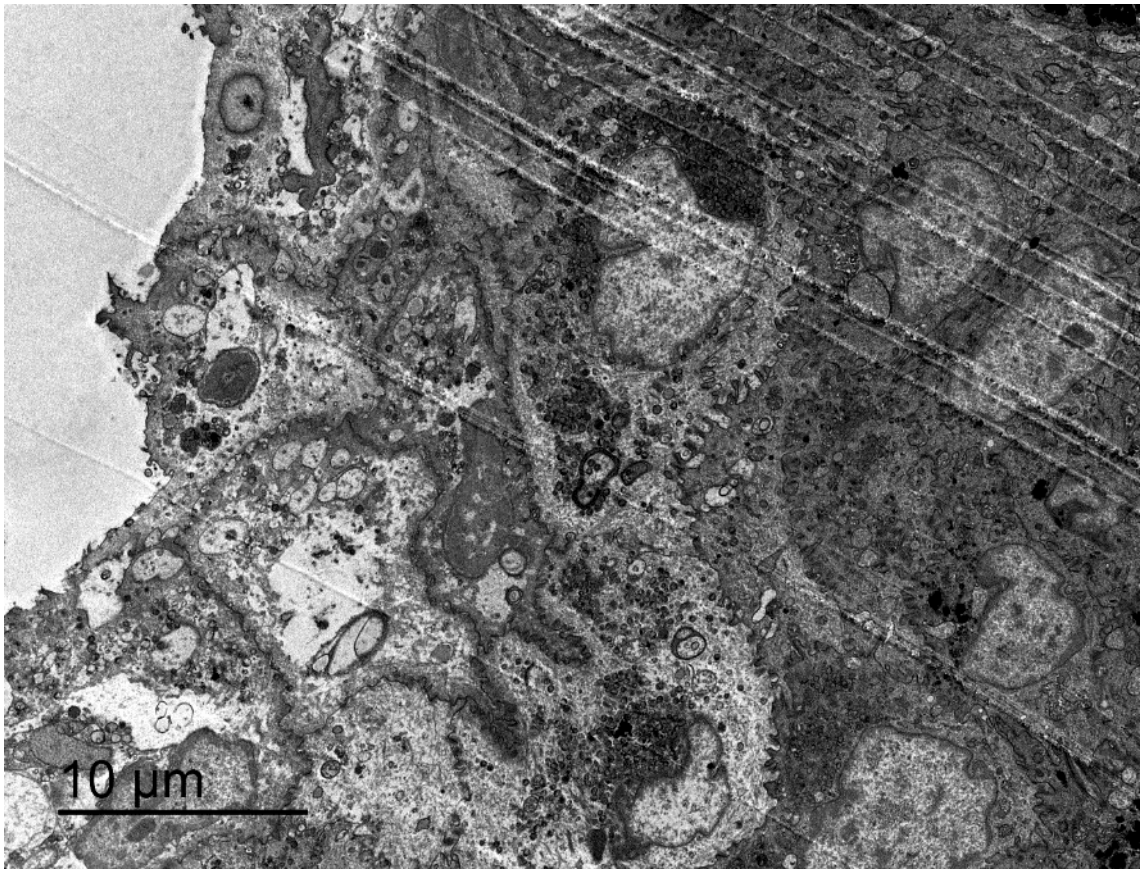

Figure 86. Overview of the epithelium with the ear canal lumen on the top left side. (TEM x 4000)

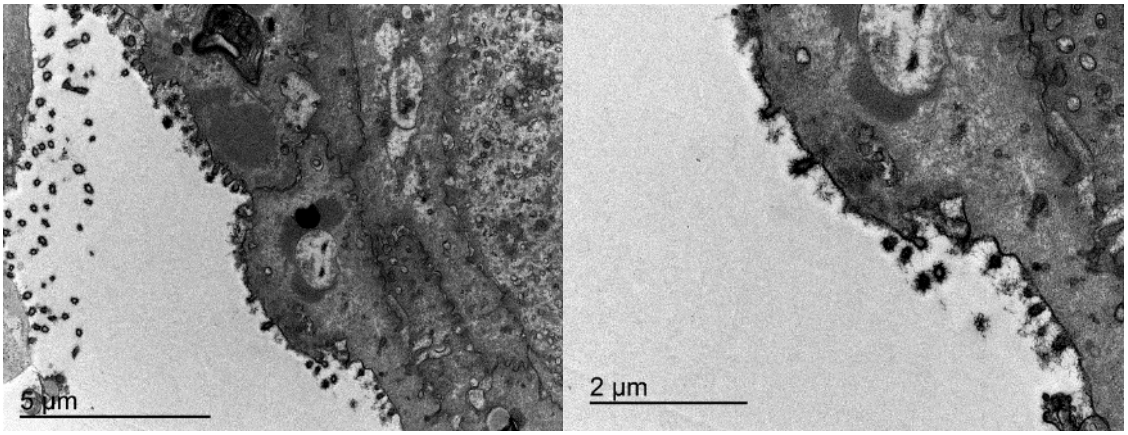

Figure 87. Lumen and superficial epithelial cells. The apical cell surface reveals an abundant glycocalyx. The cells contain nuclei with eu- and heterochromatin and multiple nucleoli and intracytoplasmic vesicles (TEM left x 12000, right x 25000 right).

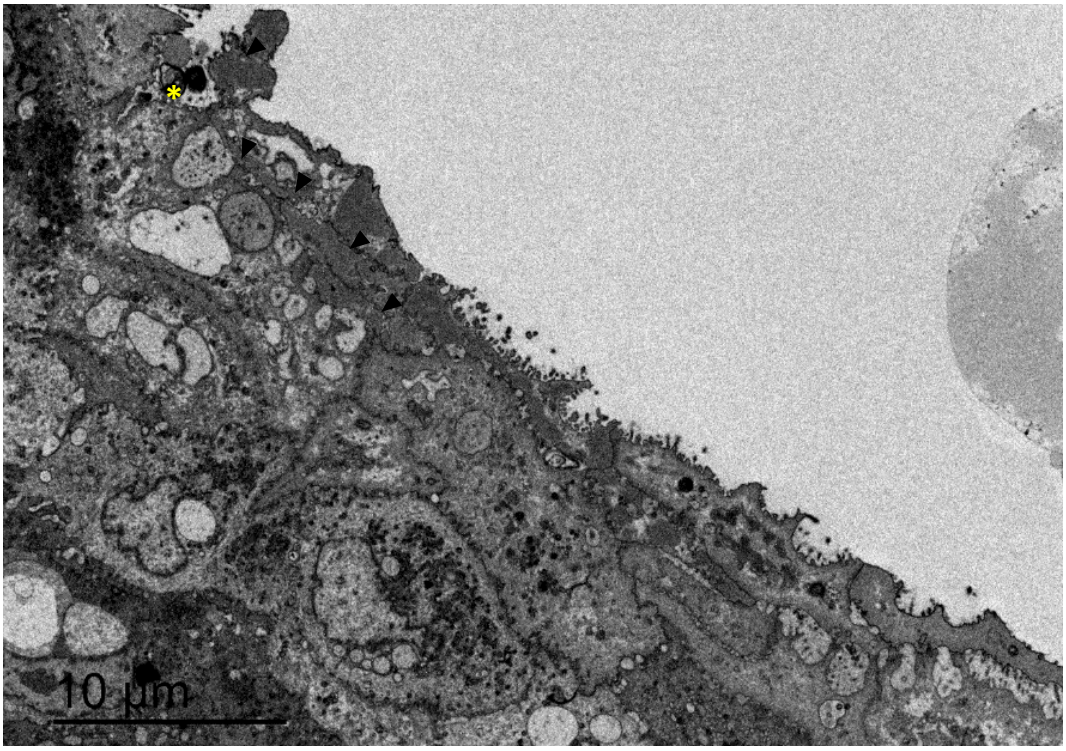

Figure 88. TEM image of the epithelium showing exchange processes on its luminal surface. In the image, five cells have a plasma membrane that is in contact with the lumen. The second cell from the left (arrowheads) does not show exchange processes and vesicles except for some sparse indications of such processes on one side of the intraluminal bulge (asterisk). (TEM x 4000)

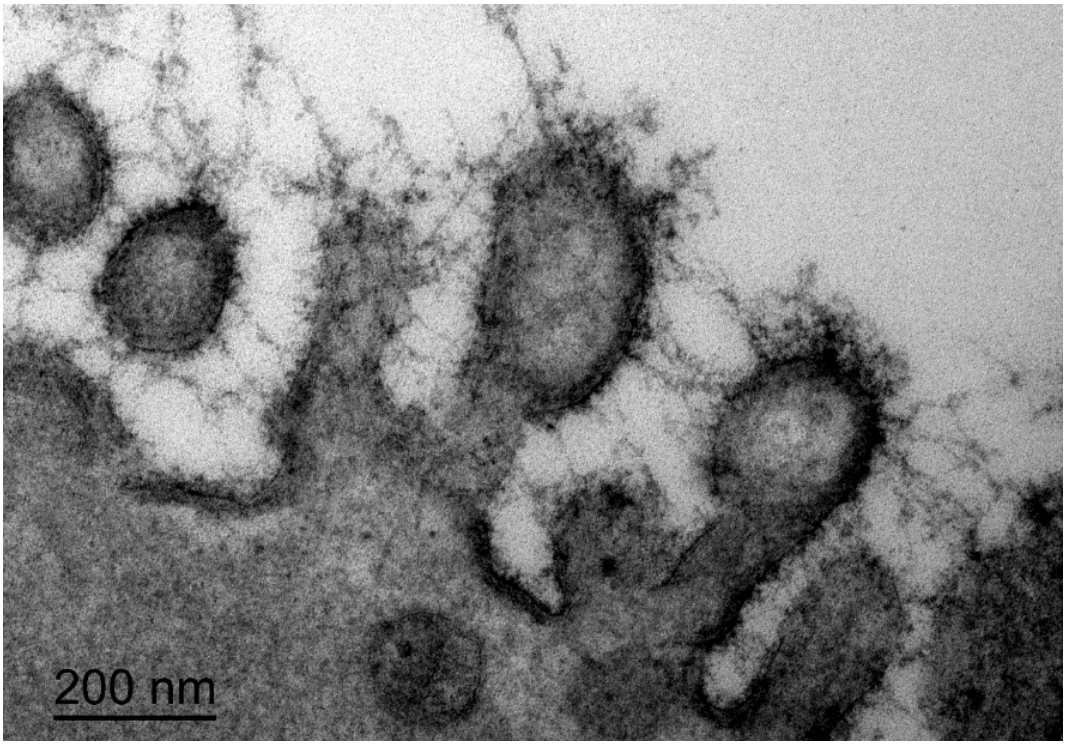

Figure 89. TEM detail image of an apical epithelial cell. Detail image of exocytotic (or endocytic) protrusions on the apical cell membrane of an epithelial cell (E) in the ear canal of a striped dolphin. There is an extensive glycocalyx connecting and interconnecting the vesicles. The content of the vesicles is relatively clear in comparison with the plasma membrane, which is electron-dense (TEM x 150.000)

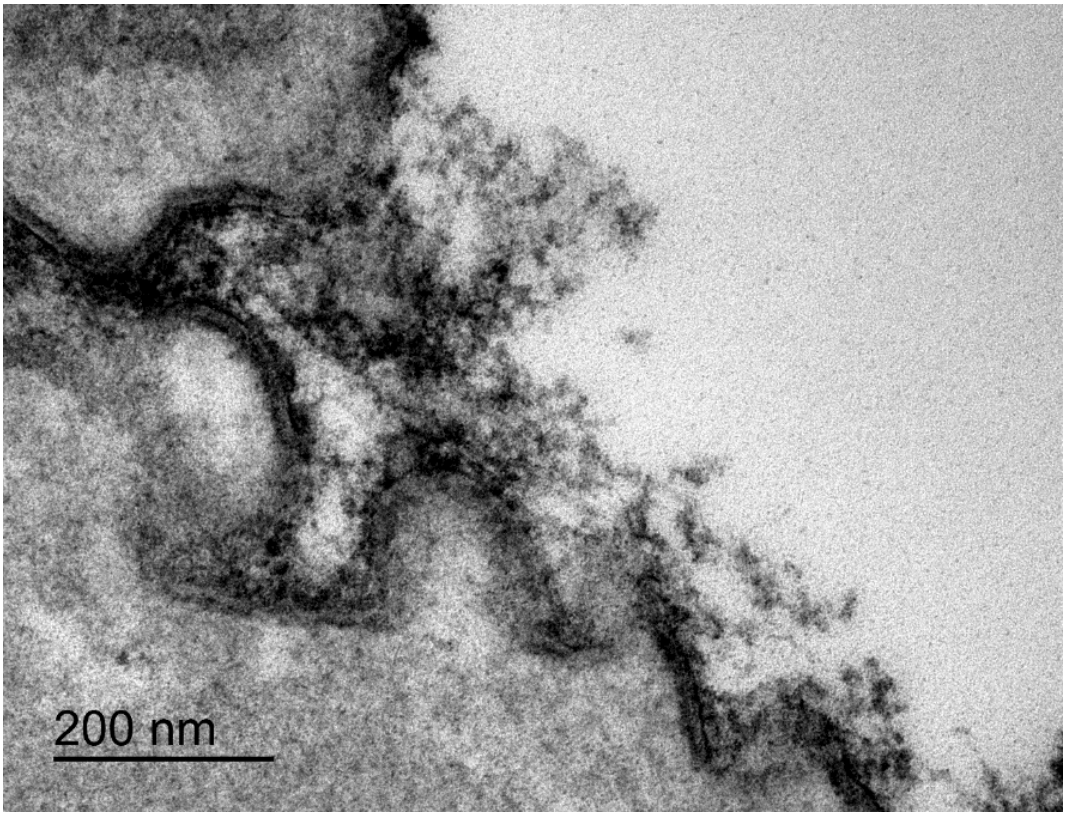

Figure 90. Extensive glycocalyx and the apical cell membrane of two adjacent cells. The glycocalyx is not necessarily associated with vesicular or nodular structures but is present over the entire apical cell surface. (TEM x 200.000)

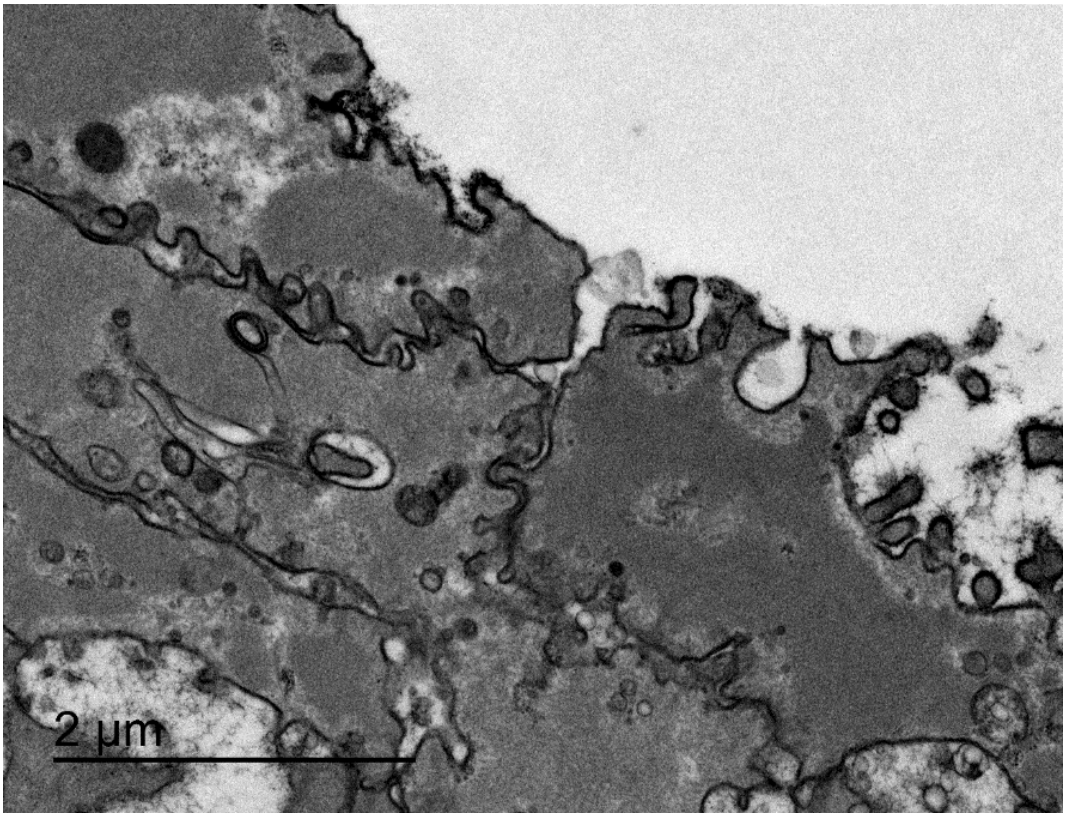

Figure 91. Detail of the intraepithelial artefactual spaces with knobs and vesicles. (TEM x 30.000)

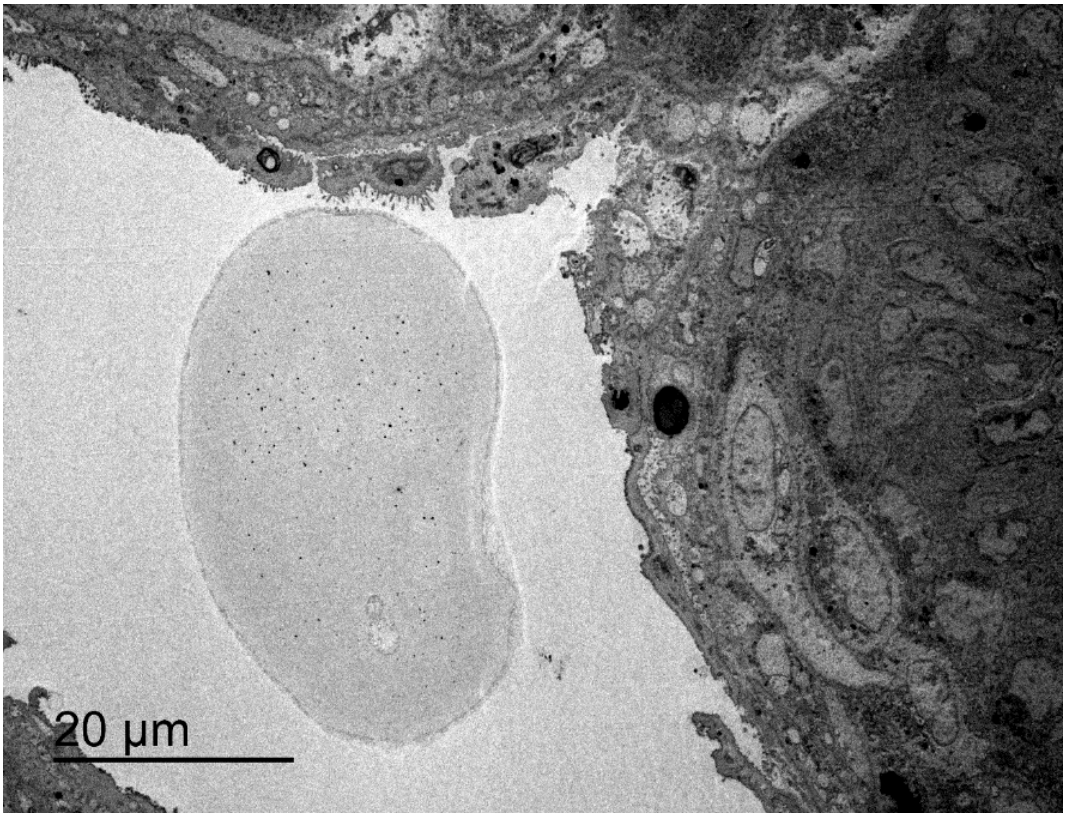

Figure 92. Lumen and superficial epithelium. (TEM x 2000)

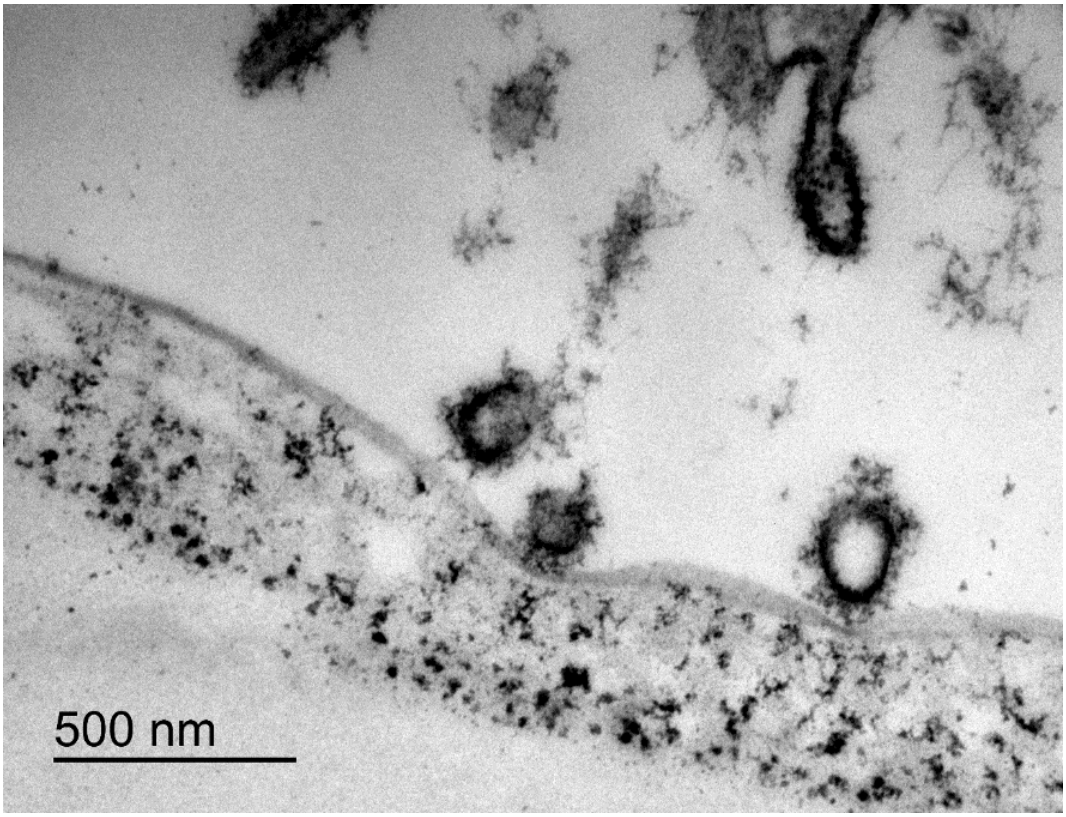

Figure 93. Detail of the previous image. (TEM x 80.000).

2.4 Connective and adipose tissue

In all animals, the ear canal was predominantly surrounded by fat tissue underneath the skin layer, corresponding to the blubber layer. In deeper tissues, the amount of fat tissue gradually decreased, and connective tissue became predominant. The other surrounding tissues were glandular tissue (tubuloacinar glands with compound excretory ducts), nervous tissue in the form of nerve fibres and lamellar corpuscles, extensive blood supply, connective tissue and fat, hyaline cartilage, well-developed muscles.

The ear canal epithelium was surrounded by a thin layer of nuclei-dense, loose connective tissue pervaded by an intense vascularization and innervation with lamellar sensory nerve formations (simple lamellar corpuscles)(Figure 94). This layer of loose connective tissue was present throughout the entire course of the canal, although in deeper sections, it was only prominent on one side of the ear canal, with the cartilage on the opposite side. Because of the presence of more densely packed nuclei, this layer generally stained more basophilic. Next, surrounding the loose connective tissue layer, and depending on the location of the section, there was fatty tissue and denser connective tissue, labelled as ´fibro-elastic tissue capsule´(´fibro-elastic lobe´ of Purves, 1966), with sparse nuclei and larger blood vessels and nerves, and in which the macroscopically visible striated muscles inserted (Figure 94, Figure 95, Figure 96).

There was a negative correlation between the amount of fat and amount of connective tissue (see also Table 10) that formed the adnexa of the ear canal, with the lateral half of the EAM, in its course through the blubber layer contained very little connective tissue (Figure 97), which then gradually increased (Figure 98) with an almost complete absence of fat at the level of the tympanic membrane (apart from the acoustic fat body that touches the tympanic bone, and which was visible in some sections in the medial half of the ear canal). Similarly, in Long-finned pilot whale and Cuvier´s beaked whale, the capsule got more pronounced going deeper (Figure 99). Also, the harbour porpoises presented a richly innervated connective tissue capsule that surrounded the ear canal, subepithelial tissue, fat tissue, and muscle, similar to Cuvier´s beaked whale (Figure 101). In bottlenose dolphin, the transition between blubber layer and the underlying soft tissue portion was more abrupt that in smaller toothed whales. As such, there was no fatty tissue around the ear canal just medial to the spiral curvature, and instead, the ear canal was embedded in a dense connective tissue that separates the canal from the cartilage. Only in the most in-depth sections, there were sparse some fat cells, together with vascular lacunae and connective tissue between the canal and the horseshoe-shaped cartilage. In contrast, in striped dolphin, there were fat cells between the ear canal and cartilage over its entire course.

This dense connective tissue capsule was made of fibrocytes and collagen fibres, single and clustered adipocytes, and also elastic fibres as shown by Weigert´s elastic stain[7] and Acid Orcein Giemsa stain[8] (Figure 102, Figure 103) in all tested species (striped dolphin, bottlenose dolphin, long-finned pilot whale, and Cuvier´s beaked whale). Interestingly, the papillary layer and loose connective tissue layer that contained the lamellar corpuscles did not show any elastic fibres (Figure 104), nor did the adipoconnective tissue around it (Figure 105). Rather, the elastic fibres were situated in the fibro-elastic tissue capsule in which the striated muscles inserted (Figure 106). In deeper sections, with the presence of cartilage, there were elastic fibres in the connective tissue in close vicinity of the canal, while they were absent in the dense connective tissue that holds the entire complex in place (Figure 107, Figure 102). As such, elastic fibres were presented throughout the entire ear canal, although with differences in conformation along its course.

In striped dolphin, the elastic fibres in the fibro-elastic tissue capsule appeared in clusters without a specific orientation. The histochemical reaction was evident in the distant connective tissue surrounding the ear canal, often associated with muscle fibres, while there was a lack of elastic in the immediate surrounding of the ear canal (Figure 105, Figure 104). In more medial slides, with the appearance of the cartilage, there were elastic fibres in the connective tissue immediately around the ear canal, associated with the cartilage, and also in clusters in the more distant connective tissue (Figure 108, Figure 102, Figure 107, Figure 109). On the other hand, in Cuvier's beaked whale, a single slide in the lateral half of the ear canal, showed no elastic fibres in and around the ear canal, only associated with muscle fascicles (peri- or epimysium), and in blood vessel walls in the subendothelial layer of the tunica interna and while it also constitutes the tunica externa together with collagen fibres (Figure 103, Figure 110).

The fibro-elastic tissue capsule was most obviously present in the lateral half of the canal, because of the density differences with the blubber. The capsule got more pronounced and thicker on its progression to the middle ear. However, it became less apparent with the gradually diminishing amount of fat until the ear canal was surrounded by dense connective tissue, cartilage, and muscle tissue running parallel to the canal and inserting into the capsule (Figure 148)(See also Macroscopic morphology of the ear canal and associated tissues).

The Cuvier's beaked whale presented a circular capsule surrounding the ear canal with the subepithelial connective and fatty tissues for the entire length of the canal, from medial to the blubber layer as deep as the sample reached close to the tympanic bulla. The capsule was surrounded by layers

[7] The Weigert – Van Gieson method stains nuclei black, elastic fibres dark blue to black, collagen various shades of red, and connectivum and erythrocytes yellow (technical sheet)

[8] The Pinkus' Acid Orcein-Giemsa Method stains nuclei deep blue, cytoplasm light blue, collagen rose pink, elastic fibres dark brown, mucoid substances and mast cell granules purple, and erythrocytes and eosinophilic granules bright red (technical sheet - Luna, 1968, Manual of Histological Staining Methods AFIP, 3rd edition, McGrawHill, 1968).

of circular and longitudinal striated muscle tissue. In this species, it was also macroscopically distinguishable from other tissues, while in smaller species the capsule was clear to the touch, but not always to the eye.

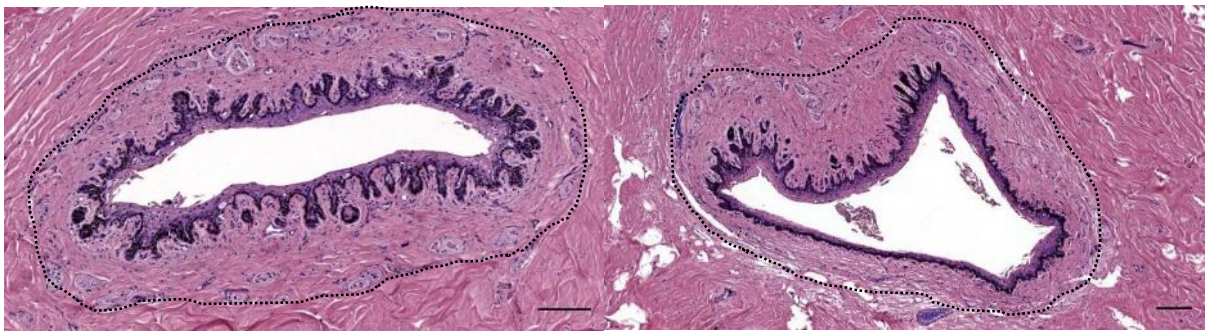

Figure 94. Histological images (HE stain) of two ear canal cross-sections in a striped dolphin. A dashed line indicates the transition between the subepithelial loose connective tissue layer and the peripheral dense connective tissue. Scale bars 100 µm

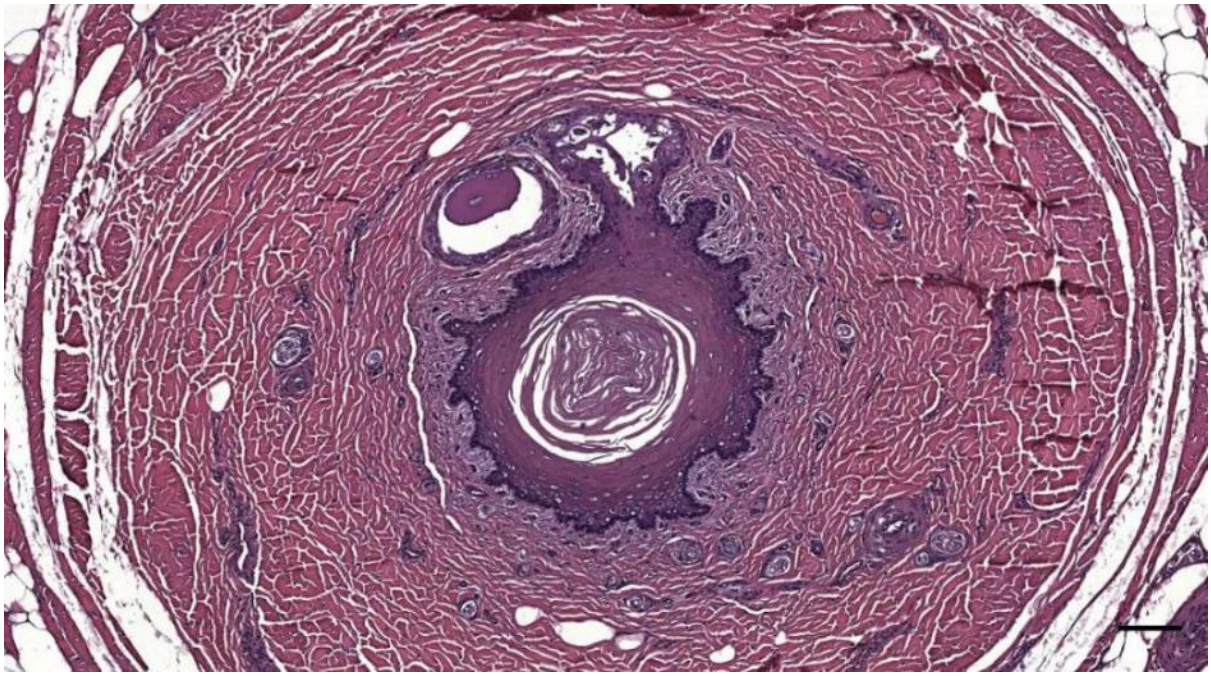

Figure 95. Histological image (HE staining) of a transverse section through the ear canal of a striped dolphin (44_17_B4). Nerves and blood vessels in the adipoconnective tissue sheath. Scale bar 100 µm

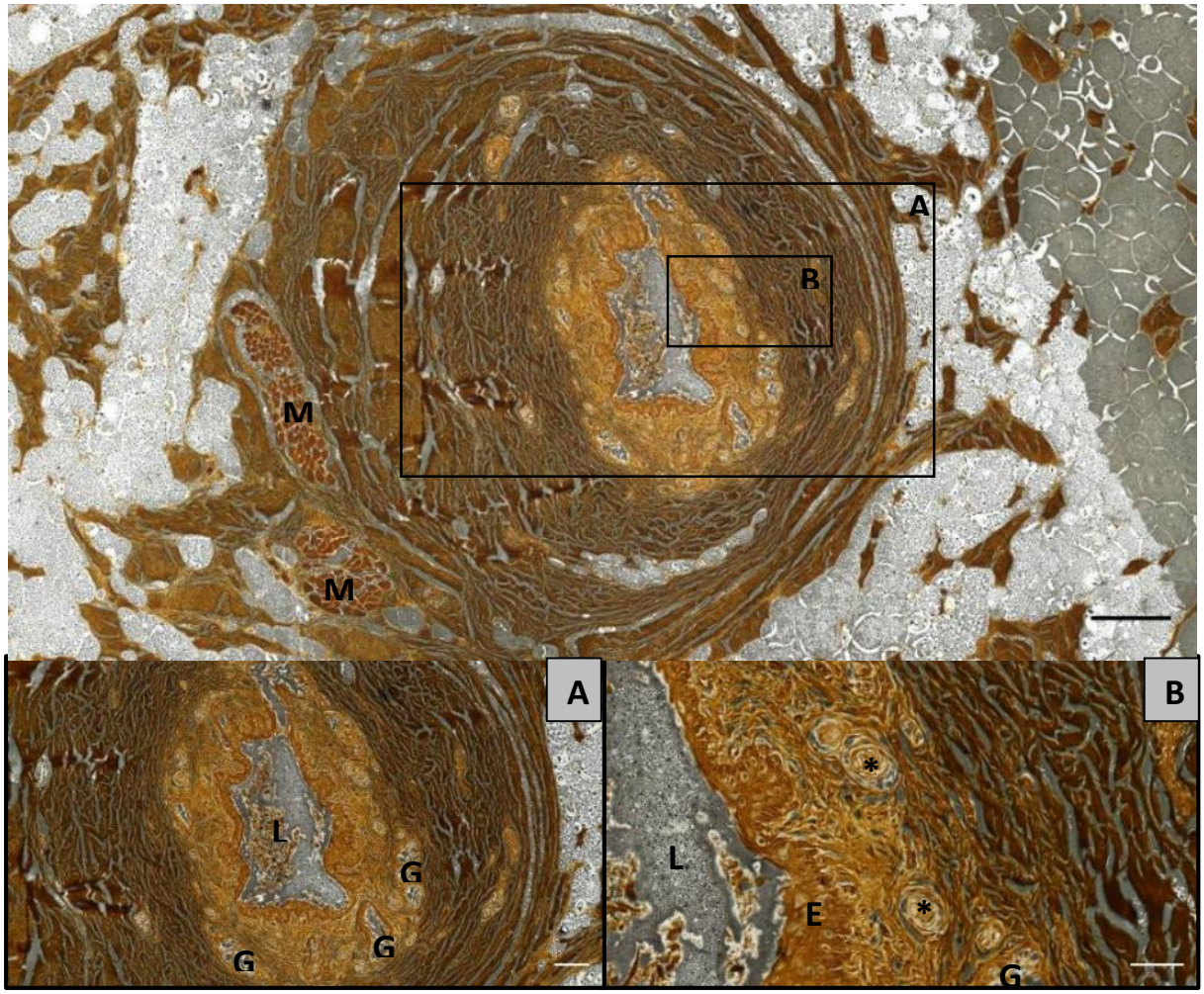

Figure 96. Palmgren´s staining of a histological cross-section through the ear canal of a striped dolphin about 1 cm beneath the surface, at the level of the deep blubber layer. L: lumen, with some desquamated epithelium and possible glandular content; E: epithelium; G: glands; M: striated muscle. Scale bars: Top: 250 µm; A: 100 µm; B: 50 µm.

Figure 97. 3D renderings of the fat and connective tissue around the external ear canal in a striped dolphin. (Caudal view; bottom of the image is lateral (skin), the top is medial (middle ear missing)). In the right image, the fat is made semi-transparent, showing the small amount of connective tissue, situated immediately around the ear canal in the blubber layer. The amount of connective tissue gradually increases until fully replacing all fat tissue at the level of the ear canal curvature. Reddish/white: connective tissue; yellowish: fat; red: muscle

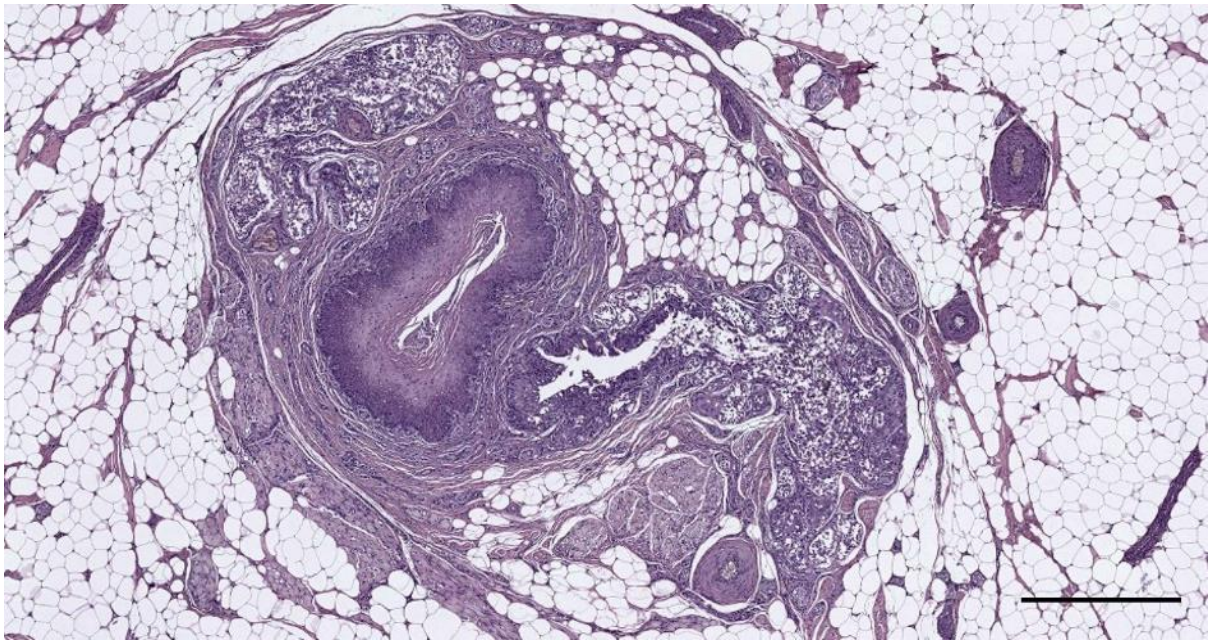

Figure 98. Histological transverse section through the external ear canal of a harbour porpoise at the level of the glands about 1.5 cm beneath the skin (UT1664). Scale bar 500 µm

Figure 99. Histological transverse section (HE staining) of the external ear canal in a Cuvier´s beaked whale at about 1.5 cm beneath the skin (ID429_03, HE) Ear canal surrounded by adipoconnective tissue and a circular connective tissue capsule. Scale bar 1 mm

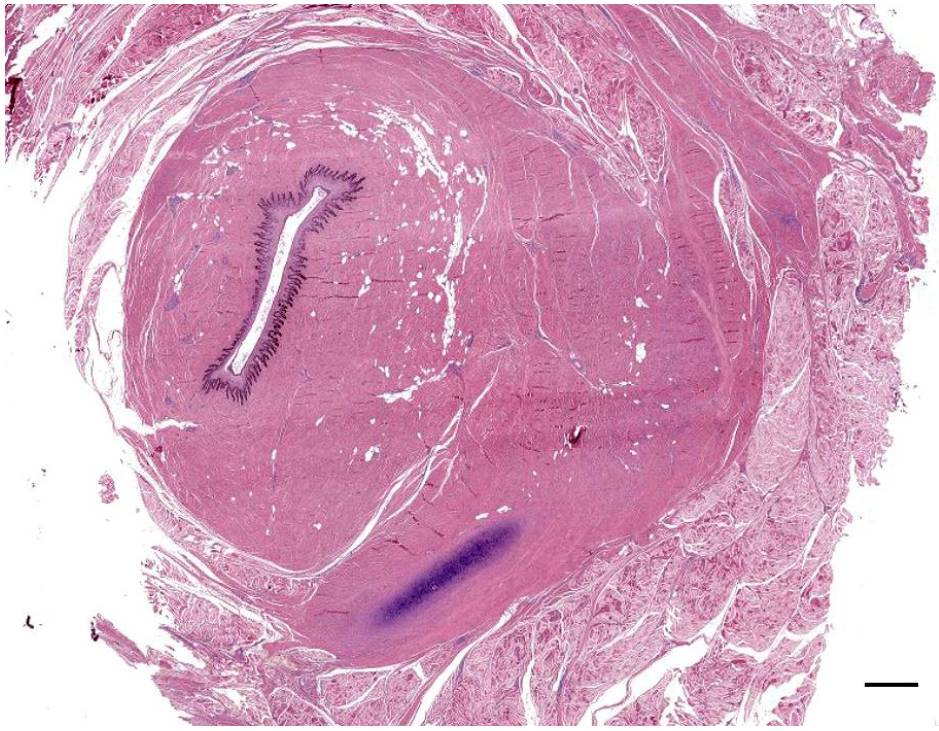

Figure 100. Histological transverse section (HE-staining) through the ear canal of a Cuvier´s beaked whale at about 5 cm beneath the skin (ID429_13) Ear canal and cartilage embedded within dense connective tissue, and surrounded by muscle and connective tissue. Scale bar 1 mm

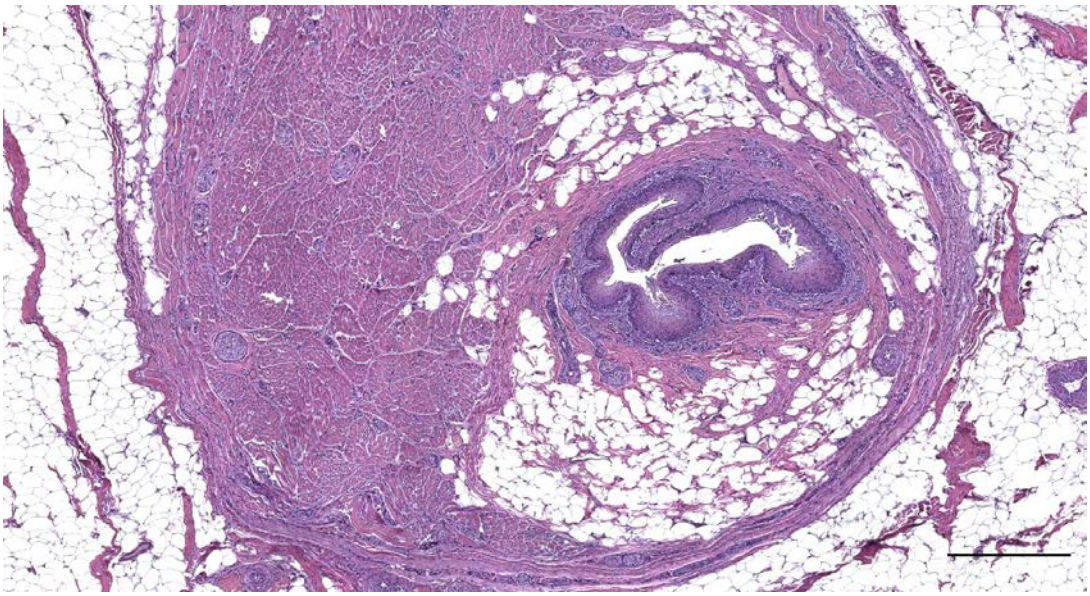

Figure 101. Histological image (HE staining) of a transverse section through the ear canal of a harbour porpoise (UT1709) The ear canal with little subepithelial connective tissue, and a fair amount of fat, is surrounded by a circular capsule in which muscle inserts, similar to the situation in Cuvier´s beaked whale. Scale bar 500 µm.

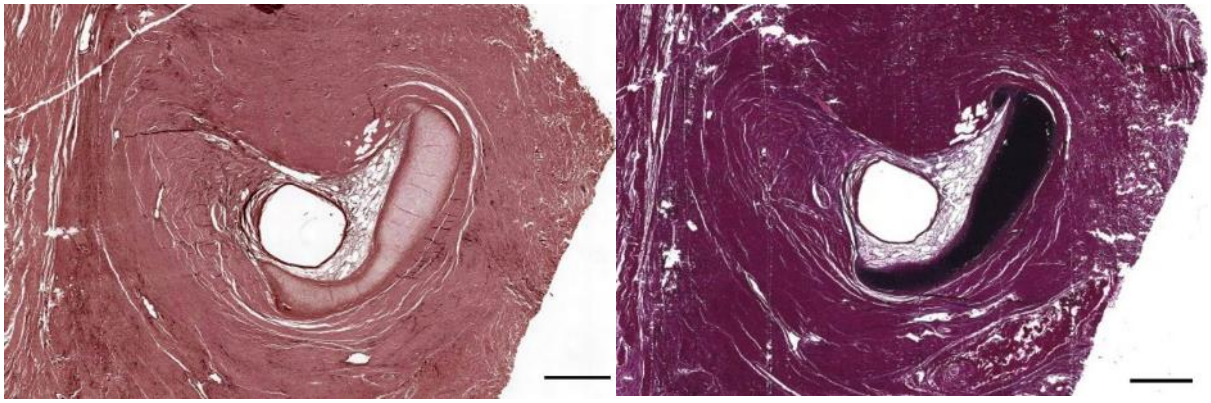

Figure 102. Acid Orcein Giemsa (left) and Weigert´s elastic stain (right) of the external ear canal of a striped dolphin (ID5386), about 5 cm beneath the skin. Scale bars 1 mm

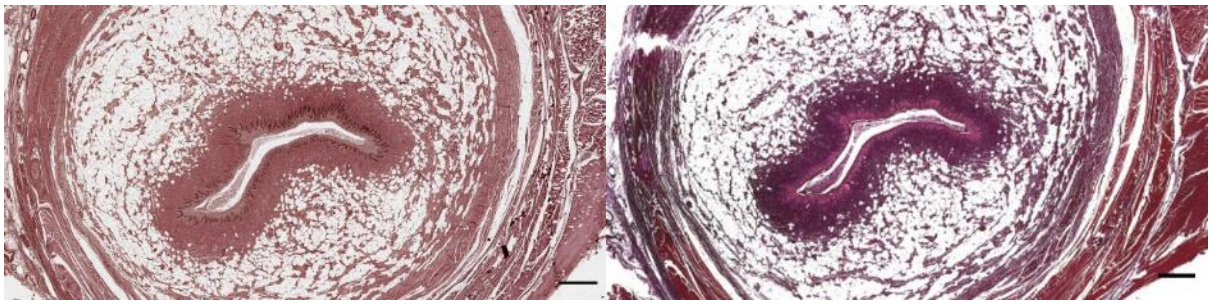

Figure 103. Acid Orcein Giemsa stain (left) and Weigert´s elastic stain (right) of the external ear canal of a Cuvier´s beaked whale (ID429). There are elastic fibres in the circular connective tissue capsule, but not in the connective tissue immediately around the ear canal. Scale bars 1 mm

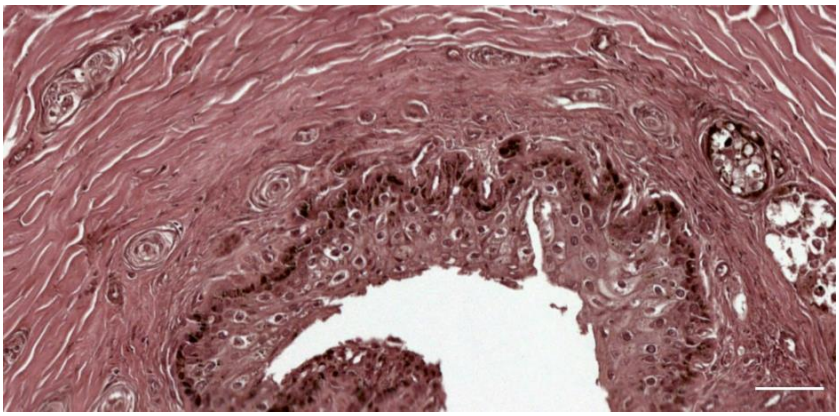

Figure 104. Detail of Figure 105. There are no elastic fibres in the subepithelial connective tissue. Scale bar 50 µm

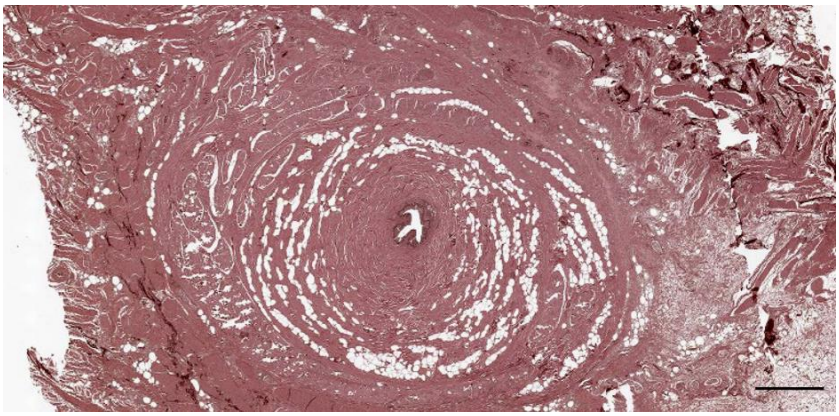

Figure 105. Acid Orcein Giemsa staining of a transverse section through the external ear canal of a striped dolphin (IDSc1), about 2 cm beneath the skin. The elastic fibres are present in the distant connective tissue, not near the external ear canal. Scale bar 1 mm

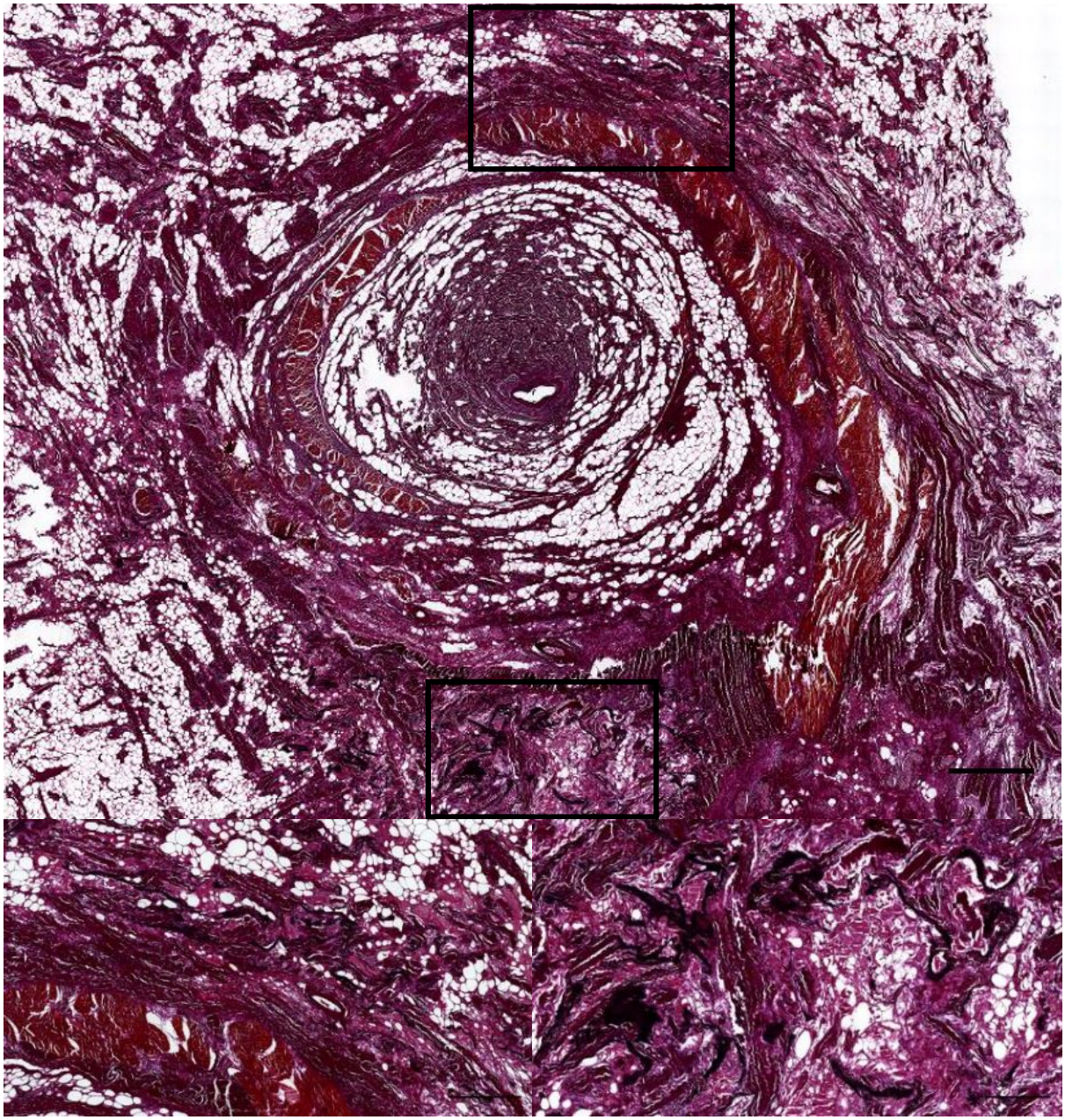

Figure 106. Weigert´s stained cross-section of the ear canal of a striped dolphin about 1.5 cm beneath the skin. The frames in the top images indicate the location of the presence of elastic fibres, as shown in detail in the bottom images. There are elastic fibres (black) in the blubber/adipoconnective tissue peripheral to the musculature (Bottom left), and running in various directions in the adipoconnective tissue sheath (Bottom right). Scale bar Top 1 mm, Bottom bars 500 µm

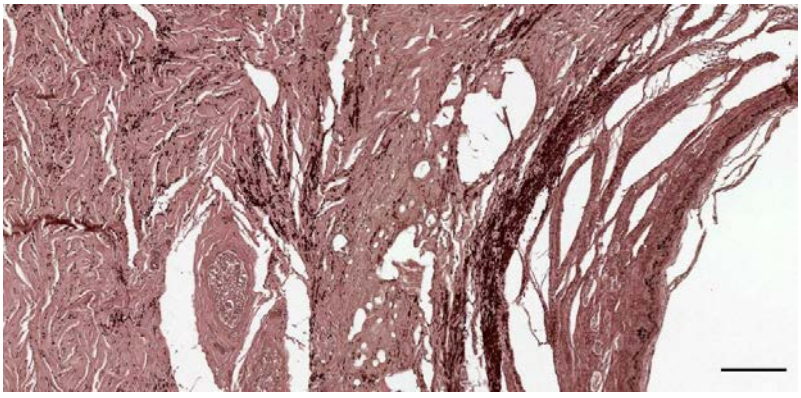

Figure 107. Detail of Figure 102. Elastic fibres in the connective tissue around the ear canal (lumen ear canal on the bottom right). Scale bar 100 µm.

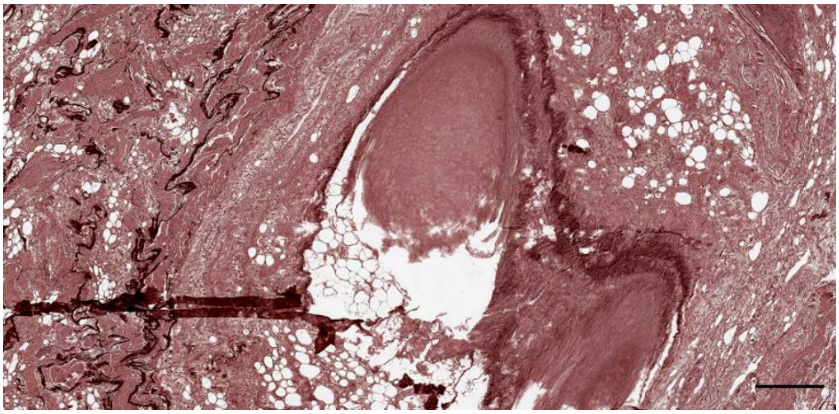

Figure 108. Acid Orcein Giemsa stain showing the presence of elastic fibres in the connective tissue associated with external ear canal of a striped dolphin (ID5386) about 5 cm beneath the skin. There cartilage and perichondrium and the adipoconnective tissue in which it is embedded do not contain elastic fibres. Scale bar 500 µm

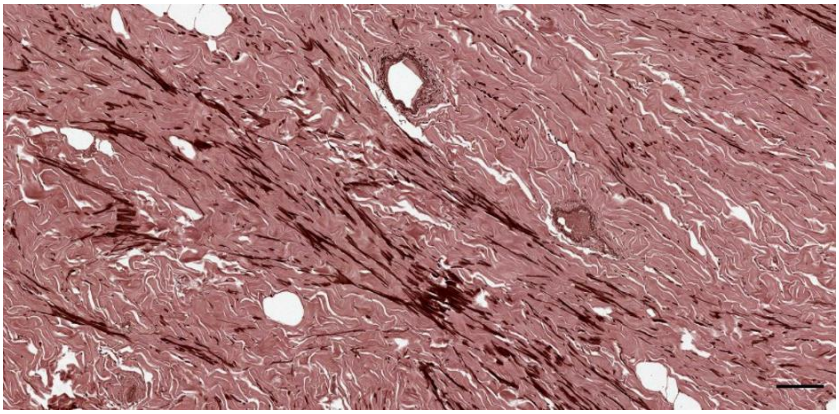

Figure 109. Acid Orcein Giemsa stain showing the presence of elastic fibres in the connective tissue associated with external ear canal of a striped dolphin (ID5386) about 5 cm beneath the skin. Scale bar 100 µm

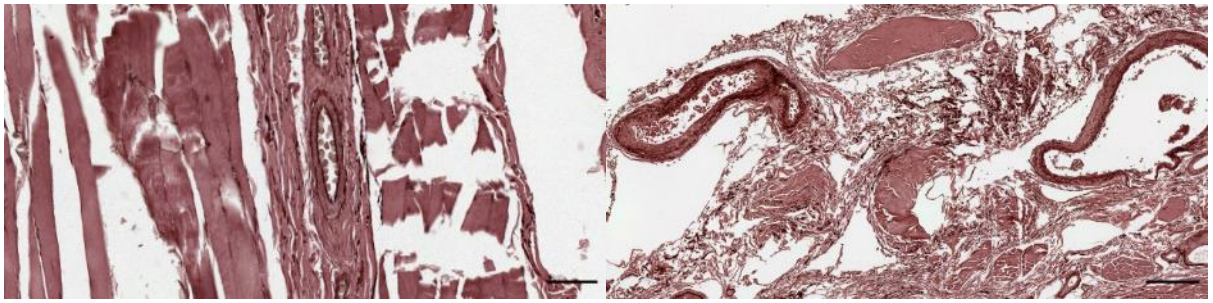

Figure 110. Acid Orcein Giemsa staining of tissues around the ear canal of a Cuvier´s beaked whale (ID429). There are elastic fibres in vascular structures. Scale bar left 50 µm, right 200 µm

2.5 Glands

The glands associated with the ear canal were present over a short distance in the deep blubber layer. The glands were identified as compound acinar or acinotubular glands that produce acidic mucinous substances (Figure 111, Figure 112), which were secreted into the ear canal through excretory ducts lined with a stratified squamous epithelium as a continuation of the ear canal epithelium (Figure 113, Figure 114, Figure 115).

The glands consisted of several secretory units, either separated and distributed on various sides of the ear canal (Figure 116, Figure 117) or combined into a seemingly single large unit with various trabeculae (Figure 118, Figure 113).

All glands in all species studied stained positive for Alcian blue (Figure 119). Alcian blue with a pH of 1 was used to stain highly acidic structures, and a pH of 2.5 to stain less acidic structures. In both tests, the cytoplasm of secretory cells stained blue, although there was a subjectively slightly more intense stain with the Alcian blue pH 1 indicating alcianophilic components as highly acidic substances. As Alcian blue stains both sulfated and carboxylated acid mucopolysaccharides and sialomucins (glycoproteins), with stain intensity differences associated the Ph, the results of the stain indicated the presence of acidic mucinous substances within the acini of the glandular structures. However, more detail about their nature could not be concluded with these techniques.

Inside the secretory units, there was often the presence of a single layer of secretory cells, indicating the method of secretion to be apocrine or merocrine, like ceruminous glands. On the other hand, there were also indications of a “greasy degeneration”, which in its turn could be an indication of holocrine secretion, a property of sebaceous glands (Figure 120). However, in all animals, there were several signs of degeneration due to post-mortem decay, including apoptotic cells with cystic degeneration, marginalization of chromatin, and cellular debris within the ducts’ lumen, all which complicated the morphological identification of types of cells and tissues. The definite nature of the glands, the secretion types and morphological distinction between excretory and secretory unit could often not be concluded with the applied techniques and due to the tissue degeneration (e.g. Figure 121). It could also not be excluded that there were various types of glands, ceruminous and sebaceous, as in the ear canal of terrestrial mammals (e.g. Figure 122, Figure 123).

Similarly, in some cases, the difference between the ear canal and its squamous epithelium, and glandular excretory ducts (and even secretory units) was not clear. Some of the smaller toothed whales, striped dolphin and common dolphin, showed a very complex lumen of the ear canal with no differences between excretory ducts of the glands and the ear canal. (e.g. Figure 124)

Of the two specimens of bottlenose dolphin in the study, both of which were in a considerate degeneration condition state, one showed the general confirmation of glandular structures as found in other delphinids and harbour porpoise. In contrast, the situation in the other animal was less clear, with less distinction between the ear canal and glandular units and an apparent change in the epithelial nature of the EAM lining (Figure 125). In this latter animal, the epithelium of the ear canal showed a transition from squamous to single columnar or pseudostratified (and likely glandular), back to squamous, for 1.5-2 cm (Figure 69, Figure 126, Figure 127, Figure 128, Figure 129)(For more details, see Annex bottlenose dolphin ID444). At the same time, there were also ´standard´ glandular

structures separate from the ear canal, with pyknotic nuclei and eosinophilic cytoplasm in the secretory units (Figure 130, Figure 131). Some aspects of this configuration were similar to the striped dolphin in degenerated states.

In all of the animals, the glandular structures showed some degree of degeneration, together with the presence of pyknotic nuclei inside the secretory units and secreted into the ear canal lumen (not known if this was a pre- or post-mortem finding)(Figure 116, Figure 132, Figure 133, Figure 131). Many sections showed the glandular epithelium with pyknotic nuclei (Figure 135), which could indicate in-vivo degenerative processes. Within the secretory units, there were cells with pyknotic nuclei in almost all animals studied, independent of sex, age, decomposition state, and general pathological findings (Figure 130, Figure 131, Figure 134).

In few animals, the glands contained a mineralized, impacted content, likely due to a prolonged stay of the secretory product within the lumen (Figure 49, Figure 70, Figure 136, Figure 137, Figure 138, Figure 139, Figure 140, Figure 141, Figure 124). The epithelium was not glandular, but a stratified squamous non-keratinized epithelium. It is unsure if this could be a form of metaplasia, or that the tissue is a non-secretory excretory duct.

We did not identify the specific innervation of the glandular structures. We did notice the presence of lamellar corpuscles in the glandular stroma, in between the secretory units and besides the excretory ducts (Figure 114, Figure 115).

The findings in the long-finned pilot whale were in line with the configuration of glands as in smaller toothed whale (e.g. Figure 142). In contrast, no glands were found in the incompletely dissected ear canal of any of the two Cuvier´s beaked whales studied. It was not excluded that these could have been missed, as there were indications of glandular product in the lumen of the ear canal in superficial sections (Figure 56, Figure 66).

The single common dolphin presented glandular structures with fresh and degenerated glandular cells, lipid content, and also mineralized content (indicating stasis) (Figure 143). Lateral to the glands, there was an artificial lumen surrounded by excretory ducts, while in deeper sections, the distinction between ear canal and glands is not clear (Figure 144, Figure 145). We based the distinction on the shape of the basement membrane, which is undulating in the superficial ear canal, compared to smooth and round in sections through glandular structures (Figure 146), while the evolution of the glands was occasionally tracked (Figure 147). Glandular content was often cellular (cells with pyknotic nuclei) in places were the basement membrane was no longer intact (artefact) and mineralized (indicating stasis). There were also glandular cells and some inflammatory cells inside the ear canal lumen.

Figure 111. Image of a 3D rendering of the ear canal epithelium and glands in a striped dolphin (ID127565). Note the ventral curvature of the ear canal on its course to the TP complex

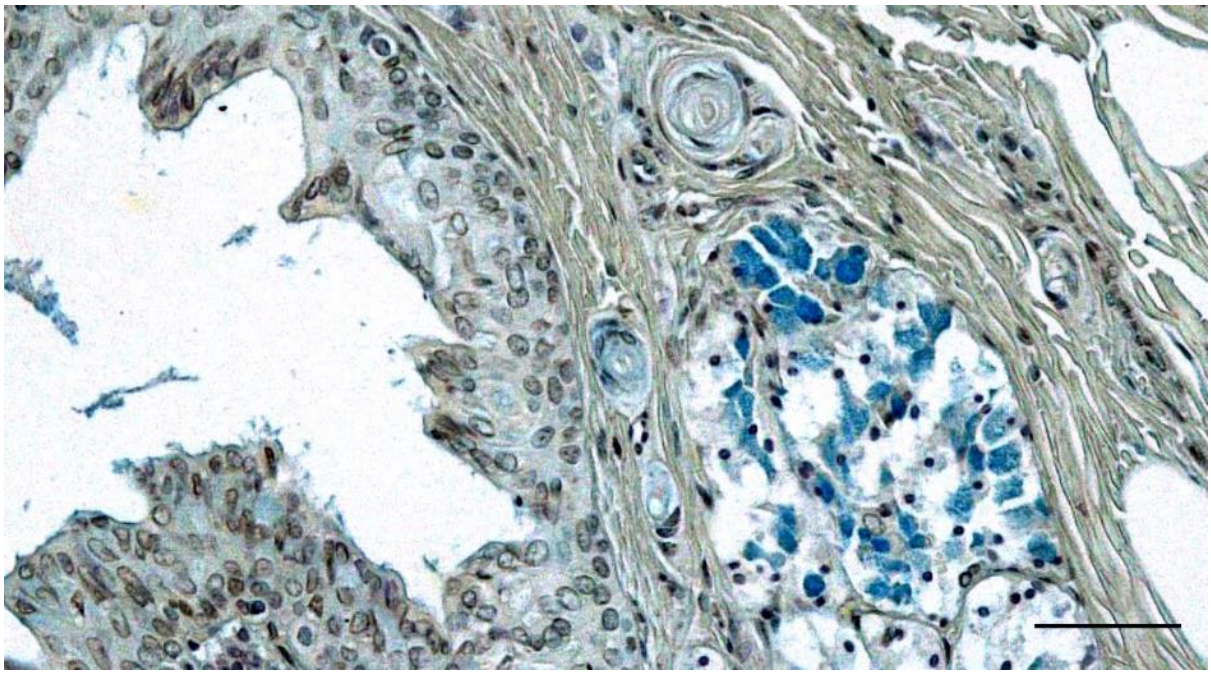

Figure 112. Histological image (Alcian blue staining) of a transverse section through the right ear canal of a striped dolphin at about 2 cm beneath the skin (ID274/18_R4). Ear canal lumen and epithelium, glands, and lamellar corpuscles. Scale bar 50 µm

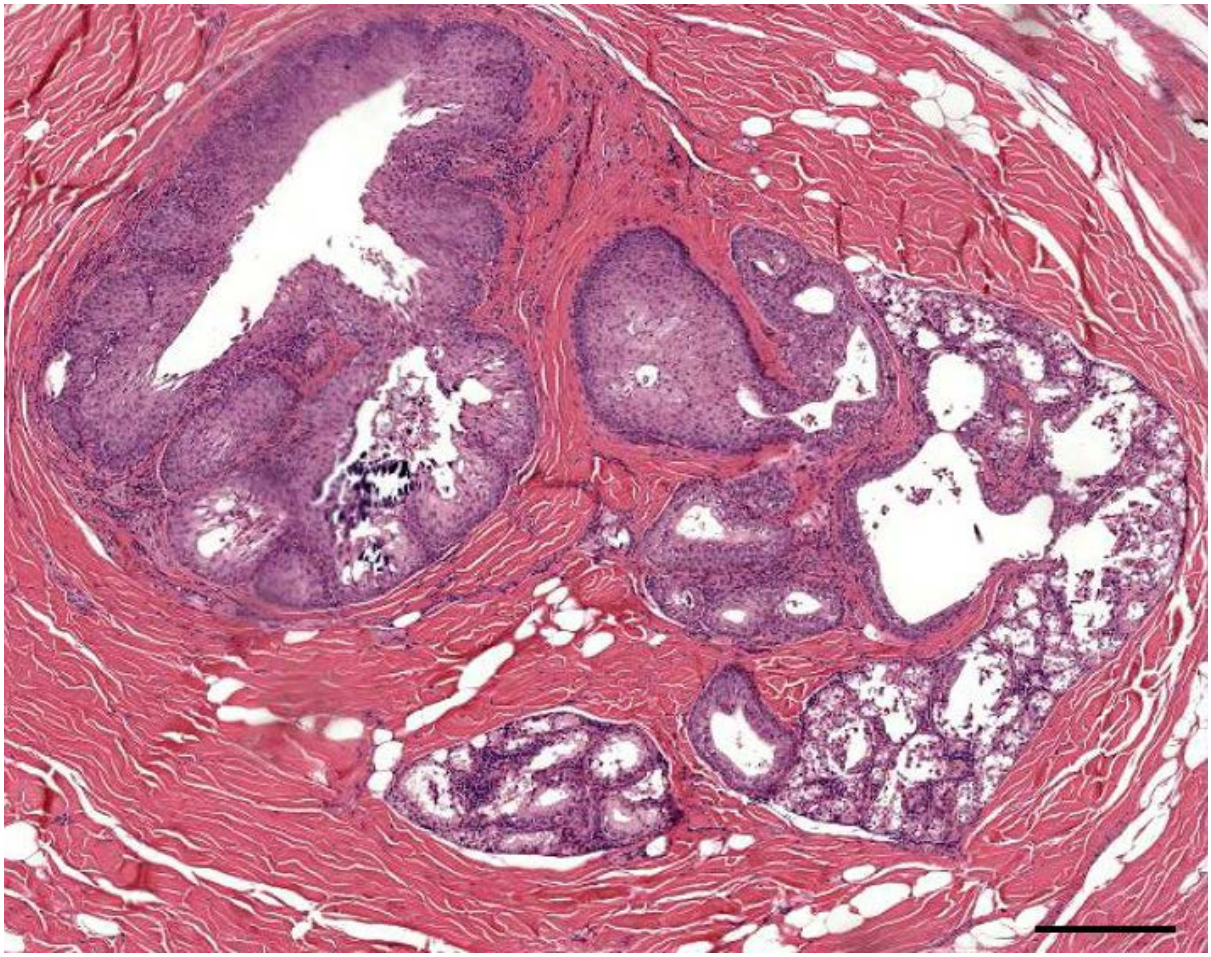

Figure 113. Histological image (HE staining) of a transverse section through the right ear canal of a common dolphin at about 1 cm beneath the skin (169_17_R4c). Note the glands and excretory ducts. Scale bar 300 µm

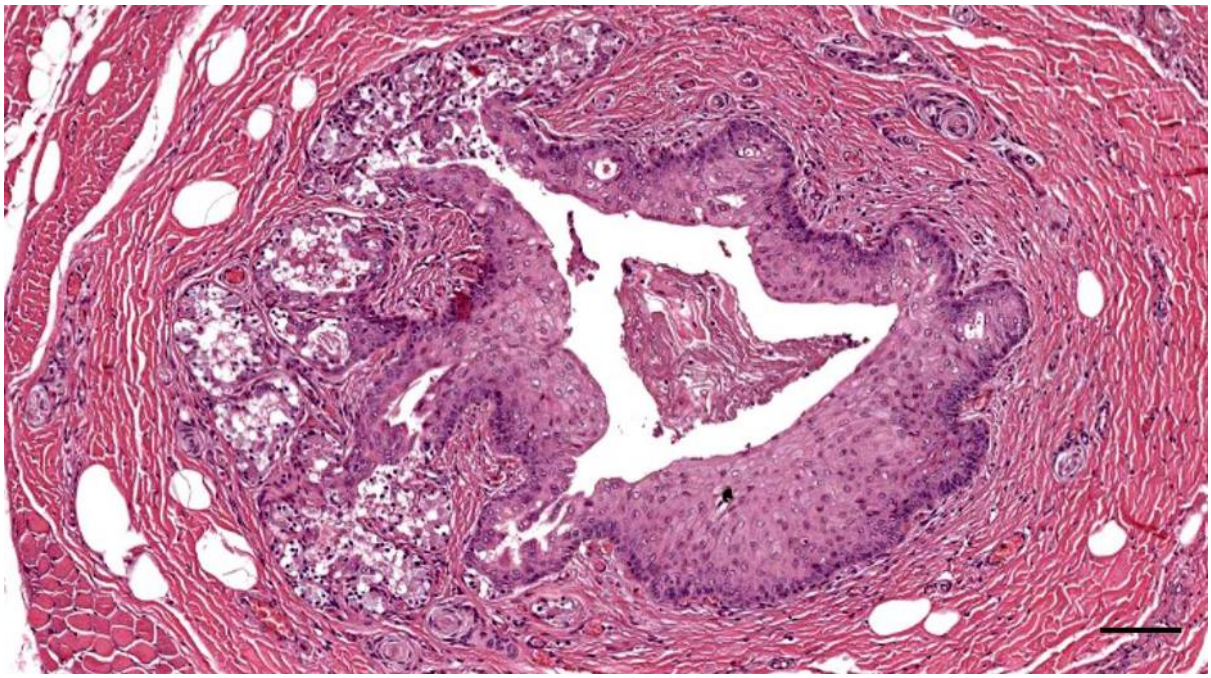

Figure 114. Histological transverse section (HE staining) through the ear canal of a striped dolphin at about 1.5 cm beneath the skin (274_18_L3). Glands with three visible excretory ducts (one is continuous in this image). Also, note the pyknotic nuclei of the glandular cells. Scale bar 100 µm

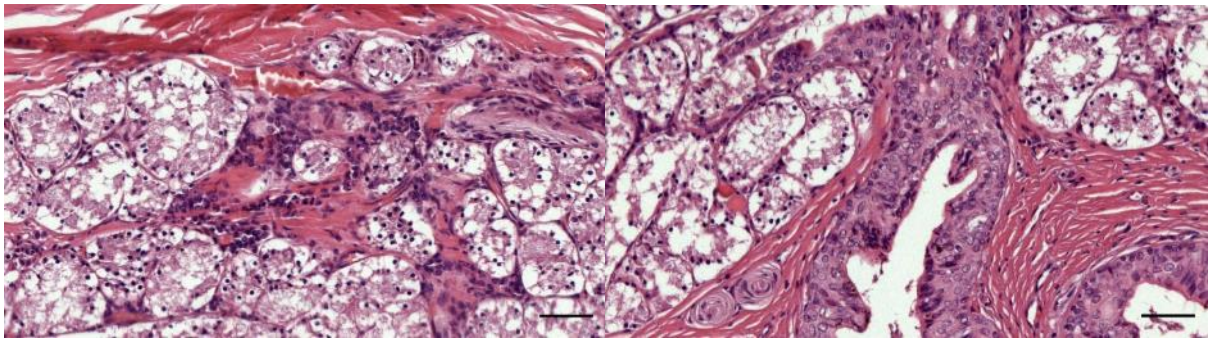

Figure 115. Two detail images (HE stain) of auricular glandular units. Note the mononuclear cells in the glandular stroma, the glandular cells pyknotic nuclei, and the excretory duct into the ear canal with the presence of lamellar corpuscles. Scale bar 50 µm

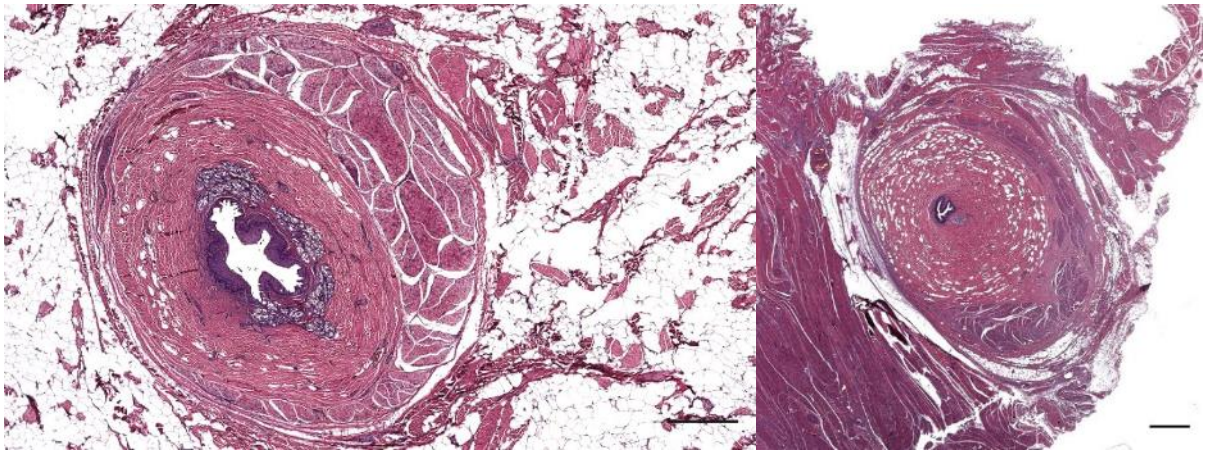

Figure 116. Histological images (HE staining) of two transverse section through the ear canal of a striped dolphin (ID44/17) at about 2.5 and 3.5 cm beneath the skin. Note the change in the ratio between fat and connective tissue that surrounds the ear canal, and also the presence of muscles inserting in the adipoconnective tissue sheath. Scale bars 500 µm

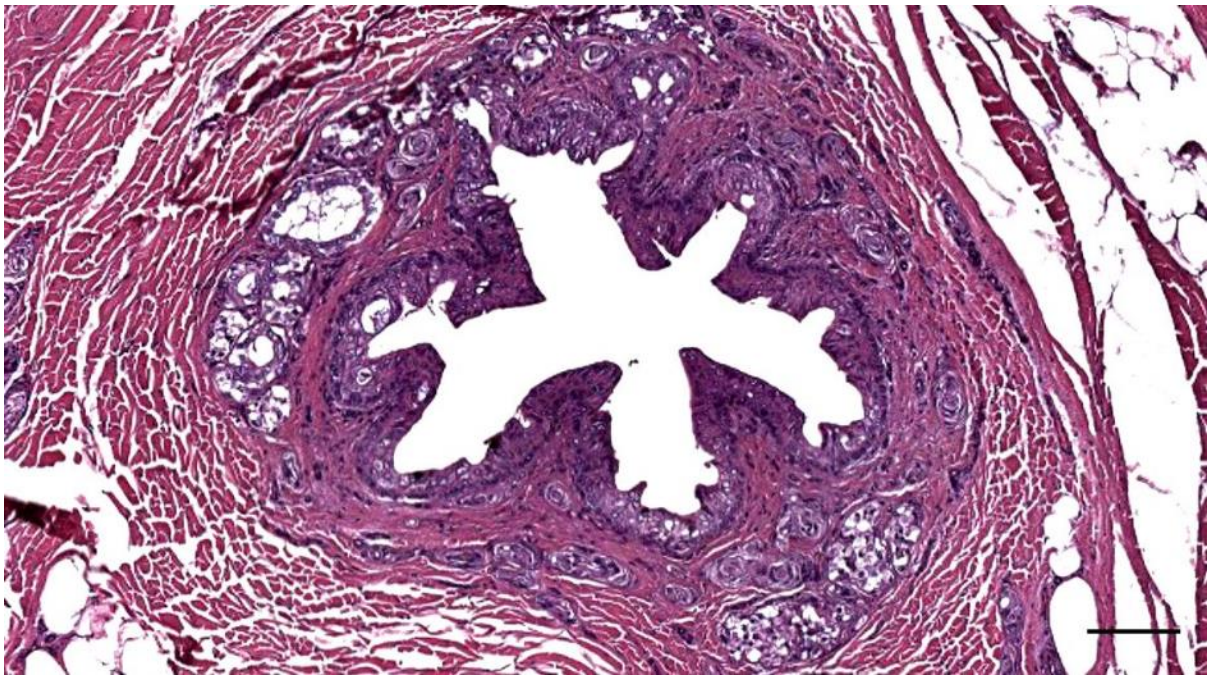

Figure 117. Histological transverse section through the ear canal of a striped dolphin at about 1 cm beneath the skin (509/17_L2). Glandular structures in the deep part of the blubber layer. (Tissue is in an advanced state of decomposition). Scale bar 100 µm.

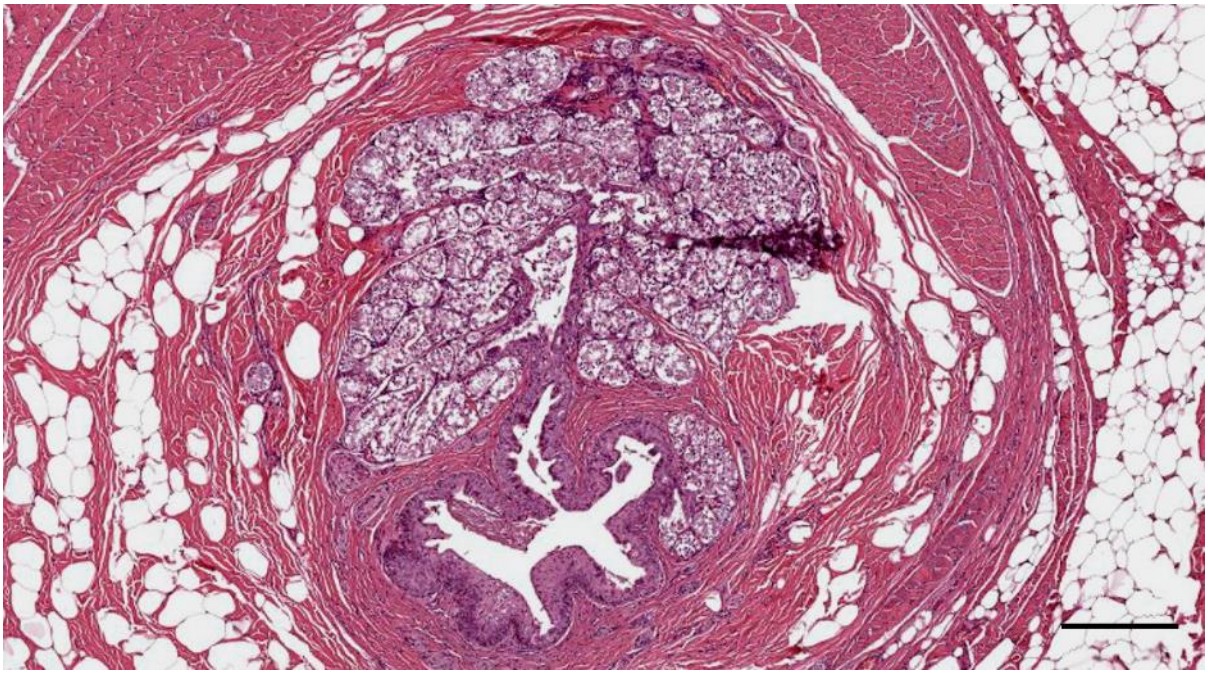

Figure 118. Histological transverse section through the ear canal of a striped dolphin at about 2 cm beneath the skin (274/18_L4). Scale bar 300 µm

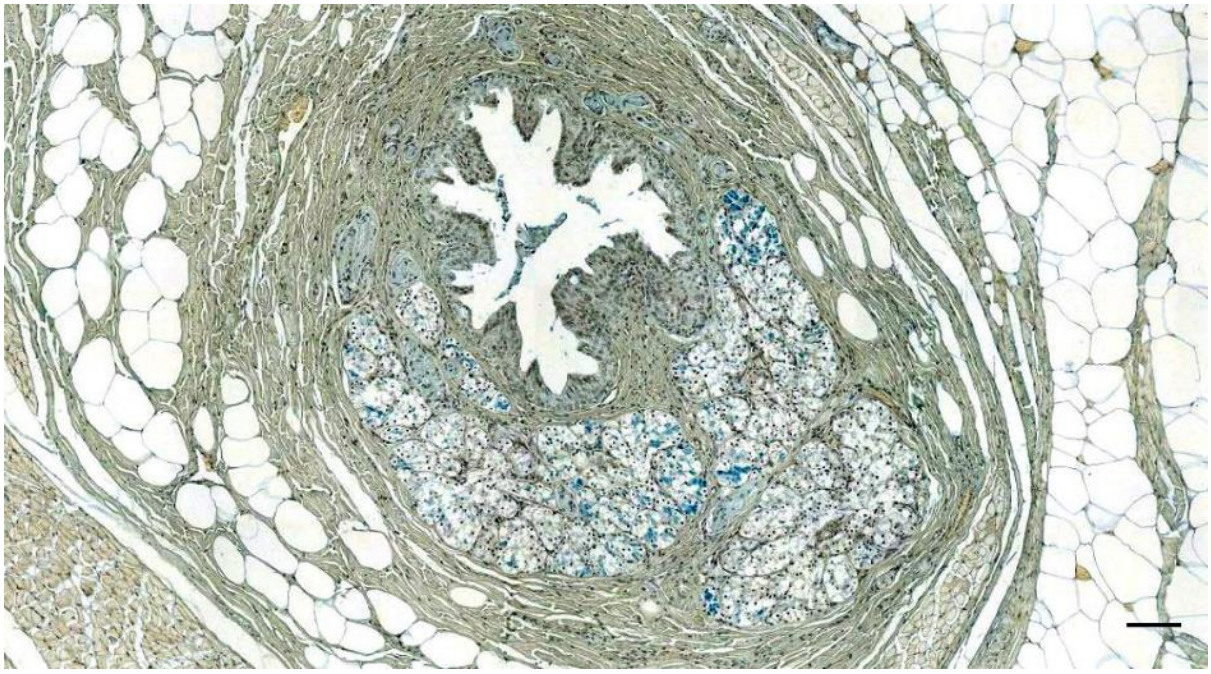

Figure 119. Histological image (Alcian blue staining) of a transverse section through the right ear canal of a striped dolphin at about 2 cm beneath the skin (ID274/18_R4). Scale bar 100 µm

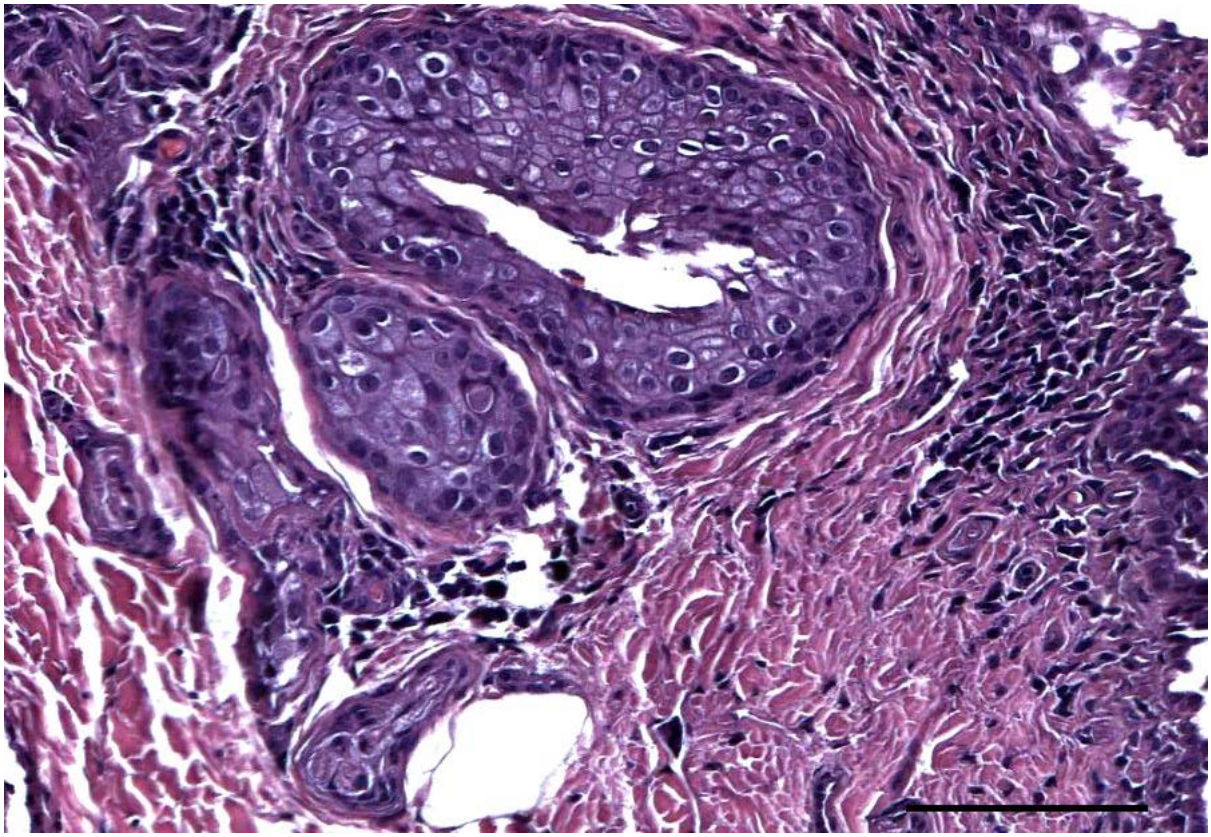

Figure 120. Histological transverse section (HE staining) through the ear canal of a striped dolphin at about 2.5 cm beneath the skin (ID77/18_R5). Excretory ducts as the epithelium with stratified squamous epithelium. Also, note the presence of mononuclear cells in the subepithelial tissue and amongst the glands. Scale bar 100 µm

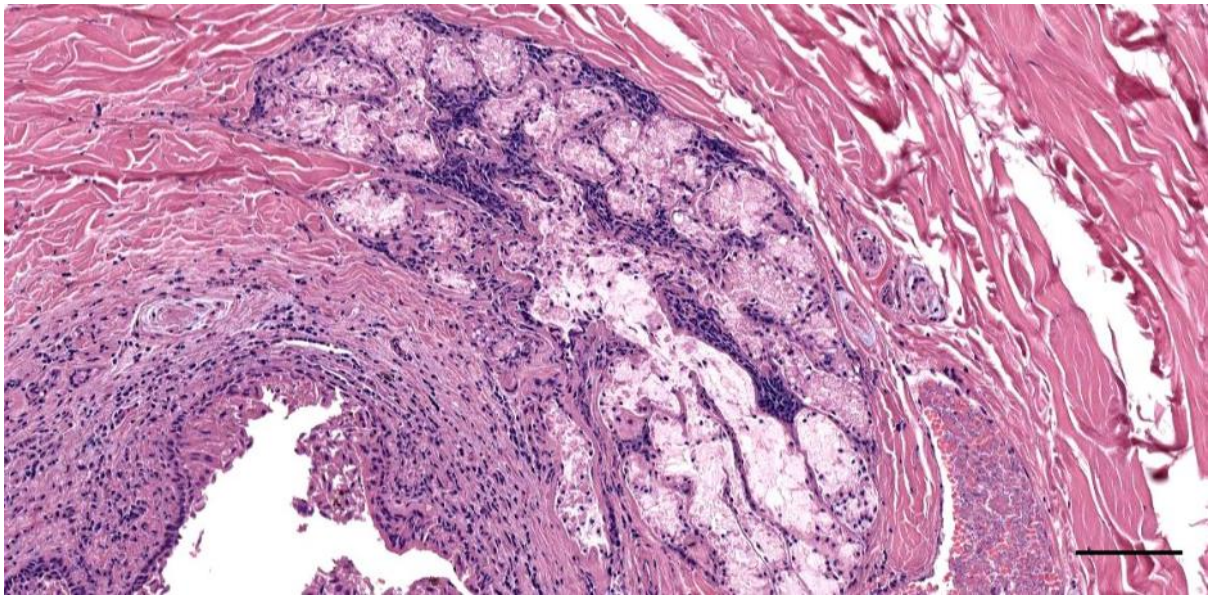

Figure 121. Histological transverse section (HE staining) through the ear canal of a long-finned pilot whale at about 5 cm beneath the skin. Note the ear canal, glandular structures, and mononuclear cells. Scale bar 100 µm

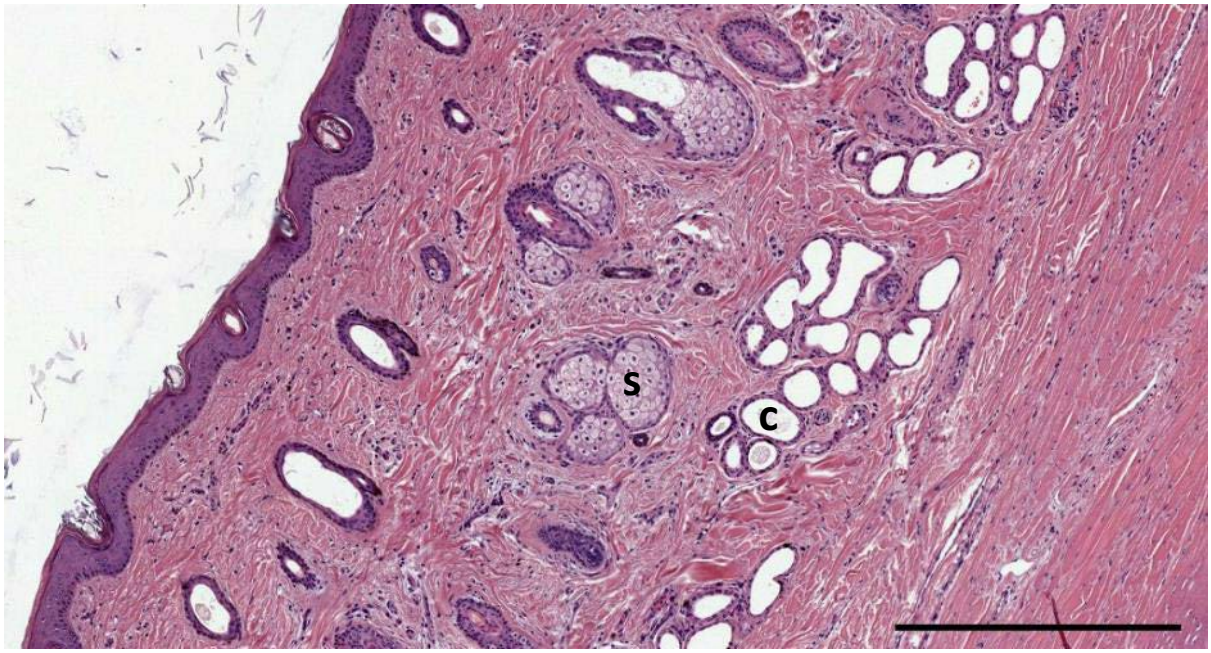

Figure 122. Histological detail image (HE) of the presence of sebaceous (s) and ceruminous (c) glands in the ear canal of a northern giraffe. Scale bar 500 µm

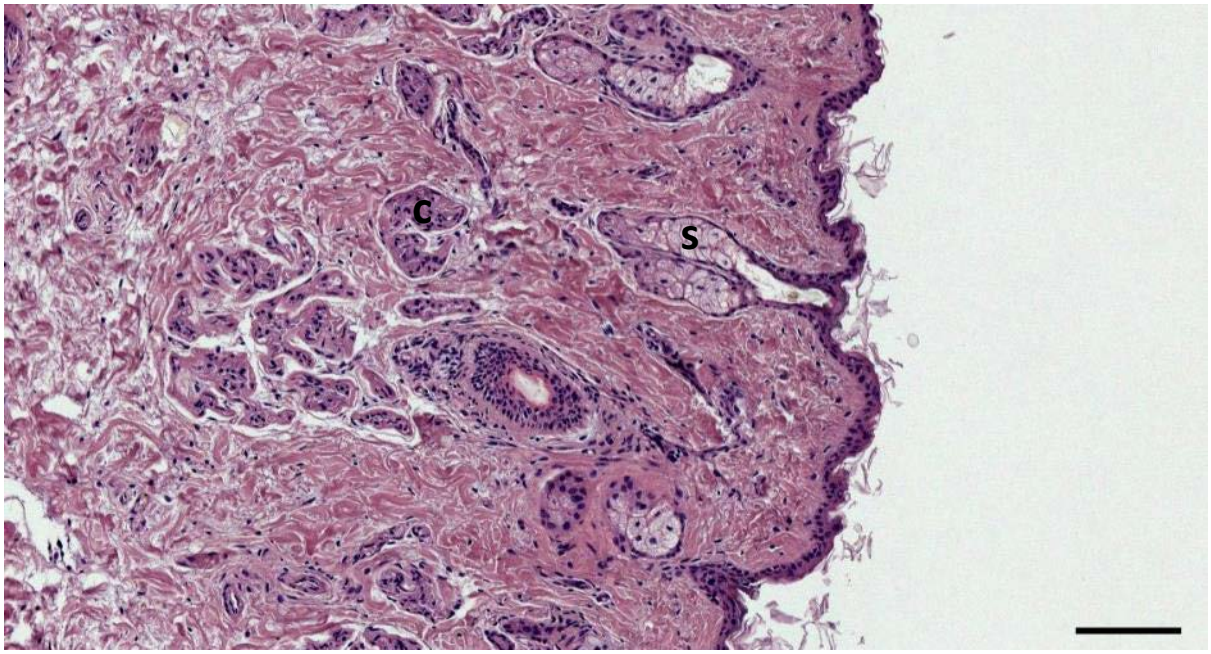

Figure 123. Histological detail image (HE) of the presence of sebaceous (s) and ceruminous (c) glands in the ear canal of a roe deer. Scale bar 100 µm

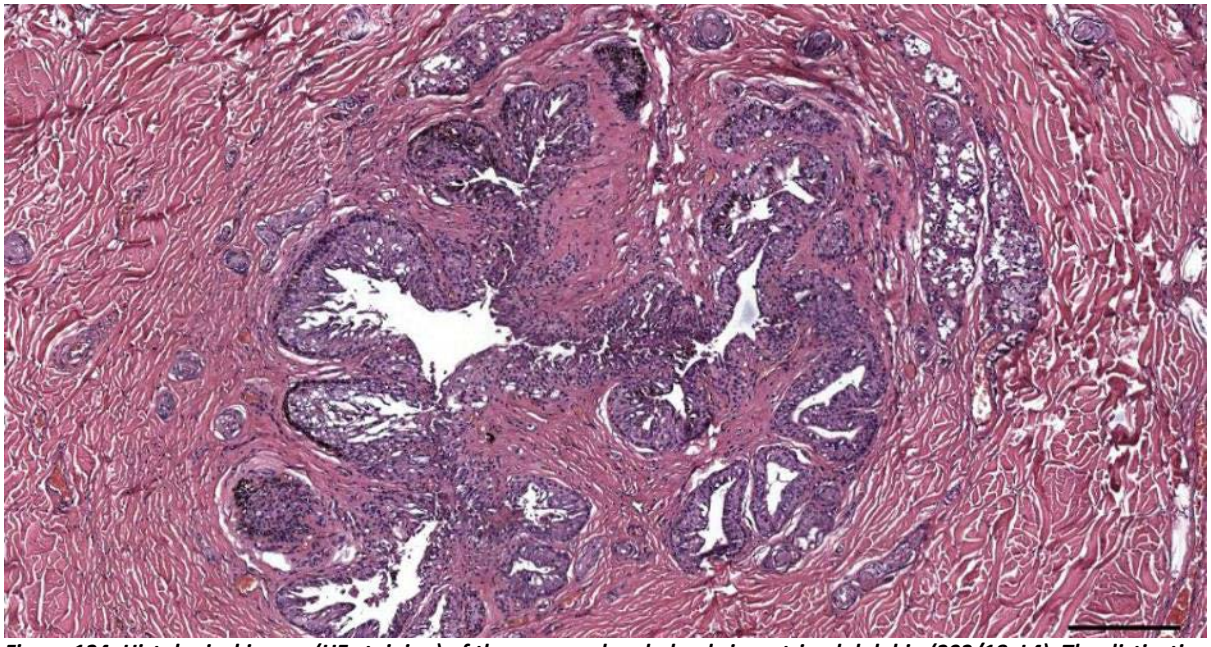

Figure 124. Histological image (HE staining) of the ear canal and glands in a striped dolphin (292/18_L4). The distinction between the two is not clear. Scale bar 200 µm

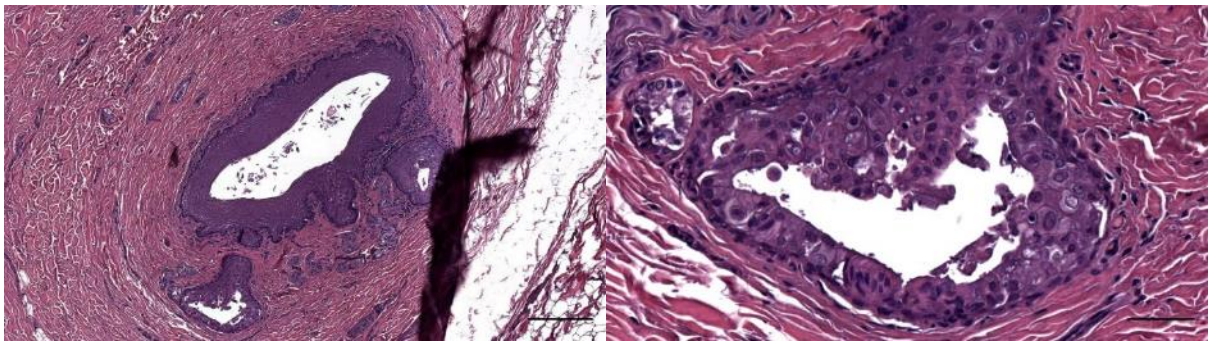

Figure 125. Histological transverse section (HE staining) through the ear canal of a bottlenose dolphin at about 3 cm beneath the skin (457_R6). Scale bar 250 µm (left), 50 µm (right)

Figure 126. Histological image (Alcian blue staining) of a transverse section through the ear canal of a bottlenose dolphin (ID444_R6) at the level of the glands, about 3 cm beneath the skin. Note the presence of glands and inflammation. Scale bar 200 µm

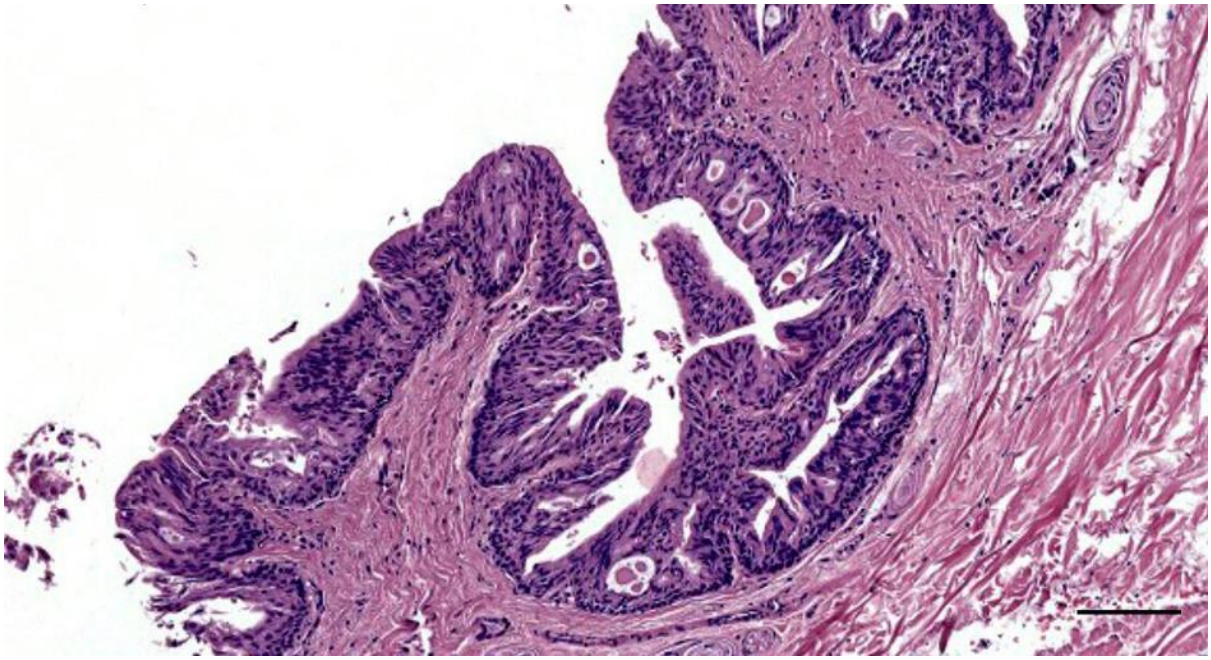

Figure 127. Histological transverse section through the ear canal of a bottlenose dolphin at about 3.5 cm beneath the skin (444_L7): Ear canal and glands. Note the apoptotic changes in the glandular epithelium. Scale bar 100 µm

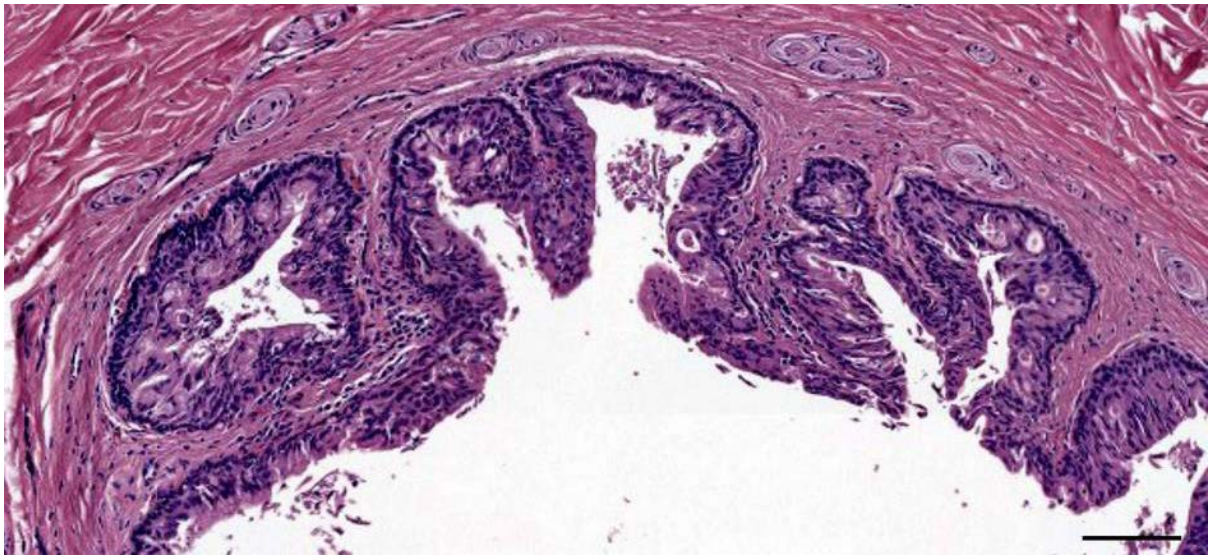

Figure 128. Histological transverse section (HE staining) through the ear canal of a striped dolphin at about 4 cm beneath the skin (444_L8). Scale bar 100 µm

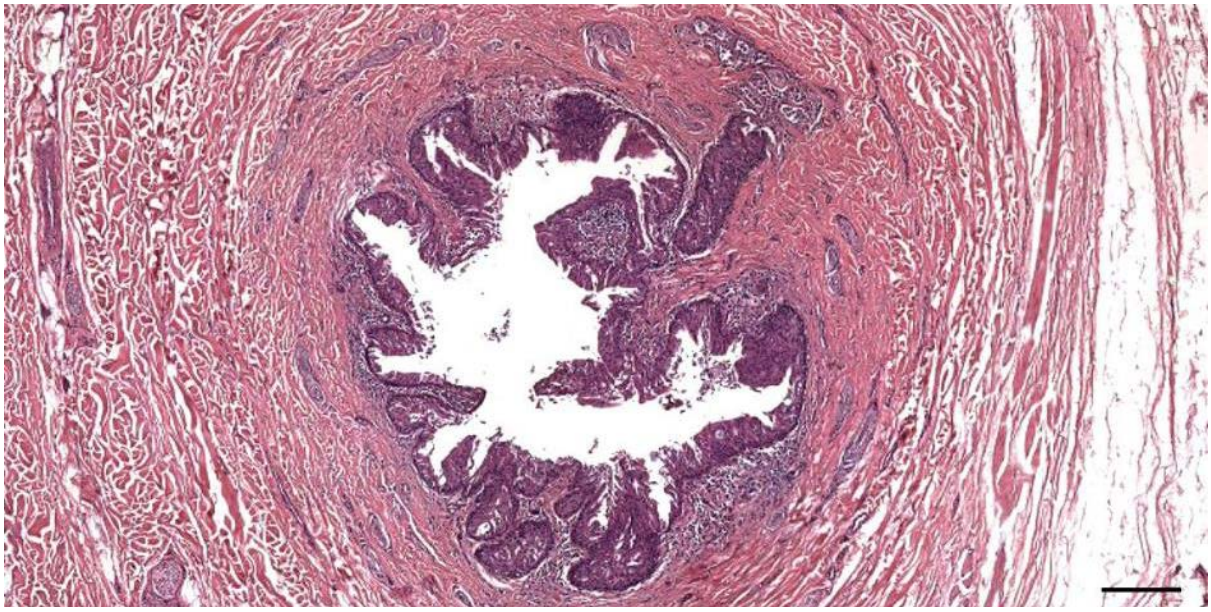

Figure 129. Histological transverse section (HE staining) through the ear canal of a striped dolphin at about 3 cm beneath the skin (444_R06). Scale bar 200 µm

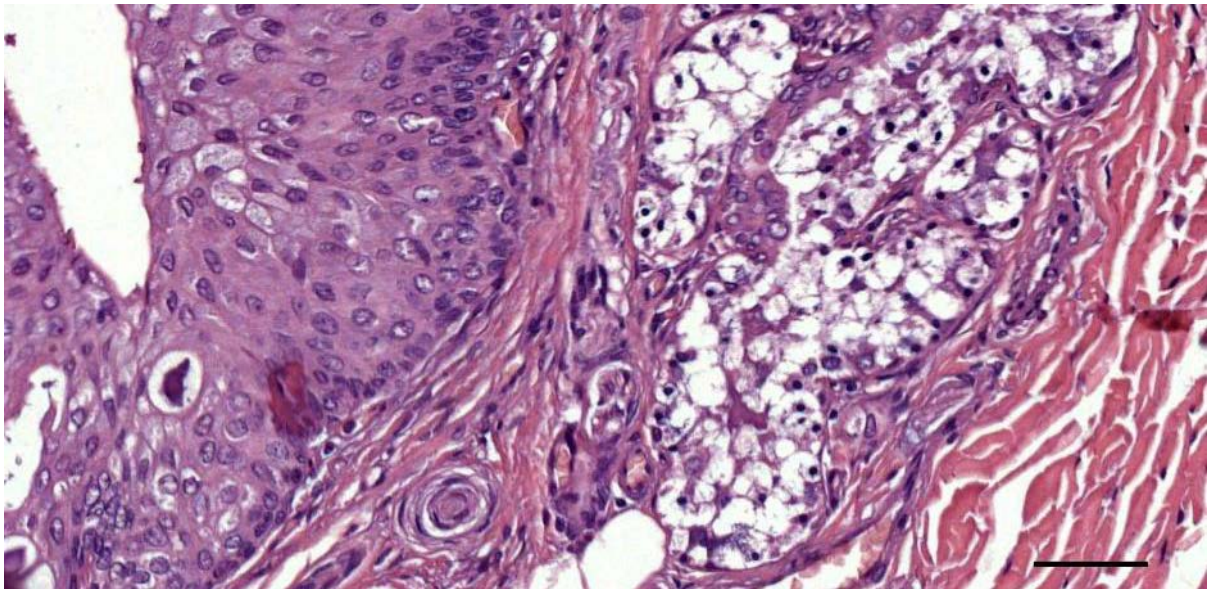

Figure 130. Histological transverse section (HE staining) through the ear canal of a striped dolphin at about 1.5 cm beneath the skin (ID274_18_R3) Glands with pyknotic nuclei. Also, note the presence of lamellar corpuscles between epithelium and glands. Scale bar 50 µm

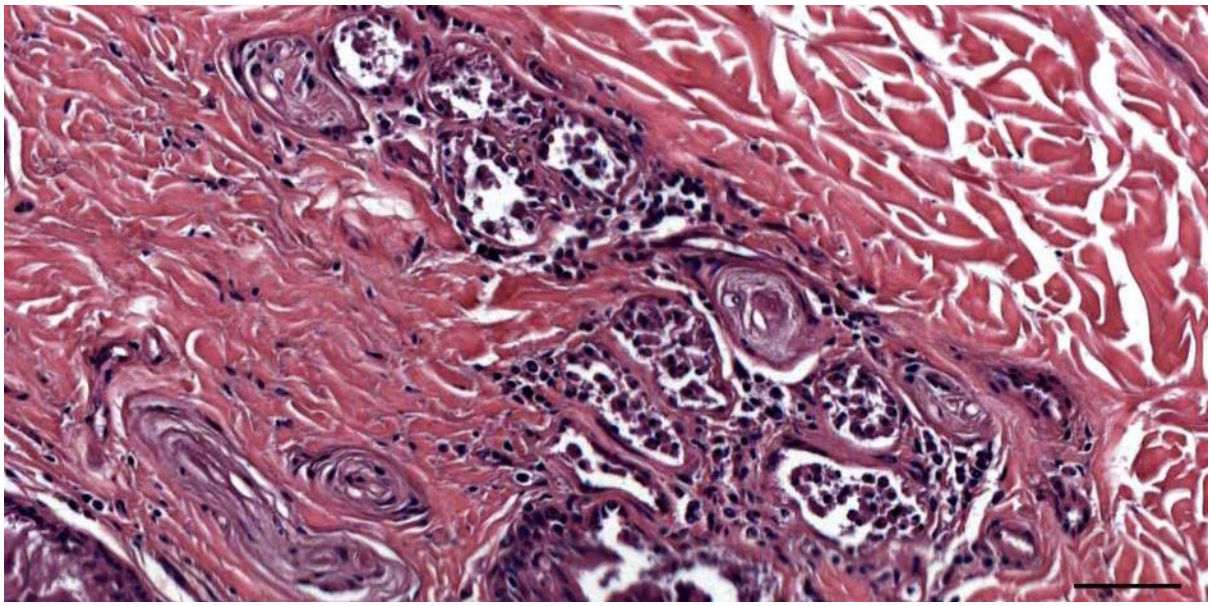

Figure 131. Histological detail image (HE staining) of glands with pyknotic nuclei associated with the ear canal of a bottlenose dolphin at about 3 cm beneath the skin (444_R06). Scale bar 50 µm

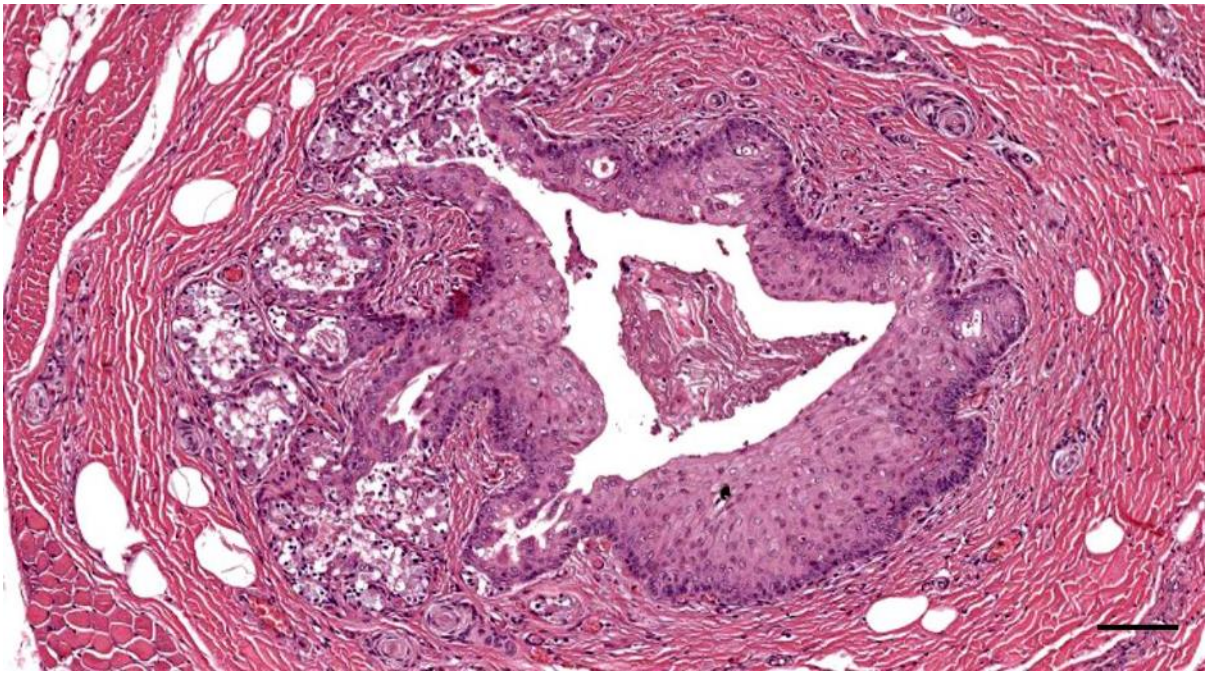

Figure 132. Histological cross-section (HE staining) of a striped dolphin ear canal and glands with pyknotic nuclei, at about 1.5 cm beneath the skin (274/18_L3). Scale bar 100 µm

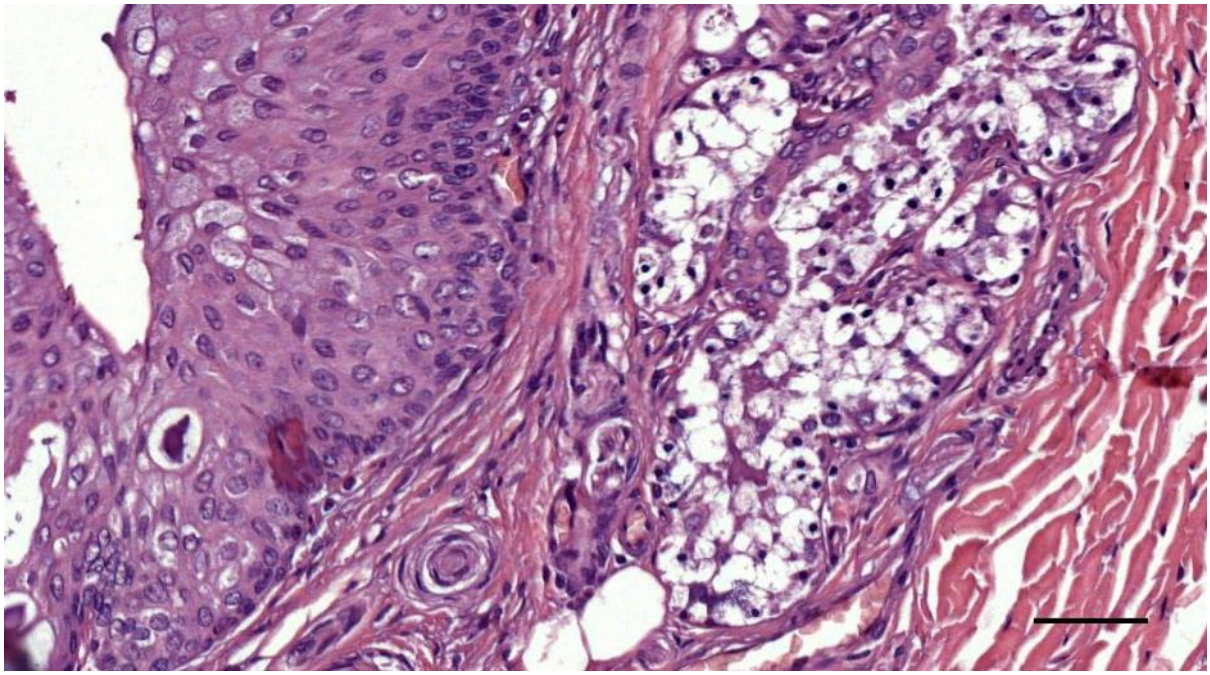

Figure 133. Histological detail (HE staining) of the auricular glands containing pyknotic nuclei in the secretory units (274/18_R3). Scale bar 50 µm

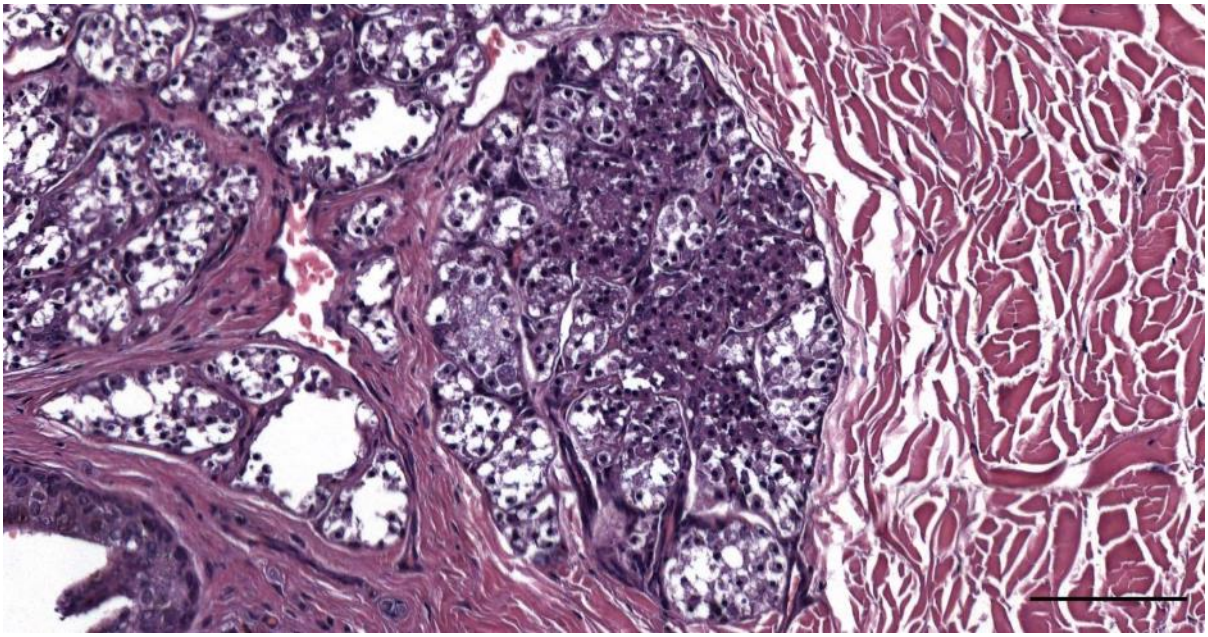

Figure 134. Histological detail image (HE staining) of glands associated with the ear canal of a striped dolphin at about 2 cm beneath the skin (44/17_B4). Scale bar 100 µm

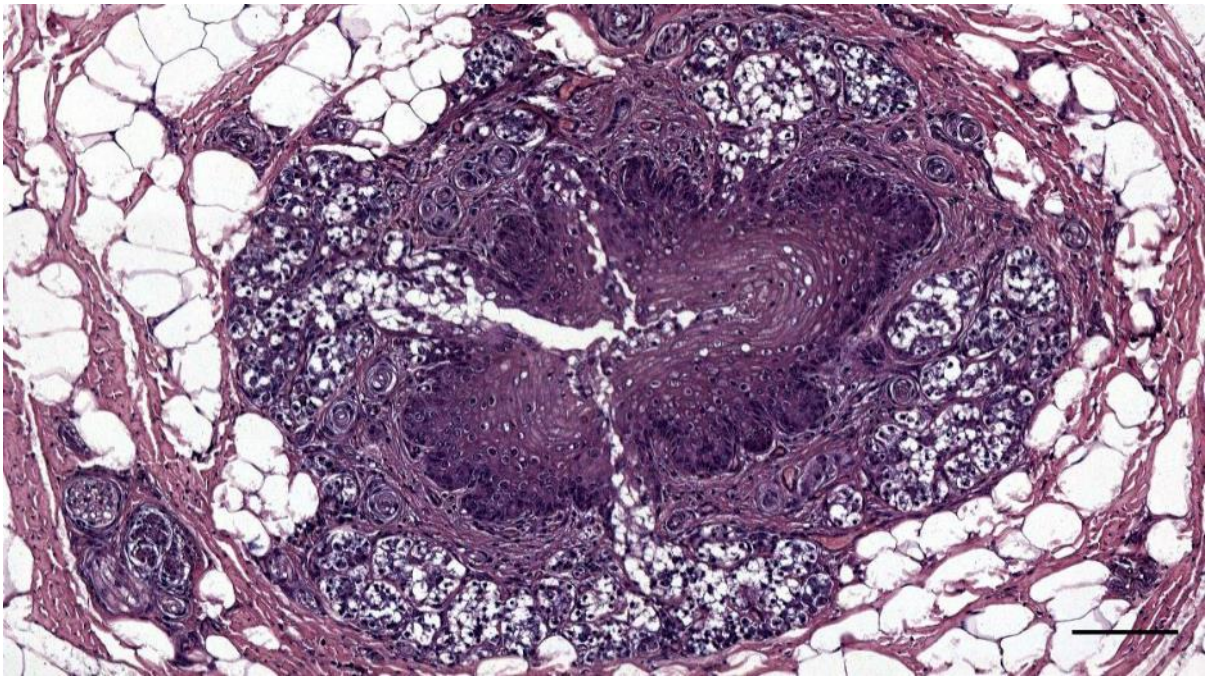

Figure 135. Histological cross-section (HE staining) of the right ear canal and glands in a striped dolphin, at about 1.5 cm beneath the skin (449_R3). Scale bar 200 µm

Figure 136. Histological transverse section (HE staining) through the ear canal of a striped dolphin at about 1 cm beneath the skin (Sc1_02). Scale bar 100 µm

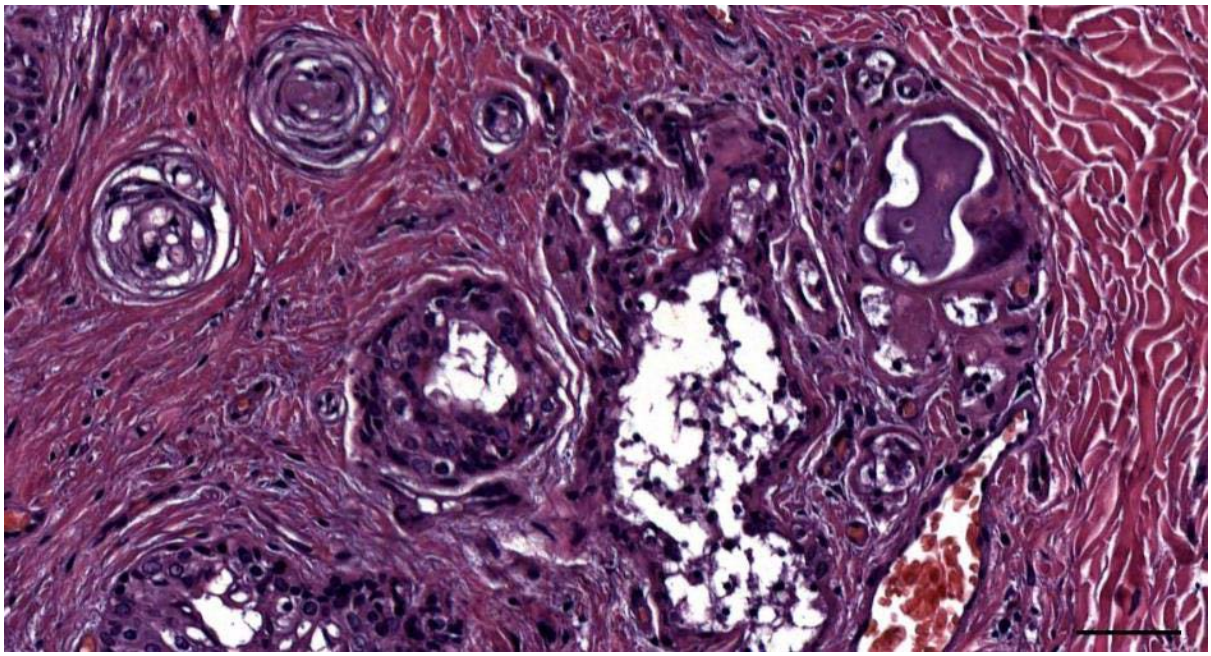

Figure 137. Histological detail image (HE staining) of glandular structures associated with the ear canal of a striped dolphin at about 1.5 cm beneath the skin (292_18_R3). Note the impacted glandular content. Scale bar 50 µm

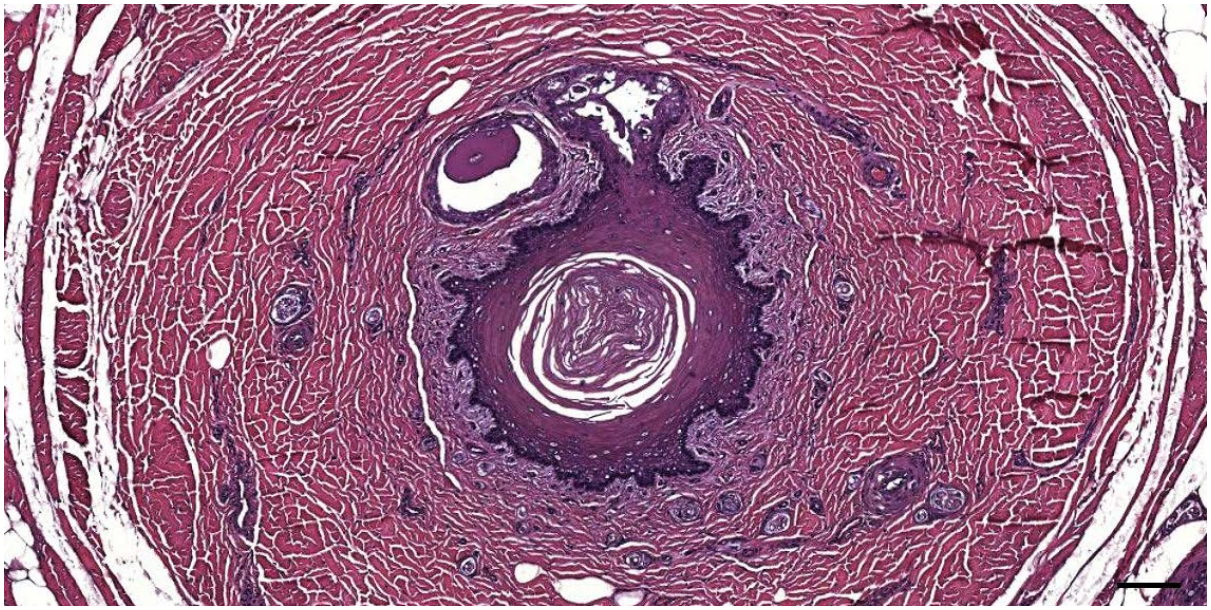

Figure 138. Histological transverse section (HE staining) through the ear canal of a striped dolphin at about 2 cm beneath the skin (44/17_B4). Scale bar 100 µm

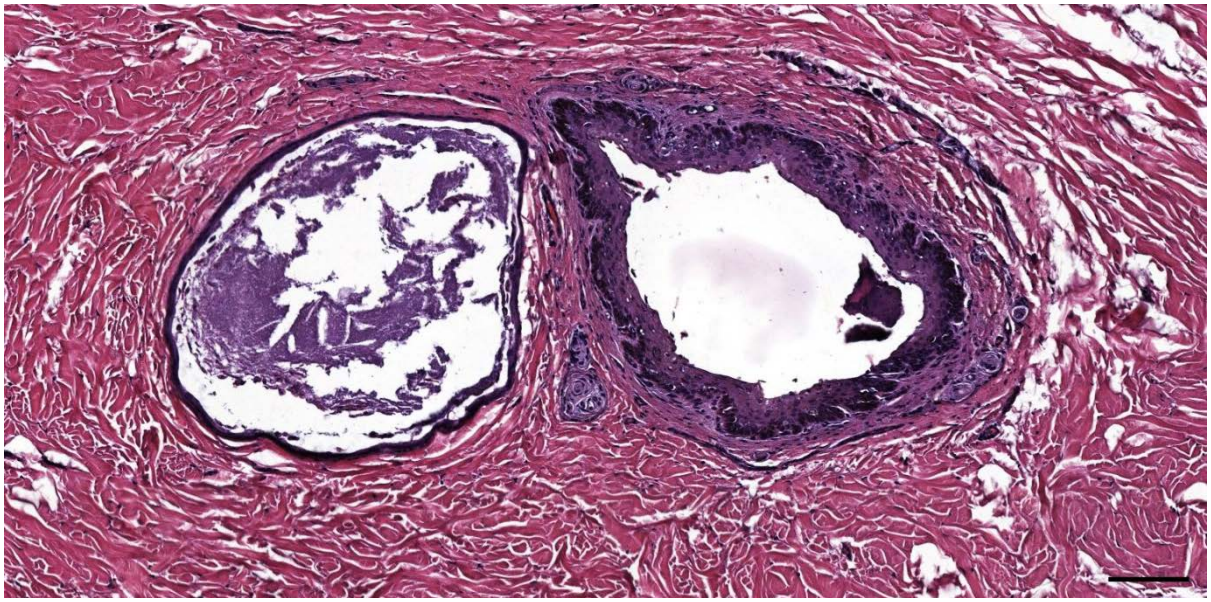

Figure 139. Histological transverse section (HE staining) through the ear canal of a striped dolphin at about 4 cm beneath the skin (44/17_B8). Scale bar 100 µm

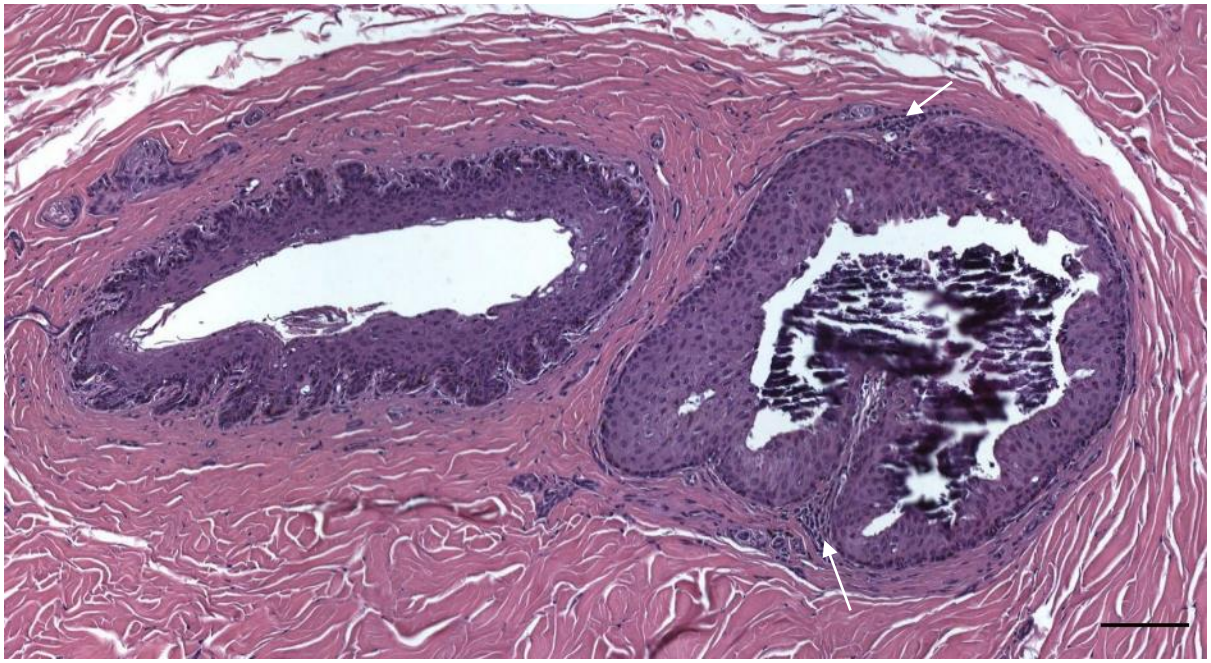

Figure 140. Histological image (HE staining) of the ear canal and glandular structure (likely excretory duct) with mineralized content in a bottlenose dolphin (ID444). Note the difference in the course of the basal membrane between the two structures: undulating with dermal papillae around the ear canal, and smooth around the glandular structure. Also note the multifocal presence of inflammatory cells (arrows)(lymphocytes, plasma cells and macrophages) in the connective tissue surrounding the glandular structures. Scale bar 100 µm.

Figure 141. Histological transverse section (HE staining) through the left ear canal of a striped dolphin, at about 1.5 cm beneath the skin, showing the ear canal complex shape and surrounding auricular glands (292/18_L3). Scale bar 200 µm

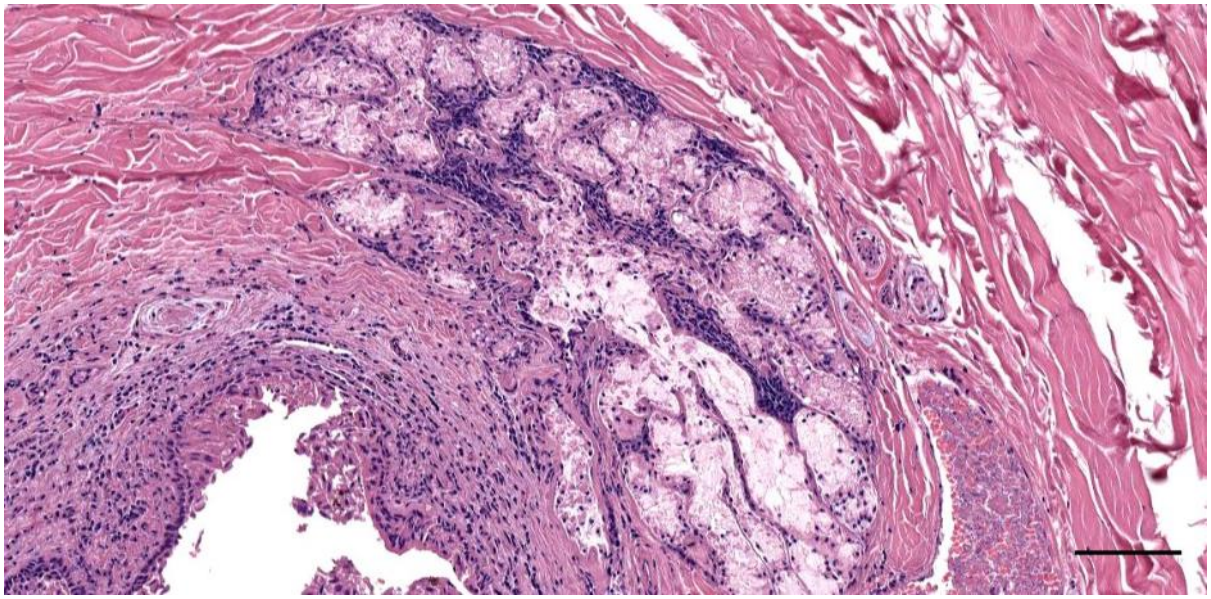

Figure 142. Histological detail (HE staining) of the ear canal and glands in a long-finned pilot whale (441_L12). Note the mononuclear cells in between the glandular structures. Scale bar 100 µm

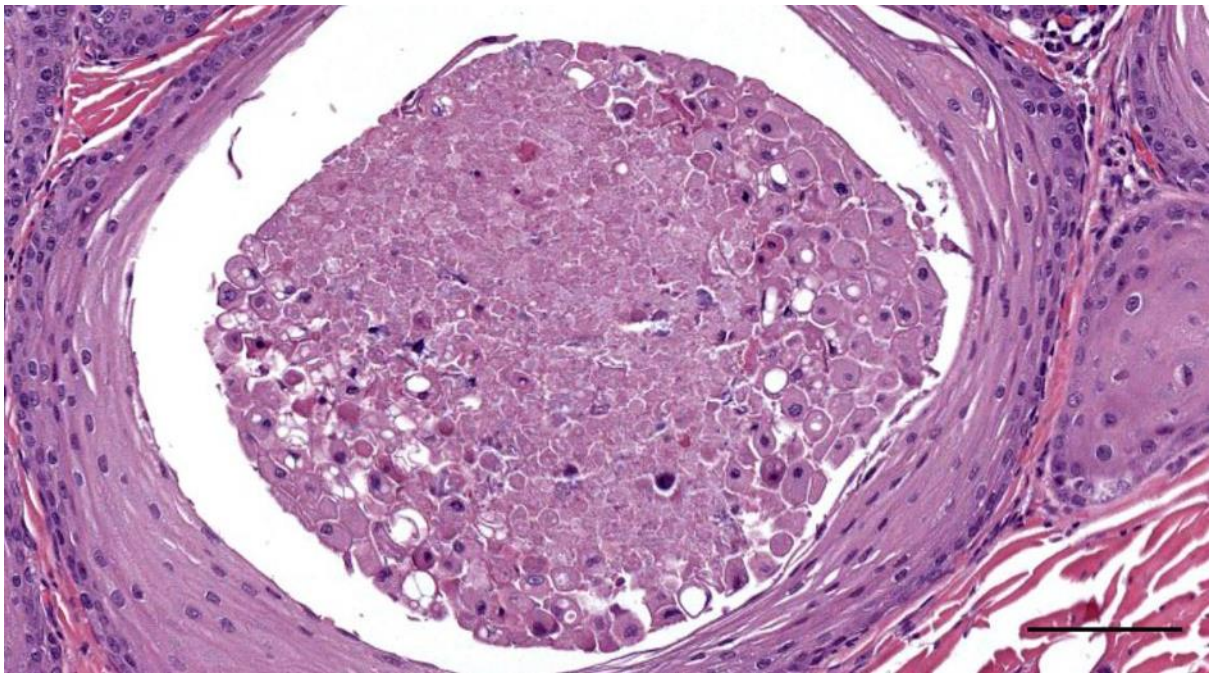

Figure 143. Histological image (HE staining) of a detail of the auricular glands in a common dolphin (Detail of Figure 63, 169/17_R2). Glandular content surrounded by a stratified squamous epithelium (likely excretory duct). Scale bar 100 µm

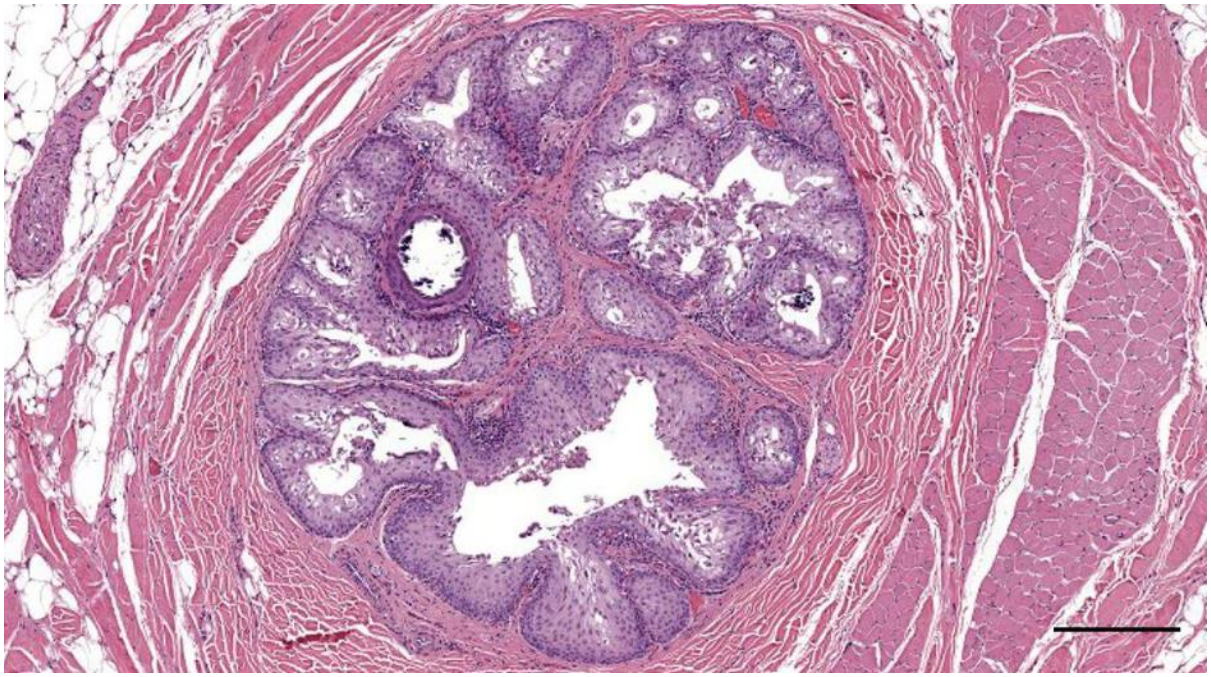

Figure 144. Histological image (HE staining) of a transverse section through the right ear canal of a common dolphin at about 1.5 cm beneath the skin (169/17_R3). The distinction between the ear canal and glands is not clear. Scale bar 300 µm

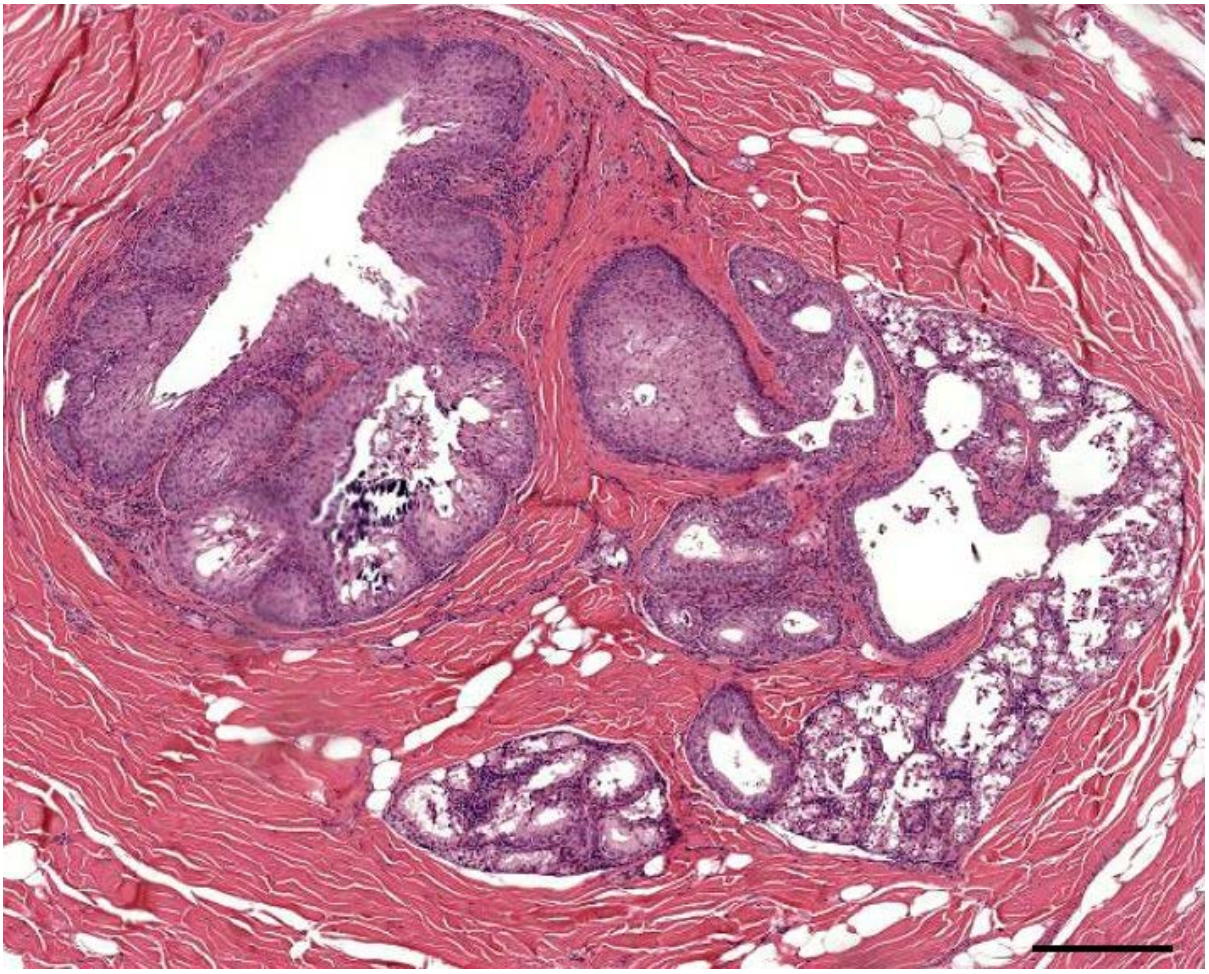

Figure 145. Histological image (HE staining) of a transverse section through the right ear canal of a common dolphin at about 2 cm beneath the skin (169/17_R4c). Ear canal and glands. Scale bar 300 µm

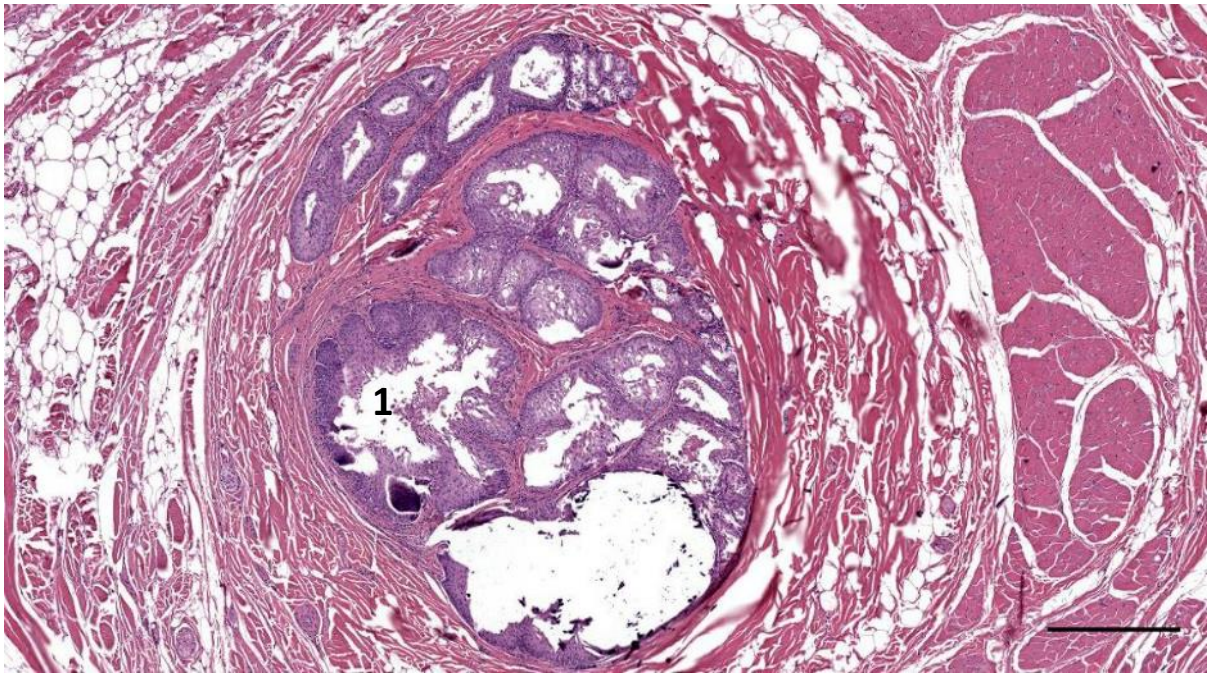

Figure 146. Histological image (HE staining) of a transverse section through the right ear canal of a common dolphin at about 2 cm beneath the skin (169/17_R4a). Ear canal (1) and glands. Scale bar 500 µm

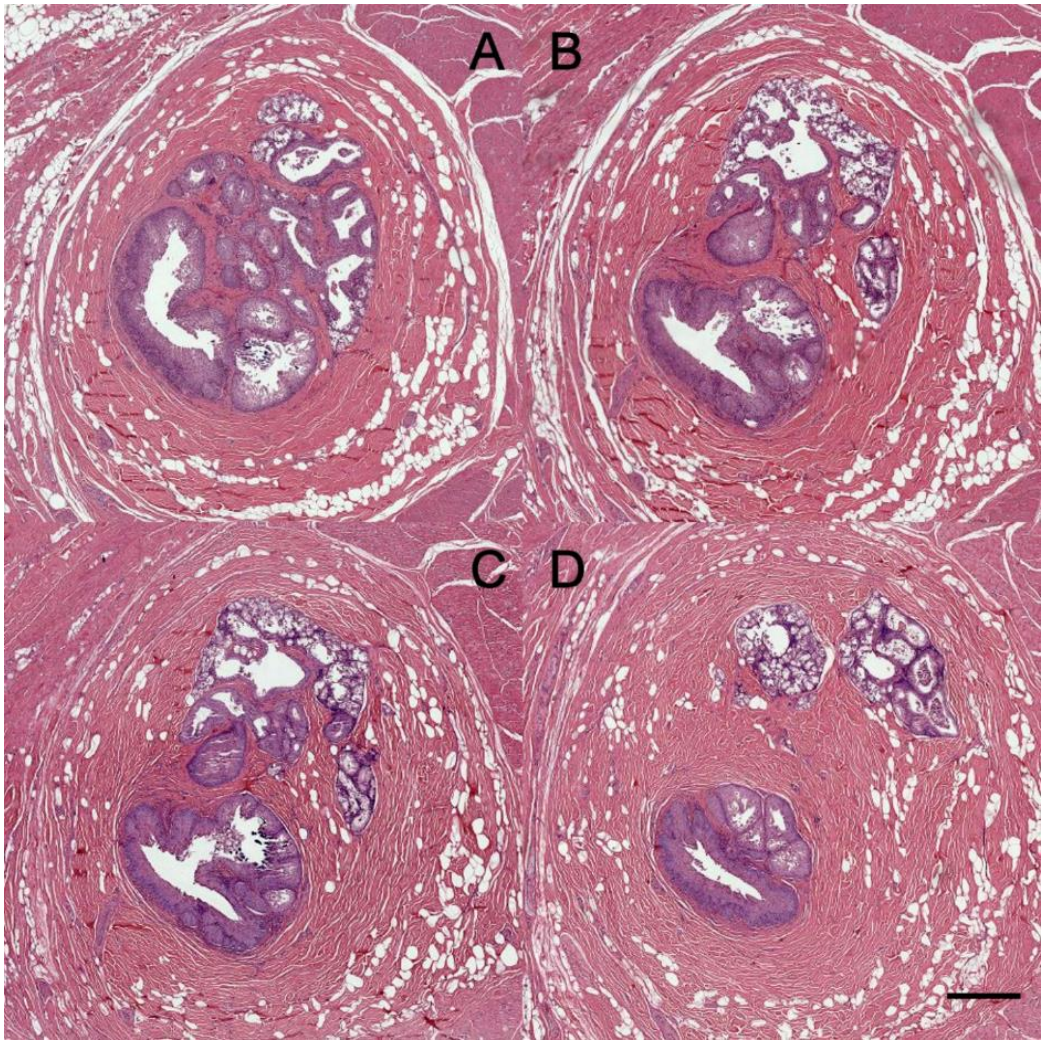

Figure 147. Consecutive histological images (HE staining) of transverse sections through the right ear canal of a common dolphin at about 2 cm beneath the skin (169/17_R4). Scale bar 500 µm

2.6 Musculature

Various striated muscles were inserting into the fibro-elastic tissue around the external ear canal. These muscles have been described in various odontocete species, with variation in nomenclature and description, see Table 12.

The most apparent muscle was the *zygomatico-auricular* muscle (Figure 25, Figure 149, Figure 150, Figure 151, Figure 152), which inserted from rostral into the adipoconnective tissue capsule at the levels of the ventral curvature of the ear canal and also deeper medial, and had even muscle fibres running parallel to the ear canal from the top of the ventral curvature towards lateral into the blubber layer to about the level of the glands (Figure 149, Figure 150). The muscle ran in the direction of the mouth commissure and the masseter muscle, but its origin was never determined.

The other apparent muscle was the (*deep) occipito-auricular muscle* (although this could have also been the *sternomastoid* or *mastohumeralis* muscle), which also inserted into the connective tissue at the level of the ventral curvature and slightly more medial, but from caudal, in contrast to rostral insertion of the zygomatico-auricular muscle (Figure 24, number 7-8). The *subcutaneous nuchae muscle* was present in all species running below and parallel to the skin as in the rest of the body, but no other muscles (*mandibulo-auricular*, *orbito-auricular*, or *superficial occipitoauricular muscle*), were identified with certainty. In general, the various muscles were tough to distinguish, and their origin was never identified. See also chapter ´Macroscopic morphology of the ear canal and associated tissues´.

Table 12. Review of the musculature in the region of the ear

Ruge, 1986 (In Hanke, 1914	auriculo-occipitalis occipito-auricularis		auriculo-labialis inferior	auricularis superior	orbito-auricularis	mandibulo-auricularis				
Murie, 1873	retrahens		attolens + attrahens							
Beauregard, 1894 (*Delphinus*)	auricularis externus (purves) / posterior (hanke)		auricularis anterior	auricularis superior		-				
Boenninghaus, 1903 (*P. phocoena*)	occipito-auricularis superficialis	occipito-auricularis profundus	zygomatico-auricularis or: "auriculo-labialis inferior = zygomatico-labialis inferior + zygomatico-auricularis"	orbito-auricularis		-				
Hanke, 1914 (*Delphinus delphis*)	occipito-auricularis superficialis	occipito-auricularis profundus	auriculo-labialis inferior	orbito-auricularis		mandibulo-auricularis	subcutaneous nuchae			
Purves, 1966 (*P. phocoena*)	occipito-auricularis		zygomatico-auricularis					sternomastoideus	mastohumeralis	tensor palati
Innervation	Small twigs from the lesser occipital branch of the second cranial nerve (Purves, 1966) Superficialis: likely VII, like all ear muscles (Boenninghaus, 1903)		VII (Purves, 1966)							
Origen	Supraoccipital crest (= parietal margin of the supraoccipital), as a strong tendon)(Purves, 1966)		An aponeurosis from the superficial facia of the m. masseter, near its origin on the zygomatic process of the squamosal (Purves, 1966)							
Insertion	Superior, distal extremity and anterior face of the antihelix (Purves, 1966); *Superficialis*: Into the purely membranous distal part of the ear canal and penetrating the subcutaneous fat layer, and continues up to or close to the skin (Boenninghaus, 1903)		- Anterior face of the antihelix (Purves, 1966) - Connective tissue surrounding EAM		Membranous part of the ear canal (Hanke, 1914)			Posterior part of Helix (Purves, 1966)	Posterior part of Helix (Purves, 1966)	Anterodorsal aspect of the bulla: processus tubaris of the periotic and the lateral margin of the osteum tympanicum tubae and Eustachian tube (Purves, 1966)
Remarks	Medial to blubber and superficial fascia; straplike muscle becomes broader and more fleshy towards insertion; passes ventrally superficial to the plenius capitis (Purves); Delicate bundle of flattened muscle at the level of its insertion (0.1-0.15 – 0.6-0.7 cm); Has direct contact with the subcutaneous nuchae (Boenninghaus, 1903)		Fan-shaped group of small muscles (Purves, 1966)							

Figure 148. Histological image of the left ear canal of a striped dolphin (ID509/17_L6), at the level of the ventral curvature. The zygomatico-auricular muscle inserts into the adipoconnective tissue capsule around the ear canal. Scale bar 1 mm

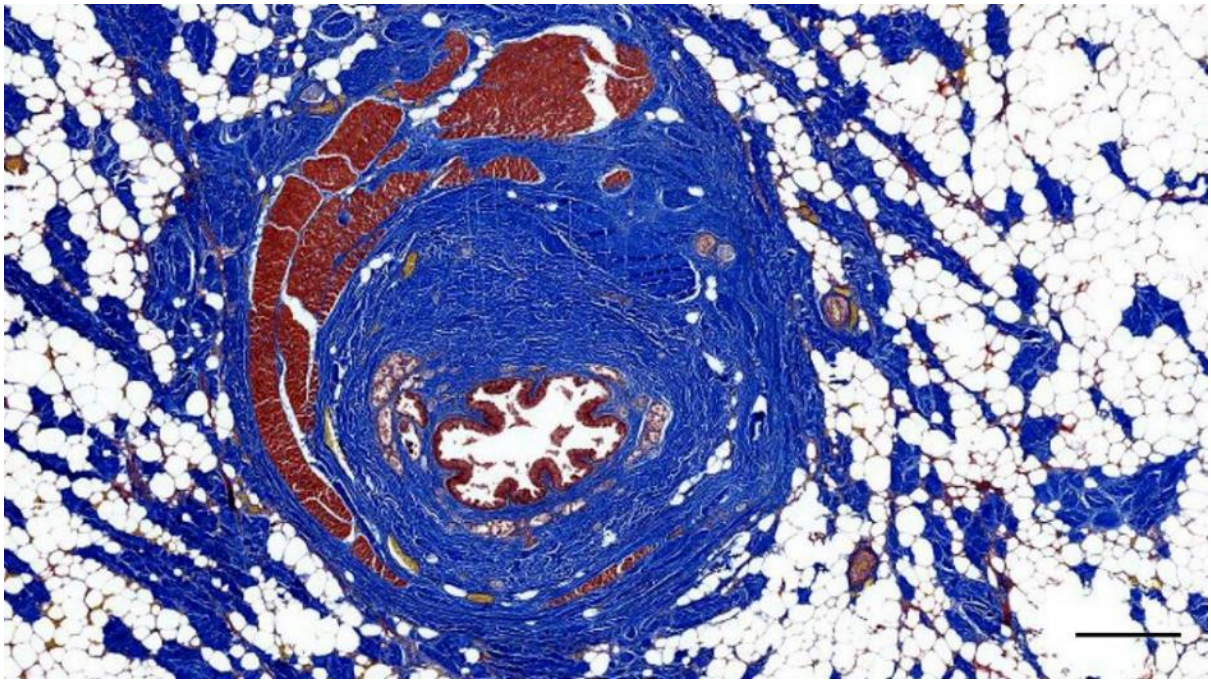

Figure 149. Masson´s trichrome staining of a cross-section through the ear canal of a striped dolphin about 0.5 cm beneath the skin surface. Note the presence of glands, and muscles within the connective tissue sheath. Scale bar 500 µm.

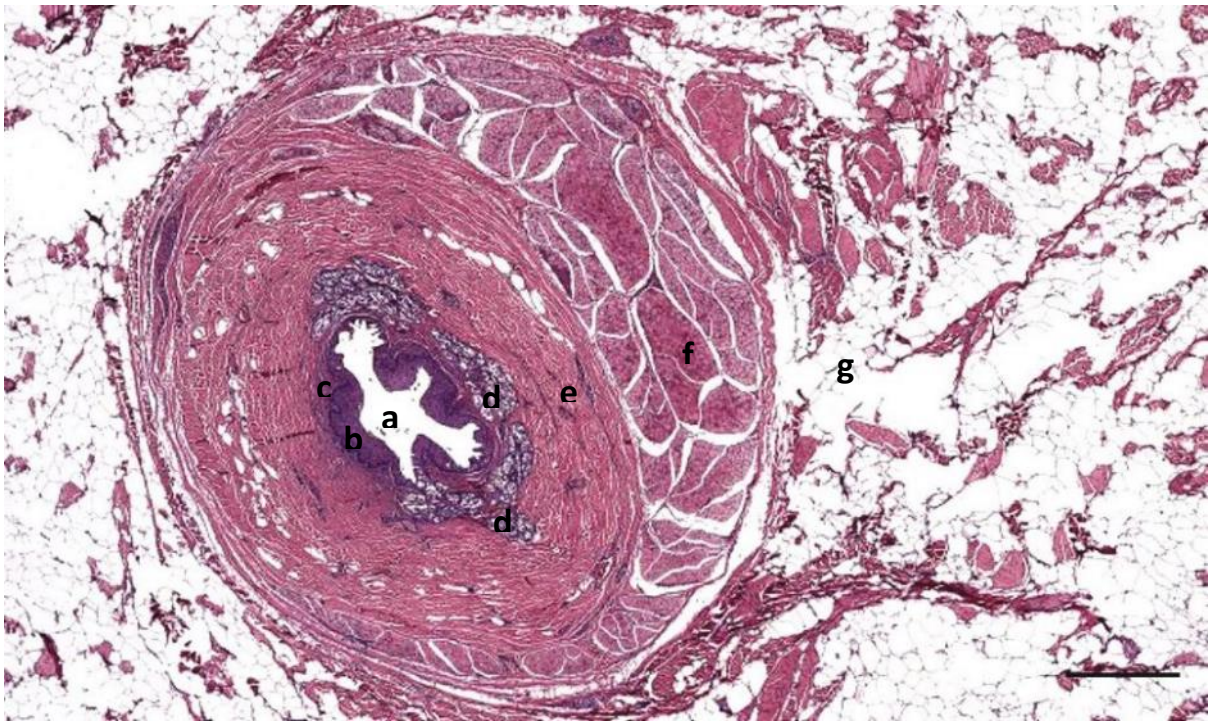

Figure 150. Overview of a cross-section through the ear canal about 1.2 cm beneath the surface (Sc 44/17). From centre to periphery there is: a) lumen, b) epithelium, c) papillary layer, d) glands, e) adipoconnective tissue sheath, f) striated muscles cut slightly medial to the insertion in the adipoconnective tissue sheath, g) blubber layer with sparse connective tissue (amount of connective tissue is larger than in more lateral sections with only adipocytes, and gets more pronounced on getting closer to the curvature of the canal)

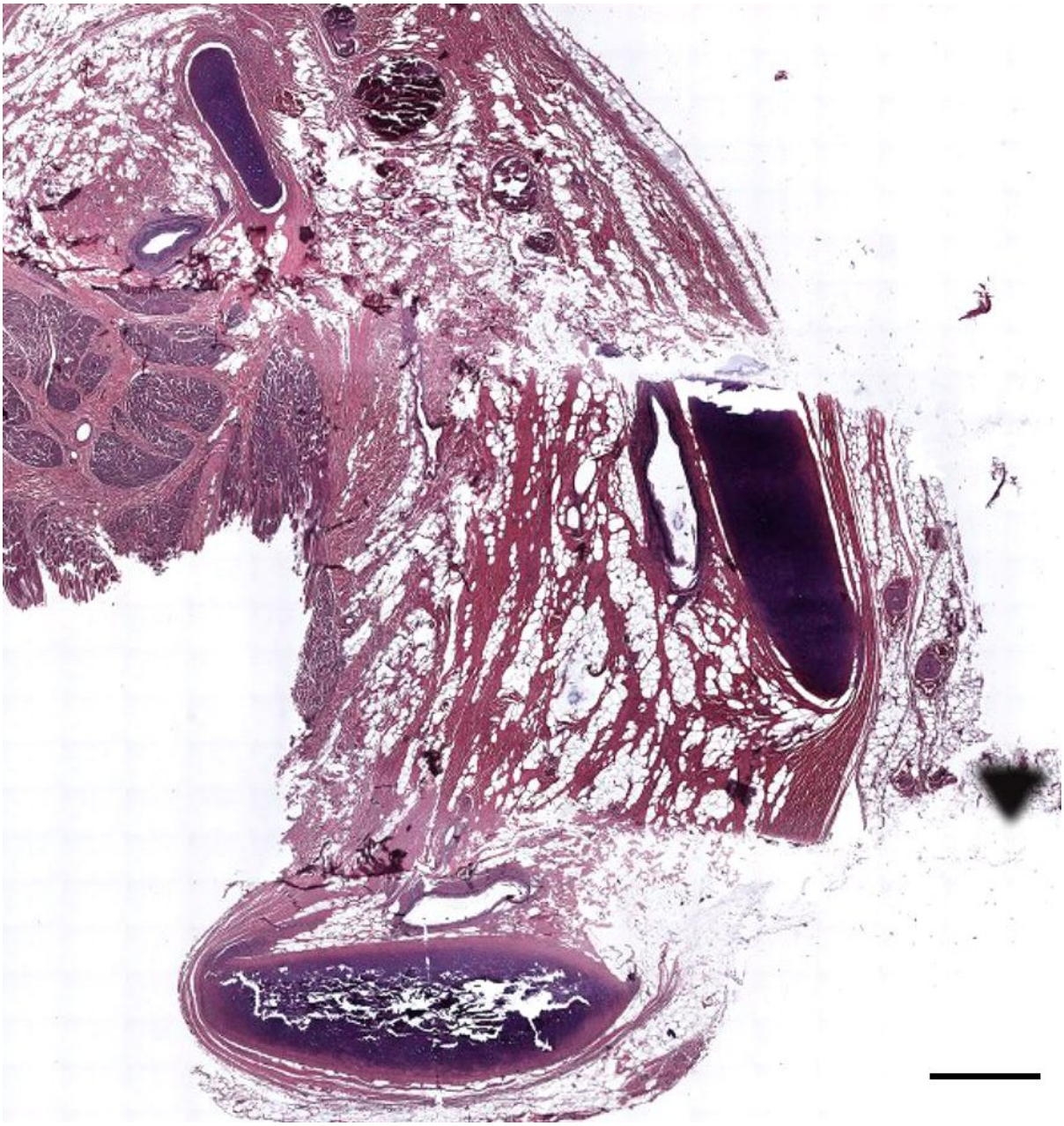

Figure 151. (509/17_L7). HE stained section of the ear canal at the level of the ventral curvature of the meatus. Note there is a triple-section through the ear canal and cartilage. Scale bar 1mm

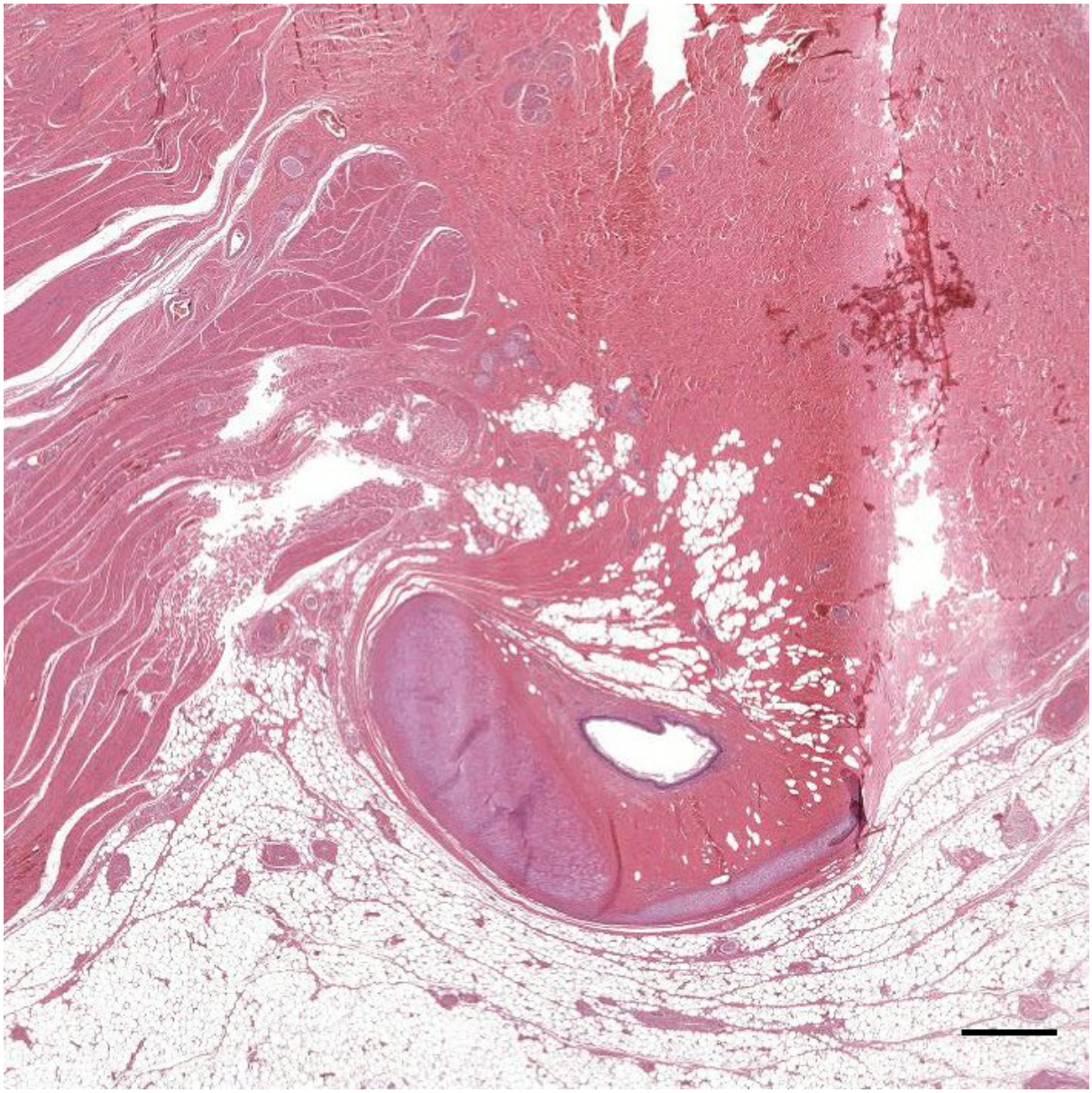

Figure 152. (274/18_L7) Medial to the ventral curvature. Zygomatico-auricular muscle inserts from rostral into the connective tissue dorsal to the ear canal, at the location where the ventral curvature of the ear canal and cartilage is located. Scale bar 1 mm

2.7 Cartilage

Hyaline cartilage was associated with the ear canal from the level of the ventrally directed curvature until the entrance of the ear canal into the tympanic aperture of the middle ear (Figure 153). The cartilage was typical hyaline cartilage with abundant matrix and lacunae with chondrocytes (Figure 154), similar to the cartilage of the trachea. It stained negative with the Acid Orcein Giemsa stain and Weigert´s elastic stain, indicating the absence of elastic fibres. There were no internal blood lacunae as found in, e.g. the northern giraffe, likely because of the small size of the cartilage.

From lateral to medial, the cartilage changed considerably in shape and size. In the sigmoid curvature, the cartilage showed laterodorsally-projecting finger-like extensions that accompanied the EAM, with significant individual variation. At the medial end of the sigmoid curvature, the cartilage was situated

ventral to the meatus, and in cross-sections, it was reniform to elongated oval (Figure 155, Figure 156). Here, the cartilage often presented a thin, dorsocaudally directed flange that originated from the rostral boundary (Figure 157, Figure 158). In some specimens, this flange grew in size towards medial and gradually covered the EAM and formed a groove in which the vascular sinuses developed (Figure 158, Figure 160, Figure 161), while in other it was present for a few millimetres before it regressed (Figure 157). In all cases, along the horizontal course in the medial third of the canal, the cartilage showed variable wave- and finger-like protrusions that stemmed from the main body of the cartilage, which was always situated more or less ventral to the EAM. The main body of the cartilage was larger the closer the cross-section was to the middle ear. Similarly, also the lumen of the EAM was more prominent, and between the ear canal and cartilage was the presence of vascular lacunae (see below). At this point, the surrounding fat tissue was almost entirely absent and replaced with connective tissue, except for a small amount. This local fat tissue was either concentrated as a body, situated caudally to the meatus in association with the cartilage or appeared more dispersed between the connective tissue fibres (Figure 158, Figure 159), although not in direct contact with it, which disappeared rapidly towards medial (Figure 157). The cartilage shape gradually changed from reniform to horseshoe-shaped, almost completely enclosing the meatus, with its opening directed towards dorsorostral (Figure 160), and accompanied the ear canal until the tympanic aperture of the middle ear (Figure 193).

There was significant individual variation in shapes of the cartilage, medial to the ventral curvature, with variety in the complexity (e.g. Figure 162). As such, two striped dolphins presented additional cartilaginous flanges running parallel to the main cartilage body (Figure 163), and so did a bottlenose dolphin which had a bifurcated cartilaginous body at the medial end of the ear canal (Figure 155, Figure 164). This animal also presented indications of ossification of the cartilage, which is considered a normal finding in old animals, and which was similar to the cartilages found in the lung: ossified, irregular in shape, and with chondroblasts like osteoclasts.

Based on the non-consecutive histological studies, it was unsure if all the protrusions and cartilaginous bulbs were interconnected, and were parts of a single continuous body of cartilage, although this was demonstrated to be the case in the 3D reconstruction of a striped dolphin ear canal (Figure 153). The shape and size of the cartilage in Cuvier´s beaked whale and Long-finned pilot whale was very similar and rather conservative compared to the cartilage of smaller toothed whales, at least in the parts of the ear canal that were subjected to investigation (Figure 165, Figure 166).

The space between the ear canal and cartilage consisted of a network of very loose connective tissue fibres, possibly reticular, and with a large amount of ground substance (Figure 193, Figure 197). Within this tissue were blood vessels, lymphoid cells (See Lymphoid tissue), and vascular lacunae.

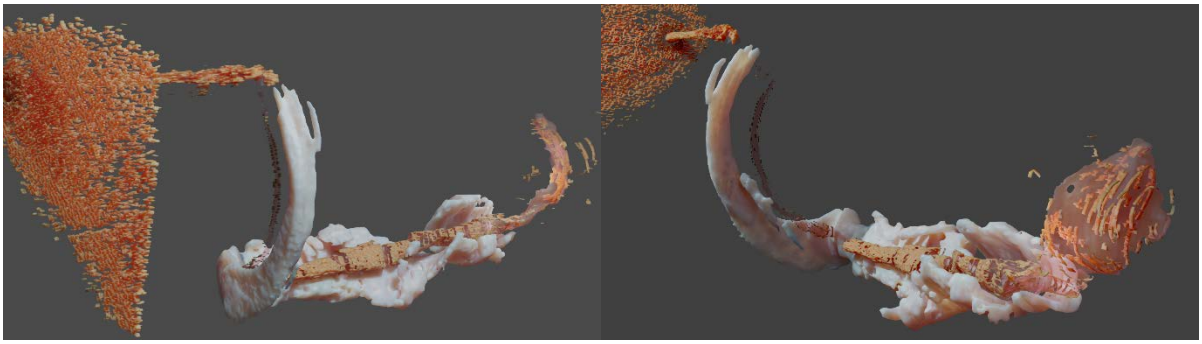

Figure 153. Two images (left: caudolateral view; right: caudomedial view) of a 3D reconstruction of the right ear canal lumen, epithelium, and cartilage of a striped dolphin. Note that the cartilage forms a trench with various flanges which supports the medial half of the ear canal. It also has a latero-dorsally orientated cartilage flange that accompanies the ear canal in the ventral curvature.

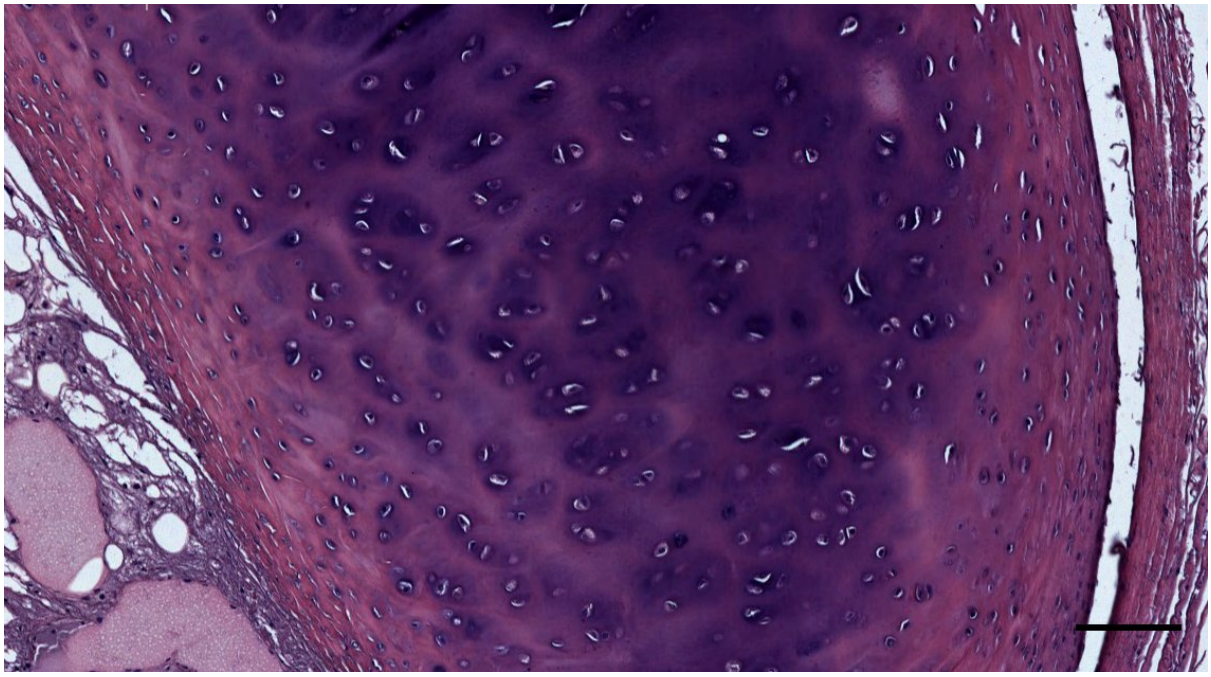

Figure 154. Histological detail image (HE staining) of the cartilage associated with the ear canal in a striped dolphin (127565_R14). Scale bar 100 µm

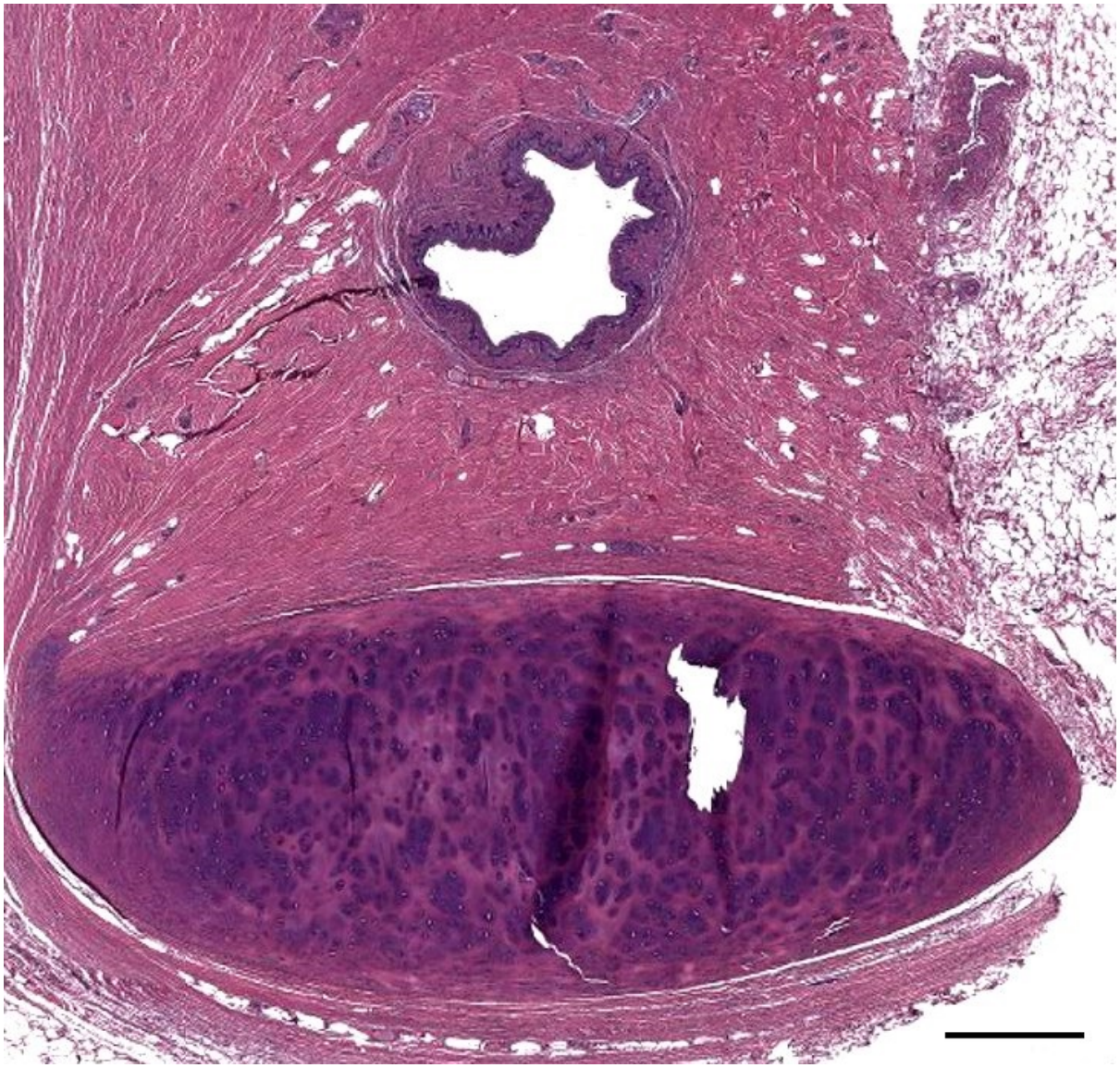

Figure 155. HE-stained cross-section of the ear canal and cartilage of a striped dolphin (457_R9). Scale bar 500 µm

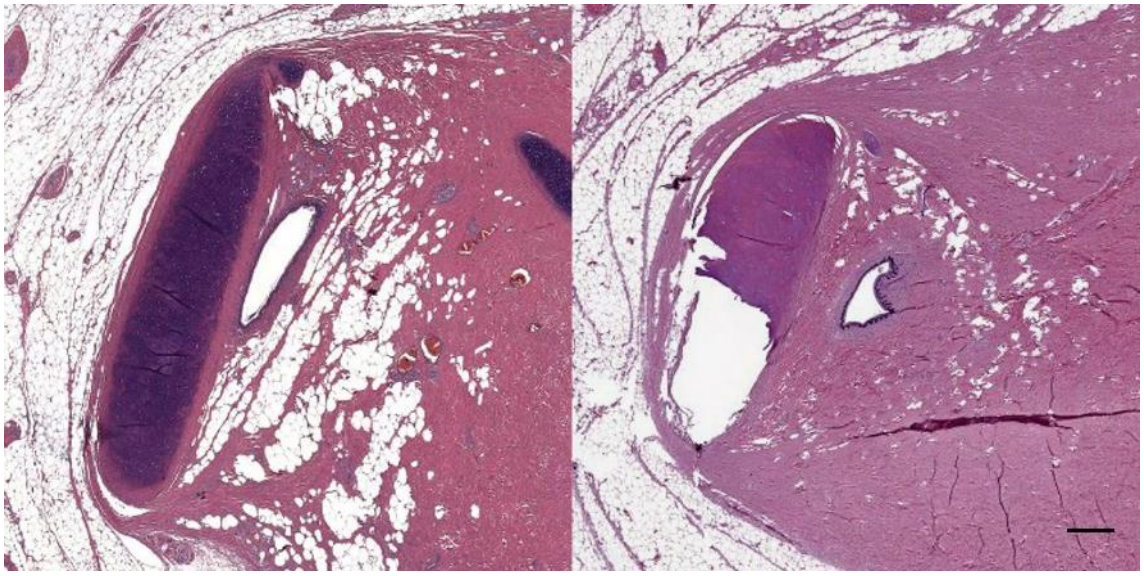

Figure 156. HE-stained section of the right ear canal of a striped dolphin (left, ID127565) and bottlenose dolphin (right, ID444) in cross-section at a similar level along the course. Note the presence of fat embedded within the connective tissue of the striped dolphin, and the absence of fat in the bottlenose dolphin (the white spaces in the latter are artefacts). Scale bar 500 µm

Figure 157. HE-stained cross-section of the ear canal and cartilage of a striped dolphin (509/17_L11). Left ear canal at the bottom of the ventral curvature. Scale bar 0.5 mm

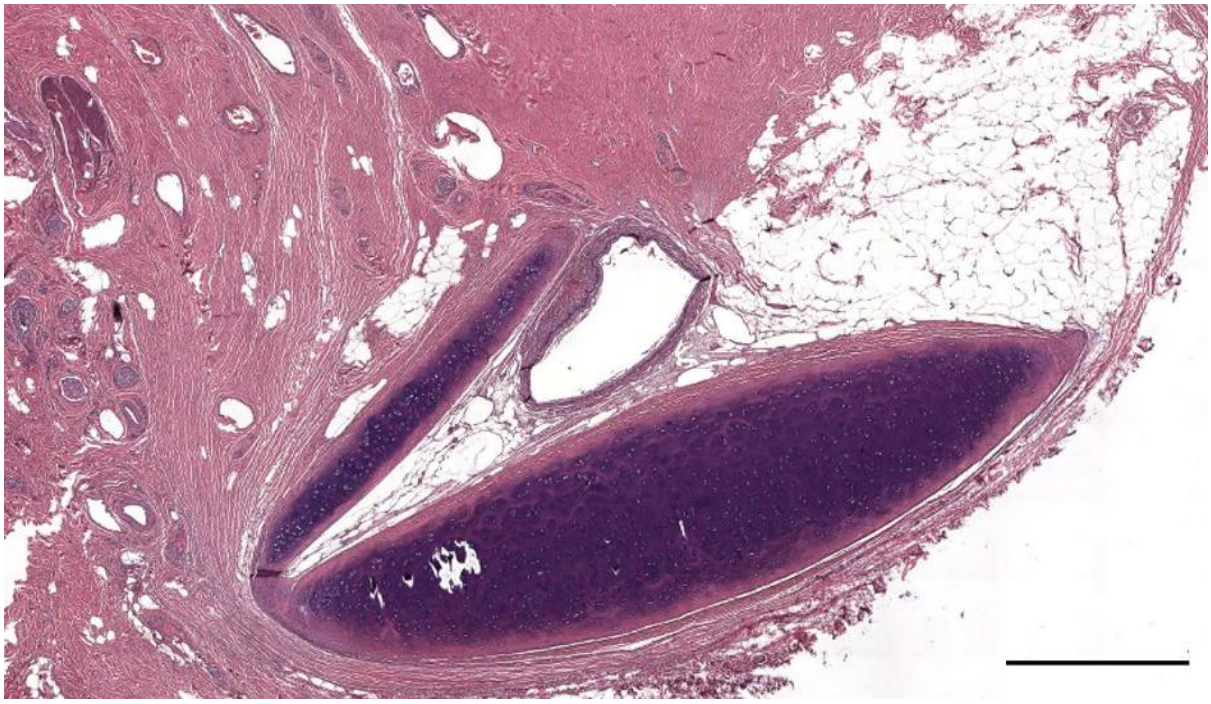

Figure 158. HE stained cross-section of the ear canal of a striped dolphin, immediately medial to the ventral curvature of the meatus. Note the dorso-caudally directed flange of cartilaginous tissue covering the meatus. Scale bar 1 mm

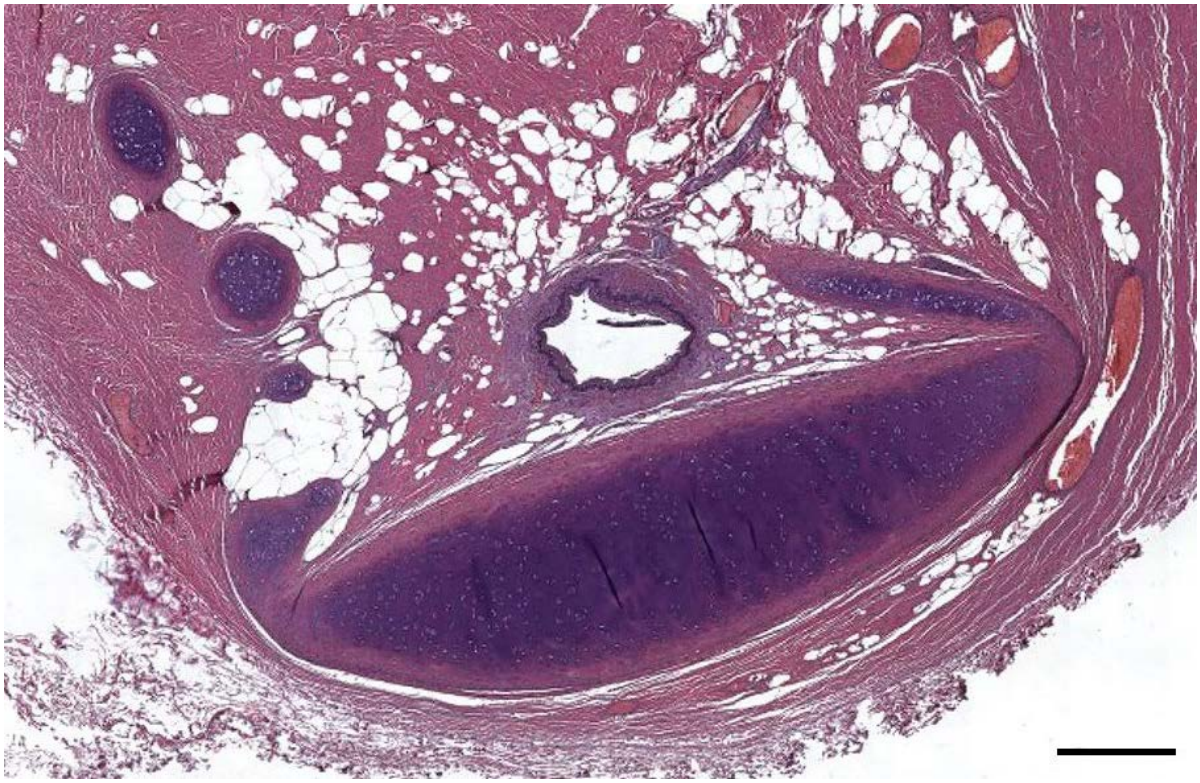

Figure 159. Histological image of the right EAM and cartilage at the bottom of the ventral curvature of the canal of a striped dolphin (42/18_R13). Note the sections through the dorsally directed cartilage on the left of the image, and the dorsocaudally directed flange of cartilage originating from the rostral extreme of the main cartilaginous body. Scale bar 0.5 mm

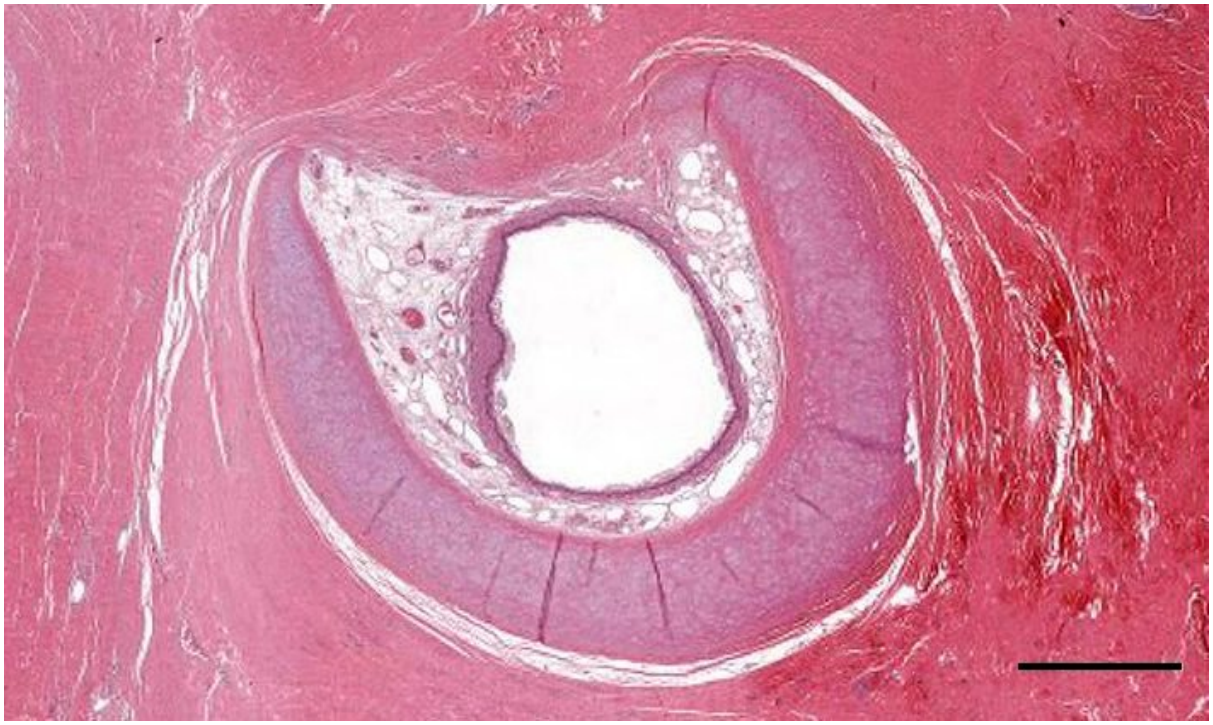

Figure 160. Histological transverse section through the ear canal of a striped dolphin at about 5.5 cm beneath the skin (274/18). Horseshoe-shaped cartilage, and the ear canal with a subtle nervous tissue ridge, and vascular sinuses. Scale bar 1 mm

Figure 161. Histological transverse section (HE staining) through the ear canal of a striped dolphin at about 5 cm beneath the skin (509/17). Scale bar 1 mm

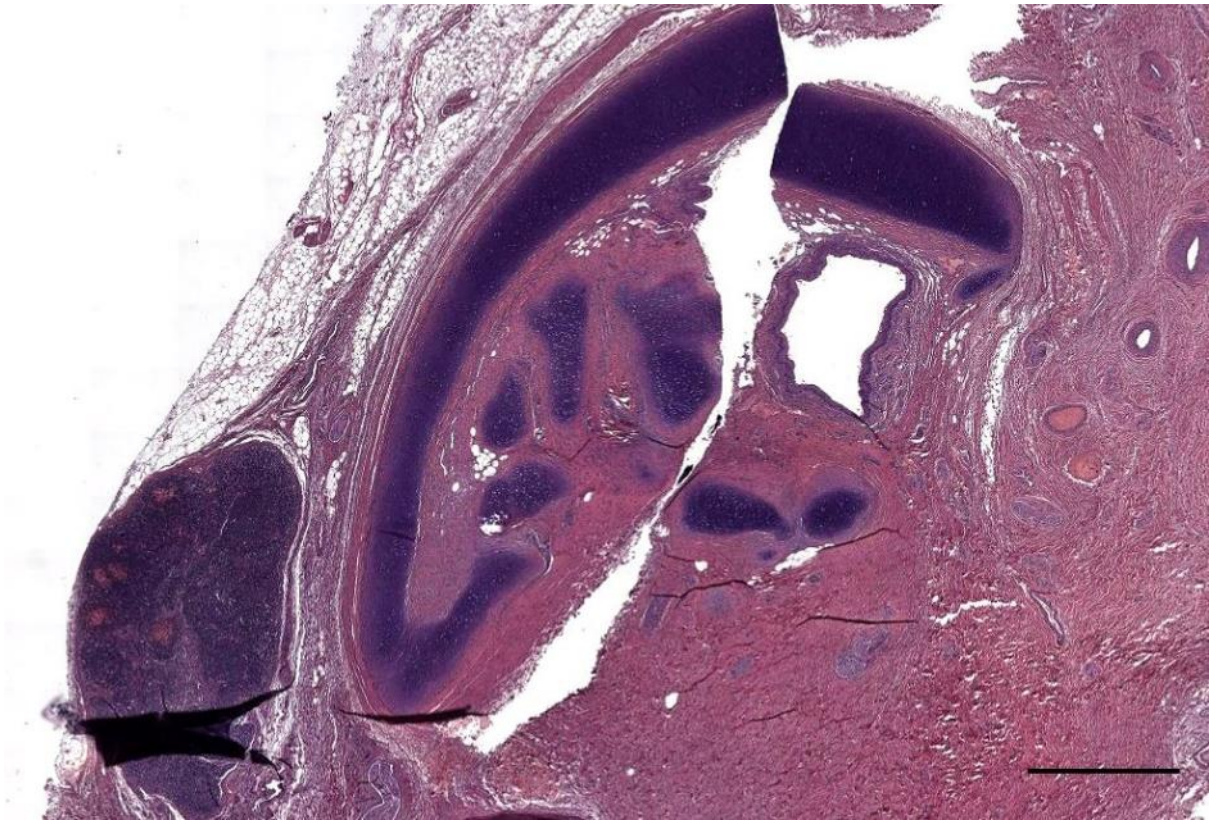

Figure 162. (ID449) Stenella coeruleoalba. (449_R8) Cross-section of the right ear canal and cartilage. Note the complex shape of the cartilage and the presence of nodular lymphoid tissue of about 1.4x2.5 mm in cross-section. Scale bar 1 mm

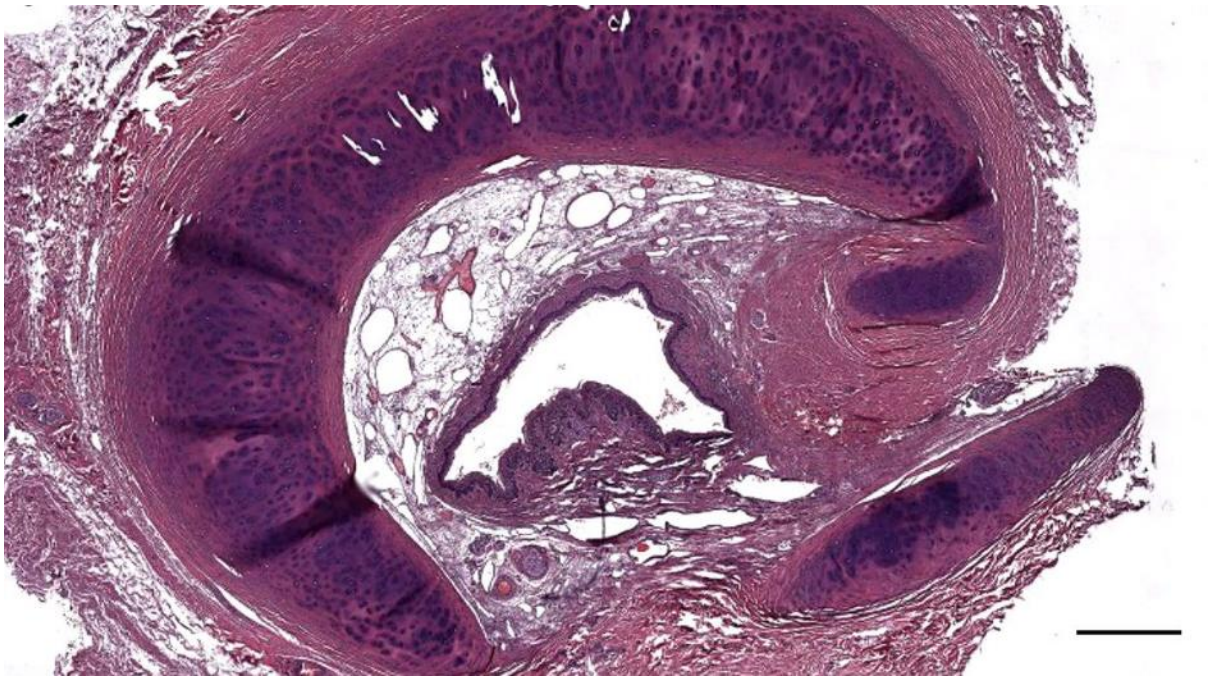

Figure 163. Histological cross-section (HE staining) of the right ear canal of a striped dolphin (292_18_R12). Note the bifurcated cartilage and the nervous tissue ridge. Scale 0.5 mm

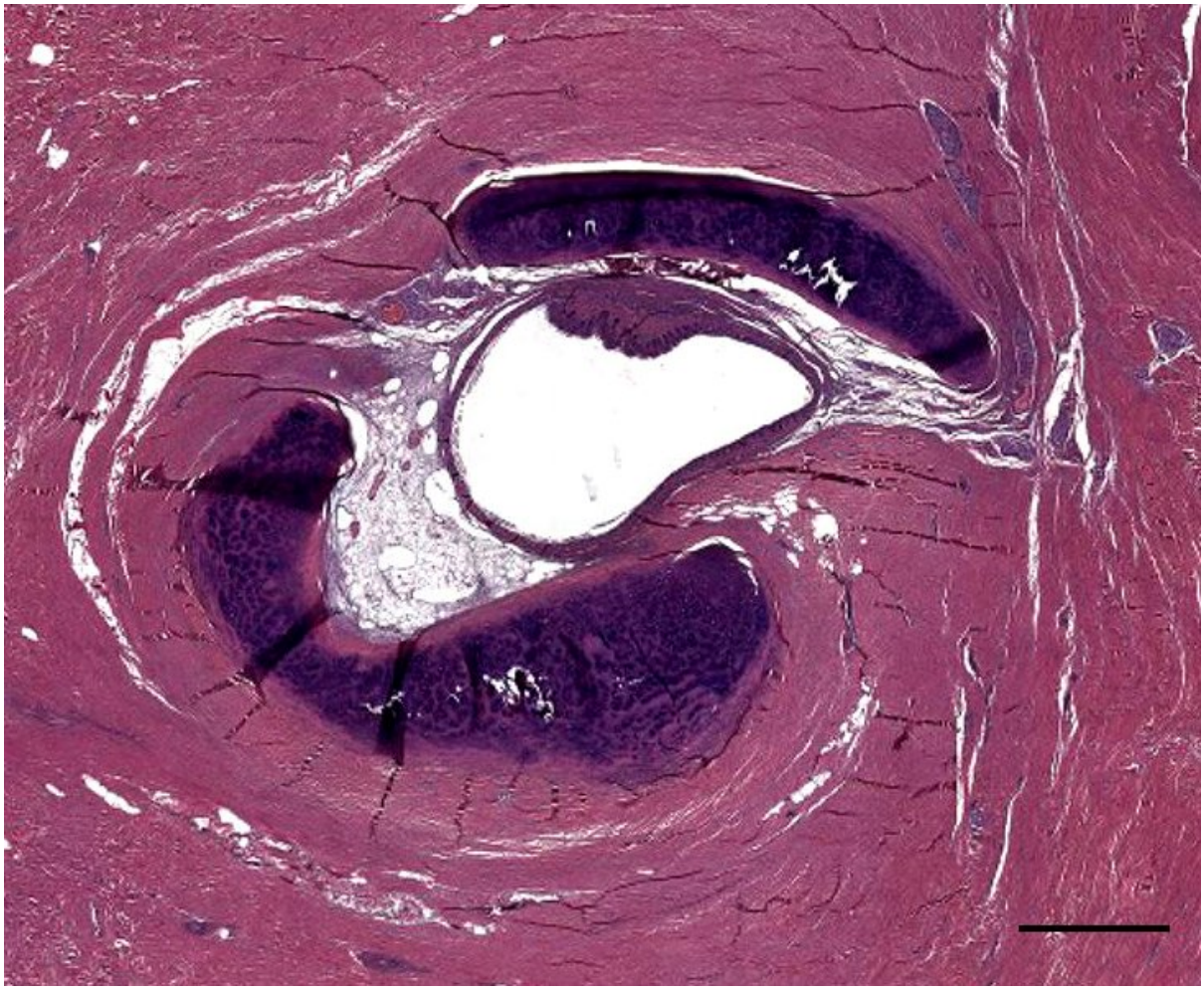

Figure 164. Histological cross-section (HE staining) of the ear canal of a bottlenose dolphin (457_R15) with prominent nervous tissue ridge and vascular lacunae with double cartilage. Scale bar 1 mm

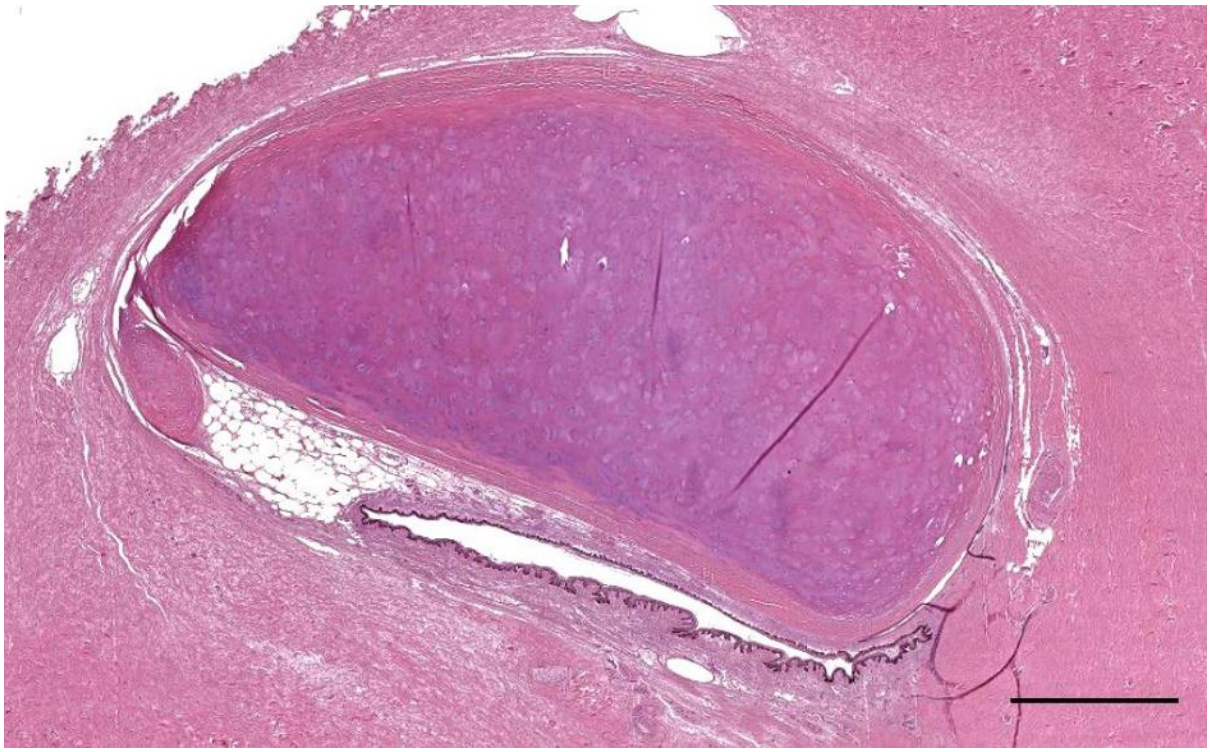

Figure 165. Histological image of the ear canal and cartilage of a long-finned pilot whale (441_L17). Scale bar 1 mm

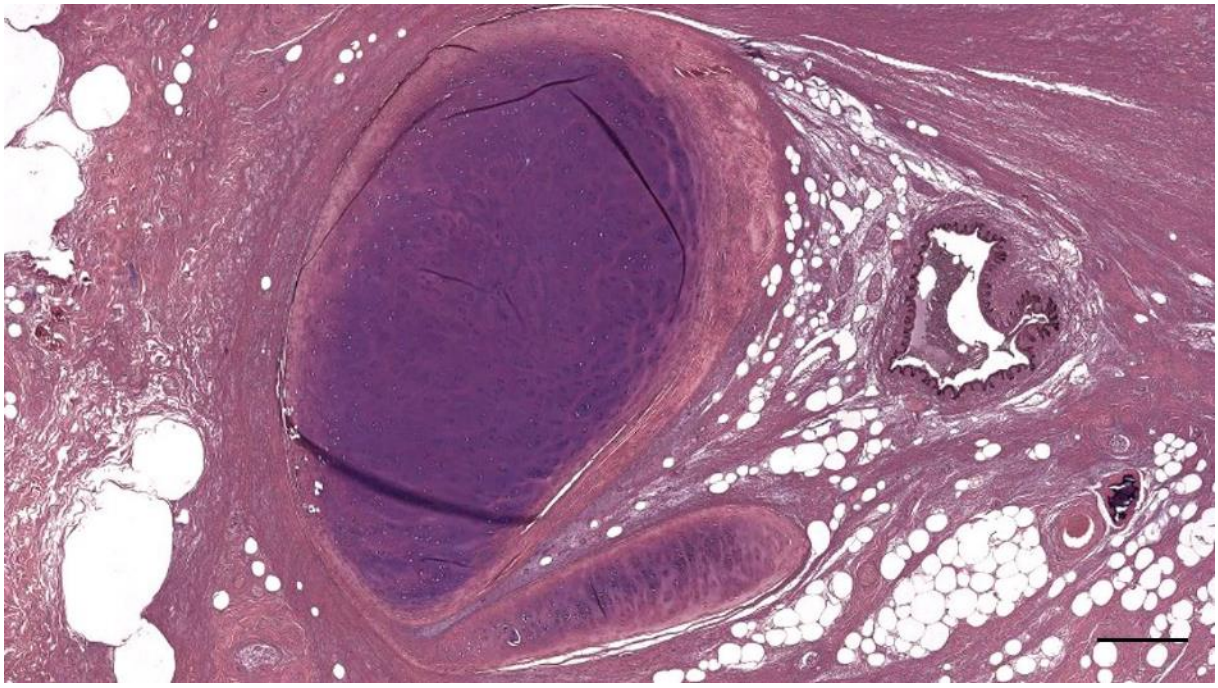

Figure 166. Histological image of the ear canal and cartilage of a long-finned pilot whale (441_R21). Scale bar 500 µm

2.8 Vascular lacunae

In all species, the histological slides showed the presence of lacunar structures in the dermal layer surrounding the entire canal in the medial half or third of the ear canal course, present in co-occurrence with the cartilage (Figure 167, Figure 168). The lining of the lacunae stained positive for von Willebrand factor (vWf)(Factor VIII) in the immunohistochemical stain, demonstrating the presence of endothelial cells (Figure 169, Figure 170). It was the small amount of cytoplasm in these cells that stained dark brown. Therefore, these lacunae could be called **vascular lacunae**. The lumen content seemed homogenous, proteinaceous on HE and Masson´s trichrome stained sections, but this could have been an artefact due to post-mortem decay. The vascular lacunae were distributed encircling the entire ear canal, but mostly seemed to be present or even fill the space of the reticular connective tissue between the canal and the cartilage and from there, they fanned out towards the extreme margins of the cartilage (Figure 171, Figure 172). The morphological characteristics of these vascular lacunae in the subepithelial tissue are similar to vascular lacunae found in the submucosa of the trachea of the striped dolphin (Figure 173)(Cozzi et al., 2005), and their function could be similar as well (See discussion).

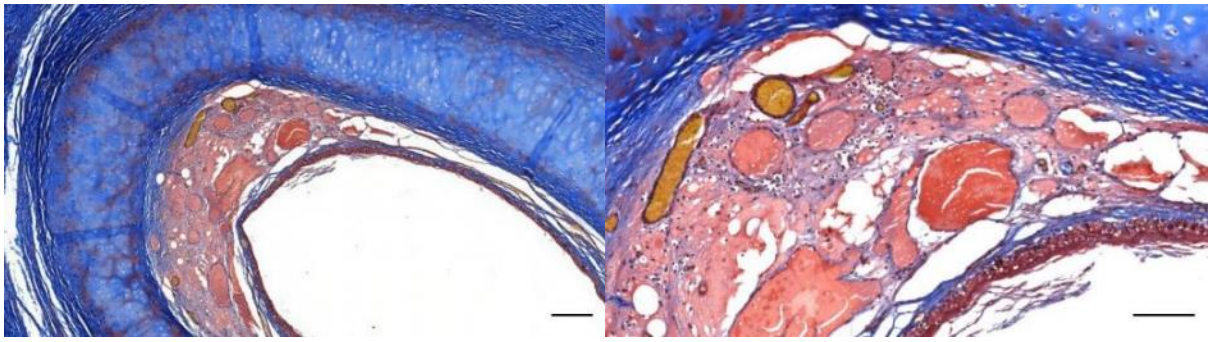

Figure 167. Histological detail image(Masson´s Trichrome) of the ear canal vascular lacunae situated between the lumen (bottom right) and the cartilage (top left) in a striped dolphin. The blood vessels with erythrocytes stain yellow. The endothelium and epithelium stain red, and so do the nuclei of all cells. The white spaces are fat cells, empty vascular lacunae, or artefacts. Scale bar 200 µm left, and 100 µm right).

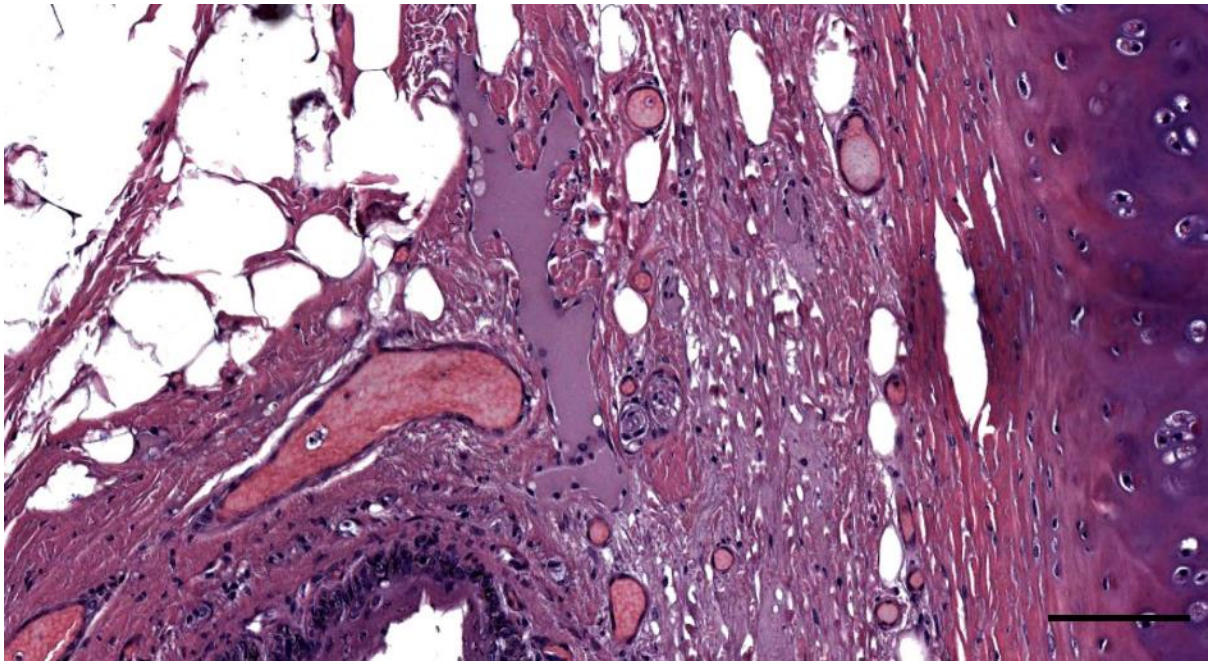

Figure 168. Histological detail (HE staining) of the vascular lacunae in a striped dolphin (42_18_R12). Scale bar 100 µm

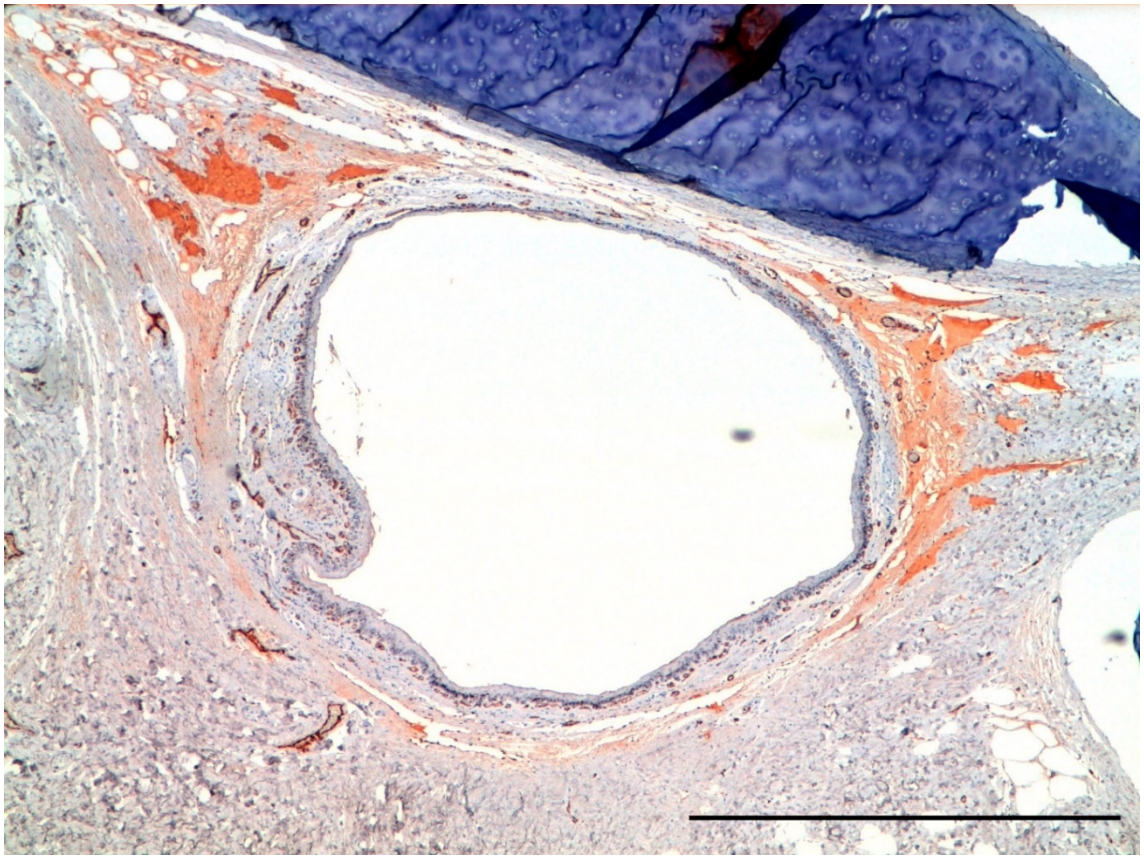

Figure 169. IHC image (anti-vWf, factor VIII) of the ear canal and cartilage with vascular lacunae in a striped dolphin. Scale bar 1 mm

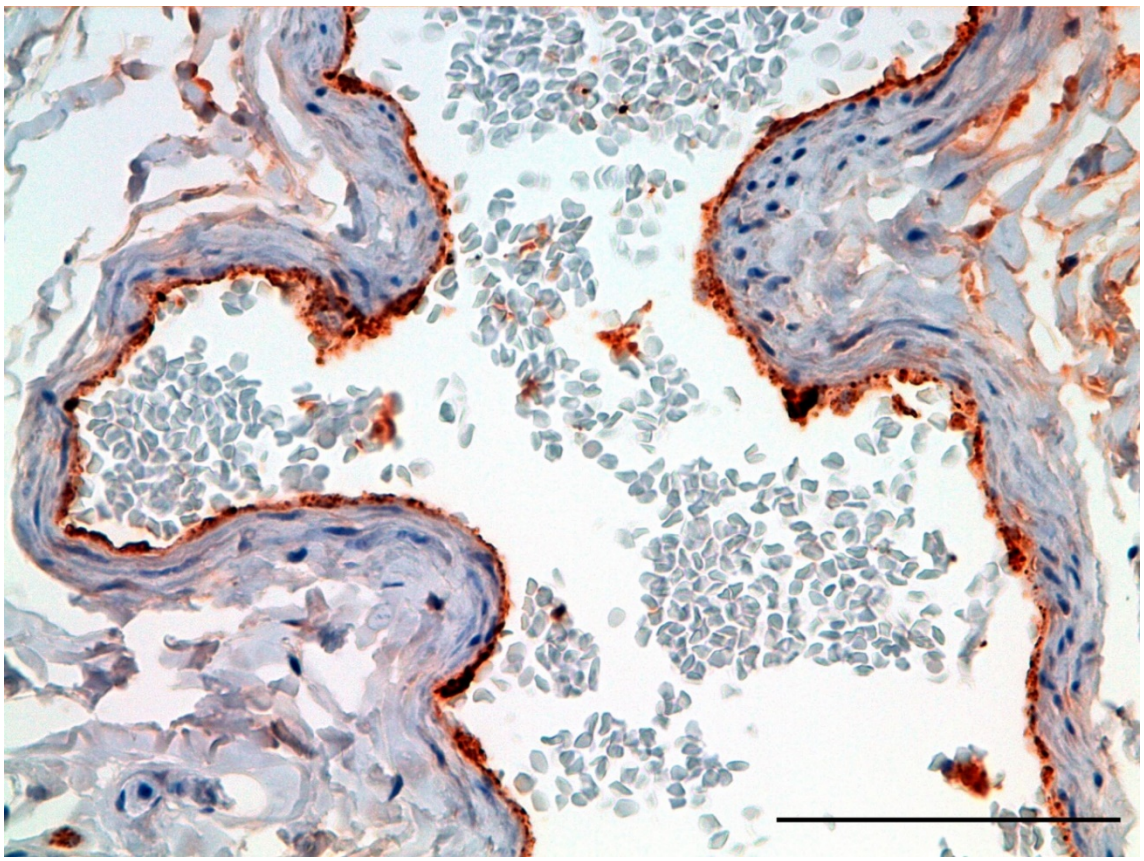

Figure 170. Detail IHC image (anti-vWf, factor VIII) of a blood vessel close to the ear canal in a striped dolphin. Scale bar 100 µm

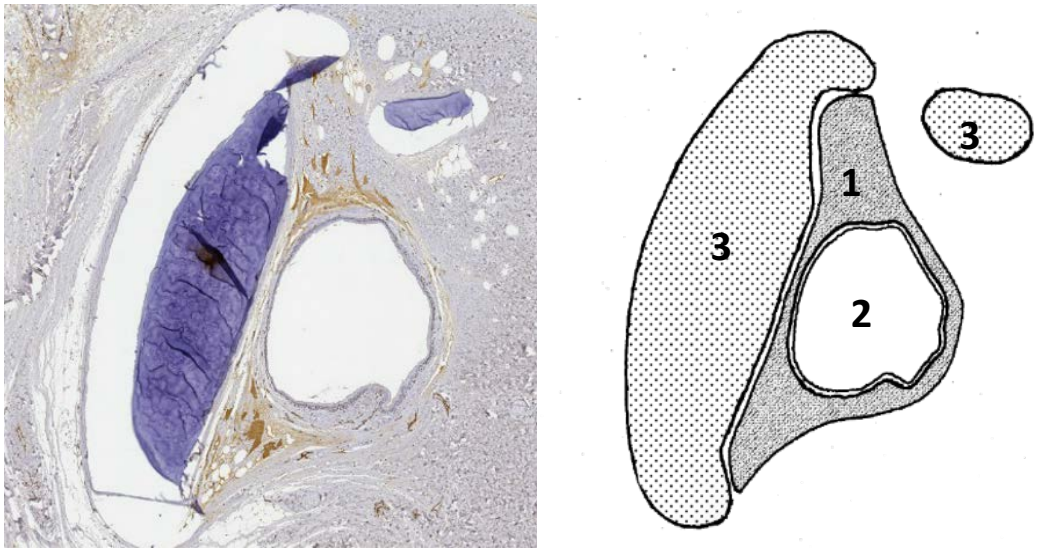

Figure 171. Left: Histological image of a transverse section through the ear canal of a striped dolphin at about 1 cm from the surface. (Immunohistochemical stain vWf (factor VIII)). Right: Schematic drawing showing the distribution of the vascular lacunae (1) in relation to the external ear canal (2) and the hyaline cartilage (3).

Figure 172. Left: Histological image of a transverse section through the ear canal of a striped dolphin at about 3 cm from the surface. (HE staining). Note the presence of large vascular lacunae surrounding the ear canal in the through created by the hyaline cartilage. Right: Schematic drawing showing the distribution of the vascular lacunae (1) in relation to the external ear canal (2) and the hyaline cartilage (3).

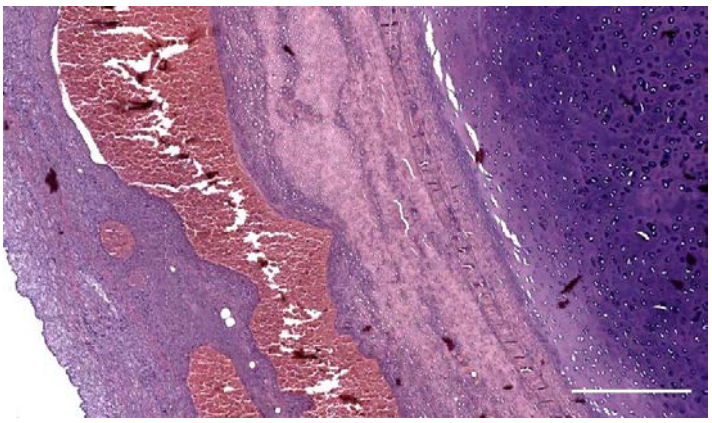

Figure 173. Histological image (HE staining) of the vasculature associated with the trachea in a striped dolphin. Scale bar 500 µm

2.9 Lymphoid tissue

There were two types of lymphoid tissue associated with the ear canal. The first is loosely arranged mononuclear cells in the ear canal´s subepithelial tissue in two locations, one at the level of the glands, and the other associated with the cartilage. The second type was clearly defined, relatively large, nodular lymphoid tissue, situated ventrocaudal to the ear canal at the level where the facial nerve passes the ear canal from ventral.

2.9.1 Ear canal-associated lymphoid tissue (ECALT)

2.9.1.1 Subepithelial, at the level of the glands

There was the presence of mononuclear inflammatory cells, mostly lymphocytes, but also plasma cells and occasionally macrophages, noted in almost all individuals, in the subepithelial tissue around the ear canal, in superficial sections, more or less at the level of the glands (e.g. Figure 174, Figure 175). In most cases, there were sparse cells, together with the other cells of the subepithelial tissue, and as such, seemed a resident population, part of a first barrier immune system, similar to resident mononuclear cells in the dermal papillae around the external ear opening. In other cases, there was an evident activation of the tissue, forming accumulations of mononuclear cells in the papillary layer and with clear signs of inflammation (See Pathology)(Figure 176).

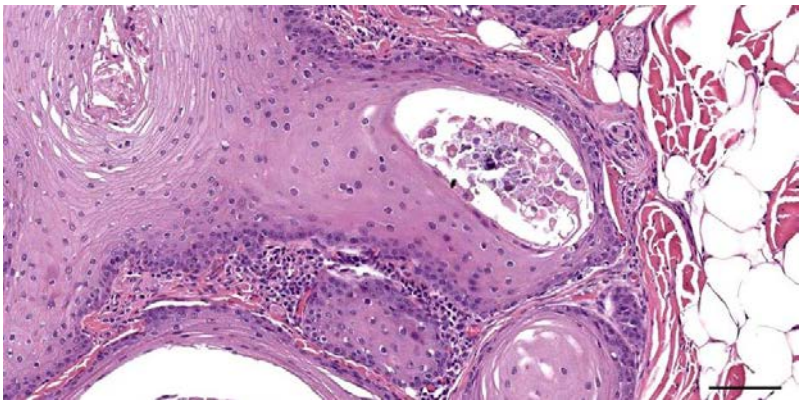

Figure 174. Histological image (HE staining) of a transverse section through the right ear canal of a common dolphin at about 1 cm beneath the skin (169/17_R2). Detail of Figure 63. Mononuclear cells in the subepithelial tissue situated between the ear canal and glandular structures. Scale bar 100 µm

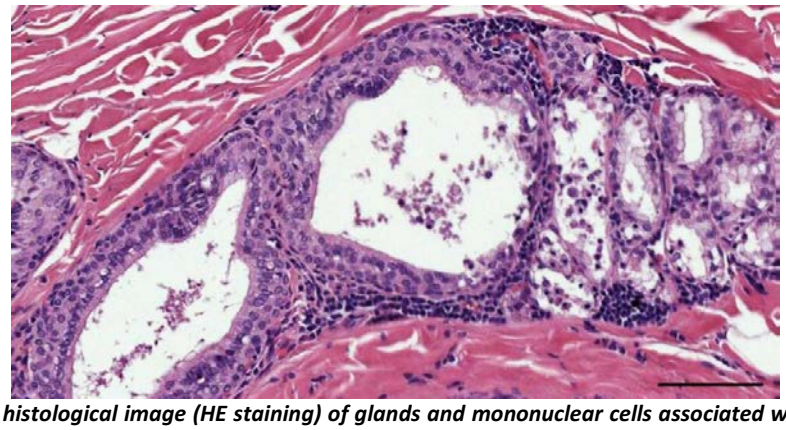

Figure 175. Detailed histological image (HE staining) of glands and mononuclear cells associated with the ear canal in a common dolphin (169/17_R4a). Scale bar 100 µm

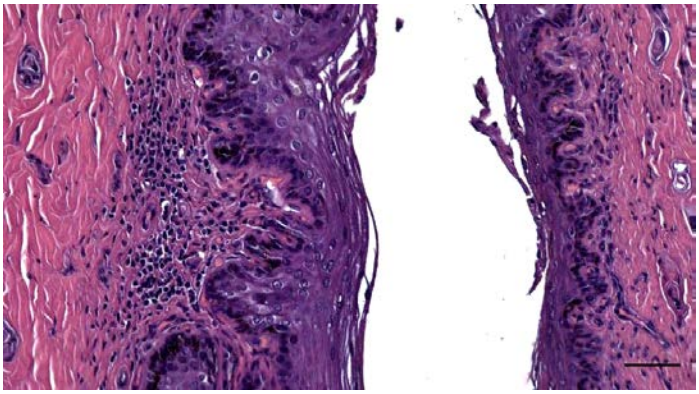

Figure 176. Histological cross-section (HE staining) of the ear canal with mononuclear infiltration in a bottlenose dolphin, at about 3 cm beneath the skin (457_R7). Ear canal with subepithelial mononuclear infiltration. Scale bar 50 µm

2.9.1.2 Between ear canal and cartilage

The second population of resident lymphocytes was present in the loose connective tissue between the ear canal and cartilage (Figure 177, Figure 178, Figure 164). This cell population was present in all individuals, in the medial third of the ear canal. In normal conditions, there were scant cells, distributed over the area, while in other cases there was an activation of the tissue with a secondary infiltration of more and other types of mononuclear cells, often with a perivascular distribution (Figure 179, Figure 180).

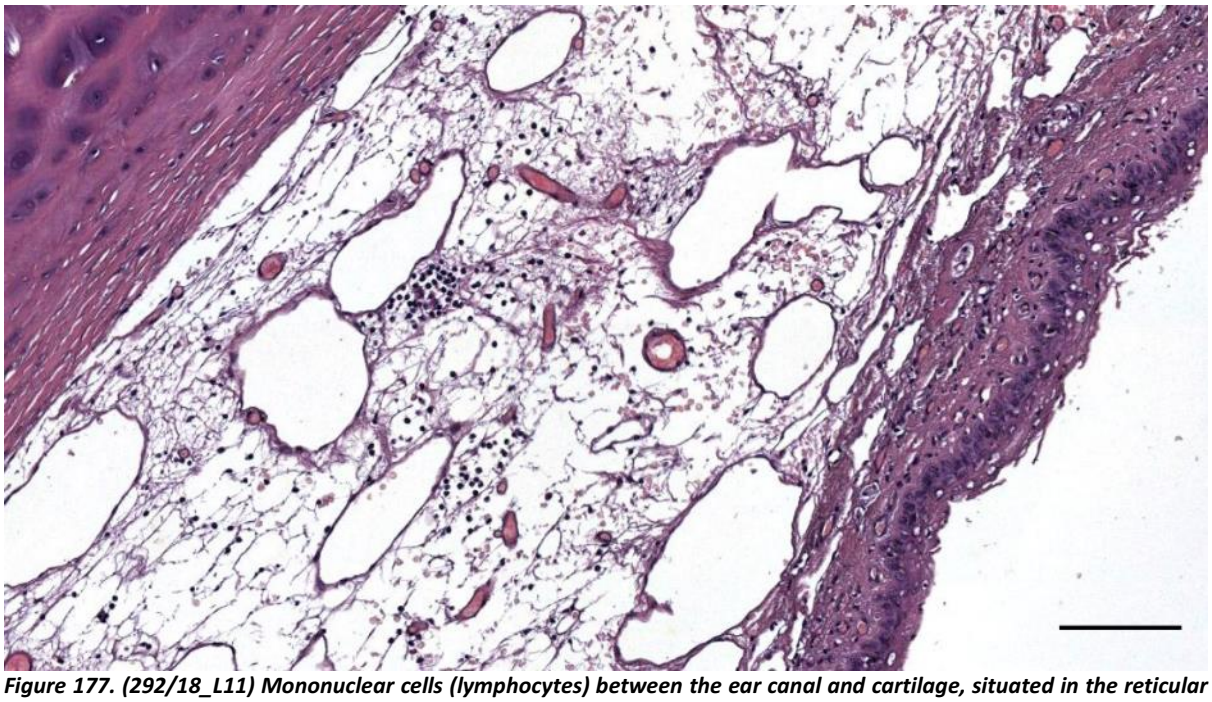

Figure 177. (292/18_L11) Mononuclear cells (lymphocytes) between the ear canal and cartilage, situated in the reticular connective tissue network with vascular lacunae. Scale bar 100 µm

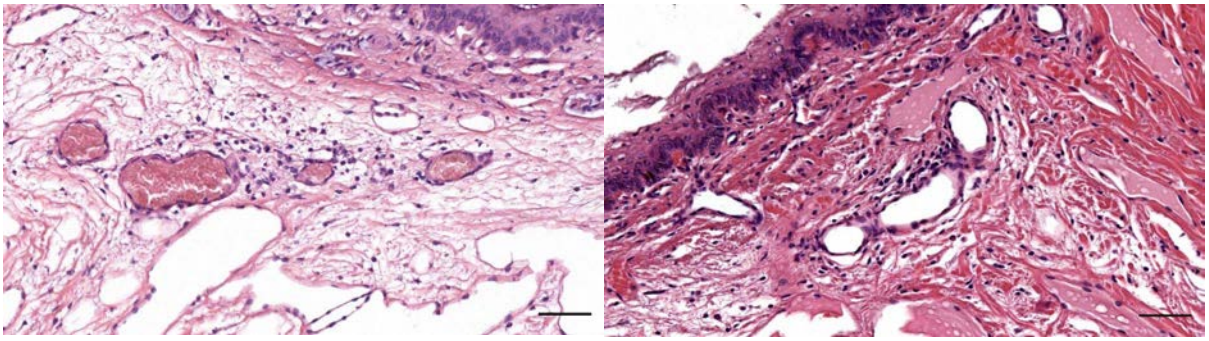

Figure 178. (274/18_R8) Mononuclear cells in the subepithelial tissue between the ear canal and cartilage in a striped dolphin, in a perivascular distribution. Scale bar 50 µm

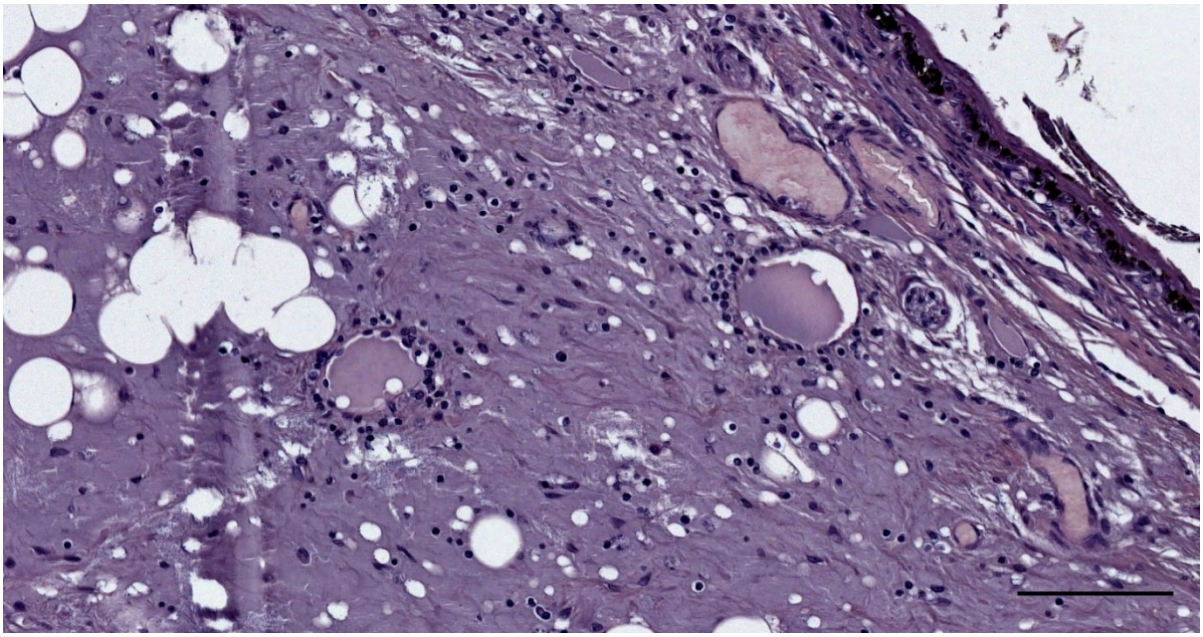

Figure 179. Histological image (HE stain) of the tissue between the ear canal and cartilage in a harbour porpoise (UT1718_L1403). There is the perivascular presence (cuffing) of lymphocytic cells and macrophages, and oedema with protein leakage associated with an inflammatory process, with the splitting of collagen fibres. Scale bar 100 µm

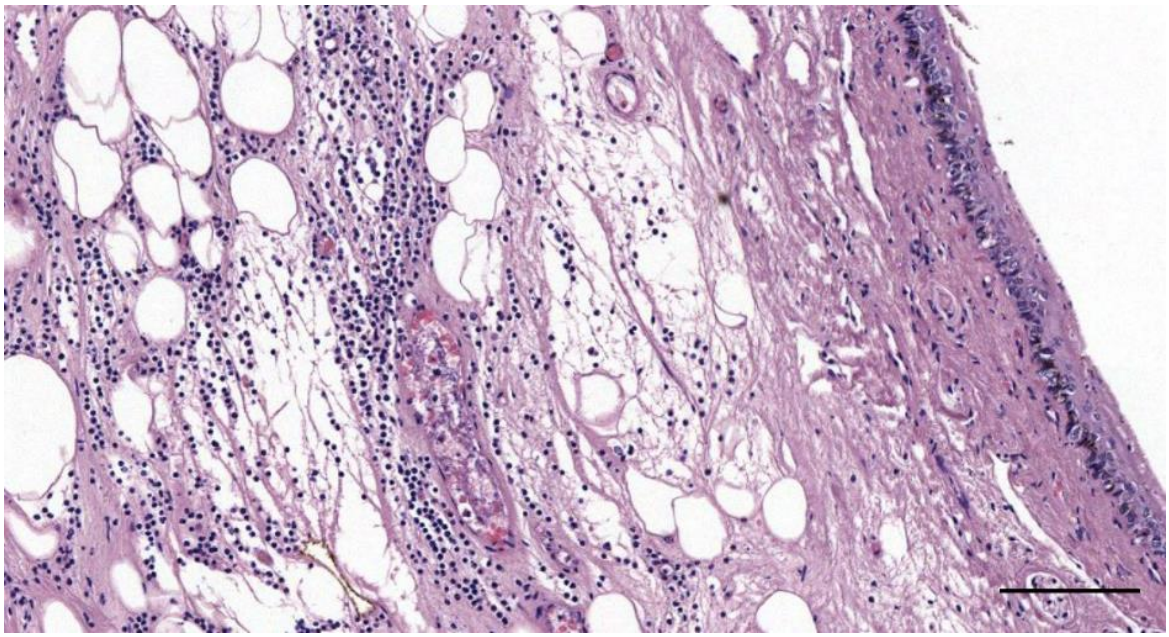

Figure 180. Histological image (HE stain) of a mononuclear infiltrate between the ear canal and cartilage in a bottlenose dolphin (444_L18). Scale bar 100 µm

2.9.2 Nodular lymphoid tissue

There was nodular lymphoid tissue in spatial association with the external ear canal in at least four striped dolphin individuals. These were found in samples that were dissected with as much surrounding tissue as would fit into a standard tissue cassette. All lymphoid nodes were situated rostroventral to the ear canal in the medial third of the ear canal, both left and right side, at about the level where the facial nerve passes ventral to the ear canal and cartilage (Figure 181). In all cases, it was located in the fat tissue ventral to the ear canal, close to the border with the triangular connective tissue capsule. Below are presented the four individual cases with an in-depth description of the morphological characteristics of the lymphoid tissue.

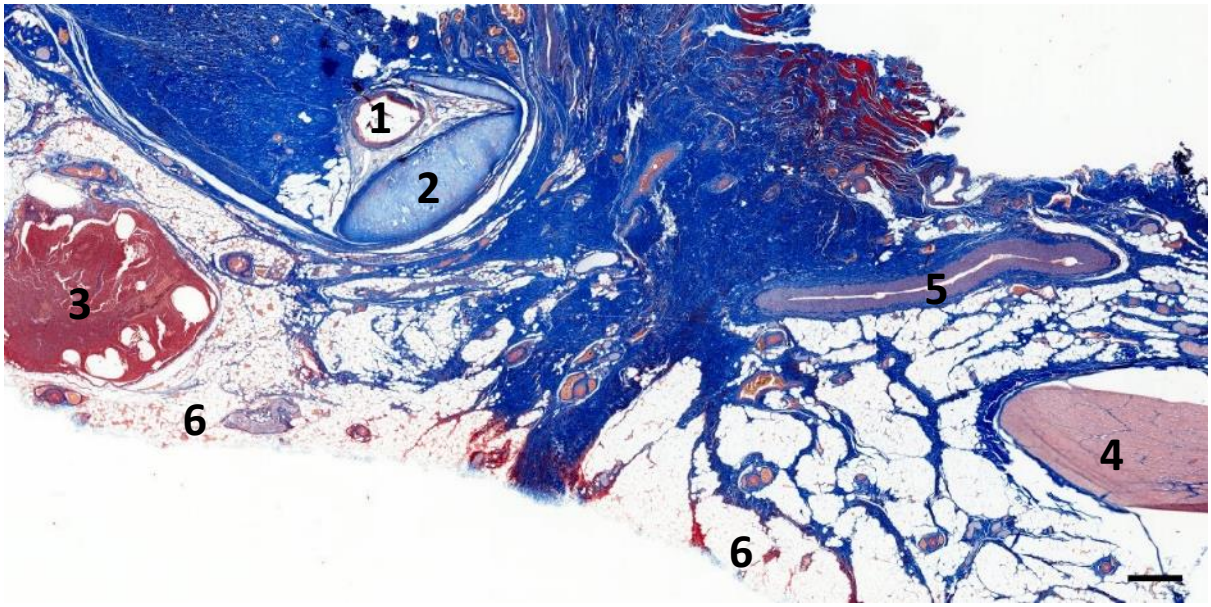

Figure 181. Parasagittal section through the region of the external ear canal of a striped dolphin (ID127565). 1. External ear canal; 2. Cartilage of the ear canal; 3. Lymph node; 4. Facial nerve; 5. Facial vein; 6. Fat body. Scale bar 1 mm

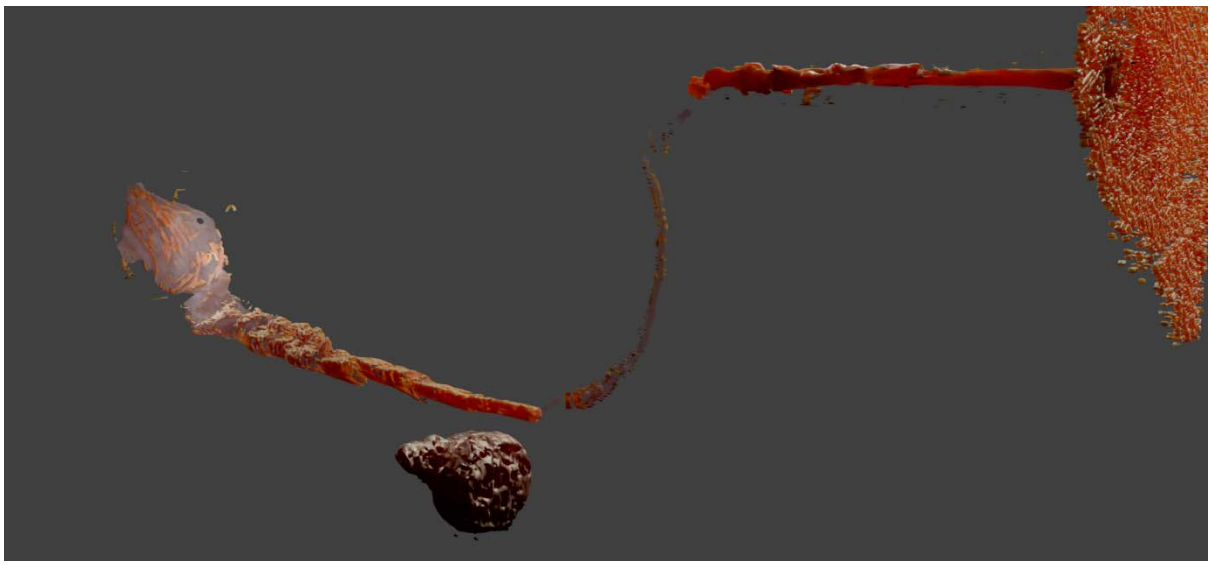

Figure 182. 3D rendering demonstrating the position of the lymph node ventral to the ear canal, at about the medial third of the course of the canal. Rostrolateral view of the ear canal lumen and epithelium.

Case striped dolphin (ID274/18)

There was bilateral lymphoid tissue located medial to the ventral curvature of the ear canal, on the rostral side of the canal, and separated from it over a distance of about 2.5-3 mm by the normal canal's subepithelial tissue, bulges of hyaline cartilage, and a dense connective tissue capsule that incompletely encircled the lymphoid tissue (Figure 183). Where the capsule was absent, there were areas of direct transition from lymphoid tissue to the neighbouring adipose tissues (Figure 184). Where it was present, we noted connective tissue strands (trabeculae) that entered into the cortex. There was a very poor delineation between cortex and medulla. The organ consisted of two main lobes with a para-lobe attached to one of them and the presence of an isolated patch of lymphoid tissue. The entire structure on the right side of the head was about 5 by 5 mm in size, while on the left it was slightly larger (7 x 5 mm) on transverse sections through the ear canal, and less than 10 mm in length.

The tissue consisted of lymphatic follicles and parafollicular tissue, with the former comprised of a mantle zone that delineated the germinal centre, which was subdivided into a light zone and a dark zone, although this was not always clear (Figure 185). There were secondary follicles with cellular depletion in some but not all germinal centres, and the deposition of hyaline material wherever active. The parafollicular tissue was poorly delineated and in some parts of the structure consisted of patched to interconnected zones of concentrated lymphocytes and other mononuclear cells. There was a large number of erythrocytes dispersed in the entire organ and concentrated in specific areas such as in the subcapsular sinuses and parafollicular tissue (Figure 185, Figure 186). We could not find any signs of erythrophagocytosis.

As for the cellular composition, there were lymphocytes, plasma cells, reticular cells (with reticular connective tissue between cells), macrophages, neutrophils, eosinophils, and megakaryocytes in the parafollicular tissue, and possibly nucleated erythrocytes within the follicles.

There were few endothelial-lined spaces within the parenchyma, and they all contained erythrocytes. In the stroma, between the main lobes of lymphoid tissue, there were arteries and veins, all containing red blood cells. The HE-stained section did not allow for the identification of any high-endothelial venules (HEV), which are typically present in lymphoid tissue.

Structurally, the tissue resembled the cetacean spleen, except for the invasion of inflammatory cells, and with more heterogeneity in the organization.

In conclusion, there was bilateral reactive lymphoid tissue with lymphadenopathy.

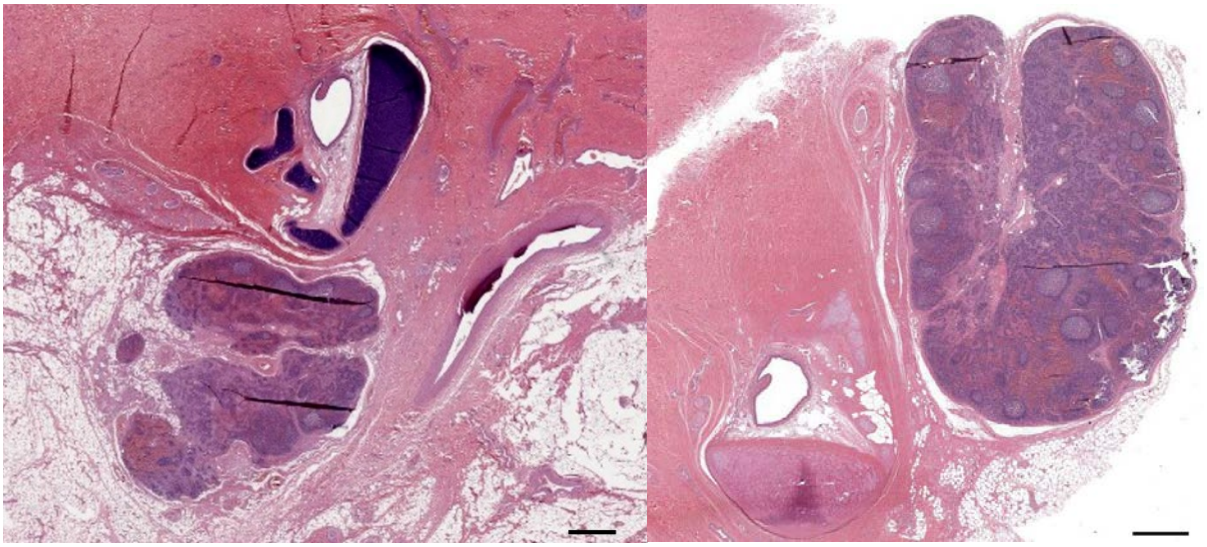

Figure 183. Histological image (HE stain) (274/18_R9) Overview of the lymphoid tissue in the close vicinity of the left and right external ear canal and a large artery. Scale bars 1 mm

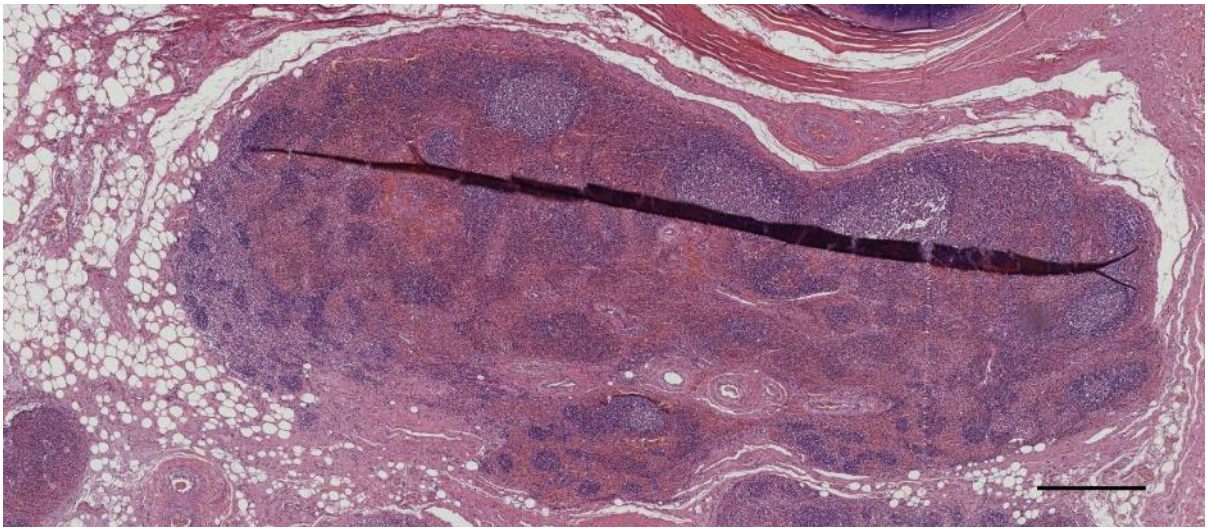

Figure 184. Histological image (HE stain) (274/18_R9) Detail of one lobe of the lymphoid tissue. Note the capsule is not present all around, and there is a region where the lymphoid tissue directly contacts the adipose tissue. There is no clear difference between cortex and medulla. There are lymphoid follicles and a parafollicular zone. Also note the overall heterogeneous distribution of erythrocytes, although, at larger magnification, we can see blood cells everywhere. Scale bar 0.5 mm

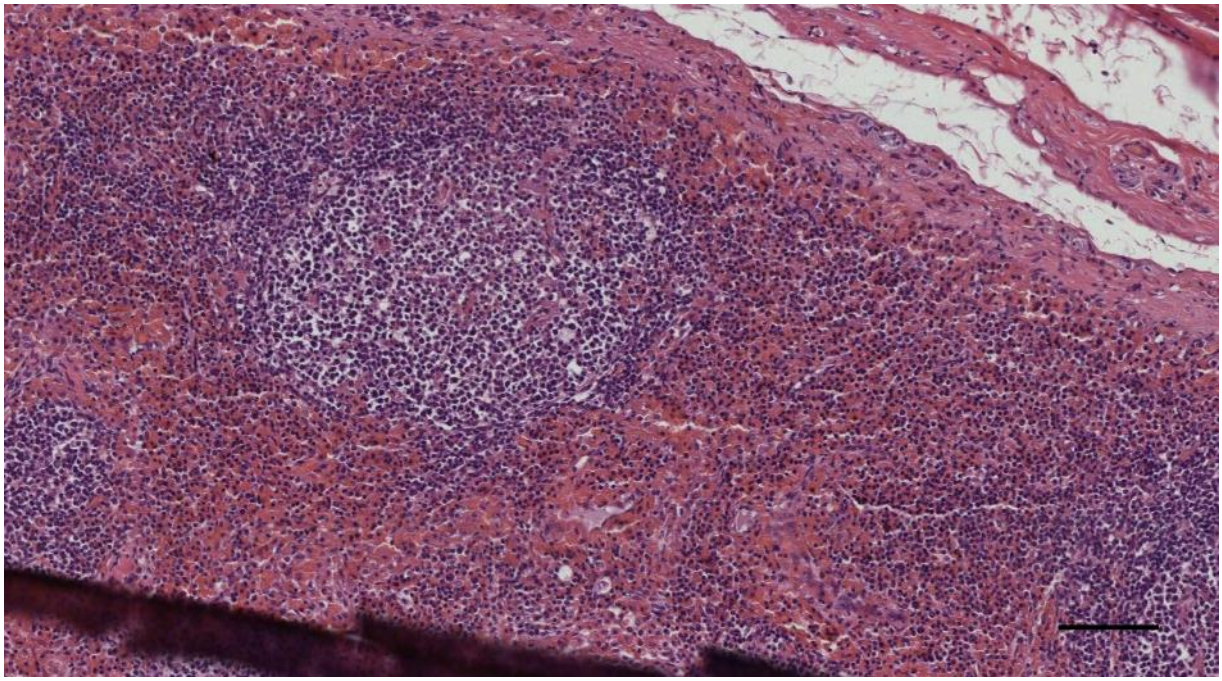

Figure 185. Histological image (HE stain) (274/18_R9) Detail of the 'cortical' zone with a connective tissue capsule, a subcapsular sinus with many erythrocytes, a follicle with mantle zone and germinal centre, and parafollicular tissue with many erythrocytes. Scale bar 100 µm

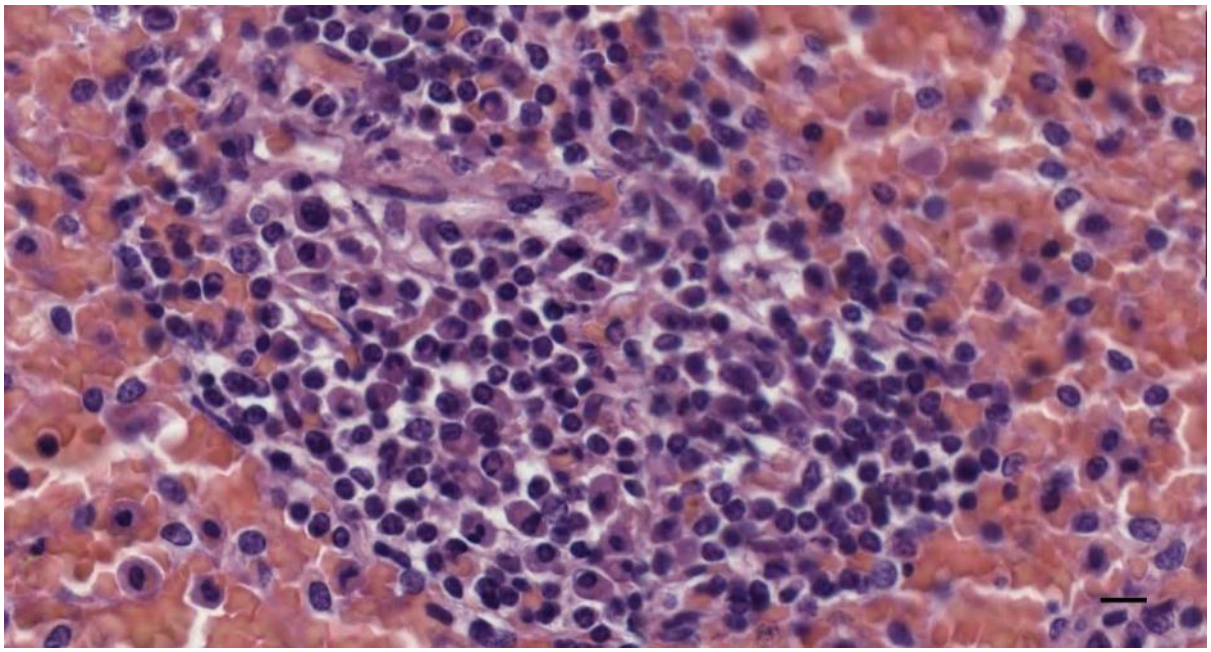

Figure 186. Histological image (HE stain) (274/18_R9) Patched folliculloid tissue and the intense presence of red blood cells. Scale bar 50 µm

Case striped dolphin ID362/18

Rostroventral to the ear canal and on the opposite side of cartilage, there were two large (1.2 x 2.5 mm on cross-section) focal nodular concentration of mononuclear cells in the adipoconnective tissue. (Figure 187, Figure 188). The structure was encapsulated, but only on one side (direction of the ear canal). It was very well vascularized. The cellular contents were lymphocytes and plasma cells (indicate of a viral infection), with a sinusoidal histiocytosis (indicating a filtering functioning, typical for

bacterial infection). There was lymphoid depletion and an eosinophilic matrix (indicative of long-term activation, possibly as a reaction to Morbillivirus infection). There were also apoptotic changes.

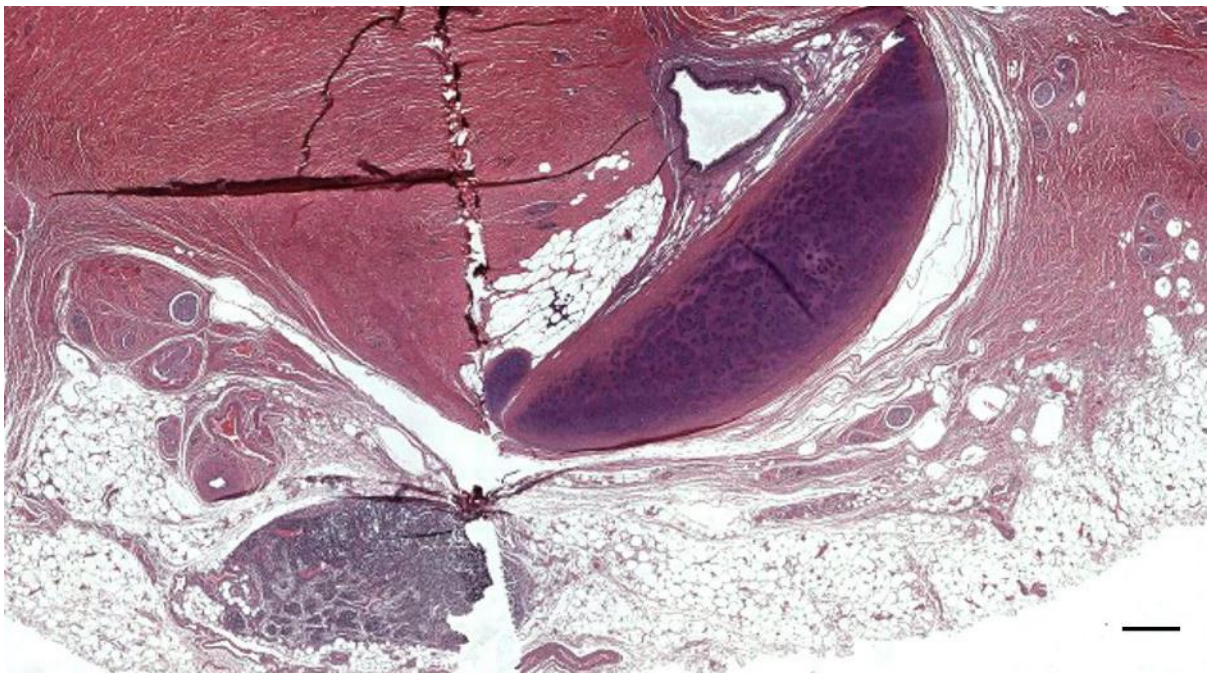

Figure 187. Histological cross-section (HE staining) through the left ear canal, cartilage, and nodular lymphoid tissue in a striped dolphin, about 5 cm beneath the skin (362/18_L11). Scale bar 0.5 mm

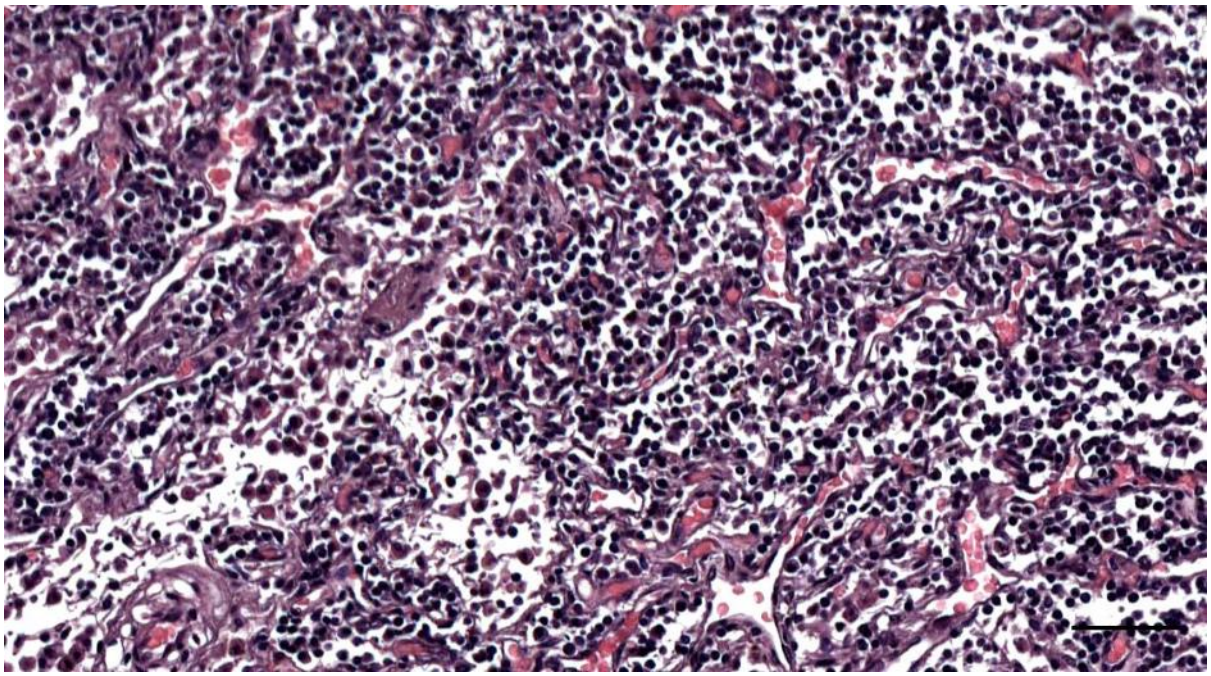

Figure 188. (362/18_L11) EAM associated lymphoid tissue. Scale bar 50 µm

Case striped dolphin ID449

The nodular lymphoid tissue was situated in the same location as in the other animals, in the medial third of the ear canal, where the facial nerve crosses the ear canal passage and separated from the ear canal by the cartilage (Figure 162). Dimensions on cross-sections were about 1.5-2.5 mm, while

the length of the tissue was not analysed. The stroma consisted of a peripheral thin collagenous capsule, with trabeculae of connective tissue projecting in the direction of the centre, both of which are predominantly inhabited by fibroblast cells, and was well-vascularized. In the centre of the node, there was similar tissue with dense vascularization in the form of many arteries. There was a marginal sinus around what was considered the cortical area, although there was no distinction between cortex and medulla, and an incomplete organization into follicles and parafollicular tissue. The peripheral areas with follicles consisted of dense populations of small, darkly stained lymphocytes. These would be considered the germinal centres containing a large number of erythrocytes, together with activated and inactivated lymphocytes. There were no signs of macrophagy, but rather hyperplastic changes with a starry sky pattern associated with apoptotic changes (Figure 189).

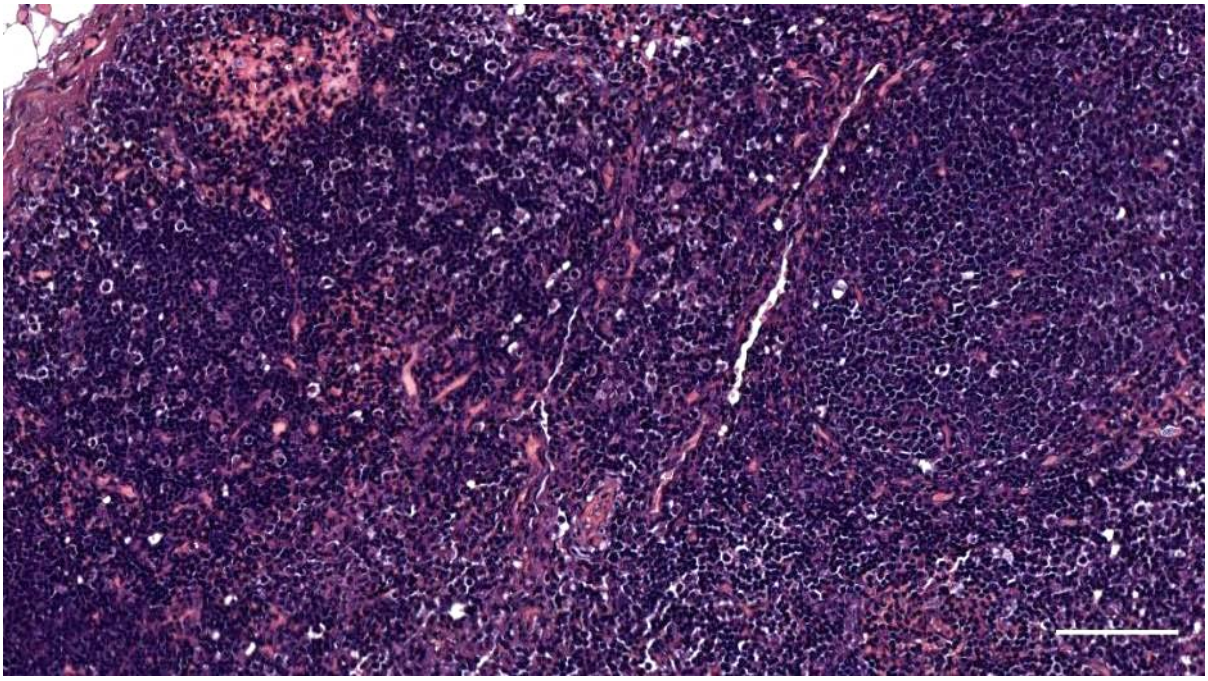

Figure 189. (ID449) Stenella coeruleoalba. (449_R8) Detail of Figure 13. Lymphoid tissue. Note the ´starry sky´ pattern of apoptotic cells. Scale bar 100 µm

Case striped dolphin ID127565

Similar to the other animals, the nodular lymphoid tissue was present more or less ventral to the ear canal, at the level where the facial nerve crosses ventral to the ear canal. The dimensions of the lymphoid node in this striped dolphin were 4.5-5 mm on histological sections and had a length of at least 3 mm (15 cross-sections with 200-micron interval) although was likely significantly larger. The stromal configuration was similar to the other animals, and the parenchyma contained lymphocytes and macrophages, and red blood cells (Figure 181 to Figure 191).

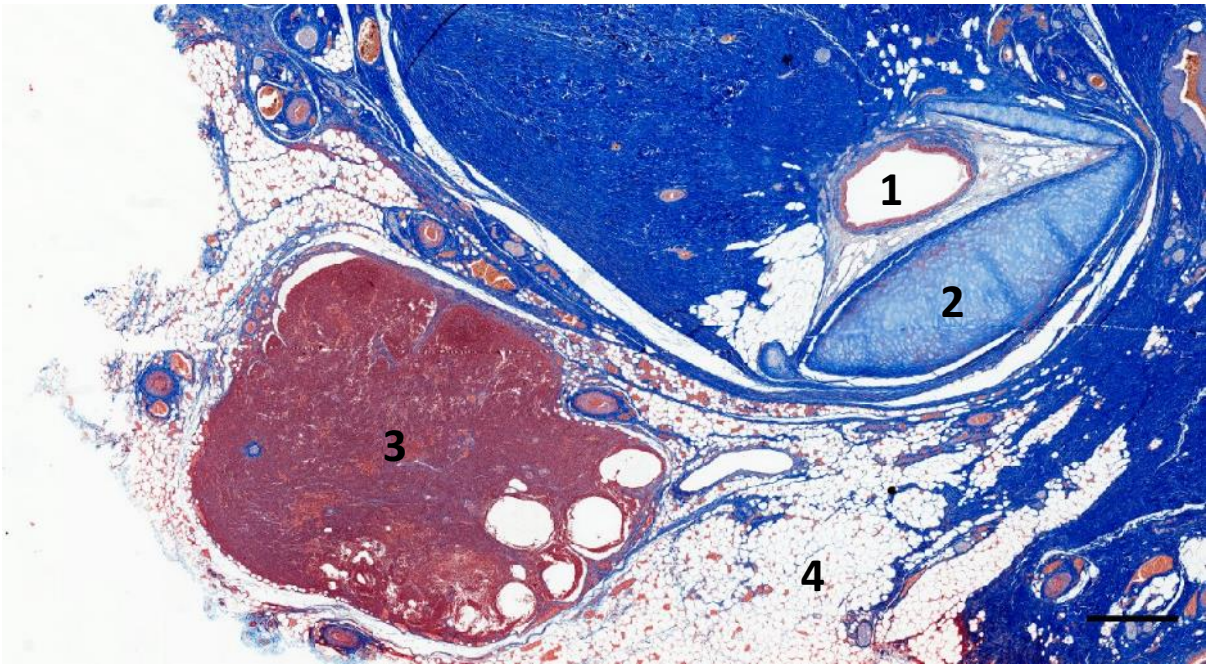

Figure 190. Parasagittal section through the region of the external ear canal of a striped dolphin (ID127565). 1. External ear canal; 2. Cartilage of the ear canal; 3. Lymph node; 4. Fat tissue. Scale bar 1 mm

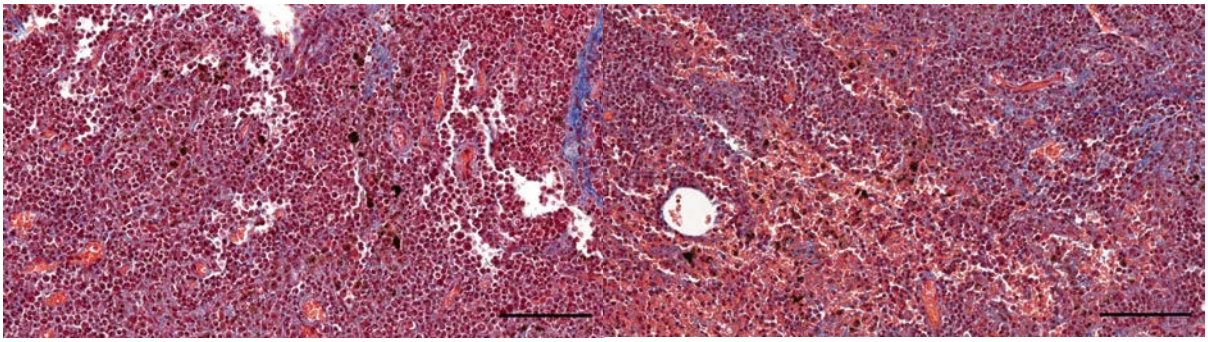

Figure 191. Detail images of Figure 190. Red blood cells, lymphocytes and macrophages. Scale bar 100 µm

2.10 Medial end of the external ear canal, and tympanic conus

We assessed the morphological features of the medial end of the ear canal in striped dolphin and bottlenose dolphin using macroscopic preparation, histological dissection and HE and Masson's Trichrome stain.

The medial end of the ear canal was surrounded by a horseshoe-shaped cartilage, which disappeared on the trajectory through the tympanic notch (*sulcus tympanicus*), i.e. between the sigmoid, conical, and posterior process of the tympanic bone (Figure 192, Figure 193, Figure 194, Figure 195, Figure 196). The canal´s lumen continued and turned around the sigmoid process (Figure 197, Figure 198, Figure 201), where it rapidly flared and broadened to a cone-shaped canal that ended blindly, overlying the tympanic conus (Figure 192).

Throughout the passage, the subepithelial connective tissue became very thin, except for a single area that abutted the sigmoid process, called the 'nervous tissue ridge'. This well-innervated and vascularized subepithelial tissue was present in the most medial part of the ear canal, from about 0.5

to 1 cm lateral to the TP complex, where it was present opposite the cartilage, and becomes gradually larger over the course to the medial end. On the canal's curvature around the sigmoid process, this tissue ridge grew rapidly in size and was at its largest at the canal´s endpoint, where it lied opposite the tympanic membrane (Figure 198).

The tympanic conus is the name for the combined structures of the tympanic membrane and tympanic ligament. The tympanic membrane was a concave structure, suspended in the bony rim of the tympanic notch. It was visible as a thin and tough membrane consisting of several layers (Figure 202): on the side of the lumen of the ear canal, in which there were desquamated epithelial cells, it had a thin squamous epithelium with melanin in the basal cells layer. Beneath it, there was a lamina propria with an extensive vascular plexus and the presence of small nerve fibres, overlying a dense organization of collagen fibres orientated in a circular and radial arrangement. Next, there was a small layer of well-vascularized loose connective tissue and a simple squamous epithelium. The height of the connective tissue layers differed depending on the location of the section through the tympanic membrane. There was a big vascular plexus in the paracentral area where the tympanic membrane transgressed into the tympanic ligament. The tympanic ligament was a seemingly though ligament with parallel orientated connective tissue fibres and scant nuclei, lined with a unicellular epithelium (Figure 203).

Figure 192. Macroscopic preparation of the medial end of the right ear canal of a striped dolphin. The ear canal is opened for visual presentation. The insert shows the identification of the three main structures: green: ear canal lumen and epithelium; blue: cartilage; orange: tympanic membrane. Scale bar 0.5 cm

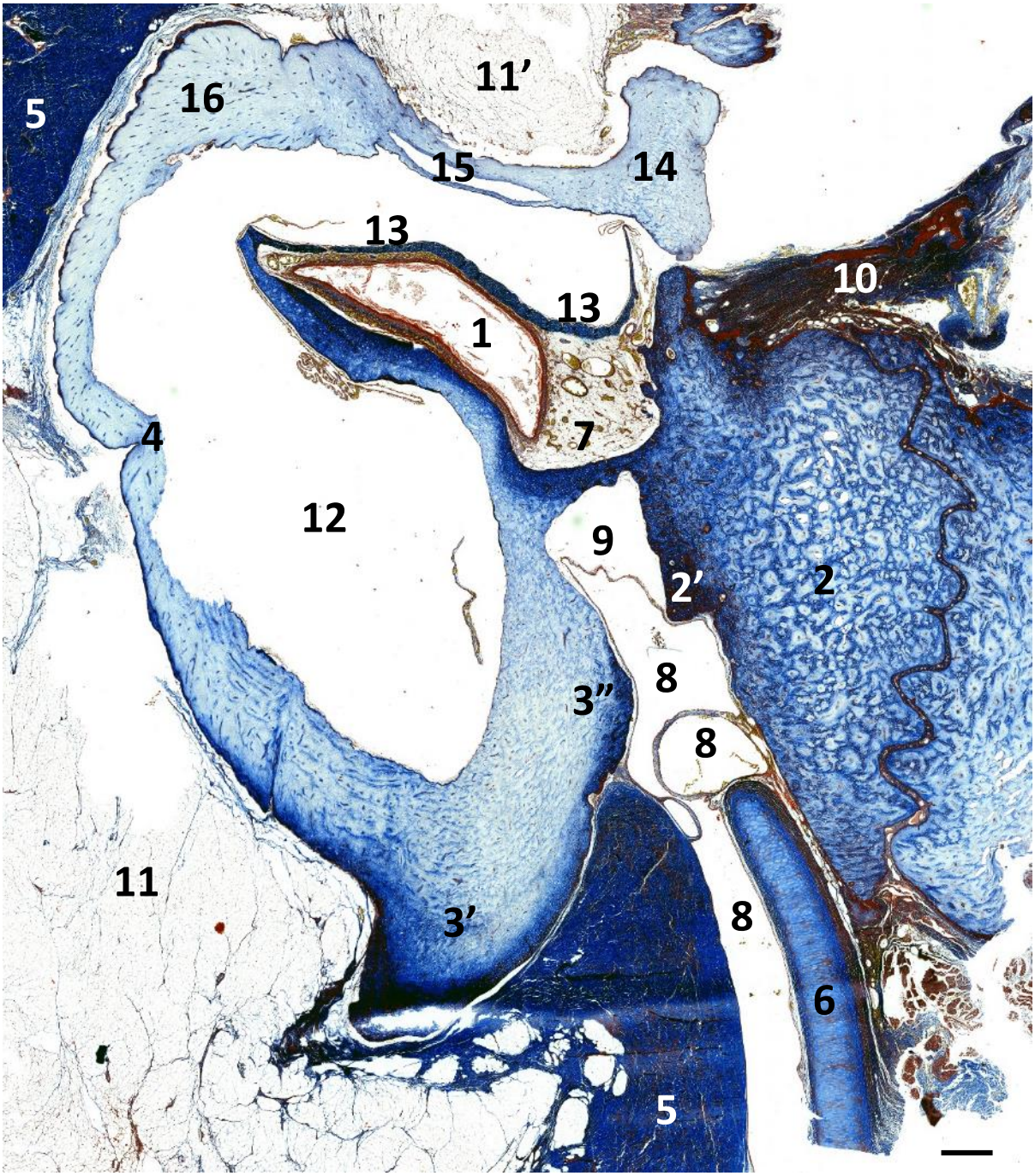

Figure 193. Masson’s trichrome staining of the left ear canal entering the TP-complex at the level of the tympanic notch in striped dolphin (N274/18). 1. Ear canal; 2. Posterior process of the tympanic (Mead and Fordyce, 2009) or processus petrosus (Nummela et al., 1999); 2’ posterior tympanic spine; 3. Sigmoid process of the tympanic; 3’ dorsal apex; 3” epitympanic border; 4. Sulcus for chorda tympani; 5. Connective tissue capsule surrounding the acoustic fat; 6. Ear canal cartilage; 7. Vascular network in a fibrine mesh; 8. Vascular sinuses accompanying the ear canal on its course through the tympanic aperture; 9. Artefactual space; 10. Ligament attaching to 2, for suspension of the TP complex in the peribullar sinus; 11. Acoustic fat contacting the sigmoid process and the malleus (11’); 12. Tympanic cavity projecting into the sigmoid process; 13. Tympanic membrane; 14. Malleus; 15. ‘blue dot in Cranford (2010) Fig.10; 16. Accessory ossicle. Scale bar 1mm.

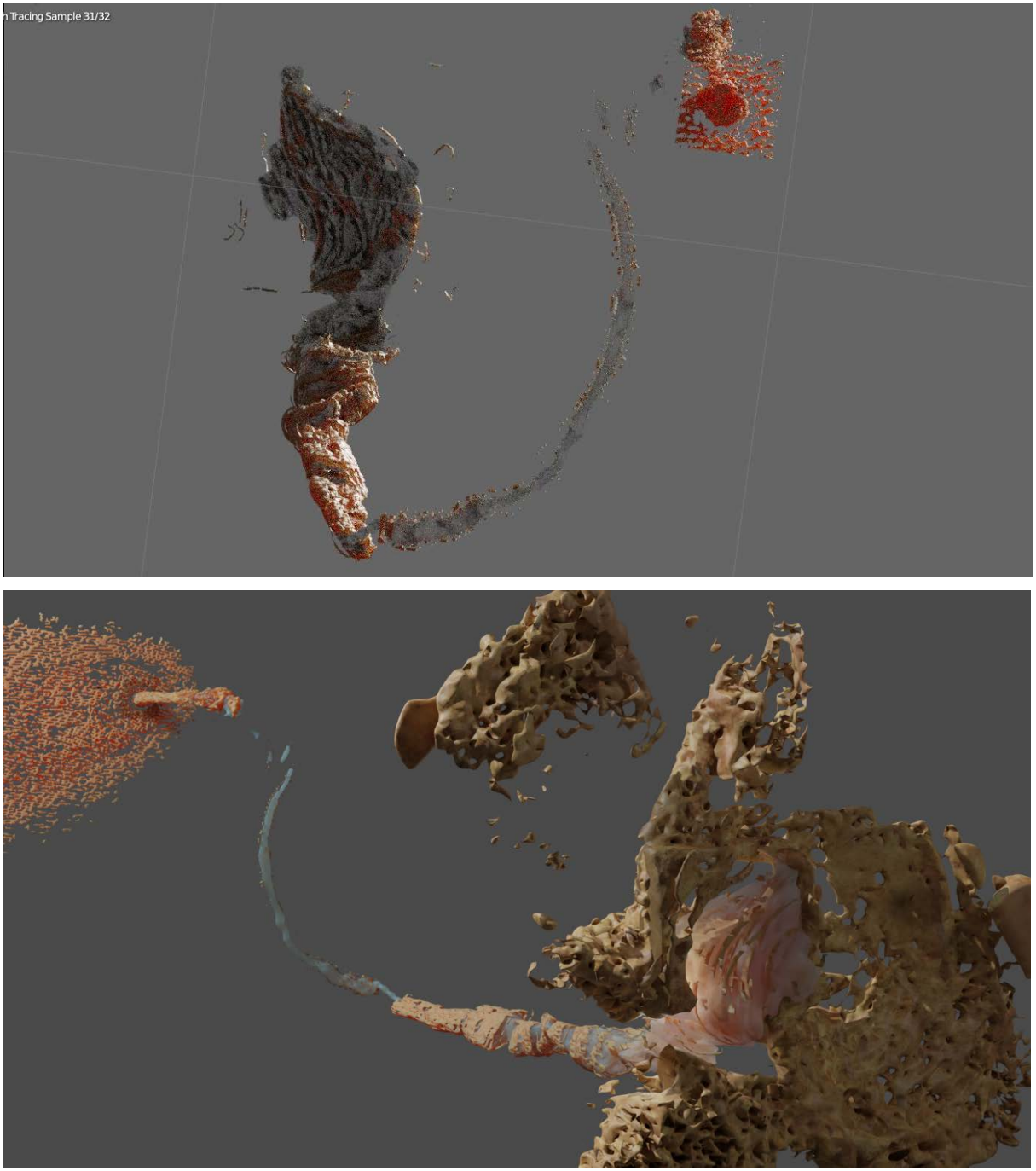

Figure 194. Images of a 3D rendering of the lumen (blue) and epithelium (pink) of the left ear canal in a striped dolphin (ID127565). Top: Lateral view of the external ear opening, the ventral curvature, and the club-shaped expansion of the ear canal at the medial end. Bottom: caudomedial view of the ear canal club-shaped expansion curving around the sigmoid process of the tympanic, together with other lateral portions of the TP-complex, reconstructed from histological slides.

Figure 195. Macroscopic preparation of the medial end of the left ear canal of a striped dolphin. The periotic has been removed, and the ossicular chain disarticulated between malleus and incus. 1. Ear canal; 2. Tympanic membrane and ligament (2’); 3. Malleus; 4. Acoustic fat; 5. Tympanic plate; 6. Involucrum; 7. Sigmoid process of the tympanic; Asterisk: tympanic cavity extension in the sigmoid process

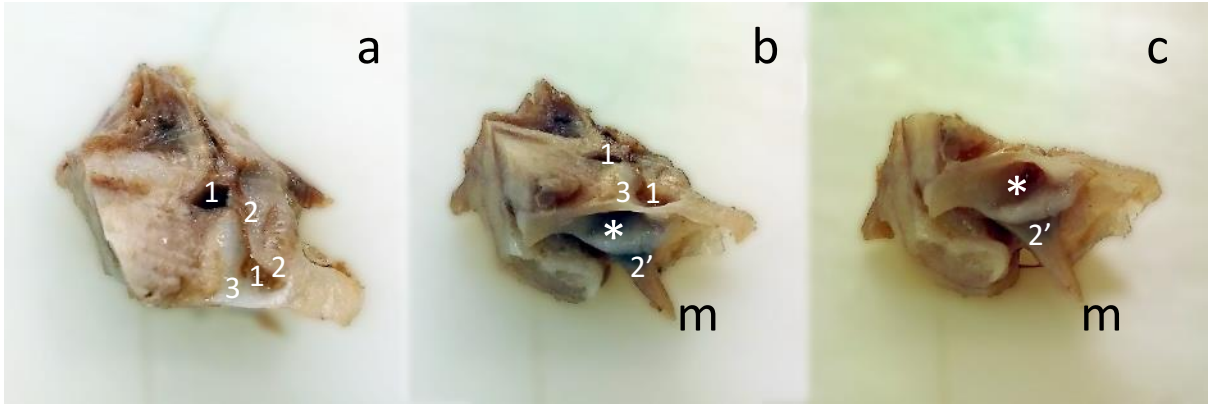

Figure 196. A lateral (a), latero-ventral (b) and ventral (c) view of a macroscopic preparation of the medial end of the right ear canal (1) and the tympanic membrane (2), and ligament (2’) of a striped dolphin. The asterisk shows a small extension of the tympanic cavity into the sigmoid process (3) which covers the far most medial end of the canal and the tympanic membrane. 4: projection of the tympanic to the malleus, which is missing.

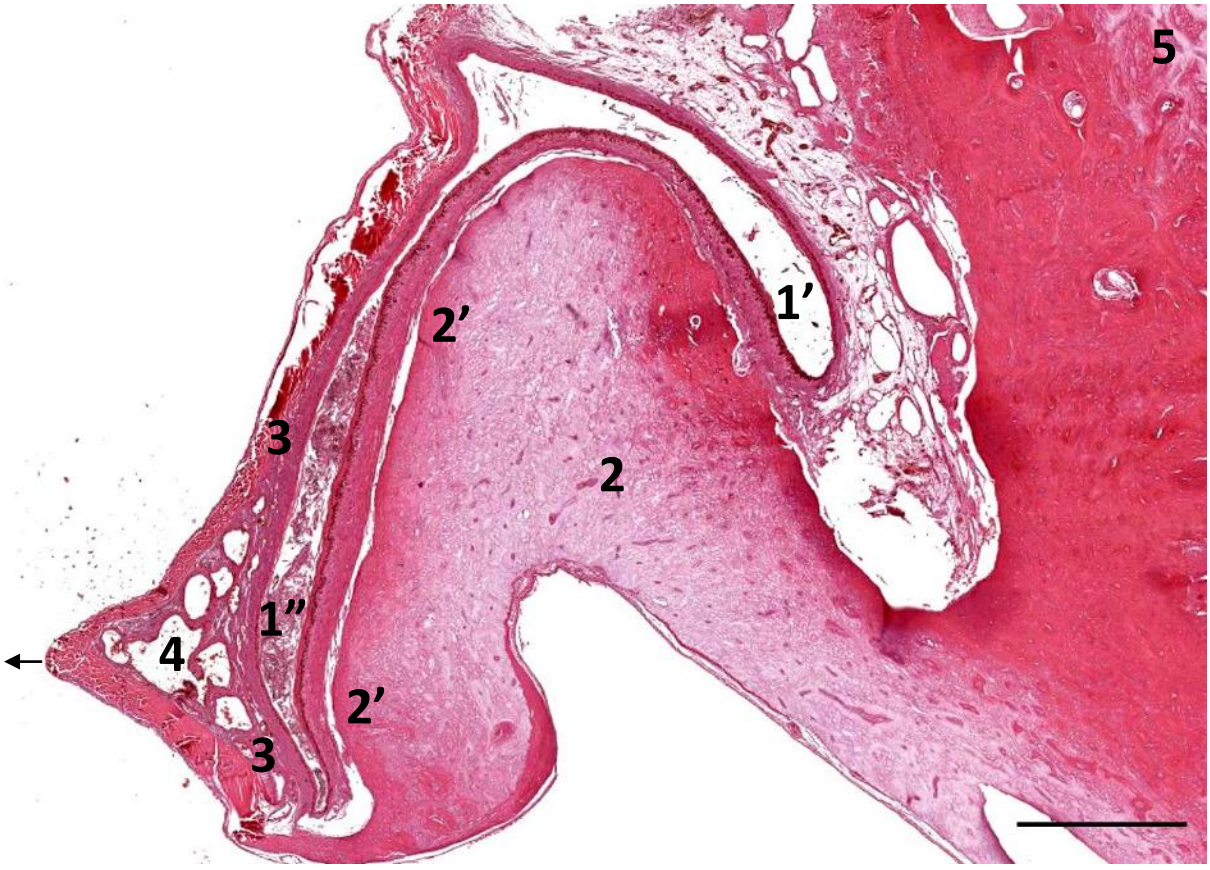

Figure 197. HE-stained histological section of the left ear canal (1) entering the TP complex. The round ear canal (1') turns around the sigmoid process (2) and broadens into a cone-shaped medial end (1")(which is flattened here because of a loss of tension and which is filled with keratine). The medial end of the ear canal abuts the epitympanic border of the sigmoid process (2') and which overlies the tympanic membrane (3). In the transition between the tympanic membrane and tympanic ligament, there is a vascular plexus (4). 5. Posterior process of the tympanic. Scale bar 1 mm

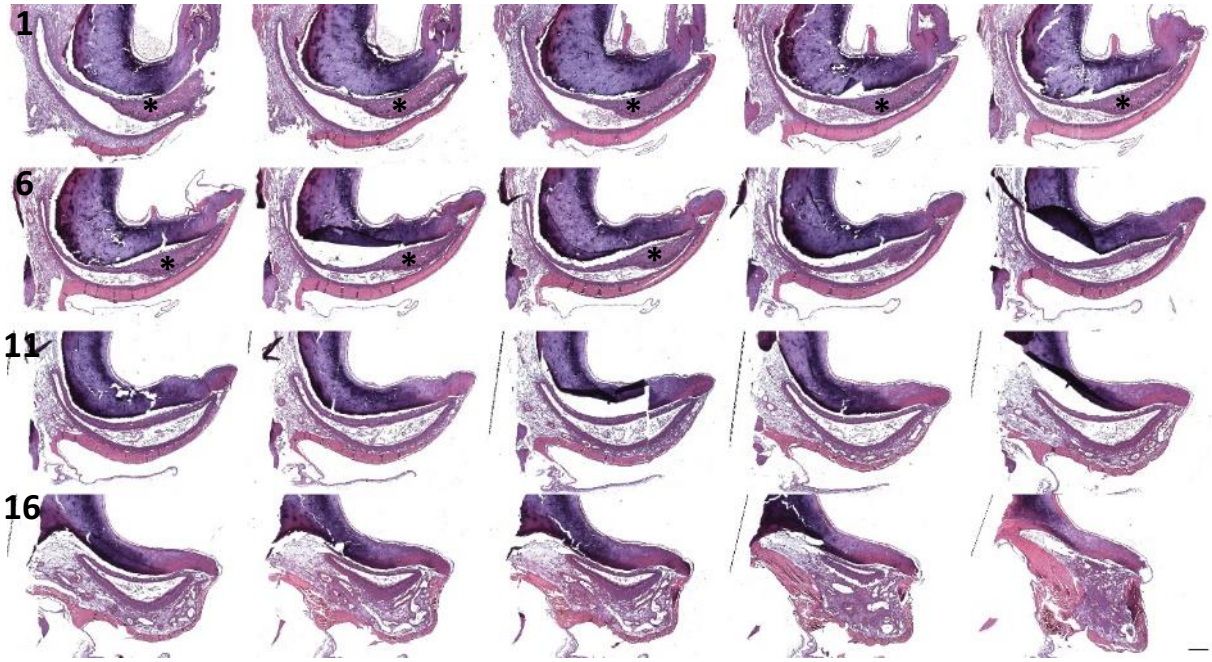

Figure 198. Series of HE sections through the medial end of the left ear canal of a striped dolphin. Note the presence of the nervous tissue ridge abutting the sigmoid process of the tympanic bull (Asterisk, slide 1-10). The presence of the vascular plexus in the centre of the tympanic conus (slide 14-20). In deeper sections, the tympanic membrane continued into the tympanic ligament, which attached to the malleus (Figure 203.)

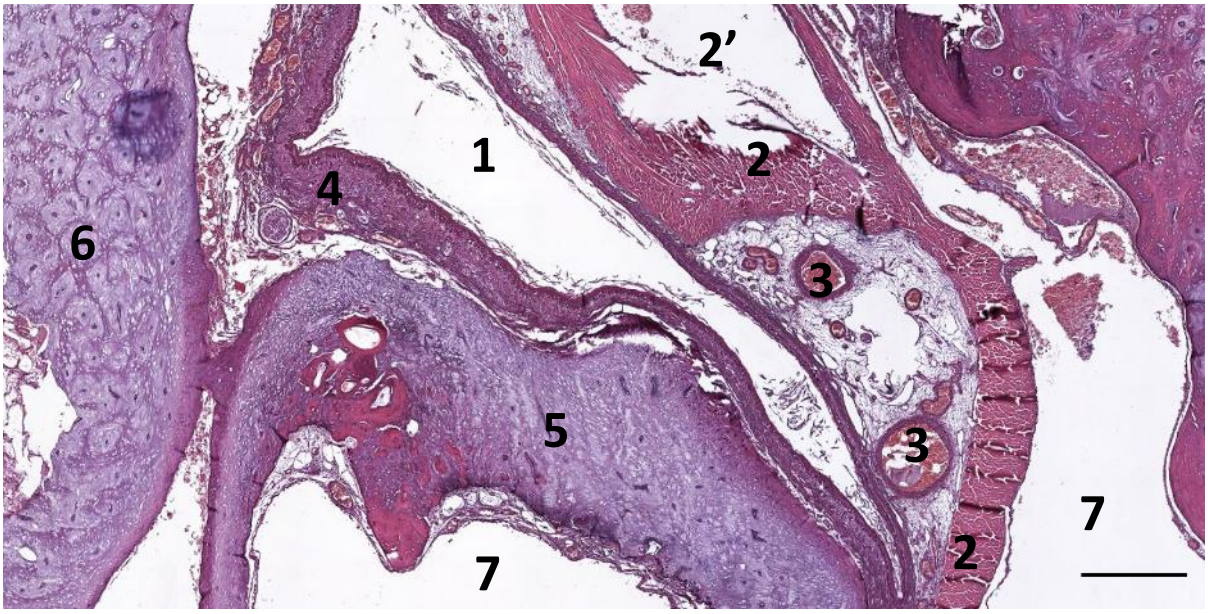

Figure 199. HE section of the right ear canal of a striped dolphin. 1. Ear canal; 2. Tympanic conus (2’ is an artefactual space); 3. Vascular plexus; 4. Subepithelial nervous network; 5. Sigmoid process; 6. Posterior process of the tympanic; 7. Tympanic cavity. Scale bar 0.5 mm

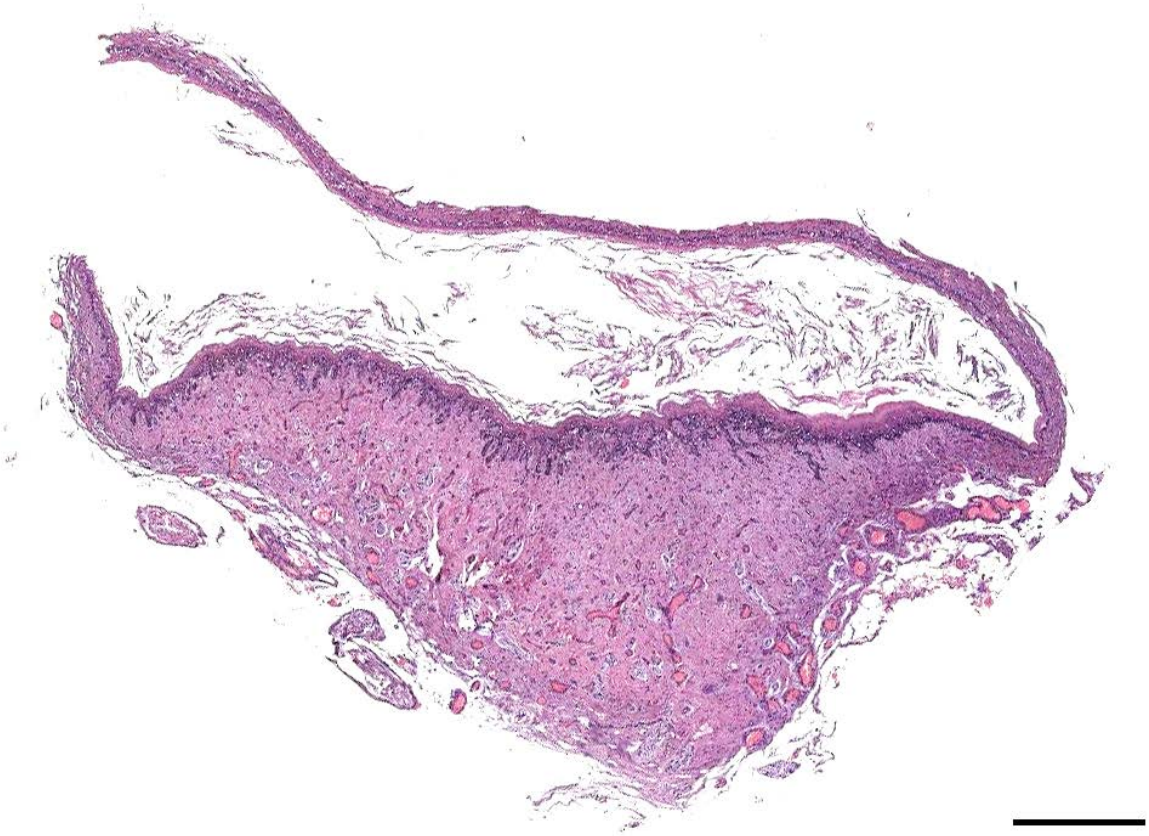

Figure 200. Histological detail (HE) of the medial end of the ear canal with large nervous tissue ridge lying opposite the tympanic membrane (the tympanic ligament got separated during dissection). Scale bar 0.5 mm

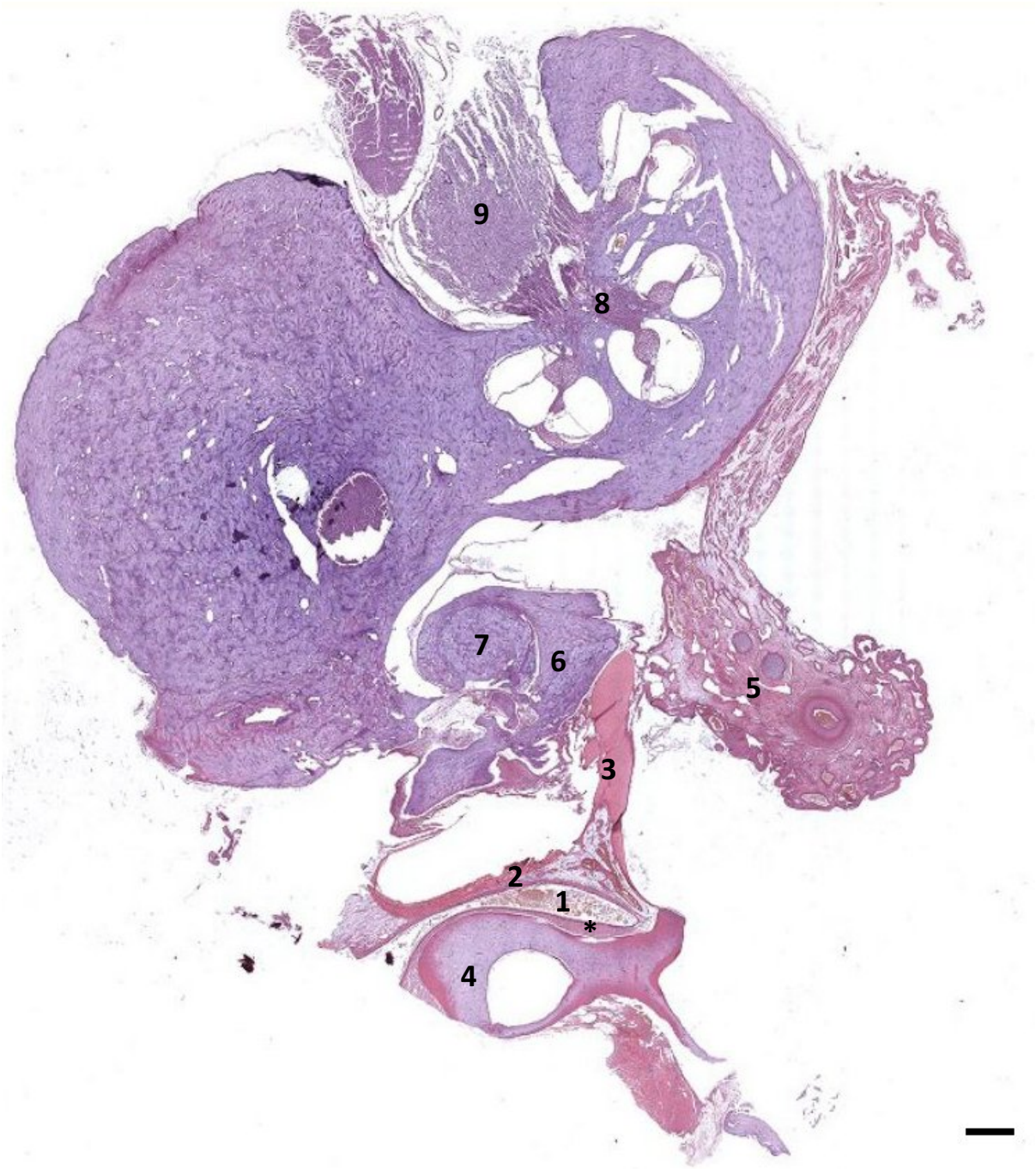

Figure 201. Histological section of the ear canal and TP-complex. 1. Ear canal (with nervous tissue ridge: asterisk); 2. Tympanic membrane; 3. Tympanic ligament; 4. Sigmoid process; 5. Corpus cavernosum tympanicum; 6. Malleus; 7: Incus; 8. Cochlea; 9. Cochlear nerve. Scale bar 1mm

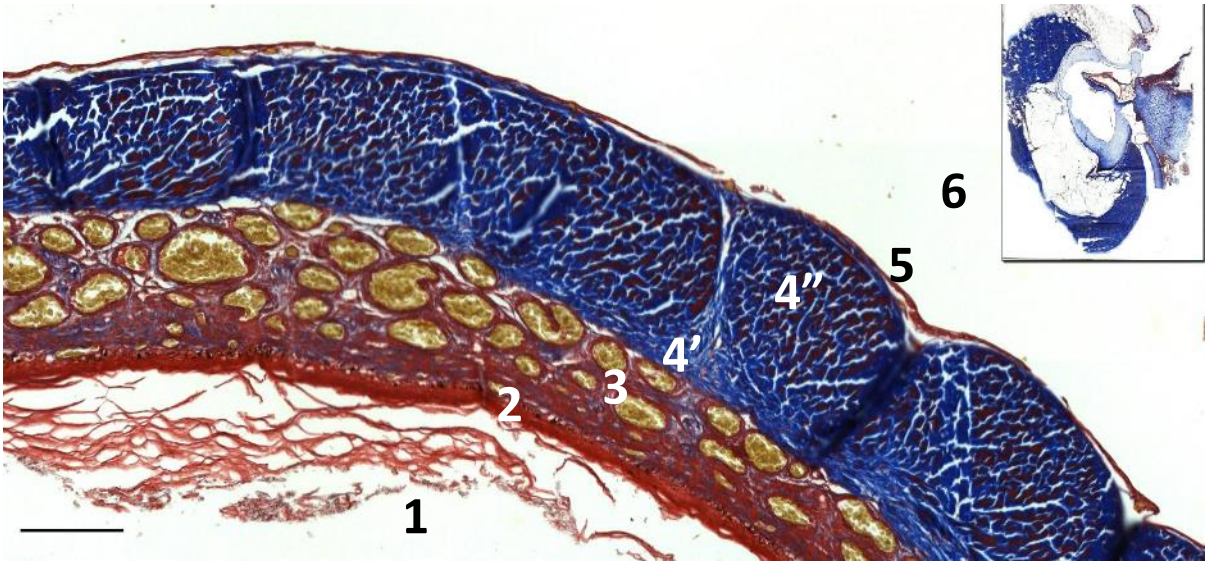

Figure 202. Detail of the tympanic membrane in Figure 193 (insert). 1. External ear canal lumen; 2. Thin squamous epithelium with melanin in the basal layer and desquamated cells in the lumen; 3. A lamina propria with an extensive vascular plexus with also the presence of small nerve fibres; 4. Collagen fibres orientated in a circular (4’) and radial (4”) arrangement; 5. Simple squamous epithelium overlying a small layer of vascularized connective tissue; 6. Tympanic cavity. Scale bar 100 µm.

Figure 203. Two images of an HE section of the tympanic ligament from the tympanic membrane and vascular sinus on the left, in the direction of the malleus (missing) on the right. Scale bar left 0.5 mm; right 100 µm

2.11 Foetus

All the features described above were present in a foetus with a length of 97 cm, weighing 6.8 kg. All tissues were heavy vascularized, as is a normal finding in developing tissue.

- Red blood cells in the lumen of the external ear opening (Figure 40)
- Ear canal content with glandular cells (artefact)(Figure 206)
- Glandular structures with pyknotic nuclei (Figure 204, Figure 205, Figure 206)
- Muscle (Figure 207)
- Nervous tissue ridge (Figure 208)
- Facial nerve

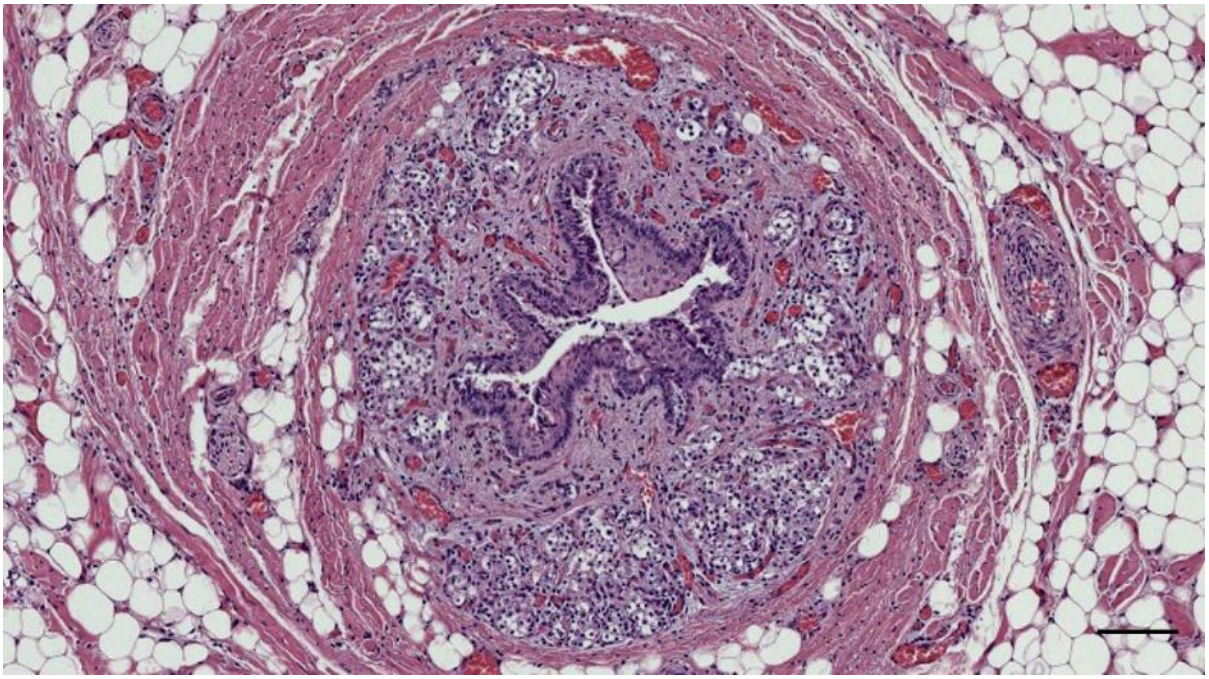

Figure 204. HE-stained section of the glandular structures around the ear canal in a striped dolphin foetus, at about 0.5 cm beneath the skin (293/18_foetus_L2). Scale bar 100 µm

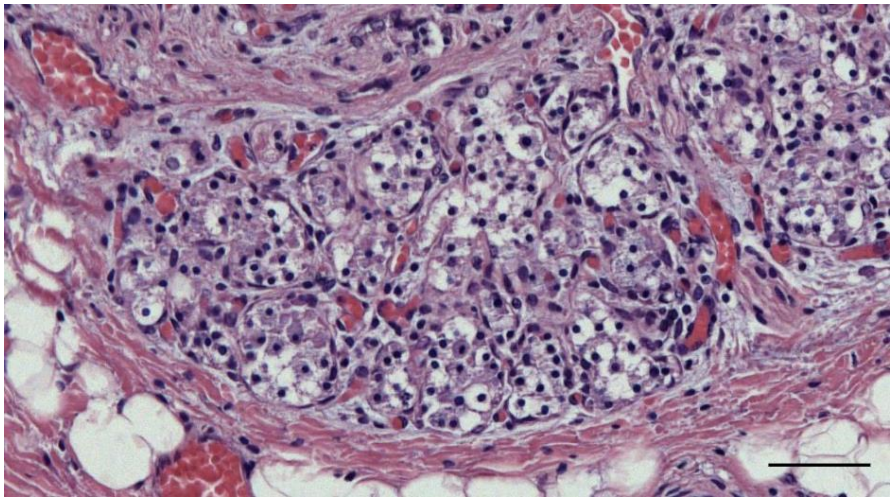

Figure 205. HE-stained detail section of the glandular structures around the ear canal in a striped dolphin foetus (293/18_foetus_L2). Scale bar 100 µm

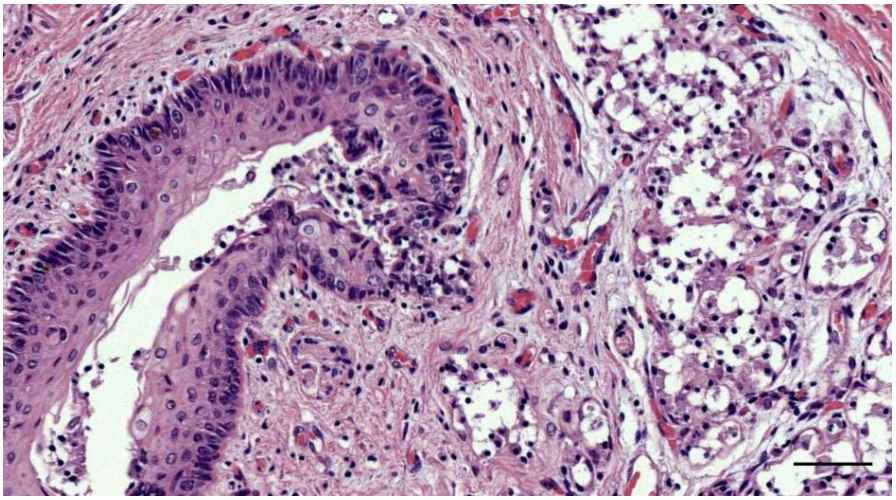

Figure 206. HE-stained detail of the ear canal and glandular structures with cellular content entering the ear canal lumen in a striped dolphin foetus at about 1 cm beneath the skin (293/18_foetus_L4). Scale bar 50 µm

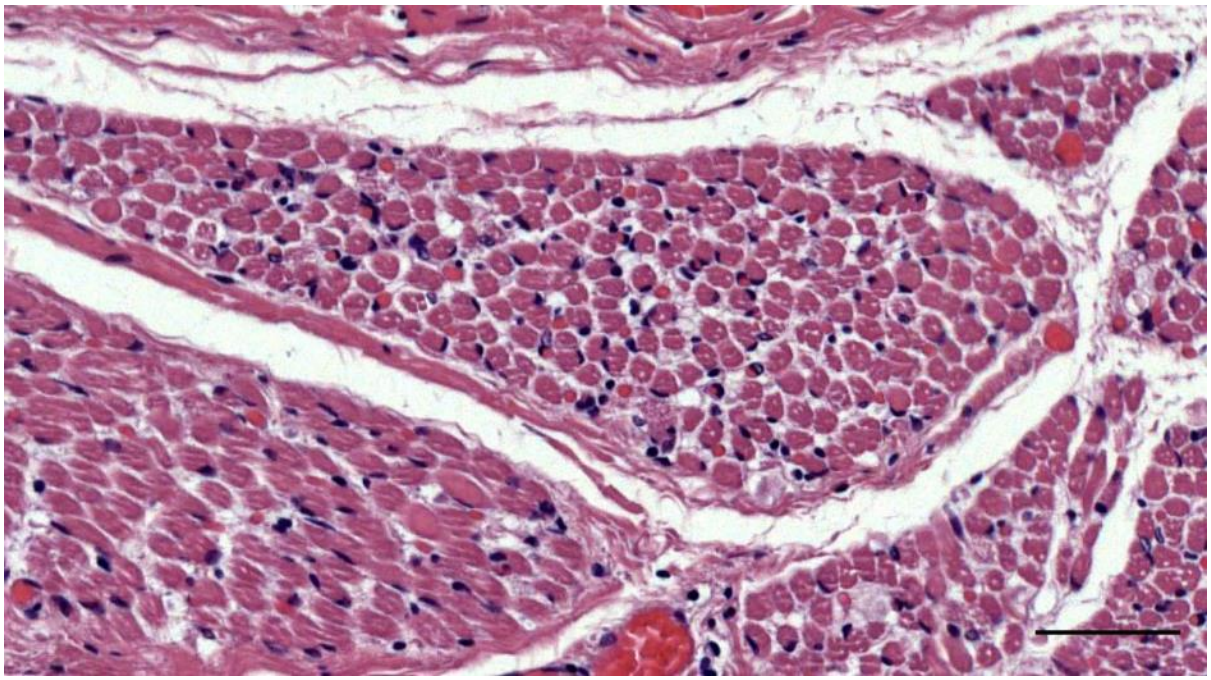

Figure 207. HE-stained detail section of the muscles around the ear canal in a striped dolphin foetus at about 1 cm beneath the skin (293/18_foetus_L3). Note the small diameter of the muscle fibres, the relatively large amount of connective tissue between fibres (similar to endomysial fibrosis), and the presence of cells with eosinophilic cytoplasm. Scale bar 100 µm

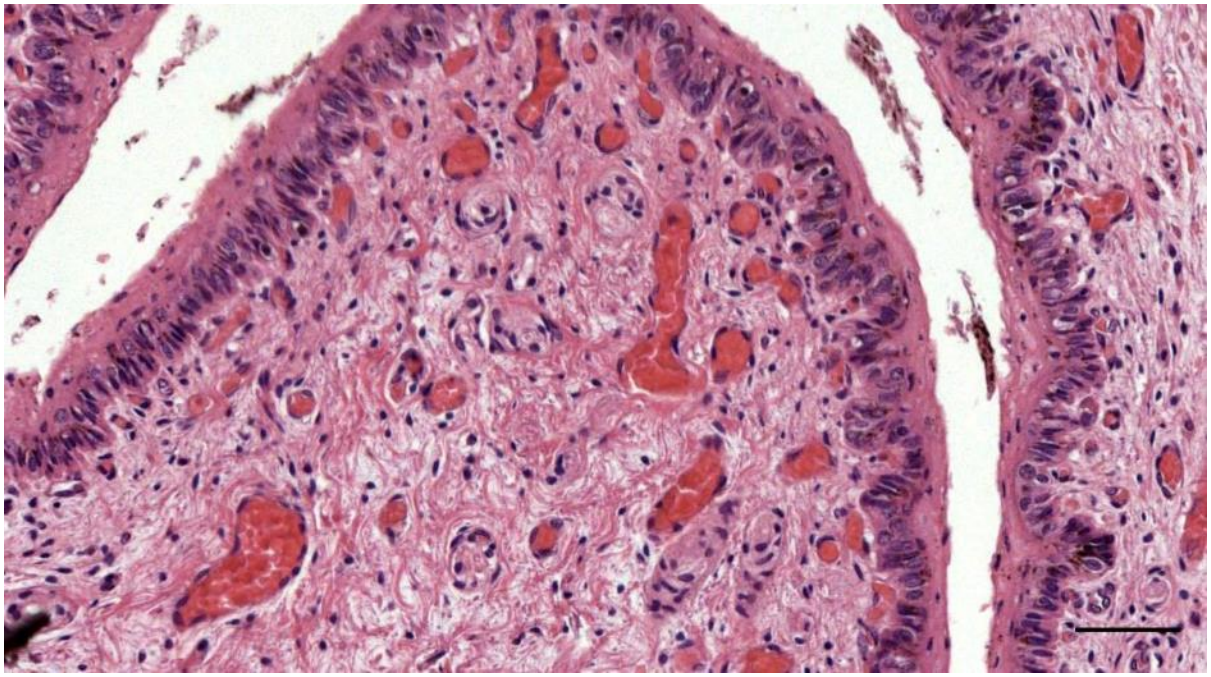

Figure 208. Histological detail (HE stain) of the nervous tissue ridge of the ear canal in a striped dolphin foetus at about 3 cm beneath the skin (293/18_foetus_L6). The ridge lies opposing the cartilage and contains abundant nervous structures. Scale bar 50 µm

3 Innervation

The external auditory meatus showed an extensive innervation over its entire course, in the form of lamellar sensory nerve formations, intrapapillary myelinated endings (IMEs), free nerve endings, and small to large nerve bundles. In the following sections, results are given on the presence and morphology of the lamellar corpuscles, using various structural and ultrastructural techniques.

3.1 Lamellar corpuscles

3.1.1 Presence and distribution

In all toothed whales in this study, lamellar corpuscles were found over the entire course of the external ear canal, from the external ear opening down to the tympanic membrane, and they were innervated by nerve fibres that gave of small centripetal branches.

In the superficial half of the ear canal, lateral to the cartilage, and down the ventral spiral, the corpuscles were distributed around the ear canal in the subepithelial tissue. In the medial half to one-third of the ear canal, the nervous tissue was concentrated on one side of the ear canal, opposite the cartilage (Figure 210). It is at this level that one area of the meatus showed a more developed epithelium and subepithelial tissue, which was more prominent the closer the cross-section was to the tympanic bulla. The epithelium in this area was thick, and there was more contact between epidermis and dermis through an undulating basement membrane (cfr. dermal papillae in the skin). In the subepithelial tissue, there was a concentration of nervous tissue (nerves and receptors), and it was also richly vascularized (Figure 211).

There was inter- and intraspecific variation in the degree to which the nervous tissue ridge was present and protruded into the ear canal lumen. In some specimens, there was no visible tissue bulge, even though the lamellar corpuscles were grouped on one side of the ear canal. E.g. one bottlenose dolphin showed a prominent nervous tissue ridge (ID457, Figure 212), while the other (ID444) also presented more nervous structures than around the rest of the ear canal, although in a less pronounced way (Figure 213). In the single specimen of common dolphin (169/17), the distribution of the nervous structures was the same as in bottlenose and striped dolphin, although there was no apparent nervous tissue ridge in either of the ear canals. In harbour porpoise, the presence, location, and morphology were similar to what was found in other toothed whales (Figure 215). In Cuvier´s beaked whale, lamellar corpuscles were found in superficial sections down to the disappearance of the blubber, at the level of the downward spiral. However, the medial half of the ear canal was not dissected correctly in either of the two animals. Also, the tissue conservation state in both animals was bad, which made it difficult to recognize the lamellar corpuscles, at least in HE-stained sections. In the Long-finned pilot whale, there were few corpuscles, mostly in deeper layers, is possibly an artefact due to the preservation state of the tissue. Where there is cartilage, the innervation was present only on the

opposite side, and concentrated in one area, cfr. ´nervous tissue ridge´ in other odontocetes (Figure 82, Figure 166, Figure 214).

The lamellar corpuscles were identified in all cetaceans in this study. While there were abundant corpuscles throughout the ear canal in striped dolphin, and bottlenose dolphin, there seemed to be only a few corpuscles in the tissues of the beaked whale. For the pilot whale, the situation seemed similar to the first two species, but we could not make any conclusions due to the conservation state of the animal.

The number of corpuscle core cross-sections in the five regions of the ear canal (B: blubber; G: glands; M: muscle; C: cartilage; N: nervous tissue ridge; See Table 13) did not present any significant interregional differences in striped dolphin. We compared the maximum values of each region among all animals, and the Spearman correlation analysis (Figure 209) showed that region B was closely associated with M (0.7353); and C and N were strongly associated (0.7420), even though although the data was sparse as can be seen in Table 14. Based on these correlations, we merged the regions into two main groups: B+G+M (Lateral group) and C+N (Medial group), to compare the lateral regions of the ear canal, with only soft tissues, to the medial regions, which contained the cartilage. The maximum corpuscle core count between the two obtained groups was compared using the dispersion in each group, which was measured using the mean absolute deviations. The results were reasonably close together (6 and 10, respectively). A ranksum test was then applied to find a difference in the median of the maximum values of Lateral versus Medial groups, which gave a p-value of 0.2035 and did not allow for a rejection of the null-hypothesis of an equal median of maximum values among groups, which was already expected based on the initial group comparison. The corpuscles count for the other species are given in Table 14 but were not subjected to any analysis due to the sparsity of data (De Vreese et al., 2020a). Due to the complex nature of the corpuscles, we did not attempt to report on the number of corpuscles along the ear canal, but rather the number of sections through corpuscles, as this could indicate the sensitivity of the canal at various levels.

Table 13. (De Vreese et al., 2020b) Schematic representation of soft tissues associated with the ear canal (rows), from left to right representing the course from the external ear opening to the tympanic conus. The columns represent the regions used for quantification.

		External ear opening	***Regions for quantification****							*Tympanic conus*
			Blubber	*Glands*		*Muscle*	*Cartilage*		*Nervous tissue ridge*	
Soft tissue	*Blubber*		*X*	*X*						
	Glands			*X*	*X*					
	Muscle				*X*	*X*	*X*			
	Cartilage						*X*	*X*	*X*	
	Button								*X*	

**Blubber: From the external ear opening to the lateral end of the glands (excluding glands); Glands: containing glandular structures; Muscle: From the medial end of the glands to the medial end of the cartilage; Cartilage: From the lateral end of the cartilage to the medial end of the ´nervous tissue ridge´; Button: from the lateral end of the nervous tissue ridge to the medial end of the ear canal*

	B	G	M	C	N
B	1	0.1579	0.7353	0.3476	-0.0966
G		1	0.3095	0.3857	0.2068
M			1	0.1506	-0.0599
C				1	0.7420
N					1
		LATERAL GROUP		MEDIAL GROUP	

Figure 209. Correlations of the number of cross-sections of lamellar corpuscles among the five regions of the external ear canal (B: blubber; G: glands; M: muscle; C: cartilage; N: nervous tissue ridge) (De Vreese et al., 2020b)

Table 14. Quantification of corpuscle cores: animals and manual *counts* (De Vreese et al., 2020b)

Animal ID	*Species*	*CC*	*Origin*	*Date of necropsy*	*Death*	*Sex*	*Length (cm)*	*Weight (kg)*	*Left/Right ear canal*	*B*	*G*	*M*	*C*	*N*
12691	*S. coeruleoalba*	*2*	*Livorno, Italy*	*19/12/2017*	*Natural*	*M*	*193*	*62*	*L*		*22*	*12*	*45*	*56*
12703	*S. coeruleoalba*	*2*	*Imperia, Spain*	*13/01/2018*	*Natural*	*M*	*133*	*34*	*L*	*18*	*25*		*26*	
12708	*S. coeruleoalba*	*2*	*Genova, Italy*	*21/01/2018*	*Natural*	*M*	*192*	*69*	*R*		*13*		*11*	
109064	*S. coeruleoalba*	*2*	*Calabria, Italy*	*13/10/2018*	*Natural*	*M*	*102*	*12*	*R*		*26*		*18*	*54*
127565	*S. coeruleoalba*	*2*	*Calabria, Italy*	*28/11/2018*	*Natural*	*M*	*200*	*na*	*R*	*14*	*29*		*19*	*32*
N-419\16	*S. coeruleoalba*	*2*	*Port de la Selva, Spain*	*16/11/2016*	*Natural*	*M*	*103*	*14*	*L*	*20*	*22*		*20*	
N-044\17	*S. coeruleoalba*	*2*	*Port Ginesta, Spain*	*10/02/2017*	*Natural*	*M*	*153*	*37*	*L*	*29*	*23*		*16*	*9*
									R	*16*	*27*	*14*	*13*	
N-168\17	*S. coeruleoalba*	*2*	*L´Escala, Spain*	*19/04/2017*	*Natural*	*M*	*193*	*79*	*L*	*24*	*19*	*17*	*5*	*15*
N-488\17	*S. coeruleoalba*	*2*	*Gavà, Spain*	*28/09/2017*	*Euth.*	*F*	*198*	*70*	*L*	*8*	*29*		*7*	
N-509\17	*S. coeruleoalba*	*2/3*	*Tarragona, Spain*	*10/10/2017*	*Natural*	*M*	*183*	*87*	*L*	*24*	*24*	*22*	*23*	*28*
N-620\17	*S. coeruleoalba*	*2*	*Vilanova i la Geltrú, Spain*	*24/07/2018*	*Natural*	*M*	*196*	*75,5*	*L*	*7*	*11*	*4*	*9*	*14*
N-042\18	*S. coeruleoalba*	*2*	*Viladecans, Spain*	*25/01/2018*	*Natural*	*M*	*178*	*62*	*L*		*43*	*21*	*13*	*12*
N-077\18	*S. coeruleoalba*	*2*	*Delta del Ebro, Spain*	*19/02/2018*	*Natural*	*M*	*220*	*97,5*	*R*	*11*		*14*	*20*	
N-145\18	*S. coeruleoalba*	*2*	*Palamós, Spain*	*26/03/2018*	*Natural*	*F*	*195*	*91*	*L*				*22*	*21*
N-274\18	*S. coeruleoalba*	*3*	*Delta del Ebro, Spain*	*24/06/2018*	*Natural*	*M*	*152*	*38*	*L*		*34*	*10*		*26*
									R	*22*	*20*		*24*	*23*
N-292\18	*S. coeruleoalba*	*2*	*Tarragona, Spain*	*06/07/2018*	*Natural*	*M*	*194*	*59,5*	*L*	*13*	*21*	*20*	*12*	*15*
N-293\18	*S. coeruleoalba*	*3*	*Port Ginesta, Spain*	*09/07/2018*	*Euth.*	*F*	*187*	*85*	*L*		*16*		*1*	*2*
N-362\18	*S. coeruleoalba*	*2*	*Riumar, Spain*	*12/09/2018*	*Euth.*	*M*	*181*	*78*	*L*	*12*	*9*		*13*	*18*
N-169/17	*D. delphis*	*2*	*L´Escala, Spain*	*20/04/2017*	*Natural*	*M*	*179*	*72*	*L*	*10*	*16*		*8*	
									R		*9*	*9*	*9*	
444	*T. truncatus*	*3*	*Pellestrina, Venezia, Italy*	*24/03/2018*	*Natural*	*M*	*264*	*260*	*L*	*33*	*30*		*40*	*30*
									R		*26*		*18*	*54*
457	*T. truncatus*	*2*	*Bibione, Venezia, Italy*	*29/01/2019*	*Natural*	*M*	*285*	*260*	*R*	*8*	*19*		*17*	*26*
429	*Z. cavirostris*	*2*	*Livorno, Italy*	*23/12/2017*	*Natural*	*M*	*503*	*na*	*L*			*18*	*12*	

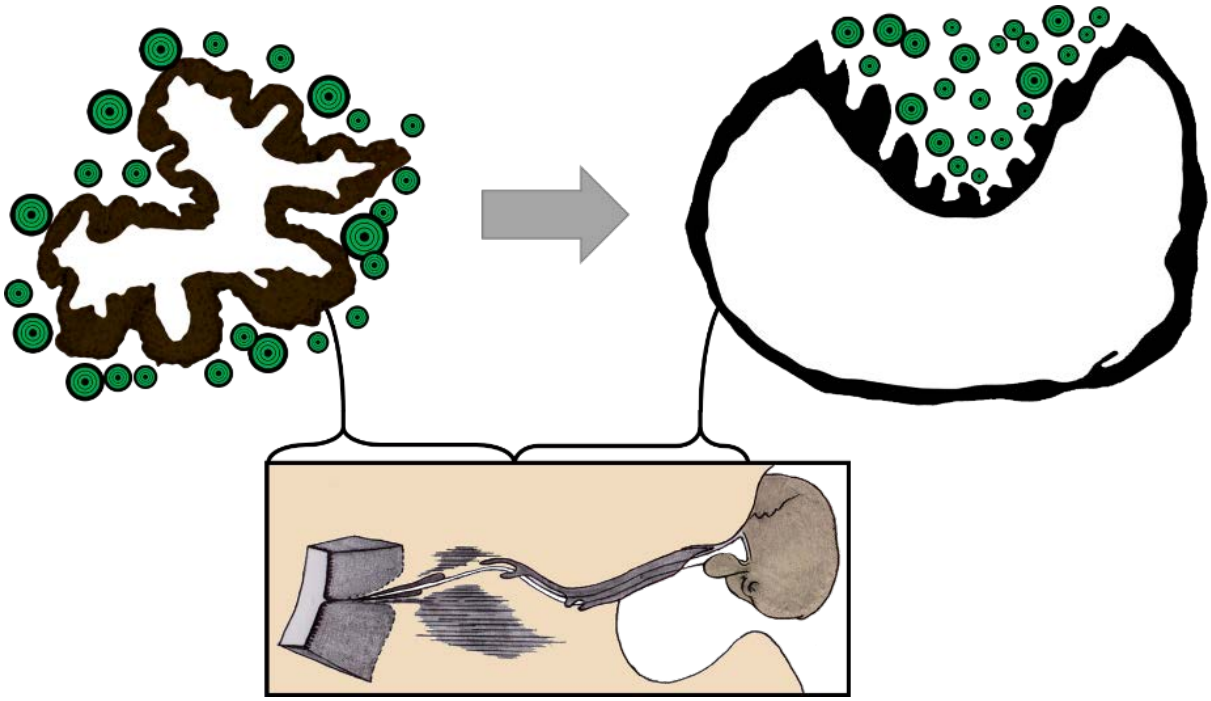

Figure 210. Schematic representation of the distribution of the lamellar corpuscles (green) associated with the external ear canal. In the superficial half of the canal (top left), the corpuscles are distributed in the subepithelial tissue around the ear canal, while in the medial half of the ear canal (right), the corpuscles are situated on one side of the canal, in the subepithelial tissue that bulges together with the epithelium (black) into the lumen of the canal, and forms what we have a called a 'nervous tissue ridge' (De Vreese et al., 2020a).

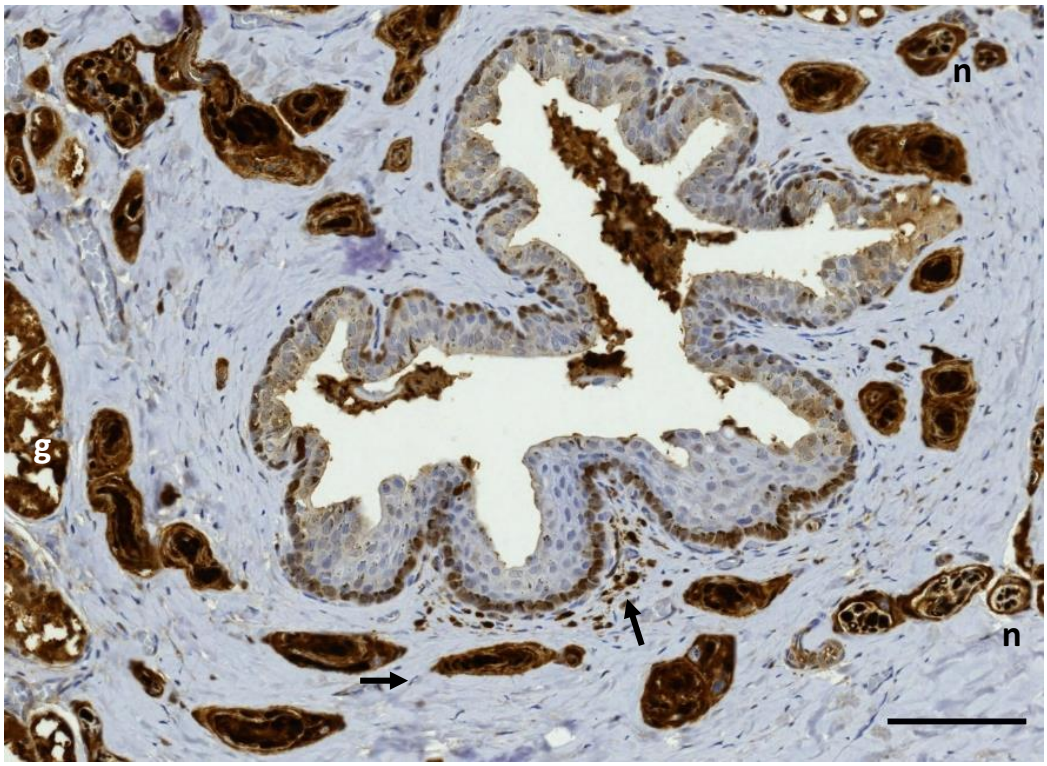

Figure 211. IHC stain with anti-S-100 (S. coeruleoalba). Note the density of corpuscles in close vicinity of the ear canal and the presence of small nerve fascicles. The central lamellae of the corpuscles stain more intensely in comparison to the peripheral lamellae. There is localized positive staining of nervous structures beneath the epithelium (arrows). Note the unspecific staining of glandular structures (g), epithelium, and the lumen content with degenerated epithelial cells. The epithelium also has melanin. Scale bar 50 µm. (Image was composed using a grid/collection stitching plugin in Jifi (Preibisch et al., 2009).

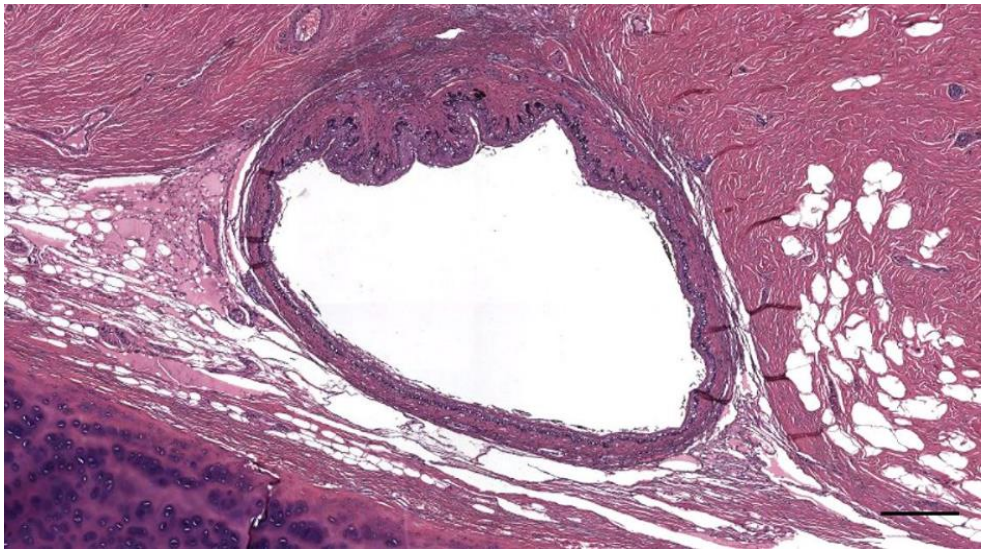

Figure 212. Histological cross-section (HE staining) of the ear canal of a bottlenose dolphin (457_R12). Note the subtle nervous tissue ridge opposing the cartilage. Scale bar 250 µm

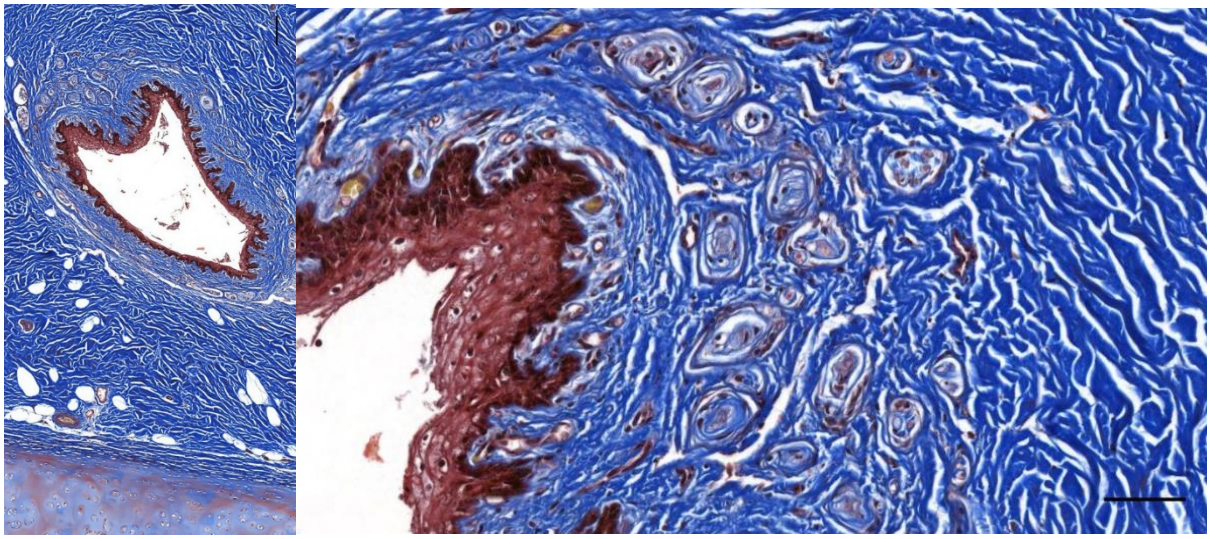

Figure 213. Histological image (Masson´s Trichrome) of the ear canal in a bottlenose dolphin (444_L12). The right image is a close-up of the left (rotated 90°). Scale bar left 100 µm, right 50 µm

Figure 214. Histological image (HE staining) of the ear canal in a long-finned pilot whale (441_R19). Nervous tissue ridge protruding into the lumen. Scale bar 200 µm

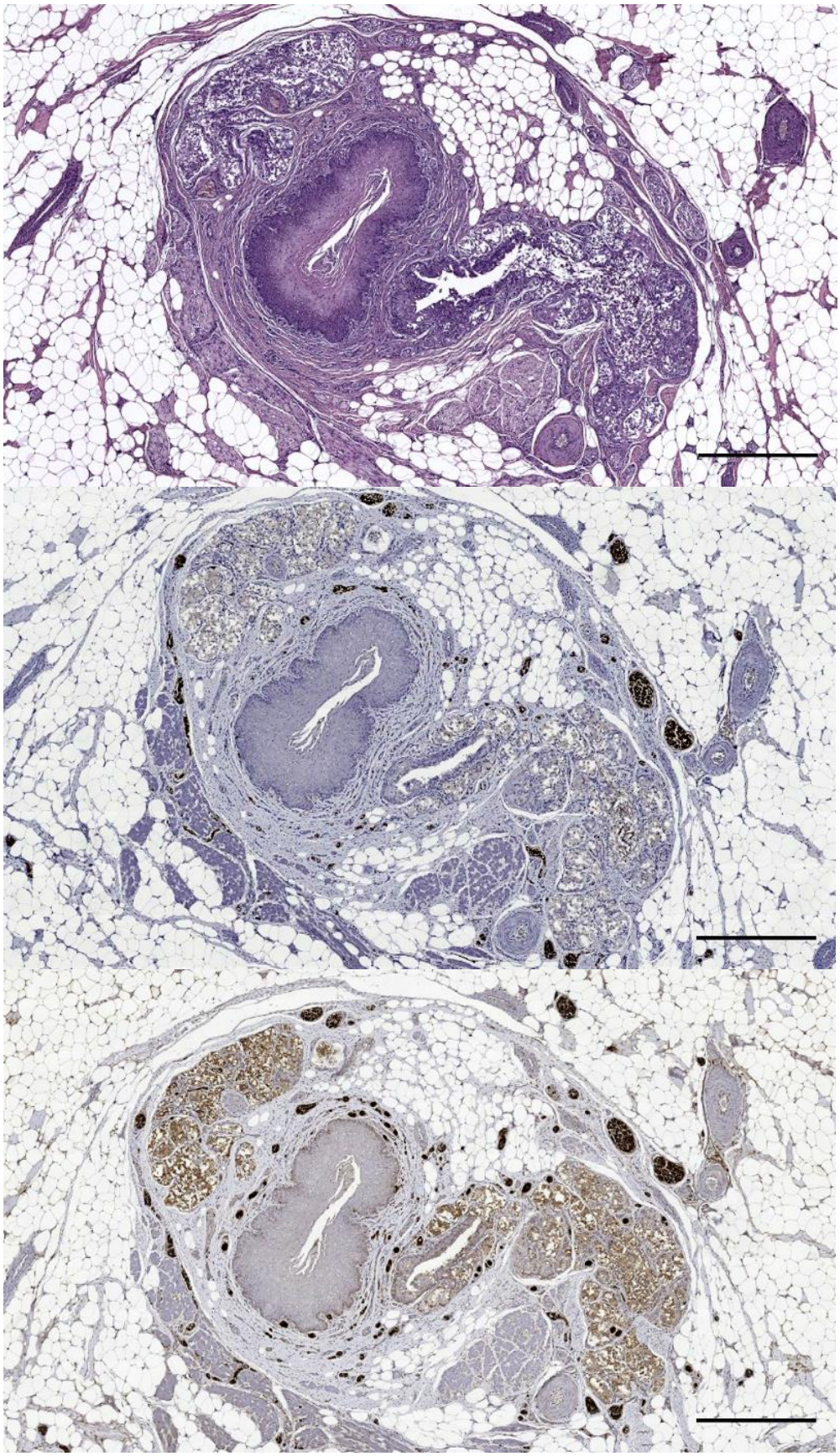

Figure 215. Histological images of a transverse section through the external ear canal of a harbour porpoise (UT1664). Top: HE stain; Middle: IHC with anti-NF; Bottom: IHC with anti-S100. Scale bars 500 µm

3.1.2 Corpuscle morphology

(Adapted and expanded from De Vreese et al., 2020a): The lamellar corpuscles were identified as *simple lamellar corpuscles,* a.k.a. *Krause cylindric corpuscles* or *Golgi-Mazzoni corpuscles* depending on the definition, according to the nomenclature by Malinovský, 1996. The corpuscles consisted of a central axon surrounded by lamellae of modified Schwann cells and were elongated with occasional convolutions and with a general course parallel to the ear canal. The diameter of the corpuscles ranged from 16 to 202 µm (geometric means, computed over the semi-minor and semi-major axes of a corpuscle, ranged from 20 to 133 µm), measured in 160 corpuscles in ten equally spaced cross-sections throughout the canal. The larger the diameter of the corpuscle, the more lamellae it contained. Most corpuscles were singular, i.e. with a single core (axon + lamellae), but there were also composite corpuscles with multiple cores, mostly two or three, and combinations of corpuscles and nerve fascicles embedded within the same peri- or epineurium (Figure 216).

The supplying myelinated nerve fibre lost its myelin sheath on entering the corpuscle. Each corpuscle consisted of a central axon showing immunoreactivity (IR) for anti-neurofilament protein (anti-NF), anti-neuron specific enolase (anti-NSE), and anti-protein gene product 9.5 (anti-PGP 9.5) (Figure 218)**.** In all sections (consecutive transverse or oblique, no perfectly longitudinal section was obtained), the terminal axon followed a straight course throughout the corpuscle, while in a single section we noted a whirling at the terminal end (Figure 218b). NF stained the central axon of the simple lamellar corpuscle dark brown, and the outer edges of the axon stained more intensely dark than the centre. There was often also a clear spot of positivity within or central to the capsular layer, which indicated the presence of single or multiple axons. NF also stained ´free´ nerve fibres and the axons of small nerves in the subepithelial tissue.

Surrounding the axon, were concentric layers (lamellae) of cells which nucleus and cytoplasm stained positive for anti-S-100 although in two gradients: the central lamellae stained more intensely positive than the peripheral ones (Figure 218f). In contrast, anti-PGP 9.5 stained the peripheral lamellar layers surrounding a less intense positive zone in the centre (Figure 218g-h). There was IR for anti-PGP 9.5 of both cytoplasm and nuclei of the peripheral layers, but only in about half of the nuclei in the central layers (with dilution 1:500, while absent with higher antibody dilutions). As such, both anti-PGP 9.5 and anti-S100 stained all lamellae but with a different zonal distribution (Figure 218), indicating that the lamellae consisted of at least two zones with a different structural composition. In transverse sections, the shape of the Schwann cell nuclei varied from round, to bean-shaped with a curvature in parallel with the lamellae, to flattened and elongated with often more dense stain in both H&E and Luxol stains. There was a general tendency that the nuclei in the centre of the corpuscle were more round and oval, and the peripheral nuclei were more flattened in cross-sections, similar to a layered

maturation of epithelial cells. A possible explanation for the difference in the shape of the lamellar cells' nuclei, might be attributed to a different kind of cellular activity depending on the location. In standard stains, the differentiation between the lamellar cells and the fibrocytes/-blasts in the peripheral layer or the surrounding stroma was not always clear.

In both corpuscles and nerves, S-100 stained the Schwann cell nuclei intensely positive and, to a lesser extent, also the cytoplasm. In small nerve bundles, the myelin sheath stained positive in a similar fashion (nuclei most intense and cytoplasm less). Interestingly, the perineurium stained positive in most cases, while the outer layer of the lamellar corpuscles usually did not, or significantly less intense in the same section. Furthermore, there was a positivity of Schwann cell nuclei in tiny nerves that were often seen in a concentric pattern around the ear canal (perpendicular to the course of the canal), and they entered into the dermal ridges/papillae (intrapapillary myelinated endings, IMEs).

The peripheral layer was thin and cellular with sparse nuclei, similar to the perineurium of small nerves (Figure 217). Besides the positivity for anti-PGP 9.5, this layer also showed IR for anti-NSE, and similarly stained the cytoplasm, although inconsistent and less intense than the staining of the axons (Figure 218d-e). See Figure 219 for a schematic representation of the IR of corpuscle and nerves to the various antibodies applied.

In many corpuscles, there was a non-stain space between the lamellae and the peripheral layer (e.g. Figure 220), possibly an artefact of the preparation.

Also, we often noted the presence of accessory axons, most clearly identifiable with anti-NF, but also with anti-NSE and anti-PGP 9.5, and which were situated central to the peripheral layer (Figure 218b, Figure 221). Occasionally, there were also small vascular structures on the inside of the peripheral layer (Figure 222)

The various histochemical stain techniques (Luxol Fast Blue / Cresyl Violet stain, Spaethe´s Silver stain modified after Richardson(Spaethe, 1984), Palmgren´s Silver stain, Bielschowski´s Silver stain(Bancroft and Gamble, 2002), Masson´s Trichrome Goldner, and Massons Trichrome with Aniline blue) confirmed the results obtained with IHC and TEM. However, they did not contribute to a deeper understanding of the morphology of the lamellar corpuscles or other components of the peripheral nervous system in the ear canal (Figure 223, Figure 224)(De Vreese et al., 2020b).

With PGP 9.5, axons stained positive in both corpuscles and nerves, and also the capsule of the corpuscles and the perineurium of the nerve bundles stained positive, although the latter was usually less intense. There was non-specific staining of Schwann cell nuclei and cytoplasm, with about half of the Schwann cell nuclei stain positive and the cytoplasm showing light brown irregular stain. With greater antibody dilution the intensity of positive staining of the lamellae reduced, while the outermost layer of the corpuscles and the perineurium of small nerves stained equally intense.

Furthermore, small arteries showed a multifocal positivity peripheral to the muscular layer possibly associated with the innervation of this layer, and we also observed a similar positivity in the close surroundings of striped muscle bundles.

The findings in all of the other toothed whale species were similar to the ones in striped dolphin. They all showed the presence of small nerve fibres, lamellar corpuscles, and the same immunoreactivity in the subepithelial tissue throughout the ear canal. The situation in common and bottlenose dolphin was similar to striped dolphin, with many lamellar corpuscles and small nerve fibres close to the epithelium in all sections. Also, the long-finned pilot whale and Cuvier's beaked whale presented lamellar corpuscles and small nerves in all sections, although difficult to distinguish from one another because of the preservation state of the tissue (De Vreese et al., 2020b). And a similar situation was found in the harbour porpoise samples.

The TEM images in striped and bottlenose dolphin also showed that there were several sensory nerve formations in the subepithelial tissue, which were identified as lamellar corpuscles (Figure 225, Figure 226, Figure 227, Figure 228, Figure 229). From central to peripheral, these mechanoreceptors were composed of an axonal sensory terminal, which had an oval to flattened shape with two opposite poles, surrounded by a lamellar core (Figure 230). To identify different regions along the longitudinal course of the lamellar corpuscles, we adopted the terminology used in Pacinian corpuscles. We also use the term '*inner core'* even if there is no *outer core* or obvious capsule, to facilitate comparison. Two 'regions of the corpuscle' were identified, namely the *body* or *terminal region* of the corpuscle and what we believe is either the '*ultraterminal region'* (according to Spencer and Schaumburg, 1973) or the medial portion of the corpuscle, which is very similar (Munger et al., 1988, 1988). It must be noted for the latter that it is not the extreme end of the corpuscle, as this has been labelled 'extreme tip', but rather refers to the region that we would call '*subultraterminal*', where the lamellae of the inner core start to reduce in number, and the radial clefts disappear. Unfortunately, no longitudinal sections through the lamellar corpuscles were acquired, and therefore, the distinction of regions within the corpuscle is based solely on comparison with Pacinian corpuscles.

In transverse sections through the body of the corpuscles, the central axon was spindle-shaped with two opposite poles (lateral spines) (Figure 231), while it turned oval in the ultraterminal region (Figure 232) (De Vreese et al., 2020b). The axon stained electron-dense due to the presence of abundant mitochondria (Figure 233, 235), and also contained electron-lucid vesicles or vesicular-like structures of varying sizes, from large structures that often contained a nucleolus-like structure, to smaller electron-dense vesicles with a double-layered membrane, resembling synaptic vesicles, to minute, single-layered vesicles in various concentrations (Figure 231, 234)(De Vreese et al., 2020b). These vesicles often contained nucleolus-like structure (Figure 234), and within their membrane there were

smaller electron-dense vesicles with a double-layered membrane, resembling synaptic vesicles (Figure 234) or even minute, single-layered vesicles in clusters. The neurite was flattened with occasional lateral spines where there were hemilamellae in the inner core, to a complex oval-shaped terminal filled with mitochondria and surrounded by continuous lamellae. Interestingly, we could not identify any axoplasm with microtubules or neurofilaments with certainty, as most terminals were either almost filled with mitochondria (cfr. ultraterminal region of the Pacinian corpuscles (Spencer and Schaumburg, 1973) or displayed a quite homogenous electron-dense centre with vesicular structures and mitochondria along the rim (Figure 226, 234). We did see indications of myelinated axons within the axonal terminal (Figure 233), but there were often indications of myelin deformations presented as myelin ovoids, similar to the findings in the nerves, although on a much smaller Scale bar (Figure 233). For detail images of the axon terminal, see Figure 225, 233, 235.

The terminal showed bilateral axonal spines projecting into the radial clefts formed by the coming together of the bilateral hemilamellae of the inner core cells (Figure 237, 238**,** 227**,** 239). These spines contained clear vesicles with a seemingly membranous infolding and a nucleolus-like structure (Figure 237) (De Vreese et al., 2020b).

The terminal lamellar core showed a bilateral conformation consisting of hemilamellae of core cells, presumably modified Schwann cells, surrounded by fully circular lamellae and cell nuclei (Figure 230). In contrast, in the distal end of the corpuscles (ultraterminal region), hemilamellae were absent, and the inner core cells fully encircled the axon several times (Figure 232) (De Vreese et al., 2020b). The number of nuclei of inner core cells ranged from one to about ten per corpuscle, although the latter number could be an overestimation due to the possibility of multiple sections through the same nucleus. The axial hemilamellae and lamellae of stacked inner core cell[9] presented double-layered plasma membranes and cytoplasm. The hemilamellae met at the radial clefts in the extension of the axonal poles (Figure 226, 236, 238). The corpuscles also comprised 'full circular' lamellae, observed peripheral to the hemilamellae, or in what was possibly the ultraterminal region of the corpuscle (Figure 241, 242, 225). The lamellae seemed to be continuous with the cytoplasm and plasma membrane of the inner core cells.

The lamellar cytoplasm contained mitochondria, abundant pinocytotic vesicles and associated membrane invaginations, and other vesicular structures, likely ribosomes, and smooth endoplasmic reticulum in the bulbous enlargement of the cytoplasm near the radial clefts (Figure 241, 243). The lamellar cytoplasm in the ultraterminal region contained more large vesicular structures with an electron-dense membrane (Figure 225) (De Vreese et al., 2020b).

[9] We opt for the nomenclature of inner core cells due to similarity with the inner core cells of Pacinian corpuscles (Zelená, 1994).

The plasma membrane was covered with an extensive glycocalyx, and there were desmosome-like junctions between adjacent lamellae (Figure 245).

The extracellular matrix in the radial clefts and interlamellar spaces of the core mainly comprised scattered collagen fibrils, in seemingly larger clusters in the more peripheral layers. The collagen fibrils were orientated in two main directions, parallel and perpendicular to the longitudinal axis of the corpuscle. They had a diameter of about 15 nm in the extracellular matrix between the hemilamellae, and between 25 and 40 nm in the clefts and between lamellae in the ultraterminal region of the corpuscle. The corpuscles did not have an outer core or distinct lamellar capsule as do Pacinian corpuscles or a distinct connective tissue capsule as in Meissner's corpuscles. Nonetheless, the peripheral, fully circular lamellae that contained the inner core cell nuclei, could be called a 'capsule', following the morphology of Golgi-Mazzoni corpuscles (Figure 230). Corpuscles were often found in close vicinity of nerve fibres, and there was a shared and continuous 'perineurium' (Figure 230), which was morphologically not distinguishable from the peripheral layer of the corpuscles (De Vreese et al., 2020b).

No elastic fibrils were identified with certainty, nor any ground substance as mentioned for the inner core of Pacinian corpuscles (Munger et al., 1988). Similarly, there was no obvious basal membrane between lamellae, nor any interlamellar junctions between plasma membranes. However, the amorphous material near the plasma membrane of the lamella is electron opaque, suggesting that it is what is known as basal lamina-like material (Watanabe et al., 2002). Moreover, basal membrane distribution might be sparse and patchy as occurs in the inner core of Pacinian corpuscles, and can, therefore, be missed easily. In Pacinian corpuscles, it is present mostly in the peripheral lamellae and around perikaryal of the inner core cells, and at the axonal spines (Zelená, 1994). Similarly, we might have missed the interlamellar junctions. There were clear differences in the size of interlamellar space between lamellae situated close to the sensory terminal or situated further away from the centre.

We could not find any morphological indications of a *lamellar 'capsule'* or 'outer core' as in Pacinian corpuscles, or *connective tissue capsule* as in Meisner corpuscles. However, for some corpuscles, there were subjectively more collagen fibres present in the extracellular space between the more peripheral lamellae (Figure 246). Nonetheless, there was a difference between the lamellar core surrounding the axon terminal and the peripheral lamellae the corpuscle, especially notable in the ultraterminal region (E.g. Figure 237). As such, the peripheral lamellae were continuous in a circular manner wherever the corpuscle was sectioned, and there was the presence of multiple nuclei of inner core cells, also positioned circularly between the peripheral layers (Figure 241, 242, 227, 230, 229). The combination of these two findings could be called the *capsule*, as has been done previously for Golgi-Mazzoni corpuscle in the human skin (Chouchkov, 1973). The peripheral layer of about 40% of the corpuscles

stained slightly positive for anti-Pan-cytokeratin, usually only for half the circumference of the corpuscle, while both the endo- and perineurium of all the nerves stained positive. Also, the lamellar corpuscles were often in close vicinity of nerve fibres, and there was a shared and continuous 'perineurium' (241, 242, 230, 229). However, when looking on greater magnification, the lamellar structure of inner core lamellae, 'capsule' and perineurium, showed high morphological similarity and were not distinguishable from one another. In any case, the lamellar corpuscles did not have a lamellar outer core/capsule similar to what has been described for Pacinian corpuscles (Figure 229) (De Vreese et al., 2020b).

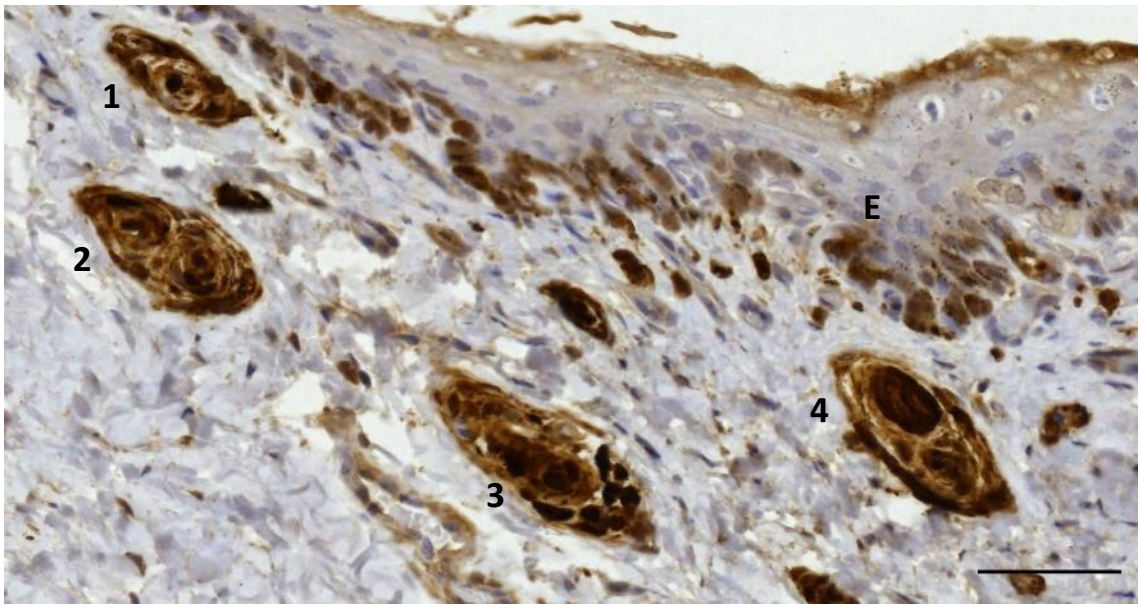

Figure 216. IHC stain with anti-S-100 of the ear canal subepithelial tissue in a striped dolphin. On the top left there is a single corpuscle (1), below that a composite corpuscle with two cores (2); (3) is a composite nervous structure in slightly oblique section, while next to it is a corpuscle with two cores (4). There are various positively stained structures in the subepithelial tissue, of which some are small nerves fascicles or single nerves, and others are nervous structures too small to identify with this antibody. E: epithelium. Scale bar 50 µm

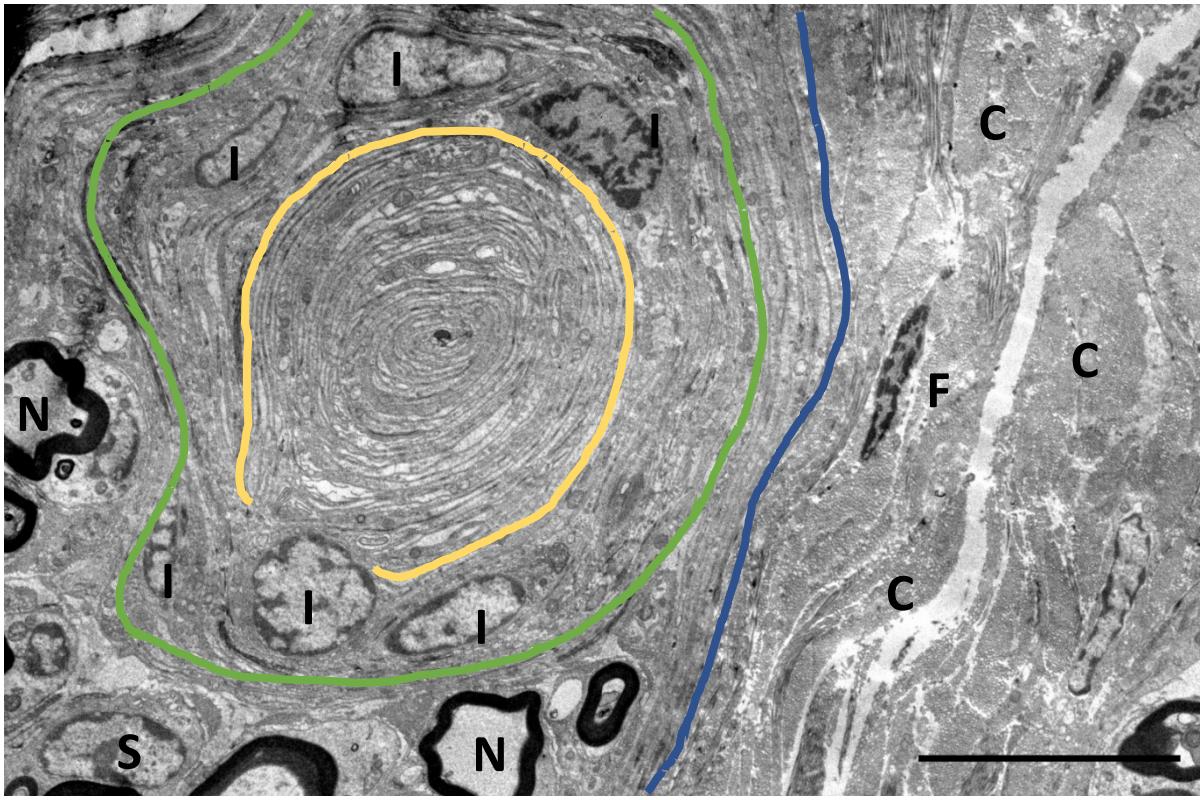

Figure 217. TEM Image: Overview of a lamellar corpuscle and nerve fibres (N) within the same perineurium (blue dashed line), and surrounded by collagenous connective tissue (C). Following the principles of Chouchkov (1973), the inner core with hemilamellar structure is delineated by the yellow dashed, while the capsule of the corpuscle, delineated by the green dashed line, contains the nuclei of the inner core cells (I). F: fibrocyte nucleus; S: Schwann cell nucleus. Scale bar 10 µm(De Vreese et al., 2020b).

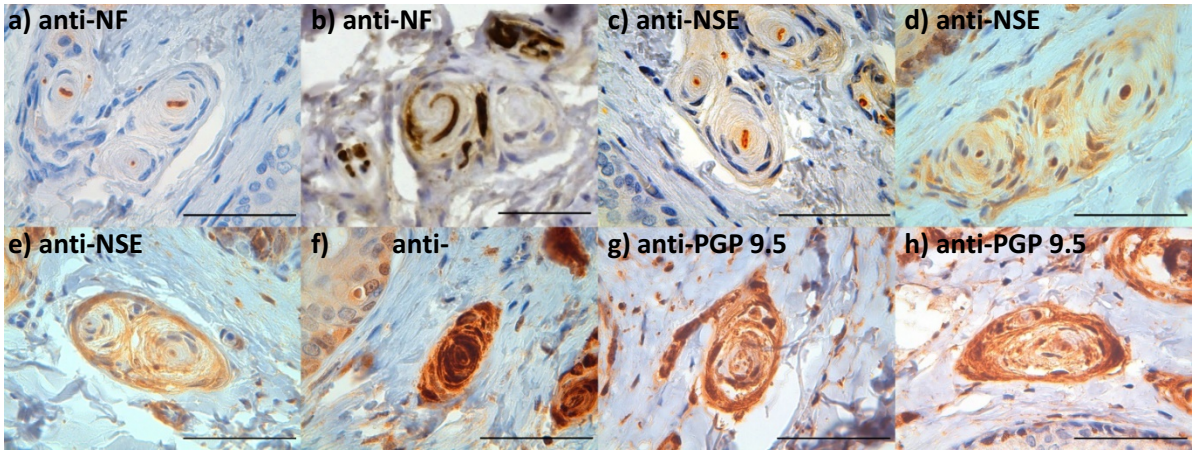

Figure 218. Immunohistochemically stained microscopic images of lamellar corpuscles in striped dolphin stained with a-b) anti-NF, in b) note the whirling course of the central axon within a composite corpuscle and several axons associated with the peripheral layer, c-e) anti-NSE, note the immunoreactivity of the central axon and inconsistent staining of the peripheral layer, f) anti-S-100, g-h) anti-PGP 9.5. Scale bars 50 µm (De Vreese et al., 2020b).

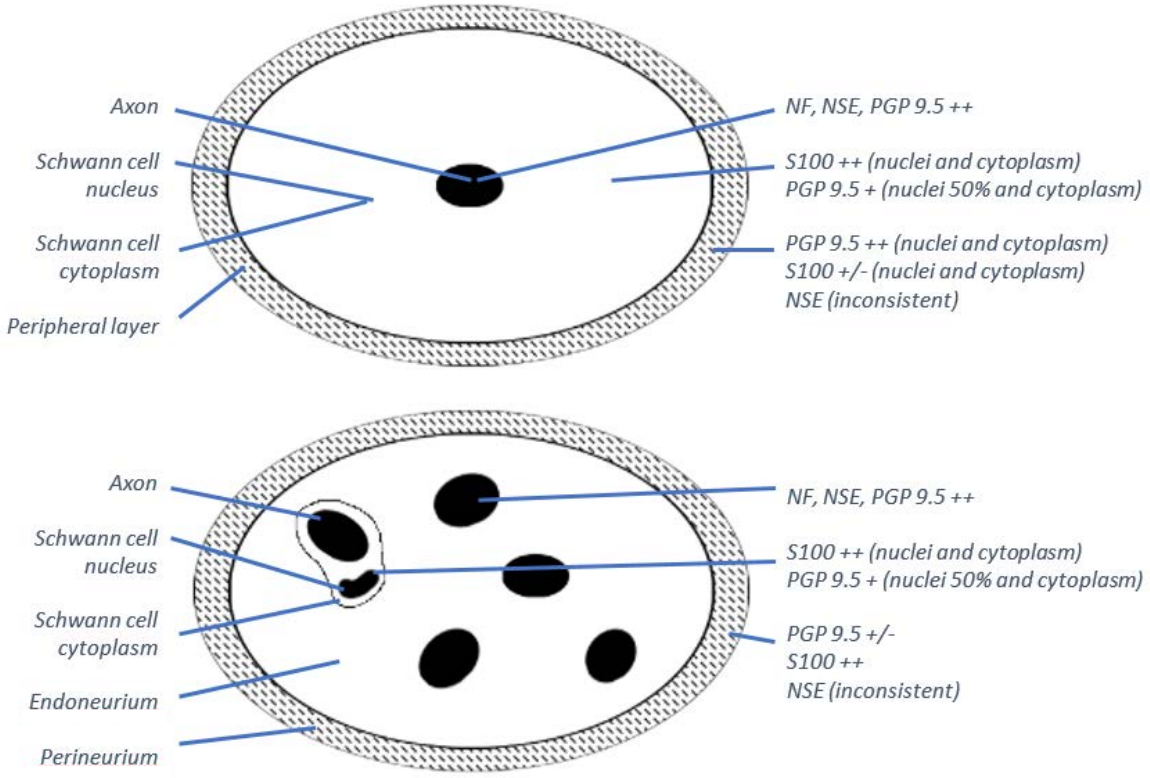

Figure 219. Schematic comparison of a transverse section through a simple lamellar corpuscle (top) and a nerve fibre (bottom, with a comparison of antibody positivity in toothed whales.

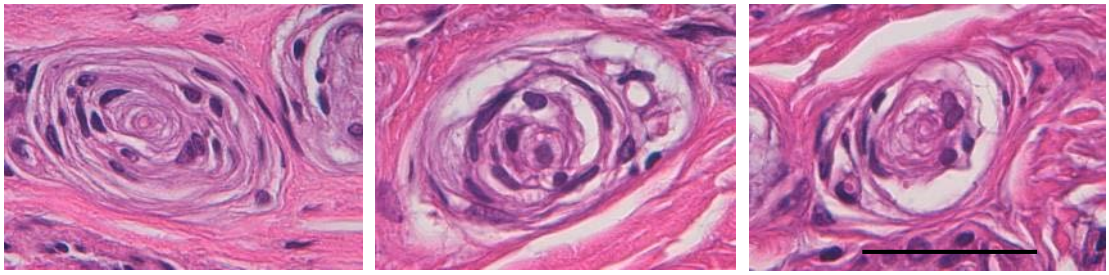

Figure 220. Three detail images of simple lamellar corpuscles of similar sizes in striped dolphin showing the degree of variability in what is probably an artefact of the tissue processing (´shrinkage´) of the core, while the size of the capsule remains the same. Scale bar: 100 µm.

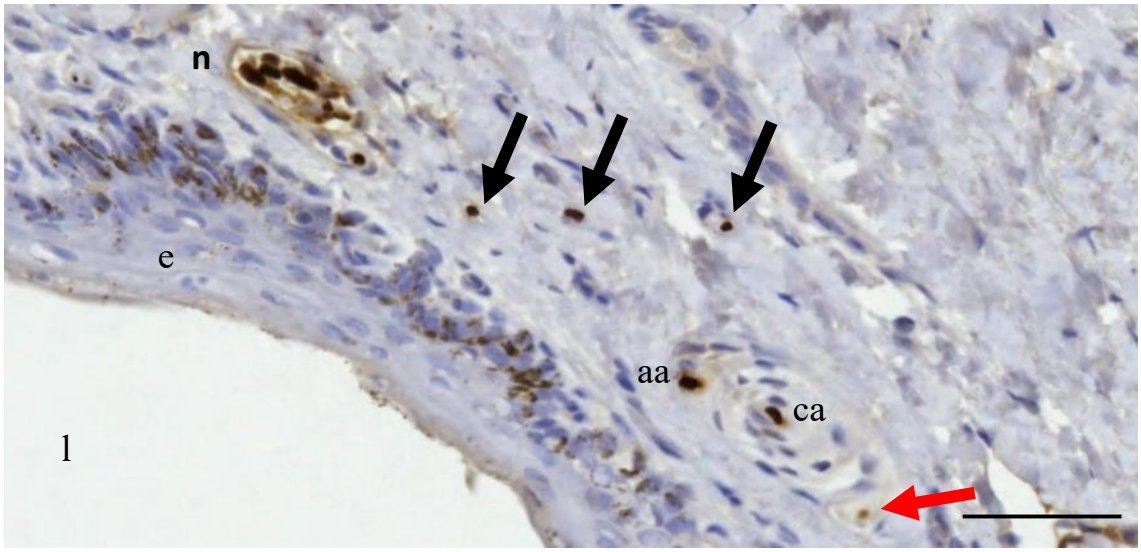

Figure 221. Anti-NF staining of the subepithelial tissue in a striped dolphin ear canal. Note the small nerve fascicle, and a lamellar corpuscle with a central axon (ca) and a possible accessory axon (aa) situated between core and peripheral layer, and several single nerve fibres (black arrows) in the subepithelial tissue. There is also a small, lesser intense stain within the peripheral layer of the corpuscle which could indicate another (accessory) axon (red arrow). l: ear canal lumen; e: epithelium; n: nerve bundle. Scale bar: 50 µm

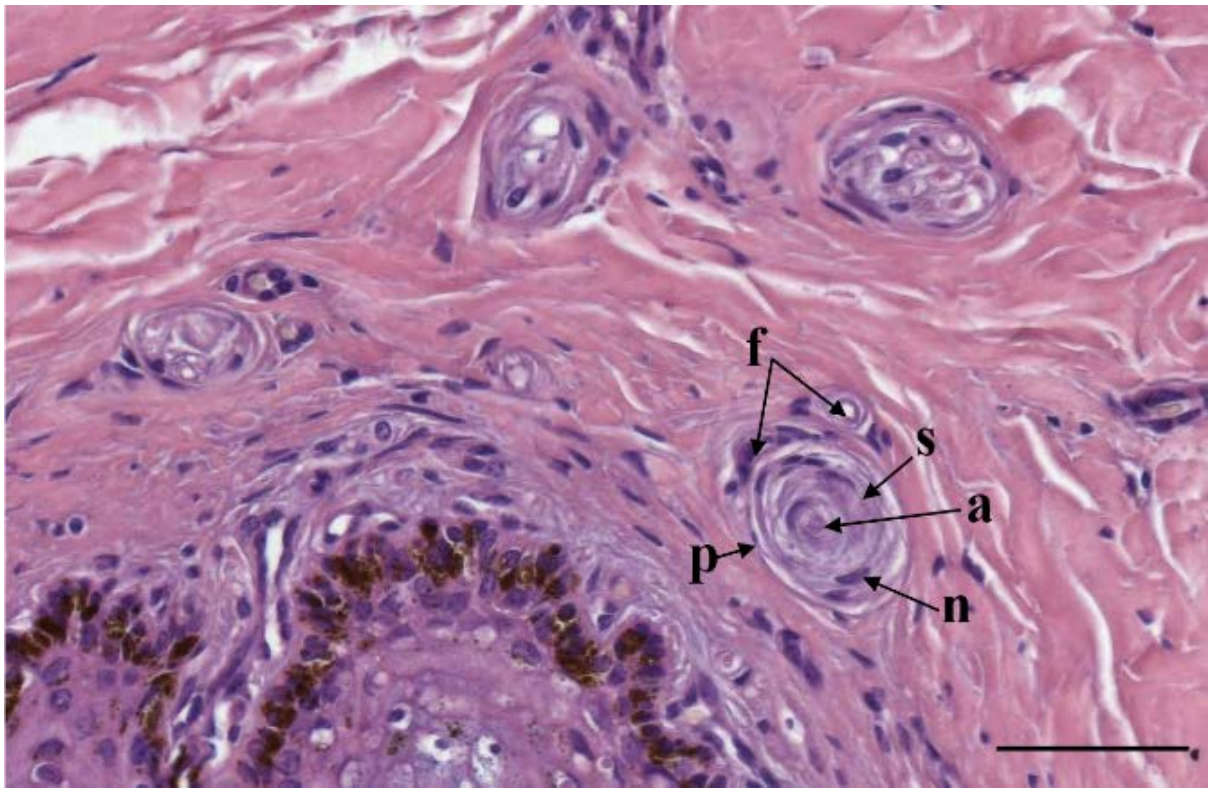

Figure 222. Histological image (HE staining) of simple lamellar corpuscles and small nerve bundles in the vicinity of the external ear canal in striped dolphin. a: central axon; n: Schwann cell nuclei; s: Schwann cell cytoplasm and cell membrane; p: peripheral layer; f: nerve fibres (or small vascular tissue) associated with the peripheral layer of the corpuscle. Scale bar 50 µm(De Vreese et al., 2020b).

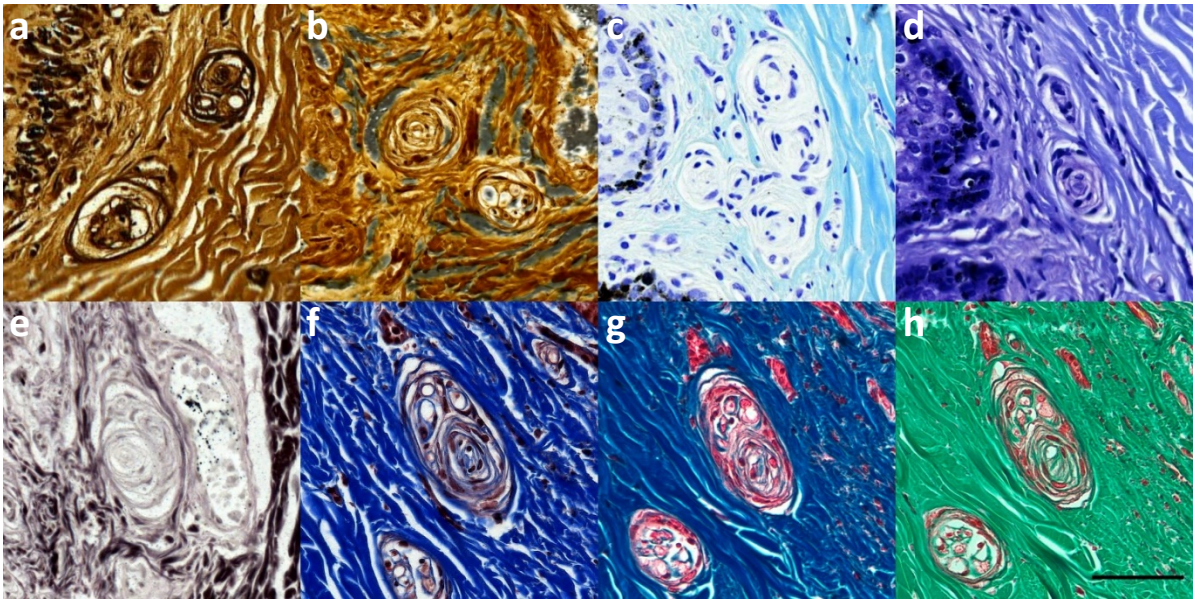

Figure 223. Various histochemical stains of lamellar corpuscles the subepithelial tissue of the external ear canal in striped dolphin. A: Palmgren´s silver stain; B: Spaethe´s silver stain; C-D: Luxol Fast Blue x2 (different stain times); E: Bielschowsky´s stain; F-G: Masson´s Trichrome with Aniline x2 (different stain times); H: Masson´s Trichrome Goldner. Scale bar 50 µm.(De Vreese et al., 2020b)

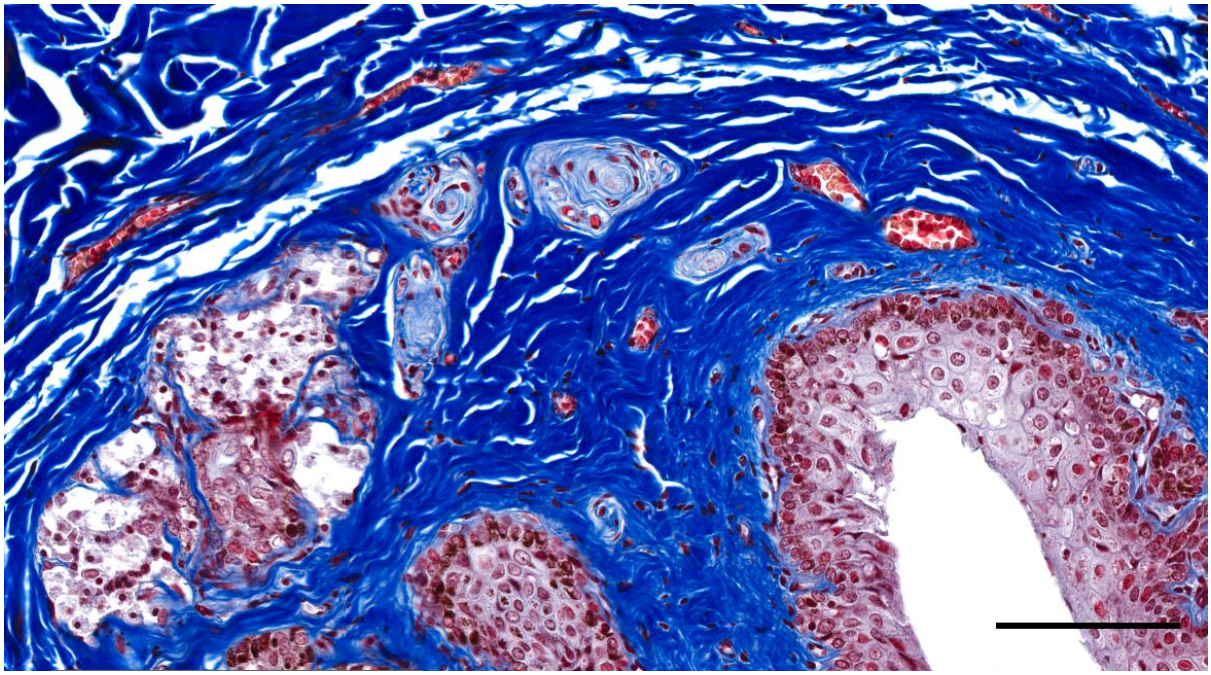

Figure 224. Histological image (Masson´s trichrome) of the ear canal subepithelial tissue with glands and lamellar corpuscles in a striped dolphin (127565_0803). Scale bar 100 µm

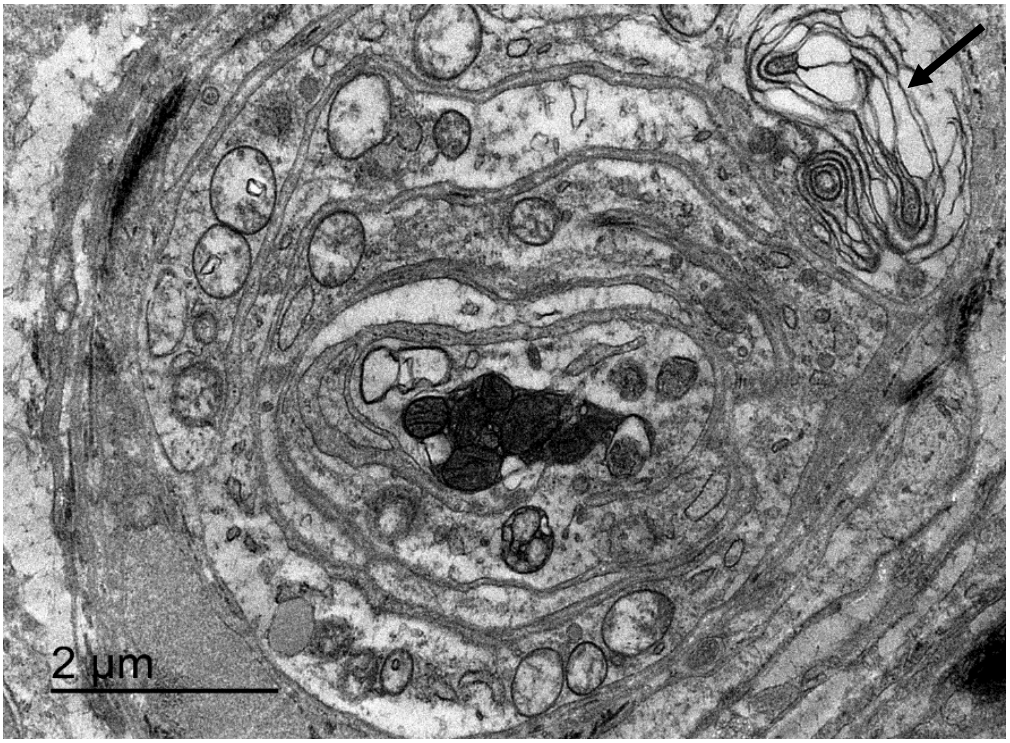

Figure 225. TEM image of a transverse section through what is likely the ultraterminal region of a lamellar corpuscle. The axon terminal is almost entirely occupied by mitochondria. (Cfr. Spencer and Schaumburg, 1973; Ide et al., 1988). This region of the corpuscles is small in comparison to the body of the corpuscle and has few inner core lamellae. Note the concentric array of endoplasmic reticulum in a bulbous enlargement of the cytoplasm of an inner core cell (arrow) (Cfr. Figure 241, 243)

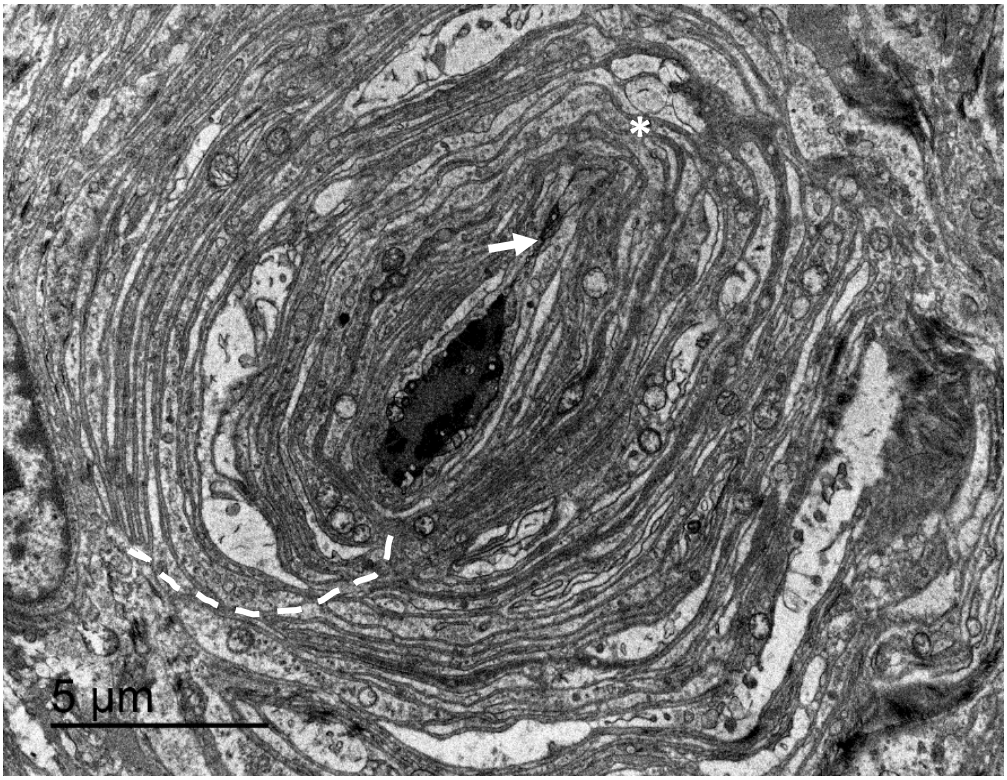

Figure 226. TEM image of a transverse section through a lamellar corpuscle. The section occurs at the transition zone between the 'terminal body' and the ultraterminal region, where the number of lamellae is not so abundant, the radial clefts is still detectable on one side (dashed line), although not so clear, while, on the side, with the lateral spine there are some hemilamellae but also lamellae that run continuously (asterisk) over the spine (arrow)

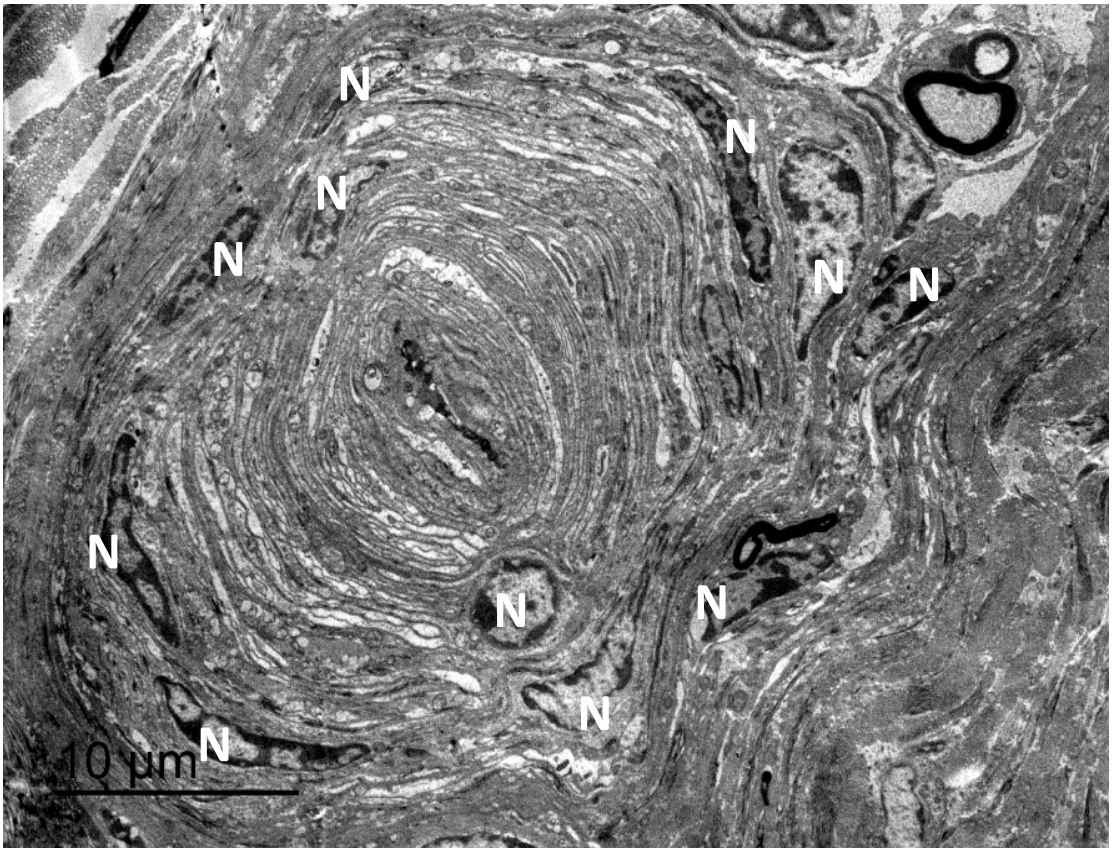

Figure 227. Detail of Figure 228, showing the lamellar corpuscle with several sections through (core cell) nuclei (N) in the periphery.

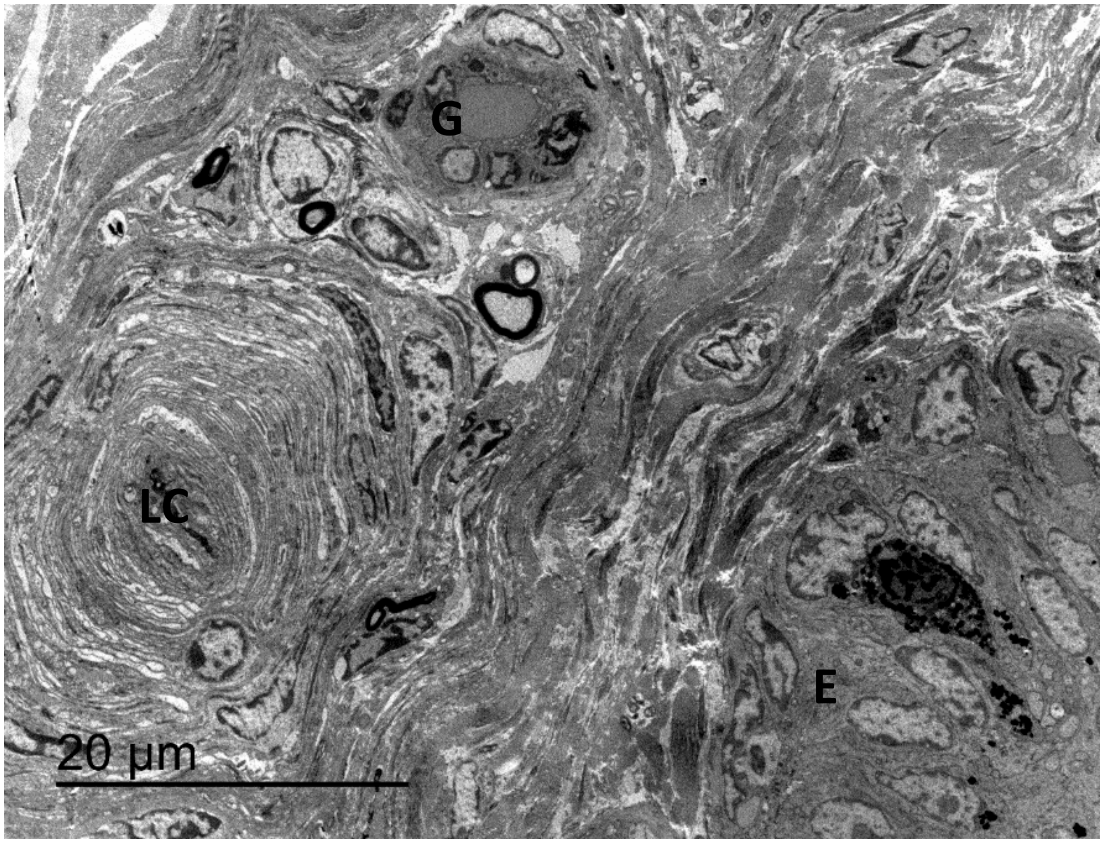

Figure 228. TEM image of a lamellar corpuscle (LC), myelinated nerve fibres, and a possible glandular duct (G) situated between the connective tissue below the epithelium of the ear canal (E).

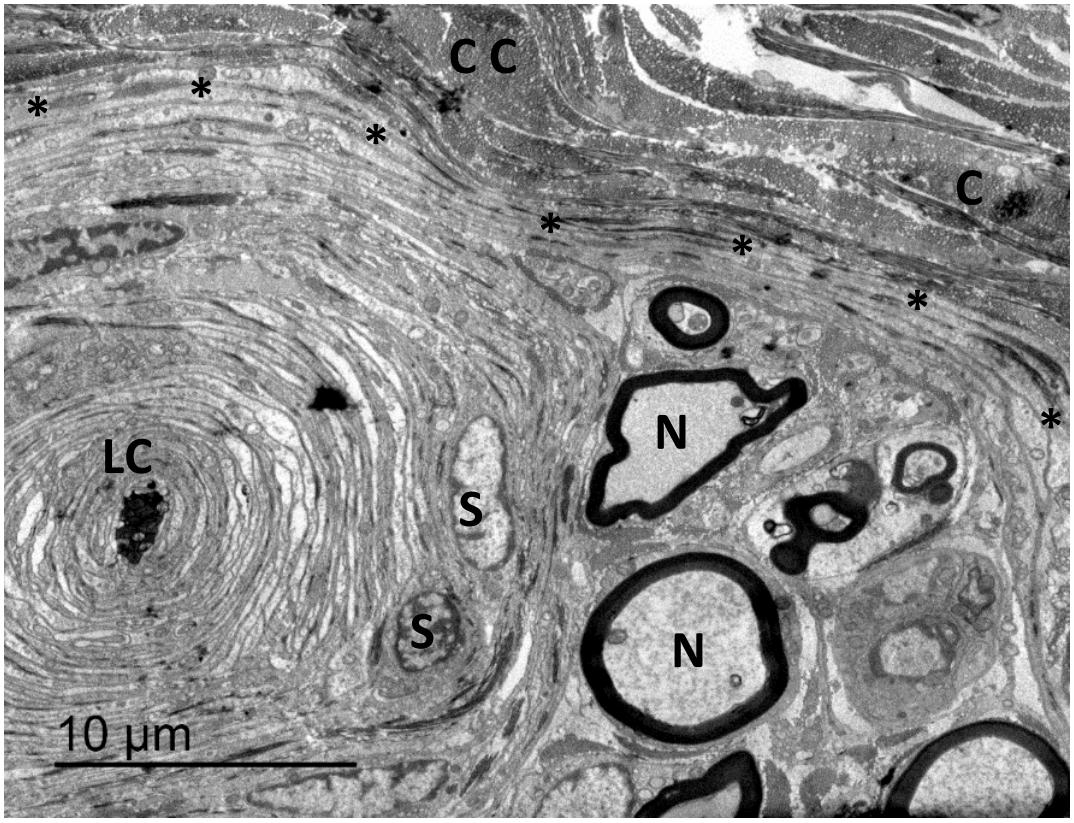

Figure 229. A lamellar corpuscle (LC) and myelinated nerve fibres (N) embedded within the same outer lamellae (asterisks). S: Inner core cell nucleus; C: collagen fibres of the subepithelial connective tissue.

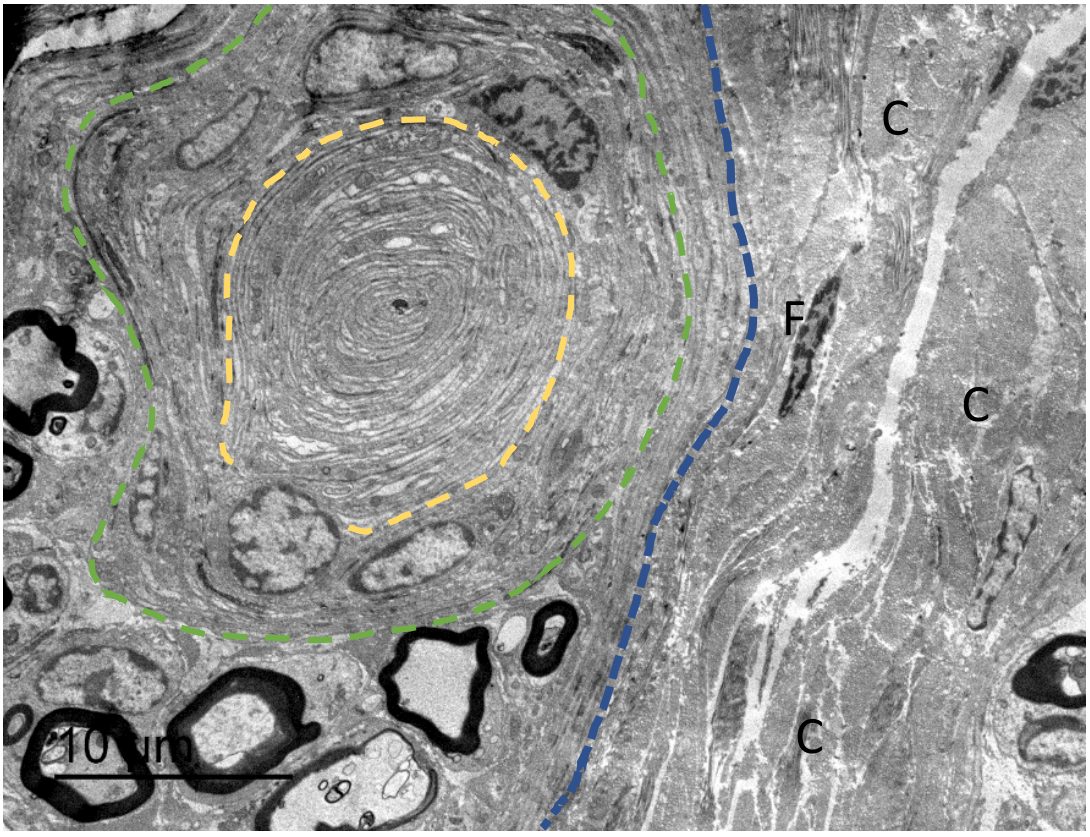

Figure 230. Overview of a lamellar corpuscle and nerve fibres within the same perineurium (blue dashed line) and surrounded by connective tissue (C). The inner core is delineated by the yellow dashed line, following the principles of Chouchkov (1973); the capsule of the corpuscle is indicated by the green dashed line, and the perineurium is indicated by the blue dashed line. F: fibrocyte/-blast. (De Vreese et al., 2020b)

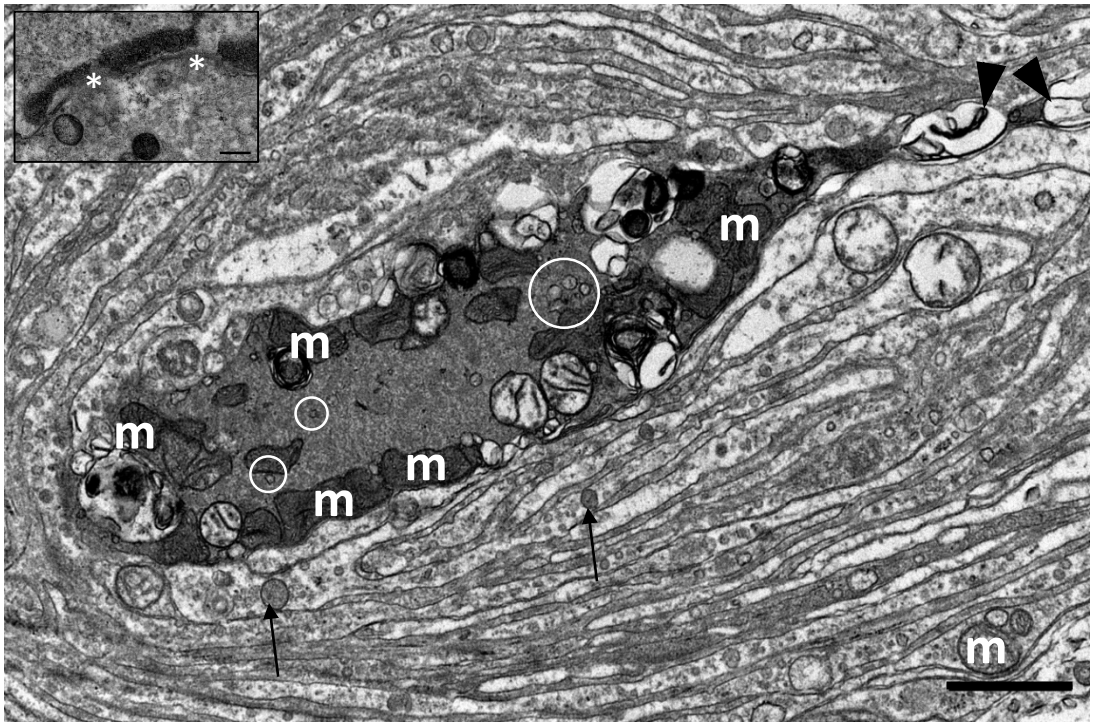

Figure 231. TEM image of the axon terminal (A) with mitochondria (m) along the rim of the neurite, and indications of microtubules (circles). The axonal spine contains large vesicular structures (arrowhead) and surrounding lamellae contain mitochondria, abundant pinocytotic vesicles, and larger vesicles (arrows). Scale bar 2 µm. The insert shows a close-up image of two adjacent inner core lamellae with desmosome-like cell-junctions (asterisks). Scale bar 0.1 µm (De Vreese et al., 2020b).

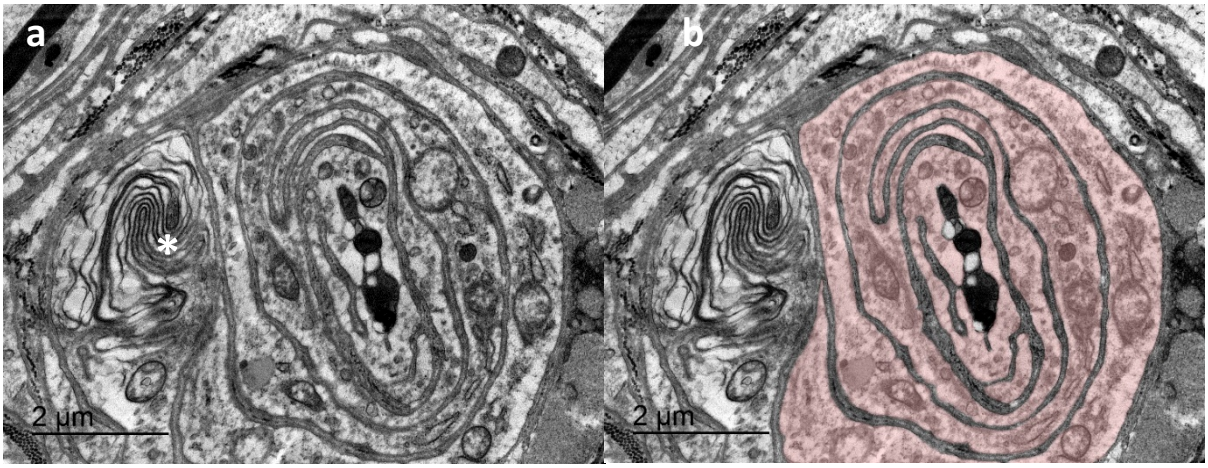

Figure 232. TEM image of a transverse section through the ultraterminal region of a simple lamellar corpuscle. Note that there is no bilateral symmetry, no radial clefts, and the axon is surrounded by several broad, continuous circular lamellae of a single core cell (see the right image where the cytoplasm is stained). There is a smooth endoplasmic reticulum (asterisk) situated in the lamellar cytoplasm. This section resembles the genital end-bulb in the rat penis as described by Munger (1971, Fig. 9b). (De Vreese et al., 2020b)

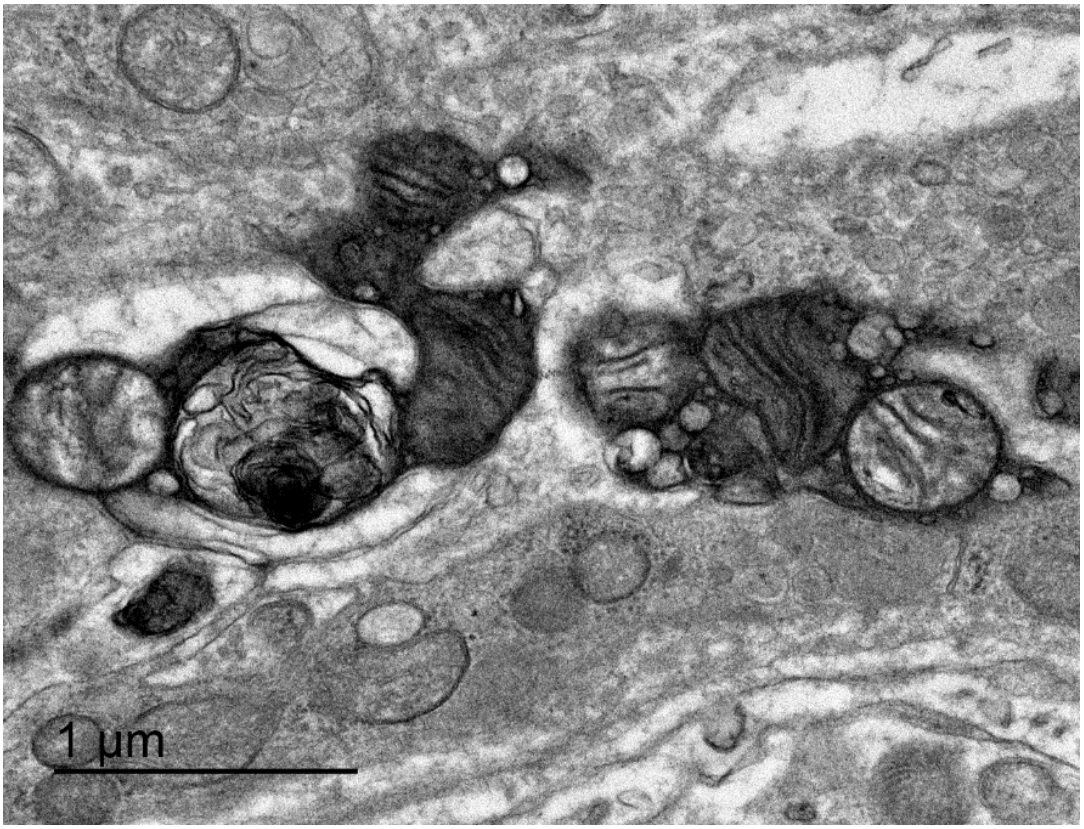

Figure 233. TEM image. Mitochondria within the axon terminal.

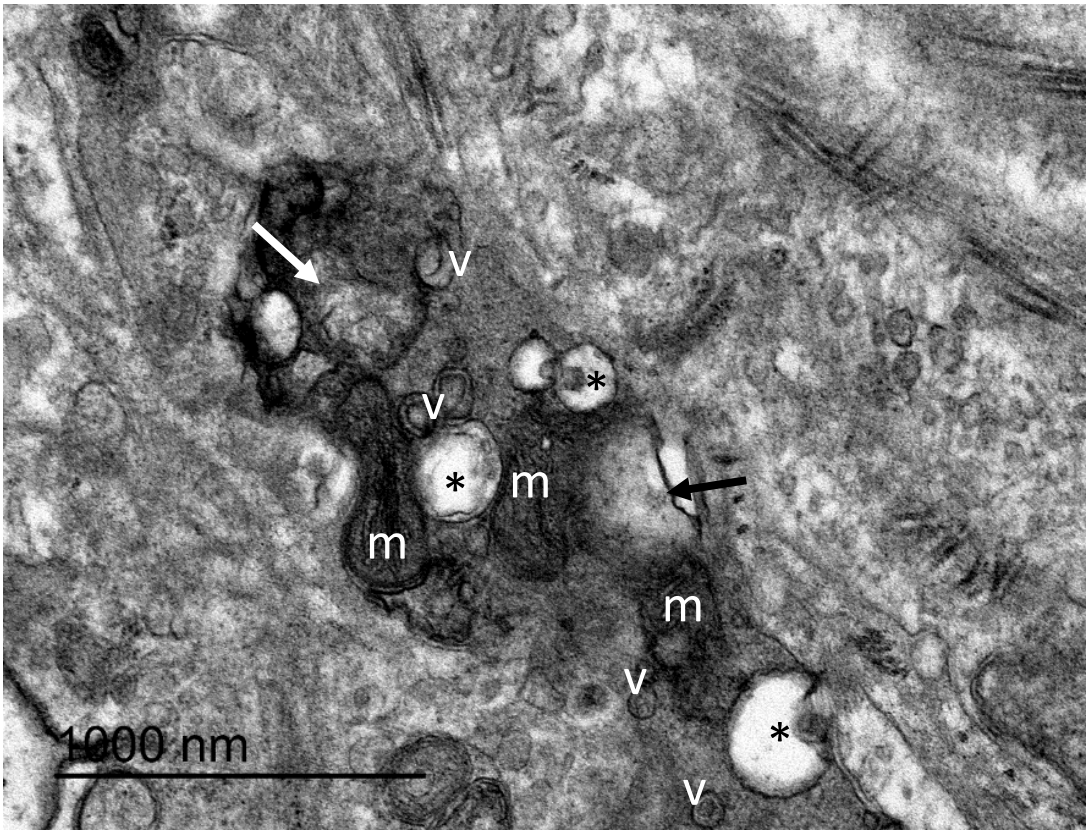

Figure 234. Detail of Figure 228. The axon terminal contains several structures including mitochondria (m), double-layered vesicles (v), and unknown electron-lucid structure with often an electron-dense 'nucleolus' (*). Arrow: degenerating mitochondria

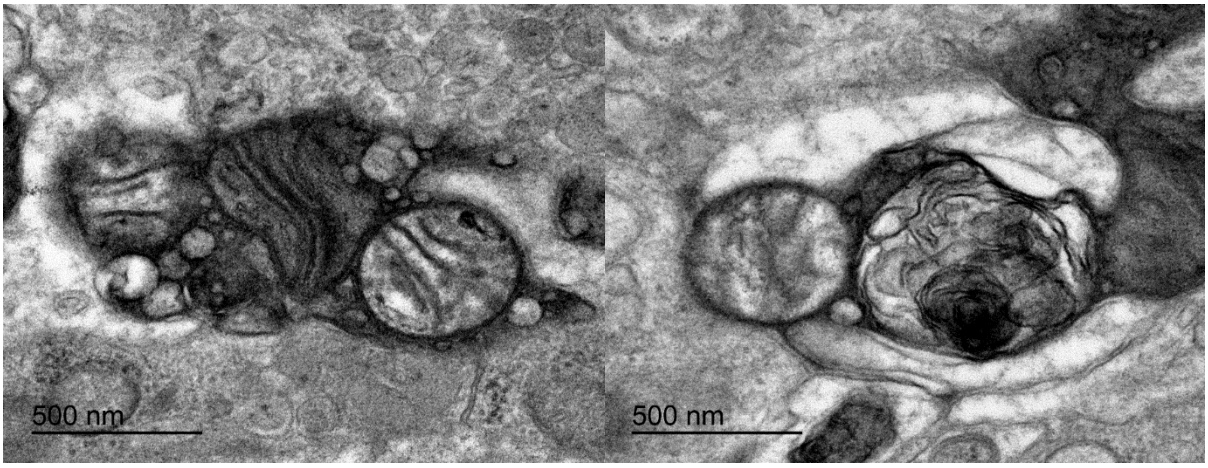

Figure 235. TEM image. Mitochondria and vesicles within the axon terminal. Right: Possibly degenerating mitochondrion within the axon terminal

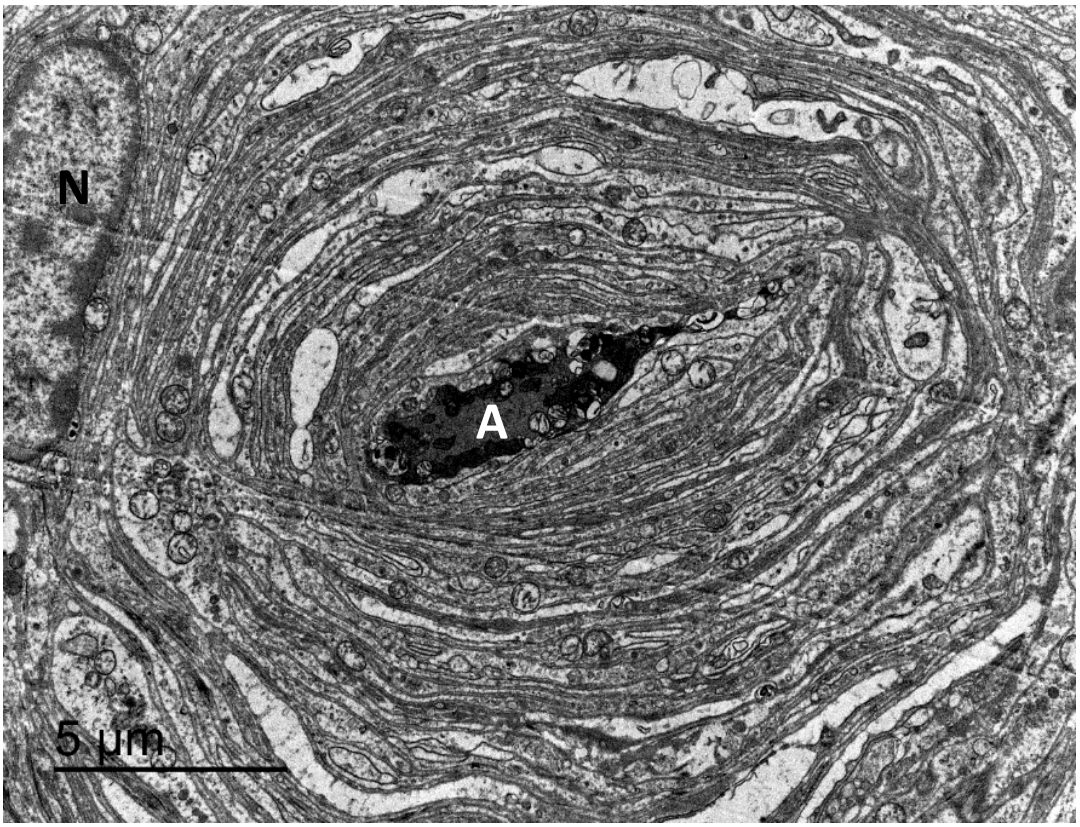

Figure 236. Overview TEM image of a cross-section through a lamellar corpuscle. Note the axon (A) in the centre, surrounded by hemilamellae made of an inner core cell cytoplasm and cell membrane. N: nucleus of the Inner core cell.

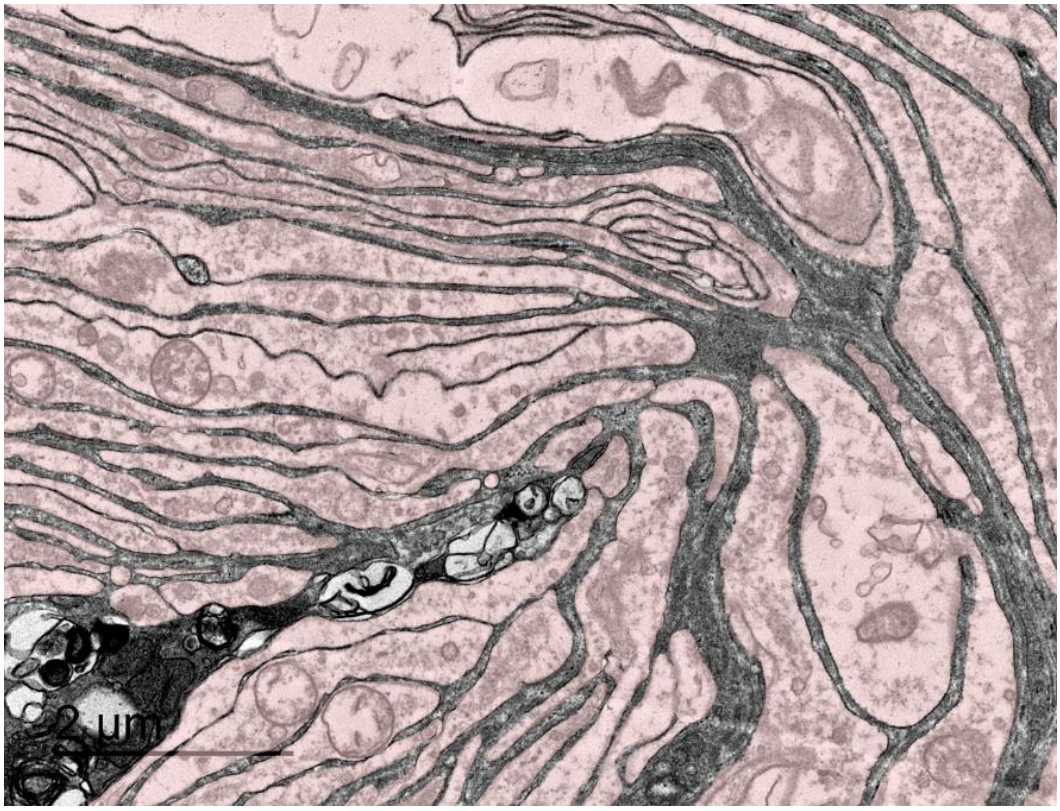

Figure 237. TEM image of the axonal spine, detail of Figure 236, showing the hemilamellar structure, with the lamellar cytoplasm manually coloured less opaque and slightly reddish. As such, it is easier to see the radial cleft, the bulbous enlargements of the lamellae near the cleft, and the full circular lamellae more peripheral (De Vreese et al., 2020a)

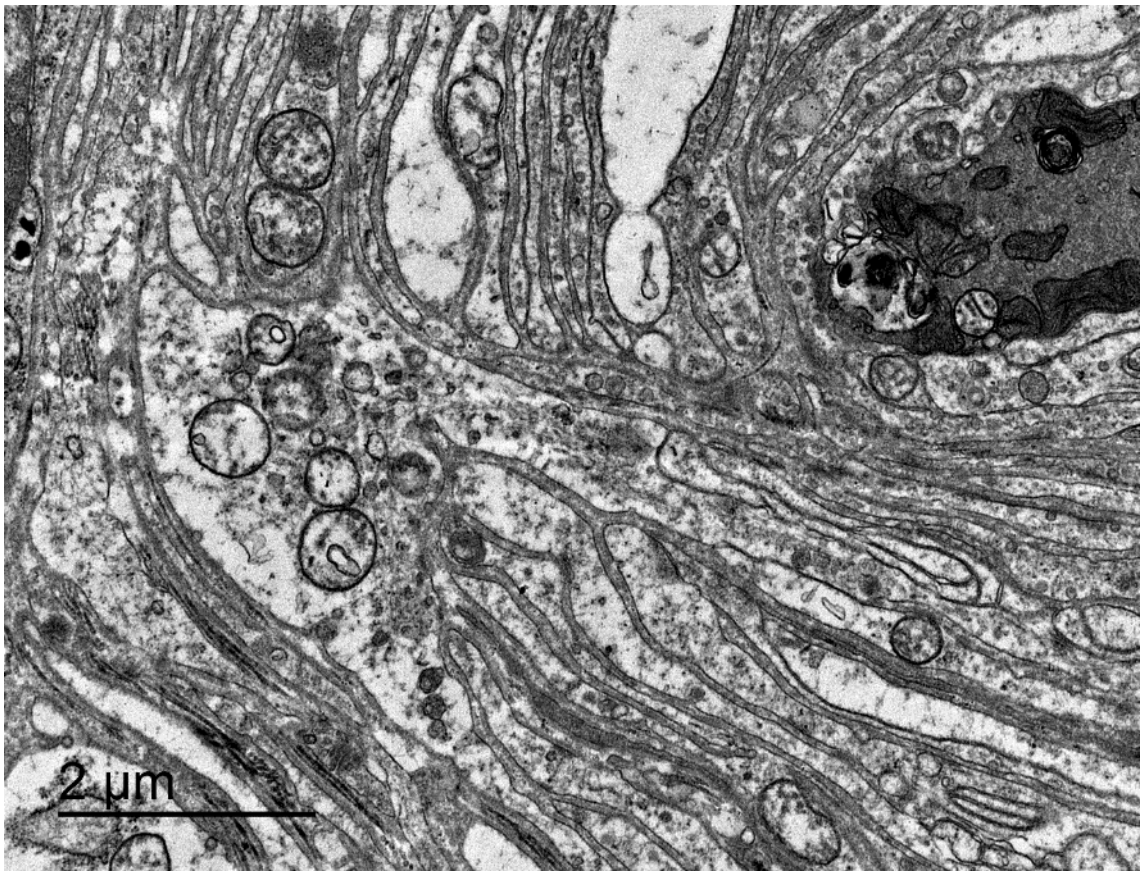

Figure 238. TEM image of the hemilamellae of the opposite pole of Figure 237.

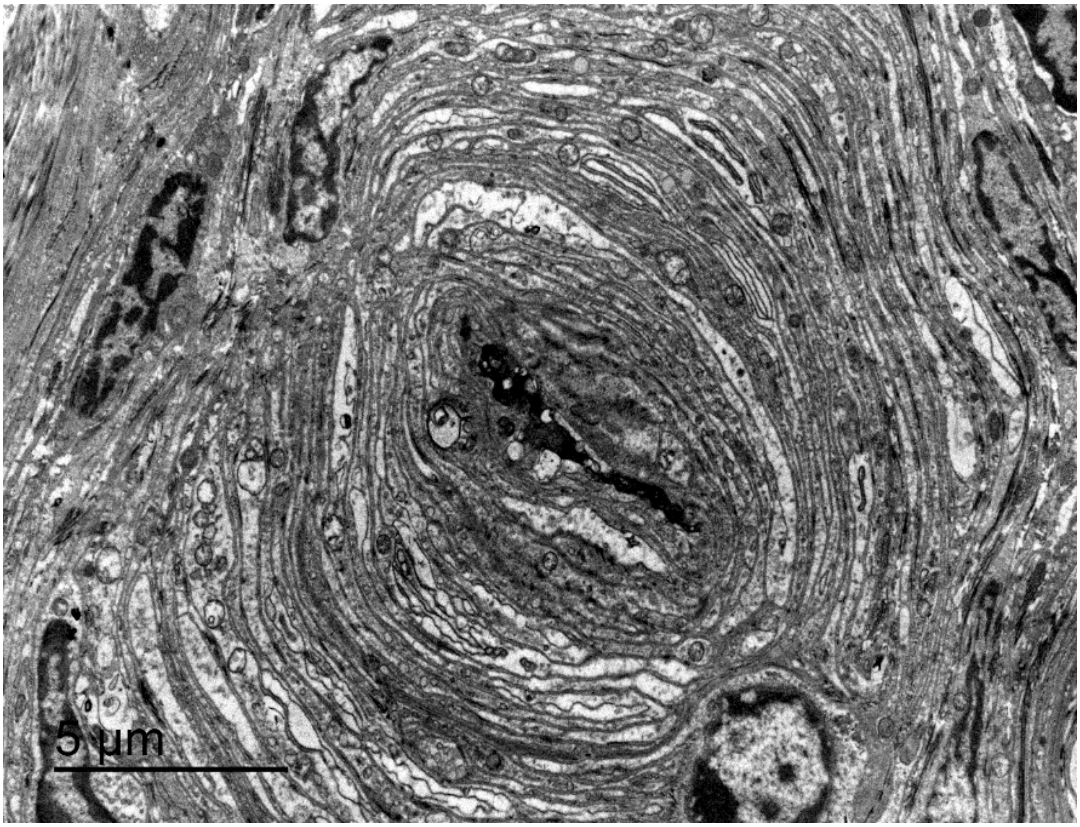

Figure 239. Detail of Figure 228, showing the hemilamellar structure of the corpuscle and the flattened axon terminal. The hemilamellae meet at the axonal poles.

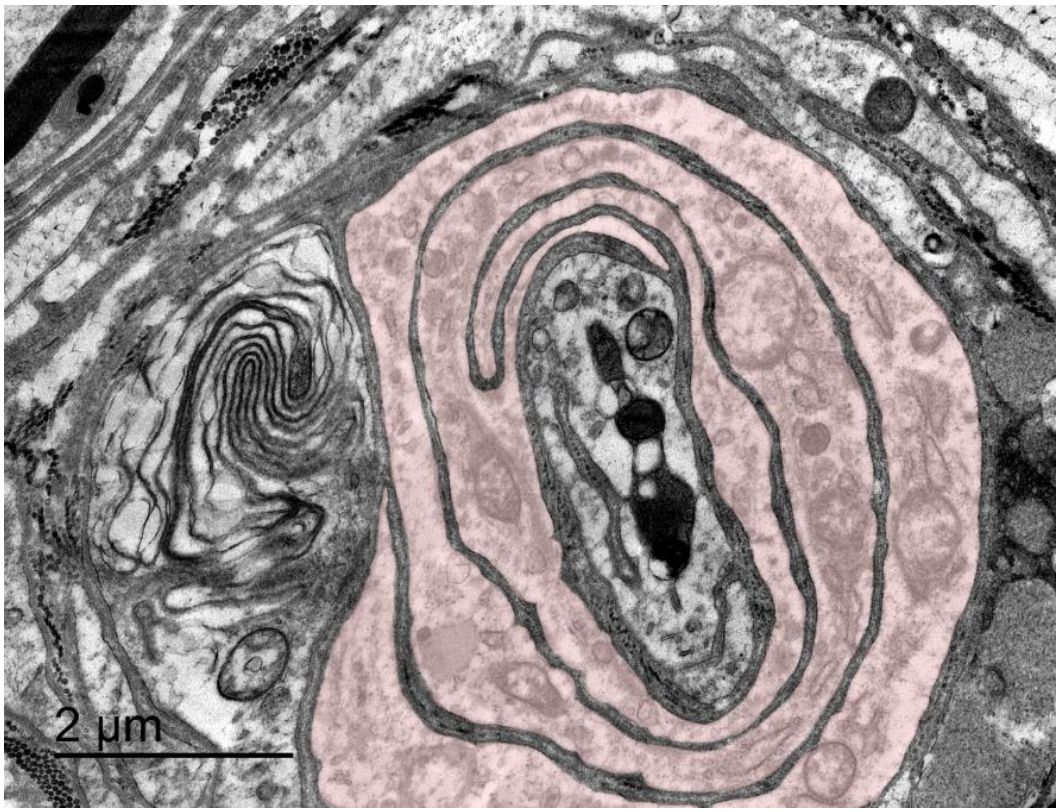

Figure 240. TEM image of a probable ultraterminal end of a corpuscle with the continuous cytoplasm of a single inner core cell highlighted in a pale reddish colour. There is no bilateral symmetry, no radial clefts, and the axon is surrounded by several broad lamellae of a single cell (See next figure). There is likely smooth endoplasmic reticulum situated in the lamellae (inside the Schwann receptor cell cytoplasm) in the close vicinity of an axon. This section resembles the genital end-bulb from a rat penis as described by Munger (1971, Fig. 9b). (De Vreese et al., 2020b)

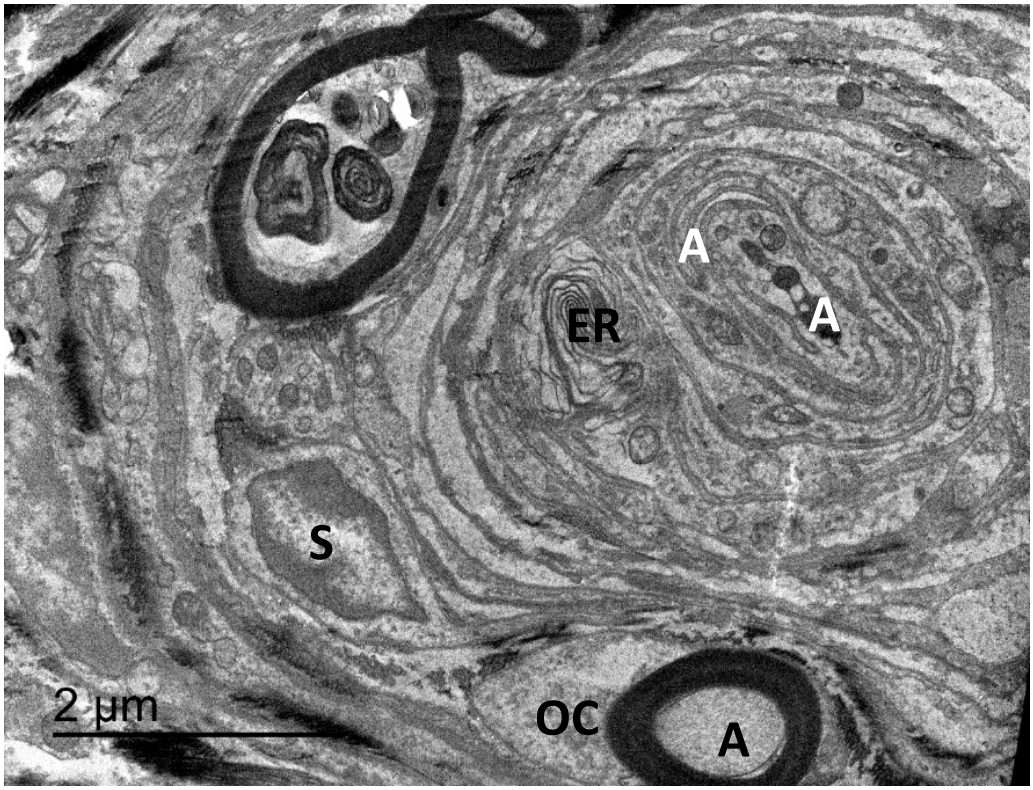

Figure 241. Lamellar corpuscle and myelinated nerve fibres; This is likely a section through the ultraterminal region of the corpuscle. S: Inner core or capsular cell nucleus; OC: Outer compartment of Schwann cell cytoplasm; A: axon; M: myelin sheath; ER: endoplasmic reticulum? Whorls in the nerve fibre at the top;

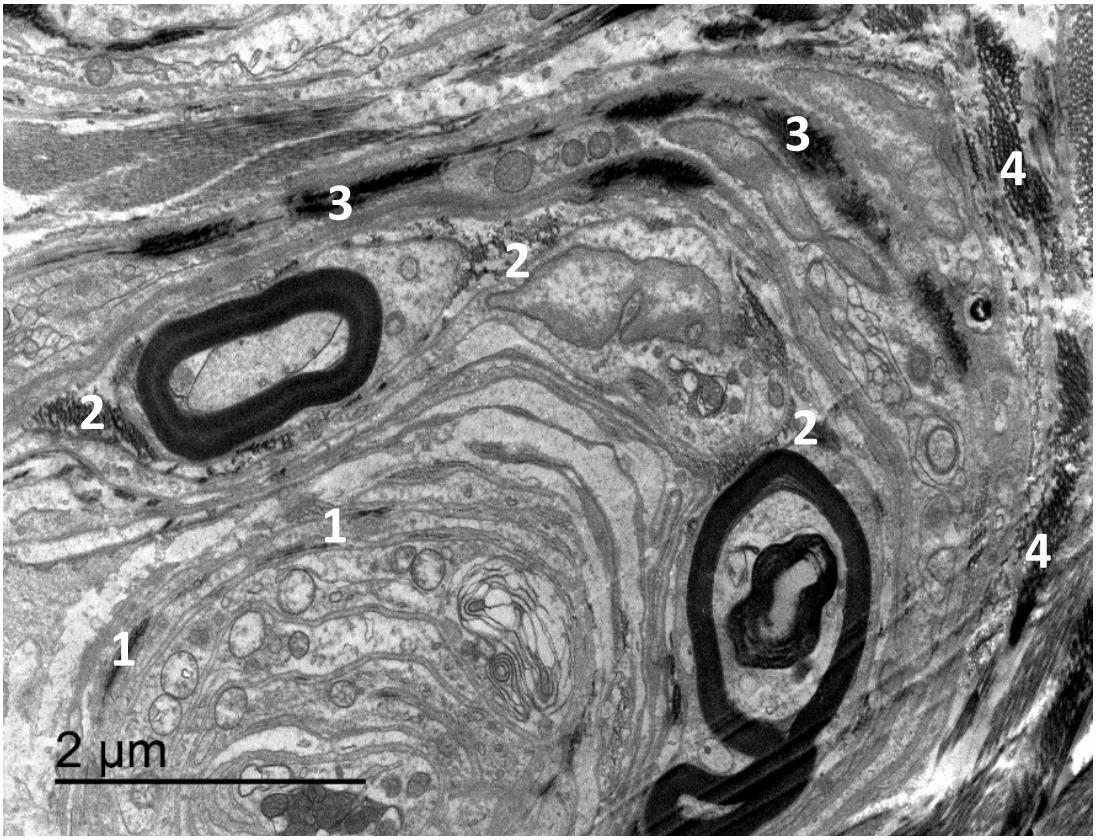

Figure 242. TEM image. Collagen fibres are present between the lamellae of the corpuscle although not near the centre (1), in the endoneurium of the nerve fibres (2), in the perineurium surrounding the nerve fibres and corpuscle (3), and in the surrounding connective tissue in which the entire structure is embedded (4).

Figure 243. TEM image of an axon terminal and surrounding lamellae. Arrows: endoplasmic reticulum; C: collagen fibrils in the extracellular matrix.

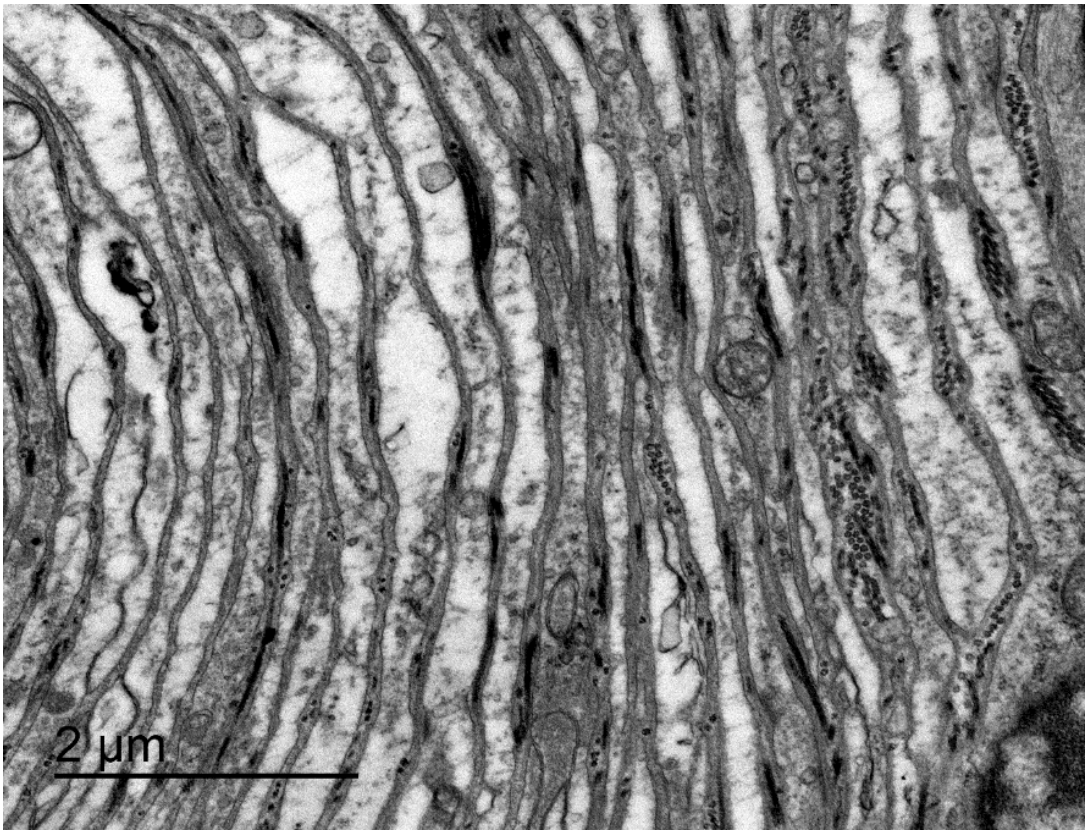

Figure 244. Detail of the core lamellae. The lamellae consist of adjoining plasma membrane and little amount of cytoplasm. There are… Collagen fibres in the extracellular spaces are oriented in two main directions and are section longitudinally and transversely in this transversely sectioned corpuscle.

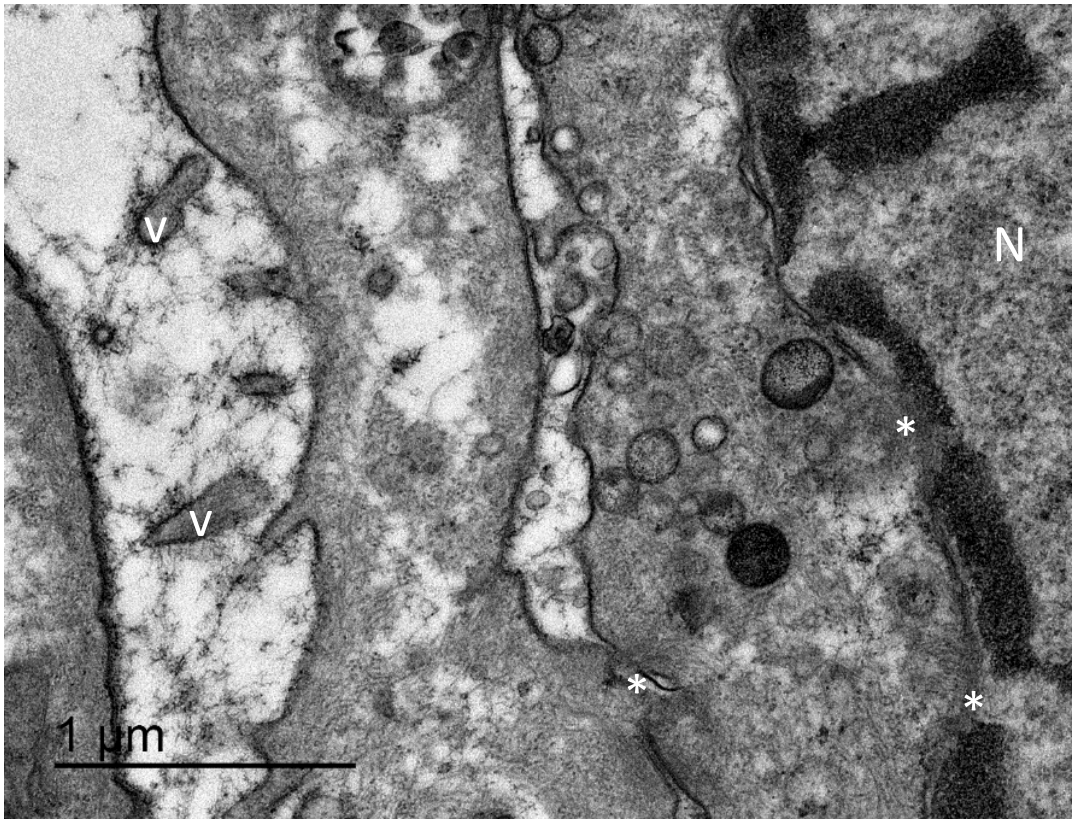

Figure 245. Close up of inner core lamellae and part of the nucleus of an inner core cell. Note the desmosome-like cell-junctions (*), and the budding/vesicular structures with extensive glycocalyx, situated between cells (v).

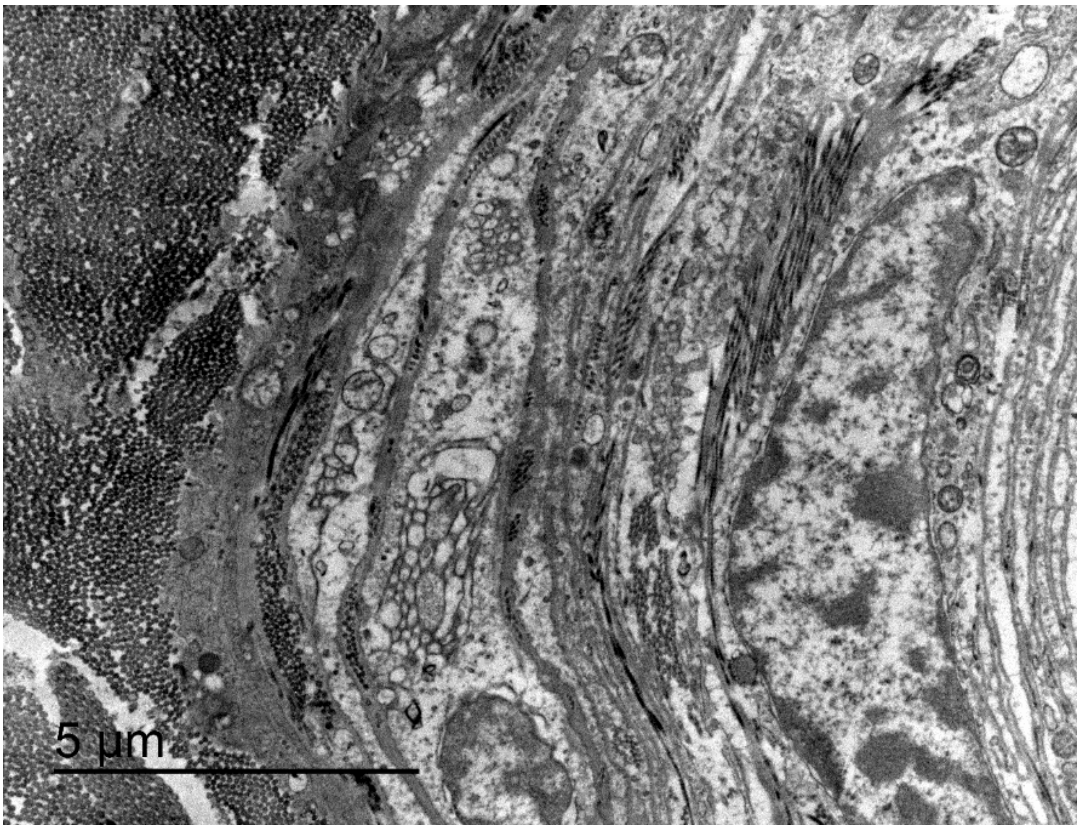

Figure 246. Detail TEM image of the capsule of a lamellar corpuscle with the inner core lamellae (L), a nucleus of an inner core cell or a capsular cell (N), capsule (C) with more collagen fibres in the extracellular space than in the core; Surrounding connective tissue consisting mainly of collagen fibres. The latter did not form a capsule but was part of the connective tissue of the environment in which the corpuscle was situated.

3.2 Other sensory nerve formations

The presence of intrapapillary myelinated nerve endings (IMEs) was shown by positive labelling with the anti-NF, anti-PGP 9.5 and anti-S-100 antibodies. All nerve fibres in the subepithelial tissue stained positive for both anti-PGP 9.5 and anti-S-100. There were positively stained singularities in the connective tissue immediately beneath the basement membrane for all antibodies except anti-NF, and there were also intraepithelial 'free' nerve endings as shown by anti-PGP 9.5 (Figure 247, Figure 248) (De Vreese et al., 2020b)

The unanimous labelling of subepithelial nervous structures is considered to be a true positive reaction although it was often granular in form, similar to the epithelial pigmentation. This feature was present in all toothed whales and absent in all terrestrial mammals. Even though the subepithelial tissue of the cow and the giraffe showed a similar reaction, this was only so only for anti-S100, which is less nervous specific as the other antibodies. However, we do not fully exclude it might be an artefact, and further investigations should be done to clarify this reactivity.

Also, the transmission electron microscopy studies did not provide any novel insights into the possible presence of other types of sensory nerve formations beside the simple lamellar corpuscles. However, as there was little tissue available after all the processing, these could have been easily missed. We gave special attention to intraepithelial nerve fibres and Merkel cell-neurite complexes, but could not identify any. Similar to Merkel cells, there were cells with a lobulated nucleus and concentrated granules near their basal pole. However, these cells were not associated with the basal membrane, nor could we find any neurite, nor any intracytoplasmic filaments associated with a desmosome, nor typical dense-core vesicles (Cfr. Orfanos and Mahrle, 1973) (Figure 86).

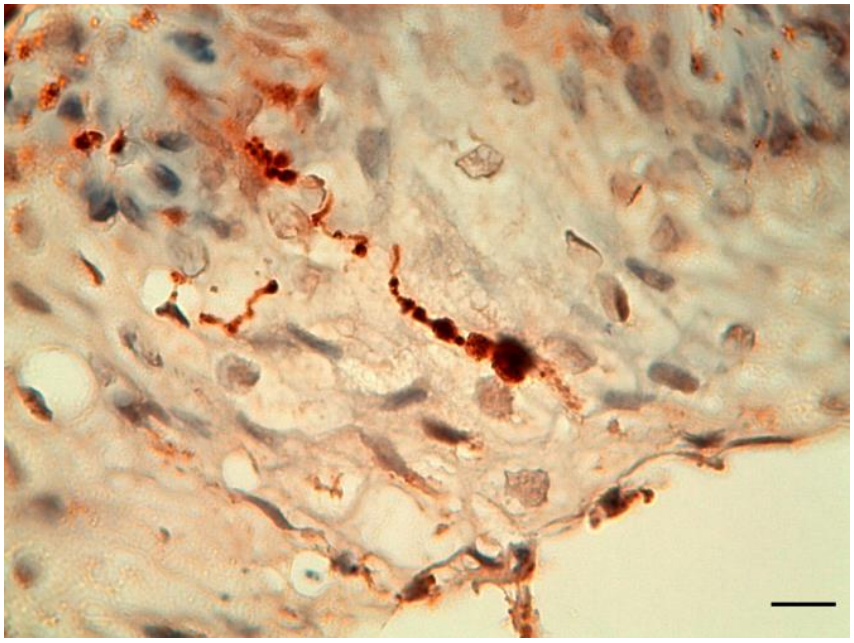

Figure 247. Detail image of an intraepithelial nerve fibre running from the germinal layer to the luminal surface of the ear canal of a striped dolphin, stained with PGP 9.5 (1:500, no block, melanin bleaching). Scale bar 10 µm(De Vreese et al., 2020b)

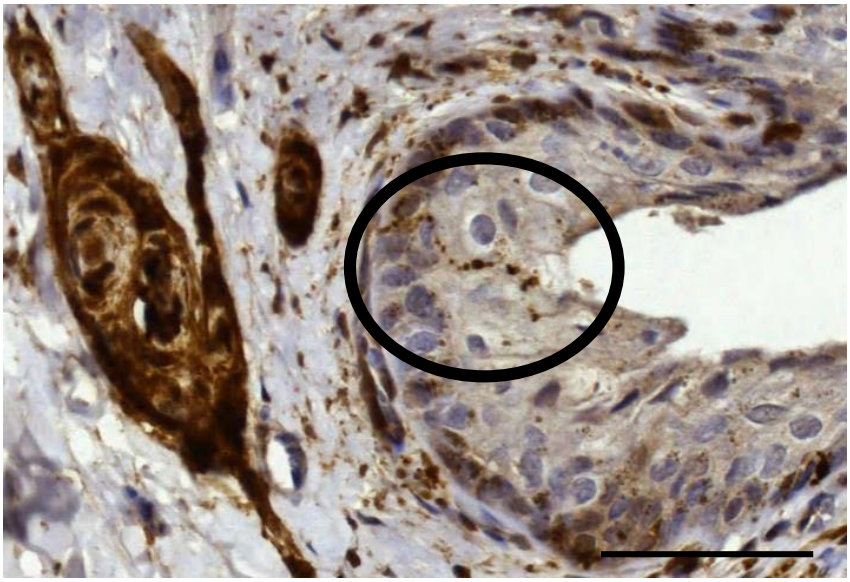

Figure 248. IHC stain with anti-PGP 9.5 (1:500, No block, no bleaching). A densely stained complex of nerve corpuscle and nerve fibres. The encircled area indicates the presence of a free nerve ending in the epithelial layer with a course from the basilar membrane to the surface and in very close proximity to the lumen. Scale bar 50 µm

3.3 Nerve fibre morphology

Nerve bundles stained similarly as the lamellar corpuscles. They comprised one or more axons and associated Schwann cells embedded in an endoneurium and surrounded by a perineurium. Axons were positive for anti-NF (Figure 249), anti-PGP 9.5 and anti-NSE. The Schwann cell nuclei and cytoplasm stained positive for anti-S100 (Figure 249), and anti-PGP 9.5, and the perineurium for anti-PGP 9.5, anti-NSE, and anti-S-100 protein. The endoneurium did not show positivity for any antibody. The major difference in immunohistochemical labelling of corpuscles and nerves was that the perineurium was labelled intensely by anti-S-100 while the peripheral layer of the lamellar corpuscles showed more IR to anti-PGP 9.5, while both the corpuscle's peripheral layer and the nerve fibre´s perineurium showed IR to anti-NSE (at least in the freshest samples)(De Vreese et al., 2020b).

The TEM images showed that the configuration of the peripheral nerves in both dolphin species followed the standard configuration as in other mammals with axons as the central unit, myelinated or not, but anyway surrounded by a Schwann cell, and embedded in endoneurium; the grouping of multiple axons formed a fascicle, which was surrounded by perineurium; and multiple fascicles were grouped into a fascicular bundle, covered by epineurium.

Inside the axoplasm, we could see microtubules and neurofilaments (although not distinguishable between the two), smooth endoplasmic reticulum, and mitochondria (Figure 250). The axolemma (plasma membrane of the axon), appeared as a delineation around the central axon consisting of two electron-dense layers separated by a lighter layer, the same as the internal mesaxon of the surrounding Schwann cell (Figure 250, Figure 251). The inner compartment of the Schwann cell cytoplasm, whenever visible, did not contain any organelles. The same fascicle could enclose both unmyelinated and myelinated axons. The myelin sheath was formed by enwinding of the Schwann cell

plasma membrane around the axon. In unmyelinated fibres, the axons were separated by single lamellae of Schwann cell cytoplasm that incompletely surrounded the axon. In the outer compartment of the Schwann cell cytoplasm we could note any cell nucleus, but only mitochondria, several unknown structures, and the external mesaxon connecting to the plasma membrane (Figure 304, Figure 252). A basal lamina surrounded the entire complex. The endoneurium consisted mainly of collagen fibres (Figure 253).

Interestingly, there was often a deformation of the myelin sheath with myelin infolding and whorling, and outfolding with sheath separation from the axon, creating peri-axonal spaces, and which sometimes involved degenerated axonal components. The infolding was often visible as myelin ovoids with wavey whirling, and focal disruption and separation of the laminae. It was also associated with the presence of round structures with little heterogeneity and contrast and with the presence of spaces that contained degeneration products (Figure 253, Figure 254). The outfolding presented with similar myelin whirling as the infolding did, also with axonal degeneration products (Figure 255). The round structures showed morphological similarities with lamellar bodies found in Type 2 alveolar cells in the lung, but could not be identified with certainty. These morphological findings concur with either an axonopathy or were associated with postmortem degeneration processes. The latter is more likely as the histological examination did not show specific indication of axonal atrophy or Wallerian degeneration. There were also indications of mononuclear cells present with the nerve fascicle, although no evidence of any phagocytosis was noted.

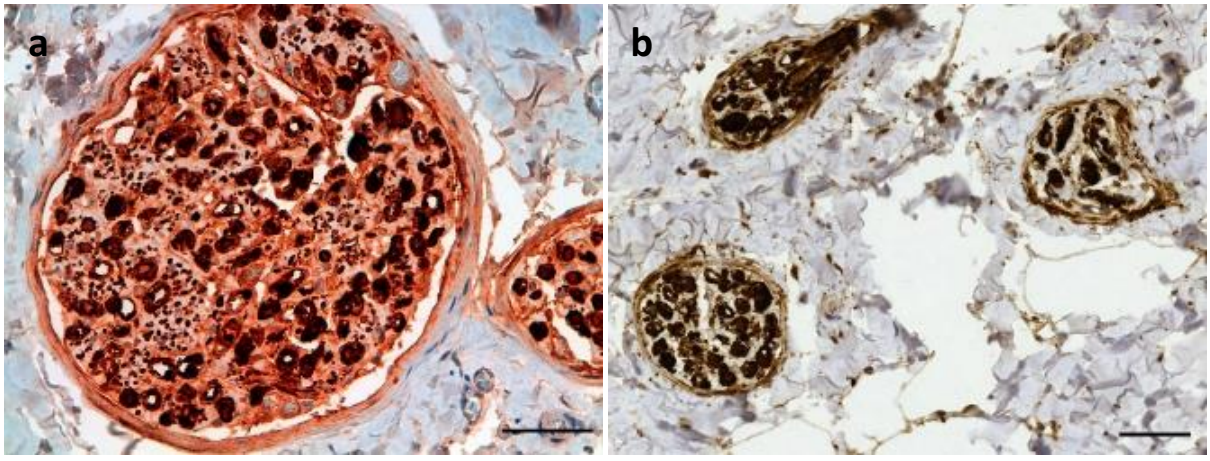

Figure 249. Detail image of a nerve fascicle in the subepithelial tissue in a striped dolphin stained with anti-NF (a) and anti-S100 (b). Scale bars 50 µm (De Vreese et al., 2020b)

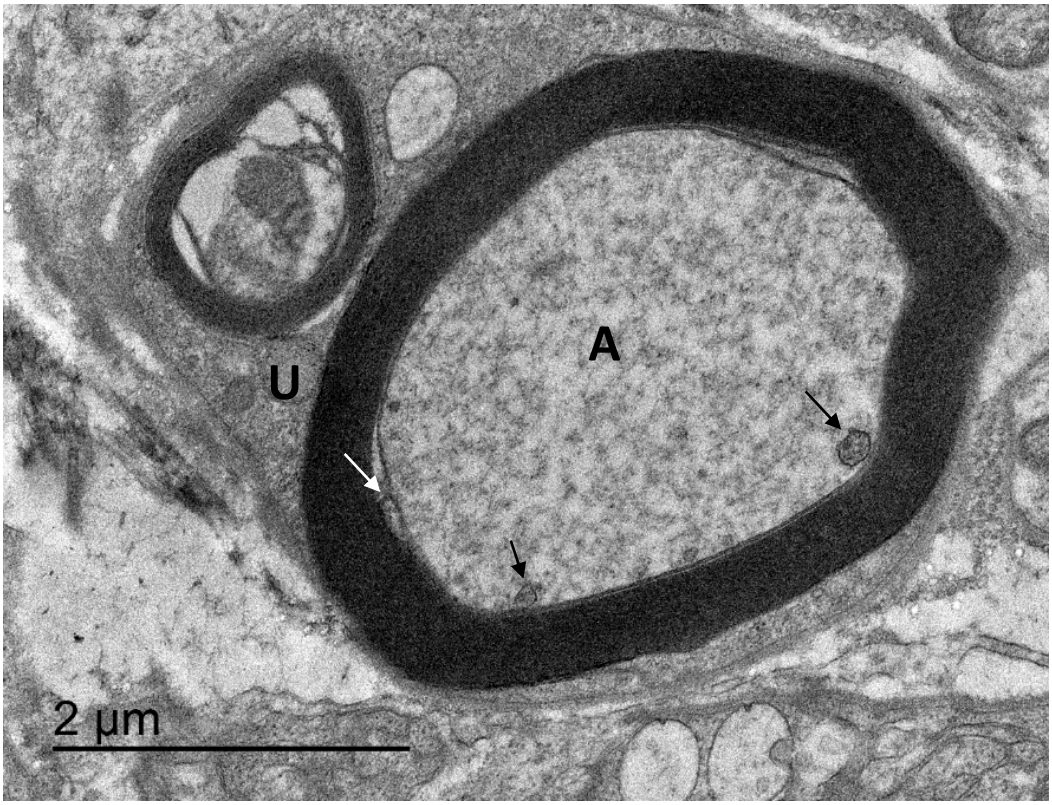

Figure 250. TEM image. Myelinated nerve fibre. A: axon; White arrow: internal mesaxon; Black arrow: mitochondrion; (Cfr. Domenech-Estevez et al., 2016 Figure 8-B-III U: unknown structures).

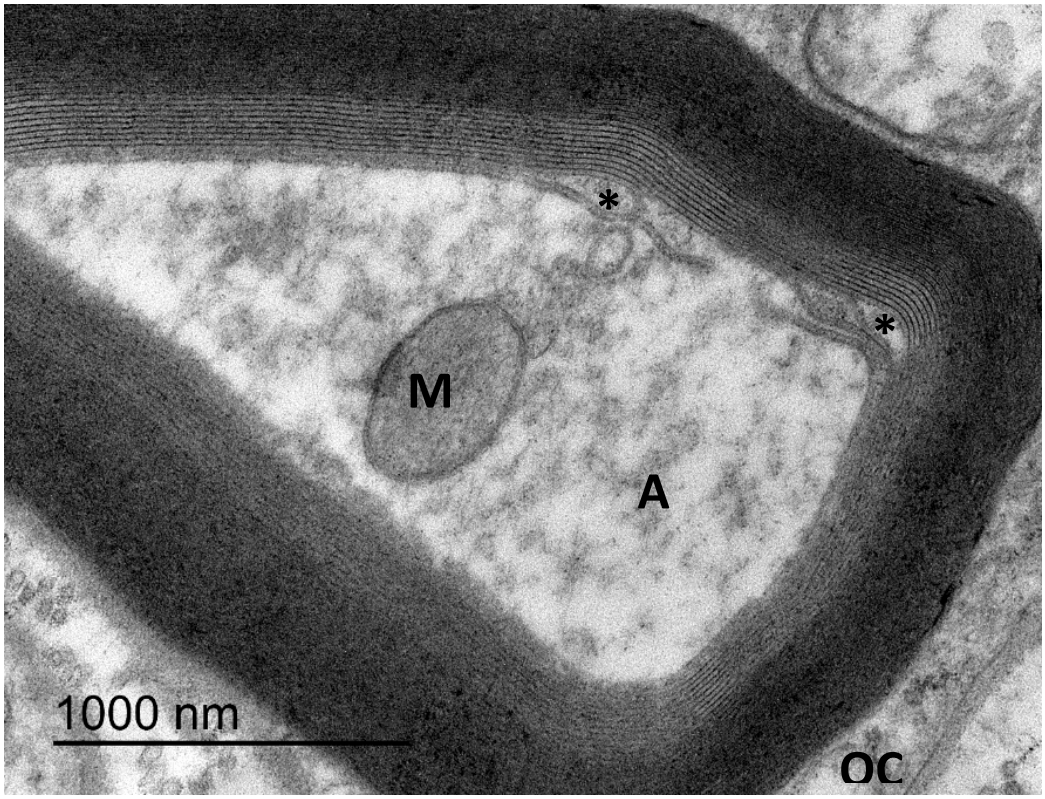

Figure 251. TEM image. Myelinated nerve fibre with the presence of a mitochondrion inside the axon (A), and a ruptured axolemma or plasma membrane of the Schwann cell. OC: outer compartment of the Schwann cell cytoplasm; M: likely mitochondrion; Asterisks: cytoplasmic pockets of the inner compartment of the Schwann cell cytoplasm indicating that this section was taken in close proximity of a node of Ranvier.

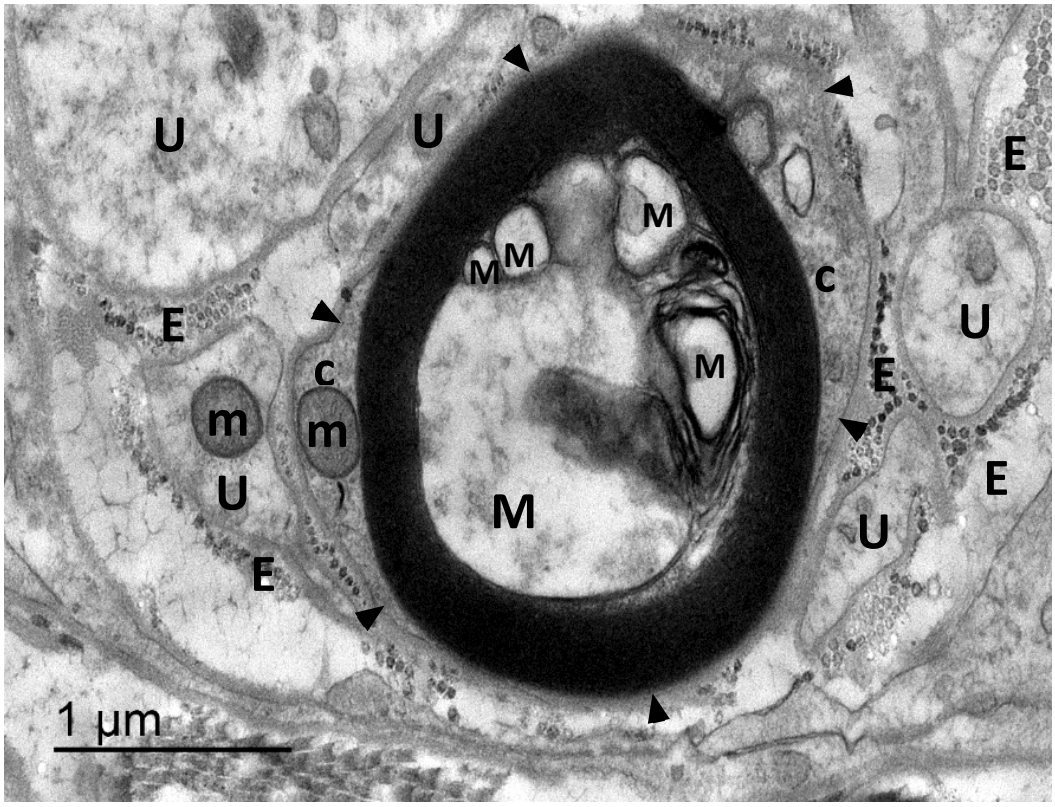

Figure 252. Myelinated (M) and unmyelinated nerve fibres (U) within the same fascicle. c: outer compartment of the Schwann cell cytoplasm; m: mitochondrion; arrowheads: Schwann cell plasma membrane; E: endoneurium with mainly collagen fibres;

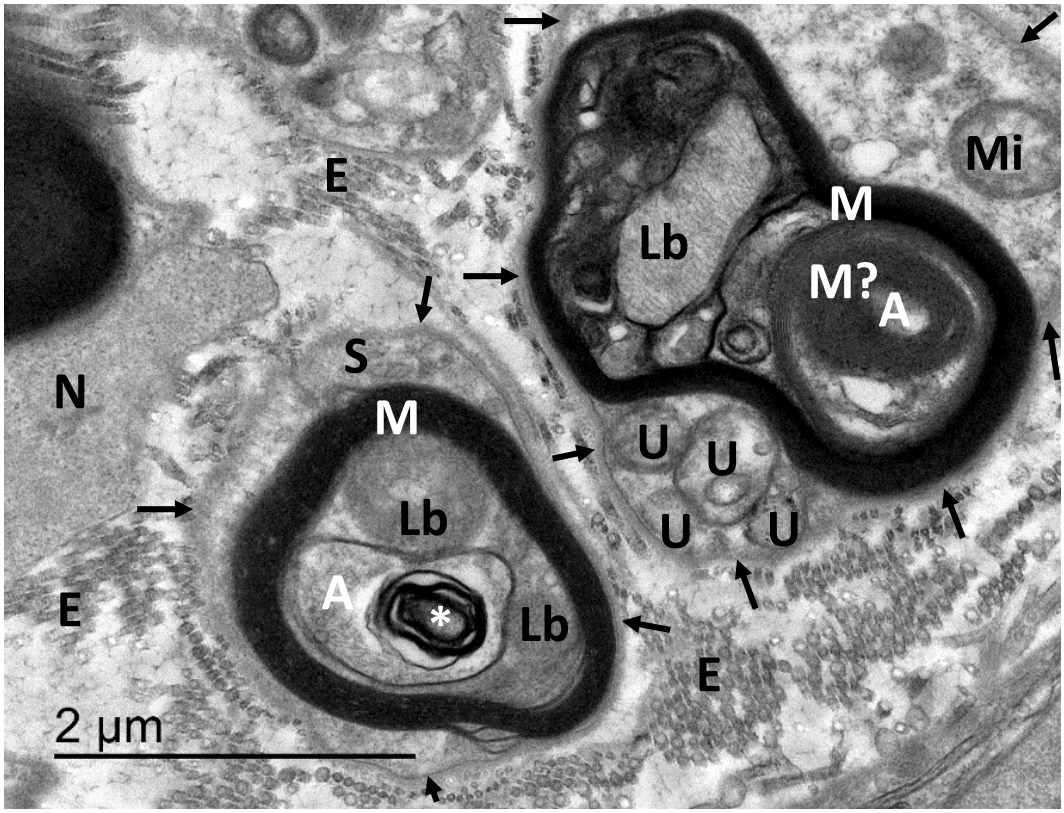

Figure 253. Detail image of two myelinated nerve fibres. A: axon;. E: collagen fibres of the endoneurium; Lb: possible lamellar bodies; M: myelin; Mi: mitochondrion; N: Inner core cell euchromatic nucleus; EC: external compartment of Inner core cell cytoplasm; U: possible multivesicular bodies; Arrows: Inner core cell plasmamembrane; Asterisk: myelin infolding. (TEM X 30000).

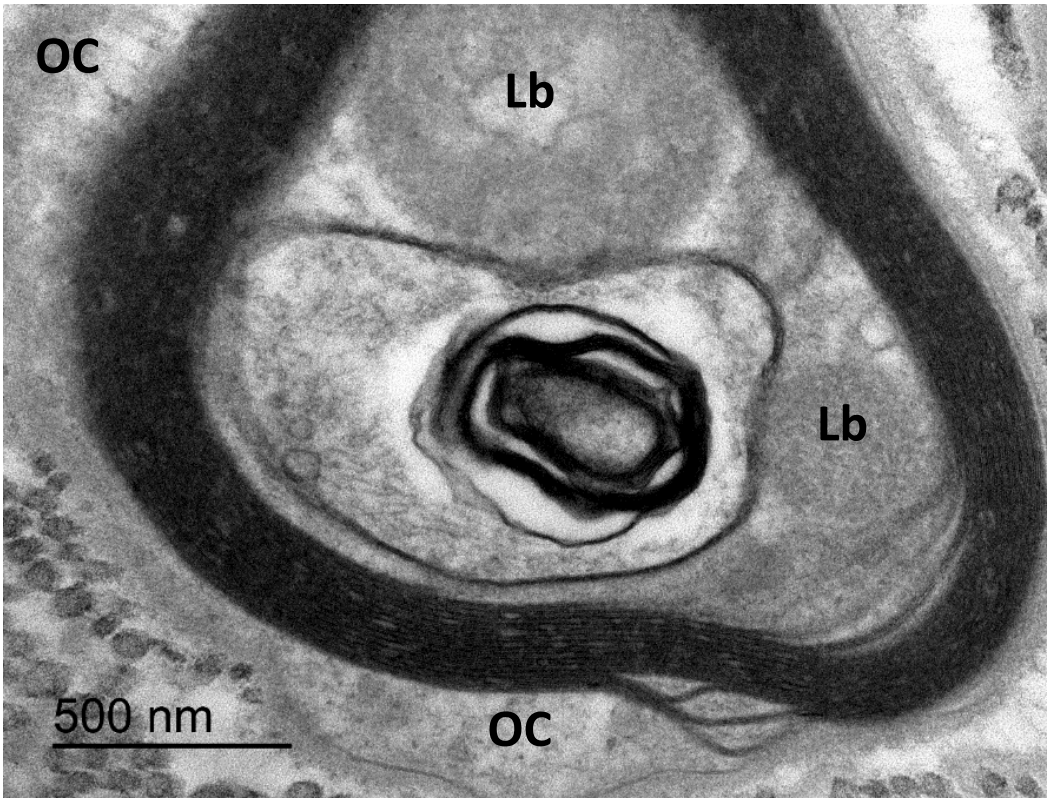

Figure 254. Detail of Figure 253. (TEM x 80000). Myelin infolding. A: axon (with sER); Arrows: basal membrane; OC: outer compartment of the Schwann cell cytoplasm; Lb: Lamellar body; C: collagen fibres of the endoneurium;*

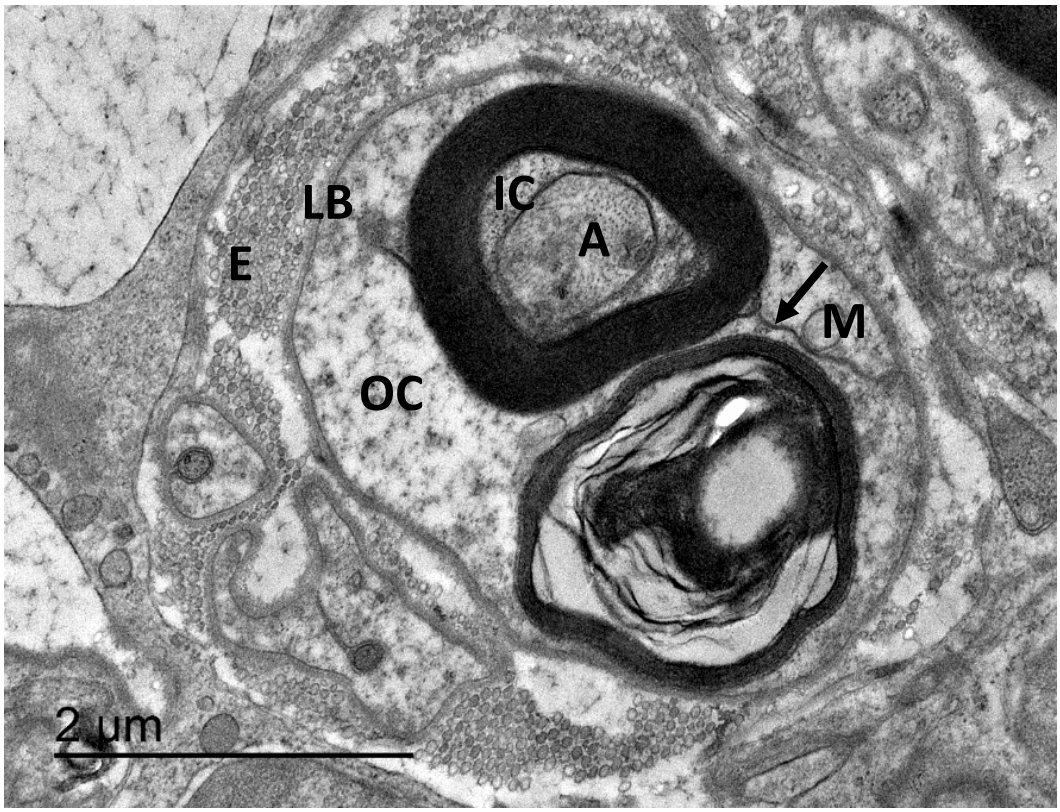

Figure 255. Two separate myelinated nerve fibres encompassed by a single Schwann cell. One depicts the normal configuration, while the other seems a myelin outfolding that encompasses a degenerated axon. A: axon; arrow: outer mesaxon of the Schwann cell. E: endoneurium with collagen fibres; OC: outer compartment of the Schwann cell cytoplasm; IC: inner compartment of the Schwann cell cytoplasm; LB: plasma membrane and lamina basalis; M: mitochondrion. (TEM x 30.000)

3.4 Intramural nervous plexus

We noted a very extensive intramural nervous plexus in which almost all of the nervous structures were interconnected, forming a network that surrounded the ear canal. The few separate structures that did not show a connection to the large 'web' might have been missed.

All corpuscles originated from small nerves with few axons. Sometimes the nerve completely transgressed into one or multiple corpuscles, while in other cases the corpuscles branched off from the nerve while the nerve continued its course. The nerves also showed many bifurcations and convergences on their course towards the periphery.

Corpuscles rapidly increased in diameter after originating from a nerve. They always presented a central axon, and often one or two axons in the periphery. The total length of 10 measured corpuscles varied from little less than 100 µm to 160 µm, with an average of 120±26 µm. They continued with the typical lamellar structures over an average distance of 90±17 µm (See Table 15).

The corpuscles ran in both directions, both from medial to lateral and vice versa. Some corpuscles ran in one direction, made a curve (up to 180°) and continued in the opposite direction. In some corpuscles, the end was unclear while most corpuscles ended as small structures with a central axon until they were untraceable in the HE stained sections. Many corpuscles were in close contact with other corpuscles, at least for part of their course. The general shape of the corpuscles was onion-like with a length about twice the width and tapering ends. In this aspect, it is similar to the shape of the inner core of Pacinian corpuscles (Loewenstein, 1971, Fig. 1).

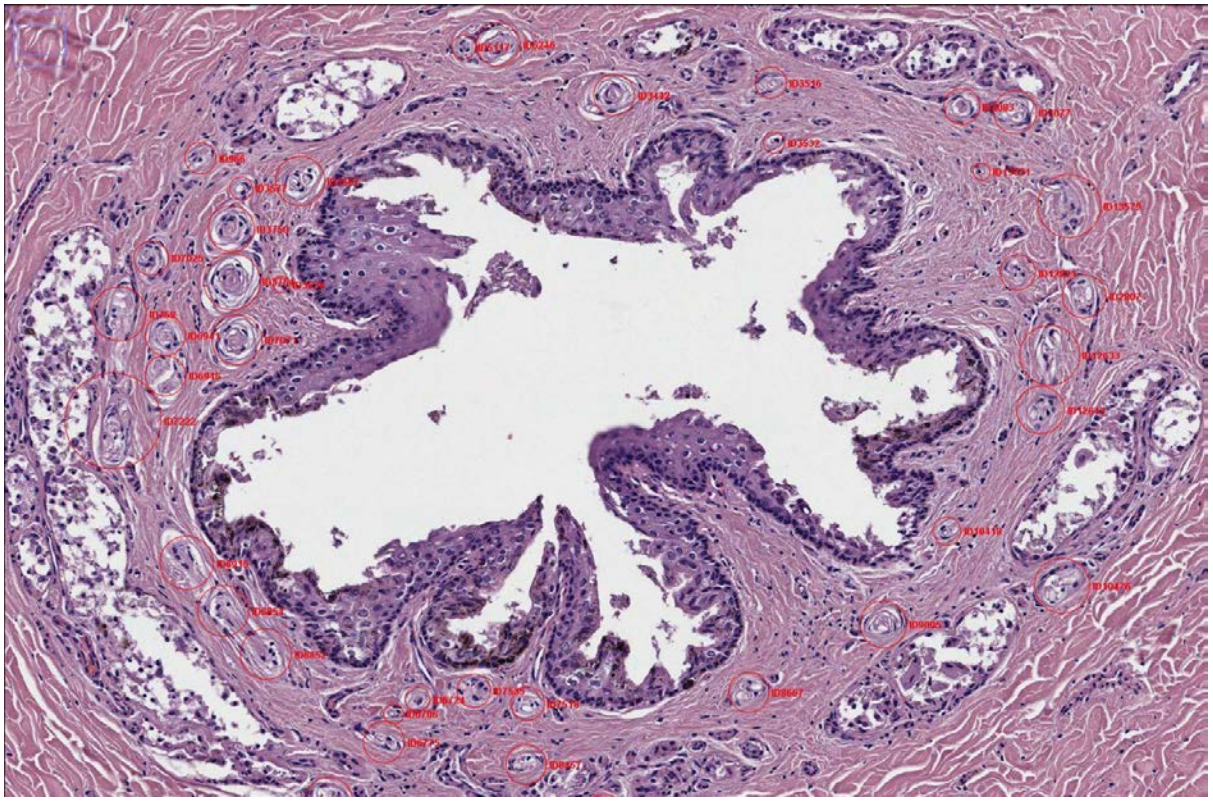

Figure 256. Histological image (HE staining) of a single histological section with the Trackmate plugin overlay of manually labelled nervous structures encircled in red with individual ID number See this LINK for a GIF of all 50 sections.

Figure 257. Overview of the links between and among nerves and lamellar corpuscles (TrackScheme output). Every horizontal line is a histological section, and each dot in the line represent one of the structures. The lines between dots represent the links between structures in consecutive sections. Different colours represent different tracks but note that almost all structures are interconnected (orange track), and the ones that do not continue before or after the sample limits so those might be connected as well. See LINK for a full view.

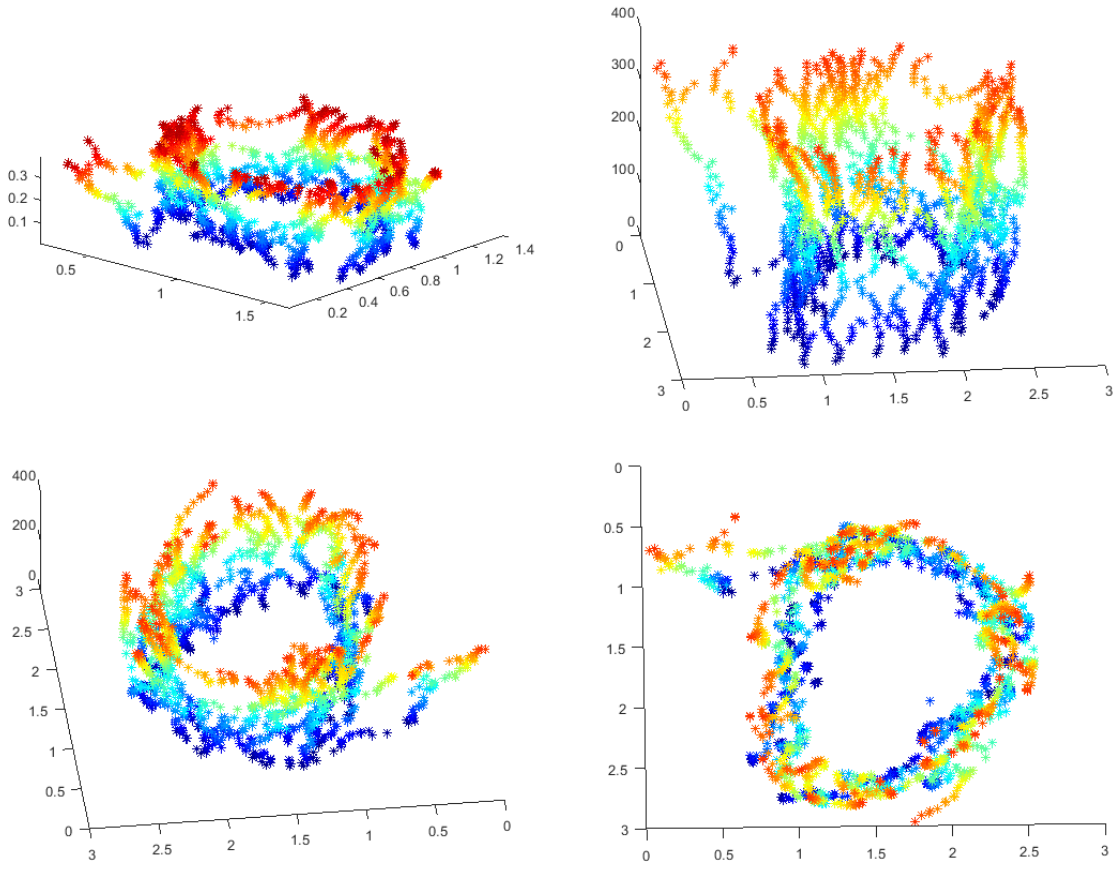

Figure 258. Matlab renderings of the nervous network. All nervous structure annotations are represented by an asterisk. In original equal scales (A), and elongated for better visual representation (B); (C) and (D) are angled and top views of (B). (E) highlights the connections between the annotated structures. Top is medial, bottom is lateral. See LINK for a video.

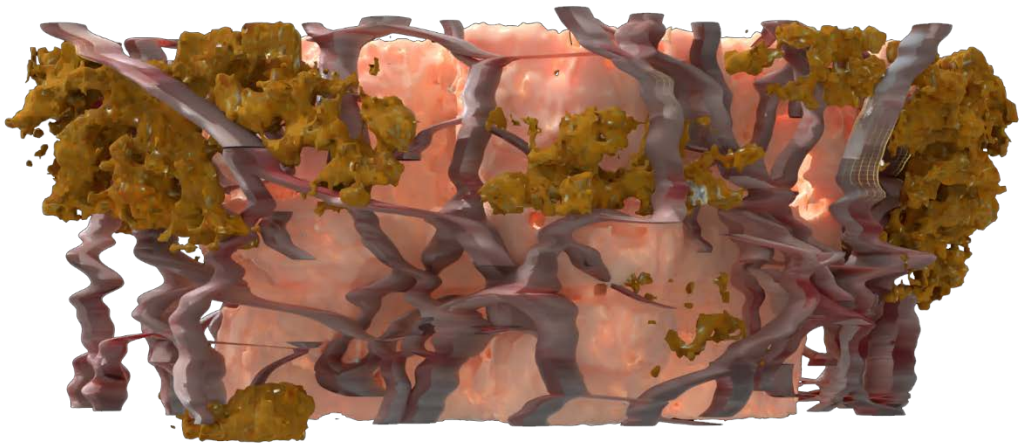

Figure 259. 3D volume rendering of a section of the ear canal (400-micron length), with the epithelium (skin colour), glands (yellow) and the intramural nervous plexus (grey). See LINK1 and LINK2 for videos of the full model.

Table 15. Measurements of corpuscle length. The number of corpuscles measured = 10. Values are in micron.

		SD	MIN	MAX
Mean total corpuscle length	120	26	96	160
Mean length of the visible lamellar part of corpuscles	90	17	72	112

3.5 Facial nerve

In almost all of the animals, we noted the facial nerve as a large nerve bundle running ventral to the ear canal at about 0.5 to 1.5 cm lateral to the TP-complex (See also Macroscopic Morphology). The nerve runs in close association to the ear canal, although separated from it by cartilage and connective tissue (Figure 260). There were no macro- or microscopically visible nerve branches from the facial nerve innervating the region around the ear canal, while there were ventral branches of the facial nerve entering the acoustic fat body.

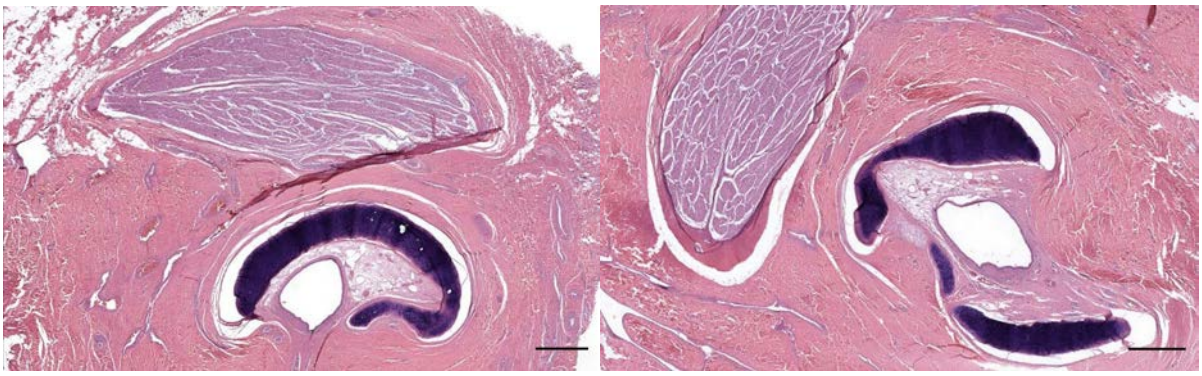

Figure 260. Histological image (HE staining) of the facial nerve near the external ear canal in a striped dolphin (N274/18_R10). The facial nerve runs ventral and in close vicinity of the ear canal, and separated from it by the cartilage of the canal. Scale bar 1 mm

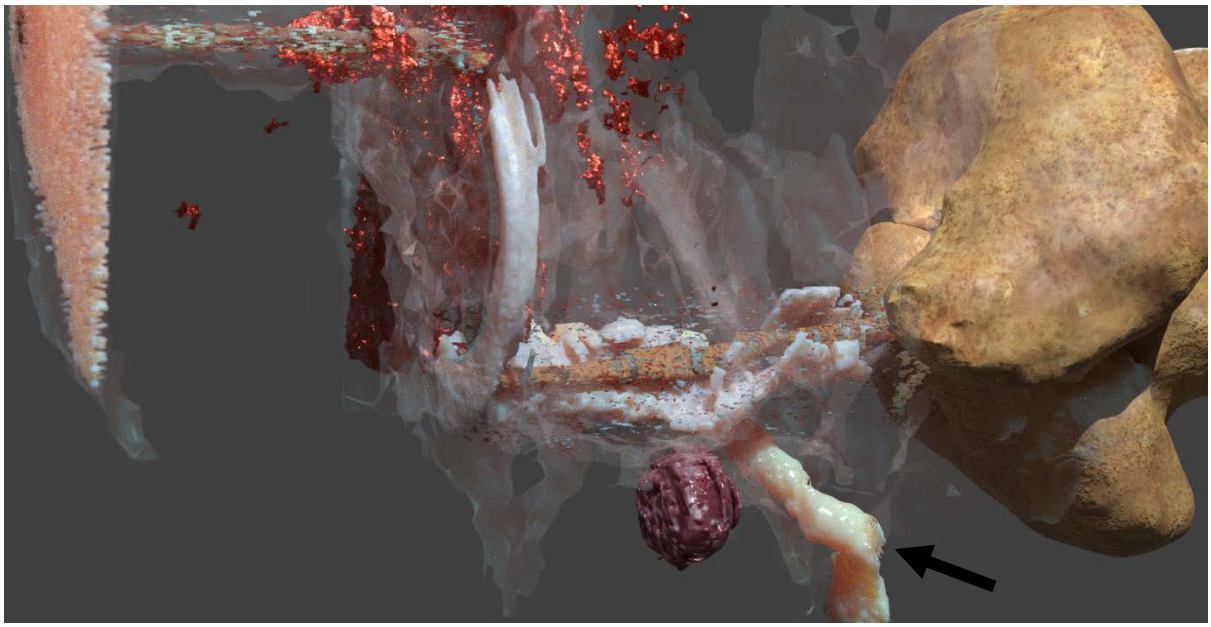

Figure 261. 3D rendering of a caudolateral view of the ear canal and associated tissues in a striped dolphin. Note a part of the facial nerve (arrow) running ventral to the ear canal, close to the TP-complex.

3.6 Terrestrial mammals

The ear canal of all terrestrial Cetartiodactyla showed innervation with nerve fibres running along the canal, small nerve fibres associated with the dermal glands and hair follicles, and intraepithelial free nerve endings (Figure 262), which were the only type of SNF we could discern with certainty. All animals showed immunoreactivity for all four antibodies used, although the nerve fascicles in the deer

labelled relatively weak for anti-NSE. Also, anti-S100 stained other structures such as the alveolar cells of the glands, the endothelium of vascular structures, and possibly Langerhans cells dispersed in the loose connective tissue of the dermis (Figure 263)(De Vreese et al., 2020b).

The ear canal of the **cow** showed innervation with nerve fibres running along the canal, small nerve fibres associated with the glands in the dermis, small nerve fibres and possible hair follicle receptors associated with the hair follicles, and free nerve endings in the epithelium (Figure 264). The nerves showed immunoreactivity for all four antibodies used (Figure 265), and we did not identify any specialized sensory nerve formations. Anti-S100 also stained other structures such as the alveolar cells of the glands, the endothelium of vascular structures, and possibly Langerhans cells dispersed in the loose connective tissue of the dermis.

In the **roe deer**, the nerve fascicles in the dermis labelled positive for all antibodies, but the intensity of the stain with anti-NSE was relatively weak and did not label all individual axons (Figure 266). The findings were very similar as in the other species, and we did not observe any sensory nerve formations associated with the ear canal. There was less intense or unspecific staining of the epithelium, stroma, some glandular structures, vascular structures, and serum for some of the antibodies, comparable to the findings in the other species.

In the **northern giraffe**, there were larger nerve fibres, showing a positive reaction for all antibodies, accompanying the ear canal and smaller nerve fibres in the dermis around the lumen, mostly associated with hair follicles and sebaceous and alveolar glands. We did not note any other nervous structures or sensory nerve formations. S100 stained the arterial wall, and there was also dispersed immunoreactive 'flakey' structures and cells in the stroma, often in focal concentrations (Figure 267).

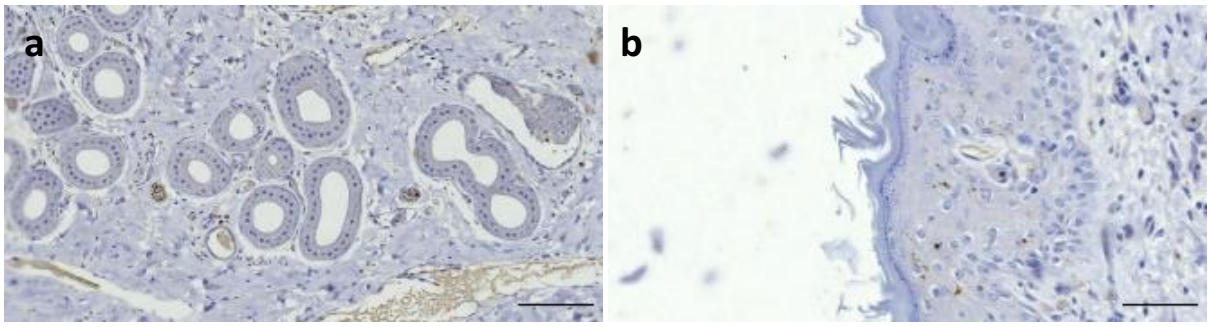

Figure 262. IHC image (anti-PGP9.5, 1:500) of the auricular dermis in a cow. A: Small nerve fibres in spatial association with alveolar glands. There is also unspecific staining of serum in the blood vessels. Scale bar 100 µm. B: intraepithelial nerve fibres. Scale bar 50 µm (De Vreese et al., 2020b).

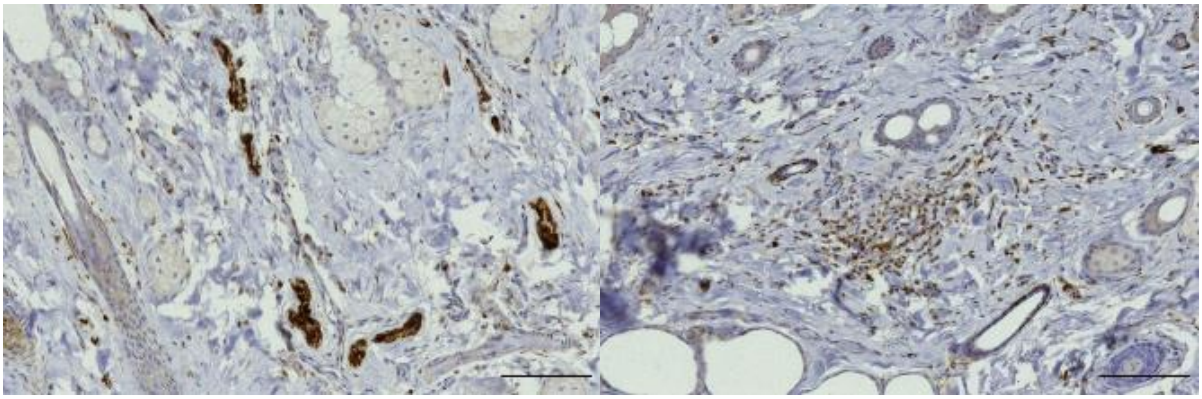

Figure 263. IHC image (anti-S100) of the auricular dermis in a giraffe. A: Immunoreactive small nerve fibres in the vicinity of sebaceous glands, and small positive reaction associated with hair follicles. B: Concentration of immunoreactive cells in the dermis. Scale bars 100 µm (De Vreese et al., 2020b).

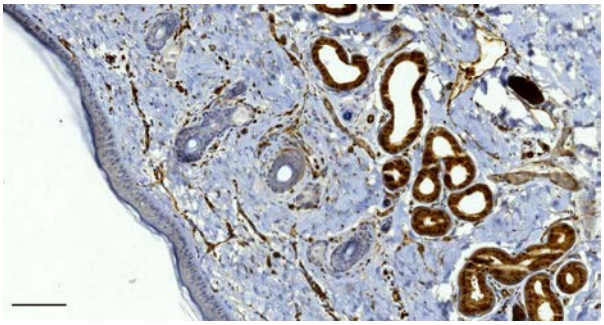

Figure 264. IHC image with anti-S100 (1:500) of the epithel8ium and surrounding tissue of the ear canal of a cow. Note the immunoreactivity of glandular epithelium, vascular epithelium, and cells and small nerve fibres in the dermis and around hair follicles. Scale bar 100 µm

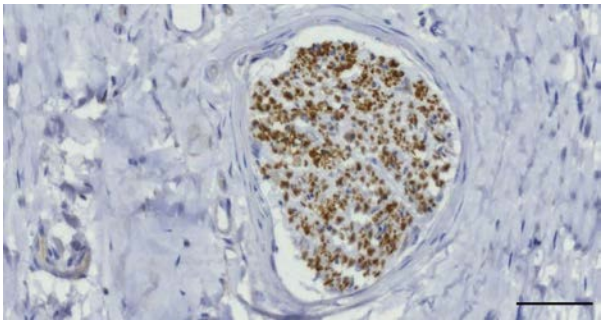

Figure 265. IHC image with anti-PGP 9.5 (1:500) of a nerve fibre in the subepithelial connective tissue around the ear canal. Scale bar 50 µm

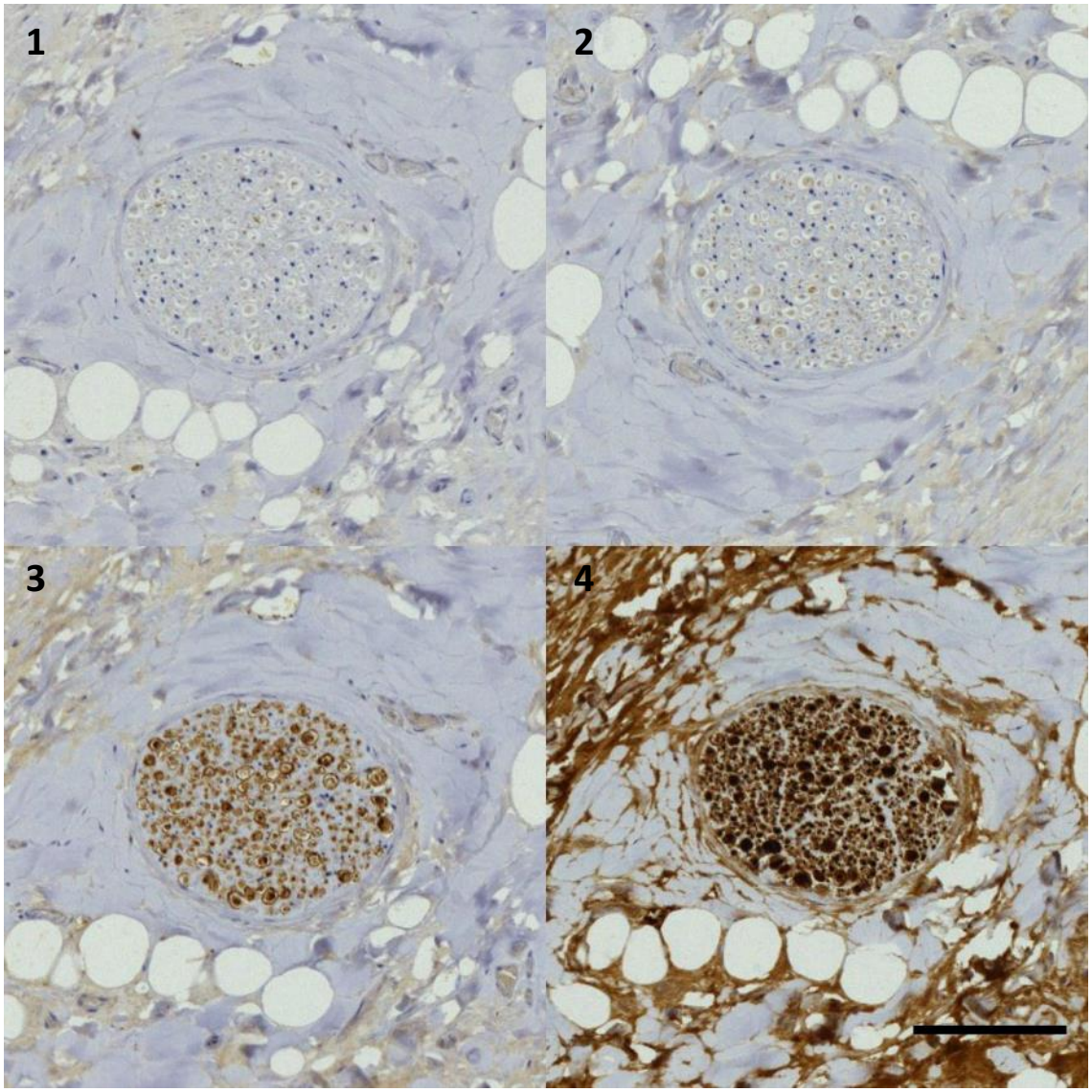

Figure 266. Montage image of transverse sections through a nerve bundle in the dermis of the ear canal of a roe deer showing weak immunoreactivity to anti-NSE (1), intermediate reactivity to anti-PGP 9.5 (2), and strong positive reaction to anti-S100 (3) and anti-NF (4). Scale: 100 µm.

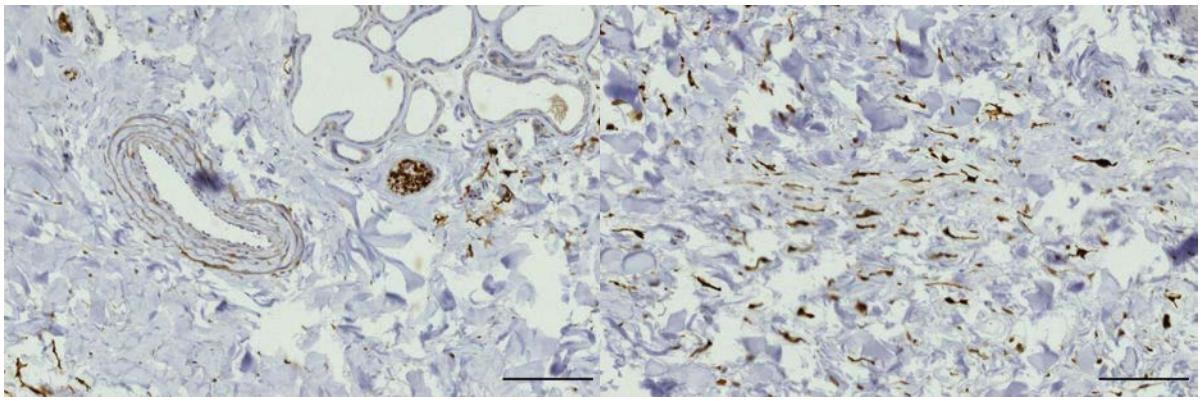

Figure 267. IHC image with anti-S100. Left: IR in the arterial wall, a small nerve fibre, and possible free nerve fibres in association with the alveolar glands. Right: 'flakey' positive structures in the stroma. Scale bar 100 µm.

3.7 Western blot

Western blot analysis performed on the protein extracts from bottlenose dolphin, striped dolphin and bovine tissues recognized all the antigens looked for. The expression of the PGP9.5 antigen was visible at around 25 kDa (Figure 268a) and of the NF antigen was evident at 150-160 kDa (Figure 268b). Anti-NSE and anti-S-100 antibody reacted to the antigens showing a signal corresponding to proteins with a molecular weight of 46 kDa (Figure 268c) and around 10 kDa (Figure 268d), respectively (De Vreese et al., 2020b).

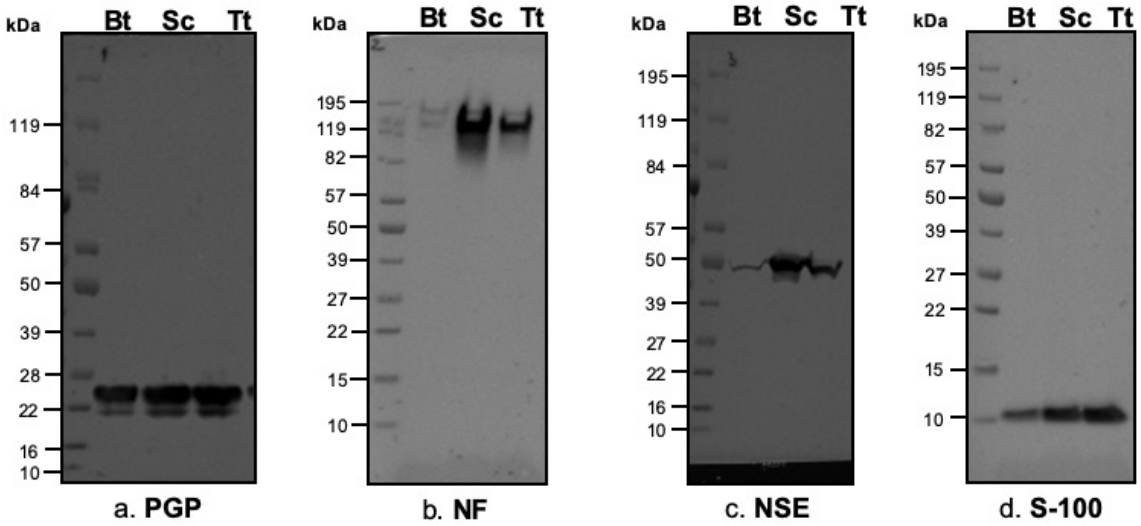

Figure 268. Western blot analyses. a) Polyclonal rabbit anti-bovine PGP antibody (code Z5116, Dako) at a dilution of 1:500.; b) Monoclonal mouse anti-human NF (Clone 2F11) antibody (code M0762, Dako) at a dilution of 1:500; c) Monoclonal mouse anti-human NSE antibody (Clone BBS/NC/VI-H14) (code M0873, Dako) at a dilution of 1:500; d) Polyclonal rabbit anti-bovine S-100 (code Z0311, Dako) at a dilution of 1:1000. *Bt: Bos taurus, Sc: Stenella coeruleoalba, Tt: Tursiops truncatus; kDa: kilodalton. (De Vreese et al., 2020b).

4 Pathology

4.1 Overview

There were various pathologies associated with the external ear canal in the toothed whales that were subject of this study. Here is presented an overview of the number of cases, together with descriptions of the most common findings. For details of individual cases, see the Annex: Anatomopathological findings and case reports.

For striped dolphin, more than a third presented some kind of pathological changes in or around the external ear canal, although most of these were not directly associated with the ear canal. There was several cases with a haemorrhage around the external ear canal, four individuals with an otitis externa, several cases with panniculitis and or dermatitis, many cases with muscle-related pathologies, and individual cases with indications of a cholesteatoma, epithelial cysts, and other.

Interestingly, there was no pathology directly associated with the external ear canal in any of the ten harbour porpoises that were subjected to the histological evaluation. The only abnormality involved a single specimen with unilateral congestion with contracted arteries, focal acute muscle degeneration, perivascular presence (cuffing) of lymphocytic cells and macrophages and oedema between the ear canal and the cartilage in the deepest parts of the ear canal (Figure 269, Figure 270).

Table 16. Overview of the pathology findings and number of cases.

Pathology	Species	Positive	Total animals	Percentage
Otitis externa	Tt	1	2	50 %
	Sc	3	21	15 %
	Gm	1	1	100 %
	Zc	1	2	50 %
	Pp	0	10	0.00%
	TOTAL	**6**	**36**	**16.67%**
Haemorrhage	Sc	3	21	14.29%
RBC in EAP	Sc	2	21	9.52%
	Pp	1	10	10.00%
Panniculitis/dermatitis	Sc	3	21	14.29%
	Gm	1	1	100.00%
Vasculitis	Sc	1	21	4.76%
Muscle atrophy / degeneration	Sc	8	21	38.10%
	Tt	1	2	50.00%
	Pp	1	10	10.00%
Peripheral nerve pathology	Sc	3	21	14.29%
Epithelial cyst / Cholesteatoma / Keratoma	Sc	2	21	9.52%

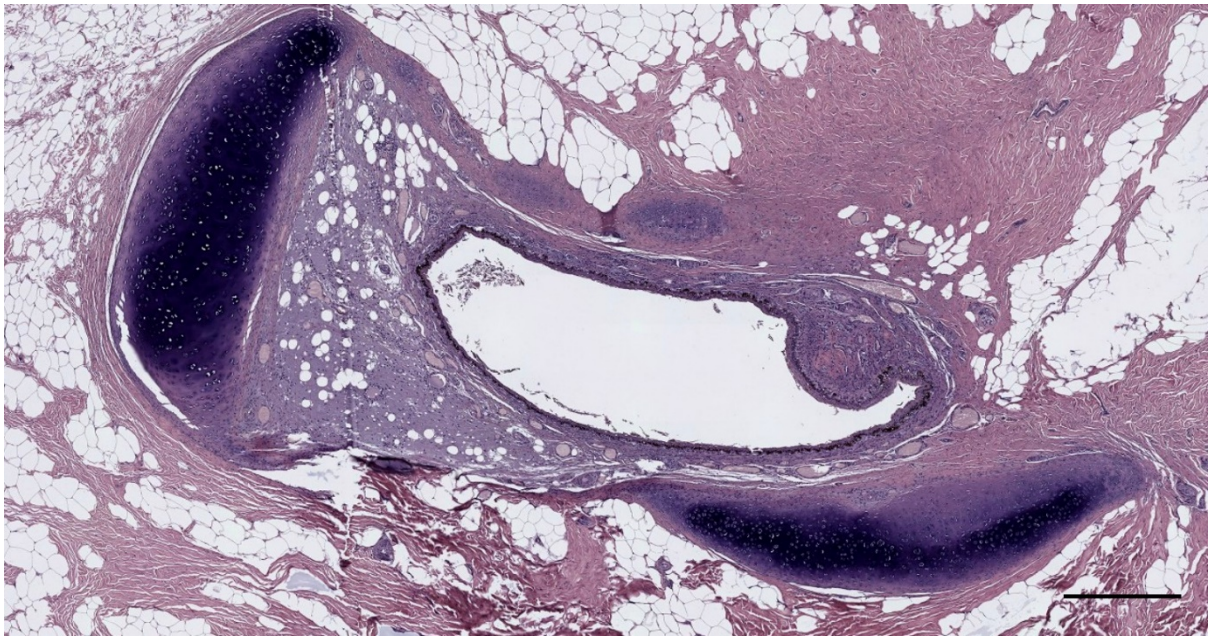

Figure 269. Histological image (HE staining) of a transverse section through the external ear canal of a harbour porpoise, about 5 cm beneath the skin (UT1718_L1402). Scale bar 500 µm

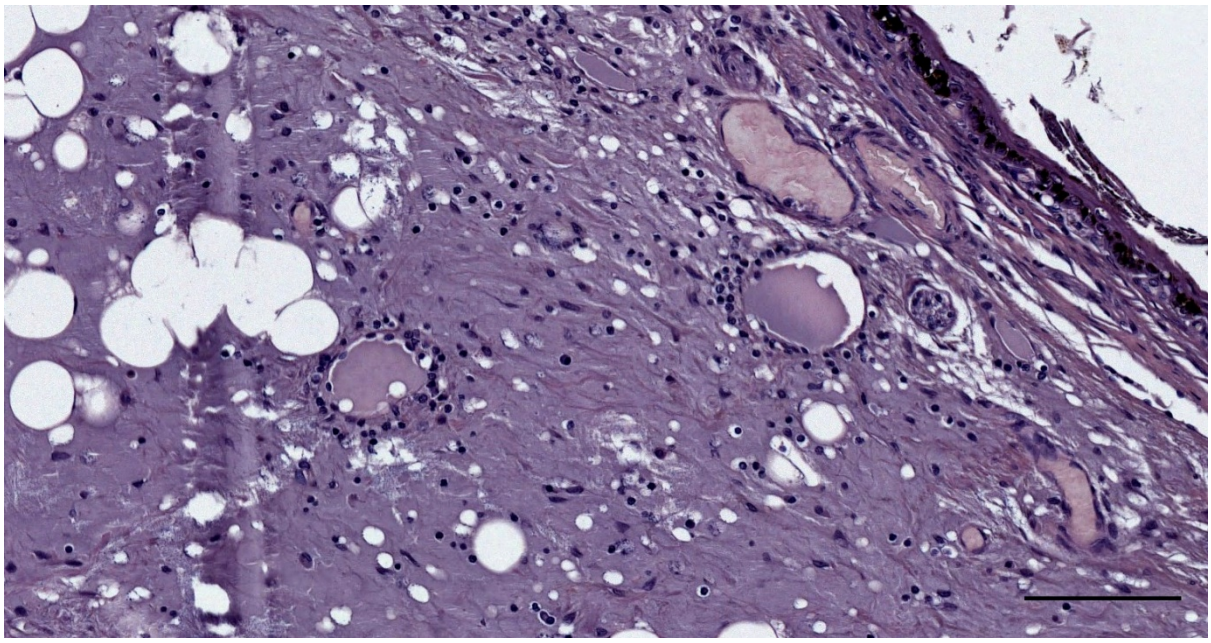

Figure 270. Detail of Figure 269. Perivascular presence (cuffing) of lymphocytic cells and macrophages; Oedema with protein leakage associated with an inflammatory process, with splitting of collagen fibres. (UT1718_L1403). Scale 100 µm

4.2 Haemorrhage

A single striped dolphin (ID292/18) presented a recent haemorrhage surrounding the ear canal in the blubber layer. It included a generalized inflammation of the adipoconnective tissue surrounding the ear canal in the superficial sections through the blubber with the presence of activated macrophages, a marginalization of inflammatory cells, and a large amount of oedema (Figure 271, Figure 272). The appearance was indicative of a disorder associated with blood cells or endothelial cells, although the haemorrhage was more likely to have been associated with a CeMV infection (with mononuclear encephalitis) and a possible blunt injury event.

In the skin and subcutaneous tissue, there was the presence of an intense inflammatory infiltrate mainly consisting of neutrophils and, to a lesser extent, macrophages, located in the subcutaneous tissue and the underlying muscle. The inflammatory cells were grouped into large aggregates (abscesses) and present in the connective tissue septa. In the subcutaneous adipose tissue, there were numerous macrophages with enlarged cytoplasm containing abundant yellowish-brown granular pigment (lipofuscin).

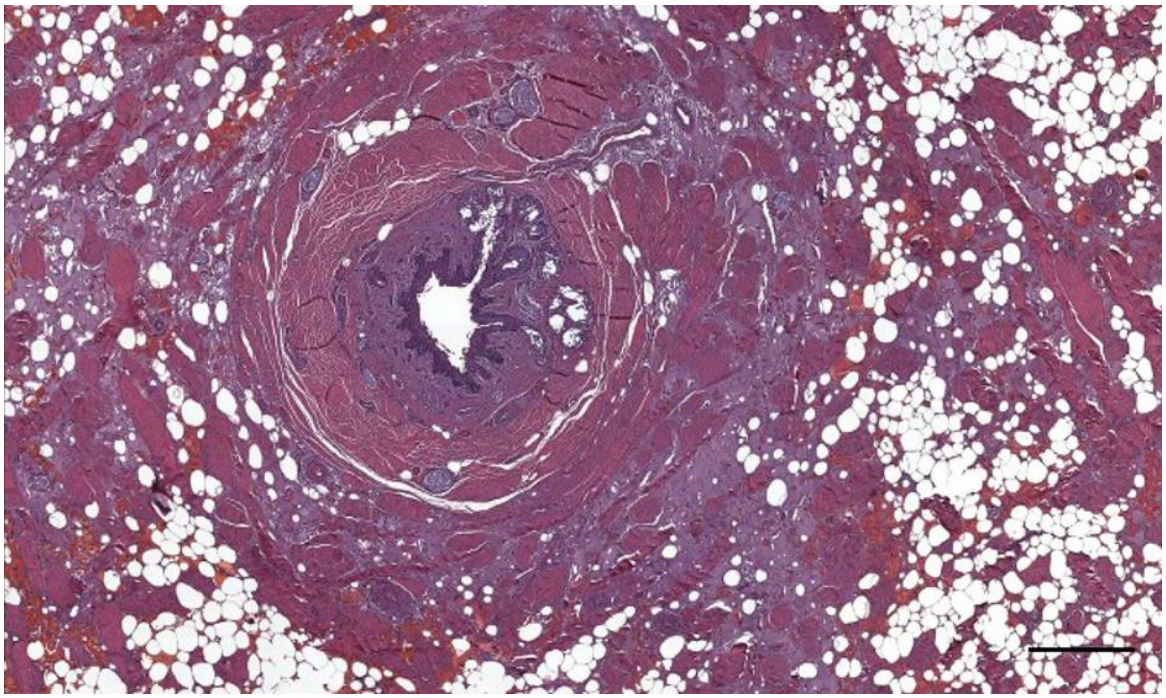

Figure 271. Histological transverse section (HE staining) through the ear canal of a striped dolphin (292/18_L2) at about 1 cm beneath the skin. The image shows the ear canal with glands and haemorrhage in the surrounding adipoconnective tissue. Scale bar 0.5 mm

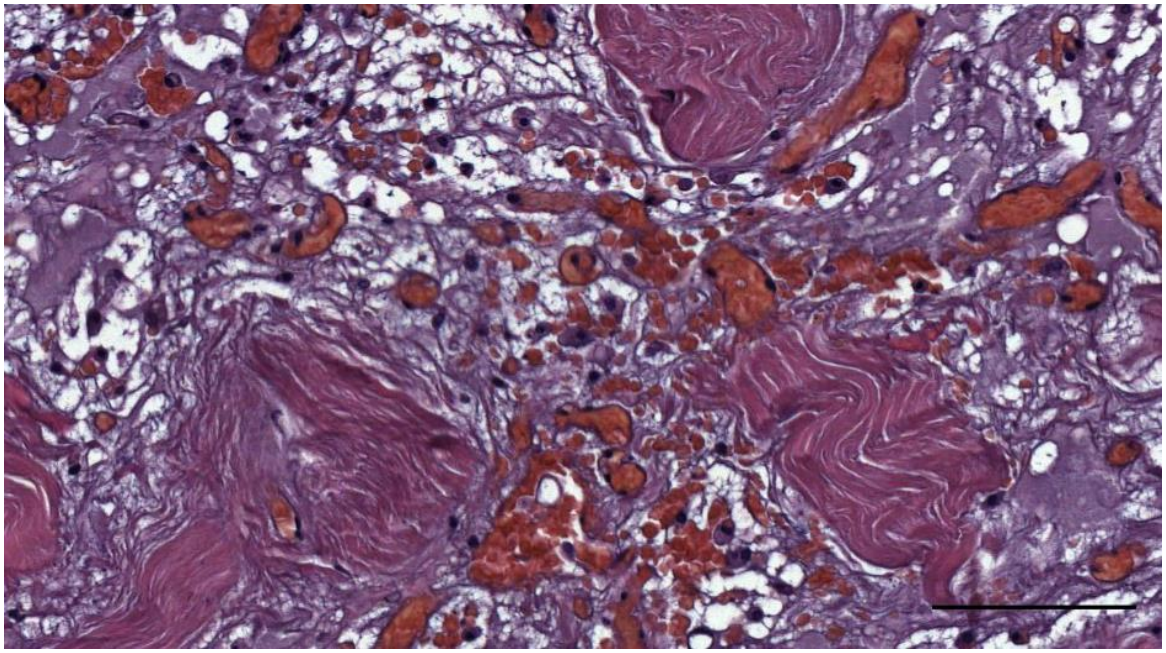

Figure 272. Histological detail image (HE staining) of inflammatory cells and haemorrhage in the adipoconnective tissue. Scale bar 100 µm

4.3 Otitis externa

Otitis externa was found in three striped dolphins, a bottlenose dolphin, a Cuvier´s beaked whale and the long-finned pilot whale. In some other cases, it was not always clear if there was inflammation, a simple activation of the diffuse ECALT, or the presence of the non-activated resident ECALT but in higher proportions than in other animals.

All cases presented a chronic inflammation, which was characterized by an activation of the resident ECALT with the presence of a multifocal mixed cell inflammatory reaction in the subepithelial tissue, often in the superficial half of the canal from the skin down to the medial end of the ventral curvature where the canal turns horizontal again (Figure 273, Figure 274). In most cases, the inflammation was bilateral, in few cases unilateral, and in others not known because only one of the two ear canals was available or analysed histologically. In three striped dolphins and the long-finned pilot whale, the otitis externa was purulent with the presence of neutrophils, macrophages, and lymphocytes in the lumen of the ear canal (Figure 275, Figure 276). Concurrent findings included (a) epithelial changes with hyperplasia, apoptotic changes, and ulceration with leakage of melanin the subepithelial tissue; (b) adenitis; (c) dermatitis and/or panniculitis. The aetiology could have been associated with either a reaction to an external influence with skin reaction (e.g. parasites: *Penella* around the ear opening), or an infectious agent with epitheliotrope character (e.g. Herpes, or a secondary infection associated with Morbillivirus) and secondary infection with bacteria in the ear canal and glands.

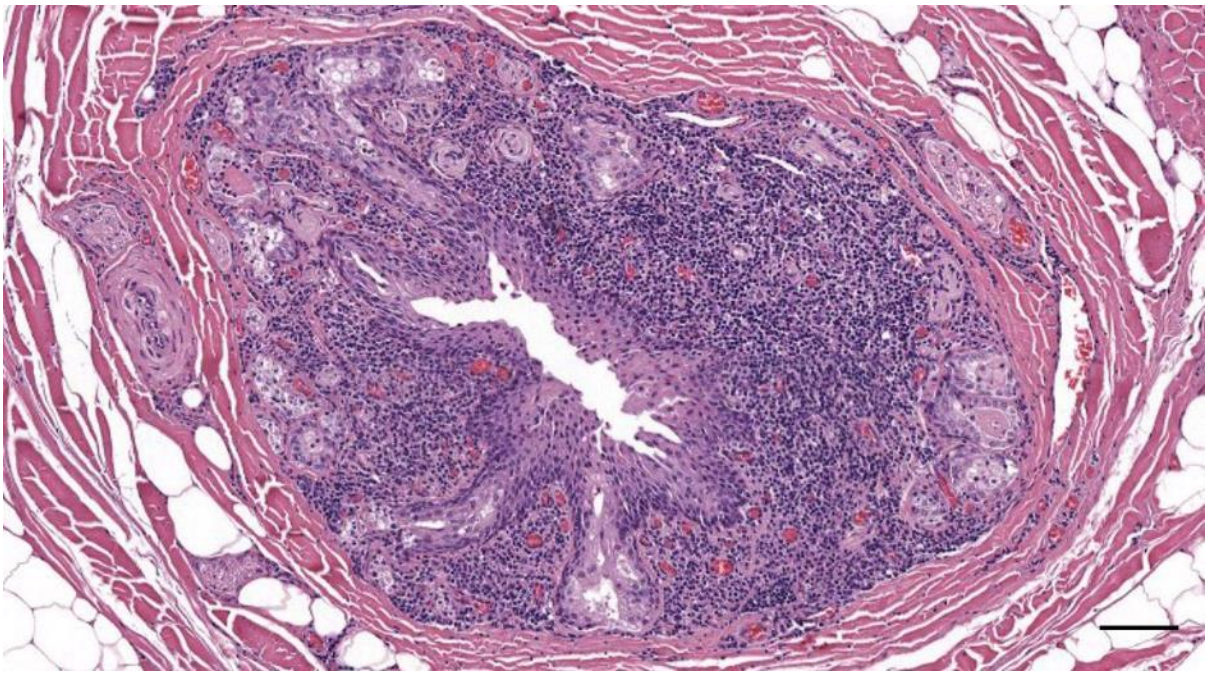

Figure 273. Histological cross-section (HE staining) of the left ear canal in a striped dolphin (293/18_L3). There is an inflammation of the ear canal and glands, with the abundant presence of mononuclear cells in the subepithelial tissue. Scale bar 100 µm

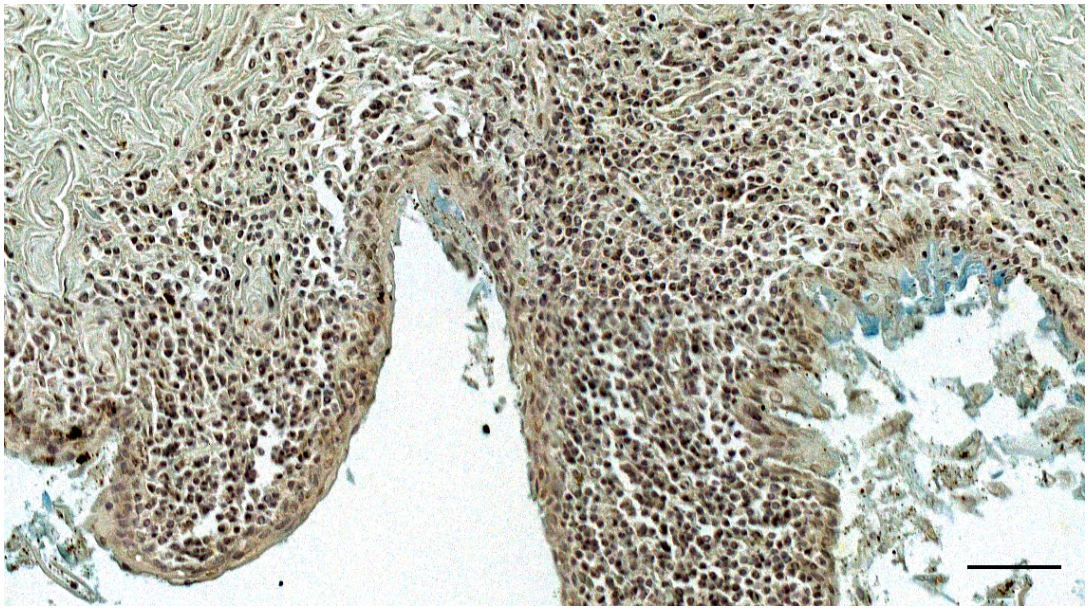

Figure 274. Histological cross-section (Alcian blue staining) of the right ear canal of a bottlenose dolphin, at about 2 cm beneath the skin (ID444_R5). Note the subepithelial abundant presence of mononuclear cells, and the abrasive epithelium of the ear canal, showing a blue staining. Scale bar 50 µm

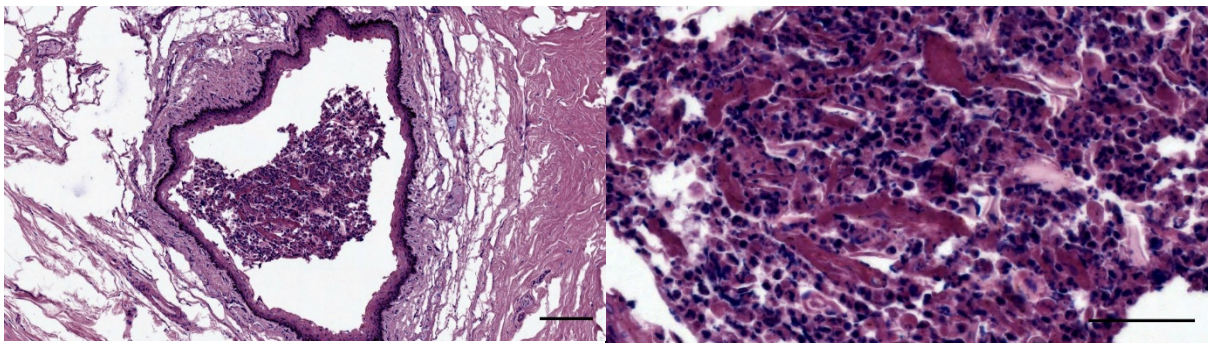

Figure 275. Histological images (Gram staining) of a transverse section through the ear canal of a striped dolphin (ID2926) with the presence of inflammatory cells such as macrophages, neutrophils and also desquamated epithelial cells within the lumen of the canal. Scale bars: left 100 µm, right 50 µm

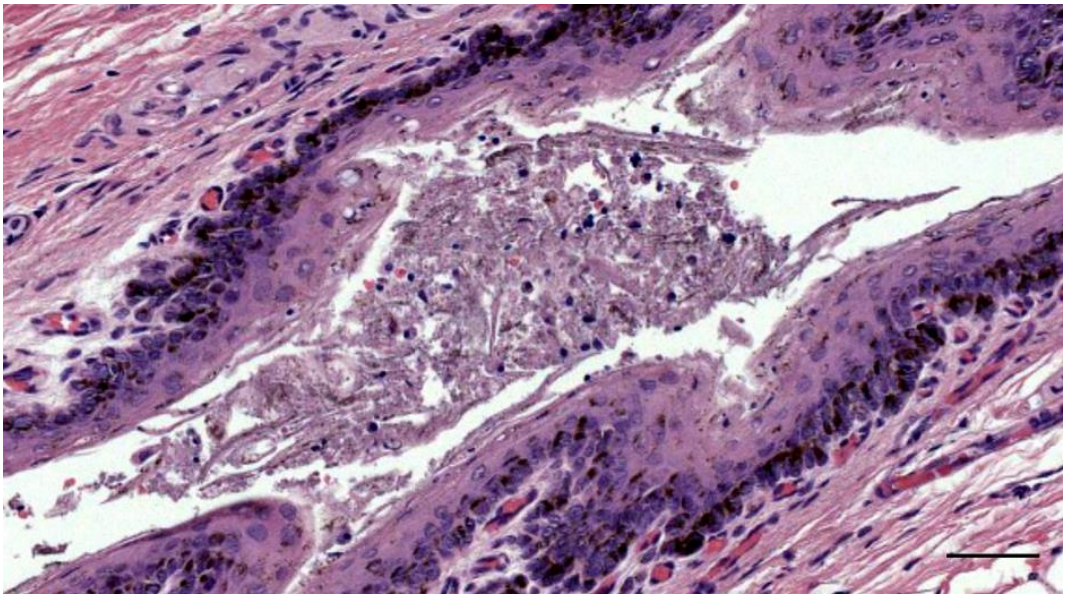

Figure 276. Histological detail (HE staining) of the ear canal content in a striped dolphin (488/17_L8) Purulent otitis: Inflammatory cells (lymphocytes, neutrophils), and cells with pyknotic nuclei (possible glandular cells), together with epithelial sloughs in the ear canal lumen. Scale bar 50 µm

4.4 Dermatitis/Panniculitis

There were six cases of striped dolphin with a chronic multifocal active (pyo-)granulomatous (mixed cell) panniculitis (Figure 277). In two cases with multifocal microgranulomas containing macrophages associated with adipocytes and macroscopic serous atrophy of the fat (Figure 278). Two other cases presented a mild mixed inflammatory reaction in the dermal papillae associated with the external ear opening and the skin (ID145/18; ID620/17)

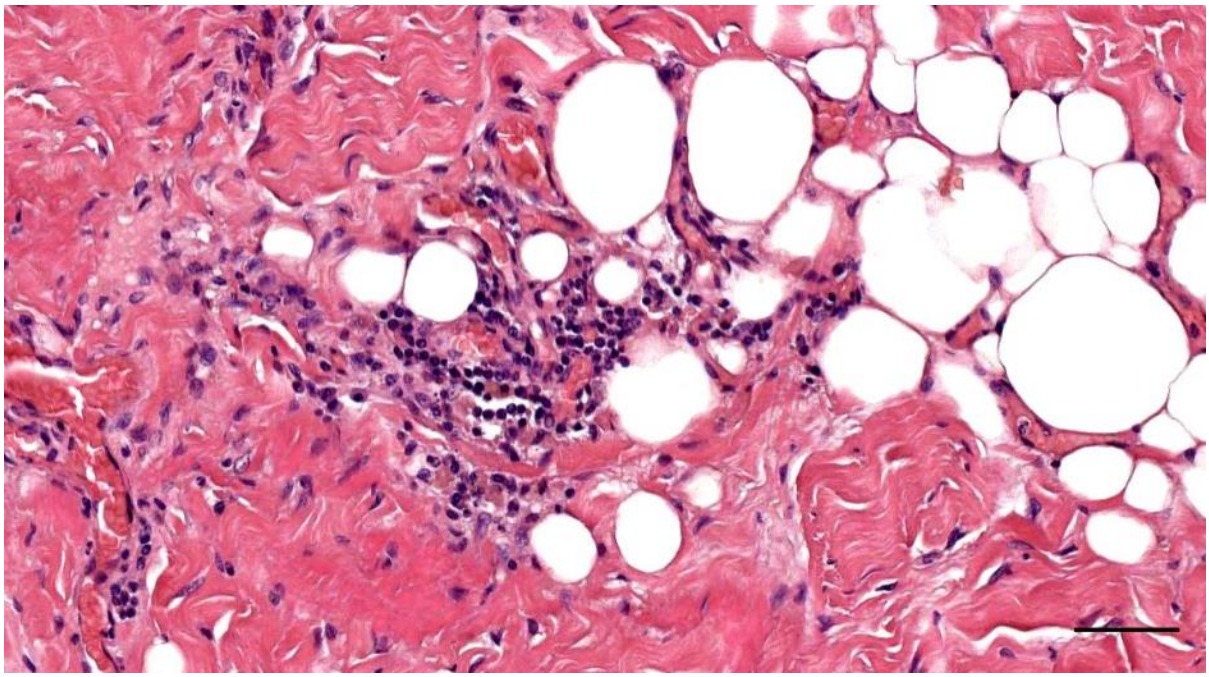

Figure 277. Histological detail (HE staining) of the chronic active mixed panniculitis (274/18_L5). Scale bar 50 µm

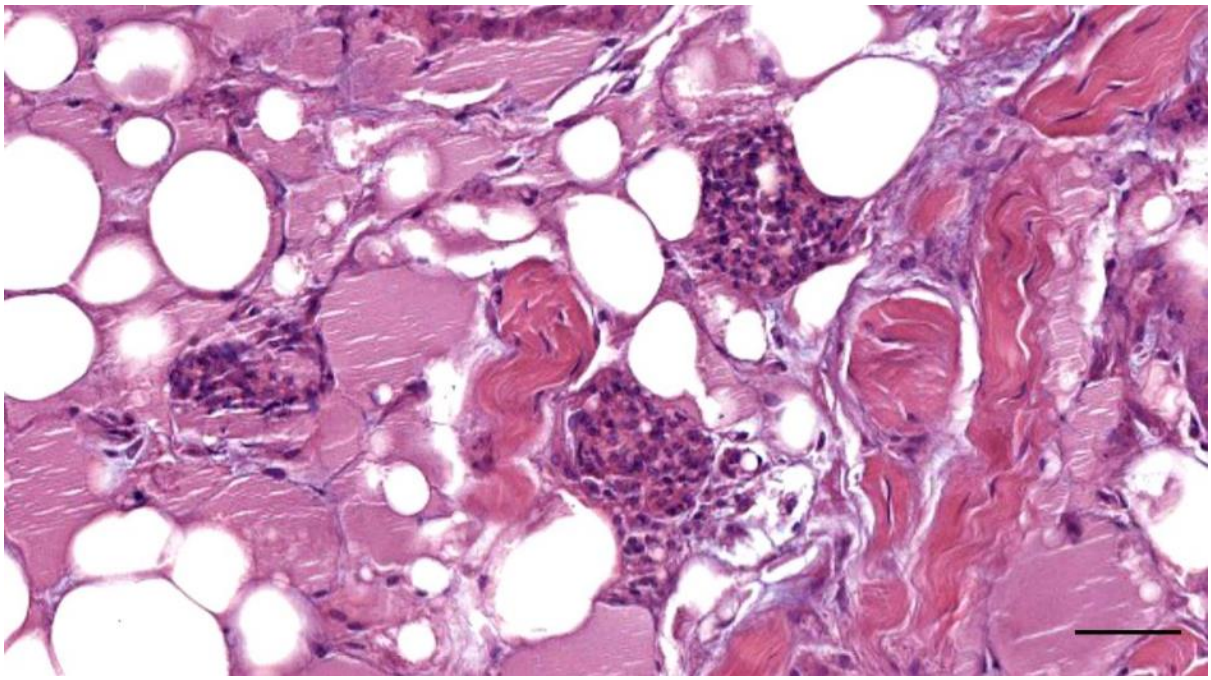

Figure 278. Histological image (HE staining) of microgranulomas in the adipoconnective tissue around the ear canal in a striped dolphin (ID5386). Scale bar 50 µm

4.5 Muscle pathology

Muscle degeneration was a common finding, as it occurred in about one-third of the striped dolphin specimens, and interestingly only in a single harbour porpoise. There was mild muscle tissue damage with fractured muscle fibres and necrotic degeneration with the infiltration of inflammatory cells (Figure 279, Figure 280), sometimes with signs of regeneration (Figure 280).

A striped dolphin and a cuvier's beaked whale presented a mild and focal muscle atrophy (Figure 281, Figure 282).

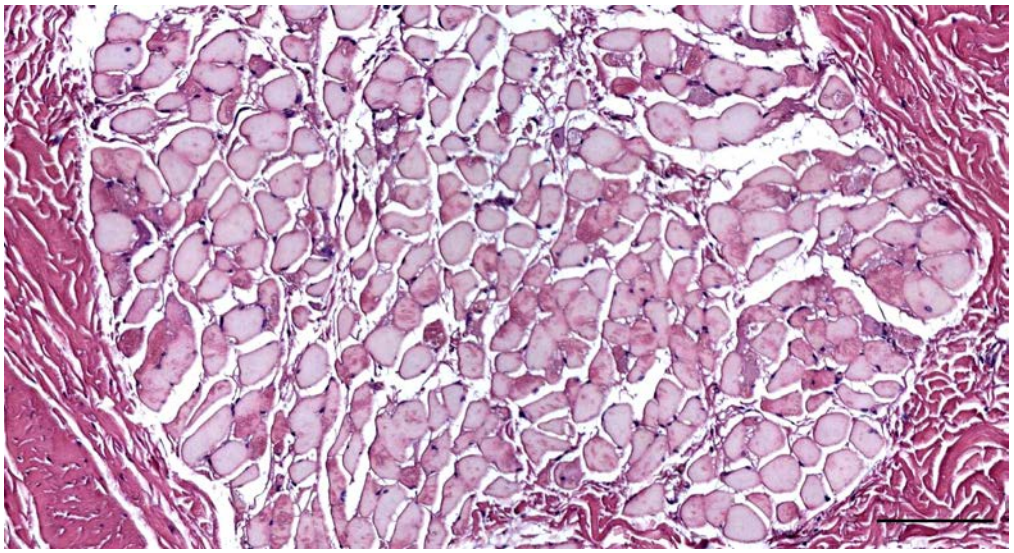

Figure 279. Histological image (HE staining) of muscle degeneration and necrosis with infiltration of inflammatory cells. Scale bar 100 µm.

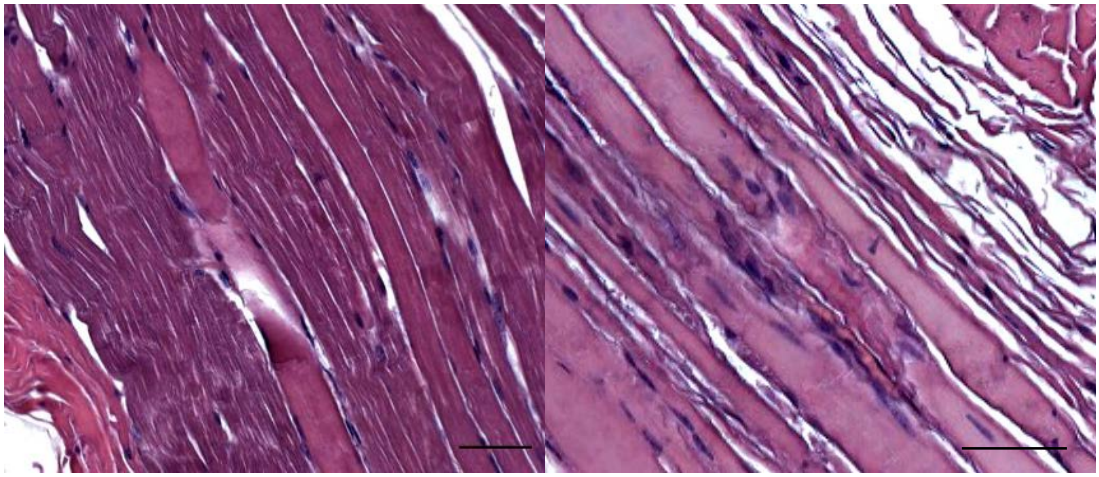

Figure 280. Histological images (HE staining) of muscle degeneration and rupture of myofibrils (left), and muscle regeneration (right). Scale bars 50 µm.

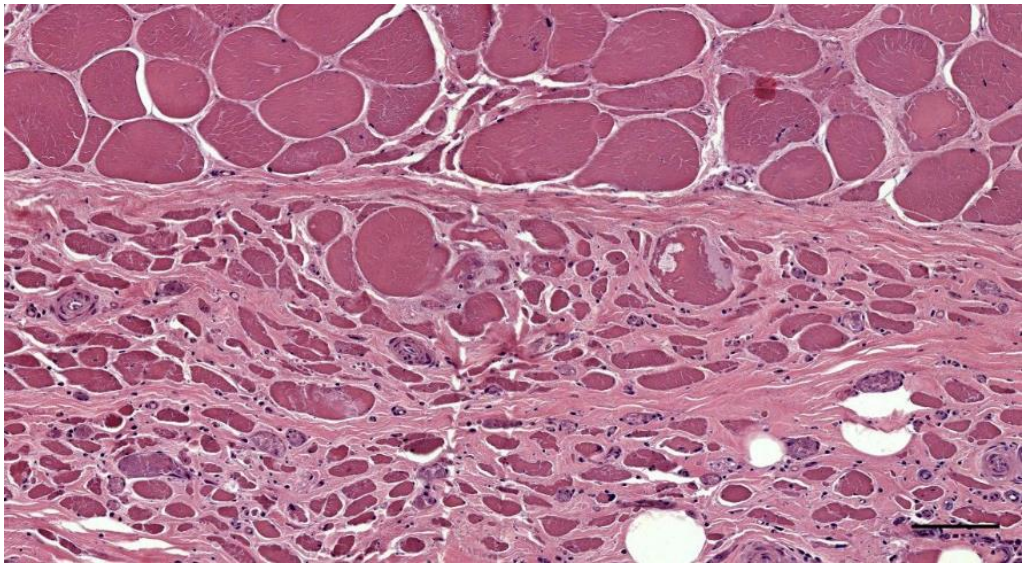

Figure 281. Muscle atrophy (HE-stained section) in the auricular muscles of a Cuvier´s beaked whale. Scale bar 100 µm

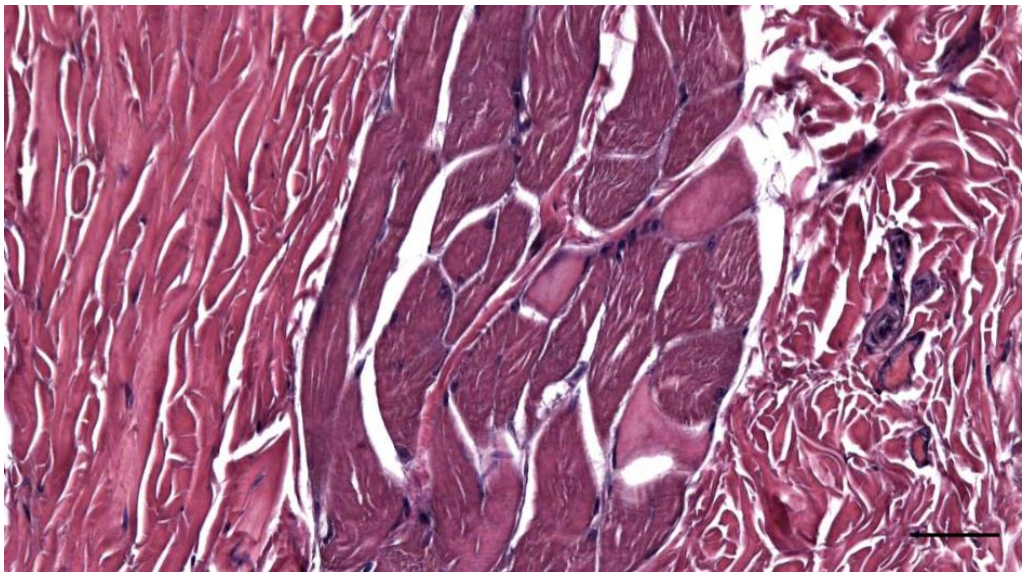

Figure 282. Histological detail image (HE staining)(Striped dolphin ID145/18) of an auricular muscle with signs of mild atrophy, and the presence of nuclear clumps (arrow). Scale bar 50 µm

4.6 Adipose tissue – effects of starvation

In various animals, we noted the effect of starvation and a bad body condition code based on the variation in size ad morphology of the fat cells surrounding the ear canal. Below are two examples.

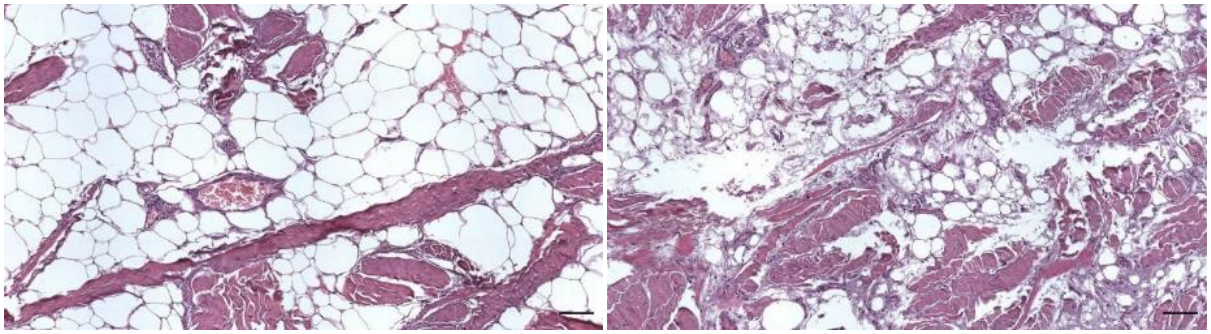

Figure 283. Comparison of two areas of the adipoconnective tissue in the same histological section (HE) around the ear canal in a striped dolphin (ID620/17-L6) Left: seemingly healthy adipoconnective tissue. Right: effects of starvation, with shrinkage of the fat cells and a decrease of the ratio fat/connective tissue. There is a marginalisation of inflammatory cells, with scant macrophages with lipid droplets in the cytoplasm. Scale bars 100 µm.

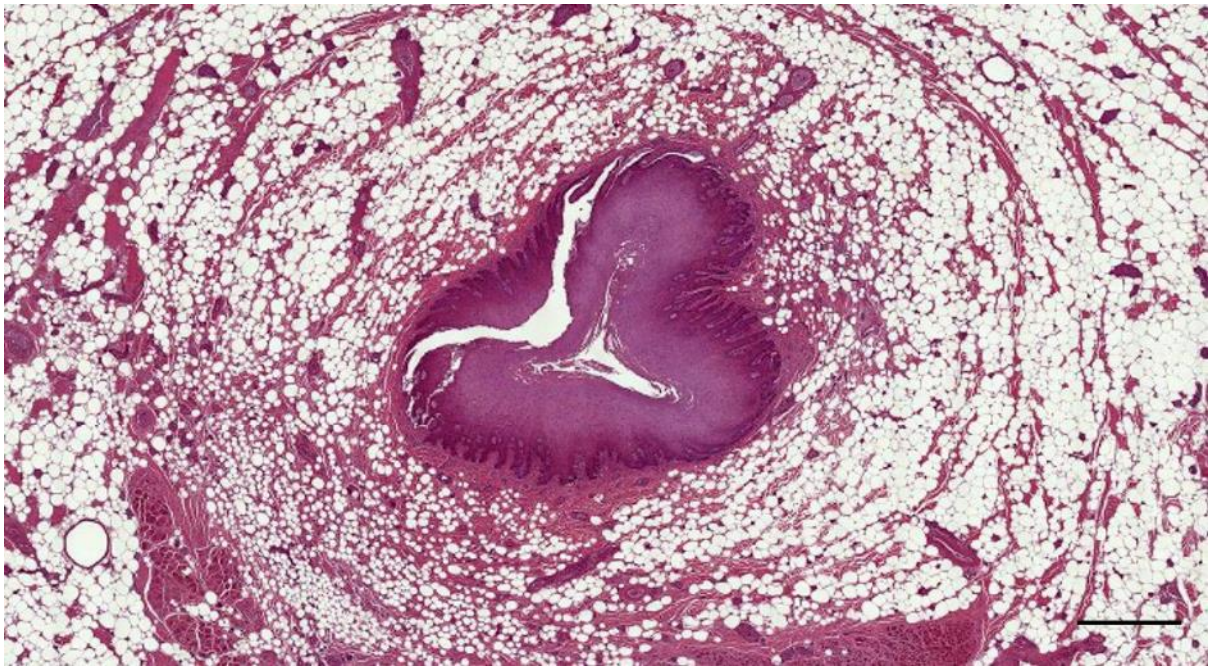

Figure 284. Histological transverse section (HE staining) through the external ear canal of a Cuvier´s beaked whale about 2 cm beneath the skin (ID177/19_R04_03). Note the variation in size of the fat cells. Scale bar 1 mm

4.7 Epithelial cyst

A single striped dolphin (ID44/17) presented an epithelial cyst in a deep section with cartilage (Figure 139). It was presented as an unusual round structure next to the ear canal, and with a diameter 0.4-0.5 mm, similar size as the ear canal. It contained desquamated and mostly nucleated epithelial cells and necrotized keratin as luminal content, and was lined by a very thin stratified (2-3 layers) squamosal epithelium. It was probably a benign malformation as there are no signs of any recent or old inflammatory process. These findings were similar to the case of another striped dolphin that presented a likely glandular structure with mineralized content, see Figure 140.

4.8 Cholesteatoma

In a striped dolphin ear canal (ID362/18), close to the tympanic conus, there was a structure, round in transverse section with a diameter of 0.23*0.29 mm, which was lined by a pigmented stratified squamous epithelium, similar to the ear canal, but with more intense in pigmentation (Figure 285). It contained a content of debris with cholesterol clefts which, and as such, showed similarities to a cholesteatoma, which is a well-delimited cystic nidus of abnormal growth of keratinized squamous epithelium (Kuo et al., 2015). This showed similarity with the content of the pilot whale ear canal (Figure 286). There was also a large number of lymphocytic cells situated between the ear canal and cartilage, closely associated with the round structure, as visible in a deep section. In this location, there were focal concentrations of inflammatory cells in the connective tissue at the location of the possible cholesteatoma. There were also inflammatory cells in a perivascular distribution in the connective tissue in the vicinity of the ear canal, indicative of an inflammatory reaction and marginalization of inflammatory cells.

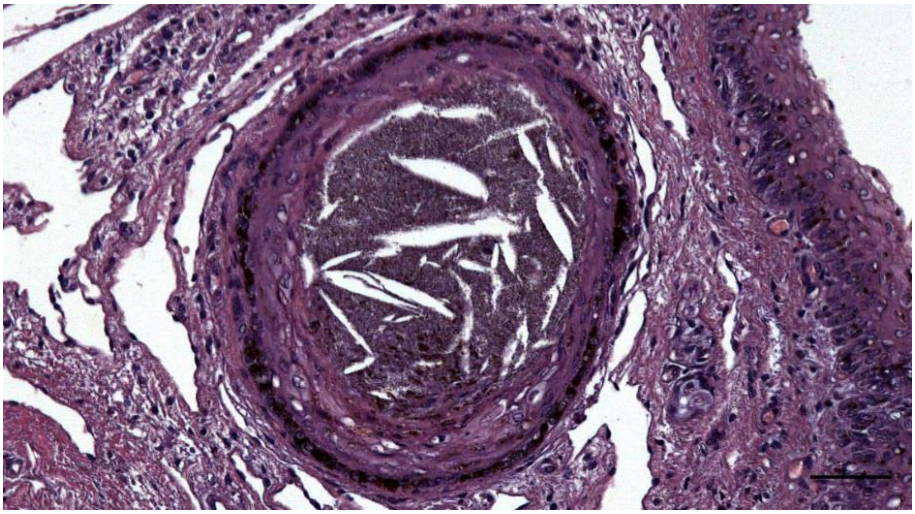

Figure 285. Histological image (HE staining) of a round structure next to ear canal (362/18_L13) (Morphological similarity with the ear canal content in a pilot whale: Figure 286). Scale bar 50 µm

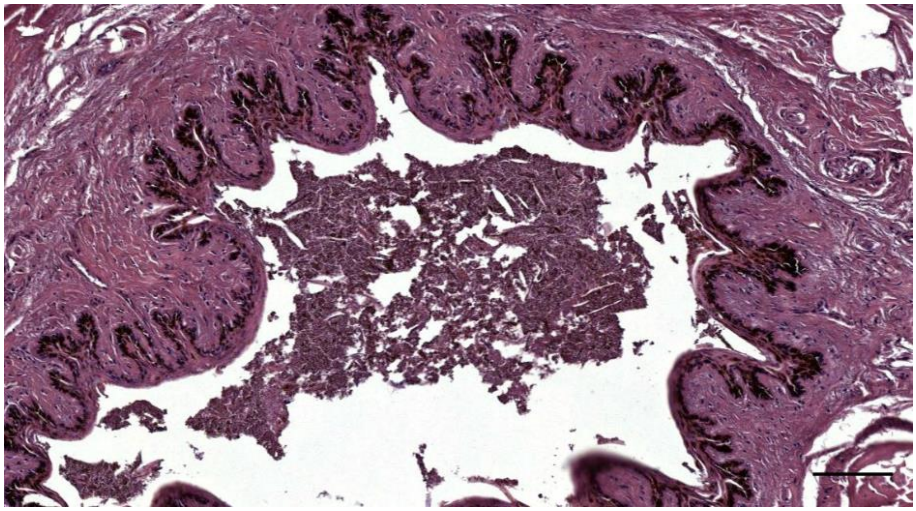

Figure 286. Histological image of the ear canal of a long-finned pilot whale (441_R17). Note the unidentified content with possible cholesterol clefts. The appearance of the content is very similar to the structure in Figure 285 (striped dolphin, Figure 285, 362/18_L13). Scale bar 100 µm.

5 Tissues of secondary interest: innervation

5.1 Density and distribution of lamellar corpuscles in other tissues

The immunoreactivity of nervous tissue (nerve fibres and lamellar corpuscles) in the ear canal was compared with the morphological characteristics of the same tissue in serial sections stained with HE. Looking at both standard histological slides and IHC stained slides of the same sample, the observer (SDV) could apprehend to discern between lamellar corpuscles and small nerve fibres in HE stained sections of all the tissues sampled. Then, a subjective assessment of the density and distribution of lamellar corpuscles in a variety of tissues was performed using light microscopy and was graded semiquantitatively as: − = no lamellar corpuscles/nerve fibres observed; + = few lamellar corpuscles/nerve fibres observed; ++ = a moderate number of lamellar corpuscles/nerve fibres observed; +++ = a large number of lamellar corpuscles/nerve fibres observed; The relative density of corpuscles is summarized in Table 17.

Table 17. The relative density of lamellar corpuscles and nerve fibres in the investigated tissues striped dolphin (Sc), bottlenose dolphin (Tt), Cuvier's beaked whale (Zc). Na = not applicable; blank = not investigated; "?" means that the lamellar corpuscles were possibly present, but could not be identified with certainty.

Tissue	**Lamellar corpuscles**				**Nerve fibres**			
	Sc	**Tt**	**Zc**	**Gm**	**Sc**	**Tt**	**Zc**	**Gm**
External ear canal	++++	++++	++	+(?)	+++	++++	+++	++
External mandibular fat body	-		?	-	+		-	+
Internal mandibular fat body	-				+			
Pterygoid sinus wall	-/+		?	-	++		+	+
Peribullar sinus wall	-				++			
Blowhole anterior lip	+				+			
Blowhole posterior lip	+				+			
Blowhole commissure	+				+			
Circumocular region	+				+			
Iridocorneal angle	++			+	+			+
Eyelid	++				++			
Eye commissures	+		+	+	+		+	+
Rostrum tip	++			+	+++			+
Vibrissal crypt	+	++			+++	+++		
Mouth commissure	++			+(?)	+			+
Throat fold (*Z. cavirostris only*)	na	na	+		na	na	++	
Urogenital fold	?		?		++		+	
Mammary gland			?				+	
Anus			-				+	
Penis	+++				+++			
Pectoral fin dorsal	+		-		+			+
Pectoral fin ventral	- (?)		-		+			+
Fluke dorsal	-				+			
Fluke ventral	-		?		+		+	
Dorsal fin	-		?		+		+	
Skin thorax (lat)				-				-
Skin level of dorsal fin (lat)				-				-
Skin abdomen (lat)				-				-
Skin peduncle (lat)				-(?)				-

The external ear canal contained the highest amount of sections through corpuscles compared to other tissues. We derived tissues of primary and secondary interest for further investigation on the morphology and location of the lamellar corpuscles. Although the penis and the rostrum tip were well innervated and presented a large number of lamellar corpuscles, these were not subjected to further investigation when taking into regard our objectives of gaining insight in the functionality of the ear canal, as these structures are sensitive for mechanosensation in the context of foraging and reproduction. Since the function of the external ear canal and the vibrissae is still subject of discussion, we chose to focus on these tissues. However, none of the tissues, besides the external ear canal, are discussed in great detail in this dissertation, while it instead provides opportunities for further investigation into the sensorial capacities of the peripheral nervous system in toothed whales.

5.2 Corpus cavernosum / fibro-venous plexus of the middle ear

The corpus cavernosum contained very scarce lamellar corpuscles or free nerve endings, and no other notable SNF.

5.3 Mandibular fat bodies

The internal mandibular fat body was poorly innervated, although it did show the presence of medium to large nerve fibres such as the inferior alveolar nerve (Figure 288). Sections throughout the fat body did not show any sensory nerve formations. The fat body was adjacent to the muscle tissue of the medial pterygoid muscle (Figure 288) which consisted of muscle fibre packets embedded in adipose tissue, which were innervated by small nerve fibres that could also be seen at the border with and inside the internal mandibular fat body.

There were very scant nervous tissue structures in the external mandibular fat body, although there were indications of lamellar corpuscles in the sparse, but well-vascularized, connective tissue (Figure 289).

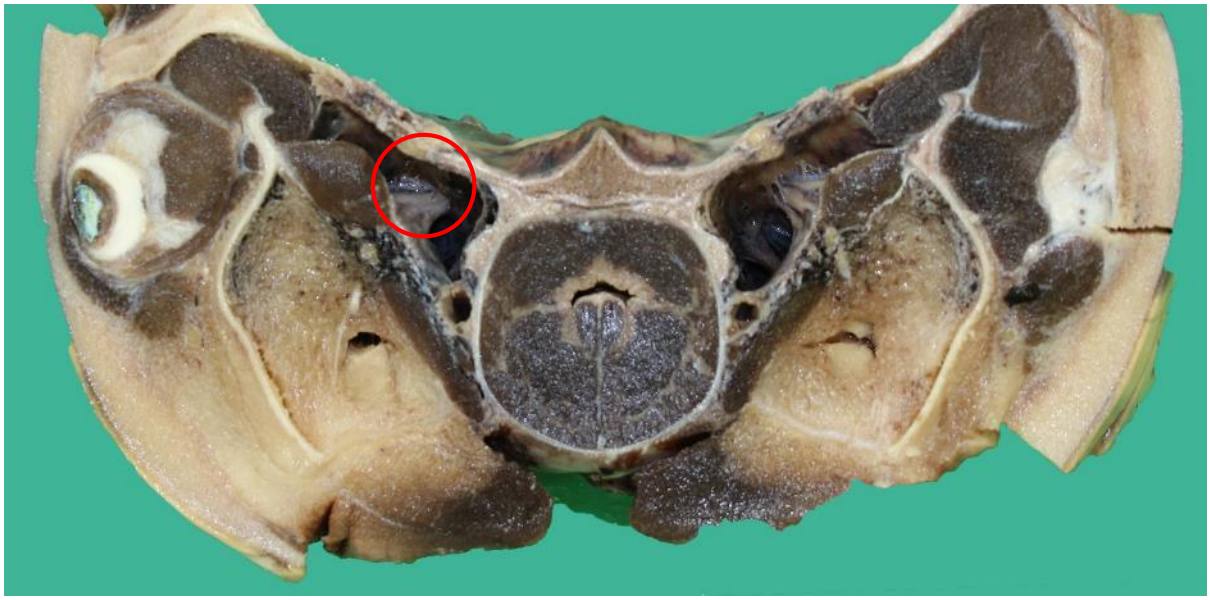

Figure 287. Macroscopic rostral view of a transverse and slightly oblique section through the head of a striped dolphin. Right side, big circle: The nervus alveolaris inferior and nervus mylohyoideus on their laterorostroventral course from the cranium, through pterygoid sinus, entering the lateral wall of the pterygoid sinus in between the lateral and medial pterygoid muscles. While the n. alveolaris inferior enters the intramandibular fat body through the periost of the medial side of the mandibula, the n. mylohyoideus stays on the medial side of the periost (see right half of the image). The n. mylohyoideus branches immediately on exiting while the nervus alveolaris inferior branches further peripheral.

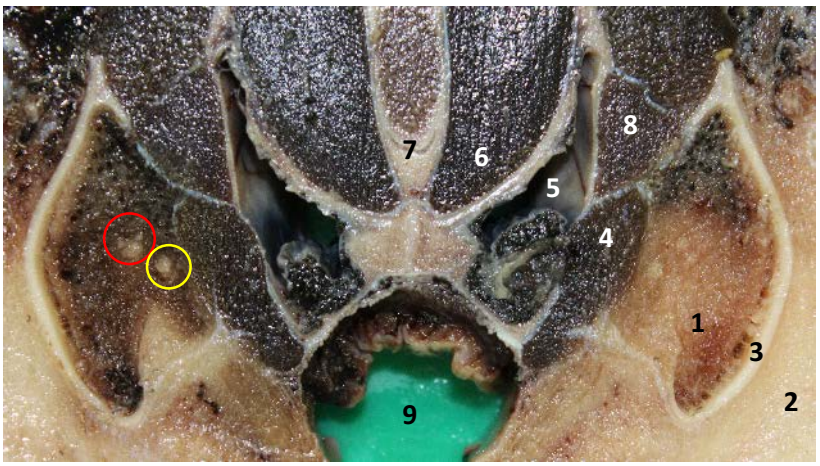

Figure 288. Caudal view of a transverse section through the head of a striped dolphin (ID5386) at about 1 cm rostral to the anterior commissure of the eye. Note the presence of multiple macroscopically visible nerve fibres of the n. alveolaris inferior (red circle) and the n. mylohyoideus (yellow circle) within the intramandibular fat bodies (1). Note the unilateral congestion of the left intramandibular fat body. 2. extramandibular fat body; 3. mandibula; 4. m. pterygoideus medialis; 5. sinus pterygoideus; 6. m. constrictor pharyngis rostralis; 7. os vomer; 8. m. pterygoideus lateralis; 9. pharynx

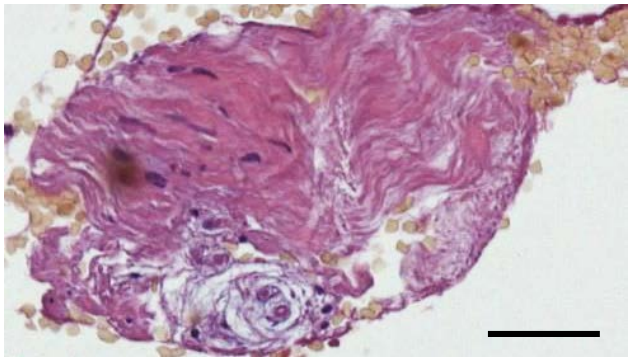

Figure 289. Histological detail (HE-staining) of a possible lamellar corpuscle within the sparse connective tissue of the extramandibular fat body. Scale bar 50 µm

5.4 Paraotic sinuses

5.4.1 Pterygoid sinus

Microscopically the pterygoid sinus wall showed several small to medium-sized (±0,25 mm) nerve fibres and also a ganglion within the loose connective tissue of the medial wall in the vicinity of the opening of the *tuba auditiva* into the sinus. There were also numerous macroscopically and microscopically visible nerve fibres in the ventrolateral of the pterygoid sinus, at the border with the internal mandibular fat body (Figure 291). In all of the walls, there were very few corpuscles, often in spatial association with vascular structures.

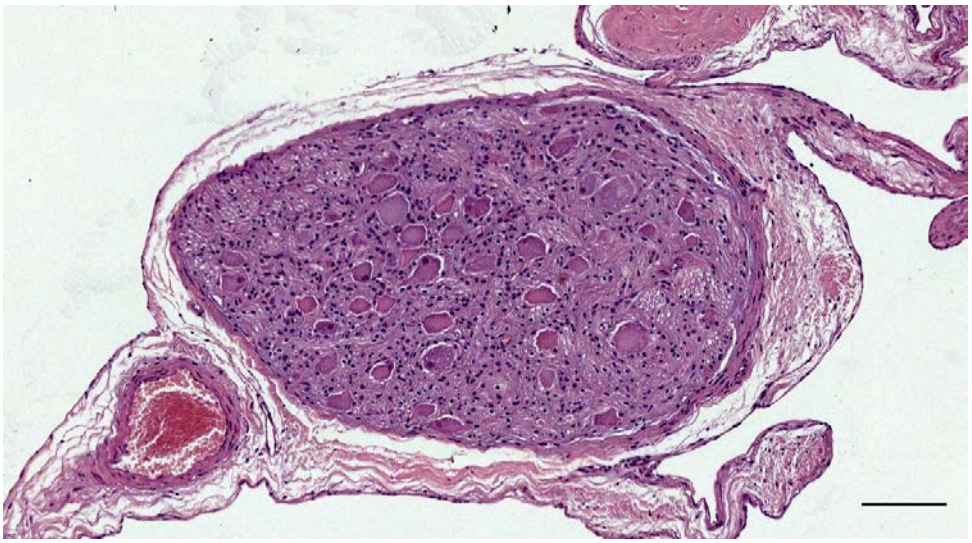

Figure 290. HE-stained section of a ganglion in the pterygoid sinus of a striped dolphin. Diameter: 0.7 x 0.4 mm. Scale bar 100 µm

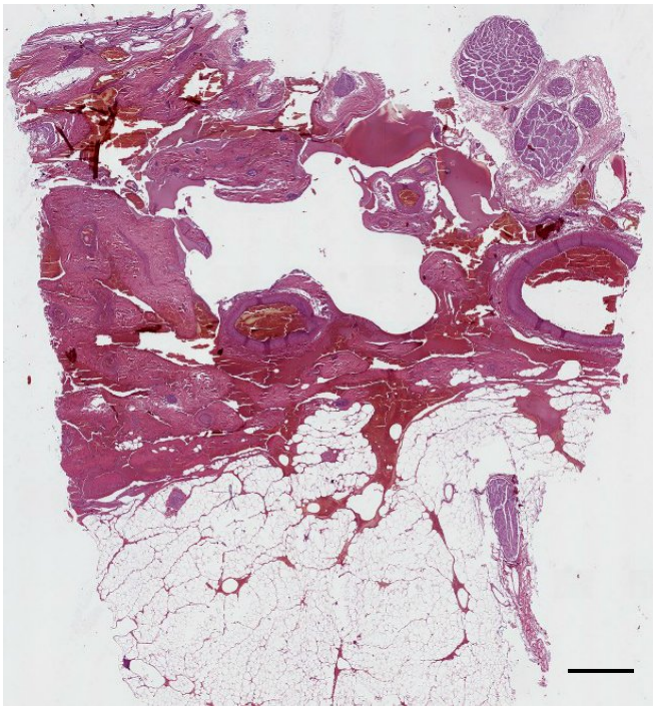

Figure 291. HE-stained section through the ventrolateral wall of the pterygoid sinus and the internal mandibular fat body (bottom) of a striped dolphin (ID5386). Note the large nerve fibres in the fibrovenous wall. Scale bar 1 mm

5.4.2 Peribullar sinus

The peribullar sinus presented several nerve fibres of small to medium size and many very small nerve fibres. The wall consisted of dense connective tissue and many large blood vessels. No sensory nerve formations could be detected.

5.5 Vibrissae

In both striped and bottlenose dolphin, there was a very rich innervation coming from branches of the infraorbital nerve. Abundant nerve fibres were running parallel and in close association with the shaft of the vibrissa, up to the epidermal layer. There were many simple lamellar corpuscles along the shaft but mostly scattered at the border of the dermal papillae (Figure 292). No other SNF could be discerned in HE-stained sections.

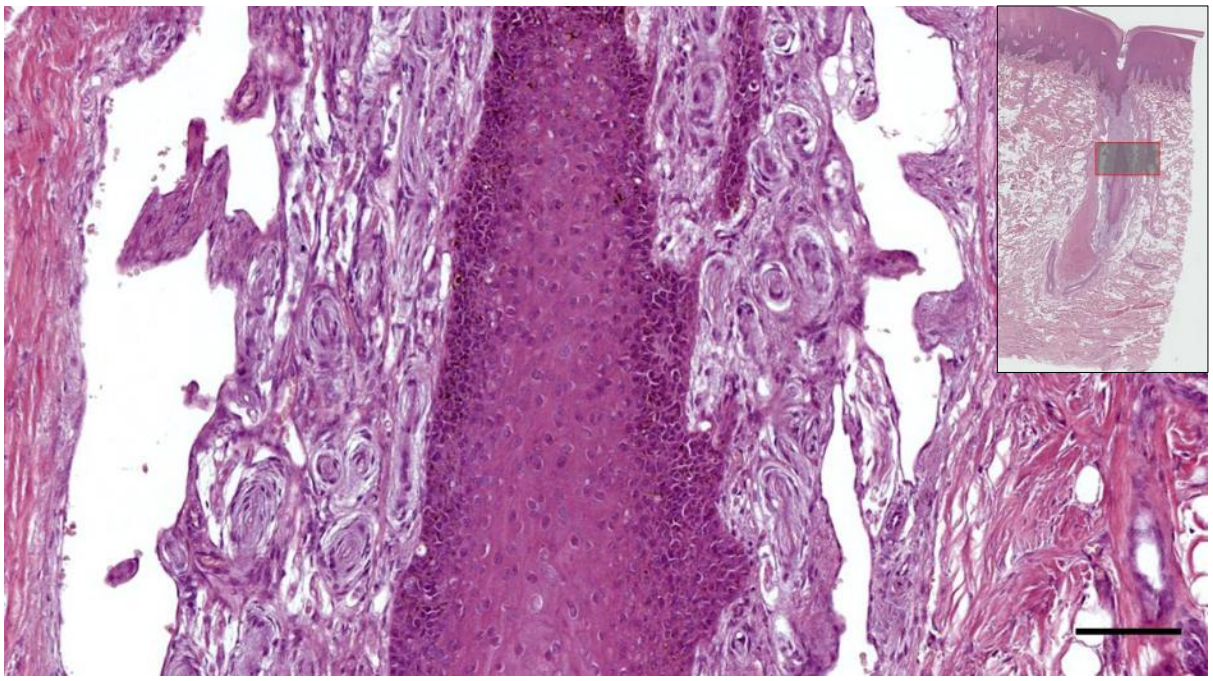

Figure 292. Histological image of a longitudinal section through a vibrissal crypt in a bottlenose dolphin (ID114). Note the high density of sections through lamellar corpuscles along the shaft. Scale bar 100 µm

5.6 Eye: eyelid, eye commissures, iridocorneal angle

There were scant receptors in the superficial skin dermis at the eye commissures and relative more corpuscles in the subpapillary layer of the dermis of the eyelid. There was little innervation by small nerve fibres. In striped dolphin, there were simple lamellar corpuscles in the iridocorneal angle, not found in a bottlenose dolphin (Figure 294, Figure 295).

Figure 293. Macroscopic image of a longitudinal section through the eye and optic nerve in a striped dolphin. Note the mandible with fat tissue and the intricate musculature of the eye and pterygoid region.

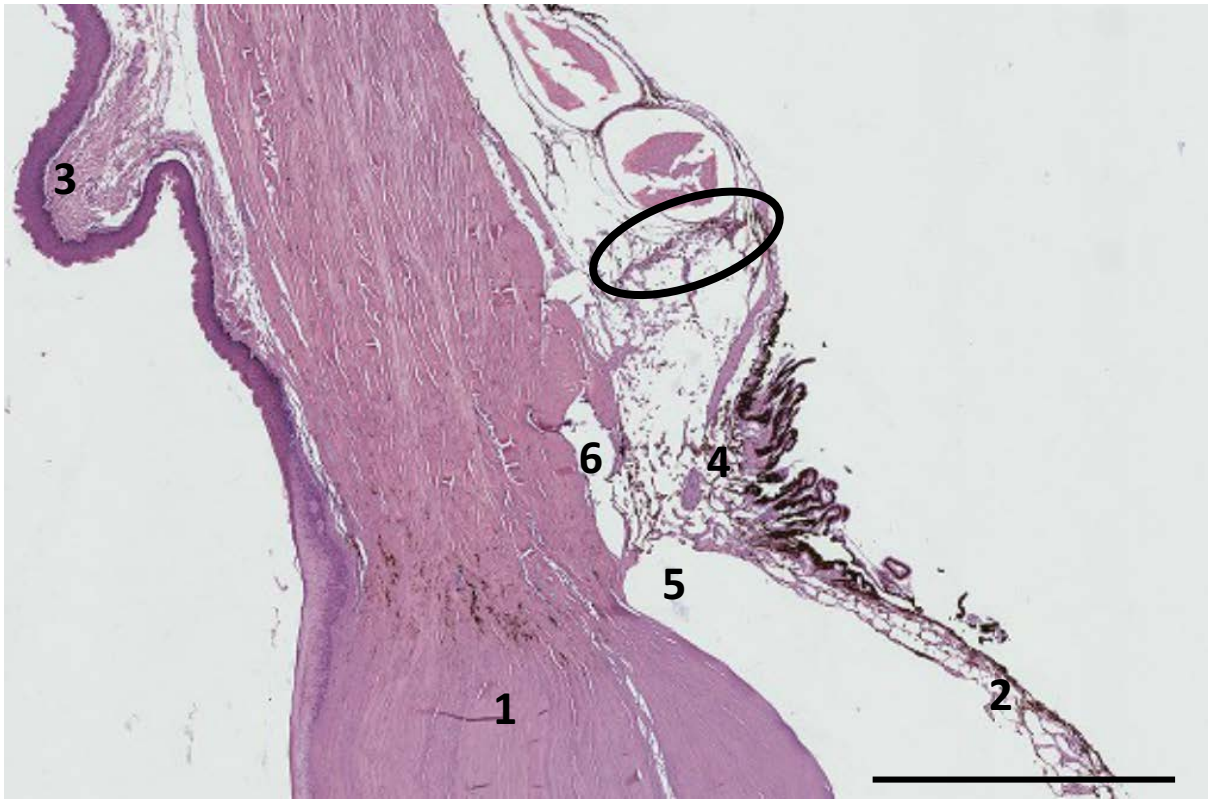

Figure 294. Histological image (HE staining) of a sagittal section through the eye of a striped dolphin (ID2926). Cornea (1), iris (2), sclera (3), ciliary body with pars plicata (ciliary processes) (4) that connect to the lens with zonular fibres (not present), anterior chamber recess (5), Schlemm's canal (6), circle: location of the simple lamellar corpuscles. Scale bar 1 mm

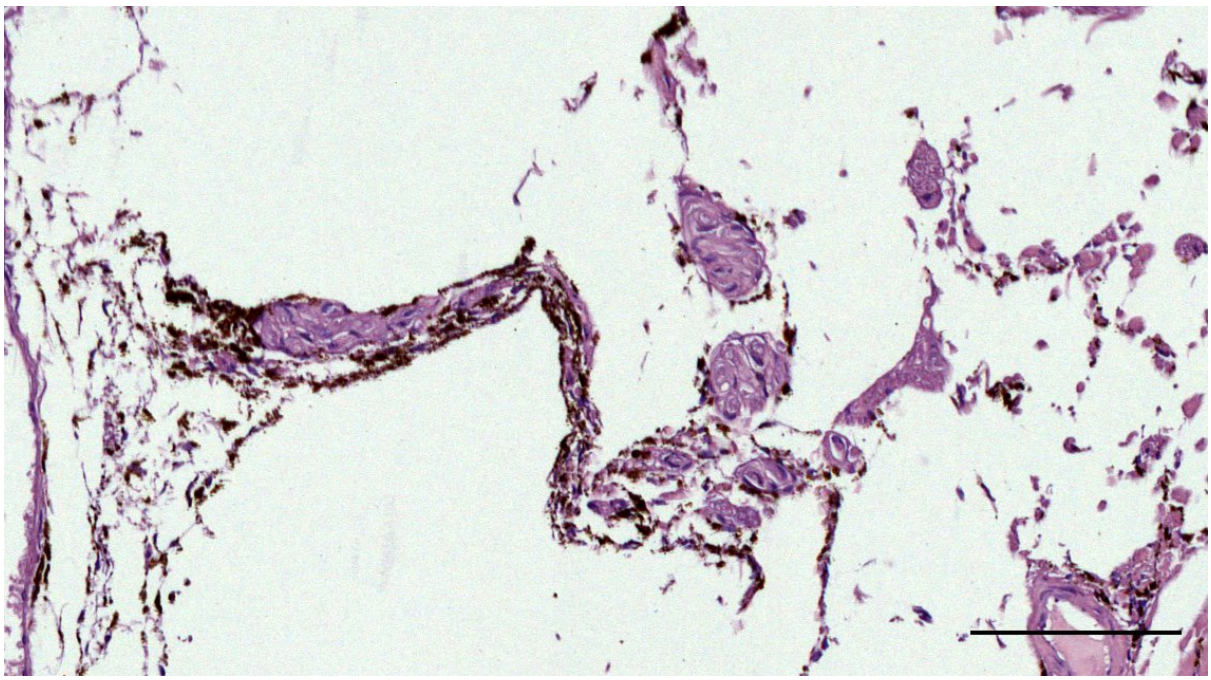

Figure 295. HE-stained section of a small nerve and various simple lamellar corpuscle complexes in the iridocorneal angle of the eye of striped dolphin. Scale bar 50

Figure 296. HE-stained cross-section of the eyelid with cornified epithelium on the outside, and uncornified on the inside. Note the large Meibomian gland (tarsal gland). Scale bar 0.5 mm (Huggenberger et al., 2019)

5.7 Blowhole

The innervation was checked in HE sections of the blowhole anterior and posterior lips and commissures in striped dolphin and Cuvier´s beaked whale. There were few lamellar corpuscles at the bottom and inside the dermal papillae in both the anterior and posterior blowhole lip, and in the lateral commissures, similar to the skin in other locations (Figure 297, Figure 298).

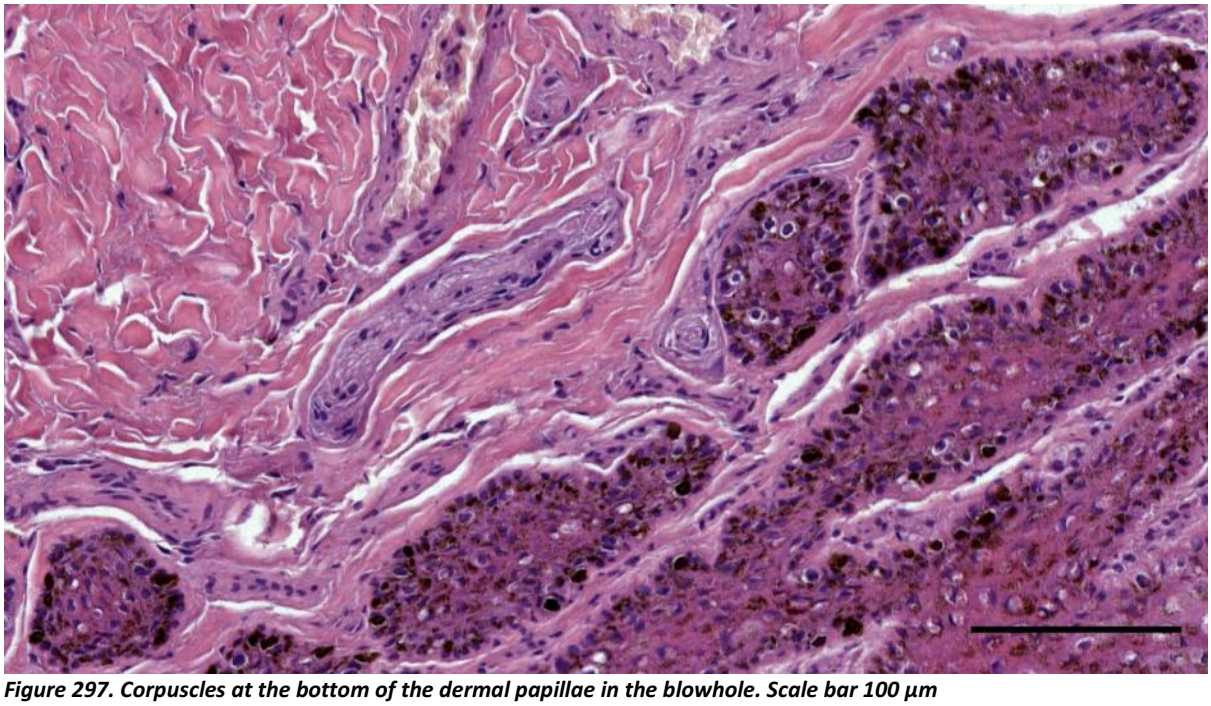

Figure 297. Corpuscles at the bottom of the dermal papillae in the blowhole. Scale bar 100 µm

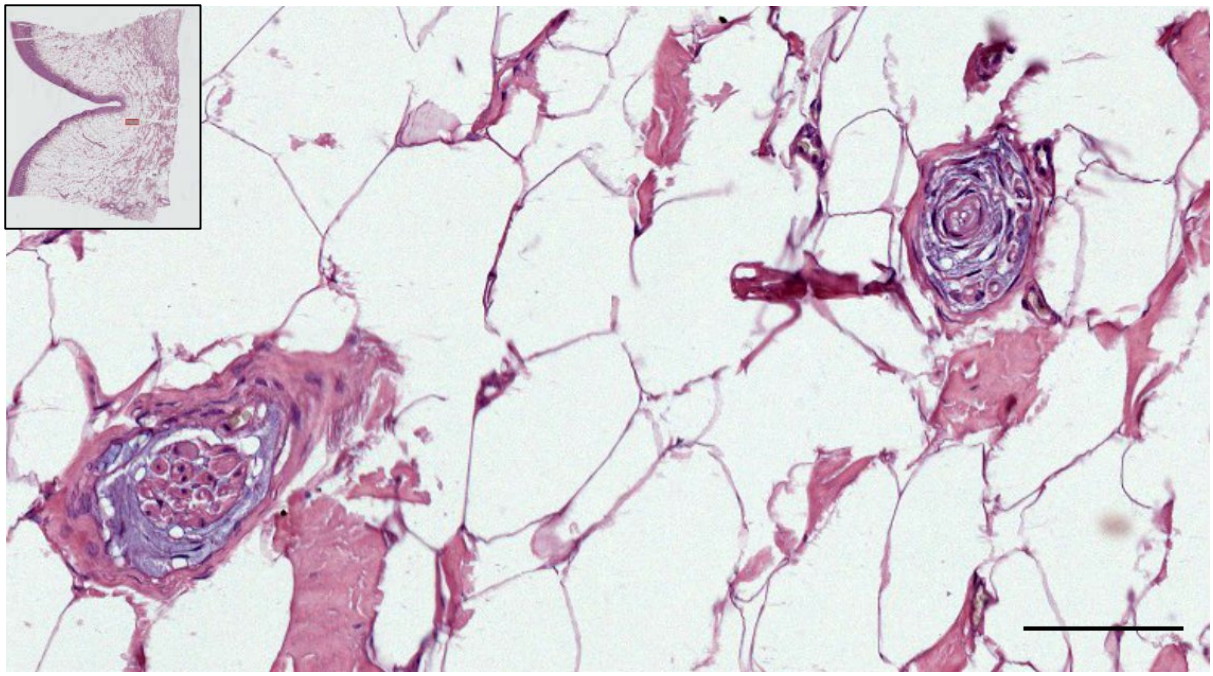

Figure 298. Small nerve fibre and a lamellar corpuscle in the adipoconnective tissue in the blowhole commissure (insert top left) of a Cuvier´s beaked whale. Scale bar 100 µm

5.8 Rostrum tip

The rostrum tip showed a rich innervation with abundant nervous structures, including lamellar corpuscles in the subpapillary layer (Figure 299), which also showed an intense vascularization. The more caudal the section, the bigger the nerve diameter and the lower the density of lamellar corpuscles.

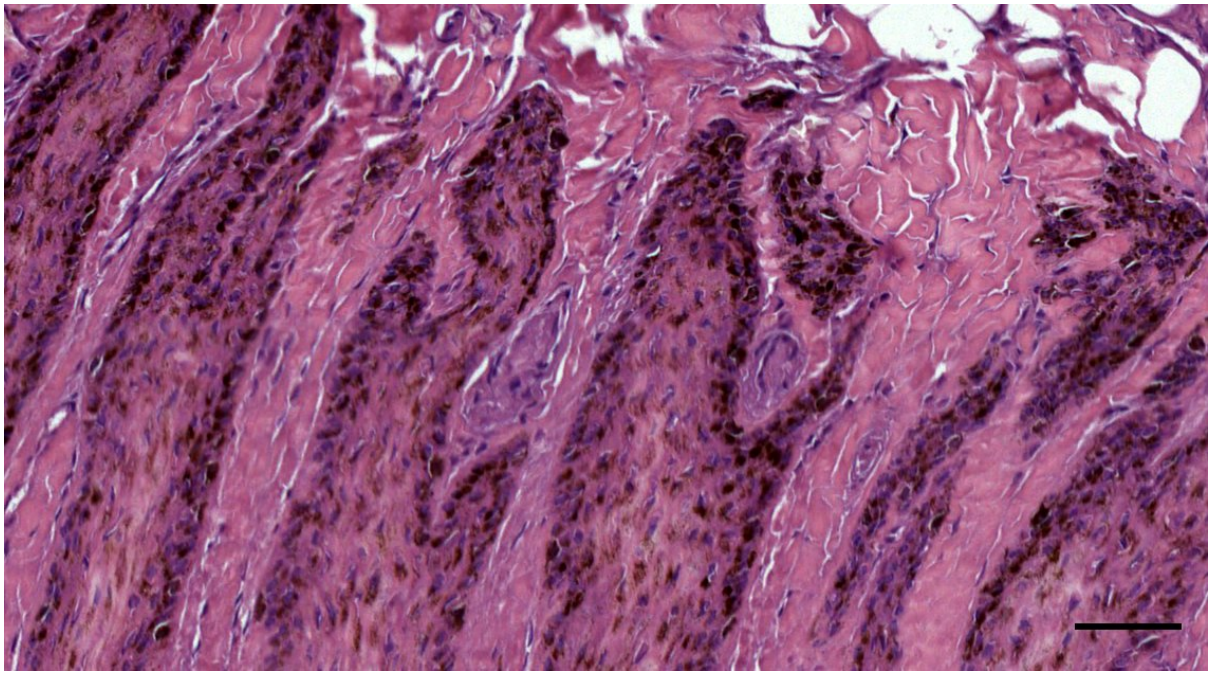

Figure 299. Two likely lamellar corpuscles at the bottom of the dermal papillae in the rostrum of a striped dolphin (Sc1). Scale bar 50 µm

5.9 Oral commissure

The oral commissure showed a very rich innervation with the presence of relatively many simple lamellar corpuscles in the papillary and subpapillary dermal layers. Most of the lamellar corpuscles were grouped per three, although there were also single and double corpuscles present.

5.10 Beaked whale throat groove

The innervation patterns were similar to those reported in skin samples, with small nerve fibres in the superficial dermis, mostly in the subpapillary but also in the papillary layers. The tissue was well-vascularized, with exceptional amounts of vascular structures in the dermal papillary layer. The presence of specialized sensory nerve formations was not clear.

5.11 Dorsal fin

No corpuscles were detected with certainty, but nerve fibres were entering the dermal papillae, as in the rest of the skin

5.12 Pectoral fin

Similar to the skin in other locations, this pectoral fin skin was poorly innervated with scarce occurrences of nerve fibres, which were mainly spatially associated with blood vessels in the reticular layer of the dermis. There were rare lamellar corpuscles, only on the dorsal side of the fins.

5.13 Fluke

The innervation of the fluke was similar to the pectoral with small nerve fibres in the dermis, often associated with blood vessels. There were no discernible sensory nerve formations in the sections examined.

5.14 Penis

The tip of the penis was very well innervated. There were many small nerve fibres throughout the entire dermis, with simple lamellar corpuscles, and sensory nerve formations that resembled Meissner corpuscles in the papillary layer (Figure 300, Figure 301).

5.15 Urogenital fold, mammary glands and anus

The urogenital fold, mammary glands and anus presented a relatively rich innervation with many small nerve fibres in the paucicellular connective tissue of the dermis. No sensory nerve formations were identified with certainty.

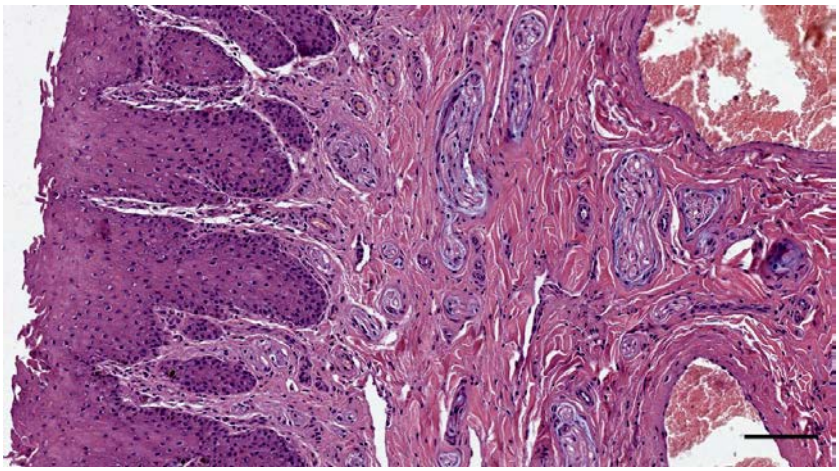

Figure 300. HE-stained histological cross-section through the penis skin. Note the very rich innervation in the dermal layer. Note the large vascular structures. Scale bar 50 µm

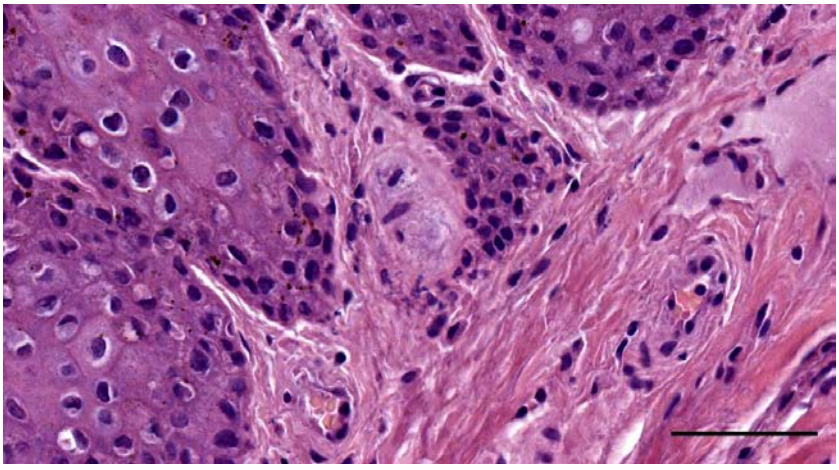

Figure 301. Histological image (HE stain) of a possible Meissner corpuscle (dimensions 23x42 µm) in the papillary layer of the dermis of the tip of the penis of a striped dolphin (Sc1). Scale bar 50 µm

6 Bibliography of Results

Bancroft, J.D., and Gamble, M. (2002). Bielschowsky's silver stain for neurofibrils, dendrites, and axons in paraffin and frozen sections, modified (Chan, unpublished). In Theory and Practice of Histological Techniques, (London), pp. 376–377.

Benninghoff, A., Drenckhahn, D., and Zenker, W. (1994). Anatomie. makroskopische Anatomie, Embryologie und Histologie des Menschen Band 2 Band 2 (München; Wien; Baltimore: Urban und Schwarzenberg).

Boenninghaus, G. (1903). Das Ohr des Zahnwales, zugleich ein beitrag zur theorie der Schalleitung: eine biologische studie. Zoologische Jahrbücher. Abteilung Für Anatomie Und Ontogenie Der Tiere *19*, 189–360.

Chouchkov, C.N. (1973). The fine structure of small encapsulated receptors in human digital glabrous skin. J Anat *114*, 25–33.

Costidis, A.M. (2012). The morphology of the venous system in the head and neck of the bottlenose dolphin (*Tursiops truncatus*) and Florida manatee (*Trichetus manatus latirostris*). PhD Thesis. University of Florida.

Costidis, A.M., and Rommel, S.A. (2016). The extracranial venous system in the heads of beaked whales, with implications on diving physiology and pathogenesis. Journal of Morphology *277*, 34–64.

Cozzi, B., Bagnoli, P., Acocella, F., and Costantino, M.L. (2005). Structure and biomechanical properties of the trachea of the striped dolphin, *Stenella coeruleoalba*: Evidence for evolutionary adaptations to diving. The Anatomical Record Part A: Discoveries in Molecular, Cellular, and Evolutionary Biology *284A*, 500–510.

Cozzi, B., Huggenberger, S., and Oelschläger, H.H.A. (2017). Anatomy of Dolphins (Academic Press).

Cranford, T.W., Mckenna, M.F., Soldevilla, M.S., Wiggins, S.M., Goldbogen, J.A., Shadwick, R.E., Krysl, P., St. Leger, J.A., and Hildebrand, J.A. (2008). Anatomic Geometry of Sound Transmission and Reception in Cuvier's Beaked Whale (*Ziphius cavirostris*). The Anatomical Record: Advances in Integrative Anatomy and Evolutionary Biology *291*, 353–378.

De Vreese, S., André, M., and Mazzariol, S. (2020a). Morphology of the external ear canal in toothed whales. Proceedings of Meetings on Acoustics *37*, 6.

De Vreese, S., André, M., Cozzi, B., Centelleghe, C., van der Schaar, M., and Mazzariol, S. (2020b). Morphological Evidence for the Sensitivity of the Ear Canal of Odontocetes as shown by Immunohistochemistry and Transmission Electron Microscopy. Sci Rep *10*, 1–17.

Domenech-Estevez, E., Baloui, H., Meng, X., Zhang, Y., Deinhardt, K., Dupree, J.L., Einheber, S., Chrast, R., and Salzer, J.L. (2016). Akt Regulates Axon Wrapping and Myelin Sheath Thickness in the PNS. Journal of Neuroscience *36*, 4506–4521.

Fraser, F.C., and Purves, P.E. (1960). Anatomy and Function of the Cetacean Ear. Proceedings of the Royal Society of London B: Biological Sciences *152*, 62–77.

Hanke, H. (1914). Ein Beitrag zur Kenntnis der Anatomie des Äusseren und Mittleren Ohres der Bartenwale. Jenaische Zeitschrifte Fur Naturwissenschaft *51*, 487–524.

Harrison, R.J., and Thurley, K.W. (1974). Structure of the Epidermis in *Tursiops*, *Delphinus*, *Orcinus* and *Phocoena*. In Functional Anatomy of Marine Mammals, R.J. Harrison, ed. (London: Academic Press), pp. 45–71.

Huggenberger, S., Oelschläger, H., and Cozzi, B. (2019). Atlas of the Anatomy of Dolphins and Whales (Elsevier Academic Press).

Kuo, C.-L., Shiao, A.-S., Yung, M., Sakagami, M., Sudhoff, H., Wang, C.-H., Hsu, C.-H., and Lien, C.-F. (2015). Updates and Knowledge Gaps in Cholesteatoma Research. BioMed Research International *2015*, 1–17.

Ling, J.K. (1974). The Integument of Marine Mammals. In Functional Anatomy of Marine Mammals, R.J. Harrison, ed. (London: Academic Press), pp. 1–44.

Loewenstein, W.R. (1971). Mechano-electric Transduction in the Pacinian Corpuscle. Initiation of Sensory Impulses in Mechanoreceptors. In Handbook of Sensory Physiology. 1. Principles of Receptor Physiology, W.R. Loewenstein, ed. (Berlin, Heidelberg, New York), pp. 269–290.

Luna, L.B. (1968). Pinkus' Acid-Orcein-Giemsa Method. Manual of Histologic Stain Methods of the Armed Foces Institute of Pathology. Third Edition, New York, pp. 77-78.

Mead, J.G., and Fordyce, R.E. (2009). The Therian Skull A Lexicon with Emphasis on the Odontocetes. Smithsonian Contributions to Zoology *627*, 261.

Munger, B.L. (1971). Patterns of Organization of Peripheral Sensory Receptors. In Principles of Receptor Physiology, W.R. Loewenstein, ed. (Berlin, Heidelberg: Springer Berlin Heidelberg), pp. 523–556.

Munger, B.L., Yoshida, Y., Hayashi, S., Osawa, T., and Ide, C. (1988). A re-evaluation of the cytology of cat Pacinian corpuscles. I. The inner core and clefts. Cell and Tissue Research *253*, 83–93.

Nummela, S., Reuter, T., Hemilä, S., Holmberg, P., and Paukku, P. (1999). The anatomy of the killer whale middle ear (*Orcinus orca*). Hearing Research *133*, 61–70.

Orfanos, C.E., and Mahrle, G. (1973). Ultrastructure and Cytochemistry of Human Cutaneous Nerves. Journal of Investigative Dermatology *61*, 108–120.

Palmer, E., and Weddell, G. (1964). The Relationship Between Structure, Innervation and Function of the Skin of the Bottlenose Dolphin (*Tursiops truncatus*). Proceedings of the Zoological Society of London *143*, 553–568.

Preibisch, S., Saalfeld, S., and Tomancak, P. (2009). Globally optimal stitching of tiled 3D microscopic image acquisitions. Bioinformatics *25*, 1463–1465.

Spaethe, A. (1984). Eine Modifikation der Silbermethode nach Richardson für die Axonfärbung in Paraffinschnitten. Verh. Anat. Ges. *78*, 101–102.

Spencer, P.S., and Schaumburg, H.H. (1973). An ultrastructural study of the inner core of the Pacinian corpuscle. J Neurocytol *2*, 217–235.

Watanabe, I., Silva, M.C.P. da, and Kronka, M.C. (2002). Sensory nerve endings in the rat cheek mucosa: an electron microscopic study. Brazilian Journal of Veterinary Research and Animal Science *39*.

Watanabe, K., Tubbs, R.S., Satoh, S., Zomorodi, A.R., Liedtke, W., Labidi, M., Friedman, A.H., and Fukushima, T. (2016). Isolated Deep Ear Canal Pain: Possible Role of Auricular Branch of Vagus Nerve—Case Illustrations with Cadaveric Correlation. World Neurosurgery *96*, 293–301.

Zelená, J. (1994). Nerves and Mechanoreceptors - The Role of Innervation in the Development and Maintenance of Mammalian Mechanoreceptors (London, UK: Chapman and Hall).

DISCUSSION

DISCUSSION

To locate a specific figure, please refer to the corresponding sections in the table of contents.

This section discusses the results obtained from the variety of studies that subjected each of the morphological structures, analyses the morphological findings, puts it into a context of a morphofunctional analysis and postulates grounded hypotheses on the various structures. This discussion aims at demonstrating not only that the ear canal in toothed whales is a functional organ, but also that it plays an unprecedented and possibly vital role in the animal's sensory perception.

- The first chapter considers the variety of anatomical components associated with the external ear canal, and how they could function individually and as a unit (p. 251)
- Next, the linchpin of this work, the assessment of the peripheral nervous system, shows that the external ear canal, once considered vestigial, could prove a crucial organ for maintaining the functionality of the hearing apparatus through mechanical and physiological responses and other homeostatic processes, essential for survival. (p. 275)
- The chapter is followed by a comparison with the external ear canal in other marine and terrestrial Cetartiodactyla (p. 306)
- The third chapter touches upon the sensory nerve formations found in other organs and around the skin (p. 308)
- Next, the pathological findings and the analysis of techniques are discussed, although the bulk of discussion can be found in the annexe (p. 311)
- The final chapter projects ideas on the future continuation of this work, on the development of novel ideas and implementation of novel techniques, and the various aspects on getting a comprehensive view in morphofunctional studies like this one (p. 313)

1 External ear canal in toothed whales

This study expands the knowledge on the morphology of the ear canal in toothed whales. The results were generally in line with previous descriptions, although they contributed an in-depth morphological analysis to many of the tissues while placing them in a comparative context. These results are essential to understand the function of the external ear canal in toothed whales. As a specialised sensory organ, it could have implications on diving physiology, pathology and possibly even underwater hearing.

The external ear canal in all mammals originates from the projection of the first two pharyngeal arches around the first pharyngeal cleft (McGeady et al., 2017). In the early organogenesis, the ear canal in all mammals is occupied with epithelial cells (Solntseva, 1990). This accumulation of cells is called the 'meatal plug', which in humans is formed by the proliferating ectoderm that intrudes into the meatal lumen. The most proximal end forms part of the tympanic membrane as a thin ectodermal membrane, while the rest of the plug gets absorbed partly and splits, creating a lumen lined with epithelium that keratinises over time (Michaels and Soucek, 1989; Nishimura and Kumoi, 1992). This plug is absent in

any adult terrestrial mammal and all marine mammals, except for the mysticetes. In these species, the ear plug is present during the entire life, and it has an intricate relation with the tympanic membrane, called the 'glove finger' in these animals due to its morphological resemblance to the finger of a glove (Trumble et al., 2013).

In cetaceans and pinnipeds, the ear canal begins to form when the embryo is 30 to 40 mm long. It starts as a short tube, which constricts in later stages (40-60 mm), and distends and acquires the typical sigmoid shape. It then expands in the proximal (embryos 70-100mm), and in the final stages, it grows in equal proportions to the overall growth of the embryo (Solntseva, 1990).

Our works confirm that the course of the external ear canal in all odontocetes describes the same pattern: a serpentine, tortuous, spiralling, which, from the skin to the tympanic membrane, runs horizontally, then ventrally, and horizontally again. Although all authors likely intended to describe the same shape, it has sometimes been labelled as sigmoid or s-shaped, which does not fully attribute to the actual three-dimensional shape of the spiralling ear canal (Boenninghaus, 1903; Fraser and Purves, 1960; Hunter, 1787; Reysenbach de Haan, 1956; Slijper, 1958)

The external ear canal is present in all toothed whales, and although its configuration can differ significantly among species, all the structural components and their relative position are very similar (Yamada, 1953; Reysenbach de Haan, 1956; Fraser and Purves, 1960; Purves, 1966; De Vreese et al., 2014, 2019). Unlike terrestrial mammals, the canal consists for the most of a membranous portion, and only the far most medial end, where the canal enters the tympanic aperture of the tympanic bone (Mead and Fordyce, 2009), could be considered bony. However, there was no histological distinction between the cartilaginous and osseous part of the external ear canal as occurring in land mammals. The osseous part in dolphins would be the part where the ear canal enters the TP complex, but this was very short, and we did not note any histological differences between the two configurations of the ear canal, as is reported in terrestrial mammals with, e.g. the presence of glands only in the cartilaginous part, which is true but only for a very short section. It is therefore not clear if the odontocete ear canal consists of a typical cartilaginous and osseous part.

1.1 External ear opening

Our findings correspond to all of the literature in which the external ear opening in cetaceans is mentioned; namely, it is located few centimetres caudoventral to the eye. The exception to this rule is the Pygmy sperm whale (*Kogia breviceps*), in which the ear opening is situated caudal to the eye, but above the eye line (Yamada, 1953). Descriptions go from ´on the side of the head and little behind the eye´ (Hunter, 1787), to quite elaborate measurements using the intersection of two imaginary circles with centres at the eye and mouth commissure (Reysenbach de Haan, 1956)

In some cases, such as well-preserved striped dolphin with a linear pigmentation, the ear opening was small but very easy to locate, while in the single specimen of long-finned pilot whale, it was not possible to locate the external ear opening, nor visual nor tactical, in various lighting conditions. This complication was partly due to the conservation code as the skin was peeling off in certain areas. Similarly, Reysenbach De Haan (1957) could not find it either in the same species. Instead, both of us had to locate and trace the ear canal in the subcutaneous tissues using visual and tactile means.

The diameter of the external ear opening was minute in all cases, maximum several millimetres, oval to spindle-shaped. The measurement of the diameter should be interpreted with caution. The opening is shaped like trumpet´s mouth, following a negative exponential curve in which the diameter decreases by a factor over distance. Therefore, it is imperative to note where and how precisely those measurements were taken. In practice, during a necropsy, there are often other priorities and little time, so we mention just a single measurement and landmark descriptions (linear pigmentation) as a method for locating the ear opening. Instead, for pathology, it is important to assess the condition of the ear opening and to check whether there is any superficial lesion, parasite or excrete present.

In none of the individuals in this study, there were indications of an epithelial structure originating from the caudal side of the external ear opening as noted in individuals of harbour porpoises and beluga and Cuvier´s beaked whale (Howes, 1880). Such a structure was also reported as a knob-shaped extension of the skin, sometimes found in the posterior wall of the ear opening in harbour porpoises (Boenninghaus, 1903). Peculiarly, only in the right ear opening, never on the left side in *Phocoena*, while it was reported to be bilateral in a beluga whale. Although these structures were sometimes described as a pinna or auricle, or at least a rudiment of the pinna, which later proved erroneous, its significance, or even presence, remains unclear to date. It has been reported to block the external ear opening and close of the ear canal from the external environment (Yamada, 1953), functionally similar to the reduced pinna in otariids (Huber, 1934)

1.2 Lumen and content of the ear canal

In all species, the lumen shape changes from oval-round in the ear opening to star-shaped with varying degrees of complexity (indications of species-dependency, but could also be individual variation). It is most convoluted at the level of the glands (from least complex in Cuvier´s beaked whale, shaped like a triple-bladed boomerang, to highly complex in the common dolphin ear canal), and changes to oval-round-spindle-shaped at the bottom of the ventral curvature, to increase in diameter but not much in shape on reaching the tympanic membrane. This configuration has been reported similarly for all toothed whales studied.

The answer to whether the ear canal in toothed whales is continuous or not is somewhat complicated as the canal appeared obstructed with epithelial and glandular content, or continuous but with a

minute lumen, or with ´collapsed´ epithelial walls. In this study, we show there is a clear continuation of the ear canal down to the tympanic membrane, although the case is nuanced.

The lumen in toothed whales is closed in one area according to some authors (Clarke, 1948; Ketten, 2000; Solntseva, 1990)(Figure 303), or "sometimes stuffed" with degenerated epithelial cells but continuous throughout its course (Yamada, 1953). Other sources report a continuous lumen, which makes the entire structure down to the tympanic conus stand in direct contact with seawater (Reysenbach de Haan, 1956). A more nuanced description, which is consistent with our results, is that the lumen is not continuously open but rather compressed and partially occluded with mucus, or *sometimes absent* in the region just below the blubber (McCormick et al., 1970).

The ear canals in this study contained cellular debris and ceruminous content in the region of the glands. Other authors reported seawater and desquamated epithelial cells without the formation of a plug, although the ear canal does taper towards the external ear opening (Reysenbach de Haan, 1956). It is currently unknown whether the external ear canal in toothed whales would be filled with seawater under normal conditions, although we believe it would rather entrap a bubble of air (See below). On the other hand, in some animals, there was no luminal content, except for a few epithelial cells. Such an absence of content might have been an artefact of the preparation in which it was washed out in the fixation or trimming passes, similar to reports in other species (White-beaked dolphin, De Vreese et al., 2015). The situation might be similar to harbour porpoises where cerumen and desquamated epithelial cells were present 'in some places', in conjunction with a lumen that was 'sometimes closed' ("*bisweilen volkommen verklebt*"(Boenninghaus, 1903). As the region of such closure would be small, we suppose these might have been overlooked by authors who do not mention it and who have drawn conclusions of a continuous canal based on such findings. This was likely the case in our data, such as for the Cuvier´s beaked whales, in which there was no closed ear canal, but also no glands, which was very likely due to an incomplete analysis of all the tissue blocks. On the other hand, it could also depend on the interpretation of the histological findings and the phrasing with which the results were described. A closed lumen, as reported by Solntseva (1990) with an apparent full closure of intact epithelium, is not the same as an ear canal that is closed because of the presence of glandular and cellular content. This vocabulary incongruency is one of the reasons why a visual representation is essential to accompany morphological descriptions.

Also, one should question whether the state of the tissues as seen with histology was representative of the in vivo state, either resting or under particular natural strain, or if it represented a biased configuration of the soft tissues. For example, the lumen could be compressed due to manipulation, or glandular content might be excreted artificially, and the state of tension of the musculature or the release of tension during sample preparation, might affect the conformation state of the canal´s

curvature and the degree of flexure of the cartilage (cfr. Purves, 1966), and therefore, could complicate the interpretation of the post-mortem morphology of the external ear canal.

In all animals, the configuration of the lumen was different from a properly closed ear canal as described in mysticetes (e.g. De Vreese et al., 2014, Fig. 7), although the single common dolphin ear canal closure was very similar to the absence of a lumen in a bottlenose dolphin (Solntseva, 1990)(Figure 303). If we assume the tissue state as seen in histology represents the in vivo configuration, in all three situations (filled lumen, minute lumen, collapsed lumen), no exogenous material such as seawater would not be able to enter the ear canal, either because of the physical obstruction or, in the case of the minute lumen, because of physical cohesion characteristics of (sea)water. However, in the cases of a minute lumen, air would be able to pass and enter the ear canal when the animal is at the surface, possibly in synergy with a peristaltic movement caused by the muscles (see below). Similarly, the collapsed wall could be opened up with the help of a physical force acting on the surrounding connective tissue sheath, as facilitated by the insertion of the striated muscles at this level of the ear canal, and could resolve to a resting state in collapse due to the elastic nature of the sheath. In the case of the completely obstructed ear canal, the same muscles might create a slight opening that could enable air to pass, although it is evident because of the unknown intercellular relations between the epithelial cells and if they were truly desquamated and lost all connections to underlying cell layers, or not. Some authors reported on a continuous lumen in all toothed whales (Fraser and Purves, 1960; Reysenbach De Haan, 1957; Slijper, 1958), while Ketten (1997, 2000) described the ear canal as filled with cerumen and cellular debris and without ´observable connection´ or ´true association´ with the tympanic membrane or middle ear, and also Solntseva (1990) reported a complete closure of the ear canal of a bottlenose dolphin. These findings might all be different states of the same configuration, although dependent on the influence of other soft tissues such as the surrounding adipoconnective, fibro-elastic tissue, and the inserting striated muscles, and possibly even environmental conditions at the time of death (cfr. Cozzi et al., 2005).

Clarke (1948) mentions that the ear canal in sperm whales is not continuous about halfway the canal. He noticed a difference between adult and physically immature adults, in that the latter showed a continued ‘stalk’ of tissue where the lumen is closed, while the mature male specimens did not show any signs of continuation between the peripheral and medial ends. It was suggested that the canal might undergo a physical change during the development, starting from a continuous lumen in foetal stages, to a closed lumen in immature specimens, and complete obliteration of ear canal tissues in adults. However, this might be an inaccuracy, as he obtained his samples from captured specimens which were sampled on deck, understandably under difficult conditions in which to work. Yamada

(1953) noticed a continuation of the ear canal, although it diminished to a closed canal with a diameter of fewer than 200 microns in sections about 10 cm beneath the skin surface.

In regards to the external ear canal in three samples of two specimens of Cuvier´s beaked whale, the proximal third of the ear canal was missing. The two animals were dissected by different persons (SM & SDV) on independent events. The TP complex is not entirely suspended in the peribullar sinus as in delphinids, but instead partially fused or showing an intricate connection with the skull. Similarly, it is possible that also the external ear canal might present a particular course that is different from the situation in smaller odontocetes. It might be that the ventral curvature of the ear canal goes further ventral than in other animals and therefore the sampling protocol was not apt for the configuration in Cuvier´s beaked whale. For now, no conclusions can be drawn, and further sampling should be done with maximum caution on this matter.

If there is indeed air in the ear canal, it could come from the external ear opening if there is no complete closure of the lumen along the canal, it could come from a gas exchange with the vascular structures (not likely), or there could be a continuation of the lumen with the air in the middle ear or peribullar sinus. It would be interesting to perform mechanical testing in the laboratory or to model the entire structure.

Reysenbach De Haan (1966) wrote that the only function of the muscles would be to cause a peristaltic movement that would help with the expulsion of epithelial cells and the interchange with seawater. Although we agree that these muscles could change the shape of the ear canal, and cause a possible peristaltic movement (Link GIF), the seawater hypothesis does not fit into our hypothesis of the ear canal as a pressure sensor with rapidly adapting SNF. Seawater that is trapped in the ear canal would not change its volume under changing pressure conditions, and would therefore not allow for a tissue deformation essential for triggering the lamellar corpuscles.

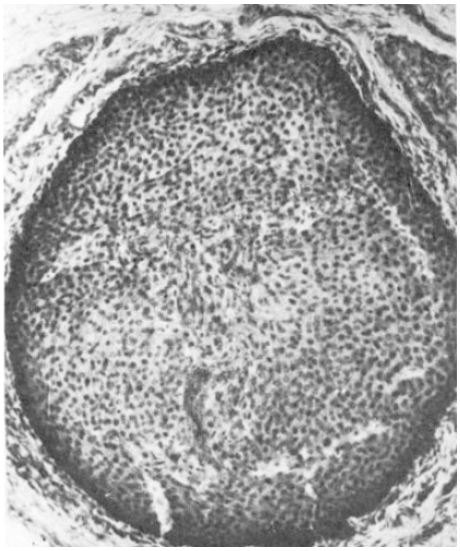

Figure 303. Closed lumen in the ear canal of a bottlenose dolphin (Solntseva, 1990). This figure shows remarkable similarity with the closed ear canal in baleen whales (De Vreese et al., 2014, Figure 7), and with some of the images in this study such as for the common dolphin.

1.3 Epithelium

In all specimens, the epithelial lining was a continuation of the skin, presented with a pigmented, stratified, squamous epithelium with incomplete keratinization (with small pyknotic nuclei), except for the beaked whale, which was the only specimen that presented a true keratinized epithelium (i.e. without nuclei in the superficial cells layer). Parakeratosis is a normal finding in mucous membranes (Kumar et al., 2014), and the configuration was the same as reported in other delphinids, as in mysticetes (De Vreese et al., 2014; Yamada, 1953).

The epithelium is a continuation of the corium, marked by squamous epithelium, with dark-coloured pigment (brown to black). However, there was interspecific and individual variation among delphinids, which correspond to the variation in the pigmentation pattern of the skin (body, head, and around the external ear opening. Also Cuvier´s beaked whale and long-finned pilot whale presented the same configuration, similar to Baird´s beaked whale (Yamada, 1953), and other reports of pilot whales (Fraser and Purves, 1960).

Similar to the skin, the epithelium is surrounded by a layer of intensely vascularized dermal papillae. On the other hand, the presence of glands indicates a mucous nature of the lining of the canal rather than a simple continuation of the skin. This situation is very similar to the spiracular cavity in odontocetes, which presents a squamous epithelium and the presence of (nasal and nasofrontal) glands (Degollada, 1998).

In the TEM images of the lamellar corpuscles, we noted desmosome-like junctions between adjacent lamellae of the lamellar corpuscles, and also in the epithelium of the ear canal of the striped dolphin. In the histological images of the epithelium, the epithelial cells desquamated at the level of the stratum corneum, which is where the desmosomal connections between cells lose their structure and

strength. Similarly, in baleen whales, there is proof of desmosomal connections in the ear canal lining of bowhead whales (*B. mysticetus*), and the authors suggested that these connections play a role in the shedding of skin layers, as they saw a difference in cadherin distribution/presence between spring- and autumn-caught whales (Rehorek et al., 2019a). Such techniques have not yet been applied to the epithelium of the ear canal in toothed whales, although they have been shown in cetacean skin (Cozzi et al., 2017; Reeb et al., 2007), and the results are likely to be similar. Toothed whales skin epithelium presents a high cellular production rate and rapid sloughing of the external cells, and has a 'self-cleaning' function as it keeps a smooth surface which assists in hydrodynamics and limits bio-fouling (together with the nano-rough skin with microscopic pores (Baum et al., 2002).

The term 'incomplete keratinization' might seem a premature term in this case, because the most apical cell layers as seen in the histological and ultrastructural slides is not keratotic, but shows active interaction with the luminal content. However, it is likely that in those images, the superficial cell layers were missing due to post-mortem tissue degeneration, or artefacts of the preparation. The presence of multiple degenerative artefacts did not allow us to get an overview image that indeed included the full epithelial thickness in many specimens. Therefore, the correct term for the epithelium, at least at the location of the samples, could indeed be incomplete keratinization.

This study involves the first ultrastructural findings on the epithelium of the external ear canal in toothed whales. The mammalian external ear canal epithelium has been subjected to few ultrastructural studies, most of which focused on the tympanic membrane (e.g. Hentzer, 1969; Lim, 1970; Kawabata and Ishii, 1971; Shimada et al., 1971; Harada, 1972, 1983)) or the epithelium of the canal closely associated with the tympanic membrane, to study epithelial migration and growth (Kakoi and Anniko, 1996a, 1996b), but none looked at the membranous of the canal. Further studies on the ultrastructural features of the epithelium (TEM in fresh species), and the composition (e.g. PanCk, cadherin) could give more insight into the processes at play, and contribute to the comparability between toothed and baleen whales.

Whether the epithelial cells show interaction with the lumen of the ear canal, is not well understood. The structures associated with the interaction with the canal lumen could be indications of various stages of interchange processes, most likely exocytosis. However, as more superficial cell layers could have been missing, and similar structures were seen in the intercellular artefactual space between epithelial cells, we cannot state with certainty that these are exocytotic products, but could be in fact signs of cell-cell interaction. However, the extensive glycocalyx on the apical plasma membrane resembles knob-like microvilli as demonstrated in several luminal organs, such as the human endometrium (Campbell, 2000), the mouse gall bladder (Kuver et al., 2000), for example. Also, according to Dahm et al. (2011), the presence of intraepithelial vesicles and various stages of

endocytotic/exocytotic protrusions along the plasma membrane would indicate exchange processes between the epithelium and lumen, at least in the vertebrate eye (Cfr. Figure 10 of Dahm et al., 2011). The glycocalyx, or pericellular matrix, is a layer of glycoproteins and –lipids, attached to a cell´s plasma membrane via transmembrane proteins. It has various functions, depending on the tissues it is associated with. In the ear canal, it might function as a barrier that protects against harmful elements or be associated with endo- or exocytotic processes. The first option could likely be valid for the external ear canal. However, the presence of vesicles within the lumen could indicate an apocrine secretion process with the cell membrane forming vesicles around (currently unknown) cytoplasmic content. The presence of intracytoplasmatic vesicles might be related to different processes, e.g. merocrine secretion (If it would be whole vesicle secretion then the intraluminal vesicles would have a double membrane, which we could not observe). The intracytoplasmic vesicles have a bright mottled content and an electron-dense membrane that is sometimes double.

Similar findings have been mentioned in the epithelium around the tympanic membrane of the rat (while absent in guinea pig), more specifically in the annular region close to the tympanic membrane (Kakoi and Anniko, 1996a, 1996b). However, in those studies, no other regions of the ear canal were investigated so we cannot conclude if this a generic feature of the entire ear canal epithelium. However, the finger-like projections seem morphologically different from our knob-like cilia with extensive glycocalyx, and the authors also say that those ´projections´ were said to be formed by the combination of *cytoplasmic protrusions and desquamation products*. Our findings agree with the former, but do not indicate to be products of desquamation processes as we consider desquamation to be a process that involves the entire cell. We do acknowledge that desquamation processes occur throughout the entire canal, but that it might be unrelated to the possible exocytotic processes described here, or to associations with adsorption or endocytotic processes.

1.4 Glandular structures

The glands are easily missed in histological preparations as they occur only in a short section of the ear canal. This was probably why Boenninghaus (1903) described the external ear canal in harbour porpoises as a *membranous tube* but did not note the presence of glands, and similarly, Reysenbach De Haan (1957) mentioned the absence of any type of glandular structure in the ear canal or skin around the external ear opening in long-finned pilot whale and harbour porpoise. In contrast, we did find glands in both species, although not in either of the Cuvier´s beaked whale samples[1], and neither did Yamada (1953). Although these were likely overlooked, it cannot be excluded that Cuvier´s beaked

[1] Sidenote: the beaked whale was the only species that presented a true keratinized epithelium, and it was also the only species in which no glandular structures were observed. Could it be that the two findings are associated? It would be interesting to do a further processing of the tissue blocks, and to apply Alcian blue stain to one of the sections with luminal content to see if there is the presence of glandular content in the lumen.

whales do not possess glands, nor that there is an individual variation in the presence or location of glands, although the latter is not considered likely.

The results in this study confirm and expand on the configuration of glands in toothed whales, which are simple to compound tubuloalveolar/-acinar glands with secretory cells of the holomerocrine secretion type, i.e. merocrine with elements of holocrine (De Vreese et al., 2014; Solntseva, 2007)(Figure 304). The secretory units were identified as of (tubulo-)alveolar nature by Solntseva (2007), although referenced by Cozzi et al. (2016) as tubuloacinar. The difference between the two is the size of the lumen, which is larger in alveoli. Our studies comply with the latter source, but also demonstrate the difficulty of a comprehensive interpretation of post-mortem structures, especially since the glands are one of the first structures to undergo post-mortem degeneration. Because the glands present such a rapid degeneration, the comparison with terrestrial mammal's glands was not performed in detail. In terrestrial mammals, the cerumen is the product of ceruminous and sebaceous glands, that present apocrine and holocrine secretion modes respectively (Stoeckelhuber et al., 2006), as also noted in northern giraffe and roe deer in this study. In contrast, in cetaceans, there is a single type of auricular glands. The secretory product, visible in the excretory ducts and the external ear canal, was similar to other descriptions, namely homogeneous eosinophilic with basophilic granules and pyknotic nuclei, only present at the level of the glands, not deeper. This finding is similar to the description in delphinids (Solntseva, 2007), but in contrast to Baird´s beaked whale Yamada (1953). The significance of glandular cells with pyknotic nuclei is not entirely clear.

The post-mortem degeneration might have also complicated the detection of myoepithelial cells, which could not be confirmed in any of the animals in this study, but has been reported associated with the secretory tubuli and acini, while absent in the excretory ducts in delphinids (Solntseva, 2007). Solntseva (2007) alluded on the possibility that the glands could participate in producing a protein-emulsion that could fill the peribullar sinuses. However, there is no direct contact between the glands in the ear canal, and the spaces of the ventral sinuses and middle ear[2], as they are separated by the tympanic membrane, which is assumed not permeable for the glandular product.

Since the ear canal is a canal that is closed on one side, there is no occurrence of natural erosion of desquamated epithelial cells through a unidirectional passage of the luminal content. In baleen whales, because the ear canal is permanently closed, this results in an accumulation of epithelial and glandular product. This is not the case in toothed whales, where the same desquamation processes

[2] The origin of the foamy substance in the ventral sinuses is not fully understood. Home (1812) found that the Eustachian tube in bowhead whale was lined with a simple glandular epithelium. Hunter (1787) noted a seemingly glandular epiuthelium near the exit in the nasopharynx. Mucous glands in the ´Eustachian sacs´ (Anderson (In Fraser and Purves, 1960). The pterygoid sinus lateral wall has mucous glands (Fraser and Purves, 1960), although we could not identify them in this study.

and glandular production takes places, but where the glandular product assists in the expulsion process of desquamated cells, similar to terrestrial mammals. Whether this process might be accompanied by an exchange with seawater, is not clear yet, although terrestrial ear wax does have water-repellent properties (Guest et al., 2004). Besides this, the glandular product could protect against frictional damage caused by internal rubbing of the epithelial walls or be associated with any type of exogenous material that might cause friction (Stoeckelhuber et al., 2006). As such, the glandular product could facilitate any movement by reducing abrasive forces. Also, it has not yet been studied whether the product in cetaceans might have other qualities, such as antimicrobial and antifungal properties, as reported for human ear wax (Lum et al., 2009; Özcan, 2005; Schwaab et al., 2011).

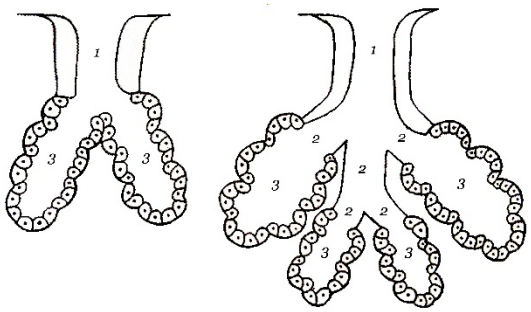

Figure 304. Schematic drawing of the basic building blocks of the auricular glands made of simple or compound tubuloacinar/alveolar or a combination (tubuloacinar in Cozzi, 2016) glands as found in a common dolphin (left) and a bottlenose dolphin (right) respectively. 1. excretory duct; 2. intercalated duct 3. alveolus/acinus; (Source: Solntseva, 2007)

1.5 Ear canal-associated lymphoid tissue

The lymphoid tissue associated with the ear canal was presented in three locations and in various states of activation. The first is the circummeatal presence of mononuclear cells at the level of the glands, in the subepithelial layers, scarce and in low concentrations, although it is sometimes visible in clusters. It likely considers a resident population forming part of a first barrier immune system, and which could also be noted in the activated state in some animals (e.g. the case of the long-finned pilot whale). The second is the presence of mononuclear cells in the medial half of the canal between the ear canal and the cartilage, also as a resident population or activated state. The third would be the more or less well-defined lymphoid tissue situated ventral to the ear canal before it reaches the tympanic bone, at about the level of the facial nerve crossing (e.g. 3D reconstruction striped dolphin). The presence of lymphoid cells in the lamina propria of the ear canal of toothed whales has been reported in few cases as a full circummeatal lymphoid organ (Baird´s beaked whale, sperm whale, and pygmy sperm whale) (Yamada, 1953), which was described in Baird´s beaked whale as subepithelial lymph follicles with “many crypts and lymphoid infiltrations of the epithelium, which has transformed into a peculiar lymphoid organ similar to the tonsils”. According to this description, it is the epithelium itself that shows transformation, and which, together with a subepithelial infiltration of lymphocytes,

forms a well-defined lymphoid organ. It is not entirely clear to what extent the epithelium itself was involved, and whether the subepithelial lymphoid infiltrations formed the tonsil-like organ. In this study, there was never any intraepithelial infiltration with lymphoid cells in any specimen, although the subepithelial infiltration was a common finding. Also, in the sperm whale, there was a very extensive peri-meatal subepithelial lymphoid organ at the level of the blubber layer, divided into lobules with deep crypts and many germinal centres. Those descriptions seem to be a combination of the findings of our study, as the subepithelial tissue does form follicles, but was never so well-defined as a tonsil-like organ, which would be the actual lymph node (see below). In any case, Yamada´s findings refer to the activated state of the circummeatal lymphoid tissue, which is consistent with this study in that we found subepithelial lymphoid tissue in almost all specimens, activated in some and latent in others.

The lymphoid tissue in the subepithelial layer forms part of the mucosa-associated lymphatic tissue (MALT) which comprises among others the gut-, nasal-, bronchus-associated lymphatic tissue. It was not organized as a well-defined structure or mass, but rather diffuse, making it part of the diffuse mucosa-associated lymphatic tissue (D-MALT). Similarly, lymphocytes associated with glandular structures occur in various cetacean mucosae such as the nasal sac system (Degollada, 1998), the larynx (Smith et al., 1999), intestines (Cowan and Smith, 1999), and anus (Cowan and Smith, 1995). Also, the presence of lymphoid cells is a common finding in the mucosa of terrestrial mammals and humans. For example, in the human pharynx, lymphocytes are frequently seen in the lamina propria lining the cavity, while they also appear in accumulations, called tonsils, situated around the opening of the digestive and respiratory passages (Lutz, 2009).

The lymphocytic populations in the connective tissue between ear canal and cartilage are likely to have a similar function and form part of the same ear canal-associated lymphoid tissue. They were not spatially associated with glandular structures, but rather with the vascular lacunae, indicative of an intricate relation with systemic functions.

In the few case description provided in the results section, there were indications of a haemolymph node (a.k.a. haemal node). To date, there are no descriptions of the presence of haemolymph nodes in cetaceans. There is one source mentioning that cetacean lymph nodes, on top of their role in the immune system, could be charged with the breakdown of old red blood cells, while the same accounts for land mammals (Slijper, 1958). There was no clear distinction between cortex and medulla, similar to the ruminant haemal node (Zidan and Pabst, 2010)(online example bovine), and there was far more heterogeneity in the general structure such as with the distribution of the presence of red blood cells, the patchy zones in the parafollicular tissue, and the partial absence of a connective tissue capsule. Interestingly, the capsule contained lamellar corpuscles amongst the connective tissue. We suspect

that in some cases, there can be organised lymph or even haemolymph nodes or activated lymphoid tissue, which might have been missed in specimens in which the circummeatal soft tissue was dissected to close to the lumen, and there might also be a variation in the location of the lymph tissue. Haemal nodes can be identified from the combination of their macroscopic and microscopic presence of blood (although this has to be distinguished from a haemorrhage, which will lead to erythrofagocytosis), and they do not have lymphatic vessels. Therefore, to distinguish between a lymph node and a haemolymph node, one should look to distinguish the presence of blood and lymph vessels. To do this, it proves useful to apply IHC with markers specific for lymphatic endothelium (Cfr. Van den Eynden et al., 2006) and a pan-endothelial marker such as anti-CD34 for control. Markers specific for lymphatic vessels include Prox-1, Lyve-1, podoplanin, and D2-40, of which the last two are considered the most specific and sensitive for lymphatic endothelium (Evangelou et al., 2005). An alternative approach, although less specific, would be to use factor-VIII (von Willebrand factor). The immunoreactivity of factor-VIII in lymphatic vessels is far less intense than in blood vessels (Noda et al., 2010), therefore, if both are present in the lymphoid tissue, there should be two distinct intensities in the endothelium-lined vessels.

To distinguish between lymphoid and non-lymphoid tissue, the presence of high-endothelial venules (HEV) could also give an indication. HEV are blood vessels with a specialized cuboidal epithelium, which are prominently present in lymphoid tissue and enable for circulating lymphocytes (B and T) to migrate from the blood circulation into the lymphoid tissue (Girard and Springer, 1995). To show the presence of HEV, the best and most specific marker for HEV is the monoclonal antibody MECA-79 (Streeter, 1988), and further studies could provide more insight into the functional morphology of lymphoid tissue in cetaceans.

We also found a diffuse lymphoid tissue in the penis and the mammary glands. It would be interesting to map the occurrence of such tissue in the body of toothed whales.

Once there is more information on the cellular composition of the tissue, one could compare the lymphoid tissue among cetaceans (cfr. Beineke et al., 2001, 2010; Díaz-Delgado et al., 2018; Centelleghe et al., 2019). For identification of the types of lymphocytes that are present in the tissue, we could distinguish between T- and B-lymphocytes using the antibodies that have already been successfully applied to cetacean tissues. That is CD3/CD5 and CD20 for T- and B- lymphocytes respectively (Centelleghe et al., 2019; Díaz-Delgado et al., 2018).

The (haemo)lymphonodal tissue described here, is not likely to be visible macroscopically under non-pathological conditions, while at the same time there might be microscopical indications. Its identification was not conclusive as it might belong to the parotid, mandibular, or superficial cervical

lymphocentre (De Oliveria e Silva et al., 2014). When encountering such nodes as described here, there was always an activation of the lymphoid tissue.

1.6 Fat and connective tissue – fibro-adipose sheath

In all species, although with variety in conformation, there was fat tissue in the close surrounding of the ear canal from just beneath the skin layer, which was gradually overtaken by connective tissue over the course of the canal to the medial end. The adipoconnective tissue and the more or less distinct fibro-elastic tissue capsule were present in all species, although more defined and separated from other tissues in some species more than others. It forms a rigid but flexible connection between the skin, blubber, musculature, cartilage, and the dense connective tissues close to the middle ear and the bones of the skull. As such, it unites the different soft tissues and renders them into a single functional unit. While it seemed to separate the ear canal tissues from the acoustic fat body situated ventral to, this relation is not fully understood yet.

Similarly, Reysenbach de Haan (1956) wrote that in the superficial part of the ear canal there is very little connective tissue in the wall of the ear canal, although it shows an intricate relation with the epithelium through the (dermal) papillae. The ear canal travels through the blubber, and only then the connective tissue increases gradually on its progression towards the middle ear. The connective tissue fibres run parallel to the ear canal. Then, muscle fibres appear, also running parallel to the ear canal, although the inclination between muscle and ear canal becomes crooked/sharp in deeper tissue, before coming to a sudden decrease until there is no longer muscle tissue present. At the level of the muscles, the connective tissue, which continually grows more prominent on the course to the middle ear, contains various cartilage tissue lobes that unite towards proximal and form a trench that never fully encloses the ear canal. Similar to the findings in this study, such a connective tissue capsule was also mentioned in harbour porpoises where it was described it as dense and “extremely strong”, and which made up the connective between the cartilage of the ear canal and the ventral side of the squamosal bone (Boenninghaus, 1903).

The presence of elastic fibres in the blubber is known in a variety of cetaceans species (e.g. Hamilton et al., 2004), and also associated with the ear canal in pinnipeds (Kastelein and Dubbeldam, 1996; Loza et al., 2019). As such, the blubber makes a pliant, composite tissue made up of an adipocytic matrix and structural fibres of collagen and elastin, which permits relatively large-scale deformations (Hamilton et al., 2004). In Cuvier’s beaked whale we noted a sheath of fibro-elastic tissue encircling the ear canal, visible in the superficial section in the blubber layer to the deeper section where it had a diameter of about 1.3 cm and where it transgressed into a fibro-muscular capsule with distinct auricular muscles in two layers, internal circular and peripheral longitudinal. This tissue is likely the same fibro-adipose tissue that was mentioned by Yamada (1953) in a *Berardius bairdii*, which gradually

grows in diameter until 2 cm just under the blubber. It consists similarly of collagenous fibres orientated in a circular direction with marked adipose tissue among the fibres, and in which the auricular muscles insert (Yamada, 1953).

Curiously, although Palmgren's stain was intended for highlighting nerve fibres and sensory nerve formations, it did show a striking difference in the connective tissue layers surrounding the ear canal by making clear differences between the loose subepithelial tissue, in which the nervous structures stained similar to the connective tissue and even the epithelium, and the dark brown staining of the peripheral connective tissue layer. The underlying reason is not apparent yet.

Although the adipoconnective tissue and the fibro-elastic capsule are present in all species, there might be differences in the composition and ratios between connective, elastic, and adipose tissue. In all species, the ratio of fat vs connective tissue is high near the surface and gradually reverses towards medial, while the concentration of elastic fibres has not been studied yet. In all species, there seems to be more flexibility and the possibility for movement in the tissues closer to the skin, while deeper tissue would be more rigid. This configuration might facilitate a graded deformation of the canal with changes in external parameters such as the pressure associated with diving depth (see hypothesis on external ear canal as a sensory organ). Although this morphofunctional unit is assumed to provide both rigidity and flexibility and resilience to mechanical deformation, this puts into question the species-specific differences and the relation with the ecological niche. For example, would the elastic tissue concentration be different in deep versus shallow divers?

Also, although its significance is still unknown, it was interesting to note that there was adipose tissue around the ear canal from its course through the fat of the blubber layer, down to deep sections close to the middle ear, where it overlayed a distinct, and likely acoustic, fat body. As such the fat formed a kind of fatty cloak around the ear canal. This conformation was similar in all odontocete species and is likely to be a general quality for odontocete species in general. The development of fatty tissues associated with the ear canal is also the case in seals, and similarly, all marine fauna, including sea turtles and marine birds, while at least in toothed whales (and possibly also baleen whales) these fat bodies are directly or indirectly associated with hearing and the sound reception pathway. It could be interesting to study the structural and molecular characteristics of the toothed whale ear canal fat, to compare with blubber fat and acoustic fat of the mandibles and the melon, to gain better insights into its function.

1.7 Relation with the acoustic fat bodies

There is a need for a better understanding of the interrelations between the external ear canal soft tissues and the mandibular fat bodies and their branches, which could be interesting in the scope of elucidating the peripheral sound conduction pathways. Multiple sound reception pathways have been described using various techniques, and the fat bodies have been described having several locations in which sound can enter from the exterior (e.g. Ketten, 2000), while also showing branching patterns and at least two points of interaction with the TP-complex (Cranford et al., 2010). Few sources describe the multiple lobes of acoustic fat bodies including the intra- and extramandibular bodies, and even fewer mention the presence of a lateral fat body that runs in parallel to the external ear canal (Ketten, 1994, 2000; Wartzok and Ketten, 1999). Although such a 'lateral pathway' was already suggested in the early '90s (Popov and Supin, 1990a, 1990b), only Ketten and colleagues described this fat body, shaped like a trumpet with its opening projecting posterolaterally, and which is also in contact with the tympanic bone (Ketten, 1994, 2000; Wartzok and Ketten, 1999). A similar structure was found in mysticetes (Yamato et al., 2012). No other studies have confirmed the presence of such a lateral fat body, while the indications given in the histological and macroscopic images in this dissertation open up the discussion on its very existence and the techniques with which it can be studied or at least detected (medical imaging, gross dissection, histology, etc.). For instance, there exist online sources of medical imagery depicting 'tri-lobed' acoustic fat bodies in odontocetes: e.g. in Atlantic white-sided dolphin (*Lagenorhynchus acutus)*: LINK; and Cuvier´s beaked whale: LINK. Rauschmann et al. (2006) explicitly stated they did not find this lateral fatty channel in medical images of perinatal dolphins, while it is mentioned by Cozzi et al. (2017) as part of a possible *(external) lateral acoustic pathway*. The morphology of the acoustic fat bodies, intra- and extramandibular and lateral, bi- or trilobed, and the exact pathways, single or segmented, are still not understood, and although the external ear canal has no role in the actual sound conduction from the exterior to the middle ear, there is an intricate spatial association between the ear canal and the fat bodies, which deserves more attention.

1.8 Cartilage

The structure of the cartilage was similar in all species, with a gutter-like entrapment of the ear canal at the proximal end, flattening out towards lateral, turning dorsally, following the canal´s curvature (Purves and Pilleri, 1983) and projecting several cartilaginous flanges, although with individual variation (cf. most studies, back to Boas, 1912). These variations included for example a split in the ventral side of the cartilaginous trench in a bottlenose dolphin. The shape was often too complex to fully grasp without a 3D visualization but concurs with the limited descriptions of cartilage shapes in other toothed whales (*Phocoena* sp. and *Delphinus spp.*) (Boenninghaus, 1903; Boas, 1912).

Even though toothed whales do not possess a pinna nor present primordial auricular hillocks during ontogenesis (Štěrba et al., 2000), the cartilaginous formations are not a rudiment of the pinna (Kükenthal, 1891). However, the cartilage, together with the ear canal embedded in fibro-elastic tissue, could be regarded as homologous to the pinna in terrestrial mammals (Purves, 1966), although not sharing the same function, i.e. a funnel that collects sound waves and directs them into the auditory canal. There is also a morphological similarity with the terrestrial mammal pinna, as the cartilage´s distal extremity projects several dorsolateral flanges in a complex configuration, but the interpretation of the shape and the link to its function is not fully clear yet.

Purves (1966) described several parts of the auricular cartilage with the terminology used for the terrestrial mammal pinna. The *helix* would be considered the cartilaginous trough containing the EAM. The anti-helix, a reniform fibro-elastic lobe that projects from the ventral aspect of the mastoid process of the squamosal, rostral to the musculature, and overlying a cartilaginous trough of cartilage that contains the ear canal in its concavity. The complex shape of the cartilage, with a main body and various fingers, plates, or flanges that can project from it or are possibly even disconnected from it, does accurately describe the situation. It is still unknown if the laterally directed flanges might be disconnected from the main body in some individuals or species, and what this would imply. The complex configuration of the cartilaginous flanges is likely the reason why there were sometimes considered several irregular cartilages, which were considered to share a common ´cellular membrane´, allowing for motion and likely lengthening and shortening of the ear canal as "the animal is more or less fat", implying seasonal variations (Hunter, 1787; Purves, 1966; Reysenbach de Haan, 1956). Although the 3D reconstructions in this study of striped dolphin and harbour porpoise only showed a single cartilage body with connecting flanges, which is also in accordance with the description made by Boenninghaus on the ear cartilage in harbour porpoise (Boenninghaus, 1903). He also regarded the ear cartilages in toothed whales as an internal pinna, which, compared to the ear cartilages of seals, are permanently 'retracted' into the internal soft tissues. The 3D configuration of the cartilaginous fingers projecting at the distal end is unknown, and further characterisation of the auricular cartilage in various toothed whale species would be interesting to understand its functions and adaptations. More information (i.e. higher resolution reconstruction) is needed to understand whether they form part of an incomplete segmentation as occurs in eared seals, or a complex shape as in true seals (Loza et al., 2019), or is more similar to the auricular cartilage in walrus (Kastelein and Dubbeldam, 1996) or other marine mammals.

Interestingly, Purves´ findings such as the mesially directed distal extremity of the cartilage and a cartilage that fully encloses the ear canal at its proximal end, does not concur with this or most studies (Purves, 1966). The incomplete sheathing of the ear canal by the cartilage at the proximal end

advocates morphological similarities with the dolphin trachea in that the cartilage is dorsally open, and secondly, there is the presence of vascular lacunae between lumen and cartilage (Cozzi et al., 2005). As such, there is likely a functional similarity in this configuration, which might be expressed as an air-trapping organ with a soft tissue distal part, and a cartilaginous proximal part, which is adapted to prevent the lumen from collapsing easily, or at least under more extreme conditions than is the case for the associated soft tissues in the distal half of the ear canal, and the lungs respectively. This supports the hypothesis that while diving, the ear canal lumen could collapse gradually from distal to proximal leaving the compressed air trapped at the medial end of the canal, abutting the tympanic conus, while there would be pressurized air on the other side of the tympanic conus, around the ossicular chain (Cozzi et al., 2017). The horseshoe-shaped cartilage would impede the ear canal to collapse, at least to a certain extent. At the same time, the vascular lacunae could act as incompressible, but expandable structures that, together with a certain elasticity of the cartilage, could cope with slight movements of the ear canal and associated soft tissue structures. This might be essential for a correct functioning of the tympanic conus, even though its function is currently still under debate.

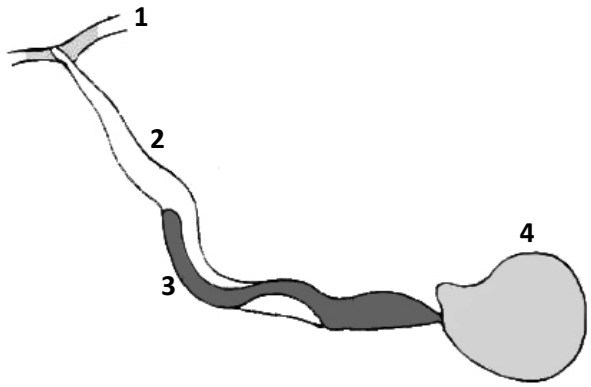

Figure 305. A simple drawing of the position of the cartilage (dark grey) associated the external ear canal in harbour porpoise. 1. skin; 2. external ear canal; 3. Cartilage; 4. TP-complex (modified from to Boas, 1912)

To date, there exists no detailed histological description of the auricular cartilage in cetaceans. The tissue composition of the auricular cartilage showed hyaline cartilage that did not stain for elastic fibres (AOG). However, this study should be repeated with more samples and a variety of staining techniques (e.g. Various Orcein stains, trichromic stains, reticulin, PAS, Giemsa, Alcian blue, etc. to thoroughly compare between species, cfr. Loza et al., 2019). According to Fraser and Purves (1960), all odontocete possess elastic fibro-cartilaginous masses, although it is not specified if the elastic fibres are inside the cartilage. It seems to contrast the general rule that auricular cartilage contains elastic fibres to some extent in most mammals, at least in one part of the ear canal, which includes the situation in most pinnipeds (Loza et al., 2019). In rats and rabbits, the auricular cartilage is composed of true elastic-lipocartilage where the chondrocytes are known as “lipochondrocytes” (Ahmed and

Abdelsabour-Khalaf, 2018; Boas, 1912; Bradamante et al., 1991). Although fat has been described around and in close association with the cartilage of toothed whales (this study), baleen whales (De Vreese et al., 2014), and pinnipeds (phocids and walrus)(Kastelein and Dubbeldam, 1996; Loza et al., 2019), no true lipocartilage has been found in any marine mammal.

It would be interesting to study the macroscopic anatomy, histology, and nature and arrangement of the chondrocytes and their territories within the extracellular matrix in a transverse and a longitudinal section, and to compare with other marine or semi-aquatic mammals and terrestrial mammals. E.g. there are significant differences between phocids and otariids with a range of intermediate configurations in between (Loza et al., 2019). We did note that in the toothed whale cartilage, independent of the size of the species, blood lacunae were not present, in contrast to the situation in the giraffe. Also, Purves (1966) described the auricular cartilage as 'practically nonvascular', which might indicate that a peripheral blood supply could be sufficient as the cartilage is relatively small, or that the cartilage is more 'alive' in terrestrial mammals than in delphinids, which could be useful for regenerative purposes.

1.9 Musculature

Although it was difficult to identify the different muscles associated with the external ear canal, especially to distinguish the origins and insertions, both the results and the difficulties we encountered are similar to previous reports in various toothed whales (e.g. Boenninghaus, 1903; Hanke, 1914; Purves, 1966). Moreover, the discrepancies in the nomenclature (e.g. Hanke, 1914, p. 17) complicated the correct classification and interpretation of the distinct muscles.

Our results indicate that the zygomatico-auricular muscle, which inserts into the adipoconnective tissue all around the external ear canal (completely encircling but with muscle fibres running longitudinally, so does not function as a constrictor/sphincter muscle) at a level lateral to the downward spiral. The cartilage, fibro-elastic tissue capsule, and external ear canal, could be considered a functional unit at this point, onto which the zygomatico-auricular muscle could exert a pulling force in rostromedial direction, and the occipitoauricular muscle in caudomedial direction, making the transverse S-shape more pronounced. We suspect that this might also exert a force on the ear canal and its lumen and might help to exert an indirect force on the glands and its production into the lumen, and might help to move any content or air over the course of the lumen with changes in diving depth (cfr. Reysenbach de Haan, 1956). Boeninghaus (1903) described in detail the musculature of the ear canal of the harbour porpoise but did not consider them to have any functional value. Fraser and Purves attributed a "sound-regulating" function to them as they considered the ear canal as having the same function as in terrestrial mammals.

In terrestrial mammals, the external ear contains several intrinsic and three extrinsic muscles. The extrinsic muscles insert into the cartilage of the pinna and serve to move the auricle in various directions (Dyce et al., 2010). The functionality of these muscle in humans remains elusive, and the muscles are considered vestigial (Liugan et al., 2018). The homologation between the auricular muscles in terrestrial mammals and cetaceans is unclear (Boenninghaus, 1903; Huber, 1934).

Regarding the function of the various muscles, Boenninghaus (1903) believed they were are evolutionary remnants without a function. Slijper (1958) speculated that the muscles, in cooperation with the sigmoid shape, might adjust the shape of the external ear canal in various condition states of the tissues, meaning that the blubber layer changes thickness with the seasons and that the shape of the canal would adapt to the thickness of this layer. However, this was framed in the hypothesis that the ear canal still served its original function as a sound conductor, similar to Fraser and Purves (1960), who assigned a sound-damping function to the muscles as they would exert traction on the walls of the canal. Reysenbach De Haan (1966) wrote that the only function of the muscles would be to cause a peristaltic movement that would help with the expulsion of epithelial cells and the interchange with seawater, as he believed the canal was filled with seawater. All authors seemed to agree that the musculature could change the shape of the curvature of the canal in some way, but the implications this might have are unknown to date.

Also, there is no knowledge of a surfactant present in the canal, so in the case of a local collapse during diving, the muscles might help to open it back up during ascend. The function of the other muscles remains elusive, although they could all have an impact on the degree of curvature of the canal, adjust the tension on the soft tissues, assist in the expulsion of content, or even act on the lumen diameter in the place of insertion (see above, Lumen and content, and below, Function) (cfr. (Fraser and Purves, 1960; Purves, 1966; Slijper, 1958).

1.10 Blood supply

In terrestrial mammals, the blood supply is provided mainly by branches of the external carotid artery, namely the posterior auricular, superficial temporal arteries, the occipital artery, and the deep auricular branch of the maxillary artery (< external carotid), while the venous drainage following the arterial descriptions. The maxillary artery plays a crucial part in the blood supply of the peripheral tissues of the head in toothed whales (Costidis and Rommel, 2016a), although its role in the supply of the external ear canal and associated tissues is still to be investigated in detail.

The vascular lacunae, situated between the ear canal and cartilage in the medial third to half of the ear canal, are a peculiar evolutionary trait uncommon to terrestrial mammals. See also ‘Cartilage’ and the functional comparison with the trachea (Cozzi et al., 2005). Reysenbach De Haan (1957) presented histological transverse sections of the ear canal of a long-finned pilot whale that contained large round

structures labelled as veins situated between the canal and cartilage. These were only seen in the images and not discussed in the text. The vascular lacunae are not filled with pure blood (See Masson's Trichrome) and are lined with an endothelium (See IHC vWf), which could point out that these are filled with serum and could be lymphatic vessels. However, such a conclusion cannot be drawn with absolute certainty.

The DAKO Rabbit Anti-Human vWf was not validated using Western blot or any other method. The used antibody (DAKO, Code A0082) does cross-react with antigens of mammals of various orders, including the cow, which belongs to the Cetartiodactyla, and was therefore assumed to show true positive staining in the striped dolphin. However, it would be interesting to investigate a further characterization of the lacunae, including the functional characteristics (mechanical (expansion) and physiological (exchange)), and to carry out WB for complete validation.

Such vascular lacunae also occur in the tunica mucosa of the nasal conchae in terrestrial mammals, where they can be seen as thin-walled, cavernous sinusoids, a.k.a. cavernous bodies (*corpora cavernosa*) (Link Histology). They are connected to shunt arteries and are functionally similar to the cavernous bodies in the genital organs, i.e. erectile tissue (Esipov, 1982; Lutz, 2009). However, while the genital cavernous bodies are lined with a non-keratinized stratified squamous epithelium, the cavernous bodies in the conchae possess vascular walls, like in the ear canal in this study. This vascular wall presents physiological adaptations with muscular tissue, which was not studied or observed here, and which would aid in preventing (or possibly facilitating) fluid loss/exchange (Esipov, 1982; Grevers and Herrmann, 1987). This would also fit in the hypothesis of the odontocete ear canal vascular lacunae being able to change dramatically in volume while avoiding any fluid loss into (the space between the cartilage and) the ear canal.

Because the vascular supply of these lacunae (and the entire ear canal, see above) is still uncertain, and so are the physiological mechanisms responsible for the fluid management (filling/emptying), it would be interesting to see if there are also nitric oxide-containing neurons associated with the lacunae as shown in the trachea (Cozzi et al., 2005), which would imply a direct, local regulation of the fluid supply stimulated by mechanical stress, tension or compression.

1.11 Medial end of the ear canal

This study confirms that the external ear canal in all studied toothed whales has its medial end abutting the tympanic membrane, situated in the annulus tympanicus (bony tympanic ring; lower tympanic aperture) of the bulla (Mead and Fordyce, 2009))(cfr. Boenninghaus, 1903). As such, the situation is similar to terrestrial mammals. Most literature presents the same results (back to Hunter,

1787) even though an absence of contact between the ear canal lumen and the tympanic membrane (or temporal bones[3]) has been reported as well (Ketten, 1997, 2000).

First of all, we adopted the nomenclature of Fraser and Purves (1960a) and Nummela et al. (1999): the tympanic membrane is the equivalent to the tympanic membrane in terrestrial mammals, and the tympanic ligament is the triangular ligament that connects the tympanic membrane to the malleus. The term tympanic conus was used to label the whole of tympanic membrane and ligament (Nummela et al., 1999), but since there is no tympanic ligament in terrestrial mammals, the whole cone would correspond to the tympanic membrane in land mammals.

It is the medial end of the ear canal itself that forms a trumpet-like, or club-shaped expansion in all species, which is common in delphinids (e.g. McCormick et al., 1970), and was also mentioned by Yamada (1953) for Baird's beaked whale while he said it was absent in Cuvier's beaked whale. Since in our beaked whales' samples, the medial end was missing, there was no opportunity to verify this finding. Yamada (1953) also mentioned that in the expansion, the lumen was filled with a grey paste-like substance, which seemed homologous to the ear-plug in mysticetes. Such content could not be seen in any of our samples, as there was only the presence of scarce epithelial cells at this level, which did not occupy the entire lumen.

Our findings confirm that the tympanic conus is a concave cone of tissue, contained in the *sulcus tympanicus* of the bulla (Reysenbach De Haan, 1957). Different from terrestrial mammals its consists of two denominated structures, the tympanic membrane and the tympanic ligament that forms the connection to the manubrium of the malleus (Fraser and Purves, 1960). The entire structure is called the tympanic conus because of its elongated and conical shape (Reysenbach De Haan, 1957). It is not considered not have any 'major' role in the sound reception process (Nummela et al., 1999), and, it is not considered to have acquired any other functional significance in any process.

The toothed whale tympanic membrane is a thin but tough layer suspended in the tympanic aperture between the tympanic (sigmoid process, conical process, and anterior face of the posterior process) and the periotic bone. The findings corresponded to the histological configuration of the terrestrial mammal tympanic membrane, consisting of an outer cutaneous or epidermal layer (stratum cutaneum), an intermediate fibrous layer (lamina propria) with radial and circular arrangement of collagen fibres, and an inner mucosal layer (stratum mucosum) with a simple squamous epithelium (Sommerauer et al., 2012; Blanke et al., 2015; Van den Broeck, 2008). The histological structure of the tympanic membrane as reported in this study, also correspond to reports for toothed whales (Boenninghaus, 1903 (harbour porpoise); Fraser and Purves, 1960a (pilot whale); Solntseva, 2007

[3] In cetaceans, there is no single temporal bone, but is comprises four osseous parts: *pars squamosa* (a.k.a. squamosal bone), *pars petrosa* (periotic bone), *pars tympanica* (tympanic bone), *pars endotympanica* (the middle ear ossicles)(Mead and Fordyce, 2009).

(delphinids)). A pars flaccida in the intermediate layer was not noted, although this could have been missed. Similarly, also, Solntseva (2007) did not observe it in toothed whales.

Although there were small nerve fibres in the tympanic conus, we did not identify naked nerve endings or other sensory nerve formations using standard histological staining techniques. For this, immunohistochemical staining would be necessary.

The experiments carried out by McCormick and colleagues (1970) are compelling in proving that the ear canal, its surrounding tissues, and the tympanic membrane and ligament do not play a significant role in conducting vibrations from the external environment to the inner ear. Artificial removal of the medial end of the canal and the tympanic membrane did not impede any stimulation of the inner ear through vibratory stimulation (23.4 kHz) of the skin in the region of the ear opening (McCormick et al., 1970). Also, an application of artificial intraluminal positive or negative air pressure, which expanded the walls of the canal and applied pressure on the wall and the tympanic membrane, on either side of the tympanic membrane, or a perforation of the tympanic membrane, did not influence the cochlear potentials, and neither did a section through the tympanic ligament when the animals were exposed to a range of sonic and ultrasonic frequencies coming from an underwater sound source in the region of the head. It was concluded that the ear canal did not play a significant role in the ultrasonic sound reception process through skin vibratory stimulation (McCormick et al., 1970).

To summarise and hypothesise on the functions of the different components, we suggest the following, starting with an overview of the morphological findings: the medial third of the ear canal is a small, air-filled, funnel-shaped space, embedded in tissue with vascular lacunar plexuses, and entrenched in a horse-shoe shaped cartilaginous trough while being equipped with a 'sensory ridge' of well innervated subepithelial tissue that protrudes into the lumen. It lies opposite the tympanic membrane, which is a tough concave structure, suspended between bony components of the tympanic, with a pyramidal-shaped vascular plexus in its centre, and which continues as a broad and tough tympanic ligament, which tapers into an insertion on the malleus. For the middle ear to function correctly in conditions of high degrees of variation in pressure, there has to be a minimum amount of air surrounding the ossicles (Cozzi et al., 2017; Fraser and Purves, 1960). This is air-contained and directed into the middle ear by the expansion of the vascular sinuses and/or medial wall of the pterygoid and entire ventral sinus complex. At the same time, the tympanic ligament acts as a tension rod that, possibly together with the tensor tympani muscle, stapedius muscle, and holds the right amount of tension on the malleus and ossicular chain for those to function correctly. Such tension could be a constant or could vary between conditions with changes pressure (e.g. Ridgway et al., 2001). In any case, during diving, we assume the following procedure of events: the pressure in the middle ear cavity rises, this would put positive pressure on the tympanic membrane and medial end

of the ear canal, which would then increase the tension on the ligament, likely making the ear less sensitive (cfr. McCormick et al., 1970). What would be needed for a correct functioning of the middle ear components, is the correct amount of tension on the ligament, which implies a correct amount of 'dent' in the concave tympanic membrane, which is feasible to achieve by regulating the pressure on the other side of the membrane, i.e. the pressure in the air-filled medial half of the ear canal, and is possibly also associated with the amount of blood in the vascular lacunae. In humans, for normal functioning of the tympanic membrane and ossicular chain, there is a need for an equal amount of pressure on both sides of the tympanic membrane, especially noticeable during massive pressure changes (e.g. during diving, or in the aeroplane). In cases of increasing pressure, we close our nose and voluntarily increase the pressure in the middle ear cavity through increasing the pressure in the nasopharynx and pushing air through the Eustachian tube. In cases of decreasing pressure, we can apply indirect actions to open the Eustachian tube to let the excess air from the middle ear escape into the nasopharynx. The situation for odontocetes is similar but different in some ways. Because there is an artificial/closed lumen in the superficial sections of the canal, the air in the medial half of the canal is trapped and therefore constant. With increasing pressure, conducted through the non-compressible soft tissues, the ear canal lumen gets compressed passively. Such compression would occur from lateral to medial because of the configuration of the ear canal. In the lateral sections, there are only connective, adipose and muscular soft tissues, which allow for the ear canal lumen to collapse. Towards medial, the cartilage appears, first on one side of the canal, and projects several flanges around the canal in more medial sections. Together with the vascular lacunae, this would create a certain relative rigidity and would allow for the peripheral parts of the ear canal to be compressed before the medial parts do. As such, all the available air in the ear canal is directed towards the medial end and the tympanic membrane. At the same time, there is the sensory ridge that could be triggered by the changes in pressure and tissue configuration of the ear canal. As such, it could sense the intraluminal pressure or the contact with the opposing wall in case of lumen collapse. As it is configured in a ridge, this could allow for a precise auto-sensation of the tissue configuration along its longitudinal axis. As such, the dolphin could attain an equal amount of pressure on both sides of the canal, while obtaining an accurate, or relative sensation of the pressure and configuration within the canal, allowing them to know the depth at which they are present (see also below).

Finally, it was not an easy process to prepare the region of the tympanic membrane from several anatomical points of view without destroying the soft and hard tissues. The first essential step was a meticulous preparation of the gross anatomical region, followed by a period in acid decalcifier for several days, checking up regularly if the tissue was soft enough for histological sectioning before

tissue processing and paraffin embedding. Leaving the tissue too long in decalcifier destroyed the soft tissues and complicated the histological interpretation.

1.12 Innervation of the external ear canal

1.12.1 Cranial nerves

The only macroscopically visible nerve that could be identified to innervate the external ear canal is the auriculotemporal nerve (< mandibular < trigeminal). These findings in Stenella species, confirm the limited descriptions of innervation of the region of the ear.

The trigeminal nerve, the largest cranial nerve in cetaceans, exists the basicranium through the large cranial hiatus close to the periotic (i.e. combined opening of the posterior lacerate foramen, jugular foramen and internal acoustic meatus). The mandibular nerve appears medial to the falciform process, through a fissure formed by the alisphenoid, the periotic and the squamosal, where it gives off the weak auriculotemporal nerve. The auriculotemporal nerve turns ventrolaterally in the direction of the tympanic bulla and turns dorsally near the mandibular joint where it gives off several thin branches into the area of the external ear canal (Rauschmann, 1992). As in Stenella species, the trigeminal ganglion is responsible for the largest part of the innervation of the ear canal, through its auriculotemporal nerve and auricular branch, but also the facial, glossopharyngeal and vagal ganglia contribute to the innervation (Folan-Curran and Cooke, 2001), which is still to be demonstrated in toothed whales.

In humans, rats, and presumably all terrestrial mammals, the external ear canal region is innervated by a neurocomplex made up of cranial, cervical and auxiliary nerves (Folan-Curran and Cooke, 2001). In this complex, the nerves are interconnected and difficult to distinguish from one another. The cranial nerves that are involved include the trigeminal nerve (V), the facial nerve (VII), the glossopharyngeal nerve (IX), and the vagal nerve (X), and possibly also the accessory nerve (XI). The branches of these nerves include the tympanic branch of the glossopharyngeal nerve (IX), the mandibular and maxillary branches of the trigeminal nerve (V), the mandibular, submandibular, chorda tympani, greater petrosal and tympanic plexus of the facial nerve (VII), and the auricular branch of the vagal nerve (X), a.k.a. Arnold's nerve. Also, the dorsal root ganglia (C2-C4) show innervation of the ear region through the greater and lesser occipital nerve, and the great auricular nerve and additional nerves from the superior cervical ganglion innervate vessels, hair and glands of the ear canal (Folan-Curran and Cooke, 2001; Folan-curran et al., 1994). This study does not go into extensive detail on the innervation of the pinna and external ear canal in terrestrial mammals, as the general scheme is as mentioned above. However, there are many interspecific differences, especially when going into greater detail. Many studies report on the innervation in dogs, cats, rats, rabbits,

monkeys, horses, and other animals, and even more detailed studies have been carried in humans (e.g. Watanabe et al., 2016).

In the rat, there is an overlapping distribution between the peripheral nerve fibres and the ganglia they are connected to, similar to humans, although more clearly separated in the latter. This complicates research that tries to identify which nerves are responsible for the innervation of which parts of the ear canal (anterior/posterior walls; superficial vs deep, etc.). The lateral surface of the tympanic membrane is innervated by the auricular branch of the vagus, the auriculotemporal nerve and the facial nerve, while the internal surface is innervated by a branch of the glossopharyngeal nerve (Mitchell, 1954). In rats, this also involves the superior cervical and glossopharyngeal ganglion (Tierney et al., 1993).

Except for the auriculotemporal nerve and limited connections higher up, no other nerve could be identified to innervate the region of the external ear canal. It is likely that there is a similar innervation as in terrestrial mammals, but that these have likely been missed as they would provide minor innervation and would therefore be small. This could have also been missed because there were few well-fixed samples in good enough condition, and because of the personal lack of experience in preparing macroscopic dissections of nerves.

A preliminary morphofunctional hypothesis could state that the signals coming from the receptors win the ear canal in toothed whales, could be conducted through the auricular branch of the auriculotemporal nerve, the mandibular nerve, the trigeminal nerve and trigeminal ganglion, from where the first-order neurons project axonal processes that are connected to the trigeminal sensory nuclear complex within the brainstem. In the brainstem, epicritic[4] sensations are associated with the principal sensory trigeminal nucleus, while protopathic (nociceptic) information is associated with second-order neurons in the nucleus (semi-)spinalis (Kandel et al., 1991). From the brainstem, the information could travel to the thalamus of the opposite side where information is further processed. The involvement of any other cranial or cervical nerves still has to be studied. It would be interesting to know if the vagal nerve would be involved, as this could assign a certain vital function to the canal, with a role in survival or autoprotection mechanisms (Carta G., personal communication). Further studies could also focus on the central nervous system regions where the information would be processed.

The peripheral nerves that innervate the ear canal possibly contained efferent and afferent fibres, with the mandibular nerve as a mixed sensory nerve (Kandel et al., 1991), which could be associated

[4] Epicritic sensations are associated with lamellar SNF and involve the ability for fine touch (topognosis; vibration detection and determination of frequency and amplitude; stereognosis; and other spatial details including surface textures; Protopathic sensation is associated with free nerve endings, and includes pain and temperature sensation (Kandel et al., 1991)

with the auricular muscles, the glandular secretion, and the sensory innervation with free nerve endings and lamellar corpuscles in the external ear canal. The trigeminal nerve in cetaceans contains an exceptionally high number of nerve fibres, and is responsible for the sensory innervation of several sensitive facial structures including the eyes, lips, and blowhole, but also the mandibles and nasal sac system (Cozzi et al., 2017; Morgane and Jacobs, 1972; Prahl, 2007; Rauschmann, 1992). It also has motor functions, and has been proposed to be associated with the regulation of the middle ear volume through the blood supply of the corpus spongiosum (Ketten, 1992), and innervates the entire facial musculature (Degollada, 1998). The external ear canal, with its lamellar corpuscles, might contribute to the size of the trigeminal nerve in cetaceans, as it is densely innervated with novel sensory nerve formations (De Vreese et al., 2020).

1.12.2 SNFs in toothed whales

Like all mammals, toothed whales feature a variety of sensory nerve formations associated with the somatosensory system. The receptors include free nerve endings and lamellar corpuscles in the skin, including the trunk, flippers and fluke, the blowhole, snout, anus, genital slit (Bryden and Molyneux, 1986; Harrison and Thurley, 1974; Ling, 1974; Palmer and Weddell, 1964) and many more tissues (see Results). The corpuscles are also present in continuations of the skin such as the nasal sac system (Khomenko, 1970, 1974, In: Degollada, 1998 and Bryden and Molineux, 1986), the external ear canal (Yamada, 1953), and the iridocorneal angle of the eye (Wickham, 1980). Other sensory nerve formations are present in the vibrissal crypts, including indications of Meissner corpuscles in the skin close to the vibrissal crypt, lamellar corpuscles, Merkel cell-neurite complexes, and presumable lanceolate endings (Czech, 2007; Czech-Damal et al., 2012a; Gerussi et al., 2020).

Khomenko (1974, in: Degollada, 1998 and Bryden and Molineux, 1988) described three types of sensory innervation in the nasal sac system: free nerve endings in spatial association with the connective tissue, vascular structures, glands, and epithelium, and functionally involved in the regulation of local blood circulation and common internal tissue metabolism functions. The second group comprises fibrillar discs in the muscle tissues, associated with muscle activity during respiration. The third group encompasses two variations of encapsulated, lamellated nerve endings, which were identified as Krause's end-bulbs and Golgi-Mazzoni corpuscles, mainly present in high concentrations in the skin of the blowhole, even more specifically in the anterior lip, in the dermal part of the papillary layer (Bryden and Molyneux, 1986). (See below for a discussion on nomenclature and identification of lamellar corpuscles)

For the skin, Palmer and Weddell (1964) mentioned large complex terminals attached to the papillary walls, and other, complex, often encapsulated, endings in various locations, from attached to the epidermis to deep in the dermis. All SNF were complex, pleomorphic, and innervated by two separate

nerves, one thick and one thin, both of which are surrounded by the same capsule, and their branched terminal processes are intimately related. Also, there are reports of sometimes high concentrations of encapsulated corpuscles in the iridocorneal angle of various toothed whales (Wickham, 1980).

For the external ear canal, there is only one study that describes the presence and structure of lamellar corpuscles in detail (Yamada, 1953), which provided, to date, the only interpretation of the fine-detail configuration of the terminal endings of peri-meatal encapsulated corpuscles in any toothed whale. Yamada (1953) described abundant lamellar corpuscles associated with the ear canal in *Berardius bairdii*, Cuvier's beaked whale and sperm whale. They were situated in great numbers in the dermal layer in the cartilaginous portion of the canal, but also present in superficial sections, such as in the capsule of the lymphoid organs in the blubber. In the deeper sections, they were most present on one side of the canal, under the convex epithelium. This description is very similar to our description of the 'nervous button', which is convexly protruding into the lumen. The corpuscles described by Yamada (1953) were long and occasionally convoluted, each of which was presumably innervated by a single myelinated nerve fibre.

In our samples of the Cuvier's beaked whale, the cartilage was not present, and in fact, based on the general morphology of the canal in odontocetes and comparison with Yamada's descriptions for the beaked whale, the entire medial half of the canal was probably not sampled. Also, we found relatively few corpuscles in the subepithelial tissue of any section, compared to other species, although this was likely affected by the tissue conservation state.

There are very few studies describing the ultrastructure of any of these sensory nerve formations. In the region of the nares (Bryden and Molyneux, 1986), the corpuscles contained several unmyelinated terminal axons, which have lost their myelin on entering the corpuscle, partly or completely covered by five to seven Schwann receptor cell lamellae, linked by desmosome-like connections. The axon terminal contains a dense matrix, neurotubules, smooth endoplasmatic reticulum, several vesicles, glycogen, and mitochondria. These last two indicate a high energy requirement. The Schwann receptor cells presented a prominent nucleus, many mitochondria at the nuclear poles, and many dilated pinocytotic vesicles. The capsule consisted of up to six cellular layers of likely perineurial cells although not specified, surrounding a capsular space with collagen fibres and unmyelinated axons. These descriptions correspond perfectly with the characteristics attributed to encapsulated lamellar corpuscles in mammals (Cherepnov and Chadaeva, 1981; Zelená, 1994), as they even appear in all vertebrates except fish, independent of the species and variety in size and conformation of the receptor (Iggo and Andres, 1982):

The axon terminal loses its myelin sheath on entering the corpuscle.

The lamellar cells that form the core are derived from Schwann cells (highly modified Schwann cells, called Schwann receptor cells).

The lamellar cells are separated by intercellular space filled with collagen fibres, and the possible presence pinocytotic vesicles, and share desmosome-like connections between neighbouring plasmalemmae (Chouchkov, 1973a). There is a subcapsular space separating the lamellar core from an outer capsule, and which contains cells and membranes. The capsule is formed by perineurial cells, which complexity can range from simple as in Ruffini endings, to elaborate as in Pacinian corpuscles.

The most striking difference between the lamellar corpuscles as described by Bryden and Molineux (1986), and the lamellar corpuscles in this study, is the presence of a capsule, and accordingly also the (sub)capsular space. This leads us to the classification of sensory nerve formations, particularly lamellar corpuscles according to the morphological characteristics.

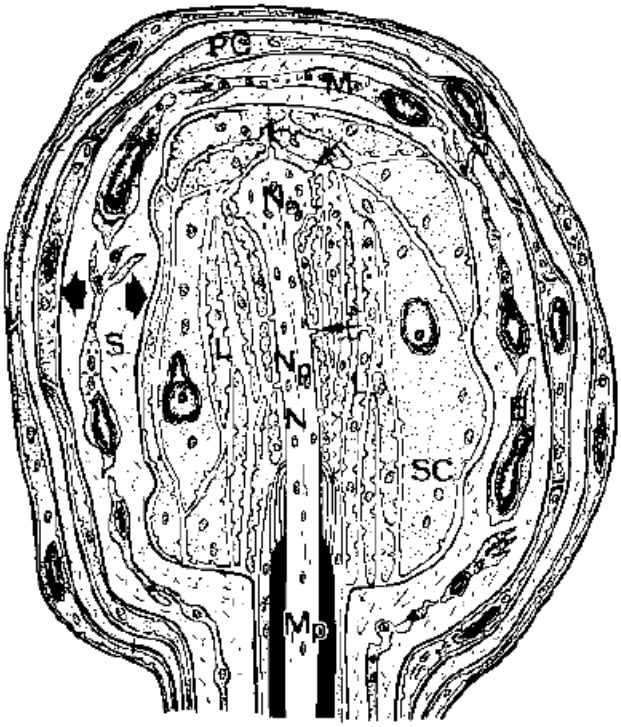

Figure 306. Drawing of a general encapsulated, lamellar corpuscle. The central axon (N: nerve terminal) loses its myelin sheath (Mp: myelinated part of the axon) at the base of the corpuscle, continues unmyelinated (Np: non-myelinated part), to end in a bulbous nerve ending (Ne). The core consists of Schwann receptor cells (SC), and their plasma membranes form the lamellae (L). The core is surrounded by a (sub)capsular space (S) with fibroblasts (F) and macrophages (M), and a capsule formed by perineurial cells (PC). (Source: Iggo and Andres, 1982)

1.12.2.1 SNF classification

The nerve ending, together with the surrounding or associated cells of ectodermal or mesodermal origin, is referred to as a sensory nerve formation (SNF), a single morphophysiological unit with a specific activity determined by its structural components (Malinovský, 1996). The terminal functions as a 'dendrite' and is sometimes referred to in that way (e.g. Loewenstein, 1971) while most authors

refer to an 'axon terminal'[5]. The axon terminal of an SNF is that of a pseudounipolar neuron that has its nucleus in the cranial (trigeminal or other, see above) or dorsal root ganglia. The structure of the terminal can have a simple arrangement 'free nerve endings' (Note: here we use this nomenclature as it is widely used, while it is not fully correct because they are not 'free' but covered by the basal lamina (and cytoplasm) of a modified Schwann cell), and as they have the most straightforward configuration of all sensory nerve formations, this is why they can also be referred to as 'simple SNF' (Malinovský, 1996)). Mechanosensitive SNF range from these simple, free nerve endings to complex and large structures like Pacinian corpuscles. As such, the hitherto used nomenclature of these sensory nerve formations has shown significant variation up to this day, and we opt for a unified nomenclature as proposed by Malinovský (1996). The SNFs are classified in literature by their morphology, the kind of sensations they perceive, and the adaptation rate.

In this brief overview, we focus on cutaneous mechanoreceptors, and there we do not mention any specialised sensory organs such as the inner ear (otosensor) and vestibulum (vestibulosensor), the eye (ophtalmosensor), the olfactory organ (olfactosensor), nor the taste buds in the oral cavity (gustosensor). We also do not include specialised interoreceptor organs such as the glomus complex (caritoid organ), Golgi-tendon organ, pulmonary stretch receptors, and others.

For the sensation of mechanical deformation, anatomic research has identified a variety of specialized mechanosensory organs, including Meissner corpuscles (tactile corpuscles), Merkel cell-neurite complexes, lanceolate and pilo-Ruffini fibres associated with hair follicles, and mechanoreceptors with free nerve endings, which are the most sensitive of all (also for heat). The classification can be addressed in several manners (Horch et al., 1977; Malinovský, 1996), and the three main types of classification are according to:

- Morphology: SNFs are grouped according to the morphological similarity of their structural components.
- Stimulus or physiological significance: Grouping according to the type of stimulus: temperature, pressure (together with touch, vibration, tension), electric fields, chemicals, or according to the sensation that is perceived (pain, touch, temperature…) and thus the function they take on: mechanosensor, thermosensor, nocisensor, electrosensor, chemosensor, barosensor, osmosensor, or combinations.
- Innervation and adaptation rate: This depends on the type of providing nerve fibre, more specifically its conductive speed, and the velocity of the adaptation rate of the axon terminal

[5] It is generally accepted that axons conduct electric potentials away from the cell body, while dendrites conduct them towards the cell body. However, in pseudo-unipolar neurons the peripheral neuronal process is structurally configured like an axon, even though it carries signals from the sensory terminal towards the cell body (Kandel et al., 1991). Its shows limited metabolic activity as it lacks ribosomes, Golgi apparatus, and endoplasmic reticulum, and contains mainly mitochondria and proteins in the form of microtubules, neurofilaments and actin filaments (Pannese, 2015).

to sustained stimuli. This subdivision is applied to cutaneous low-threshold mechanoreceptors (LTMRs) and can be divided into groups with distinct molecular, physiological, morphological (cell body, axon diameter, and myelin sheath thickness), and functional features (Burgess et al., 1968; Horch et al., 1977; Olson et al., 2016):

- slow-conducting non-myelinated C-type LTMRs (associated with social touch), e.g. lanceolate endings
- intermediate to fast-conducting, light to heavy myelinated LTMRs
  - Some free nerve endings
  - Meissner's corpuscles, Pacinian corpuscles and alike, glomerular corpuscles, simple lamellar corpuscles
- slow adaptation rate (tonic sensors)
  - Type I: Merkel cell-neurite complex
  - Type II: Ruffini corpuscle
  - Golgi-tendon SNF, neuromuscular spindles
  - (Some free nerve endings)
- intermediate (IA) to rapid adaptation rate (RA) (phasic sensors)
  - IA: Some free nerve endings
  - RA: Meissner corpuscle, Pacinian corpuscle,

As such, the lamellar corpuscles in this study can be compared to other SNF that share the same characteristics in those three areas, i.e. based on the morphological characteristics and resemblance to other well-described SNF: a lamellated structure sensitive to mechanical deformation and with a rapid adaptation rate. As such, the SNFs that meet these specifications include

- Pacinian corpuscle (Vega et al., 1996)
- Meisner's and Meisner-like corpuscle (Vega et al., 1996)
- Simple lamellar corpuscle (incl. Golgi-Mazzoni corpuscle)
- Glomerular corpuscle
- Herbst corpuscle in birds (Gottschaldt and Lausmann, 1974; Nafstad and Andersen, 1970; Zelená et al., 1997) (Are considered analogues to Pacinian corpuscles)
- Gandry corpuscle in birds (Gottschaldt and Lausmann, 1974)
- Krause's end-bulb (Krause's corpuscle) (Chouchkov, 1973b)

Next, the morphological elemental of the dendritic zones according to their origin (ecto-, endo-, mesodermal) and the organisation of the cells (e.g. lamellar), are compared and clustered into classes and subclasses (Malinovský, 1996). The corpuscles in this study have dendritic (axonal) zones that are related to elements of ectodermal origin, which demonstrate a lamellar core, therefore, belonging to

class IIIa, together with simple lamellar corpuscles (incl. Golgi-Mazzoni corpuscles), Herbst corpuscles in birds, and Pacinian corpuscles.

The accurate identification and characterisation of the types of sensory nerve formations is essential for an accurate understanding of the events that are involved in the functional sensitivity of the ear canal of dolphins. In comparing with descriptions of similar corpuscles in terrestrial mammals, we noted not only several similarities and differences in morphology but also in nomenclature. These corpuscles have been called various names, such as Krause end-bulbs, Golgi-Mazzoni corpuscles, mucocutaneous end-organs; small Vater-Pacini corpuscles; paciniform corpuscles; innominate corpuscles, amongst others. See Table 18 for a brief comparison of the nomenclature assigned to what were presumably all simple lamellar corpuscles.

Notably, most sources labelled this receptor as some kind of 'corpuscle'. The name 'corpuscle' was initially assigned to various sensory nerve formations which became relatively well-defined by Krstic (1984, In: Malinovsky, 1996): *"A corpuscle is an encapsulated ending with a well-delimited round or oval structure formed by a lamellated connective tissue capsule around one or more peripheral nerve endings in contact with either a group of specialized connective cells, intrafusal muscle fibres or tendon fibres."*. This definition corresponds very well to the properties assigned to corpuscles by Iggo and Andres (1982)(Figure 306). Similar properties were already noted by Halata (1975)(Figure 307) who described encapsulated corpuscles with an inner core, and which can exist in a vast variety of conformations. All these conformations included more or less egg-shaped corpuscles, none were stretched and complex as in this study, or as previously reported by Yamada (1953). As such, corpuscles exist in a variety of structures that all have in common a central axon with one terminal or branching in multiple terminals, surrounded by stacked lamellae of terminal Schwann cells. They can be fully capsulated, such as the Pacinian corpuscle, or partially capsulated like the Meissner corpuscle (Zelená, 1994)**.**

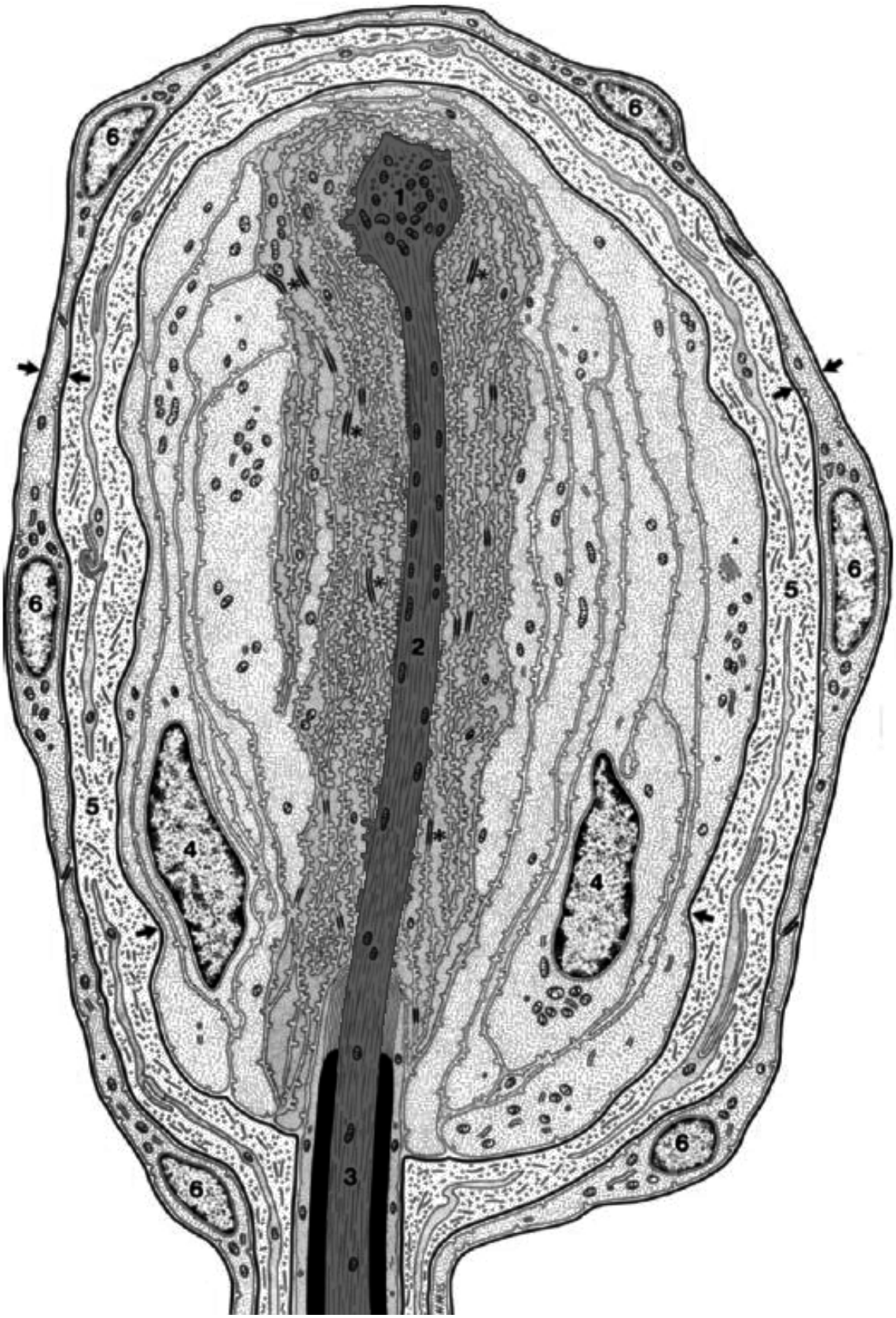

*Figure 307. Semi-schematic drawing of a lamellar corpuscle with an inner core in the nose of the mole. 1. Bulbous dilation of the axonal ending; 2. Axon; 3. Nerve fibre; 4. Receptor Schwann cells that make up the lamellar core (*desmosomal connections between lamellae); 5. Subcapsular space with fibrocytes and collagen fibres; Perineurial cells form the capsule, covered by a basal lamina (arrows). (modified after Halata, 1975)*

Simple lamellar corpuscles were described for the first time by Krause (1860) as corpuscles with an afferent nerve fibre that formed a single or branched dendritic terminal. They can be presented in different 'variants', both inter- and intraspecific (D'Andrea et al., 2014; Malinovský, 1996). The axon terminal is either singular or branched, each branch having its own lamellar core. These different cores can be encapsulated by a single capsule, or have its own 'branch' of the capsule. Sometimes these were also referred to as Krause cylindric corpuscles or bulbs, Golgi-Mazzoni corpuscles, and several other names as can be seen in Table 18. The term "Golgi-Mazzoni corpuscles" has been used as a synonym for simple lamellar corpuscles, or to describe the variant with branched axon terminals, or to encompass the variants with branched or coiled axon terminals (D'Andrea et al., 2014; Malinovský, 1996). Because the structure of the corpuscles as described in this study, is not yet entirely clear, I opted to use the term simple lamellar corpuscles and not to specify the possible morphological variants in which they could present themselves.

The overall structure of the simple lamellar corpuscles in this study showed many resemblances to the *small encapsulated receptors,* labelled as *Golgi-Mazzoni corpuscles* by Chouchkov (1973), but with significant differences, such as the single nerve fibril innervation and the morphology of the actual sensory nerve ending with cytoplasmic processes of the inner core cells, without any apparent asymmetry in our results. Based on Figure 308 and Figure 309 (D'Andrea et al., 2014; Malinovský, 1996), the difference between a simple lamellar corpuscle and a Golgi-Mazzoni corpuscle lies in the configuration of the central axon. First of all, the term simple lamellar corpuscle encompasses all types of Golgi-Mazzoni corpuscles. Specifically, only if the central axon is singular and runs a straight course, is the receptor considered not a Golgi-Mazzoni corpuscle, but labelled as a simple lamellar corpuscle, while in all other configurations (doubled axon that turns back, splitting axon, multiple axons) they can be called Golgi-Mazzoni corpuscles, independent from the presence and configuration of any accessory axons. The glomerular corpuscle is considered to be a distinct kind of corpuscle, and a morphological and functional equivalent of a simple lamellar corpuscle, and is defined as followed: "*The glomerular (Krause spheric) sensory corpuscles represent a sensory nerve formation with one or more afferent axons, branching irregularly inside the corpuscle among modified Schwann cells, which are localized irregularly, form lamellar complexes or in some zones are arranged in parallel. The capsule is variable: in simple types, it is missing, in other glomerular corpuscles (especially in genital region) it is rather thick"* (Malinovský, 1996).

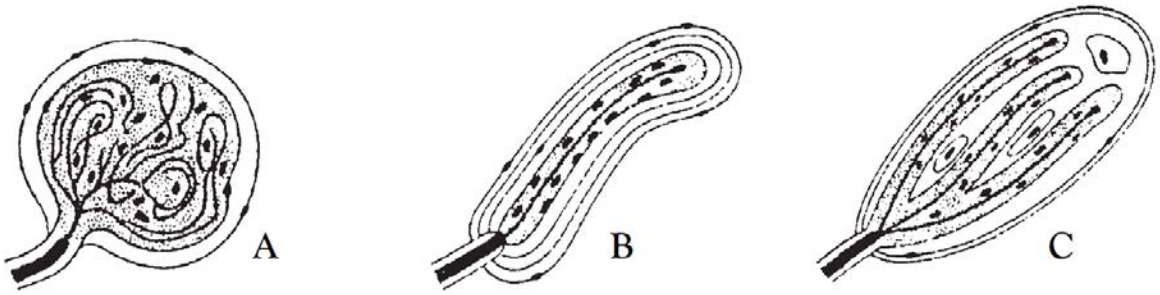

Figure 308. Schematic drawing of a glomerular (A), simple lamellar (B), and Golgi-Mazzoni (C) corpuscle (Source: D' Andrea et al., 2014)

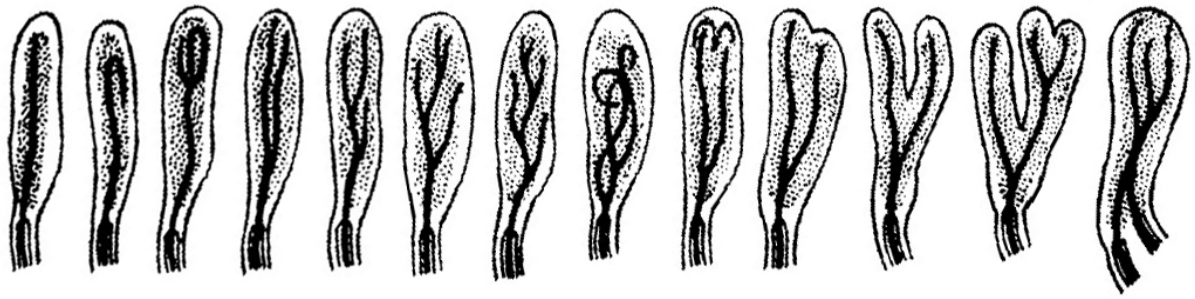

Figure 309. Variations in morphology simple lamellar corpuscles. All types, except for the first one on the left, are variants of Golgi-Mazzoni corpuscles, while the first one is the 'true' simple lamellar corpuscle (Source: Malinovsky, 1996).

Table 18. Table showing the non-exhaustive variety in nomenclature for what were possibly the same types of receptors, although with variation in the configuration.

Name	Species	Location	Size (µm)	References
Encapsulated nerve endings / genital end bulb	Rat	Penis		(Patrizi and Munger, 1965)
Encapsulated receptors	Cat	Lips		Spassova (1970)
Pacinian corpuscles	Human	Umbilical skin (dermis)		(El-Oteify et al., 2011)
Simple capsulated corpuscles	Cat	Nasolabial region		(Poláček and Halata, 1970)
	Mole	Nose	30-40 x 15-20	(Halata, 1972)
Simple encapsulated corpuscles	Rhesus monkey	Sinus		(Halata and Munger, 1980)
Simplified Pacinian corpuscles				
Small encapsulated receptors	Human	Glabrous skin		(Chouchkov, 1973a)
Small lamellated corpuscles		Vibrissal hair		(Halata, 1990)
Small lamellated Pacinian-like corpuscles	Horse	Foot	75-200 (length + width/2)[6]	(Bowker et al., 2017)
Sensory corpuscles	Horsfield's Tortoise	Upper jaw (dermis)	60-150	(Buchtová et al., 2009)
CETACEANS				
Ciliar corpuscles, which resemble Pacinian corpuscles	Humpback whale	Iridocorneal angle of the eye		(Rochon-Duvigneaud, 1940)
Corpuscles of Rochon-duvigneaud	*Amazon river dolphin, Sowerby´s beaked whale, Cuvier´s beaked whale, pygmy sperm whale, beluga whale, common dolphin, bottlenose dolphin, Pantropical spotted dolphin*			(Wickham, 1980)
Encapsulated corpuscles			10 – 50 µm	(Wickham, 1980)
		Skin of trunk, flippers and fluke		(Palmer and Weddell, 1964)
		Nasal sacs		Khomenko, 1970; In: (Degollada, 1998)
Encapsulated, lamellated receptor organs, mechanoreceptors	*Tursiops truncatus* *Pseudorca crassidens*	Blowhole lips		(Bryden and Molyneux, 1986)

[6] The authors did not mention how this was calculated (e.g. Their Figure 1 shows oblique sections through the corpuscles).

1.12.2.2 Morphology

The basic structure of the simple lamellar corpuscle follows the general rules lamellar corpuscles as described above. Most sources reference the presence of both single and composite lamellar corpuscles in toothed whales, up to seven corpuscles within the same ´capsule´ (e.g. Bryden and Molyneux, 1986), while others (e.g. Degollada, 1998) report only single-cored corpuscles. As also reported in this study, the usual configuration takes one, two, three to five cores (Wickham, 1980). Without a three-dimensional reconstruction of consecutive slides (< 8 µm interval), there is no differentiation between different corpuscles or sections through convolutions of the same corpuscle. Similar histological presentations of Pacinian corpuscles and the respective 3D configurations show either a single convoluted Pacinian corpuscle (Figure 310)(Cauna and Mannan, 1958) or a cluster of independent Pacinian corpuscles (Figure 311)(Bouley et al., 2007, Fig. 5). Also, Pacinian corpuscles can have a composite inner core (multiple axon terminals and lamellae) as a result of reinnervation after nerve damage (Zelená, 1994). The preliminary analysis of the basic 3-dimensional structure of the corpuscles showed a diameter that is conform other simple lamellar corpuscles in terrestrial and aquatic animals (e.g. Yamada, 1953; Munger, 1971; Bryden and Molyneux, 1986; Nishida et al., 2000; Buchtová et al., 2009). The elongated and tortuous course of the corpuscles, together with the uncertainties regarding ramification and possibly reuniting of nerve fibres, and the scarcity of similar studies, make a comparison of the dimensions of the corpuscles frivolous at this stage, as there is a need for more information on the 3D morphology of the structures.

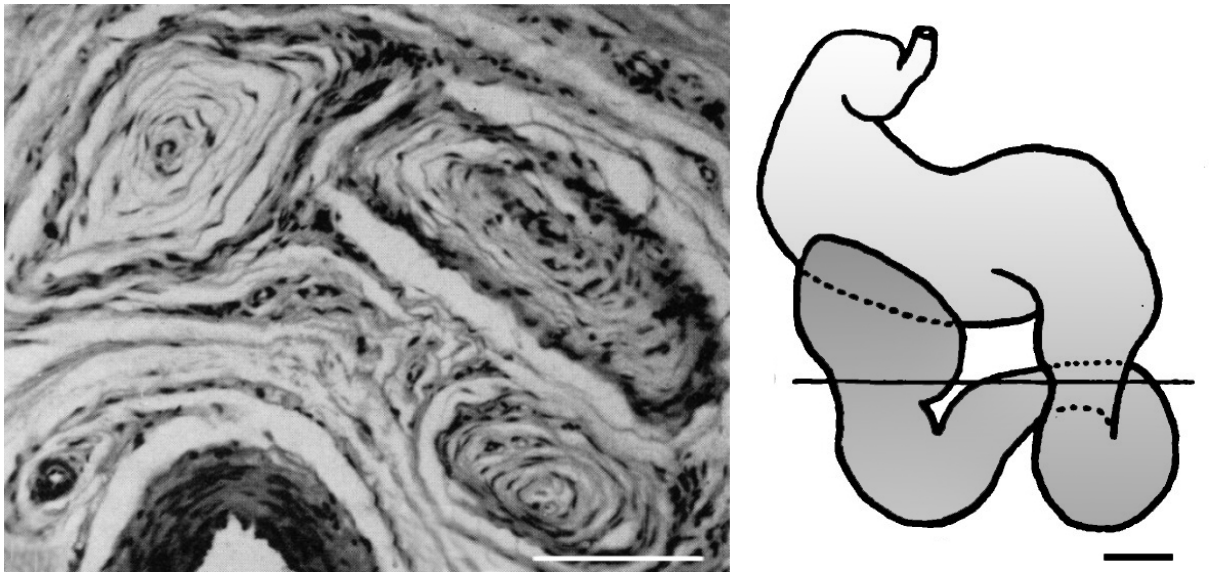

Figure 310. Histological transverse section (HE staining) through a single convoluted Pacinian corpuscle in the index finger of a 22-year-old human, with a schematic drawing of the shape of the entire corpuscle and the level of the section (horizontal line). Scale bars 100 µm (modified after Cauna and Mannan, 1959)

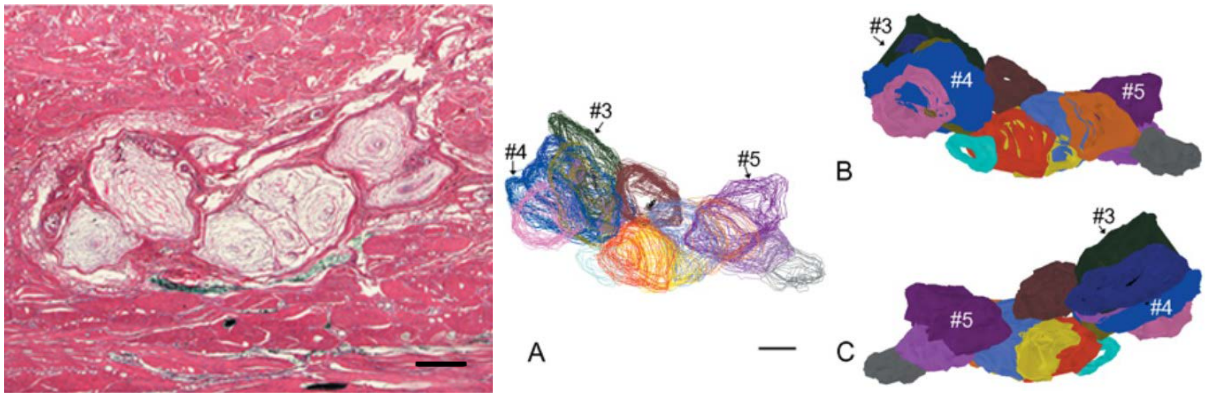

Figure 311. Histological image (HE staining) and 3D reconstruction of a Pacinian corpuscle cluster in the foot of an Asian elephant. Each core was identified as a separate corpuscle, in contrast to the findings of Cauna and Mannan (1959), see Figure 310. Scale bars 500 µm. (Source Bouley et al., 2007)

1.12.2.2.1 Nerve supply

The immunoreactivity of the central axon was similar to Pacinian and other lamellar corpuscles in terrestrial mammals (Vega et al., 1996). The supplying axon seemed to lose its myelin sheath on entering the corpuscle (cf. Wickham, 1980; Zelená, 1994), although this should be confirmed with IHC (e.g. myelin basic protein) or TEM. The course of the axon seemed to be straight throughout most corpuscles, although occasionally convoluted, similar to the corpuscles in the ear canal of Baird´sbeaked whale (Yamada, 1953). Comparatively, the central axon of lamellar corpuscles in the eye of a beluga whale also showed a tortuous course (Wickham, 1980), and so does the supplying axon on entering Pacinian corpuscles in terrestrial mammals (Zelená, 1994)(De Vreese et al., 2020).

The ultraterminal region (Spencer and Schaumburg, 1973), is, unlike its nomenclature, not the most distal part of the axon terminal, which was described later as the extreme tip of the axon by Ide et al. (Ide et al., 1988). The ultraterminal region is the region were inner core lamellae start to reduce in number and where the axolemma portrays fewer spines and becomes more smooth (Spencer and Schaumburg, 1973). In contrast, the extreme tip of the axon is no longer surrounded by any inner core lamellae and contains many spines in all directions that project into 'basal-lamina-like material' (Ide et al., 1988). If what we identified as the ultraterminal region of the corpuscle is correct, this is morphologically consistent with the same region in the Pacinian corpuscle in that it is filled with mitochondria and that the inner core has lamellae that fully encircle the axon. However, it has the difference that the axon does not enlarge to form a bulb at the end of its course, but instead gets smaller in diameter, keeps its oval shape, and does not form a complex structure with many axonal spines interacting with the lamellae of the inner core. Such a bulbous enlargement has been mentioned for practically all lamellar corpuscles, including corpuscles in the ear canal of a pygmy sperm whale (size 9x15 µm, compared to axon diameter 0.8 – 6 µm)(Yamada, 1953) and for Pacinian and other lamellar corpuscles (Zelená, 1994), although this was possibly missed it in the paucity of available tissue (De Vreese et al., 2020). As a rule, lamellar corpuscles have a single club-like expansion

(Zelená, 1994), but can also have either two or three bulbous endings (Spencer and Shaumberg, 1973 In Zelená, 1994). It most likely depends on the section, as in the ultraterminal section of Pacinian corpuscles, the axon can be branched, while in the terminal section it is not (Bell et al., 1994; Malinovský, 1986). The preterminal section is the part where the axon enters the corpuscle and is still myelinated.

The axon terminal, as seen with TEM, corresponded to the morphology of the typical axon terminal in all lamellar corpuscles. The presence of dense myelin-like bodies within the axon terminal was mentioned previously in human Golgi-Mazzoni corpuscles (Chouchkov, 1973a). There, they were assumed to be mitochondria in the process of degeneration, which could well be the case for the structures we have described. Otherwise, if there are indeed myelinated structures within the neurite terminal, this could mean two things: first, these structures were seen in sections that might have been taken at the entrance of the neurite into the corpuscle and therefore be similar to Pacinian corpuscle in that the neurite is myelinated on entering the corpuscle; however, it would be different from the Pacinian corpuscles because there, the myelin encircles the entire single axon and not several small axons within the neurite; second, this could be a novel finding that shows that there can be multiple axons in the centre of the lamellar corpuscle, similar to Golgi-Mazzoni corpuscles, and that they are myelinated, at least over some part of their course. We do consider the possibility of 'mistaken identity' to be the most likely hypothesis, and believe that these structures are degenerating mitochondria. Also, the bulbous electron-lucid vesicles within the axon terminals might be artefacts of degenerative processes. In Pacinian corpuscles, these spines contain vesicles at their base, while the rest only contains microfilaments. We did not see any modifications of the neck of the spine, namely no subaxolemmal lamina was seen, as has been described for Pacinian corpuscles, nor did we see any specialized junctions such as desmosomal plaques at this level (Spencer and Schaumburg, 1973; Zelená, 1994).

The presence of accessory axons within or associated with the peripheral layer has been described in Pacinian corpuscles (Kumamoto et al., 1993; Malinovský, 1996; Zelená, 1994), and in the capsule of tendon organs (Barker et al., 1974), and are generally accepted to be catecholaminergic fibres that can adjust the responsiveness of the corpuscles (Kumamoto et al., 1993; Zelená, 1994). However, we do not know if these are true 'accessory', as the innervation patterns of the corpuscles are not yet understood. (De Vreese et al., 2020)

The functional morphology of an accessory axon within or adjacent to the simple lamellar corpuscles is not known, but we consider three possibilities. First, it could be a ´parent axon´ from which the axons of the inner cores branch of, similar to corpuscles in the penis of the rat (Johnson and Halata, 1991). Second, it could be a nerve that passes through the corpuscle to reach the epidermis, similar

to thin-calibre intracorpuscular fibres in human Meissner corpuscles (Johansson et al., 1999). Third, it could be a kind of ´*nervus nervorum*´ that would be used for adjusting the sensitivity of the corpuscles themselves, similar to what occurs in Pacinian corpuscles (Zelená, 1994). A fourth hypothesis is that it could be useful for the interpretation of the stimulus that is received by the corpuscle in that the signal coming from the naked nerve ending and the signal coming from the axon in the corpuscle could be compared to have a relative sense of the strength, the amount or the rapidness/velocity of a mechanical deformation as the ´naked nerve´ would not have the filter that the lamellae of the corpuscle offer, and it could assist in adjusting the responsiveness of the corpuscle. In any case, it is not known if the composite corpuscles are innervated by a single myelinated axon that branches within the capsule of the corpuscles, or by multiple axons. It would require a 3D perspective to assess these innervation patterns, the topography of small nerve fibres through the soft tissues, and of the relations with the neighbouring tissues would be required to gain insight in their function.

The morphology of the lamellar corpuscles as shown by transmission electron microscopy was overall consistent with the morphology of the inner core of Pacinian corpuscles, and there were also resemblances to Golgi-Mazzoni corpuscles (Chouchkov, 1973a), but with significant differences, such as the likely single nerve fibril innervation and the morphology of the axon terminal with cytoplasmic processes of the inner core cells, which was without any obvious asymmetry in our results. We could identify at least two corpuscle regions: the terminal and ultraterminal region, both of which showed similarities to Pacinian corpuscles in the morphology of the axon terminal, its content, radial clefts and the hemilamellar structure in the terminal region, and the fully encircling lamellae in the ultraterminal region. The radial clefts were not described in previous electron microscopy studies of corpuscles in the iridocorneal angle (Wickham, 1980), and in the nasal sac system of toothed whales (Bryden and Molyneux, 1986). The lamellar and hemilamellar structures were consistent with the morphology and size of Pacinian corpuscle inner cores, including the cellular cytoplasm, glycocalyx and desmosomal connections, down to the diameter of extracellular collagen fibres (Ide et al., 1988; Munger et al., 1988; Zelená, 1994)(De Vreese et al., 2020).

1.12.2.2.2 Lamellar core

The core lamellae showed IR for anti-S100 protein, indicative of Schwann receptor cells, similar to the inner core of Pacinian corpuscles (Albuerne et al., 2000; Feito et al., 2017; Zelená, 1994). We often noted a space between lamellae and peripheral layer, similar to the acellular space between the inner core and the intermediate layer in Pacinian corpuscles (Ide and Hayashi, 1987), although we suspect this to be an artefact associated with tissue conservation and/or processing (De Vreese et al., 2020). As such, the structure of the lamellae is similar to the inner core of a Pacinian corpuscle (Zelená, 1994; Albuerne et al., 2000; Feito et al., 2017).

The presence and size of collagen fibrils in the extracellular matrix is consistent with findings in Pacinian corpuscles in the cat (Munger et al., 1988; Zelená, 1984). The collagen fibre diameter was consistent with the 15 nm fibres in the extracellular matrix of the hemilamellae in the inner core of Pacinian corpuscles of the cat, and the approximately 30 nm diameter in the vicinity of the clefts (Munger et al., 1988), and also consistent with the findings of Zelená (1984) who mentioned a maximum diameter of 40 nm, also in the cat.

The diameter of the collagen fibrils and their distribution is very similar to the endoneurial collagen, similar to previous findings in Pacinian corpuscles (Zelená, 1994). The orientation of the fibrils is reported to be lengthwise in the extracellular matrix of Pacinian corpuscle (Zelená, 1994), while we found two main orientations, both lengthwise and transverse, in the simple lamellar corpuscle. The function of this difference is unclear, although it might be that the double, perpendicular directions could provide more stability in a corpuscle that is lacking an outer core. In Pacinian corpuscles, the extracellular matrix containing proteoglycans in the interlamellar spaces would function as a mechanical filter providing flexibility to the capsule (Dubový and Bednárová, 1999), while the scattered collagen fibrils in all extracellular spaces would provide a certain degree of rigidity. This study did not allow for a distinction between types of collagen fibres such as type II and V as shown in the intermediate layer and outer layer respectively of Pacinian corpuscles (Pawson et al., 2000). It would be interesting to study the nature of the collagen fibres to estimate (and to model) the rigidity of the lamellae and their role in the transfer of the mechanical stimulus to the central axon. *We could not identify with certainty any elastic fibrils with TEM or the two elastic stains, nor was there any ground substance noted as in the inner core of Pacinian corpuscles* (Munger et al., 1988) (De Vreese et al., 2020)**.** The plasma membrane of the nerve ending is relatively elastic and confines the axoplasm that is quite incompressible (Loewenstein, 1971). The absence of elastic fibres could make these corpuscles less rapidly adapting than Pacinian corpuscles, and therefore would not be well suited to respond to vibratory stimuli in the same frequency range, but rather respond to vibratory stimuli of with longer wave-lengths.

There were often enlarged cytoplasmic spaces in the lamellae of the core, which did not show have any cytoplasmic content except for seemingly disrupted intracytoplasmic filaments. They were mostly present in a circular conformation about halfway the inner core. Chouchkov (1973b) described cytoplasmic processes of similar shape, but without intracytoplasmic content. Therefore, we considered the spaces in our images to be artefacts of degeneration processes or tissue processing. As proteoglycans are water-soluble, they are removed during the tissue processing for electron microscope imaging, which might have contributed to the tissue presentation in EM images. We do not have any information on the molecular composition of the extracellular matrix or ground

substance. For that, specific staining and fixation techniques should be used (cfr. Dubovy and Bednárová, 2000).

The Pacinian corpuscle increases in size with age due to the addition of new lamellae of the capsule (outer core)(increase in girth) and a retrograde growth of the inner core along the axon (increase in length) (Cauna and Mannan, 1958). The growth zone is separated from the inner core by intercellular space containing mainly collagen and is the region that contains the inner core cell nuclei (Ide et al., 1988; Pease and Quilliam, 1957; Zelená, 1994). This puts into question the lack of an outer core in the simple lamellar corpuscles in this study, and if there occurs any growth of the corpuscle with age. Preliminary results indicate there is no such growth in girth, no outer core lamellae in any age group. Regarding retrograde growth, there is no reason why this could not take place, although detailed studies are needed to investigate this.

The variable space between the core and peripheral layer might be explained by an artefact of the preparation (shrinkage), or it might correspond to the inner part an intermediate layer as in Pacinian corpuscles. Pacinian corpuscles have an intermediate layer between the inner and outer cores, which according to Ide and Hayashi (1987), consists of an inner, acellular space and an outer layer of endoneurial fibroblasts and connective tissue. In the lamellar corpuscles in this study, there was variation in the ´space´ without any content between the core and the peripheral layer.

To differentiate between inner core, intermediate layer and outer core, we could perform IHC according to (Pawson et al., 2000), who showed that anti-collagen II specifically stains the outer core and capsule, anti-collagen V only the intermediate, and S-100 and GFAP (glial fibrillary acidic protein) only the inner core.

1.12.2.2.3 Peripheral layer

Although the corpuscles did not have a distinct outer core/capsule, there was a continuation of the peripheral layer of some corpuscles with the perineurium of nerve fibres, and the distinction between inner core lamellae and the peripheral layer was not clear, while these did show a distinct reaction in the immunohistochemical study. The presence of myelin observed in the TEM images might have been affected by post-mortem degeneration, as the samples used for this study were fixed 22 hours post-mortem. With this delay of fixation, it is common to observe degeneration of the myelin sheath. (De Vreese et al., 2020)

The denomination of the peripheral layer in simple lamellar corpuscles as a capsule is not entirely clear. As mentioned above, all lamellar corpuscles are surrounded by a capsular layer formed by perineurial cells as a continuation of the perineurium (Halata, 1975; Iggo and Andres, 1982). The peripheral layer of the lamellar corpuscles in this study showed unexpected IR for anti-PGP 9.5, unlike the outer core of Pacinian corpuscles (Albuerne et al., 2000), and not for anti-S100, while the

perineurium of nerves displayed the opposite reaction. This would indicate a difference in nature between the peripheral layer of the corpuscles and the perineurium of nerves. As such, it might be that the peripheral layer of these corpuscles could be similar to the intermediate layer of Pacinian corpuscles, which is regarded as an endoneurium with modified endoneurial fibroblasts (Ide and Hayashi, 1987; Zelená, 1994). To differentiate between inner core, a possible intermediate layer as in Pacinian corpuscles and an outer core/capsule, future studies could look at performing IHC with e.g. anti-collagen II, anti-collagen V, anti-S-100 and GFAP(Pawson et al., 2000)(De Vreese et al., 2020).

Also, more investigation should be done to investigate the nature of the peripheral layer, its origin, and morpho-physiological and biomechanical characteristics. This could be done with IHC markers like Epithelial Membrane Antigen, Claudin-1, Glut-1, and Type IV collagen or Glucose Transporter I(Vega, 1996; Piña et al., 2015; Feito et al., 2017), with the use of SEM and TEM (Ide and Hayashi, 1987; Zelená, 1994), and through modelling (Biswas, 2015).

Chouchkov (Chouchkov, 1973a) described a capsule in Golgi-Mazzoni corpuscles, which was distinguishable from the inner core lamellae based on the number of nuclei associated with the number of lamellae, which was “appreciably” less in the core than in what was considered the capsule. If we would apply this method, a capsule could be identified. However, the exact distinction between core and capsule lamellae would still be subjective as there is no apparent morphological difference in the lamellae, besides the presence of nuclei of inner core cells. In Pacinian corpuscles, the nuclei of the inner core cells are situated at the outer margin of the inner core or in the intermediate growth layer, and in any case, central to the outer core/capsule (Pease and Quilliam, 1957). However, it is not certain if there is an intermediate layer, or something similar. The intermediate layer in Pacinian corpuscles functions as a growth layer for the outer lamellae (Pease and Quilliam, 1957; Zelená, 1994). Our findings indicate that the structure of the simple lamellar corpuscles is morphologically very similar to the Pacinian corpuscle inner core without the outer core/capsule. The capsule in the corpuscles is either absent, or ill-defined and cellular, similar to descriptions from innominate corpuscles (Quilliam, 1966), or lamellar corpuscles in the oral papillae in the snake (Nishida et al., 2000, Fig. 11).

Interestingly, the capsule of Pacinian corpuscles differentiates and develops mostly after birth (Zelená, 1994). Similarly, Pilate (1925, In: Cauna and Mannan, 1959) studied Pacinian corpuscles in the human, foetal finger, and noted that Pacinian corpuscle in early development did not have a capsule/outer core (‘devoid of a sheath’). As such, the lamellar corpuscle we described here resembles a primordial Pacinian corpuscle, as occurs in the foetal stages, and does not develop an outer core, even in adult toothed whales, as does occur in terrestrial mammals.

To understand the significance and function of the lack of a capsule, we reviewed the function of the outer core and capsule in Pacinian corpuscles. In those corpuscles, the capsule functions as a filter for the incoming stimulus. It transforms and modifies the incoming mechanical energy in several ways. First of all, it allows only the dynamical component (comparable to the kinetic energy) of the incoming mechanical impulse to be transmitted from exterior to the inner core, through fully absorbing the static component (comparable to the static energy)(Hubbard, 1958). In other words, during dynamic compression, the energy reaches the axon terminal as the dynamic component of the energy is transmitted all the way through. During static compression, there is no alteration of the morphology of the inner layers when compared to no compression being applied. Therefore, with only static compression, the sensory terminal would not trigger. In practice, there cannot be static compression without first having dynamical compression. Therefore, the capsule contributes to the rapid adaptation of Pacinian corpuscles. In fact, Loewenstein (Loewenstein, 1971) showed that with the removal of the capsule, the adaptation rate of the receptor changes from rapid to slow.

In the corpuscles described here, there could thus be a less rapid adaptation during stimulus (enhanced by the possible lack of elastic fibres in the lamellae, see above). The adaptation rate indicates what kind of trigger signal might stimulate the corpuscles, as corpuscles with a rapid adaptation rate would be more sensitive to rapid mechanical deformations, as can be caused by vibration or touch, while a slower adaptation rate could lend the corpuscle more susceptible to slowly changing or even constant triggers, such as would be the case for a deformation of the ear canal caused by pressure changes when diving.

However, this is not the only function of the capsule. It also physically modifies the signal in that it works as a band-pass filter for the range of incoming energies. For instance, Pacinian corpuscles are sensitive the frequencies in the range of 60-400 Hz, with an optimal frequency around 250 Hz (Talbot et al., 1968; Kandel et al., 1991), and Meissner's corpuscles, which are used in for sensation of light touch, are most sensitive to frequencies of about 20-50 Hz (Kandel et al., 1991). The lack of an outer core/capsule in the simple lamellar corpuscles, could then possibly imply that they could be triggered by the 'full range of frequencies' reaching the sensory terminal, although that range is still to be defined.

Next, the outer core/capsule of Pacinian corpuscles also has a function in homeostasis, as acts as a barrier for ions present in the surrounding environment (Sakada and Sasaki, 1984; Ide and Hayashi, 1987; Munger et al., 1988). As such, it functions similar to the perineurium (Peltonen et al., 2013), electrically isolating the nerve fibre. In the lamellar layers of the inner core in our corpuscles, we noted pinocytotic vesicles. Although we initially thought that these could be indications of transcytosis, allowing for the exchange of molecular material between lamellae and with the external environment,

Sakada and Sasaki (1984) showed that the vesicular membranous invaginations seen in lamellae of both inner and outer core in Pacinian corpuscles are static structures that are not involved in any pinocytosis or transcellular transport. On the other hand, the inner core lamellae of the Pacinian corpuscle do show gap junctions, especially near the radial clefts (Ide and Hayashi, 1987). Gap junctions are communicative junctions that allow the direct passage of small molecules such as inorganic ions (Dellmann and Eurell, 2000). Therefore, they are suggested to serve in keeping the lamellae at the same electrotonic potential (Ide and Hayashi, 1987). There are also tight junctions in both inner and outer core (Sakada and Sasaki, 1984), although another reference only mentions tight junctions in the innermost lamellae of the outer core, together with desmosome-like junctions (Ide and Hayashi, 1987). These junctions would allow the lamellae to function as a homeostatic barrier (Ide and Hayashi, 1987). The only type of interlamellar junctions seen in lamellar corpuscles in this study, were desmosome-like junctions. However, as there is still discussion on the presence of tight junctions in the inner core, we cannot conclude that the absence of an outer core/capsule would leave the simple lamellar corpuscles completely exposed to any molecular changes in the surrounding environment.

1.12.3 Sensory ridge

This study provides the first description of a sensory ridge, or nervous ridge, in the external ear canal of toothed whales, or any mammal. McCormick and colleagues (1970) depicted a tissue bulge protruding in the lumen of the canal in the deepest section of his Fig. 3, but they did not mention this in the text nor did they associate this with any nervous tissue.

There was variation in the degree to which the sensory ridge was present in some individuals. For instance, there was no pronounced sensory ridge in the single specimen of common dolphin. This could be because (1) it was missed but could have been present in other sections, (2) it was not present because (a) this species or individual does not have an apparent sensory ridge, (b) the tissue was fixed in a specific physiological/morphological state in which the sensory ridge was not present, (3) it was an artefact of tissue preparation (excessive manipulation or tension release during dissection) or associated with the angle of the cut through the tissue.

1.12.4 Nervous network model

The complexity and interconnectivity of the intramural nervous plexus, in which many structures would be sensitive to mechanical deformation, highlights the complexity of the external ear canal as a sensory organ. The representation shows that almost all the structures form part of the same interconnected neural sensory complex (represented by the orange colour in the diagram), as was also visualized in the video of the 3D reconstruction. The few nervous structures that were not

connected to the largest network are not connected in these sections, which does not imply they could not show a connection in histological sections further medial or lateral. The interconnectivity could allow for an action potential generated in the lamellar corpuscles, to travel in many directions, or could indicate that information processing would need multiple stimuli and action potentials for the signal to be representative of significant information. As such, it could be similar to the afferent part of the enteric nervous system

Although only a small distance of the entire course of the canal has been analysed, we believe this is representative for all sections of the ear canal in which a similar distribution of corpuscles was noted, which counts for half of the ear canal except the most medial end in which there is the presence of a nervous tissue ridge, and with it, a different type of specialization.

It would be interesting to subject the entire ear canal to such a detailed reconstruction, although it would have to be done with immunohistochemical markers that allow for a distinction between corpuscles and nerves (cf. corpuscles in the human finger: Kim et al., 2018). Although this was initially proposed for this research, for several reasons, it was not executed. Also, this could be followed by a comparative study with the nervous system of the intestinal tract, innervated by the vagus nerve, to see if there are morphological resemblances in the type and distribution of sensory nerve formations, and the connections between the peripheral nerves. Since it is currently unknown where exactly the action potentials are being created, it cannot be excluded that the action potentials could be created anywhere along the entire nervous net, both in specialized sensory nerve formations as along the nerves and in the transition between the two. As such, the usefulness of the information obtained from this, could lie in the summation of various stimuli, e.g. only when both a nerve and a corpuscle are triggered, both creating action potentials, is the information taken into account by the CNS. It would be interesting to characterise the mechanosensitive ion channels (Piezo channels 1 or 2), their location along nerves and receptors, and their threshold for stimulation, and their density along the canal (in the aspect of graded sensitivity of the ear canal).

Once the morphology of the individual corpuscles is better known, and the connections between cores are mapped into detail, further research could focus on 3D nervous network analysis systems, studying connectivity in the network, where the trigger occurs, and how the signal could travel through the peripheral tissues to the brain, in order to understand the function and significance of such an intricate nervous network associated with the external ear canal in toothed whales.

1.12.5 Other SNF

1.12.5.1 Subepithelial immunoreaction

The unanimous labelling of subepithelial nervous structures is considered to be a true positive reaction, although it was often granular in form, similar to the epithelial pigmentation (De Vreese et al., 2020). This is similar to what has been found in the oral sensory papillae of the snake, a subepithelial immunoreaction to S100 and NSE, also associated with the dermal presence of lamellar corpuscles and other SNF (Nishida et al., 2000). This feature was absent in all terrestrial mammals in this study (De Vreese et al., 2020).

1.12.5.2 Free nerve endings:

Intraepithelial free nerve endings are a common feature among all mammals. Therefore, it was not surprising to find intraepithelial free nerve endings in the ear canal of toothed whales. The single image of an intraepithelial free nerve ending in a striped dolphin showed no ramifications and a bulbous swelling, the actual axonal terminal, in the stratum intermedium. In general, they serve as nociceptors, mediating the sensation of pain associated with destructive mechanical stimuli, noxious chemical substances or extreme hot and cold temperatures (Kandel et al., 1991)(De Vreese et al., 2020).

1.12.5.3 Merkel cell-neurite complexes

There were no observations of Merkel cells (Merkel cell-neurite complexes) associated with the ear canal of any species. However, these have been seen using anti-PGP9.5 in the skin of cetaceans (Lauriano et al., 2019), and in vibrissal crypts in *Tursiops truncatus* and *Sotalia guianensis* (Czech, 2007; Gerussi et al., 2020).

Also, in the transmission electron microscopy images, we did not identify any other sensory nerve formations in the subepithelial tissue or associated with the epithelium like Merkel cell-neurite complexes or free nerve endings (as shown with immunohistochemistry). In regards to the former, we could not identify any granules or large dense-core vesicles or filaments as can sometimes be indicative of or even specific for Merkel cell complexes and which are used for differentiation with other cells such as Langerhans cells and melanocytes (Kidd et al., 1971; Orfanos and Mahrle, 1973). However, these could have been missed as there was little tissue without many artefacts after the preparation.

Merkel cell-neurite complexes are slowly adapting mechanoreceptors, sensitive to sustained touch or pressure, in contrast with lamellar corpuscles, sensitive to changes in pressure and vibration (although possibly unconscious, in contrast to Ruffini corpuscles provide a conscious sensation)(Lucarz and Brand, 2007; Young et al., 2013). The absence of Merkel-cell neurite complexes in the ear canal of

toothed whales should be investigated further using additional histochemical techniques in combination with depigmentation techniques. In light microscopy, Merkel cells have been described to appear as large clear cells with a lobulated nucleus, but as such, they could be mistaken for other dendritic cells (melanocytes or Langerhans cells situated in the basal layer)) (Kidd et al., 1971). Traditional light microscopy does not readily allow for differentiation of the Merkel cell-neurite complex with other dendritic cells that are the melanocyte and the Langerhans cell (Kidd et al., 1971). Instead, specific immunohistochemical staining should be applied, in consecutive sections to anti-PGP 9.5. Anti-Cytokeratin 20 has proven successful in a variety of species, but also antibodies against neuron-specific enolase, cytokeratins 8 and 18, chromogranin A, synaptophysin, met-enkephalin, substance P, calcitonin gene-related peptide, vasoactive intestinal polypeptide, and villin show immunoreaction (e.g. Moll et al., 1992; Tachibana and Nawa, 2005; Bowker et al., 2017; Ramírez et al., 2018).

1.12.5.4 Other

No Lanceolate endings, Meissner or other lamellar corpuscles such as Pacinian corpuscles were identified in any of the tissues with any of the techniques, except for a single indication of a Meissner corpuscle in the dermis of the penis.

It is not known to what extent the peripheral nerve fibres themselves could also act as a mechanosensor as they might have mechanosensitive ion channels, called Piezo channels (Piezo1 & 2) (Coste et al., 2010; Della Pietra et al., 2020; Gottlieb, 2017). If so, these might be triggered when the nerve is stretched, in order to prevent excessive movement and tissue damage.

1.12.6 Quantitative assessment

To our knowledge, this is the first attempt that looked at a relative quantification of lamellar corpuscles in the body and head of toothed whales. Few records describe subjective impressions of 'numerous' corpuscles in some regions of the skin, such as the blowhole, anus and genital slit (Harrison and Thurley, 1974; Ling, 1974; Palmer and Weddell, 1964).

This study comprises two types of analyses, both provide preliminary insights into the distribution of lamellar corpuscles in the skin and related tissues, and over the course of the ear canal. The first was a semi-quantitative assessment corpuscles and nerves among all superficial tissues subjected to histology (See Results: Density and distribution of lamellar corpuscles in other tissues). The second was a comparison among the number of corpuscle-core cross-sections in the five regions of the ear canal.

These results are preliminary and should be interpreted with caution, as we did not attempt to assess according to stereological principles. For such a study, the sampling procedure should be systematic

and uniform with a staining technique (IHC) that allows for unambiguous identification of the lamellar corpuscles. Such an ambiguous identification was proven impossible using the variety of histochemical stains (including silver stains) that were used in this study. Immunohistochemical techniques proved useful of the identification, although there was still room for interpretation in the distinction between lamellar corpuscles and single neurite nerve fibres. Also, before proceeding to apply stereological principles, there is an essential need for a better understanding of the basic configuration of the lamellar corpuscles in three-dimensional space.

The first study confirmed previous studies on the presence of subjectively higher numbers of lamellar corpuscles in the skin in regions that were considered to be relatively sensitive. No attempt was made to make a complete comparison, as there would be the need for more samples, taken and studied according to stereological principles, and a prior need for a better understanding of the 3-dimensional morphology of the corpuscles.

The results on the quantification of the interregional density distribution of the lamellar corpuscles in the ear canal showed indications that there are no interregional distribution differences in the number of cross-sections through lamellar corpuscle cores in striped dolphin. Unfortunately, the number of specimens from other species, and their tissue condition state, did not allow for a reliable comparative analysis. We did find lamellar corpuscles in all species, including Cuvier's beaked whale, unlike what was described for giant beaked whale where all corpuscles were concentrated in the proximal half of the ear canal (Yamada, 1953). Design-based stereological methods would be needed to investigate this further, looking at intraspecific and interspecific differences, and would help to understand the function and sensitivity of the ear canal in species with different physiological adaptations (De Vreese et al., 2020).

Also, histological processing often causes tissues to shrink in the process of embedding in paraffin. A tissue embedding in glycometacrylate (TechnoVit) would have far fewer shrinkage effects in comparison with paraffin. This can be a concern when studying the morphological characteristics of tissues and also when using the physical dissector method with a two-step count for assessing the number and size of particles (Dorph-Petersen and Lewis, 2011), although this issue can be solved by using the fractionator method. Also, we assume that shrinkage was global and non-differential (although the latter should be investigated), and depended on not only the embedding in paraffin but also the animal preservation code, which was associated with the dehydration processes in the tissues.

We are aware of the potential sources of bias that could occur throughout the entire process from tissue sampling to image analysis. As such, we took into account:

- The animal´s condition code.
- The sampling protocol and manual handling of fresh tissue.

- The fixation protocol: fresh vs frozen tissue (possibly even defrosted), time of fixation after death or after sampling, manner of fixation: with or without fixed reference points such as needles into foam, to avoid post-mortem tissue deformation through muscle contraction or overall tissue conformation (e.g. in a container that is too small), and time within fixative.
- The trimming of the tissue into blocks. For example, we tried to make each block equal in width, first manually, and later by means of the antithetic slicer.
- The tissue processing with embedding in paraffin, with associated shrinkage issues.
- The mounting step, which requires a careful positioning of the tissue.
- Slide preparation: cutting, staining and coverslipping. These are standardized ways and provide little margin for bias.
- Slides sectioning with microtome, which also requires a low temperature of the tissue blocks (preparation in fridge and freezer), which should be standardized as well.
- And more

1.12.7 The role of lamellar corpuscles in toothed whales

While the lamellar corpuscles have been described in both toothed and whalebone whales, in a variety of soft tissues, their exact function is still unknown. They have been found in the skin surrounding the blowhole and the authors associated them with the detection of 'pressure changes' when passing from water to air and vice versa (Palmer and Weddell, 1964). They are also present in the iridocorneal angle of various odontocete species, where their function could be associated with mechanical deformations, such as those caused by internal pressure differences, vascular volume change, and the author even speculated on a thermosensory function (Wickham, 1980). In mysticetes, corpuscles have been described in the skin of the fin whale, most prominently in the lips and eyelids (Giacometti, 1967a), which are considered relatively sensitive areas in dolphins (Ridgway and Carder, 1990). Corpuscles have also been demonstrated in the nasal sac system and vibrissae (Degollada, 1998; Prahl, 2007), and in the ear canal of several odontocete and mysticete species (De Vreese et al., 2014; Yamada, 1953) (De Vreese et al., 2020).

Although the mechanoreceptors could form part of a general mechanical sensing mechanism, they have been postulated to take on specific tasks in the various locations in which they are situated. In the blowhole, the tactile sensation in odontocetes is associated with sensing the difference between the air and water environment, as part of a blowhole closing reflex mechanism when water covers the region (Khomenko, 1970, In: Bryden and Molineux, 1986; Bryden and Molyneux, 1986). The authors proposed that the detection mechanisms would be associated with pressure differences. Although the outcome of such a system is reasonable, the working methods provoke several questions.

First, it assumes that the blowhole would close when in contact with water, but personal observation shows that the blowhole closes before any contact with water. The opposite function, which could be more easily understood, is that the blowhole would actively open when there is no water. As such, the outcome, and the sensitivity of the corpuscle to the density differences of the medium could be the same, but the working mechanism is reversed. Based on the musculature anatomy, it is accepted that the blowhole opens actively (Degollada, 1998). Likely, the authors were aware of this fact but simply used a misleading nomenclature. Second, the authors mention the corpuscles would detect the pressure differences at the border air-water, where in fact, there is such a minute difference in pressure between the atmospheric pressure at sea level, and the pressure at just below sea level that it seems implausible that the corpuscle would be able to detect such a difference. They could rather (also) be sensitive to any kind of mechanical deformation which could come from the differences between the vibrational stimuli caused by flowing water and the breaching through the surface into the air, where there is (practically) no disturbance in the flow of the external medium. It has been shown that superficial mechanosensors in aquatic fauna can serve to detect the turbulent-flow of water (hydrodynamic stimuli with various frequencies)(Dehnhardt and Mauck, 2008), and the same has been proposed for the dolphin skin by many researchers, which could serve both a tactile and proprioceptive function (e.g. Ridgway and Carder, 1990). Bryden & Molyneux (1986) described that the corpuscle could detect the contact with water, although the exact mechanisms were not explained. Similarly, Degollada (1998)(and also Khomenko, 1974, In: Degollada, 1998, even though this author did not specify the exact location) described the same lamellar corpuscles in the nasal sac system, particularly in the wall of the vestibular sacs, in which water could enter, and the ´contact´ with it could be detected, assisting in a reflex closure of the nasal tract. The highest concentrations of corpuscles were in the nasal plugs and the posterior wall of the spiracular cavity, both of which are considered important in the closing of the tract and the control of air passage during phonation. This would imply a precise control mechanism that could regulate both the degree of tension on the tissues, as well as the air pressure in the nasal sacs. A similar control mechanism could be present in the external ear canal.

1.12.8 Reflections on the physiology of simple lamellar corpuscles

Mechanoreceptors are involved in three known sensory systems, namely the Auditory, the Vestibular and the Somatosensory system. Within these, the modalities that receptors are involved in are Hearing, Balance and the Somatic senses, Touch and Proprioception. The energy of the associated stimuli is labelled as Sound, Balance and Pressure and Displacement respectively. In the human fingers, there are four types of well-known mechanoreceptors (Pacinian corpuscles, Meissner corpuscles, Ruffini endings, and Merkel cell-neurite complexes), the combination of which provides us

with different submodalities of touch, such as the sensation of contact with an object, steady or changing pressure on the skin, or tingling sensations or vibration (Kandel et al., 1991).

For marine mammals, which live in a completely different environment with a medium that is significantly denser than air, and which experience great variations in pressure differences when diving, the distinction between pressure, tissue displacement or deformation, and even sound (particularly in low frequencies, cfr. frequency sensitivity of lamellar corpuscles such as Pacinian corpuscles, and tactile sensitivity of dolphin skin (Ridgway and Carder, 1990)), is often not so clear as in air. For example, low-frequency sound can be perceived as a corpuscular sensation, comparable to the loud and low-frequency sounds one can feel in the belly when music is playing loud. Similarly, the elephant's 'seismic communication' fits into this scope with the earth as medium being denser than air which has consequences in the physical characteristics associated with sensing the environment. Also, the elephant foot is similarly equipped with various lamellar corpuscles and fat that could function like acoustic fat in toothed whales, both of which lend the elephant foot apt to play a part in the detection mechanisms for low-frequency signals (Bouley et al.; O'Connell-Rodwell, 2007). The question as to which modalities the elephant foot can be related, is a topic of discussion, similar as the modalities (and possible submodalities) of the sensory system of the external ear canal in toothed whales.

Each receptor is triggered by an adequate stimulus, the specific signal of a type of energy that triggers the receptors in the ear canal at low energy level (smallest amplitude) in a certain range (bandwidth) of a form of energy. All cutaneous receptors have an absolute specificity, but also a selective specificity, which refers to the high sensitivity of the receptors towards a certain form of stimulation (e.g. mechanical deformation), while in fact, other types of stimulation could also trigger the receptors, but at higher thresholds (e.g. temperature changes)(Iggo, 1977). According to Malinovský (1996), all kinds of SNF's can function as mechanosensors while each kind is linked to one or more modalities of physiological significance (e.g. sensation of pain, cold, pressure). An exception to this is the glomus complex, which is only triggered by chemical stimuli. The sensitivity of an organ, its capacity to sense a mechanical deformation of the tissue, is determined by the type, location, and density of the receptors in that area (Kandel et al., 1991). The receptive field of a sensory neuron is the space (e.g. area on the skin) in which a stimulus can trigger the firing of the neuron. The smaller the field, the more precisely the stimulus can be located in space. Pacinian corpuscles have large, poorly defined receptive fields, while Meissner´s corpuscle have small receptive fields. The receptive field of simple lamellar corpuscles is unknown. The receptive field goes hand in hand with the density of the receptor organs, which determines the precision or resolution of the receptiveness of the tissue

in which they are embedded. It would be interesting to elaborate the studies of the ear canal, to be able to specify the apparent extraordinary sensitivity of the canal.

Specifically, these systems provide four basic types of information of the stimulus: modality, location, intensity, and timing, all embedded in the action potentials conveyed to the central nervous system. Since the sensory nerve formations of the ear canal in toothed whales are mainly associated with the ability for mechanosensation, the focus for a preliminary functional interpretation/hypothesis will be put on the morphological characteristics that could indicate a sensitivity towards the type of signal that could trigger the corpuscles, together with the specific characteristics embedded in that signal. All of these specialized nerve endings transform mechanical to electrical energy through a change in the membrane permeability after which the electrical signal gets transmitted over afferent nerve fibres to a ganglion and to the central nervous system. The generated action potentials form part of the neural code in which the frequency patterns and amplitude carry the information, which science is starting to decipher. The information embedded in that code is then perceived and interpreted by the CNS, but only as imperfect shadows of reality, framed into a context with complementary sensory input, to form a temporary and incomplete interpretation of the environment.

In this preliminary hypothesis, we do not exclude that the receptors could be sensitive to multiple types of stimuli, but the commonly accepted one, also consistent with our results, is that of mechanical deformation. Among the main stimuli that can trigger deformation of the soft tissues of the ear canal in cetaceans, we consider (a) changes in ambient hydrostatic pressure, (b) vibratory or pulsed stimuli coming from the natural environment and/or from other animals such as conspecifics, and unnatural sources such as anthropogenic noise (this would allow them to hear or feel the environment, depending on the perspective), and finally, (c) touch, although an associated behaviour has never been reported. For the detection of ambient pressure, the suited type of mechanoreceptors would have a slow adaptation rate, while for transient deformation such as vibration, it would be rapidly adapting. The lamellar corpuscles described here, show an immunohistochemical and ultrastructural resemblance to the inner core of a Pacinian corpuscle, a rapidly adapting, low-threshold mechanoreceptor (Ide et al., 1988; Munger et al., 1988; Vega, 1996; Zelená, 1994). However, an artificial removal of the outer core of the Pacinian corpuscle lowers its adaptation rate (Loewenstein, 1971). This could allow the corpuscles described here to be stimulated by (more or less) constant stimuli (Kandel et al., 1991)(De Vreese et al., 2020). Also, the absence of the outer lamellar core would omit the amplitude and frequency filtering mechanism it accommodates (Iggo, 1976; Zelená, 1994), leading to a corpuscle that can be stimulated by smaller deformations over a wider frequency range. Also, it is generally easier for animals to detect changes in the environment than it is to assess static conditions in the same environment. Therefore, although we cannot make definite conclusions on the

adaptation rate of the lamellar corpuscles described here, we hypothesise they could be appropriate for the sensation of changes in pressure, and the associated perception of depth.

Such information would be essential to accommodate physiological responses associated with diving, through general body responses, after processing in the central nervous system, or through arched reflexes in structures that are connected to the same neural ganglia. One of the most striking adaptations of toothed whales is the ability to cope with significant pressure differences through vascular perfusion and the presence of extensive arterial and venous plexuses and retia mirabilia (Costidis and Rommel, 2016a, 2016b; Cozzi et al., 2017). Connected to the same neural ganglia, are the middle ear and its corpus spongiosum, and the mandibular fat bodies and accessory sinus complex with extensive venous plexuses and prominent arterial supply (Costidis and Rommel, 2012), which are all novel evolutionary structures subjected to large pressure differences and showing considerable physiological flexibility, and are essential for a correct functioning of the hearing apparatus at depth. While there are indications of pressure-related redistributions of blood, at least in the middle ear and pterygoid sinuses, it is not yet known how those might be regulated. For comparison, there are indications of active vasodilation of the vascular lacunae in the dolphin trachea with nitric oxide as chemical messenger (Cozzi et al., 2005), possibly coordinated through a centrally stimulated parasympathetic innervation (Kandel et al., 1991). It would be interesting to study how the blood supply in the middle ear and associated tissues is controlled.

To get a better understanding of the biomechanical properties of the corpuscles, further immunohistochemical characterisation could be achieved with the use of antibodies for neuronal and neurotransmitter-related molecules, possibly using confocal microscopy as this would also provide information on the 3-dimensional structure. Such information could be used for modelling and to mimic the response of these corpuscles to various stimuli (De Vreese et al., 2020).

Based on the morphological resemblances to well-described lamellar corpuscles such as Pacinian and Meissner corpuscles, we can assume the triggering mechanism are the same, which are the mechanosensitive ion channels in the plasma membrane of the axon terminal. A mechanical deformation causes the ion-channels to open, which causes Na-K –ion exchange and the creation of an electric generator potential. The deformation happens in a direction that is perpendicular to the longitudinal axis of the sensory corpuscle (Figure 312)(Loewenstein, 1971). The configuration of the tortuous lamellar corpuscles in the ear canal of toothed whales would render them suitable to be stimulated from various directions, which corresponds to the convoluted nature of the ear canal and the possibly multidirectional vectors of its motion.

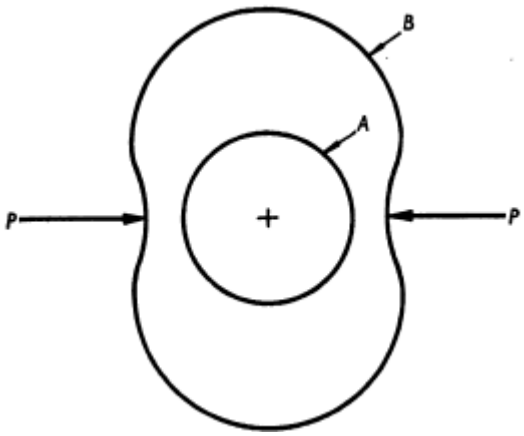

Figure 312. Drawing of a mechanical stimulus on a Pacinian corpuscle in cross section. Any steady displacement would not deform the inner core (A), but would pass on the forces (P) after amplitude and frequency filtering in the outer core (B). In simple lamellar corpuscles, however, there could be a deformation of A, since B is not present. (Source: Loewenstein and Skalak, 1966).

1.12.9 The role of lamellar corpuscles in the ear canal

In terrestrial mammal external ear, the role of the (mechano)receptors is to maintain chemical, temperature, bacteriological and ionic homeostasis. Hence, when a movement happens in the external ear canal, it is perceived as a threat to the homeostasis by these mechanoreceptors (Carlson, 2004). The presence of simple lamellar corpuscles observed here in the ear canal in several delphinid species, a long-finned pilot whale and a Cuvier's beaked whale, together with literature references for several other species, including baleen whales (De Vreese et al., 2014; Yamada, 1953), make plausible that these constitute a common characteristic among cetaceans. The lack of such SNF in terrestrial mammals indicates that this feature may be considered an evolutionary adaptation of the ear canal of cetaceans to life in an aquatic environment. In comparison, there is an online mentioning of Pacinian corpuscles, Meissner corpuscles and hair follicle receptors in the ear canal of humans, associated with a reflex mechanism that would serve to expel foreign objects by means of glandular secretion and muscular contraction (Chartrand, 2005), while we could not find morphological evidence of such SNF in the cited literature (Grennes, 1999; Kress and Zeilhofer, 1999; Spray, 1986). Moreover, a recent study that used immunohistochemistry with NF, S100, and MBP (myelin basic protein), concluded that there were no SNF in the cavum conchae or cartilaginous portion of the external ear canal in humans (Bermejo et al., 2017). However, it is reasonable to assume that the presence of lamellar corpuscles in the stroma in between glandular units in the external ear canal of toothed whales, could confer a propriosensory role which could influence the glandular secretion and/or the excretion into the ear canal (e.g. with muscular contraction). The ear canal of all terrestrial mammals that have been studied is well-innervated (Alvord and Farmer, 1997; Folan-curran et al., 1994; Miller et al., 1964; Sommerauer et al., 2012; Watanabe et al., 2016), but how it is triggered by external stimuli is not clear (De Vreese et al., 2020).

Based on morphological data, we hypothesise the tissue shapes under a variety of circumstances: The mechanoreceptors are possibly triggered by the combination of external pressure and associated tissue deformation, or by the current tension/pressure on the tissues relative to the resting state of the tissue at the surface. Supposing that the ear canal is filled with air, at least in its medial half, we suppose the resting state of the tissue would be the state of conformation at the surface boundary air-water, as this would allow the animal to get a consistent reference pressure level of 1 atm. The resting state of the tissue would be consistent with the absence of a lumen distal to the glands, closed by the collapsed epithelium, or simply strong epithelial production, or filled with glandular content and desquamated epithelial cells. At the same time, the orbito-auricular and superficial occipito-auricular muscle could exert a force on the adipoconnective tissue sheath, which could create a lumen that is continuous between the exterior medium and the tympanic membrane. As such, air could be exchanged between the exterior atmosphere and the interior of the ear canal, while water would not enter such a small lumen because of its cohesion characteristics. As the animal dives, the superficial muscles relax, the lumen closes, and the air is trapped inside the canal. According to Boyle´s law, the volume of the air varies inversely with the pressure (at constant temperature). As such, the air could get compressed gradually along the course of the canal, with the canal collapsing progressively from the superficial soft tissue to the spiraling curvature where it is surrounded by a denser connective tissue and supported by a cartilage on one side. The compressed air accumulates at the medial end of the canal, where the lumen is greatest and is supported by cartilage trench, and the presence of vascular lacunae, which could allow for controlled closure of the lumen, structurally similar to the dolphin trachea (Cozzi et al., 2005). In this process, the gradual deformation and possible collapse of the ear canal, and the gradual compression of the soft tissues, would allow for triggering of the mechanoreceptors along its course, in which the topographical distribution could serve as a ´measuring tape´ for the pressure conditions, and therefore the depth at which the animal is present. Further information on the topographical distribution of the lamellar corpuscles, based on unbiased stereological techniques and possibly supported by three-dimensional data, within and among species, would be needed to understand this process better. In deeper waters, all air would be trapped on the lateral side of the tympanic membrane, while the air pressure inside the middle ear could be regulated via the very muscular auditory tube that is connected to the nasopharynx. For us humans, it is essential to maintain an equilibrium between the air pressures on both sides, and, although unknown, so could be the case for toothed whales. In fact, (Fraser and Purves, 1960) stated that the cetacean middle ear is under positive pressure at the surface, causing tension on the tympanic ligament and strain on the malleus if not for the compensating forces acted out by the tensor tympani muscle. We believe this muscle alone could not handle the pressure changes and forces acted upon

the tympanic ligament during diving if not for a pressure compensating mechanism on the other side of the tympanic membrane, through the deformation of the ear canal soft tissues and the entrapped air. Moreover, the elaborate presence of mechanoreceptors along the entire course of the ear canal indicates that there is a need for a detailed sensation at high resolution of the conformation of the canal. The current pressure-monitoring hypothesis would allow for the soft tissue associated with the external and middle ear, and possibly also the tissues that are innervated by the same cranial nerve (V3) to adapt to the changing environment, which could be essential for a correct functioning of the various soft tissues associated with the hearing apparatus, and possibly with more general physiological mechanisms. The exact trigger or ´modus´ of the lamellar corpuscles is not known up to date. It is known that these corpuscles also occur in other soft tissue in cetaceans, such as in the nasal sac system, the iridocorneal angle and throughout the skin, although not in such high concentrations and specific formations such as the distribution around the ear canal in its lateral half, and concentrations into a ´sensory ridge´ in the medial part**.** The working hypothesis, supported by our results and literature findings (e.g. Yamada, 1953), is that the ear canal has acquired a new sensory role and would be able to detect the changes in ambient pressure, while the topographical distribution of the lamellar corpuscles, and the intricate association with a complex configuration of the lumen and the surrounding soft tissues, could allow for a graded sensation. (De Vreese et al., 2020).

To conclude, I sympathise with a quote from the great James G. Mead: "*I have drawn functional conclusions from the basis of this comparative study, but these are largely unsupported by experimental data"* (Mead, 1975).

2 Innervation of the external ear canal in other species

2.1 Baleen whales

In brief, the general configuration of the external ear canal in baleen whales is similar to the one in toothed whales, with two major differences. First, it is completely and permanently closed in the deeper blubber layer. As a consequence, there is an accumulation of glandular and epithelial desquamated products inside the external ear canal, forming what is called the 'earplug'. This earplug is present from before birth, during the entire lifetime of the animal, grows with the years, and can even be used in post-mortem and museum specimens for age estimation and hormonal analyses, similar to dendrochronology studies (Trumble et al., 2013). Second, the tympanic membrane is not a flat surface, but protrudes extensively into the external ear canal, taking on the shape (and the corresponding epithet) of a 'glove finger' (Ketten, 1997). All other characteristics, including the glandular structures, striated musculature, cartilage, lymphoid tissue, and nervous tissue including the presence of simple lamellar corpuscles, are similar to the situation in toothed whales (Boas, 1912;

Clarke, 1948; De Vreese et al., 2014; Fraser and Purves, 1960; Hanke, 1914; Home, 1812; Ketten, 1997, 2000; Rehorek et al., 2019b; Reysenbach de Haan, 1956; Solntseva, 2007; Yamada, 1953).

Baleen whales also possess similar sensory nerve formations in the skin, which were labelled as "Small Vater-Pacini corpuscles" in a higher level of the dermis in fin whale, scantly in the skin of the back and belly, but high in numbers in the lips and eyelids, and Winkelmann mucocutaneous end organs, visible as ´round masses of neurofibrils situated in the rete ridges´ (Giacometti, 1967b)[7].

The function of the baleen whales external ear canal is equally enigmatic as in toothed whales. It is assumed to have lost its function in the sound reception process with the development of other pathways. Although there is still discussion on the pathways, it likely includes both bone and soft tissue conduction (Cranford and Krysl, 2015; Yamato et al., 2012). The function of the ear canal in this or other contexts, nor the role of the earplug and glove finger are known.

2.2 Pinnipeds

The external ear canal in pinnipeds resembles the ear canal in terrestrial mammals more than cetaceans. All pinnipeds feature the same morphological characteristics of the external ear canal although with minor differences between and among families. True seals (phocids) have a long and narrow ear canal with several bends and consists of a cartilaginous and osseous part. The content consists of cerumen, hairs and epithelial cells. The lumen is lined by a non-keratinized, pigmented, stratified, squamous epithelium, and sebaceous and ceruminous glands. The lumen can be closed by musculature in two locations, externally at the external ear opening, and internally at the tragus. The hypodermis contains adipose tissue, connective tissue with collagen and elastic fibres, fibroblasts, and vasculature. The latter presents 'blood sinuses' associated with the cartilage and in the bony region of the ear canal, very similar in distribution and configuration to the vascular lacunae in toothed whales. There are various cartilaginous plates, into which striated muscles insert, allowing for a movement of the ear canal, and mechanisms for closing the canal when diving. The cartilage plates consist of a hyaline core while peripherally, it is composed of elastic fibres (Ramprashad et al., 1972).

Eared seals (otariids) and walruses (odobenids) do have an external pinna, while the ear canal is very similar to the ear canal in true seals (Loza et al., 2019; Wartzok and Ketten, 1999).

There exist no detailed descriptions of the innervation of the ear canal in pinnipeds, nor of any sensory nerve formations in the external ear canal. The innervation was described as ´poor´ in Otariids, and ´rich´ in Phocids (except in elephant seal), especially in the proximal region of the cartilaginous part of the ear canal (no attention was given to the osseous part), and all innervation was associated with glands and muscles (Loza et al., 2019).

[7] I assume the term ´rete ridges´ can be interpreted as ´dermal papillae/ridges´ as can be seen in his Figure 6

When in air, pinnipeds use the external ear canal to conduct sound to the middle ear as in terrestrial mammals, while in water, the ear canal closes and the animals are believed to rely on both soft tissue and osseous sound conduction (Nummela, 2008; Reichmuth et al., 2013).

2.3 Sirenians

Sirenians have a tiny external opening dorsocaudal to the eyes, without a pinna, similar to cetaceans. The external ear canal is a slightly curved, very narrow canal that is at least partially occluded with debris and epithelial cells (Bullock et al., 1980; Chapla et al., 2007; Ketten et al., 1992).

2.4 Terrestrial cetartiodactyla

The results on the morphology of the external ear canal in the terrestrial mammals in this study are in line with the general morphology of the terrestrial mammal ear canal, although differences between species, such as the large size differences, and with strikingly different innervation patterns than in toothed whales. The absence of lamellar corpuscles or other distinct sensory nerve formations indicated that the lamellar corpuscles in toothed whales (and in cetaceans in general) are an evolutionary adaptation, acquired after the return to the aquatic environment. In common with toothed whales, and with other terrestrial mammals, are the intraepithelial free nerve endings. They serve as nociceptors, mediating the sensation of pain associated with destructive mechanical stimuli, noxious chemical substances or extreme hot and cold temperatures (Kandel et al., 1991). Finally, we did not note any other types of SNF such as Merkel cells associated with the ear canal of any species, although these have been seen in the skin of cetaceans using PGP9.5 (Lauriano et al., 2019). (De Vreese et al., 2020).

3 SNF in tissues of secondary interest

The presence of SNF, and particularly lamellar corpuscles, in tissues of secondary interest, was generally in line with literature findings, such as for the skin, or, for tissues that were not yet studied before, the results were in the same line as reported before. In all of the tissues of secondary interest, mostly investigated in striped dolphin, and several tissues also in bottlenose dolphin and Cuvier´s beaked whales, the number of nervous structures was relatively low in comparison to the external ear canal. The exception to the rule were the penis and vibrissal crypts. Although no absolute quantitative comparison has been made, the preliminary results highlight the exceptional innervation of the external ear canal, which stood out in the number of corpuscles and nerve fibres. Further research could investigate this in detail, using fresh tissues of various species, dissected and prepared using a study design with the application of stereological principles, and the unambiguous histological identification of nervous structures using immunohistochemical techniques.

3.1 Penis

The organ was cut transversely at three levels, and the histological aspect of the dermis was very similar in all cases. Besides lamellar corpuscles, there were few indications of Meissner's corpuscles in histological (HE-stained) images of cross-sections of the penis in striped dolphin. This should be investigated more, using immunohistochemical techniques, as they might occur in other organs as well, which could contribute to the knowledge of the mechanosensory system in cetaceans. If they are indeed Meissner's corpuscles, and in what other locations they might be present. Lamellar corpuscles, including genital end-bulb, simple, Pacinian and Ruffini corpuscles, have been described in the human glans penis, together with numerous free nerve endings, (isolated and in the corpuscular form) and dermal (!) Merkel cells. The absence of Meissner corpuscles, together with the absence of Merkel-cell neurite complexes, makes the glans penis different from the human fingers in terms of thresholds for tactile and painful stimuli (Halata and Munger, 1986). The simple lamellar corpuscles were very similar to the corpuscles described in the ear canal in toothed whales. The morphology included the central axon with lamellar core and the lack of a capsule (e.g. Fig. 12 in the article).

Similarly, in the glans penis of the rat, there are abundant free nerve endings, small lamellar corpuscles, and Ruffini corpuscles; while no Merkel cell-neurite complexes, Meissner or Pacinian corpuscles found (Johnson and Halata, 1991). The distribution of lamellar corpuscles, including Meissner, is not the same in the entire penis. For example, there are Meissner's corpuscles in the human prepuce (Martín-Alguacil et al., 2015), but only in small numbers, which decrease with attaining sexual maturity (Cox et al., 2015).

3.2 Anus, urogenital fold, mammary gland

It was unsure if there where sensory nerve formations present in the skin around the anus and urogenital fold in dolphins, while there were relatively abundant small nerve fibres.

In Cuvier´s beaked whale the mammary gland was well innervated with many small nerve fibres embedded in the connective tissue of the superficial dermis, from just below the epidermis to the transition with the adipose tissue, while it was not clear if the were SNF's present.

3.3 Extremities: pectoral fins, dorsal fin, and fluke

Our limited findings concur with the literature on the innervation of the skin of toothed whales (Palmer and Weddell, 1964; Ridgway and Carder, 1990) in that there is a distribution of sensory nerve formations over the entire body, although very scarce in certain areas and therefore could be missed in histological examination. This could explain the difference found between the ventral and dorsal side of the pectoral fin innervation.

3.4 Blowhole

There were abundant lamellar corpuscles in the skin around the blowhole, in the anterior and posterior lip and the commissures, as previously reported (Khomenko, 1970, In: Bryden and Molineux, 1986; Bryden and Molyneux, 1986).

3.5 Throat groove

Cuvier´s beaked whale was the only species to present a throat groove, as do all beaked whale species, which allows for the throat region to expand during suction feeding (Heyning and Mead, 1996). The ultrastructure of the throat groove was very similar to that of the skin, except that it was very well-vascularized, with exceptional amounts of vascular structures in the dermal papillary layer. The presence of SNF's was not apparent in HE-stained sections. There was also a rich innervation with small nerve fibres with an apparent different composition that in other areas, in that there was a more considerable amount of *basophilic connective tissue* between and surrounding the axon support cells, while the perineurium stained as in other tissues and species. Although likely an artefact, it could be interesting to do a characterization of the nature of the tissues and to compare with nerves fibres in other locations and other species.

3.6 Vibrissal crypt in toothed whales

Czech (2007)(and also Czech-Damal et al., 2012b, 2013) found single and clustered encapsulated lamellar corpuscles in the cavernous sinus peripheral to the capsule of the vibrissal crypt in the neonate bottlenose dolphin, but could not say if all corpuscles shared a common axon, or were individually innervated. Interestingly, there were no corpuscles found in adult bottlenose dolphin, while in harbour porpoise there were lamellar corpuscles in all age groups. Also, in Franciscana dolphins, there were lamellar corpuscles, close to the stem of the vibrissal crypt. Lamellar corpuscles were also found in the mesenchymal sheath of adult bottlenose dolphin together with Merkel-cell neurite complexes, lanceolate endings, and free nerve endings along the entire vibrissal crypt (Gerussi et al., 2020). Intraepithelial nerve fibres were common in the upper third of the vibrissal crypt in harbour porpoise, although only in adult animals, while they were found throughout the entire crypt in Guiana dolphin, although absent in Franciscana dolphin. This species also did not present intraepithelial nerve endings or Merkel-cell neurite complexes, while there were low numbers of Merkel cell-neurite complexes in bottlenose dolphin and Guiana dolphin. There were lanceolate endings in the vibrissal crypts of Guiana dolphin (*Sotalia guianensis*). Similar, in Franciscana dolphin, there were presumable lanceolate endings in the upper half of crypt and along the stem.

More in-depth descriptions of the presence and distribution of various SNF's, including lamellar corpuscles, and comparison among age groups in bottlenose dolphin, can be found in a recent publication (Gerussi et al., 2020).

3.7 Mandibular fat bodies and ventral sinus complex

There was difficulty in obtaining relevant samples of the peribullar and posterior sinus wall for several reasons. First, because the tympanoperiotic complex had to be removed before sampling was possible. As such, the connective tissue structures that hold it in place had to be cut, together with the vestibulocochlear nerve. In this process, it was impossible not to damage the peribullar sinus wall. Second, the wall in itself was very thin and intensely associated with the skull making it hard to remove the soft tissue by itself. As such, the samples often contained bone tissue and were, therefore decalcified. The pterygoid sinus walls were much easier to samples in this respect. No corpuscles were identified with certainty in any of the sinus walls, although there was a relatively rich innervation with small nerve fibres. The same counted for the intra- and extramandibular fat bodies. It cannot be excluded that SNF's have been missed, due to the limited sampling size and the histological techniques applied.

3.8 Eye

In the eyelid and commissures, there were lamellar corpuscles and small nerves as expected for the most sensitive regions of the head (blowhole and circumocular skin) (Ridgway and Carder, 1990).

We confirmed the presence of lamellar corpuscles in the iridocorneal angle of the eye in striped dolphin and long-finned pilot whale, in addition to all the other odontocete species in which this has already been reported (exc. spinner dolphin) (Vrabec, 1972; Wickham, 1980). The presence of lamellar corpuscles has also been reported in the eye of aquatic birds (Vrabec, 1961; Vrabec, 1972).

4 Analysis of Techniques

All of the techniques that were applied in this study, from macroscopic dissection to histological staining, ultrastructural analyses, software, etc. are revised in the Annex. There, the validation of the techniques for their specific purposes is demonstrated. Although most of the techniques proofed successful, others did not (entirely) for the respective objectives. Also, there are further recommendations for the applications of similar techniques for future studies.

5 Pathology

We describe various pathologies associated with the external ear canal. Strikingly, there was a significant number of cases with otitis externa. There was an ear canal inflammation in at least six animals, comprising four different species. Our conservative approach might have led to an underestimation, because the degree to which the activation of the ECALT was considered a pathological finding, was not always evident. We considered a scant number of resident lymphocytes in the subepithelial tissue, diffusely arranged or in clusters, associated with the glands and between ear canal and cartilage, together with scant other mononuclear cells such as plasmacells, to be a

normal finding. Activation of the tissue would present a wider variety of inflammatory cells, including lymphocytes, mast cells, plasma cells, macrophages, neutrophils. There were often inflammatory cells in the glandular excretory ducts and inside the ear canal lumen.

It is not known what effect the various pathologies, such as otitis externa could have on the sensory function of the ear canal. An inflammation could cause higher tension in the tissues due to the influx of cells and fluids into the connective tissues. It could be accompanied by the release of inflammatory mediators causing vasodilation, increased permeability of the vasculature, and the influx of plasma proteins and fluid into the tissue. Such a compression might have an effect on the various SNF's, specifically the free nerve endings, with nociceptic capacities and the possible sensation of pain. The implications for the lamellar corpuscles are challenging to anticipate since the lack of knowledge on the functional morphology and their significance in the external ear canal. However, it can be assumed that any pathological process that could impede the normal function of an organ, especially when it regards the somatosensory system, could have severe consequences for the vitality of the animal. More attention should be dedicated to pathological processes in the external ear canal of cetacean species around the world.

The single pathological findings in one ear canal of a harbour porpoise, which included an acute, local inflammation of the tissue between ear canal and cartilage, together with local muscle degeneration, was likely due to tissue damage associated with a live stranding event. It is interesting to note, that there was no pathology specific for the external ear canal in any of harbour porpoises. It is too early to speculate on the differences in pathological findings between harbour porpoise and the other species, in which there was often some kind of pathology or at least activation of the ECALT.

There were various lesions associated with live stranding events, such as muscle degeneration and contracted arteries, while in the few cases that presented a haemorrhage around the ear canal, it was not known if they might have stranded alive. A haemorrhage is considered a common and non-specific finding in stranded odontocetes, although specific events such as barotrauma could cause haemorrhages in the middle ear canal and rupture of the tympanic membrane (NOAA/NMFS and US Navy, 2001). It is currently not known if the external ear canal is sensitive to barotrauma or acoustic overexposure, while it could be possible if contains gas. As such, the ear canal lumen could resonate to a vibration or change rapidly change in conformation with abrupt pressure differences, which could cause changes in tissue stress, and could lead to the rupture of membranes on a cellular or tissues, e.g. the epithelium of the ear canal, endothelium of vascular structures. For an deeper discussion on the various pathological findings, see Annex case reports. Currently, there is only speculation on the aetiology of the lesions, on the role of the pathogens, or the effects they could have on the health of the animal.

There is a need for a deeper investigation on the impact that the described pathologies and diseases can have on the animal, even if the external ear canal is a secondary location in which the lesions manifest. This is essential for gaining insight in the aetiology, and the actual pathological processes, in the scope of anthropogenic and natural acoustic exposure and pressure changing events, marine mammal diseases and pathogens. In any case, these results strongly recommend the sampling and histological analysis of the external ear canal in routine postmortem investigations. It could provide information on the general health status of the animal, on the stranding conditions (alive or dead), and on specific pathological constitutions. As such, there are on-going discussions that advocate the needs for new research and investigation on the sensitivity of marine fauna, which could be useful to get a more comprehensive understanding of the possible impacts of anthropogenic sounds on marine biota. (e.g. JPI Oceans: Strategy Framework beyond 2020)

6 Future research

This research addresses the lack of basic knowledge on the peripheral nervous system in the head of cetaceans and opens the path for more detailed studies regarding the understanding of the functionality of their somatosensory system. The same is valid for the morphology and functionality of the external ear canal and its associated soft tissues. Future research could focus on these two aspects in a non-exclusive manner.

It also highlights the need for comprehensive studies on cetacean post-mortem assessment, and for a basic understanding of their normal physiology, which will support the development of an all-inclusive forensic approach

6.1 Confocal microscopy studies

In this study, we have already undertaken preliminary steps to gain a better understanding of the intramural nervous plexus and the 3D morphology of its lamellar corpuscles.

Based on the validated immunohistochemical techniques using antibodies for PGP9.5, S100, and NF, combined with DAPI for the staining of cell nuclei, a protocol has been developed and fine-tuned for the study of about 0.5 mm of tissue, similar to the dimensions of the nervous network reconstruction in this study, which was based on HE stained slides. The leverage of the use of antibodies would allow for an in-detail insight into the tissue that makes up the corpuscles in 3D, to differentiate between corpuscles and nerve, the transition between the two, and the connections, ramifications, bifurcations and possibly also the coalescence between these structures (See e.g. Link video). Preliminary results at the current stage, show that the protocol is valid and that the indications regarding the complexity of the auricular intramural plexus as given by the HE-studies, are legitimate and require an in-depth analysis.

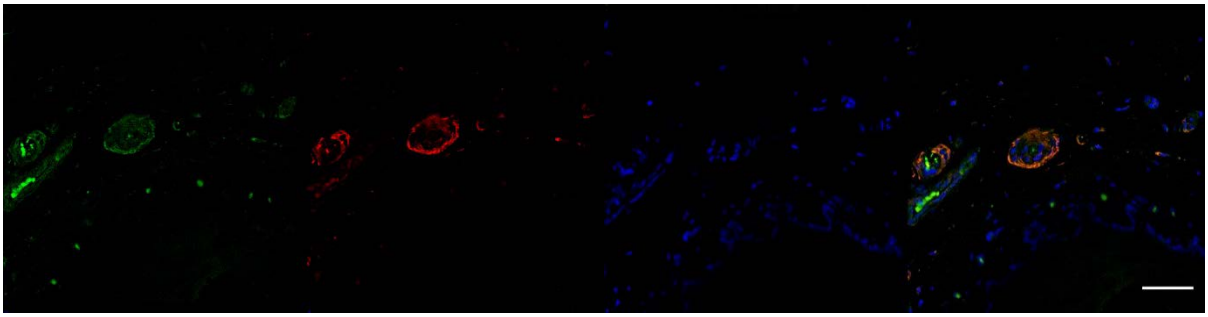

Figure 313. Immunofluorescent confocal microscopy images of a section of a small subepithelial region of the external ear canal of a striped dolphin, showing a lamellar corpuscle stained with (1) anti-NF, (2) anti-S100, (3) DAPI, and the composite image of the three (4). Scale bar 50 µm

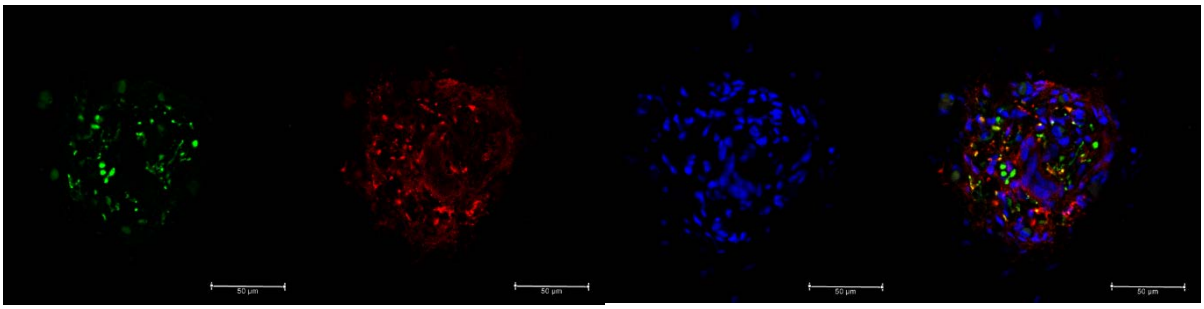

Figure 314. Immunofluorescent confocal microscopy images of a cross=section of a nerve fibre stained with (1) anti-NF, (2) anti-PGP9.5, (3) DAPI, and the composite image of the three (4).

6.2 Dynamic modelling of the ear canal and associated tissues

Ted Cranford and Peter Krysl (e.g. Cranford & Krysl, 2012, 2015) developed protocols that allow for *finite element modelling* (FEM) of the vibroacoustic environment inside a whale's head (e.g. Cranford et al., 2010; Cranford & Krysl, 2015; Escobar, 2016). These methods have had various applications in studying both the sound production (Aroyan et al., 1992) and reception mechanisms in cetaceans. These techniques have been applied successfully in studies on hearing in terrestrial mammals as well (E.g. (Wada et al., 1992). Similarly, the combination of morphological data obtained from medical imaging techniques such as DICECT (https://dicect.com/), (Synchrotron-based) micro-CT (Descamps et al., 2014), (micro-)MRI, DTI (Jambawalikar et al., 2010), or high-resolution sonography of the ear canal (Peer and Gruber, 2013), could be used to create a biodynamic model for physical simulation of the tissues (Aroyan, 2001; Aroyan et al., 1992). If possible, this could be combined with acoustic propagation models derived from data obtained from the measurement of the physical properties of the tissues of interest, which can include: sound speed, density, elasticity, hysteresis (i.e. energy loss during elastic tissue deformation), etc. (e.g. Soldevilla, 2005), which contribute greatly to validating, adjusting, and perfecting the models to the real-life complexity of the sound reception mechanisms. If possible, data could be extrapolated, as associations have already been demonstrated between e.g. the Hounsfield units (HU) of CT scans and the physical sound speed measurements in the tissue (Soldevilla, 2005).

6.3 Mechanical testing of the ear canal lumen

It could be interesting to test whether air or sea-water could pass through the lumen of the ear canal. This would require a sealed double-chamber space with the intact ear canal including tympanic membrane, suspended in the wall between the spaces. The test could apply pressure differences between the two spaces, investigating the tension on the tympanic membrane, the tendency for the ear canal curvature to change shape, and correlated with a centrifugal change in tension on the soft tissues where the musculature inserts. Similarly, McCormick et al. (1970) applied artificial intraluminal air pressure to the medial end of the ear canal (160-mm Hg), which 'expanded the walls of the canal'.

6.4 Morphofunctional features of sensory nerve formations (lamellar corpuscles) and the intramural nervous plexus

Here, we propose to identify and map the cranial nerves contribution to various parts of the external ear canal, using retrograde neuronal tracers (e.g. fluorogold) and the appropriate microscopic visualization techniques (Folan-Curran and Cooke, 2001; Folan-curran et al., 1994; Tierney et al., 1993). This could provide insight into the various nervous ganglia that are responsible for the innervation of the ear canal, and which cranial nerves are they connected to. Also, medical imaging techniques such as diffusion-weighted MRI and tractography could be useful in this process (Hiltunen et al., 2005; Khalil et al., 2010), and could provide information on pathologies such as nerve degeneration (Simon and Kliot, 2014). As in the case of working with cetaceans, the research will likely involve fixed tissue rather than live specimens. Therefore, standard DT-MRI methods using diffusion-weighted spin-echo might not provide the best results (Miller et al., 2012), while alternatives such as diffusion-weighted steady-state free precession might be better suited (McNab et al., 2009).

Next, would be a characterisation of the nature of the peripheral nerves, to differentiate between motor and sensory nerves and their activity patterns using (immuno)histochemical techniques (e.g. Karnovsky's staining for choline acetyltransferase activity, Hansson's staining for carbonic anhydrase; IHC with Agrin, vasoactive intestinal polypeptide, calcitonin gene-related peptide, annexin V, tyrosine hydroxylase), possibly in combination with fluorescence microscopy (e.g. Cavallotti et al., 2004). This could also be applied to the lamellar corpuscles, together with other antibodies such as myelin-basic protein (García-Suárez et al., 2009), and vimentin and epithelial membrane antigen (EMA) for the identification of the nature of the corpuscle's peripheral layer (Del Valle et al., 1998). These antibodies, or the antibodies already applied in this study, could be used with confocal microscopy, together with applying mechanical forces. As such, dynamic response data of the corpuscles could be obtained (cfr. Pitts-Yushchenko et al., 2013; Summers et al., 2018).

If there is truly an absence of an outer core and capsule in the lamellar corpuscles, this might allow for studying the mechanisms of transduction using patch-clamp techniques to study electrophysiology

of the axon and the lamellar cells, which might have a sensory function themselves (Nikolaev et al., 2020), something that not fully understood in lamellar corpuscles and which is complicated in Pacinian corpuscle due to the presence of an outer core.

Also, more research could be done on the investigation of other sensory nerve formations such as Merkel-cell neurite complexes in various organs (cfr. Ramírez et al., 2018).

6.5 Post-mortem assessment

The current study also draws the attention to the importance of anatomy and pathology in the context of veterinary evidence-based medicine. We have developed protocols for postmortem tissue sampling of the ear canal and associated tissue, and if these can be implemented and performed on a large scale, this would provide the basis for various studies that comprehend morphology and pathology. A postmortem investigation involves a well-coordinated, interdisciplinary approach, and with respect to the assessment of the impact of noise, it is essential to carry out a full necropsy protocol (IJsseldijk et al., 2019), and a comprehensive evaluation of the tissues of the entire auditory pathway (even if not fully understood). This would include a macroscopic inspection of the tissues of the peripheral hearing apparatus, histological analysis of the external ear canal, macroscopic inspection of the ventral sinus complex including peribullar spaces, and inner ear and central nervous system assessment (Sacchini et al., 2020). There is an urgent need to understand the biologically-significant effects, or impact, of sound exposure on marine ecosystems in order to establish correct regulatory noise exposure criteria and policy guidelines. In this regard, this assessment would contribute to the understanding of the physiological effects of noise exposure.

7 Bibliography of Discussion

Ahmed, Y.A., and Abdelsabour-Khalaf, M. (2018). Adipochondrocytes in rabbit auricular cartilage. Assiut Veterinary Medical Journal *64*, 105–109.

Albuerne, M., Lavallina, J.D., Esteban, I., Naves, F.J., Silos-Santiago, I., and Vega, J.A. (2000). Development of Meissner-like and Pacinian sensory corpuscles in the mouse demonstrated with specific markers for corpuscular constituents. The Anatomical Record *258*, 235–242.

Alvord, L.S., and Farmer, B.L. (1997). Anatomy and orientation of the human external ear. Journal-American Academy of Audiology *8*, 383–390.

Aroyan, J.L. (2001). Three-dimensional modeling of hearing in *Delphinus delphis*. The Journal of the Acoustical Society of America *110*, 3305–3318.

Aroyan, J.L., Cranford, T.W., Kent, J., and Norris, K.S. (1992). Computer modeling of acoustic beam formation in *Delphinus delphis*. The Journal of the Acoustical Society of America *92*, 2539–2545.

Barker, D., Hunt, C.C., and McIntyre, A.K. (1974). Muscle Receptors (Berlin Heidelberg: Springer-Verlag).

Baum, C., Meyer, W., Stelzer, R., Fleischer, L.-G., and Siebers, D. (2002). Average nanorough skin surface of the pilot whale (*Globicephala melas*, Delphinidae): considerations on the self-cleaning abilities based on nanoroughness. Marine Biology *140*, 653–657.

Beineke, A., Siebert, U., Wünschmann, A., Stott, J.L., Prengel, I., Kremmer, E., and Baumgärtner, W. (2001). Immunohistochemical Investigation of the Cross-reactivity of Selected Cell Markers from Various Species for Characterization of Lymphatic Tissues in the Harbour Porpoise (*Phocoena phocoena*). Journal of Comparative Pathology *125*, 311–317.

Beineke, A., Siebert, U., Wohlsein, P., and Baumgärtner, W. (2010). Immunology of whales and dolphins. Veterinary Immunology and Immunopathology *133*, 81–94.

Bell, J., Bolanowski, S., and Holmes, M.H. (1994). The structure and function of pacinian corpuscles: A review. Progress in Neurobiology *42*, 79–128.

Bermejo, P., López, M., Larraya, I., Chamorro, J., Cobo, J.L., Ordóñez, S., and Vega, J.A. (2017). Innervation of the Human Cavum Conchae and Auditory Canal: Anatomical Basis for Transcutaneous Auricular Nerve Stimulation. BioMed Research International *2017*, 1–10.

Biswas, A. (2015). Characterization and Modeling of Vibrotactile Sensitivity Threshold of Human Finger Pad and the Pacinian Corpuscle. PhD Dissertation. Indian Institute of Technology.

Blanke, A., Aupperle, H., Seeger, J., Kubick, C., and Schusser, G.F. (2015). Histological Study of the External, Middle and Inner Ear of Horses. Anatomia, Histologia, Embryologia *44*, 401–409.

Boas, J.E.V. (1912). Ohrknorpel und äusseres ohr der Säugetiere; eine vergleichend-anatomische Untersuchung (Kopenhagen: [Nielsen & Lydiche (A. Simmelkiær)]).

Boenninghaus, G. (1903). Das Ohr des Zahnwales, zugleich ein beitrag zur theorie der Schalleitung: eine biologische studie. Zoologische Jahrbücher. Abteilung Für Anatomie Und Ontogenie Der Tiere *19*, 189–360.

Bouley, D.M., Alarcón, C.N., Hildebrandt, T., and O'Connell-Rodwell, C.E. The distribution, density and three-dimensional histomorphology of Pacinian corpuscles in the foot of the Asian elephant (*Elephas maximus*) and their potential role in seismic communication. J Anatomy *211*, 428–435.

Bowker, R.M., Lancaster, L.S., and Isbell, D.A. (2017). Morphological evaluation of Merkel cells and small lamellated sensory receptors in the equine foot. American Journal of Veterinary Research *78*, 659–667.

Bradamante, Z., Jostovic-Knezevic, L., Levak-Svajger, B., and Svajger, A. (1991). Differentiation of the secondary elastic cartilage in the external ear of the rat. Int. J. Dev. Biol. *35*, 311–320.

Bryden, M.M., and Molyneux, G.S. (1986). Ultrastructure of encapsulated mechanoreceptor organs in the region of the nares. In Research on Dolphins, M.M. Bryden, and R. Harrison, eds. (Oxford: Clarendon Press), pp. 99–107.

Buchtová, M., Páč, L., Knotek, Z., and Tichý, F. (2009). Complex Sensory Corpuscles in the Upper Jaw of Horsfield's Tortoise (*Testudo horsfieldii*). Acta Veterinaria Brno *78*, 193–197.

Bullock, T.H., Domning, D.P., and Best, R.C. (1980). Evoked Brain Potentials Demonstrate Hearing in a Manatee (Trichechus inunguis). Journal of Mammalogy *61*, 130–133.

Burgess, P.R., Petit, D., and Warren, R.M. (1968). Receptor types in cat hairy skin supplied by myelinated fibers. Journal of Neurophysiology *31*, 833–848.

Campbell, S. (2000). Mosaic characteristics of human endometrial epithelium in vitro: analysis of secretory markers and cell surface ultrastructure. Molecular Human Reproduction *6*, 41–49.

Cauna, N., and Mannan, G. (1958). The structure of human digital Pacinian corpuscles (corpuscula lamellosa) and its functional significance. Journal of Anatomy *92*, 24.

Cauna, N., and Mannan, G. (1959). Development and postnatal changes of digital Pacinian corpuscles (corpuscula lamellosa) in the human hand. Journal of Anatomy *93*, 271–286.

Cavallotti, C., Tranquilli Leali, F.M., Galea, N., and Tonnarini, G. (2004). Catecholaminergic nerve fibers in bronchus-associated lymphoid tissue: age-related changes. Archives of Gerontology and Geriatrics *39*, 59–68.

Centelleghe, C., Da Dalt, L., Marsili, L., Zanetti, R., Fernandez, A., Arbelo, M., Sierra, E., Castagnaro, M., Di Guardo, G., and Mazzariol, S. (2019). Insights Into Dolphins' Immunology: Immuno-Phenotypic Study on Mediterranean and Atlantic Stranded Cetaceans. Front. Immunol. *10*.

Chapla, M.E., Nowacek, D.P., Rommel, S.A., and Sadler, V.M. (2007). CT scans and 3D reconstructions of Florida manatee (*Trichechus manatus latirostris*) heads and ear bones. Hearing Research *228*, 123–135.

Chartrand, M.S. (2005). Identifying Neuro-reflexes of the External Ear Canal Max Stanley Chartrand.

Cherepnov, V.L., and Chadaeva, N.I. (1981). Some characteristics of soluble proteins of Pacinian corpuscles. Bull Exp Biol Med *91*, 346–348.

Chouchkov, C.N. (1973a). The fine structure of small encapsulated receptors in human digital glabrous skin. J Anat *114*, 25–33.

Chouchkov, C.N. (1973b). On the Fine Structure of Krause's Bulbs in Human Skin, Oral Cavity and Rectum. Arch. Histol. Jap., Arch. Histol. Jpn *35*, 365–375.

Clarke, R. (1948). Hearing in Cetacea. Nature, London *161*, 979–980.

Coste, B., Mathur, J., Schmidt, M., Earley, T.J., Ranade, S., Petrus, M.J., Dubin, A.E., and Patapoutian, A. (2010). Piezo1 and Piezo2 Are Essential Components of Distinct Mechanically Activated Cation Channels. Science *330*, 55–60.

Costidis, A., and Rommel, S.A. (2012). Vascularization of Air Sinuses and Fat Bodies in the Head of the Bottlenose Dolphin (*Tursiops truncatus*): Morphological Implications on Physiology. Frontiers in Physiology *3*, 1–23.

Costidis, A.M., and Rommel, S.A. (2016a). The extracranial arterial system in the heads of beaked whales, with implications on diving physiology and pathogenesis. Journal of Morphology *277*, 5–33.

Costidis, A.M., and Rommel, S.A. (2016b). The extracranial venous system in the heads of beaked whales, with implications on diving physiology and pathogenesis. Journal of Morphology *277*, 34–64.

Cowan, D.F., and Smith, T.L. (1995). Morphology of complex lymphoepithelial organs of the anal canal ("anal tonsil") in the bottlenose dolphin, *Tursiops truncatus*. Journal of Morphology *223*, 263–268.

Cowan, D.F., and Smith, T.L. (1999). Morphology of the lymphoid organs of the bottlenose dolphin, *Tursiops truncatus*. J Anat *194*, 505–517.

Cox, G., Krieger, J.N., and Morris, B.J. (2015). Histological Correlates of Penile Sexual Sensation: Does Circumcision Make a Difference? Sexual Medicine *3*, 76–85.

Cozzi, B., Bagnoli, P., Acocella, F., and Costantino, M.L. (2005). Structure and biomechanical properties of the trachea of the striped dolphin, *Stenella coeruleoalba*: Evidence for evolutionary adaptations to diving. The Anatomical Record Part A: Discoveries in Molecular, Cellular, and Evolutionary Biology *284A*, 500–510.

Cozzi, B., Huggenberger, S., and Oelschläger, H.H.A. (2017). Anatomy of Dolphins (Academic Press).

Cranford, T.W., and Krysl, P. (2012). Acoustic Function in the Peripheral Auditory System of Cuvier's Beaked Whale (*Ziphius cavirostris*). In The Effects of Noise on Aquatic Life, A.N. Popper, and A. Hawkins, eds. (New York, NY: Springer New York), pp. 69–72.

Cranford, T.W., and Krysl, P. (2015). Fin Whale Sound Reception Mechanisms: Skull Vibration Enables Low-Frequency Hearing. PLOS ONE *10*, e0116222.

Cranford, T.W., Krysl, P., and Amundin, M. (2010). A New Acoustic Portal into the Odontocete Ear and Vibrational Analysis of the Tympanoperiotic Complex. PLoS ONE *5*, e11927.

Czech, N. (2007). Functional Morphology and Postnatal Transformation of Vibrissal Crypts in Toothed Whales (Odontoceti). Fakultät für Biologie und Biotechnologie der Ruhr-Universität Bochum.

Czech-Damal, N.U., Liebschner, A., Miersch, L., Klauer, G., Hanke, F.D., Marshall, C., Dehnhardt, G., and Hanke, W. (2012a). Electroreception in the Guiana dolphin (*Sotalia guianensis*). Proceedings of the Royal Society B: Biological Sciences *279*, 663–668.

Czech-Damal, N.U., Liebschner, A., Miersch, L., Klauer, G., Hanke, F.D., Marshall, C., Dehnhardt, G., and Hanke, W. (2012b). Electroreception in the Guiana dolphin (*Sotalia guianensis*). Proceedings of the Royal Society of London B: Biological Sciences *279*, 663–668.

Czech-Damal, N.U., Dehnhardt, G., Manger, P., and Hanke, W. (2013). Passive electroreception in aquatic mammals. J Comp Physiol A *199*, 555–563.

Dahm, R., van Marle, J., Quinlan, R.A., Prescott, A.R., and Vrensen, G.F.J.M. (2011). Homeostasis in the vertebrate lens: mechanisms of solute exchange. Philosophical Transactions of the Royal Society B: Biological Sciences *366*, 1265–1277.

D'Andrea, V., Malinovsky, L., Troccoli, R., Malinovska, I., and Artico, M. (2014). Sensory innervation of the upper lip in the Domestic pig (*Sus scrofa f. domestica*). Journal of Mountain Ecology *3*.

De Oliveria e Silva, F.M., Guimarães, J.P., Vergara-parente, J.E., Carvalho, V.L., De Meirelles, A.C.O., Marmontel, M., Ferrão, J.S.P., and Miglino, M.A. (2014). Morphological Analysis of Lymph Nodes in Odontocetes From North and Northeast Coast of Brazil. Anat. Rec. *297*, 939–948.

De Vreese, S., Doom, M., Haelters, J., and Cornillie, P. (2014). Heeft de uitwendige gehoorgang van walvisachtigen nog enige functie? Vlaams Diergeneeskundig Tijdschrift *83*, 284–292.

De Vreese, S., Doom, M., Haelters, J., and Cornillie, P. (2015). Poster presentation: The external ear canal of cetaceans, vestigial or not? (European Cetacean Society Conference - Malta), p. 1.

De Vreese, S., André, M., and Mazzariol, S. (2019). Morphology of the external ear canal in toothed whales. Proc. Mtgs. Acoust. *37*, 010016.

De Vreese, S., André, M., Cozzi, B., Centelleghe, C., van der Schaar, M., and Mazzariol, S. (2020). Morphological Evidence for the Sensitivity of the Ear Canal of Odontocetes as shown by Immunohistochemistry and Transmission Electron Microscopy. Sci Rep *10*, 1–17.

Degollada, E. (1998). Anatomía e Histología Funcionales del Sistema de Sacos Nasales en los Odontocetos (Superfamilia Delphinoidea). PhD Dissertation. Autonomous University of Barcelona.

Dehnhardt, G., and Mauck, B. (2008). Mechanoreception in Secondarily Aquatic Vertebrates. Sensory Evolution on the Threshold: Adaptations in Secondarily Aquatic Vertebrates 295–314.

Del Valle, M.E., Harwin, S.F., Maestro, A., Murcia, A., and Vega, J.A. (1998). Immunohistochemical analysis of mechanoreceptors in the human posterior cruciate ligament: a demonstration of its proprioceptive role and clinical relevance. The Journal of Arthroplasty *13*, 916–922.

Della Pietra, A., Mikhailov, N., and Giniatullin, R. (2020). The Emerging Role of Mechanosensitive Piezo Channels in Migraine Pain. IJMS *21*, 696.

Dellmann, H.D., and Eurell, J.A. (2000). Istologia e anatomia microscopica veterinaria (Milan: C.E.A. Casa Editrice Ambrosiana).

Descamps, E., Sochacka, A., De Kegel, B., Van Loo, D., Van Hoorebeke, L., and Adriaens, D. (2014). Soft tissue discrimination with contrast agents using micro-CT scanning. Belg. J. Zool. *144*, 20–40.

Díaz-Delgado, J., Ressio, R., Groch, K.R., and Catão-Dias, J.L. (2018). Immunohistochemical investigation of the cross-reactivity of selected cell markers in formalin-fixed, paraffin-embedded lymphoid tissues of Franciscana (*Pontoporia blainvillei*). Veterinary Immunology and Immunopathology *200*, 52–58.

Dorph-Petersen, K.-A., and Lewis, D.A. (2011). Stereological Approaches to Identifying Neuropathology in Psychosis. Biological Psychiatry *69*, 113–126.

Dubový, P., and Bednárová, J. (1999). The extracellular matrix of rat Pacinian corpuscles: An analysis of its fine structure. Anatomy and Embryology *200*, 615–623.

Dyce, K.M., Sack, W.O., and Wensing, C.J.G. (2010). Textbook of veterinary anatomy (St. Louis, Mo: Saunders/Elsevier).

El-Oteify, M., El-Dien, H.M.S., and Mubarak, W. (2011). Sensory nerve endings in the human female umbilical skin: light and electron microscopic study. Egyptian Journal of Histology *34*, 57–68.

Escobar, I. (2016). Sound reception mechanism analysis of a Cuvier's beaked whale (Ziphius cavirostris). UC San Diego.

Esipov, A.L. (1982). Nature of the corpora cavernosa of the conchae nasales. Arkh Anat Gistol Embriol *83*, 68–72.

Evangelou, E., Kyzas, P.A., and Trikalinos, T.A. (2005). Comparison of the diagnostic accuracy of lymphatic endothelium markers: Bayesian approach. Modern Pathology *18*, 1490–1497.

Feito, J., Cobo, J.L., Santos-Briz, A., and Vega, J.A. (2017). Pacinian Corpuscles in Human Lymph Nodes. The Anatomical Record *300*, 2233–2238.

Folan-Curran, J., and Cooke, F.J. (2001). Contribution of cranial nerve ganglia to innervation of the walls of the rat external acoustic meatus. Journal of the Peripheral Nervous System *6*, 28–32.

Folan-curran, J., Hickey, K., and Monkhouse, W.S. (1994). Innervation of the Rat External Auditory Meatus: A Retrograde Tracing Study. Somatosensory & Motor Research *11*, 65–68.

Fraser, F.C., and Purves, P.E. (1960). Anatomy and Function of the Cetacean Ear. Proceedings of the Royal Society of London B: Biological Sciences *152*, 62–77.

García-Suárez, O., Montaño, J.A., Esteban, I., González-Martínez, T., Alvarez-Abad, C., López-Arranz, E., Cobo, J., and Vega, J.A. (2009). Myelin basic protein-positive nerve fibres in human Meissner corpuscles. J Anat *214*, 888–893.

Gerussi, T., Graïc, J., De Vreese, S., Grandis, A., Tagliavia, C., De Silva, M., Huggenberger, S., and Cozzi, B. (2020). The follicle-sinus complex of the bottlenose dolphin (*Tursiops truncatus*). Functional anatomy and possible evolutional significance of its somato-sensory innervation. J Anat *00*, 1–14.

Giacometti, L. (1967a). The skin of the whale (*Balaenoptera physalus*). The Anatomical Record *159*, 69–75.

Giacometti, L. (1967b). ABSTRACT - The skin of the whale (*Balaenoptera physalus*). Anat. Rec. *159*, 69–75.

Girard, J.-P., and Springer, T.A. (1995). High endothelial venules (HEVs): specialized endothelium for lymphocyte migration. Immunology Today *16*, 449–457.

Gottlieb, P.A. (2017). A Tour de Force: The Discovery, Properties, and Function of Piezo Channels. Curr Top Membr *79*, 1–36.

Gottschaldt, K.-M., and Lausmann, S. (1974). The peripheral morphological basis of tactile sensibility in the beak of geese. Cell Tissue Res. *153*, 477–496.

Grennes, M.J. (1999). Mapping morphologic change in the external ear. Master thesis. University of Tasmania.

Grevers, G., and Herrmann, U. (1987). Cavernous tissue of the nasal mucosa. Laryngol Rhinol Otol (Stuttg) *66*, 152–156.

Guest, J.F., Greener, M.J., Robinson, A.C., and Smith, A.F. (2004). Impacted cerumen: composition, production, epidemiology and management. QJM *97*, 477–488.

Halata, Z. (1972). Innervation der unbehaarten Nasenhaut des Maulwurfs (*Talpa europaea*). Cell and Tissue Research *125*, 108–120.

Halata, Z. (1975). The mechanoreceptors of the mammalian skin: ultrastructure and morphological classification (Berlin: Springer).

Halata, Z. (1990). Specific Nerve Endings in Vellus Hair, Guard Hair, and Sinus Hair. In Hair and Hair Diseases, (Springer, Berlin, Heidelberg), pp. 149–164.

Halata, Z., and Munger, B.L. (1980). Sensory nerve endings in rhesus monkey sinus hairs. J Comp Neurol *192*, 645–663.

Halata, Z., and Munger, B.L. (1986). The neuroanatomical basis for the protopathic sensibility of the human glans penis. Brain Research *371*, 205–230.

Hamilton, J.L., Dillaman, R.M., McLellan, W.A., and Pabst, D.A. (2004). Structural fiber reinforcement of keel blubber in harbor porpoise (Phocoena phocoena). Journal of Morphology *261*, 105–117.

Hanke, H. (1914). Ein Beitrag zur Kenntnis der Anatomie des Äusseren und Mittleren Ohres der Bartenwale. Jenaische Zeitschrifte Fur Naturwissenschaft *51*, 487–524.

Harada, Y. (1983). Atlas of the Ear: By Scanning Electron Microscopy (Dordrecht: Springer Netherlands).

Harrison, R.J., and Thurley, K.W. (1974). Structure of the Epidermis in *Tursiops*, *Delphinus*, *Orcinus* and *Phocoena*. In Functional Anatomy of Marine Mammals, R.J. Harrison, ed. (London: Academic Press), pp. 45–71.

Hiltunen, J., Suortti, T., Arvela, S., Seppä, M., Joensuu, R., and Hari, R. (2005). Diffusion tensor imaging and tractography of distal peripheral nerves at 3 T. Clinical Neurophysiology *116*, 2315–2323.

Home, E. (1812). An Account of Some Peculiarities in the Structure of the Organ of Hearing in the Balaena Mysticetus of Linnaeus. Philosophical Transactions of the Royal Society of London Series I *102*, 83–88.

Horch, K.W., Tuckett, R.P., and Burgess, P.R. (1977). A Key to the Classification of Cutaneous Mechanoreceptors. J Invest Dermatol *69*, 75–82.

Howes, G.B. (1880). Some Points in the Anatomy of the Porpoise (*Phocoena communis*). J Anat Physiol *14*, 467–474.

Hubbard, S.J. (1958). A study of rapid mechanical events in a mechanoreceptor. J Physiol *141*, 198-218.1.

Huber, E. (1934). Contribution to palaeontology IV: Anatomical notes on pinnipedia and cetacea. Publ. Carnegie Inst. *447*, 105–136.

Hunter, J. (1787). Observations on the struture and oeconomy of whales, Esq. F. R. S. communicated by Sir Joseph Banks, Bart., F. R. S. Phil. Trans. R. Soc. Lond. B *77*.

Ide, C., and Hayashi, S. (1987). Specializations of plasma membranes in Pacinian corpuscles: Implications for mechano-electric transduction. Journal of Neurocytology *16*, 759–773.

Ide, C., Yoshida, Y., Hayashi, S., Takashio, M., and Munger, B.L. (1988). A re-evaluation of the cytology of cat Pacinian corpuscles. II.The extreme tip of the axon. Cell and Tissue Research *253*, 83–93.

Iggo, A. (1976). Is the Physiology of Cutaneous Receptors Determined by Morphology? In Progress in Brain Research, (Elsevier), pp. 15–31.

Iggo, A. (1977). Cutaneous and subcutaneous sense organs. British Medical Bulletin *33*, 97–102.

Iggo, A., and Andres, K.H. (1982). Morphology of Cutaneous Receptors. Ann. Rev. Neurosci. *5*, 1–31.

IJsseldijk, L.L., Brownlow, A., and Mazzariol, S. (2019). Best practice for cetacean post mortem investigation and tissue sampling. ASCOBANS/AC25/Inf.3.2/Rev1 71.

Jambawalikar, S., Baum, J., Button, T., Li, H., Geronimo, V., and Gould, E.S. (2010). Diffusion tensor imaging of peripheral nerves. Skeletal Radiol *39*, 1073–1079.

Johnson, R.D., and Halata, Z. (1991). Topography and ultrastructure of sensory nerve endings in the glans penis of the rat. The Journal of Comparative Neurology *312*, 299–310.

JPI Healthy and Productive Seas and Oceans (2020). Draft Strategy Framework beyond 2020. 31 pages. http://www.jpi-oceans.eu/draft-strategy-framework-beyond-2020, consulted on Nov 11 2020.

Kakoi, H., and Anniko, M. (1996a). Auditory Epithelial Migration: II: Morphological Evidence for Auditory Epidermal Cell Migration in Rat. Acta Oto-Laryngologica *116*, 850–853.

Kakoi, H., and Anniko, M. (1996b). Auditory Epithelial Migration: IV. Light- and Scanning Electron-Microscopic Studies of the Tympanic Membrane and External Auditory Canal in the Mouse. ORL *58*, 136–142.

Kandel, E.R., Schwartz, J.H., and Jessell, T.M. (1991). Principles of neural science (Elsevier).

Kastelein, R.A., and Dubbeldam, J.L. (1996). The anatomy of the walrus head (*Odobenus rosmarus*). Part 4: The ears and their function in aerial and underwater hearing. Aquatic Mammals *22*, 95–125.

Ketten, D.R. (1992). The cetacean ear: form, frequency, and evolution. In Marine Mammal Sensory Systems, J.A. Thomas, R.A. Kastelein, and A.Y. Supin, eds. (New York: Springer Science+Business Media), pp. 53–75.

Ketten, D.R. (1994). Functional analyses of whale ears: adaptations for underwater hearing. In OCEANS'94.'Oceans Engineering for Today's Technology and Tomorrow's Preservation.'Proceedings, (IEEE), p. I–264.

Ketten, D.R. (1997). Structure and Function in Whale Ears. Bioacoustics *8*, 103–135.

Ketten, D.R. (2000). Cetacean Ears. In Hearing by Whales and Dolphins, W.W.L. Au, A.N. Popper, and R.R. Fay, eds. (New York: Springer-Verlag), pp. 43–108.

Ketten, D.R., Odell, D.K., and Domning, D.P. (1992). Structure, Function, and Adaptation of the Manatee Ear. In Marine Mammal Sensory Systems, J.A. Thomas, R.A. Kastelein, and A.Ya. Supin, eds. (Boston, MA: Springer US), pp. 77–95.

Khalil, C., Budzik, J.F., Kermarrec, E., Balbi, V., Thuc, V.L., and Cotten, A. (2010). Tractography of peripheral nerves and skeletal muscles. European Journal of Radiology *76*, 391–397.

Khomenko, B.H. (1970). The histostructure and innervation of the sound apparatus-nasal sacs- in dolphins. Dopovidi Akad. Nauk. Ukrayinskoy, R.S.R., 32, 83-87. English Abstract. In: Bryden, M. M., and Molyneux, G. S. (1986). "Ultrastructure of encapsulated mechanoreceptor organs in the region of the nares," in Research on Dolphins, eds. M. M. Bryden and R. Harrison (Oxford: Clarendon Press), 99–107.

Khomenko, B.G. (1974). A morphological and functional analysis of the structure of the supracranial respiratory passage as a possible echolocation signal generator in the dolphin. Bionika 8: 40-47 (in Russian). In: Bryden, M. M., and Molyneux, G. S. (1986). "Ultrastructure of encapsulated mechanoreceptor organs in the region of the nares," in Research on Dolphins, eds. M. M. Bryden and R. Harrison (Oxford: Clarendon Press), 99–107.

Khomenko, B.G. and Khadzinskiy, V.G. (1974). Morphological and functional principles underlying cutaneous reception in dolphins. *Bionika*, **8**, 48-57 (In Russian). In: Bryden, M. M., and Molyneux, G. S. (1986). "Ultrastructure of encapsulated mechanoreceptor organs in the region of the nares," in Research on Dolphins, eds. M. M. Bryden and R. Harrison (Oxford: Clarendon Press), 99–107.

Kidd, R.L., Krawczyk, W.S., and Wilgram, G.F. (1971). The merkel cell in human epidermis: its differentiation from other dendritic cells. Archiv Für Dermatologische Forschung *241*, 374–384.

Kim, J.H., Park, C., Yang, X., Murakami, G., Abe, H., and Shibata, S. (2018). Pacinian Corpuscles in the Human Fetal Finger and Thumb: A Study Using 3D Reconstruction and Immunohistochemistry. Anat. Rec. *301*, 154–165.

Krause, W. (1860). Die terminalen Körperchen der einfach sensiblen Nerven (Hahn´sche Hofbuchhandlung).

Kress, M., and Zeilhofer, H.U. (1999). Capsaicin, protons and heat: new excitement about nociceptors. Trends in Pharmacological Sciences *20*, 112–118.

Krstic, R.V. (1984). Illustrated Encyclopedia of Human Histology. Springer Verlag, Heidelberg. In: Malinovský, L. (1996). Sensory nerve formations in the skin and their classification. *Microsc. Res. Tech.* 34, 283–301.

Kükenthal, W. (1891). On the Adaptation of Mammals to Aquatic Life. The Annals and Magazine of Natural History *Ser. 6*, 153–178.

Kumamoto, K., Ebara, S., and Matsuura, T. (1993). Noradrenergic Fibers in the Pacinian Corpuscles of the Cat Urinary Bladder. Cells Tissues Organs *146*, 46–52.

Kumar, V., Fausto, N., and Abbas, A. (2014). Robbins and Cotran - Pathologic Basis of Disease (Elsevier).

Kuver, R., Klinkspoor, J.H., Osborne, W.R.A., and Lee, S.P. (2000). Mucous granule exocytosis and CFTR expression in gallbladder epithelium. Glycobiology *10*, 149–157.

Lauriano, E.R., Pergolizzi, S., Aragona, M., Spanò, N., Guerrera, M.C., Capillo, G., and Faggio, C. (2019). Merkel cells immunohistochemical study in striped dolphin (*Stenella coeruleoalba*) skin. Tissue and Cell *56*, 1–6.

Ling, J.K. (1974). The Integument of Marine Mammals. In Functional Anatomy of Marine Mammals, R.J. Harrison, ed. (London: Academic Press), pp. 1–44.

Liugan, M., Zhang, M., and Cakmak, Y.O. (2018). Neuroprosthetics for Auricular Muscles: Neural Networks and Clinical Aspects. Front. Neurol. *8*, 752.

Loewenstein, W.R. (1971). Mechano-electric Transduction in the Pacinian Corpuscle. Initiation of Sensory Impulses in Mechanoreceptors. In Handbook of Sensory Physiology. 1. Principles of Receptor Physiology, W.R. Loewenstein, ed. (Berlin, Heidelberg, New York), pp. 269–290.

Loewenstein, W.R., and Skalak, R. (1966). Mechanical transmission in a Pacinian corpuscle. An analysis and a theory. The Journal of Physiology *182*, 346–378.

Loza, C.M., Krmpotic, C.M., Galliari, F.C., Andrés Laube, P.F., Negrete, J., Scarano, A.C., Loureiro, J., Carlini, A.A., and Barbeito, C.G. (2019). Adaptations to a semiaquatic lifestyle in the external ear of southern pinnipeds (Otariidae and Phocidae, Carnivora): Morphological evidences. Zoology *133*, 66–80.

Lucarz, A., and Brand, G. (2007). Current considerations about Merkel cells. European Journal of Cell Biology *86*, 243–251.

Lum, C.L., Jeyanthi, S., Prepageran, N., Vadivelu, J., and Raman, R. (2009). Antibacterial and antifungal properties of human cerumen. The Journal of Laryngology & Otology *123*, 375.

Lutz, S. (2009). Blue Histology - Respiratory System (https://www.lab.anhb.uwa.edu.au/mb140/CorePages/Respiratory/respir.htm accessed on 10/10/2020).

Malinovský, L. (1986). ABSTRACT Mechanoreceptors and Free Nerve Endings. In Biology of the Integument, (Springer, Berlin, Heidelberg), pp. 535–560.

Malinovský, L. (1996). Sensory nerve formations in the skin and their classification. Microsc. Res. Tech. *34*, 283–301.

Martín-Alguacil, N., Cooper, R.S., Aardsma, N., Mayoglou, L., Pfaff, D., and Schober, J. (2015). Terminal innervation of the male genitalia, cutaneous sensory receptors of the male foreskin. Clin Anat *28*, 385–391.

McCormick, J.G., Wever, E.G., Palin, J., and Ridgway, S.H. (1970). Sound Conduction in the Dolphin Ear. The Journal of the Acoustical Society of America *48*, 1418–1428.

McGeady, T.A., Quinn, P.J., Fitzpatrick, E.S., Ryan, M.T., Kilroy, D., and Lonergan, P. (2017). Veterinary Embryology (Chichester, West Sussex ; Ames, Iowa: Wiley-Blackwell).

McNab, J.A., and Miller, K.L. (2008). Sensitivity of diffusion weighted steady state free precession to anisotropic diffusion. Magnetic Resonance in Medicine *60*, 405–413.

McNab, J.A., Jbabdi, S., Deoni, S.C.L., Douaud, G., Behrens, T.E.J., and Miller, K.L. (2009). High resolution diffusion-weighted imaging in fixed human brain using diffusion-weighted steady state free precession. Neuroimage *46*, 775–785.

Mead, J.G. (1975). Anatomy of the external nasal passages and facial complex in the Delphinidae (Mammalia, Cetacea) / (City of Washington : Smithsonian Institution Press,).

Mead, J.G., and Fordyce, R.E. (2009). The Therian Skull A Lexicon with Emphasis on the Odontocetes. Smithsonian Contributions to Zoology *627*, 261.

Michaels, L., and Soucek, S. (1989). Development of the stratified squamous epithelium of the human tympanic membrane and external canal: The origin of auditory epithelial migration. American Journal of Anatomy *184*, 334–344.

Miller, K.L., McNab, J.A., Jbabdi, S., and Douaud, G. (2012). Diffusion tractography of post-mortem human brains: Optimization and comparison of spin echo and steady-state free precession techniques. NeuroImage *59*, 2284–2297.

Miller, M.E., Christensen, G.C., and Evans, H.E. (1964). Anatomy of the Dog (Philadelphia - London: W.B. Saunders Company).

Mitchell, G.A. (1954). The autonomic nerve supply of the throat, nose and ear. J Laryngol Otol *68*, 495–516.

Moll, R., Lowe, A., Laufer, J., and Franke, W.W. (1992). Cytokeratin 20 in Human Carcinomas. American Journal of Pathology *140*, 21.

Morgane, P.T., and Jacobs, M.S. (1972). Comparative anatomy of the cetacean nervous system. In Functional Anatomy of Marine Mammals, R.J. Harrison, ed. (New York: Academic Press), p.

Munger, B.L. (1971). Patterns of Organization of Peripheral Sensory Receptors. In Principles of Receptor Physiology, W.R. Loewenstein, ed. (Berlin, Heidelberg: Springer Berlin Heidelberg), pp. 523–556.

Munger, B.L., Yoshida, Y., Hayashi, S., Osawa, T., and Ide, C. (1988). A re-evaluation of the cytology of cat Pacinian corpuscles. I. The inner core and clefts. Cell and Tissue Research *253*, 83–93.

Murri, A. (1890) Di un nuovo organo nervoso terminale e sulla presenza dei corpuscoli Golgi-Mazzoni nel connettivo sottocutaneo dei polpastrelli delle dita del'uomo. Mem. R. Acad. Lincei, ser. 4, vol. 7, pp 398-410

Nafstad, P.H.J., and Andersen, A.E. (1970). Ultrastructural investigation on the innervation of the Herbst corpuscle. Z. Zellforsch. *103*, 109–114.

Nikolaev, Y.A., Feketa, V.V., Anderson, E.O., Gracheva, E.O., and Bagriantsev, S.N. (2020). Lamellar cells in Pacinian and Meissner corpuscles are touch sensors (PREPRINT). BioRxiv - Https://Doi.Org/10.1101/2020.08.24.265231.

Nishida, Y., Yoshie, S., and Fujita, T. (2000). Oral Sensory Papillae, Chemo- and Mechano-Receptors, in the Snake, *Elaphe quadrivirgata*. A Light and Electron Microscopic Study. Archives of Histology and Cytology *63*, 55–70.

Nishimura, Y., and Kumoi, T. (1992). The embryologic development of the human external auditory meatus. Preliminary report. Acta Oto-Laryngologica *112*, 496–503.

NOAA/NMFS and US Navy (2001). Joint Interim Report Bahamas Marine Mammal Stranding Event of 15-16 March 2000 (Washington, D.C.: NOAA/NMFS and U. S. Navy).

Noda, Y., Amano, I., Hata, M., Kojima, H., and Sawa, Y. (2010). Immunohistochemical Examination on the Distribution of Cells Expressed Lymphatic Endothelial Marker Podoplanin and LYVE-1 in the Mouse Tongue Tissue. Acta Histochemica et Cytochemica *43*, 61–68.

Nummela, S. (2008). Hearing in aquatic animals. In Sensory Evolution on the Threshold: Adaptation in Secondarily Aquatic Vertebrates, J.G.M. Thewissen, and S. Nummela, eds. (San Diego: University of California Press), pp. 211–224.

Nummela, S., Reuter, T., Hemilä, S., Holmberg, P., and Paukku, P. (1999). The anatomy of the killer whale middle ear (*Orcinus orca*). Hearing Research *133*, 61–70.

O'Connell-Rodwell, C.E. (2007). Keeping an "Ear" to the Ground: Seismic Communication in Elephants. Physiology *22*, 287–294.

Olson, W., Dong, P., Fleming, M., and Luo, W. (2016). The specification and wiring of mammalian cutaneous low-threshold mechanoreceptors. Wiley Interdiscip Rev Dev Biol *5*, 389–404.

Orfanos, C.E., and Mahrle, G. (1973). Ultrastructure and Cytochemistry of Human Cutaneous Nerves. Journal of Investigative Dermatology *61*, 108–120.

Özcan, Z. (2005). Some histochemical properties of the ceruminous glands in the meatus acusticus externus in cats and dogs. Turkish Journal of Veterinary and Animal Sciences *29*, 917–921.

Palmer, E., and Weddell, G. (1964). The Relationship Between Structure, Innervation and Function of the Skin of the Bottlenose Dolphin (*Tursiops truncatus*). Proceedings of the Zoological Society of London *143*, 553–568.

Pannese, E. (2015). Neurocytology: Fine Structure of Neurons, Nerve Processes, and Neuroglial Cells (Springer International Publishing).

Patrizi, G., and Munger, B.L. (1965). The cytology of encapsulated nerve endings in the rat penis. Journal of Ultrastructure Research *13*, 500–515.

Pawson, L., Slepecky, N.B., and Bolanowski, S.J. (2000). Immunocytochemical identification of proteins within the Pacinian corpuscle. Somatosensory & Motor Research *17*, 159–170.

Pease, D.C., and Quilliam, T.A. (1957). Electron microscopy of the Pacinian corpuscle. The Journal of Cell Biology *3*, 331–342.

Peer, S., and Gruber, H. (2013). Atlas of peripheral nerve ultrasound: with anatomic and MRI correlation (Heidelberg; New York: Springer).

Peltonen, S., Alanne, M., and Peltonen, J. (2013). Barriers of the peripheral nerve. Tissue Barriers *1*, e24956-1–6.

Pilate, M. (1925). Contribution a l'etude de la structure et du developpement des corpuscles de Vater-Pacini. Arch. Russ. Anat. histol. embryol. 3, 225-278 (full text in Russian); 427-435 (French summary). In: Cauna, N., and Mannan, G. (1959). Development and postnatal changes of digital Pacinian corpuscles (corpuscula lamellosa) in the human hand. *Journal of Anatomy* 93, 271–286; Also in: Ahmed, Y.A., and Abdelsabour-Khalaf (2018). Adipochondrocytes in rabbit auricular cartilage. Assiut Veterinary Medical Journal, **64** (156), 105-109

Pilleri, G. and Wandeler, A. (1964). Ontogenese und funktionelle Morphologie des Auges des Finnwals, *Balenoptera physalus* L. (Cetacea, Mysticeti, Balaenopteridae). Acta Anat Suppl **50**, 1-73. In: Wickham, M. G. (1980). Irido-corneal angle of mammalian eyes: Comparative morphology of encapsulated corpuscles in odontocete cetaceans. *Cell Tissue Res. **210**, 501–515.*

Piña, A.R., Martínez, M.M., and de Almeida, O.P. (2015). Glut-1, Best Immunohistochemical Marker for Perineurial Cells. Head and Neck Pathology *9*, 104–106.

Pitts-Yushchenko, L., Dale, J., Winlove, P., and Summers, I. (2013). Dynamic response of Pacinian corpuscles (poster presentation). (Montpellier, France), p. 1.

Poláček, P., and Halata, Z. (1970). Development of simple encapsulated corpuscles in the nasolabial region of the cat. Ultrastructural study. Folia Morphol (Praha) *18*, 359–368.

Popov, V., and Supin, A. (1990a). Localization of the Acoustic Window at the Dolphin's Head. In Sensory Abilities of Cetaceans, (Springer, Boston, MA), pp. 417–426.

Popov, V.V., and Supin, A.Y. (1990b). Location of an acoustic window in dolphins. Experientia *46*, 53–56.

Prahl, S. (2007). Untersuchungen zum Bau der epicranialen Atemwege beim Schweinswal (*Phocoena phocoena* Linnaeus, 1758) - Doctoral Dissertation.

Purves, P.E. (1966). Anatomy and Physiology of the Outer and Middle Ear in Cetaceans. In Whales, Dolphins and Porpoises, K.S. Norris, ed. (Berkeley, California, USA: University of California Press), pp. 320–380.

Purves, P.E., and Pilleri, G. (1983). Echolocation in whales and dolphins (London; New York: Academic Press).

Quilliam, T.A. (1966). Unit Design and Array Patterns in Receptor Organs. In Novartis Foundation Symposia, A.V.S. de Reuck, and J. Knight, eds. (Chichester, UK: John Wiley & Sons, Ltd.), pp. 86–116.

Ramírez, G.A., Rodríguez, F., Suárez-Bonnet, A., Herráez, P., Castro-Alonso, A., Rivero, M., and Espinosa de los Monteros, A. (2018). Study of Merkel cells in the dog through the immunohistochemical expression of five different commercial antibodies: comparative analysis. Journal of Applied Animal Research *46*, 417–421.

Ramprashad, F., Corey, S., and Ronald, K. (1972). Anatomy of the seal's ear (*Pagophilus groenlandicus*) (Erxleben, 1777). In Functional Anatomy of Marine Mammals, R.J. Harrison, ed. (London: Academic Press), pp. 264–305.

Rauschmann, M.A. (1992). Morphologie des Kopfes beim Schlanken Delphin *Stenella attenuata* mit besonderer Berücksichtigung der Hirnnerven. Makroskopische Präparation und moderne bildgebende Verfahren - Dissertation. Johann Wolfgang Goethe-Universität.

Rauschmann, M.A., Huggenberger, S., Kossatz, L.S., and Oelschläger, H.H.A. (2006). Head morphology in perinatal dolphins: A window into phylogeny and ontogeny. Journal of Morphology *267*, 1295–1315.

Reeb, D., Best, P.B., and Kidson, S.H. (2007). Structure of the integument of southern right whales, *Eubalaena australis*. The Anatomical Record: Advances in Integrative Anatomy and Evolutionary Biology *290*, 596–613.

Rehorek, S.J., Stimmelmayr, R., George, J.C., Suydam, R., McBurney, D.L., and Thewissen, J.G.M. (2019a). The role of desmosomes in the ear plug formation in the bowhead whale (*Balaena mysticetus*). Anat Rec ar.24338.

Rehorek, S.J., Stimmelmayr, R., George, J.C., Suydam, R., McBurney, D.M., and Thewissen, J.G.M. (2019b). Structure of the external auditory meatus of the Bowhead whale (*Balaena mysticetus*) and its relation to their seasonal migration. Journal of Anatomy *234*, 201–215.

Reichmuth, C., Holt, M.M., Mulsow, J., Sills, J.M., and Southall, B.L. (2013). Comparative assessment of amphibious hearing in pinnipeds. J Comp Physiol A *199*, 491–507.

Reysenbach De Haan, F.W. (1957). Hearing in whales. Acta Otolaryngol Suppl *134*, 1–114.

Reysenbach De Haan, F.W. (1966). Listening Underwater: Thoughts on Sound and Cetacean Hearing. In Whales, Dolphins and Porpoises, K.S. Norris, ed. (Berkeley and Los Angeles: University of California Press), pp. 583–596.

Reysenbach de Haan, W.F. (1956). De ceti auditu: over de gehoorzin bij walvissen. Dissertation. Universiteit Utrecht.

Ridgway, S.H., and Carder, D.A. (1990). Tactile Sensitivity, Somatosensory Responses, Skin Vibrations, and the Skin Surface Ridges of the Bottle-Nose Dolphin, *Tursiops Truncatus*. In Sensory Abilities of Cetaceans: Laboratory and Field Evidence, J.A. Thomas, and R.A. Kastelein, eds. (Boston, MA: Springer US), pp. 163–179.

Ridgway, S.H., Carder, D.A., Kamolnick, T., Smith, R.R., Schlundt, C.E., and Elsberry, W.R. (2001). Hearing and whistling in the deep sea: depth influences whistle spectra but does not attenuate hearing by white whales (*Delphinapterus leucas*)(Odontoceti, Cetacea). Journal of Experimental Biology *204*, 3829–3841.

Rochon-Duvigneaud, A.J.F. (1940). L'oeil des cétacés. Arch. Mus. Hist. Nat. Paris *16*, 57–90.

Sacchini, S., Díaz-Delgado, J., Monteros, A.E. de los, Paz, Y., Quirós, Y.B. de, Sierra, E., Arbelo, M., Herráez, P., and Fernández, A. (2020). Amyloid-beta peptide and phosphorylated tau in the frontopolar cerebral cortex and in the cerebellum of toothed whales: aging vs hypoxia. Biology Open.

Sakada, S., and Sasaki, T. (1984). Blood-nerve barrier in the Vater-Pacini corpuscle of cat mesentery. Anatomy and Embryology *169*, 237–247.

Schwaab, M., Gurr, A., Neumann, A., Dazert, S., and Minovi, A. (2011). Human antimicrobial proteins in ear wax. European Journal of Clinical Microbiology & Infectious Diseases *30*, 997–1004.

Simon, N.G., and Kliot, M. (2014). Diffusion weighted MRI and tractography for evaluating peripheral nerve degeneration and regeneration. Neural Regen Res *9*, 2122–2124.

Slijper, E.J. (1958). Walvissen (Amsterdam - Hilversum - den Helder: C. de Boer Jr. N.V.).

Smith, T.L., Turnbull, B.S., and Cowan, D.F. (1999). Morphology of the complex laryngeal gland in the Atlantic Bottlenose dolphin, Tursiops truncatus. The Anatomical Record *254*, 98–106.

Soldevilla, M.S. (2005). Cuvier's beaked whale (*Ziphius cavirostris*) head tissues: physical properties and CT imaging. Journal of Experimental Biology *208*, 2319–2332.

Solntseva, G.N. (1990). Formation of an Adaptive Structure of the Peripheral Part of the Auditory Analyzer in Aquatic, Echo-locating Mammals During Ontogenesis. In Sensory Abilities of Cetaceans: Laboratory and Field Evidence, J.A. Thomas, and R.A. Kastelein, eds. (New York: Plenum Press), pp. 363–385.

Solntseva, G.N. (2007). Morphology of the auditory and vestibular organs in mammals, with emphasis on marine species (Bulgaria: Russian Academy Of Sciences & Pensoft Publishers & Brill Academic Publishers).

Sommerauer, S., Muelling, C.K.W., Seeger, J., and Schusser, G.F. (2012). Anatomy and Anaesthesia of the Equine External Ear Canal. Anatomia, Histologia, Embryologia *41*, 395–401.

Spencer, P.S., and Schaumburg, H.H. (1973). An ultrastructural study of the inner core of the Pacinian corpuscle. J Neurocytol *2*, 217–235.

Spray, D.C. (1986). Cutaneous Temperature Receptors. Ann. Rev. Physiol. *48*, 623–638.

Štěrba, O., Klima, M., and Schildger, B. (2000). Embryology of dolphins: staging and ageing of embryos and fetuses of some Cetaceans (Berlin ; New York: Springer).

Stoeckelhuber, M., Matthias, C., Andratschke, M., Stoeckelhuber, B.M., Koehler, C., Herzmann, S., Sulz, A., and Welsch, U. (2006). Human ceruminous gland: Ultrastructure and histochemical analysis of antimicrobial and

cytoskeletal components. The Anatomical Record Part A: Discoveries in Molecular, Cellular, and Evolutionary Biology *288A*, 877–884.

Streeter, P.R. (1988). Immunohistologic and functional characterization of a vascular addressin involved in lymphocyte homing into peripheral lymph nodes. The Journal of Cell Biology *107*, 1853–1862.

Summers, I.R., Pitts-Yushchenko, S., and Winlove, C.P. (2018). Structure of the Pacinian Corpuscle: Insights Provided by Improved Mechanical Modeling. IEEE Transactions on Haptics *11*, 146–150.

Tachibana, T., and Nawa, T. (2005). Immunohistochemical reactions of receptors to met-enkephalin, VIP, substance P, and CGRP located on Merkel cells in the rat sinus hair follicle. Arch. Histol. Cytol. *68*, 383–391.

Talbot, W.H., Darian-Smith, I., Kornhuber, H.H., and Mountcastle, V.B. (1968). The sense of flutter-vibration: comparison of the human capacity with response patterns of mechanoreceptive afferents from the monkey hand. Journal of Neurophysiology *31*, 301–334.

Tierney, S., Russell, J.D., Walsh, M., and Folan-Curran, J. (1993). Innervation of the rat tympanic membrane from the superior cervical and glossopharyngeal ganglia. Journal of Anatomy *182*, 355.

Trumble, S.J., Robinson, E.M., Berman-Kowalewski, M., Potter, C.W., and Usenko, S. (2013). Blue whale earplug reveals lifetime contaminant exposure and hormone profiles. Proceedings of the National Academy of Sciences *110*, 16922–16926.

Van den Broeck, W. (2008). Begeleidende notas bij de cursus bijzondere weefselleer van de huisdieren (Ghent University).

Van den Eynden, G.G., Van der Auwera, I., Van Laere, S.J., Colpaert, C.G., van Dam, P., Dirix, L.Y., Vermeulen, P.B., and Van Marck, E.A. (2006). Distinguishing blood and lymph vessel invasion in breast cancer: a prospective immunohistochemical study. British Journal of Cancer *94*, 1643–1649.

Vega, J.A. (1996). Cutaneous sensory nerve formations: An overview. Microsc. Res. Tech. *34*, 281–282.

Vega, J.A., Haro, J.J., and Del Valle, M.E. (1996). Immunohistochemistry of human cutaneous Meissner and pacinian corpuscles. Microsc. Res. Tech. *34*, 351–361.

Vrabec, F. (1972). Encapsulated sensory corpuscles in the sclerocorneal boundary tissues of the killer whale Orcinus orca L. Acta Anat (Basel) *8*, 23–29. In: Wickham, M. G. (1980). Irido-corneal angle of mammalian eyes: Comparative morphology of encapsulated corpuscles in odontocete cetaceans. Cell Tissue Res. *210*, 501–515.

Wada, H., Metoki, T., and Kobayashi, T. (1992). Analysis of dynamic behavior of human middle ear using a finite-element method. The Journal of the Acoustical Society of America *92*, 3157.

Wartzok, D., and Ketten, D.R. (1999). Marine Mammal Sensory Systems. In Biology of Marine Mammals, J. Reynolds, and S. Rommel, eds. (Smithsonian Institution Press), pp. 117–175.

Watanabe, K., Tubbs, R.S., Satoh, S., Zomorodi, A.R., Liedtke, W., Labidi, M., Friedman, A.H., and Fukushima, T. (2016). Isolated Deep Ear Canal Pain: Possible Role of Auricular Branch of Vagus Nerve—Case Illustrations with Cadaveric Correlation. World Neurosurgery *96*, 293–301.

Wickham, M.G. (1980). Irido-corneal angle of mammalian eyes: Comparative morphology of encapsulated corpuscles in odontocete cetaceans. Cell and Tissue Research *210*, 501–515.

Yamada, M. (1953). Contribution to the Anatomy of the Organ of Hearing of Whales. The Scientific Reports of the Whales Research Institute *8*, 79.

Yamato, M., Ketten, D.R., Arruda, J., Cramer, S., and Moore, K. (2012). The Auditory Anatomy of the Minke Whale (Balaenoptera acutorostrata): A Potential Fatty Sound Reception Pathway in a Baleen Whale. The Anatomical Record: Advances in Integrative Anatomy and Evolutionary Biology *295*, 991–998.

Young, B., Woodford, P., and O'Dowd, G. (2013). Wheater's Functional Histology E-Book: A Text and Colour Atlas (Elsevier Health Sciences).

Zelená, J. (1984). The effect of long-term denervation on the ultrastructure of Pacinian corpuscles in the cat. Cell and Tissue Research *238*.

Zelená, J. (1994). Nerves and Mechanoreceptors - The Role of Innervation in the Development and Maintenance of Mammalian Mechanoreceptors (London, UK: Chapman and Hall).

Zelená, J., Halata, Z., Szeder, V., and Grim, M. (1997). Crural Herbst corpuscles in chicken and quail: numbers and structure. Anat Embryol *196*, 323–333.

Zidan, M., and Pabst, R. (2010). Histology of hemal nodes of the water buffalo (Bos bubalus). Cell and Tissue Research *340*, 491–496.

CONCLUSIONS

CONCLUSIONS

- The external ear canal, although minute in size compared to terrestrial mammals, shows a complex spiralling shape, and is accompanied by many active structures such as ceruminous glands and striated muscles. The general conformation of the ear canal was the same in all species, even though there are still uncertainties regarding elusive species such as Cuvier's beaked whale.
- The ear canal has a content consisting of glandular product and desquamated epithelial cells, which can occupy the entire lumen in superficial cross-sections, while it is still unknown of the medial end of the canal contains air under and under which physiological conditions. Also, the continuity of the ear canal with the external environment is still not fully understood.
- The mechanosensory nature of the simple lamellar corpuscles is confirmed, and its morphology is consistent with that of Pacinian corpuscles without an outer core or capsule.
- The presence of these lamellar corpuscles has been confirmed in various peripheral organs and all cutaneous tissues, although in highest relative abundance in the external ear canal. In the external ear canal, the corpuscles form part of a complex intramural nervous plexus present around the ear canal in the lateral half, and concentrated in a sensory ridge in the medial half.
- The ear canal has its associated lymphoid tissue (ECALT), present in the subepithelial tissue in two specific locations, one superficial and one deep.
- There were various pathologies associated with the ear canal, including several cases of otitis externa (inflammation of the ear canal), haemorrhage, muscle degeneration, and epithelial cysts or cholesteatoma. The significance of these lesions and its impact on the animal's health is still unknown.
- The results indicate not only that the ear canal in toothed whales is a functional organ, but also that it plays an unprecedented and possibly vital role in the animal's sensory perception. As such, it could have a function in the adaptation of the hearing apparatus, or to diving physiology in general, providing information for adaptive responses associated with changes in external pressure.